THE APPLICATION OF ABSORPTION SPECTROSCOPY, PARTICULARLY INFRARED TO THE STUDY OF CLAY MINERALS, SOIL ORGANIC MATTER, SOIL ADDITIVES, AND RELATED COMPOUNDS

JAMES DENNIS RUSSELL

D.Sc.
University of Edinburgh
1981

ABSTRACT

The infrared spectroscopy (IR) group at the Macaulay Institute has gained international recognition for research that has led to increased knowledge of weathering phenomena and the pedological development of soil profiles, and to a better understanding of many of the processes that have a bearing on the fertility of agricultural soils. The investigations have concerned both inorganic and organic soil constituents, and have sought to establish the structures and properties of these components, and their possible roles in soil chemistry.

Thus, in the inorganic field, IR has made significant and frequently unique contributions to the identification of new minerals, and to the elucidation of their structures. This is particularly true of the poorly crystallized minerals such as imogolite and allophane which are now recognized as products formed during the development of podzolic soils.

While it is necessary to know the bulk structures of soil clay minerals, it is even more important to know the structure of the surfaces, because it is there that adsorption and exchange of nutrient ions, fertilizers, herbicides etc. occurs. Investigations of the surfaces of many clay minerals by IR have given an insight into their reactivities. For example, it has been shown that the surfaces of swelling layer silicates like montmorillonite are acidic, and that basic molecules such as ammonia gas, widely used as a nitrogenous fertilizer, or aminotriazole, a systemic herbicide, are protonated on contact with these surfaces and are adsorbed there as cations. A different type of surface reactivity is exhibited by the oxide and hydroxide minerals. For them, adsorption occurs by ligand exchange of surface hydroxyl groups, and IR has identified for the first time, a singly coordinated OH group on the goethite (α-FeOOH) surface, that is replaced by fertilizer ions such as phosphate, sulphate and nitrate. Goethite occurs widely in soils, but more significantly, it has a surface structure that is thought to be closely related to those of the more amorphous iron oxides that occur commonly in coatings on mineral grains in soils.

Soil organic matter, although complex, can be separated into various fractions. Some of them, because of their solubility in water, are capable of movement in soil, where they have a role in profile development, and are partly responsible for soil characteristics such as crumb structure. IR has had major success in the characterization of some of these fractions; one of the water-soluble fulvic acids for example has been shown to be a polycarboxylic acid with aliphatic rather than aromatic character, containing negligible amounts of carbohydrate and nitrogenous components. This fulvic acid is very similar to synthetic polymaleic anhydride, an observation which may help to more fully elucidate the structure of the natural material which is thought to be involved during the intermediate stages of podzol development.

Ultraviolet absorption spectroscopy has been used less extensively, but it has given insights into the metabolic pathways by which lignin is degraded by soil fungi, and has highlighted the existence of an extracellular alcohol oxidase that is probably involved in the early attack of the lignin in wood. These observations are pedologically significant, because degraded lignin is a likely source of some of the phenolic compounds that are implicated in the early leaching and weathering of rocks.

CONTENTS

A. Contribution made by the author to the publications presented

B. Detailed Summary

C. Publications

	Paper No.
I Infrared Spectroscopy	
a Techniques	28
b Layer Silicates	11, 13
i Structure	5, 9, 12, 22, 23, 24, 42, 49
ii Hydration/dehydration	6, 18*, 25
iii Surface studies	
1. Reaction with organic compounds	10, 19*, 20*, 21*
2. Reaction with inorganic compounds	8, 27, 46, 51, 53
c Oxide and Hydroxides	32, 50
i Surface structure	31, 37, 52
ii Surface reactivity	
1. Reaction with organic compounds	43, 44
2. Reaction with inorganic compounds	35, 45
d Aluminosilicates	
i Imogolite structure	15, 29, 41
ii Characterization of podzol constituents	59
e Identification and characterization of minerals, clay minerals, and soil extracts	14, 36, 38, 58, 60, 61, 62
f Identification and characterization of organic substances	
i Soil organic matter fractions	30, 40, 47, 54
ii Plant glycosides	7
iii Aphid wax	34
iv Fungal pigment	57
II Ultraviolet/visible Spectrophotometry	
a Decomposition of lignin-related organic compounds by soil microfungi	1 - 3
b Determination of cation exchange capacity of clay minerals	17

* Publications while on leave of absence in U.S.A.

		Paper No.
III	Critical Commentaries	
	a Clay minerals	16, 56
	b Soil organic matter	33, 39, 48, 55
IV	Miscellaneous	
	a Adsorption of water and aromatic compounds on alkali halides	4
	b Reaction of silica with boron compounds from glass	26

A. CONTRIBUTION

Because of the unique concentration within the Institute of expertise in most of the major physical and chemical methods of analysis used in modern research, most of the research work is collaborative. This has resulted in our active collaboration in any project in which infrared (IR), or ultraviolet (UV) spectroscopy might provide useful information. Conversely, we have naturally sought the help of any other technique in solving problems arising in our own projects.

During my earlier years at the Institute, my colleague, Dr. V. C. Farmer, Head of the IR section of the Department of Spectrochemistry, guided, supervised, and gave advice on my research work, and on the preparation of manuscripts for publication. More recently, responsibility for the work and its publication has become increasingly mine, although Dr. Farmer and I are still involved in joint research and publication.

I have personally been responsible for writing twenty-six of the sixty-two papers presented in this thesis. Of those in which I am the senior author, two-thirds have been written by me, as have the IR sections in the more recent of the multiauthor papers.

All practical IR and UV spectroscopic work has been done either by me directly or, in a few instances, has been done under my supervision.

None of the papers submitted here, nor any part thereof, has been previously submitted for any other degree or diploma.

B. DETAILED SUMMARY

As a practical research tool, infrared spectroscopy made its earliest and most rapid advances in the field of organic chemistry, where the spectra of pure crystalline or gaseous compounds of known composition could be fully interpreted on the basis of classical group theory. Correlations between spectra and structure were rapidly established and functional group analysis emerged as a powerful analytical method. Progress in the application of IR to inorganic compounds was much slower, partly because of the lack of instrumentation capable of covering the low-frequency end of the spectral range below 400 cm^{-1} in which most inorganic exhibit absorption bands, and partly because of the absence of pure, well crystallized samples of known composition. Isomorphous substitution is widespread in nature, for example in the silicates and oxides present in clays, and as a consequence correlations between the spectra of these minerals and their composition was not immediately obvious to the early investigators. Indeed it was not until the need for pure analysed minerals was recognised, and then satisfied by the synthesis of such systems, that progress became possible. With the information gained from investigating synthetic compounds, it became possible to recognise correlations between spectra and structural composition of natural minerals, to identify for example the spectral changes brought about by the isomorphous replacement of aluminium for silicon in tetrahedral sheets of layer silicates, or the shift in stretching and bending frequencies of hydroxyl groups effected by coordination to different octahedral cations.

Dr. Farmer was one of the pioneers in this field and, in sharing a research project with him, I was privileged to become involved in the early innovation and development of IR techniques necessary to the study of clay minerals (Paper No. 28). The availability of analysed minerals permitted several fundamental studies to be undertaken. A wide variation of spectra was recognized for the different types of layer silicates; for example dioctahedral and trioctahedral, 1:1 minerals such as kaolinite and 2:1 minerals like montmorillonite. Different spectra were also recognized for the various isomorphous structures generated by

cation substitution within one mineral type, for example pyrophyllite ($Si_8Al_4O_{20}(OH)_4$) with no substitution, and muscovite ($K_2.Si_6.Al_2.Al_4O_{20}(OH)_4$) with one in four of its tetrahedral silicon atoms replaced by aluminium, and with potassium ions present to maintain charge balance (5). Of considerable importance was the recognition of the influence of particle size and shape on the appearance of the IR spectrum (9), but of equal value in spectral interpretation was the identification of absorption bands arising from structural hydroxyl groups (12). A more rigorous approach to this latter problem involved the exchange by deuterium of the protons in hydroxyl groups in layer silicates, a procedure which allowed a more complete identification of hydroxyl bands to be made (22). With the experience gained from the earlier structural studies, the nontronite group of minerals, iron-rich montmorillonites, was shown to be divided into two sub-groups, one, in which tetrahedral silicon was replaced by aluminium (1 in 8), and the other, in which silicon was replaced by iron III (42). In an extension of this line of work, it was established that the b axis of the nontronite was related to its iron content and to its Si-O stretching frequency (49).

One of the most important groups of layer silicates is the smectites or swelling clays. Their role in the soil is as cation exchangers having a very large surface area, much of which is internal, the so-called interlayer region. It is in this region that neutral, basic, polar or non-polar molecules, organic or inorganic, may be adsorbed, the thickness of the interlayer region measurable by XRD reflecting the size and orientation of the molecules present. The mechanism by which water is adsorbed in this region in smectites, and the role that the exchange cations play in this reaction have been studied in detail, the most important finding being that water molecules are coordinated to the exchange cations in the interlayer space, and that when the cations are small, for example Mg, the water molecules are strongly polarized, giving rise to, in this case, very acidic protons (6). Orientation studies further showed that these protons occur in hydroxyl groups that are directed at large angles to

the silicon-oxygen surfaces of the interlayer region, and that the water molecules in this region perform the function of a charge-compensating linkage between the negatively charged site of isomorphous substitution in the structure, and the positively charged exchange cations (25).

These results have been of central importance in understanding the mechanisms by which other molecules are adsorbed in the interlayer region; mechanisms which have an obvious bearing on those which are likely to occur in natural systems in the soil. A neutral organic molecule such as nitrobenzene has been shown to be adsorbed in the interlayer by replacing hydration water molecules and become coordinated to exchange cations directly, or be adsorbed to them through a water bridge. Similarly, benzoic acid may be adsorbed either as a neutral molecule or as benzoate anion (10). In investigations relating more directly to adsorption of herbicides, to some of which these molecules mentioned above are closely related, it was shown that protonation played an important part in the adsorption mechanism, usually occurring at a nitrogen atom in an amino or similar group (21).

Infrared studies also proved to be of fundamental importance in establishing that a certain class of herbicide - the s-triazines - were protonated on adsorption at the montmorillonite surface, then hydrolysed, a reaction of considerable significance, because the product was then biologically inactive (19, 20).

In studies designed to investigate these acidic surface properties of smectites still further, the agriculturally important ammonia molecule was used as a probe. IR spectroscopy is particularly well suited to detect changes in the state of the ammonia molecule, and it was shown that the gas was adsorbed by three different mechanisms; one, physical adsorption; two, direct coordination to metal cations; three, protonation to produce ammonium cations held on exchange sites. These mechanisms were demonstrated for the swelling clays montmorillonite and saponite (8) and for vermiculite (27), a mineral that occurs widely in Scottish soils. Because it retains relatively large amounts of stable ammonium

ions ammonia-treated vermiculite was investigated as a possible source of slowly released nitrogen for plant uptake (46). A sensitive colorimetric method for the determination of ammonia N was also developed (17).

Further studies of the surface reactions of smectites, particularly those that contained structural ferric ions have shown that this ion is susceptible to partial reduction by hydrazine vapour, a relatively mild reagent, and to much more extensive reduction by dithionite. The reduction is manifest in a shift in frequency of those hydroxyl groups that were coordinated to iron (III) as a result of the reduction to iron (II). Marked colour changes from yellow to blue-green that accompany the reduction are similar to those observed in gleyed (reduced) soil profiles (51). Yet another reaction that involves Fe(III) in swelling clays is one with alkali metal hydroxides, compounds which are used in the stabilization of certain soils. It was found that certain of the hydroxides were able to abstract the proton from those OH groups that were coordinated to Fe(III) in smectites, particularly nontronite. This was deduced from the disappearance of absorption bands of FeFeOH groups in the IR spectrum which also shows large shifts in Si--O vibrations, suggesting perturbation of the silicate framework, particularly by the larger cations but not by Li^+. Large increases in spacings on X-ray diffraction patterns, and shifts in Mossbauer peaks also support the deprotonation reaction, a completely novel one for clay minerals, that was shown to be partly reversible (53).

IR studies have been made of the hydroxides, oxyhydroxides and oxides, a group of minerals whose importance in soil arises because of their occurrence in coatings on other soil particles, and their effect on soil properties. It is subsequently shown here that they play a vital role in controlling the availability of agriculturally important anions such as phosphate, sulphate and nitrate among others. Before the surface reactions of these oxide minerals can be understood, their bulk structure must be fully elucidated. In a general approach to this problem IR studies of a disordered form of the silica polymorph cristobalite, and of the aluminium oxyhydroxide boehmite were made (32, 50). From band assignments for the latter mineral, an alternative space group was proposed for

the boehmite structure.

Natural hydroxides seldom are sufficiently pure, or have clean, uncontaminated surfaces, to permit unambiguous conclusions to be made about their surface structure. Although they are frequently different from their natural analogues in particle size and shape, synthetic samples of, for example, goethite (α-FeOOH) or gibbsite ($Al(OH)_3$) provide the only opportunity for successful surface investigations. By applying our well established evacuation and D_2O vapour exchange techniques to such specimens, spectra were obtained in which absorption bands arising from three different types of OH groups on the principal (100) face of the goethite crystals were identified. These groups are singly, doubly and triply coordinated to Fe(III) ions and in the air-dry state are hydrogen bonded to water molecules. They exchange very rapidly with D_2O, and one of them, the singly bound type, readily undergoes ligand exchange with acid phosphate giving a binuclear complex (31), the nature of which was subsequently more completely elucidated (37).

The surface of synthetic goethite proved to be exceptional, in that, in addition to the surface OH groups, it was shown that atmospheric CO_2 was also present, adsorbed on the surface as carbonate or bicarbonate species. Application of a modest vacuum was sufficient to desorb the CO_2, thus indicating a very weak form of bonding analogous to that of a purely physical nature. The CO_2 is nevertheless chemisorbed, possibly acting as a linkage between sites of opposite charge (35).

To more fully characterize the properties of these surface groups, they were reacted with a range of organic and inorganic anions, and it was established that, as with phosphate, these ions exchanged with the singly coordinated OH groups to give a) binuclear complexes (sulphate, selenite and oxalate), and b) monodentate complexes (fluoride, chloride and benzoate) (43, 45). Surface OH groups were also detected on the gibbsite surface, and similar studies on the absorption of oxalate, benzoate and phosphate established that, in contrast to what occurred with goethite, these anions were adsorbed only on edge faces of the crystals (44).

Ferrihydrite is another example of an iron oxide mineral likely to be present in some soils, podzols for example, as films and coatings. It is formed from solution and was thought to have a structure closely related to that of hematite but with vacancies at some of the iron sites. An IR investigation provided unambiguous proof of the presence of both surface and bulk hydroxyl groups (52), thereby suggesting that the mineral may possess reactive sites for the adsorption of anions. This is of considerable importance in the context of the probable occurrence of this mineral as a product of the pedogenesis of podzols.

Another important group of minerals that occur in soils, probably in coatings, are the aluminosilicates. These compounds are usually amorphous, or have at most short-range order, for example allophanes, but one member of the group, imogolite, now known to occur widely in Scottish soils, is cryptocrystalline, having a fibrous morphology, and a tubular structure. An earlier investigation of the structure established the presence of more than one type of hydroxyl group, and their rapid exchange with D_2O indicated that they were easily accessible, probably on surfaces (15). In this study it was suggested from IR spectra that the imogolite structure contained a pyrosilicate anion, but in a subsequent investigation using X-ray crystallography and a trimethylsilylation technique to support the IR work (29), it was unambiguously proved that the structure was tubular and that the silicate was present as orthosilicate. It was shown that the structure must contain Si-OH groups projecting into the pore of the tube, and Al-OH groups in a gibbsite-like arrangement projecting from the outer surface (29). A detailed knowledge of the structure of this mineral is vital to an understanding of its reactions in soil and the possible role it plays in the nutrient cycle. The identification of a mineral with this type of structure in a soil clay is difficult, but the recognition of a characteristic IR absorption band at 348 cm^{-1} has proved extremely valuable (41), particularly in the early recognition of short-range imoglite-like organization in both synthetic and natural preparations. This method of recognising imogolite structures has

been used extensively in characterizing the inorganic products occurring in the various horizons of podzols. From the amounts of imogolite and protoimogolite allophane - a non-crystalline form of imogolite with the same chemical composition - in these horizons, and with the help of chemical extraction data it was concluded that one of the most important mobile phases involved in the development of a podzol must have been an aluminosilicate solution with the protoimogolite composition. This is in marked contrast to the organic-based mechanism which has until now been held responsible for the translocation of aluminium down the profile (59). Work is continuing in an investigation into the possible use of the appearance of protoimogolite as an indicator of the onset of podzolization.

IR spectroscopy plays a vital role in conjunction with X-ray diffraction and electron microscopy in the identification of new and unexpected minerals in soils and rocks, where they may be present as primary minerals or as weathering products. In an earlier study, IR confirmed the presence of pyrophosphate and oxalate in alkaline extracts of several soils (14). Although it was not possible to identify the original compounds from which these anions arose, in a more recent study, a possible contributor to the oxalate was identified as glushinskite - magnesium oxalate dihydrate - a product resulting from the attack of a serpentinite rock by oxalic acid exuded by a lichen (58). Alkaline earth oxalates have very low solubilities in water and are likely to have considerable residence times in soil. Some microorganisms are known to metabolise oxalate however, thereby releasing in this case magnesium for utilization by plants.

In other studies, IR has played minor but indispensible roles in identifying for example, goethite in yellow podzols, and goethite and hematite in red (36), and in confirming the basic hydroxy-carbonate component in a nickeloan pyroaurite mineral in a serpentinite rock (38).

The IR technique has performed a much more substantial role in complementing X-ray diffraction in the characterization firstly, of minerals in weathered rocks at the earth's surface, and secondly, of products formed in deeply weathered rock. Minerals in these categories are frequently interstratified,

and the IR technique generally sees them as mixtures of the individual components. Nevertheless, the identification of the components from their spectra provides essential information to a full understanding of the structure. Thus, in a study of the weathering of a basalt, IR and XRD combined to show the presence of a three-component interstratification of montmorillonite, illite, and dioctahedral vermiculite in the weathered clay (60). In the fresh rock, a chlorite-like mineral with a composition intermediate between those of swelling chlorite and saponite was identified, its IR spectrum providing clues vital to an understanding of the island structure of the interlayer region of this little-known mineral (61).

Similarly, in an investigation of an unusual, swelling, hematitic mineral of probably pedogenic origin in deeply weathered granite beneath a podzol, the IR spectrum provided fundamental information concerning its platy morphology and its mixed hematite-silicate composition. Differential IR spectra showed that the mineral contained structural OH groups coordinated to iron(III), and this in conjunction with XRD and electron microscopy allowed the proposal of a unique structure to be made. It comprises twelve iron-oxygen octahedral sheets in a hematite array, bounded on each side by a silicate tetrahedral sheet, giving a basal spacing of 35.5A (62).

Because of its heterogeneous and complex nature, soil organic matter does not lend itself to definitive study by IR spectroscopy in that complete structures can seldom be identified. Instead, IR is used to make a functional group analysis of fairly well defined fractions of soil organic matter, fractions isolated by a combination of chemical dissolution and fractionation on various adsorbents. Using this method, some very important broad classifications of soil organic matter have been possible. The most common method of fractionation is that based upon alkaline extraction, then precipitation by acidification to give an insoluble fraction referred to as humic acid, and a soluble one called fulvic acid. Spectra of humic acids are generally very broad and diffuse,

indicating a rather complex composition. Nevertheless, aromatic functionality attributable to lignin residues is occasionally observed, particularly in spectra of humic acids from organic-rich upper horizons. Fractionation on the basis of molecular weight or size has not proved helpful in elucidating the structure of humic acids. The fulvic fraction however can be readily separated on a variety of adsorbents into two main fractions, one with the IR characteristics of carbohydrate, the other with those of a polycarboxylic acid. In the characterization of this latter fraction, the so-called fulvic B, a comparison was made between its composition and that of a synthetic polymer of maleic anhydride. The close similarity of their spectra in showing no detectable aromatic character, and essentially only carboxylic acid groups on an aliphatic or alicyclic framework, and their almost identical chemical compositions, led to the proposal of polymaleic anhydride (PMA) as a model for fulvic acid (40). Although the two substances must differ in structural detail, the broad similarity between them represents an important advance in understanding the structure of at least one part of soil organic matter. In a broader study of the organic matter in a podzol, while the humic and fulvic B components were recognized, it was the polysaccharide-rich fraction - fulvic C - that provided another important result. The spectrum shows the carbohydrate nature of the fraction, and also that ester and possibly carboxylic acid groups are present. Spectra of a series of these fractions taken from increasing depths in the profile clearly indicated a steady decrease in ester/carboxylic acid and an increase in secondary amide groups, subsequently shown chemically to be due to proteinaceous material. Although the soil polysaccharide spectra are not generally recognizable as belonging to well defined polymers, one fraction from this podzol had a spectrum with very close analogies to that of pectic acid. The identification of protein- and pectic-like materials in these horizons is surprising in view of their known instability in soil, and must suggest their presence in a protected form, possibly as an adsorption complex (47).

In an attempt at a more detailed structural study of soil polysaccharide, IR spectroscopy was used to follow the course of its methylation and subsequent

hydrolysis. It was shown that sugar residues and proteinaceous material are both methylated, the latter yielding the easily recognizable absorption band of the tertiary amide group (54). Knowledge of the presence of methylated amino acids in the hydrolysis products of methylated soil polysaccharide could be of importance in deciding whether the protein and carbohydrate are bonded, or are merely co-precipitated.

A thermal decomposition-IR study of the soil protein showed that, apart from its intrinsic value as a nitrogen source, it decomposes just above 100°C to yield NH_3 which is trapped at acidic adsorption sites as NH_4^+, easily identified from its IR absorption band (30). This reaction could partly explain the increased fertility of soil following burning of stubble for example.

As a preliminary to studying that fraction of soil organic matter that is not soluble in alkali in the usual extraction procedure, the humin fraction, a study was made of a black fungal melanin thought to be sufficiently resistant to accumulate in soil in the form of fungal debris, and to contribute to the humin fraction. Using a combination of IR spectroscopy, methylation, and chemical analysis, it was concluded that the melanin probably had a structure similar to that of oxidatively polymerized catechol. The spectra were interpreted to show the presence of very strongly hydrogen bonded conjugated carboxylic acid groups as well as normal acid groups (57), both of which might be involved in cation exchange in soil.

Ultraviolet (UV) and visible spectroscopy has played a relatively minor part in the overall research programme, but it nevertheless made a significant contribution to a better understanding of the mode of action of the white-rot fungus Polystictus versicolor. This fungus metabolizes the lignin component in wood and, in order to understand the mechanisms involved, the action of the fungus on simple aromatic compounds was studied. By measuring the UV spectra of culture filtrates it was shown that the fungus reduced certain aromatic acids to aldehydes and alcohols, a metabolic pathway not previously reported in biological systems (1). It was also noted that the organism produced an extracellular

alcohol dehydrogenase,and, in a subsequent study, it was shown that the enzyme, probably a flavoprotein, oxidized a range of primary aromatic alcohols, but did not affect secondary aromatic or primary aliphatic alcohols, carbohydrates or L-amino acids (2). These observations suggest that the enzyme might somehow be involved in the primary attack of the lignin in wood, and to try to substantiate this, the metabolisms of a number of synthetic model compounds by the fungus and its extracellular enzyme were studied. While the organism was able to utilize those models with a free phenolic hydroxyl group but not those with only methoxyls, the enzyme oxidized none of them over the duration of the experiment. The operation of a much slower oxidation reaction cannot be ruled out however (3).

In response to several examples of serious misinterpretation of IR spectra in the literature concerning both soil organic matter and clay minerals, a number of critical notes have been written in the hope that these errors might be avoided in the future (16, 13, 39, 48, 55, 56). Particular concern was expressed in one of these notes (39), because erroneous conclusions drawn from IR spectra concerning the existence of an ester linkage between soil polysaccharide and humic acid has been incorporated into the new edition of an authoritative text-book on soil science. If such errors arising from misinterpretation of IR spectra are not corrected and drawn to the attention of the scientific community, real progress towards a better understanding of the structures of soil organic matter and clay minerals will be unnecessarily delayed. Indeed, to know of such work and remain silent is to do a disservice to science.

Reprinted from Biochim. Biophys. Acta, Vol. 35 (1959)

REDUCTION OF CERTAIN AROMATIC ACIDS TO ALDEHYDES AND ALCOHOLS BY *POLYSTICTUS VERSICOLOR*

V. C. FARMER, MOIRA E. K. HENDERSON AND J. D. RUSSELL
Macaulay Institute for Soil Research, Aberdeen (Scotland)

(Received December 1st, 1958)

SUMMARY

1. *Polystictus versicolor* reduced the following acids to the corresponding aldehydes and alcohols: *m*-, *p*-methoxybenzoic, 3:4-dimethoxybenzoic, β-naphthoic. Only the alcohols were detected from *o*-methoxybenzoic and benzoic acids. *o*- and *p*-Hydroxybenzaldehydes were reduced to alcohols. The following acids were not reduced: 2:4-dimethoxybenzoic, phenylacetic and α-naphthoic.

2. The rate of conversion varied with the position and nature of ring substituents.

3. There was a small amount of demethoxylation of the following with production of the corresponding hydroxy acids: *o*-, *m*- and *p*-methoxybenzoic and 2:4-dimethoxybenzoic acids. The following were hydroxylates in the *para* position: cinnamic, benzoic, and phenylacetic acids, the last two in only small amounts. Some breakdown of the aromatic structure occurred during metabolism of cinnamic, β-naphthoic, *p*- and *o*-hydroxybenzoic acids.

4. The fungus produced an extracellular alcohol dehydrogenase.

References p. 211.

INTRODUCTION

Following an investigation into the metabolism of methoxylated aromatic compounds by micro-fungi[1] a similar study was made with the wood-rotting basidiomycete *Polystictus versicolor*. Using preformed mats of this fungus a type of metabolism was obtained which differed markedly from that previously found. Whereas micro-fungi converted methoxybenzoic acids to the corresponding hydroxybenzoic acids which were then further metabolised through cleavage of the ring, the predominant system in *P. versicolor* was one of reduction of these acids to their corresponding aldehydes and/or alcohols. Several other aromatic acids and aldehydes were found to be reduced by this fungus. The presence of an extracellular enzyme system was also detected which could dehydrogenate the aromatic alcohols formed to regenerate the aldehydes.

METHODS

Organism

Polystictus versicolor was isolated from fructifications collected from a tree-stump.

Cultural conditions

Mats of the fungus were obtained by the technique used previously for the micro-fungi[1]. In the present work the inocula were discs cut from the periphery of cultures growing on potato dextrose agar plates, four discs being added to each flask. After 12 days incubation, mats were obtained which completely covered the surface of the culture medium. The medium beneath the mat was then replaced by the substrate as described by KLUYVER AND VAN ZIJP[2].

Preparation of substrates

Substrates were made up at a concentration of 0.004 *M*, unless stated otherwise, for the solutions analysed spectrochemically, and at 0.01 *M* for those analysed chromatographically, and were adjusted to pH 6.5 before autoclaving at 15 lb./sq. in. pressure for 20 min. Since the aldehydes were volatile, weighed amounts were autoclaved at 22.5 lb./sq. in. in small bottles with tightly screwed caps. After autoclaving, the contents were added to sterile water and aliquots then taken aseptically from each solution to determine the concentration as described below.

Spectrochemical analysis

The course of metabolism was followed by studying the u.v. absorption of suitably diluted aliquots from the culture solution, and by examining the infrared spectra of the ether-soluble products. In estimating the concentration of substituted benzoic acids, use was made of the change in absorption on going from acidic to alkaline solution (0.05 *N* in H_2SO_4 or NaOH), corresponding to a change from the undissociated acid to the anion. As the absorption of other components of the culture solutions was generally insensitive to pH, their overlapping absorption did not interfere. The wavelengths at which $\Delta\varepsilon$, the change in molar absorption coefficient, were measured are given in Table I for the various acids studied. Metabolic products from *o*-hydroxybenzoic acid were sensitive to pH and this method of estimation could not be applied. Estimations of this acid were based on measurements at 297 mμ in alkaline solution after an approximate correction for background absorption.

References p. 211.

TABLE I

THE DIFFERENCE IN MOLAR ABSORPTION COEFFICIENT, $\Delta\varepsilon$, BETWEEN ACID AND ALKALINE SOLUTION AT WAVELENGTH λ (mμ) FOR VARIOUS AROMATIC ACIDS

Compound	λ	$\Delta\varepsilon$
p-Methoxybenzoic acid	265	7,800
m-Methoxybenzoic acid	300	1,330
	245	2,790
o-Methoxybenzoic acid	300	2,700
	240	3,900
3:4-Dimethoxybenzoic acid	300	3,700
	265	5,900
Benzoic acid	235	4,700
β-Naphthoic acid	240	18,240
p-Hydroxybenzoic acid	285	15,625
Cinnamic acid	250	4,360
p-Hydroxycinnamic acid	340	17,400

TABLE II

THE MOLAR ABSORPTION COEFFICIENT, ε, AT WAVELENGTH λ (mμ) FOR VARIOUS AROMATIC ALDEHYDES AND ALCOHOLS

Compound	λ (mμ)	ε
p-Methoxybenzaldehyde	290	15,000
m-Methoxybenzaldehyde	310	2,550
o-Methoxybenzaldehyde	320	4,000
o-Methoxybenzyl alcohol	230	2,380
p-Hydroxybenzaldehyde	330*	26,400
p-Hydroxybenzyl alcohol	245*	11,800
o-Hydroxybenzaldehyde	375*	5,750
o-Hydroxybenzyl alcohol	290*	3,500
β-Naphthaldehyde	250	33,800
β-Naphthyl carbinol	223.5	90,000

* ε values at these wavelengths refer to alkaline solution.

Aldehydes and alcohols in culture solutions were estimated at wavelengths where their absorption was high relative to other constituents whose absorption was corrected for where necessary. The selected wavelengths, together with approximate molar absorption data, are given in Table II. Total amounts of *p*-methoxybenzaldehyde plus *p*-methoxybenzyl alcohol were estimated at 225 mμ, where their absorption is equal and $\varepsilon = 10{,}000$.

Paper chromatographic analysis

For this, 0.01 *M* solutions of the substrates were used. Analyses of the culture solutions were made at intervals of a few days, using the method previously described[1].

RESULTS

Reduction of mono-methoxybenzoic acids by P. versicolor

The general pattern of metabolism is well-illustrated by the 3 monomethoxybenzoic acids. The concentration of all three acids fell as shown in Table III. The

References p. 211.

TABLE III

METABOLISM OF MONO-METHOXYBENZOIC ACIDS BY *P. versicolor*

Days	*Residual acid as percentage of original concentration (0.004 M)*		
	p-Methoxybenzoic	*m-Methoxybenzoic*	*o-Methoxybenzoic*
1	60	62	84
2	32	32	—
3	14	17	73
4	—	5	—
5	4	—	67
7	—	3	—
8	4	—	—
9	—	—	48
15	—	—	20
21	—	—	10

— = No analysis

para and *meta* acids disappeared at a similar rate, but the *ortho* acid was metabolised much more slowly. During the disappearance of *p*-methoxybenzoic acid the absorption spectrum of *p*-methoxybenzaldehyde appeared in the culture medium (Table IV). The concentration of aldehyde varied erratically, ranging from 21 to 46%, over 8 days. The culture solution remaining on the 8th day was extracted with ether. The infrared spectra of the ether-soluble material showed it to be a simple mixture of *p*-methoxybenzyl alcohol and *p*-methoxybenzaldehyde in a ratio of about 1.75:1. This material gave a 2:4-dinitrophenylhydrazone whose infrared spectrum was identical with that of the dinitrophenylhydrazone of *p*-methoxybenzaldehyde.

TABLE IV

FORMATION OF *p*-METHOXYBENZALDEHYDE FROM *p*-METHOXYBENZOIC ACID BY *P. versicolor*

Days	*Percentage of p-Methoxybenzaldehyde*
1	21
2	31
3	46
5	45
8	33

In 4- and 7-day samples from *m*-methoxybenzoic acid cultures a new maximum insensitive to pH appeared at 255 mμ, which corresponded to about 2% *m*-methoxybenzaldehyde. Its presence was confirmed, in a separate experiment, by the identification of its 2:4-dinitrophenylhydrazone by its infrared spectrum. An ether extract made after 7 days incubation contained a product whose infrared spectrum showed *m*-methoxybenzyl alcohol to be the chief constituent but an impurity (not the aldehyde) was present which absorbed at 9.04 μ.

The formation of *o*-methoxybenzaldehyde from *o*-methoxybenzoic acid could not be detected by ultraviolet analysis of the culture solution nor was any precipitate obtained with 2:4-dinitrophenylhydrazine. After 22 days incubation, an ether extract

References p. 211.

of the culture solution yielded an oil whose infrared spectrum was identical with that of *o*-methoxybenzyl alcohol.

TABLE V

METABOLISM OF MONO-METHOXYBENZALDEHYDES BY *P. Versicolor*

Days	*Residual aldehyde as percentage of original concentration*		
	p-Methoxybenzaldehyde $2.6 \cdot 10^{-3}$ *M**	*m-Methoxybenzaldehyde* $2.0 \cdot 10^{-3}$ *M**	*o-Methoxybenzaldehyde* $2.1 \cdot 10^{-3}$ *M**
1	60	37	0
2	60	—	—
4	44	—	—
5	78	15	0
6	65	25	—
8	46	25	—
10	48	—	—
12	73	17	—
13	—	32	—
14	56	22	—

* Original concentration.

Starting with the aldehydes, at initial concentrations as given in Table V, it was found that only the *ortho* form disappeared (Table V). With the *meta* and *para* forms, after the concentration had fallen to a certain level, no further reduction took place. The *o*-methoxybenzaldehyde culture solution was extracted with ether on the 6th day and *o*-methoxybenzyl alcohol was identified in the extract by infrared analysis. The experiment with *o*-methoxybenzaldehyde was repeated and u.v. analyses of the culture solutions made at more frequent intervals. After 4, 8 and 24 h the concentration had been reduced to 70, 45 and 5 % respectively of the initial concentration of $2.4 \cdot 10^{-3}$ *M*, while *o*-methoxybenzyl alcohol accumulated in amounts which indicated that there was a quantitative conversion of aldehyde to alcohol. Further analyses after 6 and 10 days showed that there was no re-accumulation of the aldehyde. *o*-Methoxybenzyl alcohol was again identified on examining an ether extract of the culture solution prepared on the 13th day after inoculation. The experiment with *p*-methoxybenzaldehyde was also repeated and ether extracts prepared after 2 and 7 days. A mixture of *p*-methoxybenzyl alcohol and aldehyde was identified by infrared analysis in both extracts. The presence of a readily available substrate, 1 % glucose, was found to have no effect on the rate of reduction of *p*-methoxybenzaldehyde, or on the final equilibrium reached.

Dehydrogenation of p-*methoxybenzyl alcohol by* P. versicolor

Examination of Table V shows that the concentrations of aldehyde tended to fluctuate in successive samples. It was found that this could be attributed to an increase in aldehyde concentration during the time that a sample was stored in the refrigerator before analysis. For example the 5- and 12-day samples, in which the aldehyde concentration was particularly high, were stored for 2 days before analysis. To confirm this, a mat of *P. versicolor* was incubated over *p*-methoxybenzoic acid for 5 days, when the acid was completely reduced, and 37.5 % of *p*-methoxybenzaldehyde had been formed. On storing a cell-free sample from this culture in the refriger-

References p. 211.

ator for 2 days, the proportion of aldehyde increased to 53 % at the expense of the alcohol, but no increase occurred in a sample autoclaved at 15 lb./sq. in. pressure for 20 min. These results indicate that an extracellular alcohol dehydrogenase is produced by the fungus.

Confirmation of the ability of *P. versicolor* to dehydrogenate *p*-methoxybenzyl alcohol was obtained by following the conversion of the alcohol to *p*-methoxybenzaldehyde under a fungal mat. The alcohol solution (0.004 *M*) was sterilised by filtration. Analyses over 8 days showed that conversion of alcohol to aldehyde varied between 24 and 35 %. There was no overall loss of the methoxyphenyl group and no acid was formed.

Formation of acetals

Ether extracts from *p*-methoxybenzoic acid and *p*-methoxybenzaldehyde cultures generally gave a mixture of the alcohol and aldehyde. Sometimes, however, the acetal formed by reaction between the components of the mixture was obtained, *i.e.* $R.CHO + 2\ R.CH_2OH \longrightarrow R.CH(OCH_2R)_2 + H_2O$. It is presumed that some accidental contaminant catalysed the formation of the acetal in these extracts. Synthetic mixtures of *p*-methoxybenzyl alcohol and *p*-methoxybenzaldehyde did not react at room temperature, even on long standing, but the acetal was obtained when the reagents were heated together with $CaCl_2$ and NH_4Cl crystals[3]. It was then isolated as waxy crystals, melting point 34–35° on crystallising from light petroleum. The impurity associated with *m*-methoxybenzyl alcohol obtained from cultures of *P. versicolor* on the corresponding acid may also have been an acetal, but efforts to synthesise this material failed.

Reduction of dimethoxybenzoic acids by P. versicolor

The metabolism of 3:4- and 2:4-dimethoxybenzoic acids was followed by the same method as was that of the mono-methoxybenzoic acids. The former was metabolised in a similar way to the monomethoxy acids, only 5 % remaining after 8 days. A 2:4-dinitrophenylhydrazone prepared from a carbon tetrachloride extract made on the 9th day was identical with that obtained from 3:4-dimethoxybenzaldehyde. An ether extract made after extracting the culture solution with carbon tetrachloride was shown by infrared analysis to contain 3:4-dimethoxybenzyl alcohol together with some aldehyde.

2:4-Dimethoxybenzoic acid was metabolised very slowly. An intermediate product, which reached a maximum after 2 days, was formed. This product had a strong absorption at 270 mμ in alkaline solution probably due to a phenolic substance. Its presence prevented estimation of residual acid, but chromatography showed that considerable amounts remained unchanged after 8 days. Chromatographic analysis (see below) also showed the formation of phenolic products. Carbon tetrachloride and ether extracts of the neutral solution, which would have extracted any 2:4-dimethoxy-benzaldehyde or -benzyl alcohol formed, yielded no products. Similarly, on incubation for 3 weeks no products could be obtained.

Reduction of other aromatic acids and aldehydes by P. versicolor

Benzoic acid: The concentration fell steadily and only 5 % remained after 7 days. On the 8th day the culture solution was extracted with carbon tetrachloride and

References p. 211.

ether. Benzyl alcohol was identified in the ether extract. Benzaldehyde was not detected although its characteristic smell was clearly evident during the course of the experiment.

Phenylacetic acid: This acid did not appear to be attacked by the fungus. No marked change in the u.v. spectrum occurred up to 7 days. No neutral products were obtained from either carbon tetrachloride or ether extractions, indicating that this acid was not reduced. Chromatography confirmed that much of the acid remained unattacked.

Cinnamic acid: Only 12 % of this acid remained after 11 days under the mat. The absorption of *p*-hydroxycinnamic acid, which appeared as a transient intermediate, reached a maximum corresponding to 18 % of the original acid on the fourth day, but fell off to only 2.5 % after 11 days. No other aromatic product was detectable. In a separate experiment the neutralised culture solution was extracted with ether when the concentration of cinnamic acid had fallen to 44 %. This extract yielded very little material, indicating that no significant amounts of cinnamyl alcohol or aldehyde were present.

α- and β-Naphthoic acids: 0.0025 *M* solutions of these acids were used. α-Naphthoic acid was not attacked. β-Naphthoic acid was converted until 49 % remained after 4 days, after which it was not changed further (Table VI). At this time 27 % β-naphthaldehyde was present. On the 8th day the culture solution was extracted with ether. A 2:4-dinitrophenylhydrazone prepared from the extract had an infrared spectrum which was identical with that of the 2:4-dinitrophenylhydrazone of β-naphthaldehyde. In the culture solution a new band at 223 mμ rose to its maximum on the 2nd day. Although β-naphthaldehyde has a maximum at 223 mμ, this does not account for the maximum at this wavelength from 2 days onwards. β-Naphthyl carbinol was synthesised from its aldehyde by reduction with $LiAlH_4$ and was found to have a very strong absorption band at 223.5 mμ. On the basis of its u.v. absorption at this wavelength, the percentage of the carbinol present in the samples was estimated (Table VI).

TABLE VI

METABOLISM OF β-NAPHTHOIC ACID BY *P. versicolor*

Days	*Percentage residual acid*	*Percentage aldehyde formed*	*Percentage carbinol formed*
1	71	6.5	4
2	52	11.5	19
4	49	27	4
5	42	30	8
7	48	30	4
8	47	30	5

The failure to reduce the acid completely in this experiment is probably due to the formation of toxic products in the culture solution. A lower initial concentration of acid (0.0013 *M*) was completely reduced in 4 days, with the formation of 47 % aldehyde and 20 % β-naphthyl carbinol. The low yield of products indicates that there was some attack on the naphthyl nucleus. This was confirmed when the fungus was incubated over 0.0004 *M* β-naphthyl carbinol. After 6 days 35 % had been oxidised

References p. 211.

to aldehyde, but only 5 % of the carbinol remained. No β-naphthoic acid was formed.

p-*Hydroxybenzaldehyde:* This compound was metabolised steadily and fairly rapidly, only 6 % remaining after 4 days. *p*-Hydroxybenzyl alcohol was produced and estimation of the amounts of aldehyde and alcohol present in the culture solution showed that there was a quantitative conversion. The alcohol was extracted with ether at pH 6.5 since it polymerises in acid conditions. It was purified by recrystallisation and gave an infrared spectrum identical with that of *p*-hydroxybenzyl alcohol synthesised by reduction of *p*-hydroxybenzaldehyde by $LiAlH_4$.

p-*Hydroxybenzoic acid:* This acid was metabolised very slowly, 10 % remaining after 14 days. U.v. analysis showed that no significant conversion to *p*-hydroxybenzyl alcohol occurred. On the 16th day the culture solution was neutralised with bicarbonate, extracted with ether and the ether extracts washed with bicarbonate solution to remove any acid present. The resulting product was too small for analysis.

o-*Hydroxybenzaldehyde:* Table VII shows the course of metabolism of *o*-hydroxybenzaldehyde, starting with an initial concentration of 0.002 *M*. The aldehyde was rapidly converted to the alcohol which was further metabolised. In order to extract the alcohol for identification by infrared analysis four flasks each containing 100 ml of $3.5 \cdot 10^{-3}$ *M* *o*-hydroxybenzaldehyde were incubated for 1 day, extracted at pH 7 with carbon tetrachloride to remove aldehyde, then with ether to extract the alcohol. The identity of the alcohol was confirmed from its infrared spectrum, melting point and mixed melting point.

TABLE VII

METABOLISM OF *o*-HYDROXYBENZALDEHYDE BY *P. versicolor*

Days	*Residual aldehyde as percentage of initial concentration*	*o-Hydroxybenzyl alcohol*
1	24	50
2	6	35
4	0	7

o-*Hydroxybenzoic acid:* At an initial concentration of 0.004 *M*, this acid was metabolised very slowly. The concentration dropped to 86 % of the original after 1 day, but after 10 days 63 % still remained. The acid was probably toxic at this level and when its initial concentration was lowered to 0.001 *M* it was metabolised slowly and steadily, less than 13 % remaining after 11 days. The corresponding aldehyde and alcohol could not be detected in the culture solution. The u.v. spectrum indicated that a complex phenolic product had been formed.

Effect of aeration on the reduction of p-*methoxybenzoic acid by* P. versicolor

The experimental results point to the existence of a strong reducing system in *P. versicolor*. It was considered possible that the conditions in the culture flasks might have been conducive to an anaerobic type of metabolism. However, even when a steady stream of air was bubbled through a solution of *p*-methoxybenzoic acid under a mat of the fungus, *p*-methoxybenzaldehyde was formed. This indicates that lack of oxygen was not a governing factor in the reduction of the acid. In another

References p. 211.

experiment the metabolism of *p*-methoxybenzoic acid under air and nitrogen was compared. After 7 days under air the concentration of acid fell to 3 %, while under nitrogen it fell to 60 % of the initial concentration. *p*-Methoxybenzaldehyde was formed in both flasks, 53 % being present in the air flask and 11 % in the nitrogen flask after 7 days. These results indicate that anaerobic conditions were not responsible for the reducing reactions which were taking place, and actually slowed down the rate of reduction considerably. *p*-Methoxybenzaldehyde was extracted from both cultures and its identity was confirmed by examining the infrared spectra of the 2:4-dinitrophenylhydrazones.

Analysis of culture solutions by paper chromatography

Results obtained by paper chromatography indicated that demethoxylating and hydroxylating systems were present in *P. versicolor*. Thus the formation of *p*-, *m*- and *o*-hydroxybenzoic acids from the corresponding methoxybenzoic acids was indicated. 2:4-dihydroxybenzoic acid was detected in the extract from a culture solution containing 2:4-dimethoxybenzoic acid. In addition a strong pink-orange spot, considerably larger than the spot of 2:4-dihydroxybenzoic acid, was obtained with diazotised sulphanilic acid spray. When the solvent was *n*-propanol–ammonia–water (80/5/15 vol.) this unidentified phenolic compound had an R_F value of 0.536. There was no indication of demethoxylation or hydroxylation of 3:4-dimethoxybenzoic acid. Benzoic acid was hydroxylated to form *p*-hydroxybenzoic acid and phenylacetic acid to form *p*-hydroxyphenylacetic acid. Extracts from β-naphthoic acid cultures yielded only traces of coloured compounds when sprayed with diazotised sulphanilic acid. Spectrochemical analysis revealed that the naphthalene nucleus was being attacked, but these results show that the main attack did not lead to naphthol formation. Similarly, traces of coloured products were obtained with α-naphthoic acid cultures. Cinnamic acid was partly hydroxylated to *p*-hydroxycinnamic acid and an additional unidentified phenolic compound of R_F 0.813 with butanol–ammonia–water (80/5/15 vol.) was detected as a yellow spot with diazotised sulphanilic acid.

These results show that several different enzyme systems were acting in the mycelium under the conditions operating in the culture flasks. U.v. absorption analysis indicated that the hydroxy acids were present only in very small quantities except in the case of 2:4-dimethoxybenzoic and cinnamic acids.

DISCUSSION

A survey of the results reveals that there is a general pattern of reduction involving the conversion of aromatic acids and aldehydes to alcohols by *P. versicolor*. The reduction of aldehydes to alcohols is a common metabolic step, and has been reported for several aromatic aldehydes[4,5] but the reduction of acids does not appear to have been reported previously in biological systems. The rates of conversion vary with the position and nature of ring substituents. In particular there is evidence that the steric effect of *ortho* substituents may interfere with the reduction of the aromatic acids. Thus *m*- and *p*-methoxybenzoic acids are much more rapidly reduced than the *ortho* isomer. Again β-naphthoic acid is readily reduced, but α-naphthoic acid is not attacked and 3:4-dimethoxybenzoic acid is reduced but the corresponding 2:4 isomer is not. A marked reduction in metabolic rates when *ortho* substituents are present

References p. 211.

has been reported in the β-oxidation of various aryloxy-propionic and butyric acids[6], in the demethoxylation of mono-methoxybenzoic acids and in the decomposition of hydroxybenzoic acids[1]. Steric factors, however, do not appear to inhibit reduction of the methoxybenzaldehydes, since the *ortho* isomer is rapidly reduced to the alcohol.

Apart from the above instances where steric effects may operate, reduction products were not obtained from four of the acids, namely, *o*- and *p*-hydroxybenzoic, phenylacetic and cinnamic acids. The first two are of interest in that the corresponding aldehydes are readily reduced. The aromatic rings of both hydroxy acids are attacked by the fungus: nevertheless it can be concluded that no significant reduction of *p*-hydroxybenzoic acid could have occurred, since this would have led to *p*-hydroxybenzyl alcohol, which is not attacked. It is uncertain, however, whether *o*-hydroxybenzoic acid is reduced, since the expected reduction products are also attacked by the fungus.

Phenylacetic and cinnamic acids differ from the other acids examined in that their carboxylic acid groups are not directly attached to the ring, although in cinnamic acid this group is conjugated with the ring through the C = C bond of the side chain. No significant reduction of phenylacetic acid could have occurred, as much of this acid remained unmetabolised in the experiment. Cinnamic acid, however, was rapidly metabolised, so that reduction of this acid, with subsequent attack on the reduction products, cannot be excluded.

In several instances only partial reduction of aldehyde to alcohol occurred, the final ratio of the two varying with the different compounds. This is clearly seen for *m*- and *p*-methoxybenzaldehydes in Table VI. Other aldehydes not completely reduced were 3-4-dimethoxybenzaldehyde and β-naphthaldehyde. The persistence of aldehydes in the culture solution can probably be ascribed to the action of the extracellular dehydrogenase found there, and further investigations on it are being carried out. In contrast to the above, *o*-methoxybenzaldehyde, *p*-hydroxybenzaldehyde and, presumably, benzaldehyde itself were quantitatively reduced to alcohols. *o*-Hydroxybenzaldehyde was also reduced to the alcohol, but the alcohol was further metabolised.

Paper chromatography revealed that the ability possessed by micro-fungi to demethoxylate aromatic acids, with formation of hydroxylated compounds, was by comparison only weakly developed in *P. versicolor*.

REFERENCES

[1] M. E. K. HENDERSON, *J. Gen. Microbiol.*, 16 (1957) 686.
[2] A. J. KLUYVER AND J. C. M. VAN ZIJP, *Antonie van Leeuwenhoek J. Microbiol. Serol.*, 17 (1951) 47.
[3] W. J. HICKINBOTTOM, *Reactions of Organic Compounds*, Longmans Green & Co. London, 1948, p. 181.
[4] T. HIGUCHI, *Physiol. Plantarum*, 10 (1957) 633.
[5] T. HIGUCHI, *4th Intern. Congr. Biochem., Vienna*, 1958, Symposium No. 11, Preprint No. 4.
[6] D. M. WEBLEY, R. B. DUFF AND V. C. FARMER, *J. Gen. Microbiol.*, 18 (1958) 733.

Printed in The Netherlands

[FROM THE BIOCHEMICAL JOURNAL, VOL 74, No. 2, pp. 257–262, 1960]

PRINTED IN GREAT BRITAIN

Aromatic-Alcohol-Oxidase Activity in the Growth Medium of *Polystictus versicolor*

BY V. C. FARMER, MOIRA E. K. HENDERSON AND J. D. RUSSELL
The Macaulay Institute for Soil Research, Craigiebuckler, Aberdeen

(*Received* 20 *July* 1959)

To gain a better understanding of the changes which plant lignins undergo in the soil the fungal breakdown of aromatic compounds related to lignin has been studied. Previous work has shown that the wood-rotting basidiomycete *Polystictus versicolor* is able to reduce many aromatic acids to the corresponding alcohols, or to mixtures of aldehydes and alcohols (Farmer, Henderson & Russell, 1959). The persistence of aldehydes after complete reduction of the acids appeared to be due to an extracellular oxidase acting on the alcohols, and this was confirmed for *p*-methoxybenzyl alcohol. The properties and substrate specificity of this system are more fully examined here.

MATERIALS AND METHODS

Organism. *Polystictus versicolor* as used previously (Farmer *et al.* 1959) was isolated from fructifications collected from a tree stump.

Buffers. Sørensen's phosphate (Clark, 1928) and 2-amino-2-hydroxymethylpropane-1:3-diol (tris) buffer (Gomori, 1955) were used.

Production of enzyme. The fungus was grown in 250 ml. conical flasks containing 100 ml. of mineral salts solution ($NaNO_3$, 0·3%; $MgSO_4$, 0·05%; KH_2PO_4, 0·1%; KCl, 0·05%) to which were added 1·0 g. of glucose and 0·5 g. of yeast extract. Each flask was inoculated with four disks, cut from the periphery of a culture of the fungus on potato-dextrose–agar, and incubated at 22°, usually for 10–12 days. Hyphae from these disks spread over the surface of the medium to form a firm mat. During growth of the fungus the enzyme accumulated in the growth medium, and this solution was used directly in many experiments. A further supply of enzyme could be obtained by pouring off the medium at the end of the growth period, washing the mats three times with sterile water and then pouring 100 ml. of sterile water under them. After further incubation enzyme diffused from the mycelium into the water.

An enzyme concentrate was obtained by saturating growth solutions with $(NH_4)_2SO_4$. The saturated solution was allowed to stand overnight and the resulting precipitate was centrifuged down at 38 000 *g* for 20 min. It was then suspended in 3–5 ml. of water and dialysed for 21 hr. against Sørensen's phosphate buffer (KH_2PO_4–Na_2HPO_4, pH 6·2) at 5°. Under these conditions the volume did not change appreciably.

Enzyme activity. The activities of enzyme solutions were compared spectrophotometrically by measuring the rates at which they oxidized *p*-methoxybenzyl alcohol to the aldehyde, and are reported as μmoles of aldehyde produced by 1 ml. of enzyme solution in 1 hr. (μmoles/ml./hr.). The assay solution contained 1 ml. of 0·067 M-phosphate buffer (pH 6·2), 4 μmoles of *p*-methoxybenzyl alcohol, *x* ml. of enzyme solution and water to 3 ml. The change in absorption per minute (ΔE/min.) was measured at 290 mμ in

1 cm. cells with a Beckman DU spectrophotometer. The temperature of the cell housing was not controlled. The reference cells contained buffer, water and either enzyme or alcohol. The activity, in terms of μmoles of aldehyde/ml./hr., is given by $1{\cdot}8 \times 10^5$ $(\Delta E/\text{min.})/\epsilon x$ (ϵ, the molar extinction coefficient of *p*-methoxybenzaldehyde at 290 mμ, being taken as 15 000). Similar methods were used to estimate the activity of enzyme solutions towards other aromatic alcohols, differing wavelengths and appropriate ϵ values being used (Table 1). As the aldehydes have carbonyl groups conjugated with the aromatic ring, they all absorb at longer wavelengths than the alcohols, and therefore small amounts could be detected in the presence of excess of the alcohols.

Enzyme activity was also indicated by oxygen uptake in the Warburg apparatus at 25°. Enzyme solution (1 ml.) and 1 ml. of phosphate buffer, pH 6·2, were added to the main compartment of the flasks, and 0·5 ml. of 0·01 M solutions of alcohols were tipped in from the side arms. β-Naphthylcarbinol, because of its low solubility, was added in aqueous suspension. This method was less sensitive than the photometric method. Oxidation of 1 μmole of *p*-methoxybenzyl alcohol/hr. in a 3 ml. assay solution causes a change in absorption at 290 mμ of 0·0833/min., and an oxygen uptake of 11·2 μl./hr., assuming that oxygen is used only in oxidizing alcohol.

Enzymes and coenzymes. The following preparations were also used: alcohol dehydrogenase and horseradish peroxidase (C. F. Boehringer und Söhne, Mannheim, Germany); glucose oxidase and triphosphopyridine nucleotide (TPN; Sigma Chemical Co., St Louis, Mo., U.S.A.); diphosphopyridine nucleotide (DPN; L. Light and Co. Ltd., Colnbrook).

Chemicals. Most of the compounds examined were commercial samples, recrystallized where necessary, or were prepared from commercial samples. Melting points reported are uncorrected. Reduction of the aldehydes by $LiAlH_4$, by the procedure of Larsson (1950), gave β-naphthylcarbinol, m.p. 79°, *p*-hydroxybenzyl alcohol, m.p. 116°, *m*-methoxybenzyl alcohol (b.p. 90–100°/0·01 mm. Hg) and 3:4-dimethoxybenzyl alcohol, b.p. 140°/0·5 mm. Hg. This last was an oil which slowly changed on standing into a crystalline solid without hydroxyl groups, thought to be the di-ether (Lindgren, 1950). By a procedure used to reduce acetylated ethyl ferulate (Allen & Byers, 1954), ferulic acid was reduced directly by $LiAlH_4$ to give 4-hydroxy-3-methoxycinnamyl alcohol, m.p. 71–73°, in poor yield. Reduction of the appropriate aldehydes and ketones (1 g.) in aqueous 2% (w/v) NaOH (plus ethanol where necessary to achieve complete solution) by $NaBH_4$ (0·45 g.) at room temperature (Adler & Hernestam, 1955) gave 4-hydroxy-3-methoxybenzyl alcohol, m.p. 113–114°, 1-(4-hydroxy-3-methoxyphenyl)ethanol, m.p. 100–102°, 1-(*p*-methoxyphenyl)ethanol and 1-(3:4-dimethoxyphenyl)-ethanol. The two last-named were oils which were not further purified because of their instability (Stedman & Stedman, 1929). Reductions by $NaBH_4$ were followed spectrophotometrically, and were all complete within 18 hr. Phenolic aldehydes and ketones were more slowly reduced than the fully methylated compounds (Smith, 1955). Melting points and boiling points of the various preparations were close to published values, except for *p*-hydroxybenzyl alcohol (Heilbron & Bunbury, 1946, quote 125°).

RESULTS

Activity of preparations. Activity in growth solutions reached a maximum after 10 days (Fig. 1, curves *A*). Most of the work was done with solutions obtained after 12 days' growth, whose activity, i.e. rate of oxidation of *p*-methoxybenzyl alcohol, ranged from 0·6 to 1·4 μmoles/ml./hr. On replacement of the growth solution with water, a further amount of enzyme diffused from the mycelial mat as shown in Fig. 1, curves *B*. Such solutions were generally used after 7 days' incubation under the mat, when they showed activities ranging from 0·1 to 1·6 μmoles/ml./hr.: most were near 0·3 μmole/ml./hr. Concentration of the enzyme from 300 ml. of growth solution by precipitating it with $(NH_4)_2SO_4$, followed by resolution in 5 ml. of water, gave activities ranging from 8 to 38 μmoles/ml./hr. However, only about 38% of the total initial activity was recovered by this technique. On one occasion, 28% of the initial activity was found to be in the supernatant after $(NH_4)_2SO_4$ saturation. Enzyme activity was also found in an extract of a mycelial mat of which the cells had been disrupted. A 14-day-old mat was well washed, ground with silver sand and extracted with 7 ml. of phosphate buffer, pH 6·2. After centrifuging and filtering, the supernatant showed an activity of 0·53 μmole/ml./hr. initially. This enzyme preparation differed from the others in that its rate of oxidation was not linear, but fell off to only one-seventh of its initial value after 28 min.

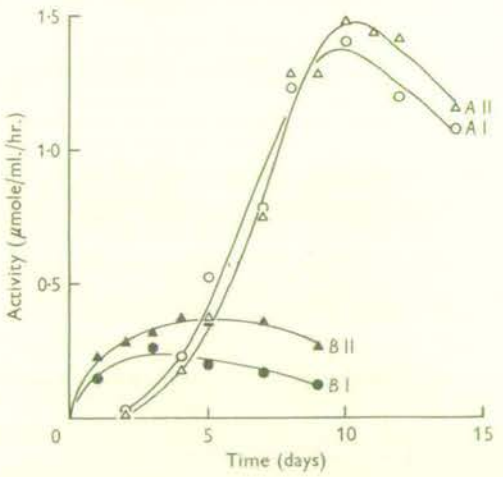

Fig. 1. Results of two experiments, I and II, showing the development of oxidase activity from *Polystictus versicolor*: *A*, in growth solution; *B*, in water to which the mycelium was transferred after 14 days' growth. Activity was estimated spectrophotometrically as described in the Materials and Methods section.

Table 1. *Relative rates of oxidation of various aromatic alcohols by the extracellular oxidase from* Polystictus versicolor

The aldehydes or ketones formed were estimated at wavelengths [λ (mμ)] where they had molar-extinction coefficients ϵ.

Alcohol	Concn. (mM)	λ (mμ)	ϵ	Relative oxidation rates (μmoles/hr.)
p-Methoxybenzyl alcohol	1·33	290	15 000	1·00
m-Methoxybenzyl alcohol	1·77	310	2 550	0·32
3:4-Dimethoxybenzyl alcohol	1·11	310	10 300	0·056
4-Hydroxy-3-methoxybenzyl alcohol	1·33	310	8 800	0·12
o-Hydroxybenzyl alcohol	1·33	245	7 200	0·003
p-Hydroxybenzyl alcohol	1·33	300	8 880	0·0007
Benzyl alcohol	1·33	240	9 600	0·036
4-Hydroxy-3-methoxycinnamyl alcohol	1·33	342·5	56 800	0·008
β-Naphthylcarbinol	0·67	245	34 000	1·14
1-(3:4-Dimethoxyphenyl)ethanol	1·33	300	8 340	<0·0004
1-(4-Hydroxy-3-methoxyphenyl)ethanol	1·33	305	8 050	<0·00001
1-(4-Methoxyphenyl)ethanol	1·33	290	11 250	<0·00001

Range of substrates. The enzyme was found to dehydrogenate all the primary aromatic alcohols examined, and also the unsaturated alcohol, 4-hydroxy-3-methoxycinnamyl alcohol (coniferyl alcohol), although at very different rates. No activity was detected with secondary aromatic alcohols, even when enzyme concentrates were used (Table 1). The formation of *o*- and *p*-hydroxybenzaldehyde, vanillin and 4-hydroxy-3-methoxycinnamaldehyde from the alcohols was confirmed by the appearance of their characteristic ultraviolet-absorption maxima in the range 330–400 mμ on making the test solutions alkaline (Lemon, 1947; Aulin-Erdtman, 1953). In the Warburg apparatus oxygen uptakes of 83, 52 and 6 μl. in 30 min. were obtained with *p*-methoxybenzyl alcohol, β-naphthylcarbinol and water. The uptake for *p*-methoxybenzyl alcohol exceeds the theoretical maximum (56 μl.), probably owing to the formation of hydrogen peroxide (see below). The enzyme concentrates gave no oxygen uptake with glucose, the primary alcohols ethanol and butanol or the L-forms of the amino acids leucine, methionine and proline. Conversely, glucose oxidase, which gave an oxygen uptake of 324 μl. in 25 min. in the presence of 0·1 M-glucose, did not oxidize *p*-methoxybenzyl alcohol, nor did the DPN-coupled alcohol dehydrogenase of yeast. The relative rates of oxidation of 0·2 M-ethanol and 0·66 mM-*p*-methoxybenzyl alcohol by the yeast dehydrogenase were found to be not less than 4000:1.

General properties. The rate of oxidation of *p*-methoxybenzyl alcohol followed the Michaelis equation up to substrate concentrations of 1·3 mM, but inhibition by substrate occurred at higher concentrations. As a result, the rate of oxidation of alcohol was almost independent of the concentration between 1·3 and 5·0 mM (Fig. 2). An alcohol concentration of 1·33 mM was selected for enzyme assay, as at higher concentrations absorption by the alcohol itself became troublesome at 290 mμ, where the aldehyde formed was estimated. The rate of oxidation of *p*-methoxybenzyl alcohol was directly proportional to enzyme concentration in the usual working conditions. Under these conditions, the oxidation of alcohol was linear with time, but at very high enzyme concentrations the rate of oxidation decreased with time, perhaps due to exhaustion of dissolved oxygen in the test solution. At such high enzyme concentrations, the formation of aldehyde was followed at 310 mμ, where the aldehyde absorbs less strongly. Measurements at this wavelength were also used to show inhibition

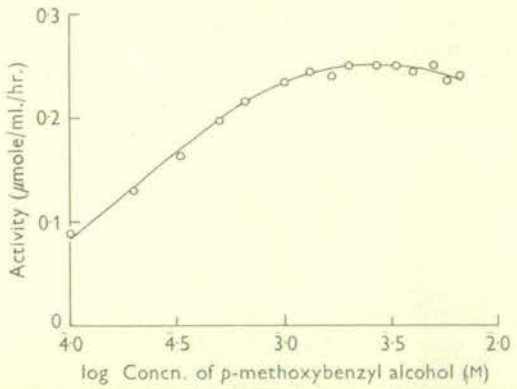

Fig. 2. Effect of the concentration of *p*-methoxybenzyl alcohol on its rate of oxidation by the oxidase from *Polystictus versicolor*. The source of enzyme was water to which the mycelium had been transferred from growth solution 5 days previously. Rates of oxidation were estimated spectrophotometrically, as described in the Materials and Methods section. The alcohol concentration was varied while the enzyme concentration remained constant.

of the oxidation of *p*-methoxybenzyl alcohol by the presence of *p*-methoxybenzaldehyde (Fig. 3). The enzyme showed its maximum activity between pH 6·0 and 6·5 in 0·022 M-phosphate buffer (Fig. 4). Activity fell off rapidly above pH 7·0, but was higher in tris buffer than in phosphate buffer.

Enzyme solutions were stable, and could be kept at room temperature for many days without marked loss in activity. Heating for 5 min. at temperatures up to 45° had no effect, but above this temperature activity rapidly fell off, the enzyme being totally inactivated after heating to 55° for 5 min. Activity was unaffected by 0·67 mM-*p*-chloromercuribenzoate in the test solution, indicating that SH groups do not contribute to the activity. Also no heavy-metal ions appear to be involved, as activity fell by only 12% in the presence of 2 and 4 mM-KCN, and by only 9% in the presence of 2 and 4 mM-NaN_3. No diffusible cofactor is involved, as the activity of an enzyme solution was unaffected by dialysis against 0·067 M-phosphate buffer for 24 hr. The activity of the enzyme was found to be unaffected by the addition of 0·15 μmole of DPN or TPN to the usual test solution.

Formation of hydrogen peroxide. The formation of hydrogen peroxide during oxidation of *p*-methoxybenzyl alcohol by the enzyme was indicated by the appearance of a red–brown when *o*-dianisidine and peroxidase were present (Huggett & Nixon, 1957). To 1·5 ml. of reagent solution [1–2 mg. of peroxidase and 0·5 ml. of 1% (w/v) *o*-dianisidine in 95% (v/v) ethanol, in 29·5 ml. of phosphate buffer, pH 7·0] were added 0·5 ml. of 5 mM-*p*-methoxybenzyl alcohol and 1 ml. of growth solution of activity 0·74 μmole/ml./hr. After 1·5 hr. the test solution had an extinction of 1·015 at 420 mμ. No colour developed in a control from which *p*-methoxybenzyl alcohol was omitted. Oxidation of *p*-methoxybenzyl alcohol by the enzyme ceased after bubbling nitrogen through the usual test solution for 15 min. On adding 0·15 μmole of DPN or TPN to the anaerobic solution, no formation of reduced DPN or TPN could be detected by absorption measurements at 340 mμ. On bubbling oxygen through an anaerobic solution, oxidation began again. In solutions saturated with oxygen at atmospheric pressure, the rate of oxidation was only 10% higher than when saturated with air.

These results indicate that the enzyme transfers hydrogen from aromatic alcohols directly to molecular oxygen, but cannot transfer hydrogen to

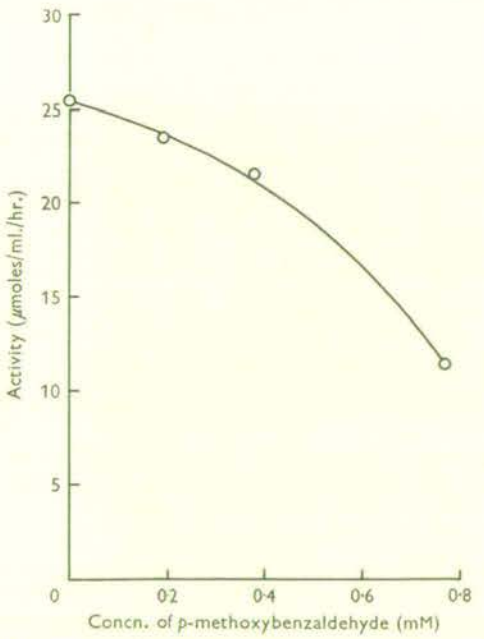

Fig. 3. Inhibitory effect of *p*-methoxybenzaldehyde on the rate of oxidation of *p*-methoxybenzyl alcohol by oxidase from *Polystictus versicolor*. The source of enzyme was a 50-fold dilution of a concentrate prepared from a 10-day-old growth solution. The rate of oxidation was determined spectrophotometrically, aldehyde being added to the usual assay solution before making up to 3 ml. (see Materials and Methods section).

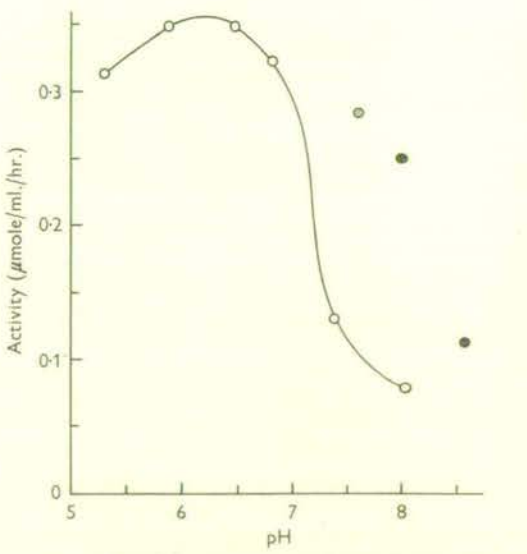

Fig. 4. Effect of pH on the rate of oxidation of *p*-methoxybenzyl alcohol by the oxidase from *Polystictus versicolor*, the source of enzyme being water to which the mycelium had been transferred from growth solution 7 days previously. The buffers used, Sørensen's KH_2PO_4–Na_2HPO_4 (○) and tris (●), were substituted for the usual phosphate buffer in the assay solution used for spectrophotometric determination of oxidation rates.

DPN or TPN. Transfer of hydrogen to methylene blue was observed under anaerobic conditions. A portion (1 ml.) of enzyme concentrate was added to 1 ml. of phosphate buffer, pH 6·2, 0·5 ml. of 0·534 mM-methylene blue and 0·5 ml. of 0·04 M-*p*-methoxybenzyl alcohol or 0·5 ml. of water in Thunberg tubes, after evacuating and filling the tubes with nitrogen three times. After incubation for 4 hr. at 22° in daylight or in the dark the methylene blue was reduced 60 % in the presence of the alcohol and was unchanged in the control. The rate of transfer of hydrogen to methylene blue by the enzyme was only about one-fiftieth of the rate of transfer to oxygen.

Polyphenoloxidase activity was absent from a growth solution and an enzyme concentrate. The former was tested by the method of Dion (1952), with 1 ml. of 10 days' growth solution and 5 ml. of 0·1 % (w/v) solutions of catechol, guaiacol, phenol and *p*-cresol. After incubation for 24 hr. at 25° no coloured products were formed. The enzyme concentrate was tested for oxygen uptake in the Warburg apparatus. Portions (1 ml.) of enzyme solution and 1 ml. of phosphate buffer, pH 6·2, were added to the main compartments of the flasks and 0·5 ml. of 0·02 M solutions of catechol and *p*-cresol were tipped in from the side arms. No oxygen uptakes were recorded nor were any coloured products formed.

DISCUSSION

The aromatic-alcohol oxidase of *Polystictus versicolor* differs from alcohol dehydrogenase in not oxidizing ethanol and butanol and in being independent of DPN. Ose & Hironaka (1957) reported an alcohol dehydrogenase which reduced benzaldehyde and which was not identical with, but was very similar to, ethanol dehydrogenase. Gillette (1959) presented evidence of an aromatic-alcohol dehydrogenase, from rabbit liver, which oxidized *p*-nitrobenzyl alcohol to *p*-nitrobenzaldehyde, but this enzyme was also dependent on DPN. Various aromatic aldehydes, including some which have been examined in the present work, have been found to be reduced to give the corresponding alcohols when added to cultures of brewer's yeast which were vigorously fermenting sugars (Neuberg, 1949; Higuchi, Kawamara & Ito, 1955). The reduction is linked with the fermentation.

The enzyme of *Polystictus versicolor* has not yet been obtained in sufficient concentration and purity to identify its prosthetic group with certainty. However, its general properties suggest that it is a flavoprotein, as they closely resemble those of known enzymes of this type, such as the amino acid oxidases, and glucose oxidase. Like these it is scarcely inhibited by cyanide or azide, and transfers hydrogen directly to molecular oxygen to give hydrogen peroxide. It transfers hydrogen to methylene blue rather slowly, as does, for instance, the D-amino acid oxidase of kidney (Krebs, 1935). The L-amino acid oxidase of kidney is known to oxidize α-hydroxy acids, including the aromatic phenylglycollic acid (Ratner, 1955), but it is certainly distinct from the enzyme examined here, which does not oxidize L-amino acids.

The release of this aromatic-alcohol oxidase into solutions in contact with mats of the fungus provides an explanation of previous observations made with the Kluyver technique (Farmer *et al.* 1959). It was then found that solutions of *m*- and *p*-methoxybenzoic acid and of 3:4-dimethoxybenzoic acid were completely reduced in the presence of fungal mats to give mixtures of the corresponding alcohols and aldehydes, but benzoic acid gave only the alcohol. These observations can be interpreted as being the result of a dynamic equilibrium in which the aldehydes were reduced to alcohols within the cells of the fungus, while the alcohols were re-oxidized to the aldehydes by the extracellular enzyme. The relative rates of these two processes must determine the ratio of aldehyde to alcohol at equilibrium. Our present observations give information only on the rates of oxidation of the alcohols, so these do not exactly parallel the amounts of aldehyde formed on reducing the corresponding acids by fungal mats.

Polystictus versicolor is a white rot, attacking the lignin of wood. Henderson (1955) found that vanillic acid and syringic acid could be extracted from a hardwood sawdust after this fungus had been growing on it for some weeks, but that only vanillic acid could be extracted from a softwood sawdust, in agreement with the known aromatic structure of the lignin of these woods (Brauns, 1952). The initial attack on the lignins must be by extracellular enzymes, causing a degradation of the lignin to water-soluble substances which can be absorbed by the fungal cells. The possibility that the extracellular enzyme examined here plays some part in the breakdown of the lignin is being further investigated.

SUMMARY

1. Growth media of *Polystictus versicolor*, or water left in contact with mycelial mats of this fungus, contained an enzyme system which transferred hydrogen from aromatic alcohols to molecular oxygen, with the formation of aromatic aldehydes and hydrogen peroxide. No phenoloxidase activity was detected.

2. Activity was estimated either by spectrophotometric estimation of the rate of aldehyde formation, or by oxygen uptake.

3. The enzyme system could be concentrated from growth media, though with some loss, by ammonium sulphate precipitation.

4. Of the substances tested, all the primary aromatic alcohols, which included β-naphthylcarbinol, benzyl alcohol and seven other ring-substituted benzyl alcohols, were oxidized, but three secondary 1-phenylethanols were not. Glucose, ethanol, butanol and the L-amino acids tested were not oxidized.

5. Enzyme activity was little affected by *p*-chloromercuribenzoate, cyanide or azide ions.

6. There was no evidence for pyridine nucleotide participation in the reaction.

We are indebted to Dr D. M. Webley for valuable discussions during the course of this work.

REFERENCES

Adler, E. & Hernestam, S. (1955). *Acta chem. scand.* **9**, 319.
Allen, C. F. H. & Byers, J. R. (1954). U.S. Patent 2,692,269.
Aulin-Erdtman, G. (1953). *Svensk Papp-Tidn.* **56**, 91.
Brauns, F. E. (1952). *The Chemistry of Lignin.* New York: Academic Press Inc.
Clark, W. M. (1928). *The Determination of Hydrogen Ions*, 3rd ed., p. 210. London: Baillière, Tindall and Cox.
Dion, W. M. (1952). *Canad. J. Bot.* **30**, 9.
Farmer, V. C., Henderson, M. E. K. & Russell, J. D. (1959). *Biochim. biophys. Acta*, **35**, 202.
Gillette, J. R. (1959). *J. biol. Chem.* **234**, 139.
Gomori, G. (1955). In *Methods in Enzymology*, vol. 1, p. 144. Ed. by Colowick, S. P. & Kaplan, N. O. New York: Academic Press Inc.
Heilbron, I. & Bunbury, H. M. (1946). *Dictionary of Organic Compounds.* London: Eyre and Spottiswoode.
Henderson, M. E. K. (1955). *Nature, Lond.*, **175**, 634.
Higuchi, T., Kawamara, I. & Ito, Y. (1955). *J. Jap. For. Soc.* **37**, 239.
Huggett, S. St G. & Nixon, D. A. (1957). *Lancet*, ii, 368.
Krebs, H. A. (1935). *Biochem. J.* **29**, 1620.
Larsson, E. (1950). *Chalmers tek. Högsk. Handl.* **94**, 15.
Lemon, H. W. (1947). *J. Amer. chem. Soc.* **69**, 2998.
Lindgren, B. O. (1950). *Acta chem. scand.* **4**, 1356.
Neuberg, C. (1949). *Advanc. Carbohyd. Chem.* **4**, 75.
Ose, S. & Hironaka, J. (1957). In *Proc. int. Symp. Enzyme Chem., Tokyo and Kyoto*, p. 457. London: Pergamon Press.
Ratner, S. (1955). In *Methods in Enzymology*, vol. 2, p. 211. Ed. by Colowick, S. P. & Kaplan, N. O. New York: Academic Press Inc.
Smith, D. C. C. (1955). *Nature, Lond.*, **176**, 927.
Stedman, E. & Stedman, E. (1929). *J. chem. Soc.* i, 614.

METABOLISM OF LIGNIN MODEL COMPOUNDS BY *POLYSTICTUS VERSICOLOR*

J. D. RUSSELL, MOIRA E. K. HENDERSON AND V. C. FARMER
Macaulay Institute for Soil Research, Aberdeen (Great Britain)

(Received March 10th, 1961)

SUMMARY

Mats of *Polystictus versicolor* metabolized the lignin model compounds α-guaiacylglycol-β-guaiacyl ether (III) and α-guaiacylglycerol-β-guaiacyl ether (IV) but not the compounds α-veratrylglycol-β-guaiacyl ether (I) and α-veratrylglycerol-β-guaiacyl ether (II). Veratryl alcohol was formed from III. Veratraldehyde and veratryl alcohol were also formed when solutions of *p*-hydroxybenzoic acid, protocatechuic acid, vanillin and vanillyl alcohol were metabolized by the fungus. Smaller amounts of veratraldehyde were liberated by the growing fungus and by preformed mats. None of the model compounds I to IV was oxidized by the aromatic-alcohol oxidase of *P. versicolor*.

INTRODUCTION

Under the influence of soil microorganisms, plant lignins undergo modification and decomposition leading to products which form an important part of soil organic matter. Neither the mechanism of the initial cleavage of the lignin molecule nor the enzyme systems involved are understood. In a study of this problem, HENDERSON[1] showed that incubation of spruce and birch sawdust with the white rot fungus *Polystictus versicolor* resulted in the release of vanillic acid from the first, and a mixture of vanillic and syringic acids from the second, consistent with attack on side-chains in the lignin molecule present in these woods[2]. Subsequently cell-free growth medium of *P. versicolor* was found to contain an oxidase system capable of converting aromatic alcohols to aldehydes[3]. Among the alcohols oxidized were coniferyl, vanillyl and veratryl alcohol all of which are structurally related to lignin. The secondary aromatic alcohols examined were not oxidized by the enzyme system.

Since the initial attack on the lignin molecule must be effected by extracellular enzyme systems released by the fungus, the possibility of the participation of the alcohol oxidase from *P. versicolor* arose. This paper describes an investigation into the possible attack by this oxidase system on lignin model compounds, and the influence of the fungus itself on these compounds.

The lignin model compounds studied are closely related and may be represented by the following structure:

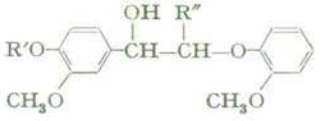

The compounds are, I ($R' = CH_3$, $R'' = H$), α-veratrylglycol-β-guaiacyl ether,
II ($R' = CH_3$, $R'' = CH_2OH$), α-veratrylglycerol-β-guaiacyl ether,
III ($R' = R'' = H$), α-guaiacylglycol-β-guaiacyl ether,
IV ($R' = H$, $R'' = CH_2OH$), α-guaiacylglycerol-β-guaiacyl ether.

Compounds II and IV were synthesized by ADLER, LINDGREN AND SAEDEN[4] and ADLER AND ERIKSOO[5] respectively. These compounds behave similarly to lignin in sulphonation and ethanolysis reactions and are believed to be good models for the B′ group in the lignin molecule. This group contains a benzyl alcohol residue etherified either to other lignin monomers or to carbohydrate material in the proto-lignin molecule[6]. I and III are new compounds and although they are not probable lignin models, having an aromatic ring with a two-carbon side-chain, their structural relationship to II and IV makes their study of some interest.

EXPERIMENTAL

Apparatus

Infrared absorption spectra were recorded on a Grubb-Parsons double beam infrared spectrometer, type S4, equipped with a NaCl prism. Ultraviolet measurements were made on a Beckman model DU spectrophotometer using 1-cm silica cells.

Procedure

As far as possible, aqueous solutions of substrates were employed but compounds I and II required aqueous solvents containing 8.5 and 5 % (v/v)ethanol. Allowance

was made for the consequent deactivation of the aromatic alcohol oxidase: 0.5 % ethanol caused a deactivation of 10.5 %, 1 % ethanol 15.8 %, 5 % ethanol 36.8 %, 10 % ethanol 52.6 %, 20 % ethanol 73.7 % and 30 % ethanol 94.7 % deactivation, measured using *p*-methoxybenzyl alcohol as substrate. For the estimation of rates of enzymic oxidation of substrates I to IV relative to *p*-methoxybenzyl alcohol, the absorption cells contained Sörensen's phosphate buffer pH 6.2 (1 ml), $4 \cdot 10^{-3}$ *M* substrate solution (1 ml) and enzyme solution (1 ml), consisting of either cell-free growth solution from *P. versicolor*, or a concentrate of this growth solution[3]. Conditions of growth of *P. versicolor* and of its incubation with substrates were those described in a previous paper[9].

Three flasks, each containing 25 g sawdust and 60 ml growth medium[1], were inoculated with *P. versicolor* and then incubated for 3 months at 22° by which time the fungus had completely permeated the sawdust. The mixture was washed with ethanol and sucked dry on a Buchner. The amber ethanol solution was evaporated under reduced pressure to a small volume and poured into 10 volumes of diethyl ether. After precipitated waxes, protein etc., had been filtered off, the pale yellow ether solution was washed with dilute NaOH solution and water, dried over anhydrous Na_2SO_4 and evaporated to dryness under reduced pressure to give a waxy residue (4 mg). The dry sawdust was further extracted with ethanol–benzene in a soxhlet apparatus, the resulting extract being worked up as described above to give about 5 mg residue. The infrared spectra of both products were recorded in $CHCl_3$ solution.

Preparation of lignin model compounds

Melting points are uncorrected. α-Veratrylglycerol-β-guaiacyl ether (II) was synthesized by the method of ADLER *et al.*[4], the product being a thick oil which was not further purified. The last step involved reduction by $NaBH_4$ of β-hydroxy-α-(2-methoxyphenoxy)propioveratrone, m.p. 115–116.5°, $\varepsilon_{310} = 8660$. Found: C, 65.2; OCH_3, 28.0. Calc. for $C_{13}H_{20}O_6$: C, 65.1; OCH_3, 28.0 %.

Compound I, α-veratrylglycol-β-guaiacyl ether, was obtained by $NaBH_4$ reduction, under the conditions described by ADLER *et al.*[4], of α-(2-methoxyphenoxy)-acetoveratrone, m.p. 92–92.5°, $\varepsilon_{300} = 8710$, an intermediate compound in the synthesis of II. I is a buff crystalline compound, m.p. 130–132°. Found: C, 67.0; OCH_3, 30.1. $C_{17}H_{20}O_5$ requires: C, 67.1; OCH_3, 30.6 %.

FREUDENBERG AND EISENHUT[10] describe the synthesis of α-guaiacylglycerol-β-coniferyl ether. Appropriate modifications of this method yielded compounds III and IV, α-guaiacylglycol-β-guaiacyl ether and α-guaiacylglycerol-β-guaiacyl ether. Reaction of ω-bromoacetovanillone benzyl ether with guaiacol gave ω-(2-methoxyphenoxy)acetovanillone benzyl ether, m.p. (EtOH) 94°, (ligroin) 103–105°. Hydrogenolysis of each form of this product gave the keto-phenol ω-(2-methoxyphenoxy)-acetovanillone, an amber liquid ($\varepsilon_{305} = 9260$). Subsequent reduction of the carbonyl group of this compound in alcoholic solution with $NaBH_4$ gave α-guaiacylglycol-β-guaiacyl ether (III), colourless needles from EtOH, m.p. 128.5–129.5°. Found: C, 65.7; OCH_3, 20.8. $C_{16}H_{13}O_5$ requires: C, 66.2; OCH_3, 21.4 %.

Treatment of ω-(2-methoxyphenoxy)acetovanillone benzyl ether with formalin gave β-hydroxy-α-(2-methoxyphenoxy)propiovanillone benzyl ether, white prisms from C_6H_6-ligroin, m.p. 93–95°, which yielded β-hydroxy-α-(2-methoxyphenoxy)-propiovanillone after hydrogenolysis. This compound was a light oil ($\varepsilon_{310} = 9280$)

from which IV, α-guaiacylglycerol-β-guaiacyl ether, a thick colourless oil (Found: C, 63.6; OCH_3, 17.0. Calc. for $C_{17}H_{30}O_6$: C, 63.8; OCH_3, 19.4 %) was obtained by reduction with $NaBH_4$.

RESULTS

No evidence was found for the oxidation of any of the four model compounds, I to IV, by enzyme concentrates from cell-free growth medium of *P. versicolor*. A spectrophotometric method was used whereby the ketones, produced by oxidation of the secondary alcohol grouping in these compounds could be detected by their distinctive absorption near 305 mμ. The sensitivity of the method was such that the rate of enzymic oxidation of these alcohols must be less than that of *p*-methoxybenzyl alcohol by a factor of 3000. In the case of phenolic compounds III and IV this factor was shown to exceed 6000 by using a more sensitive test: after action of the enzyme for 16 h no characteristic absorption due to the ionized ketophenols was observed in the region of 350 mμ on making the test solutions alkaline.

Solutions (100 ml) of the neutral compounds I ($2.5 \cdot 10^{-4}$ *M*) and II (10^{-3} *M*) were not metabolized after incubation for 10 days with preformed mats of *P. versicolor*, the course of the incubation being followed from ultraviolet absorption measurements on suitable samples. Compounds I and II were recovered and identified by infrared spectroscopy. The phenolic compounds, III and IV (10^{-3} *M*), were fairly rapidly metabolized when they were incubated with *P. versicolor* (see Table I). Estimation of residual III and IV was made from $\Delta\varepsilon$, the difference between molar extinction coefficients of these compounds in acid and alkaline solution at 250 mμ. $\Delta\varepsilon_{250}$ values for III and IV are approx. 8500 and 7000. After 7 days incubation with *P. versicolor* the solution which had contained compound III was extracted with $CHCl_3$. Evaporation of the $CHCl_3$ solution gave a residue which was identified from its infrared absorption spectrum as veratryl alcohol (1.6 mg was produced from 26 mg III). The corresponding residue from IV was too small to be identified. Further evidence of the ability of *P. versicolor* to methylate phenolic hydroxyl groups was obtained by the formation of veratraldehyde, alone or admixed with veratryl alcohol, when some simpler phenolic compounds (100 ml of $4 \cdot 10^{-3}$ *M* solutions) were metabolized by mats of the fungus. Sodium protocatechuate solution gave 3.2 mg veratraldehyde and 1.6 mg veratryl alcohol; *p*-hydroxybenzoate gave 5.2 mg aldehyde and 1 mg alcohol; vanillyl alcohol gave 1.7 mg aldehyde, and so also did vanillin at $2 \cdot 10^{-3}$ *M* concentration. This last was toxic at the higher concentration. At most, only 10 % of these phenolic compounds was converted to methylated end-products, the remainder being metabolized with destruction of the aromatic ring. About 1 mg veratraldehyde was formed when mats of the fungus were incubated over some distilled water for 8 days. This may well have been formed from tyrosine liberated during autolysis of aging cells. Veratraldehyde and veratryl alcohol were identified and estimated from the infrared spectrum of the neutral fraction obtained from the above solutions by chloroform or ether extraction, and veratraldehyde was confirmed from the infrared spectrum of its 2,4-dinitrophenylhydrazone. These were always the major components, but a small amount of anisaldehyde was present in the product from *p*-hydroxybenzoate. Small amounts of an unidentified aromatic aldehyde were sometimes present. It was distinguished principally by its carbonyl absorption band at 5.89 μ in chloroform; veratraldehyde absorbs at 5.94 μ.

TABLE I

METABOLISM OF LIGNIN MODEL COMPOUNDS α-GUAIACYLGLYCOL-β-GUAIACYL ETHER (III) AND α-GUAIACYLGLYCEROL-β-GUAIACYL ETHER (IV) BY *P. versicolor*

Compounds expressed as percent original concentration of 10^{-3} *M*.

Days	*Residual lignin model compound*	
	III	*IV*
2	69.8	44.6
5	10.3	9.3
6	0	0

As DL-methionine is a well-known source of methyl groups in transmethylation reactions of biological systems[7], it was added in 0.0125 *M* concentration, to a solution of *p*-hydroxybenzoate before incubation with a mat of the fungus in an attempt to increase the yield of veratraldehyde. No increase resulted. Similarly no increase in yield was obtained when *p*-hydroxybenzoate and DL-methionine were added to the growth medium of the fungus. The occurrence of a strong mercaptan-like smell throughout the experiment indicated decomposition of methionine by the fungus.

The identification of veratraldehyde as a product from the action of *P. versicolor* on compounds which are structurally related to lignin suggested that this aldehyde might accumulate from attack on proto-lignin in wood by this fungus. An ethanol extract of spruce sawdust (75 g) after incubation with *P. versicolor* for 3 months, yielded about 4 mg of a waxy alkali-insoluble residue. Its infrared spectrum showed strong aliphatic wax absorption bands, which tended to obscure some of the detail of the spectrum, and a well defined aromatic absorption pattern which agreed with that of veratraldehyde. Attempts to separate the wax from the aromatic material were unsuccessful and reaction with 2,4-dinitrophenylhydrazine was inconclusive. A further extraction of the sawdust in a soxhlet apparatus with ethanol–benzene (1:1) yielded a similar product with a higher proportion of wax. The total amount of veratraldehyde was estimated at not more than 1 mg, and so may well have arisen by the natural metabolism of the fungus rather than as a breakdown product of the lignin.

DISCUSSION

Although the aromatic-alcohol oxidase from *P. versicolor* can use a variety of primary aromatic alcohols as substrate it does not oxidize the secondary alcoholic groupings present in 1-(3,4-dimethoxyphenyl)ethanol, 1-(4-hydroxy-3-methoxyphenyl)ethanol and 1-(4-methoxyphenyl)ethanol[3]. In agreement with this the secondary alcohol groups in the lignin model compounds investigated here were not oxidized by the enzyme. Steric blocking of the >CHOH group by neighbouring substituents, rendering it inaccessible to the enzyme, could account for this. Since the number of primary aromatic alcohol groups in lignin is probably very small, no clear role can be ascribed to the enzyme during primary attack of the lignin molecule. However, lignin decomposition is a slow process, extending over several months, so that reactions, which are too slow to be detected under the conditions used here, may still play a part.

P. versicolor was shown to be capable of cleaving the aliphatic side-chain of model compound III α-guaiacylglycol-β-guaiacyl ether, which contains a free phenolic hydroxyl group. The compound isolated from this reaction was veratryl alcohol. The methylation which had taken place must have followed fission of the chain because compound I, which differs from III only in having the phenolic hydroxyl group etherified, was not attacked by the fungus. The chain-splitting outlined here could involve one of the processes which is in operation when vanillin is released from spruce sawdust by *P. versicolor*[1]. The isolation of veratryl alcohol from α-guaiacylglycol-β-guaiacyl ether and veratraldehyde from vanillin and vanillyl alcohol indicates in the fungus a weakly developed ability to methylate free phenolic groups, and in addition methoxylation was shown by the production of both veratraldehyde and veratryl alcohol from *p*-hydroxybenzoic and protocatechuic acids.

This behaviour may be compared to that of the brown-rot fungus, *Lentinus lepideus*, which synthesizes methyl *p*-methoxycinnamate when growing on wood or on a glucose medium[8]. This compound is thought to arise from a side-reaction in the synthesis of alanine. The formation of veratraldehyde by *P. versicolor* under similar circumstances indicates more powerful oxidizing systems in this fungus.

Previous work has shown that veratryl alcohol and veratraldehyde are interconvertible in solutions in contact with *P. versicolor*[3,9]. The aldehyde generally predominates at equilibrium. The predominance of veratryl alcohol in the product from the lignin model compound III suggests that its solution may have contained an inhibitor of the extracellular aromatic-alcohol oxidase which oxidizes the alcohol to the aldehyde.

REFERENCES

1 M. E. K. HENDERSON, *Nature*, 175 (1955) 634.
2 F. E. BRAUNS, *The Chemistry of Lignin*, Academic Press, Inc., New York, 1952.
3 V. C. FARMER, M. E. K. HENDERSON AND J. D. RUSSELL, *Biochem. J.*, 74 (1960) 257.
4 E. ADLER, B. O. LINDGREN AND U. SAEDEN, *Svensk Papperstidn.*, 55 (1952) 245.
5 E. ADLER AND E. ERIKSOO, *Acta Chem. Scand.*, 9 (1955) 341.
6 P. E. T. BAYLISS, *Sci. Progr. Twent. Cent.*, 48 (1960) 409.
7 F. CHALLENGER, D. B. LISLE AND P. B. DRANSFIELD, *J. Chem. Soc.*, (1954) 1760.
8 W. J. SCHUBERT AND F.-F. NORD, *Ind. Eng. Chem.*, 49 (1957) 1387.
9 V. C. FARMER, M. E. K. HENDERSON AND J. D. RUSSELL, *Biochim. Biophys. Acta*, 35 (1959) 202.
10 K. FREUDENBERG AND W. EISENHUT, *Ber.*, 88 (1955) 626.

Printed in The Netherlands

Spectrochimica Acta, 1962, Vol. 18, pp. 461 to 466. Pergamon Press Ltd. Printed in Northern Ireland

Infrared study of adsorption of water and aromatic compounds on alkali halides

V. C. Farmer and J. D. Russell
Department of Spectrochemistry, The Macaulay Institute for Soil Research, Craigiebuckler, Aberdeen

(*Received* 24 *September* 1961)

Abstract—Grinding aromatic hydrocarbons and quinones containing three or more condensed rings with alkali halides leads to markedly increased water adsorption on the alkali halide particles. Changes in the spectrum of 1,2-benzanthraquinone indicate that the increased adsorbed water is associated with adsorption of the quinone on the alkali halide during the grinding process. 1,2-Benzanthraquinone is also adsorbed from the vapour phase on to finely divided KBr prepared by freeze-drying.

The alkali-halide pressed-disk technique is of considerable value in the study of solid natural products, such as clays and humic acids, by infrared spectroscopy. A disadvantage of this technique is that rather variable amounts of water are adsorbed on the finely ground alkali halides, and this water can introduce uncertainties in the study of the hydroxyl absorption of the sample. It has been suggested, however, that this uncertainty can be reduced or eliminated by heating the prepared disk to 100° or more overnight, as pressed disks of most alkali halides are sufficiently porous to allow water adsorbed on the alkali halide or on the sample to be driven off by this means [1, 2]. Doubts are raised on the efficacy of this procedure by the observation of Durie and Szewczyk [3] that KCl disks containing aromatic compounds show much higher hydroxyl absorption than does a blank KCl disk prepared under the same conditions. Their work led them to believe that the hydroxyl absorption was not due to adsorbed water. This phenomenon is re-examined here with a wider range of alkali halides and of aromatic compounds, and using more vigorous grinding conditions.

Results

Whereas Durie and Szewczyk [3] mixed their samples with potassium chloride by hand grinding, a vibratory ball mill has been used here. The aromatic compound (1 mg) was ground with 300 mg of alkali halide, previously dried at 150°, and the mixture pressed at 8 tons to give a disk of 12·5 mm diameter, using apparatus already described [4]. It was confirmed that a marked increase in hydroxyl absorption in the 3 μ region was shown by KBr, KCl and KI disks containing aromatic hydrocarbons and quinones with three or more fused rings, but not by disks containing benzoquinone, naphthalene or α-naphthoquinone (Table 1). As

[1] A. W. Baker, *J. Phys. Chem.* **61**, 450 (1957).
[2] V. C. Farmer, *Mineral. Mag.* **31**, 829 (1958).
[3] R. A. Durie and J. Szewczyk, *Spectrochim. Acta* **15**, 593 (1959).
[4] V. C. Farmer, *Spectrochim. Acta* **8**, 374 (1957).

the highest hydroxyl absorption appeared in spectra from disks containing 1,2-benzanthraquinone, this compound was selected for more detailed study of the effect.

Table 1. Percentage absorption of the 3 μ band of adsorbed water in alkali-halide disks containing aromatic compounds

Compound	Alkali halide		
	KCl	KBr	KI
Violanthrone	88	66	74
Iso-violanthrene	86	66	79
Pyranthrone	90	79	85
1,2-2′,1′-Anthraceno-anthracene	87	86	65
1,2-Benzanthracene	56	83	70
2,3-Benzanthracene	74	80	49
1,2-Benzanthraquinone	90	91	92
Benzanthrone	88	65	60
Anthracene		73	73
Anthraquinone		76	53
Naphthalene	47	35	19
α-Naphthoquinone	69	31	35*
Benzoquinone	31	25	24*
None	60	36	29

* Some oxidation of the iodide by these quinones occurred.

Origin of hydroxyl absorption

Markedly increased hydroxyl absorption was shown by CsCl and CsBr disks containing 1,2-benzanthraquinone, just as with disks of the potassium salts. NaCl disks containing the quinone showed less hydroxyl absorption (53 to 79%) than did a disk of pure salt (83 per cent). Increased hydroxyl absorption near 3 μ was always associated with increased infrared absorption of bands near 6·1 μ and near 4·9 μ, and as these last two are undoubtedly water absorption bands, it seemed likely that the absorption at 3 μ also arose from water. This was confirmed by heating the potassium halide disks to temperatures between 150 and 200° for periods of 16 to 48 hr. Under these conditions, the hydroxyl absorption at 3 μ was reduced from over 90 per cent to less than 12 per cent, and in some cases to less than 2 per cent absorption.

The positions of its absorption bands indicated that the water was adsorbed on the alkali halides, and not on the quinone itself. The wavelengths of the absorption bands due to OH stretching of water molecules have been shown to vary according to the alkali halide on which they are adsorbed [5], and we have found the same to be true for the absorption due to HOH bending, which lies at 6·07 μ, 6·12 μ and 6·18 μ in KCl, KBr and KI disks respectively. These absorption bands were intensified, but were unchanged in position in presence of the quinone.

[5] W. C. Price, W. F. Sherman and G. R. Wilkinson, *Proc. Roy. Soc.* (*London*) A **247**, 467 (1958).

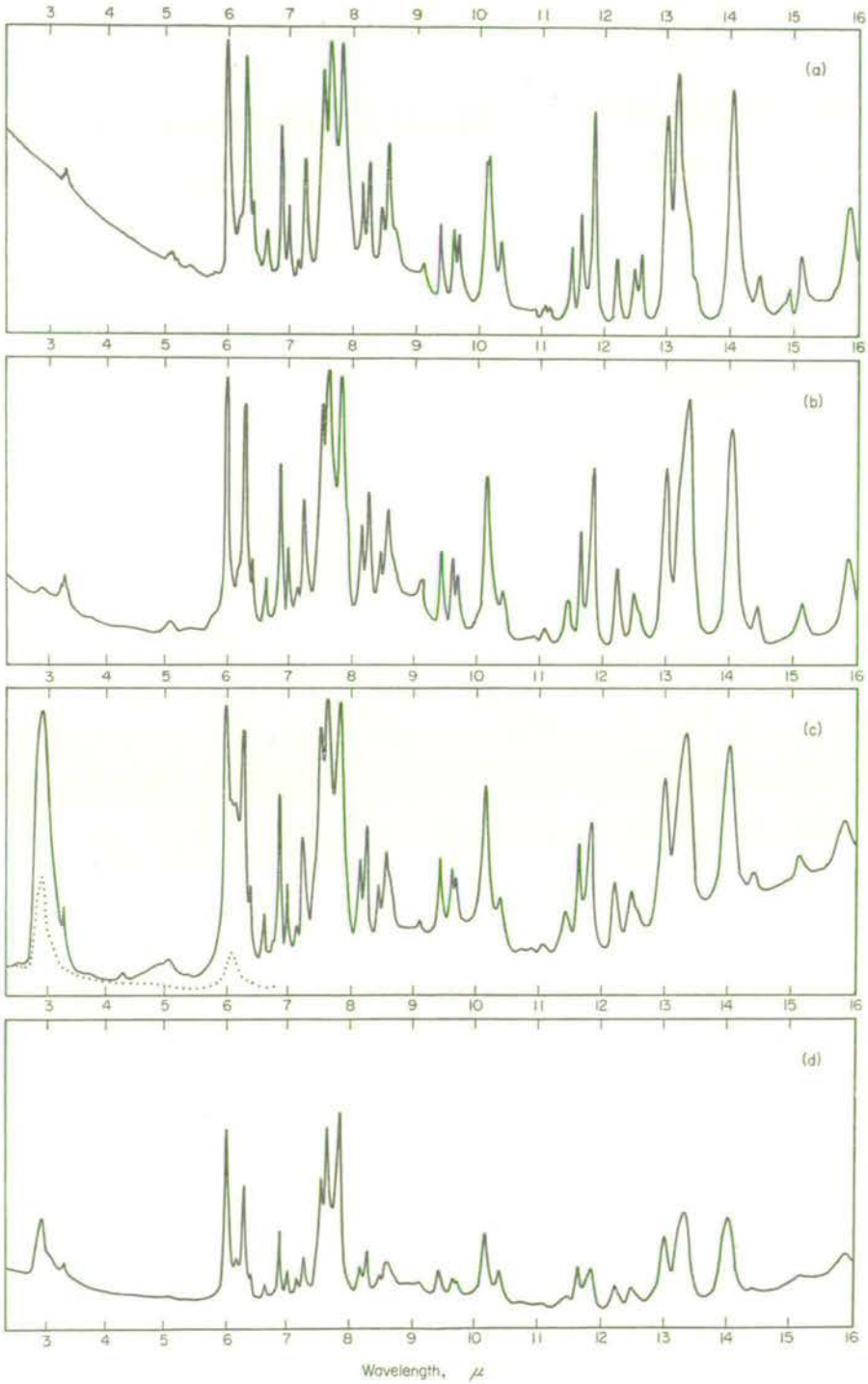

Fig. 1. 1,2-Benzanthraquinone in KBr disks: (a) Crystalline form I. (b) Amorphous supercooled melt. (c) Amorphous state produced by 8 min grinding in KBr. Dotted curve shows water absorption in pure KBr disk. (d) Adsorbed from the vapour phase on freeze-dried KBr. Spectra were recorded on a Grubb Parsons Double-Beam Spectrometer type S.4 equipped with NaCl prism.

Adsorption of 1,2-*benzanthraquinone on alkali halides*

The increased adsorption of water by the alkali halides suggested that grinding causes some interaction between the alkali halides and 1,2-benzanthraquinone, and changes in its spectrum did in fact indicate that the quinone was adsorbed on the alkali halides. The original crystalline form was usually completely destroyed by grinding for 8 min with the alkali halides. No change occurred when the quinone was ground alone. The spectrum of the altered form in a KBr disk (Fig. 1c) is typical of that obtained from KI, CsCl, and CsBr disks: it is distinguished from the spectrum of the original crystalline form (Fig. 1a) by a number of details, but principally by a shift of an absorption band at 13·20 μ in the spectrum of the crystalline form to 13·37 μ in that of the altered form. The spectrum is, however, closely similar to that of 1,2-benzanthraquinone in the form of an amorphous supercooled melt (Fig. 1b and Table 2). The only marked difference is the lower

Table 2. Wavelengths (μ) of absorption bands of 1,2-benzanthraquinone which are sensitive to physical state

Crystalline I	Crystalline II	Supercooled melt	Adsorbed on KBr from vapour
13·02	12·95 13·02	13·02	13·00
13·20	13·39	13·37	13·33
14·07	14·05	14·04	14·02

intensity of an absorption band at 11·82 μ in the spectrum of the altered form produced by grinding. The supercooled melt was obtained by heating a KBr disk containing finely ground crystals of the quinone above the melting point, and then cooling the disk quickly. Some difficulty was found in obtaining a completely amorphous phase by this means, as the quinone tended to recrystallize to some extent, usually giving some mixture of the original crystalline form (I) with a second crystalline form (II), which was obtained pure when the molten quinone cooled in bulk.

The spectra given by the quinone in pressed disks of NaCl and KCl following 8-min grinding differed somewhat from that given by a KBr disk. They could be interpreted as arising from mixtures of the amorphous form with both crystalline phases.

The amorphous state produced by grinding with the alkali halides was metastable. Complete reversion to a mixture of the two crystalline forms occurred spontaneously in CsCl disks a few minutes after pressing: this change was signalled by a dense fogging which moved slowly from some centre across the originally very clear disk. Reversion to the original crystalline form (I) occurred when a ground mixture of the quinone with KBr was exposed to air of 76 per cent humidity for 23 hr before pressing the disk. Heating KBr and KI disks containing the amorphous quinone to between 100 and 150° sometimes induced its recrystallization. In all these cases, recrystallization was associated with increased light scattering by the disk and with a decrease in the amount of adsorbed water to normal levels or below, showing that the amorphous condition was intimately associated with

and necessary for the increased water adsorbed on the alkali halides. These results suggested that the amorphous phase might in fact be adsorbed on fresh surfaces of the alkali halides produced by the vigorous grinding. To test this, the spectrum of the quinone was obtained in an undoubtedly adsorbed state. This was achieved by adsorption from the vapour phase following the method used by TOLK [6] in studying the adsorption of benzoic acid by alkali halides: 1 mg of the quinone was sealed in an evacuated tube containing 300 mg finely divided KBr prepared by freeze-drying, and the whole heated at 150° in an oven for 48 hr. The KBr powder became uniformly coloured yellow by adsorbed quinone and a pressed disk prepared from it gave the spectrum in Fig. 1(d). Exposure of the freeze-dried potassium bromide powder to atmospheric moisture led to a rapid loss of adsorptive capacity. The spectrum of this adsorbed state differs from that of the supercooled melt (Fig. 1b) by a broadening of some of the absorption bands, particularly those at 11·41 and 11·82 μ, by enhancement of bands at 7·82 and 10·36 μ and by a marked depression of the band at 11·82 μ. Some small shifts in band positions (Table 2) also occurred. The spectrum of the adsorbed form produced by grinding (Fig. 1c) is intermediate between those of the supercooled melt and of the form adsorbed from the vapour phase. This can be explained if grinding leads to both mono- and multilayer adsorption, whilst adsorption from the vapour phase gives rise to essentially a monolayer.

Effects of crystalline form

The results reported above were obtained using the crystalline form of 1,2-benzanthraquinone which is stable at room temperature (I). A second crystalline form (II) which was obtained on cooling the melt had a spectrum closer to that of the supercooled melt (Fig. 1b), and distinguished from it by only small displacements of the absorption bands and a doubling of the 13 μ band (Table 2). When crystals of type II were ground with potassium bromide, relatively little was converted to the adsorbed form, and there was only a small increase in adsorbed water in the disk (58 per cent absorption at 3 μ, cf. Table 1). Crystals of form II were readily converted to form I by grinding alone, but when ground with the alkali halides, form II was still predominant in the disk obtained. Apparently, crystals of type II provide seeds on which the amorphous state formed by grinding can more readily recrystallize than on seeds of type I. The observation is of importance in showing that the more pronounced effects observed with 1,2-benzanthraquinone compared with other aromatic compounds (Table 1) are a consequence of its crystal structure, and not of its molecular structure. The spectra of those aromatic compounds which caused enhanced water absorption in alkali halide disks (Table 1) showed evidence for partial destruction of their crystal structure due to grinding with the alkali halides but in no case were the spectral changes so marked as with 1,2-benzanthraquinone in form I.

DISCUSSION

KARAGOUNIS and PETER [7] have observed that the amorphous state of aromatic compounds is stabilized when these compounds are dispersed on the surface of

[6] A. TOLK, *Spectrochim. Acta* **17**, 511 (1961).
[7] G. KARAGOUNIS and O. PETER, *Z. Elektrochem.* **61**, 827, 1094 (1957); **63**, 1120 (1959).

powdered carriers. In infrared studies using AgI, AgCl, NaCl and KBr as carriers, they found marked changes in the relative intensity of the absorption bands of the dispersed substance on going from higher to lower surface coverages, as in the present study of 1,2-benzanthraquinone. Pronounced shifts in absorption bands only occurred with molecules containing polar groups, such as amino groups. Adsorption, induced by grinding, of phenols, amides and carboxylic acids on alkali halides has been established by infrared spectroscopy [4, 7]. The spectral changes which occur indicate that acids and phenols are adsorbed principally by hydrogen bonding between their hydroxyl groups and the halide ions, although some additional interaction between the aromatic rings of these compounds and the alkali halides is not excluded [4]. Precise assignments of the adsorption bands which are most affected when 1,2-benzanthraquinones are adsorbed on the alkali halides should assist in identifying the orientation of the adsorbed molecules, but unfortunately this has not been possible.

Conversion of crystalline compounds to the amorphous state during the preparation of alkali-halide pressed disks has been reported previously [1, 8] and appears to be common with steroids [9]. It has been shown that crystalline steroids may be rendered amorphous when ground alone [8], but it is noteworthy that the amorphous phase produced in alkali-halide disks is always associated with enhanced water adsorption by the alkali halide [9], as has been found with the aromatic compounds studied here. It seems possible, therefore, that adsorptive forces play a part in rendering the steroids amorphous. Although amorphous steroids can be induced to recrystallize by heating disks containing them to about 100° [9] this technique was not always successful with 1,2-benzanthraquinone.

It is at first sight surprising that adsorption of organic compounds on alkali-halide particles causes an increase in the amount of water adsorbed by these particles. On grinding pure alkali halides under normal conditions of humidity, the amount of adsorbed water increases rapidly at first, and then levels out. Two factors at least operate to limit the amount of water adsorbed. Firstly, the impact of the balls in the vibratory mill, as well as breaking down larger particles, causes fine particles to coalesce, and an equilibrium will be reached. Secondly, a high concentration of adsorbed water leads to continuous films through which ions can migrate, and so to recrystallization of the alkali halide with a loss of active centres. As a consequence, the amount of adsorbed water in finely ground alkali halides is generally reduced after exposing them to higher humidities. The action of adsorbed organic molecules may be to prevent finer particles from coalescing during grinding and to prevent the formation of continuous water films.

The conditions used in preparing the alkali-halide disks studied here were more vigorous than is necessary for qualitative studies. With a shorter grinding time (1 min) and a higher ratio of sample to alkali halide (1 mg–170 mg), spectral changes in the sample, and water adsorption by the alkali halide are much reduced. Doubts on the origin of hydroxyl absorption in alkali halide disks can generally be resolved by heating the pressed disk to 100° or over.

---

[8] V. C. FARMER, *Chem. & Ind. (London)* 1306 (1959).
[9] G. ROBERTS, *Anal. Chem.* **29**, 911 (1957).

Spectrochimica Acta, 1964, Vol. 20, pp. 1149 to 1173. Pergamon Press Ltd. Printed in Northern Ireland

The infra-red spectra of layer silicates

V. C. Farmer and J. D. Russell
Department of Spectrochemistry, The Macaulay Institute for Soil Research, Craigiebuckler, Aberdeen

(*Received* 22 *November* 1963)

Abstract—The infra-red absorption bands arising from the structural hydroxyl groups of a number of dioctahedral and trioctahedral layer silicates are reported with grating resolution in the 3750–3500 cm^{-1} region. The frequency differences and orientation behaviour of these bands are discussed in terms of the known structures of the minerals. The effect of the deviation from hexagonal symmetry shown by the tetrahedral layers of dioctahedral minerals on their vibrations is theoretically analyzed, and shown to account for some of the principal differences between the spectra of dioctahedral and trioctahedral layer silicates in the 1300 to 400 cm^{-1} region. Comparison of the spectra of random and oriented specimens of dioctahedral layer silicates in this region permits an assignment of some of the principal absorption bands to particular vibrational modes of the crystal lattice, and reveals some surprising differences between corresponding vibrational frequencies in related structures. Effects on the spectra of Al-for-Si substitution in the lattice of both dioctahedral and trioctahedral minerals are reported. A striking effect of particle size on the appearance and position of some of the stronger absorption bands of the kaolin minerals is related to the direction of the dipole moment change associated with these vibrations. Minerals examined include pyrophyllite, beidellite, rectorite, muscovite, margarite, montmorillonite, nontronite, celadonite, lepidolite and kaolins in the dioctahedral series, and talc, hectorite, saponite, phlogopite and biotite in the trioctahedral series.

Introduction

The present study of pure well characterized layer silicates has been undertaken to provide some of the background information necessary for the interpretation of the infra-red spectra of soil clays. The absorption spectra of most of the common layer silicates have already been broadly surveyed in the frequency range from 4000 to 650 or 400 cm^{-1} [1, 2], and it has been established that the spectra are sensitive both to structural and to compositional variations in the minerals. As the resolution used in studying the hydroxyl absorption of these minerals has generally been inadequate, a survey of their hydroxyl stretching vibrations under grating resolution has been undertaken with a view to revealing additional distinguishing features. In addition, an assignment of absorption bands in the 1300 to 400 cm^{-1} region has been attempted.

Difficulties are often encountered in assigning the causes of differences in the spectra of related minerals, as such minerals may differ in several ways, for example in the geometry and regularity of their structure and in the nature and site of ionic substitution. Study of the spectra of synthetic minerals of controlled composition has proved valuable [3, 4], but there remain many features of the spectra which are not well understood. A correlation of the absorption bands with the particular

[1] R. J. P. Lyon, *Minerals in the Infra-red.* Stanford Research Institute, California (1962).
[2] H. Moenke, *Mineralspektren.* Akademie-Verl., Berlin (1962).
[3] V. Stubičan and R. Roy, *Am. Mineralogist* **46**, 32 (1961).
[4] V. Stubičan and R. Roy, *Z. Krist.* **115**, 200 (1961).

vibrational modes of the crystal lattice which give rise to them would be a valuable conceptual tool in the interpretation of variations in spectra, and such a correlation is attempted here for dioctahedral layer silicates, along lines previously developed for the discussion of the trioctahedral layer silicates [5]. The assignment of absorption bands is assisted by the study of differences between the spectra of randomly oriented specimens (dispersed in alkali halide disks) and those of oriented films.

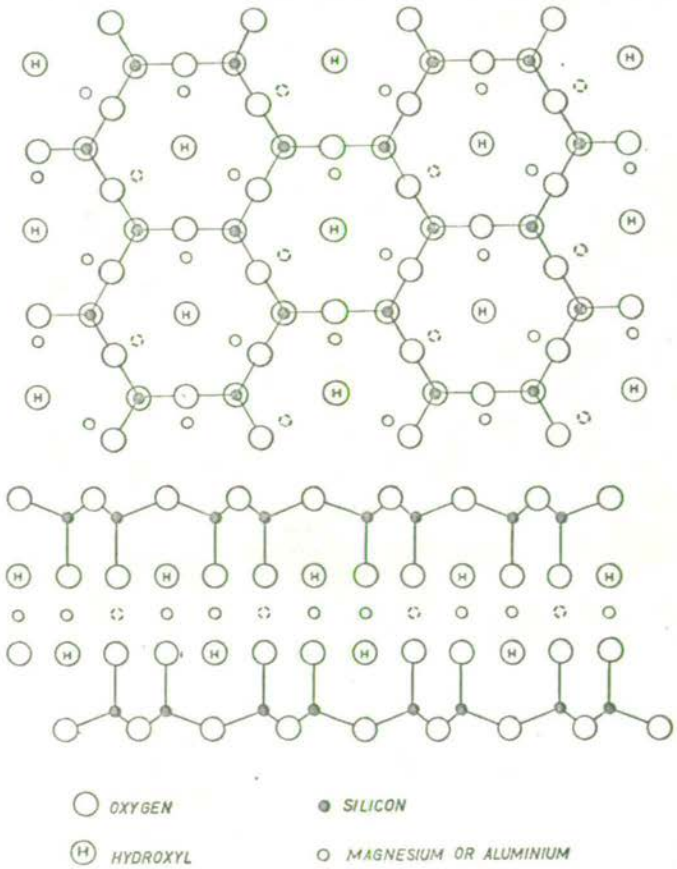

Fig. 1. The structures of talc ($Mg_3Si_4O_{10}(OH)_2$) and pyrophyllite ($Al_2Si_4O_{10}(OH)_2$). For clarity only one of the silicate anions is shown in the plan: the other is related to it by centers of symmetry at the dotted sites. This site is occupied by Mg^{2+} in talc, but is not occupied in pyrophyllite.

STRUCTURE AND NOMENCLATURE

The general features of the structure of layer silicates are illustrated in Fig. 1. They contain anions composed of condensed silicate tetrahedra in the form of infinite sheets of approximately hexagonal symmetry. In the *triphormic* (2:1) minerals, two such sheets are linked together by di- or tri-valent ions in octahedral co-ordination to give a layer structure. In talc, a typical *trioctahedral triphormic*

[5] V. C. FARMER, *Mineral. Mag.* **31**, 829 (1958).

mineral, all the octahedral sites are occupied by Mg^{2+}, whereas in pyrophyllite, the corresponding *dioctahedral* mineral, only two out of three sites are occupied by Al^{3+}: the unoccupied site is dotted in Fig. 1. Each octahedrally co-ordinated ion is linked to four oxygens at the apices of silicon–oxygen tetrahedra, and to two hydroxyl groups. In the trioctahedral minerals, the ideal hexagonal symmetry of the silicate anion is largely preserved, but the composite layer does not have hexagonal symmetry, as the two silicate anions are displaced relative to each other: they are related to each other by a centre of symmetry lying at the octahedral site that is unoccupied in the pyrophyllite structure. In the dioctahedral minerals, the silicate anion is distorted as shown in Fig. 5.

In talc and pyrophyllite, each composite layer in the structure is neutral, and successive layers are held together only by weak van der Waals forces. Substitutions such as Al^{3+}-for-Si^{4+} in the tetrahedral layers, or of Mg^{2+}-for-Al^{3+} in the octahedral layers result in a negative charge on the composite layers, which is compensated for by cations lying between the layers. The anhydrous micas have a high layer charge. The smectite minerals, saponite, hectorite, montmorillonite, beidellite and nontronite have a lower layer charge, and in these the interlayer cations are exchangeable, and are associated with a water layer of variable thickness.

In the *diphormic* (1:1) minerals, one of the silicate anions of the triphormic minerals is replaced by a layer of hydroxyl groups. Those of the kaolin group are *diphormic dioctadehral* minerals. In all these groups of layer silicates, one or more polymorphs of each mineral type may exist, differing in the way successive layers are stacked together.

This investigation is concerned principally with the hydroxyl vibrations and lattice vibrations of the diphormic and triphormic dioctadehral minerals, and with the hydroxyl vibrations of the triphormic trioctahedral minerals. The lattice vibrations of the latter have been discussed in an earlier publication [5].

Materials and Methods

The minerals examined are listed in Table 1. Many of them belong to species which cover a range of compositions, and for most of these analyses are given. The infra-red spectrum of the lepidolite shows it to have low Al-for-Si substitution in the tetrahedral layer, which is estimated as near $(Si_{7.6}Al_{0.4})$ in composition, from a comparison with Lyon's series of spectra [6]. The nontronite spectrum is close to one published by Stubičan and Roy [4] for which the composition shown in Table 1 is given. It is not known, however, to what extent the nontronite spectrum is affected by chemical composition.

Spectra were recorded using a sodium chloride prism for dispersion in the region 4000 to 630 cm^{-1} and a potassium bromide prism in the 700 to 400 cm^{-1} region [5]. Improved resolution in the 4000 to 3000 cm^{-1} region was achieved with a grating of 2,500 lines per inch. Randomly oriented preparations were obtained by the potassium-bromide pressed-disk technique, and oriented specimens by deposition on potassium bromide plates from isopropyl alcohol, or on silver chloride sheets from aqueous

[6] R. J. P. Lyon, *Evaluation of Infra-red Spectrophotometry for Compositional Analysis of Lunar and Planetary Soils*. Stanford Research Institute, California (1962).

Table 1. Composition and source of minerals investigated

Mineral	Characterization	Composition
Kaolinite: St. Austell, Cornwall	X-ray, optical	$Si_4Al_4O_{10}(OH)_8$
Dickite: Bodorgan Shore, Anglesey	Smithson and Brown [37]	$Si_4Al_4O_{10}(OH)_8$
Nacrite: Germany	X-ray, optical	$Si_4Al_4O_{10}(OH)_8$
Kaolin: Pugu, Tanganyika	Robertson, Brindley and Mackenzie [22]	$Si_4Al_4O_{10}(OH)_8$
Pyrophyllite: Graves Mount, Georgia	Heller *et al.* [8]	$0{\cdot}07M^+(Si_{7.90}Al_{0.10})(Al_{3.91}Fe_{0.04}Mg_{0.01}Ca_{0.07})O_{20}(OH)_4$*
Montmorillonite: Wyoming, U.S.A.	Heller *et al.* [8]	$0{\cdot}93M^+(Si_{7.70}Al_{0.30})(Al_{3.12}Fe^{3+}_{0.27}Fe^{2+}_{0.06}Mg_{0.39})O_{20}(OH)_4$*
Montmorillonite: Woburn, England	Mackenzie [38]	$0{\cdot}70M^+(Si_{7.77}Al_{0.16}Fe^{3+}_{0.07})(Al_{2.60}Fe^{3+}_{0.72}Fe^{2+}_{0.05}Mg_{0.73})O_{20}(OH)_4$*
Montmorillonite: Skyrvedalen, Norway	Rosenqvist [39]	$0{\cdot}98M^+(Si_{7.74}Al_{0.26})(Al_{3.24}Fe^{3+}_{0.04}Mg_{0.72})O_{20}(OH)_4$*
Beidellite: Black Jack Mine, Idaho	Weir and Greene-Kelly [40]	$0{\cdot}92M^+(Si_{6.96}Al_{1.04})(Al_{3.86}Fe_{0.04}Mg_{0.02})O_{19.96}(OH)_4$*
Nontronite: Dade Co., Georgia, U.S.A.	C. S. Ross	$0{\cdot}70M^+(Si_{7.0}Al_{1.0})(Fe_{4.04}Al_{0.06})O_{20}(OH)_4$
Rectorite (=Allevardite): Allevard, France	Brindley [41], Brown and Weir [9]	$Na_{0.62}K_{0.20}Ca_{0.15}(Si_{6.40}Al_{1.60})(Al_{3.78}Fe_{0.14}Mg_{0.08})O_{19.40}(OH)_{4.60}$*
Muscovite: unknown	X-ray, optical	$K_2(Si_3Al)_2Al_4O_{20}(OH)_4$
Margarite: Chester, Massachusetts	X-ray, optical	$Ca_2(Si_2Al_2)_2Al_4O_{20}(OH)_4$
Lepidolite: Yavapai County, Arizona, U.S.A.	Infra-red spectrum	$K_2(Al_ySi_{4-y})_2(Li,Al)_{4-6}O_{20}(OH,F)_4$
Ferric Celadonite: Reno, Nevada, U.S.A.	Foster [24]	$(K_{1.84}Ba_{0.06}Ca/2_{0.04})Si_{8.00}(Al_{0.14}Fe^{3+}_{1.86}Fe^{2+}_{0.46}Mg_{1.54})O_{20}(OH)_4$*

* By analysis.

[37] F. SMITHSON and G. BROWN, *Mineral. Mag.* **31**, 381 (1957).
[38] R. C. MACKENZIE, *Silicates Ind.* **25**, 12, 71 (1960).
[39] I. Th. ROSENQVIST, *Norsk. Geol. Tiddskr.* **39**, 350 (1959).
[40] A. H. WEIR and R. GREENE-KELLY, *Am. Mineralogist* **47**, 137 (1962).
[41] G. W. BRINDLEY, *Am. Mineralogist* **41**, 91 (1956).

suspension. Grinding moistened powders in a vibrating ball mill was effective in reducing particle size without altering the structure of the minerals [7].

Hydroxyl Stretching Frequencies

Dioctahedral minerals

The absorption bands due to the OH-stretching vibrations of a series of triphormic dioctahedral minerals, randomly oriented, are shown in Fig. 2. Pyrophyllite can be considered the parent mineral of this series, as the other members are considered to be derived from it by ionic substitution. In this structure, each pair of aluminium ions shares two hydroxyl groups which are related by a centre of symmetry between the aluminium ions. Coupling between the vibrations of the two hydroxyl groups can give rise to two frequencies of vibration: one in which the two hydroxyl groups are 180° out-of-phase (antisymmetrical with respect to the centre of symmetry), and the other an in-phase vibration (symmetric). The antisymmetric vibration is infra-red active, and is the origin of the strong band at 3675 cm^{-1} (Fig. 2A). The symmetric vibration is infra-red inactive, but would be active in the Raman spectrum, which has not yet been examined. The weak band at 3647 cm^{-1} could arise from this vibration, if the symmetry of the structure is not ideal. An alternative assignment is that it arises from hydroxyl groups shared between Al and Fe ions, as the octahedral layer does contain a small proportion of Fe ions. In support of the latter assignment, it may be noted that pyrophyllite-like structures containing a higher proportion of iron show stronger absorption than pure pyrophyllite at 3640 cm^{-1} [8]. Progressively increasing substitution of aluminium for silicon in the tetrahedral layer of pyrophyllite, with the introduction of interlayer cations to balance the resulting charge deficiency, gives first beidellite and then muscovite or paragonite. Their hydroxyl absorption (Fig. 2B and D) has two components at 3660 and 3627 cm^{-1}, the lower-frequency band increasing in intensity with increasing aluminium substitution, and the higher-frequency component decreasing. Rectorite (Fig. 2C), in which the substitution is also principally in the tetrahedral layer, gives one rather broad band at an intermediate frequency, but its structure has some unusual features, discussed later, which distinguish it from the other three minerals in this group [9]. The OH group in these structures is expected to be directed away from the octahedral aluminium ions to which it is attached, so that the proton may interact with the oxygens at the apices of adjacent tetrahedra (O_4 and O_5 in Fig. 5). The lower-frequency band can be correlated with Al-for-Si substitution in one of the tetrahedra, and the higher-frequency absorption with sites where both tetrahedra are occupied by silicon. In margarite (Fig. 2E), one of every pair of tetrahedra is occupied by aluminium, and the higher-frequency band is absent. Displacement of the OH stretching vibration to lower frequencies associated with band-broadening is commonly ascribed to hydrogen bonding, but this explanation is unlikely here. It might be

[7] W. M. Tuddenham and R. J. Lyon, *Anal. Chem.* 32, 1630 (1960).

[8] L. Heller, V. C. Farmer, R. C. Mackenzie, B. D. Mitchell and H. F. W. Taylor, *Clay Minerals Bull.* 5, 56 (1962).

[9] G. Brown and A. H. Weir, *Proc. Intern. Clay Conf., Stockholm*, vol. 1. *International Series of Monographs on Earth Sciences*, vol. 14, p. 27, Pergamon Press, London (1963).

anticipated that hydrogen bonding could occur between the hydroxyl group and the oxygens of tetrahedra containing aluminium ions, as these oxygens would be expected to carry a residual negative charge, but in fact a detailed X-ray study of muscovite [10, 11] has shown that the OH—O distances in this structure (3·45 and 3·50 Å) are almost identical with the corresponding distances (3·41 and 3·47 Å) in dickite [12], in which no Al-for-Si substitution occurs. It seems rather that the low-frequency component in these minerals arises from a crystalline field effect due to Al^{3+}-for-Si^{4+} substitutions. Electrostatic field effects have been shown to have a marked influence on hydroxyl frequencies [13]. The breadth of both components in these minerals, compared with the narrowness of the hydroxyl absorption in pyrophyllite, can reasonably be ascribed to structural irregularities arising from the random nature of the Al-for-Si substitution, leading to a range of hydroxyl–oxygen distances. Further, each hydroxyl group is surrounded by the apical oxygens of six tetrahedra, and although Al-for-Si substitution in only two of these causes a marked change in frequency, substitution in one of the other four may cause minor shifts and so contribute to the band width.

Beidellite is an end-member in the range of composition of the dioctahedral smectites; the montmorillonite from Skyrvedalen closely approaches another end-member in which only Mg-for-Al substitution occurs in the octahedral layer. This is also the principal substitution in the Wyoming montmorillonite, which has in addition some Fe-for-Al substitution. The hydroxyl absorption of these two montmorillonites (Figs. 2F and G) has a maximum close to that of the lower-frequency component of beidellite, but is weaker and more diffuse at higher frequencies, and has a broad shoulder on the low-frequency side. This pattern of absorption is not affected by changing the interlayer cation, and is only slightly changed by removing interlayer water. In the Skyrvedalen montmorillonite at most 36 per cent of the hydroxyl groups are shared between Al and Mg ions in the octahedral layer, the remainder being shared between two Al ions, as in pyrophyllite: accordingly, the marked difference between the hydroxyl absorption of this montmorillonite and pyrophyllite cannot be ascribed to a direct effect of the magnesium ions on the hydroxyl groups, since this would leave 64 per cent of the hydroxyl groups unaffected. Rather, the shift to lower frequencies of the hydroxyl absorption in these montmorillonites must again arise from field effects due to residual negative charges on adjacent oxygen atoms, as a result of Mg^{2+}-for-Al^{3+} substitution; the broadening can be ascribed to the range of hydroxyl-oxygen distances which are a likely consequence of distortions resulting from substituting the larger Mg^{2+} for Al^{3+} in the octahedral layer. A further factor, valid for both beidellite and montmorillonite, is that hydroxyl frequencies in crystals are determined not only by direct bonding forces and static fields effects, but also by electrical dipole-dipole coupling forces between the vibrating hydroxyl groups [13]. Lack of parallelism of the hydroxyl groups in smectites can therefore cause frequency shifts by changing these coupling forces. When Wymoing and Skyrvedalen montmonillonites are dehydroxylated at

[10] E. W. Radoslovich, *Acta Cryst.* **13**, 919 (1960).
[11] L. Gatienau, *Compt. Rend.* **256**, 4648 (1963).
[12] R. E. Newnham, *Mineral. Mag.* **32**, 683 (1961).
[13] H. H. Caspers and R. A. Buchanan, *Spectrochim. Acta* **18**, 1361 (1962).

700°–750° and then rehydroxylated in steam, the hydroxyl groups which are recovered, amounting to about 50 per cent of the original, show a much sharper absorption with a peak position identical with that of pyrophyllite [8]. According to the present interpretation, this implies that migration of Mg and Al ions occurs in the octahedral layer during dehydroxylation and rehydroxylation, leading to small regions which approach the pyrophyllite composition.

The hydroxyl absorption of nontronite (Fig. 2J), a smectite in which the octahedral sites are occupied by ferric ions, is displaced about 90 cm^{-1} to lower frequency compared with that of beidellite, its aluminium analogue. The Woburn montmorillonite, in which about 18 per cent of the octahedral sites are occupied by ferric ions, also shows evidence of a proportion of groups with absorption at this low frequency (Fig. 2H). Absorption in this region is also characteristic of celadonite (Fig. 2K), a mica in which half the octahedral sites are occupied by ferric ions, the remainder being occupied by mangesium and ferrous ions, but there the hydroxyl absorption has a sharp three-banded pattern. The sharpness of the absorption bands indicates a very well-ordered structure with the divalent and trivalent ions occupying crystallographically different sites, each hydroxyl group being shared between a divalent and a trivalent ion [14]. It is possible that the two strongest absorption bands of celadonite arise from two types of hydroxyl groups: those shared between Fe^{2+} and Fe^{3+} and those shared between Mg^{2+} and Fe^{3+}. The low frequency of these FeOH groups may be in part due to hydrogen bonding, as the O(H)—O distances in celadonite (3·01 Å) are rather shorter than those found for muscovite (3·45–3·50 Å). The sharpness of the absorption bands, however, argues against any significant degree of hydrogen bonding; also, shorter hydrogen bonds occur in dickite (O—O distances 2·97 Å and 2·94 Å), and in this mineral the lowest observed frequency (3622 cm^{-1}) is higher than those of celadonite. Clearly other factors must be of importance, peculiar either to the ions to which the hydroxyl groups are linked, or to the structure in which they are incorporated. A further example of anomalous absorption by $Fe^{III}OH$ groups is that of synthetic leucophosphite [15] which in its anhydrous form ($KFe_2(PO_4)_2 \cdot OH$) gives a very sharp band of half-width only 12 cm^{-1} at 3507 cm^{-1}.

The hydroxyl absorption of all these minerals is essentially unaffected by the angle at which the radiation is incident upon the sheets, showing that all the hydroxyl groups are oriented at a considerable angle to the normal to the sheets. Observations on a single muscovite flake [16] have indicated that the dipole oscillation lies at 16° to the plane of the sheet. Radoslovich [17] has argued that this angle would be nearer to 60–70° if it were not for repulsion of the protons of the hydroxyl groups by the interlayer potassium ions in muscovite. Our observations on pyrophyllite, which has no interlayer cations, contradict this supposition of Radoslovich. In contrast to these triphormic minerals, the diphormic kaolin group of minerals show a complex pattern of sharp absorption bands of which one in kaolinite and two in nacrite and dickite show marked orientation effects (Fig. 3). Almost identical results have been

[14] B. B. Zvyagin, *Kristallographiya* 2, 393 (1957). Eng. Transl. p. 388.
[15] E. Z. Arligde, V. C. Farmer, B. D. Mitchell, and W. A. Mitchell, *J. Appl. Chem.* (*London*) 13, 17 (1963).
[16] W. Vedder and R. S. McDonald, *J. Chem. Phys.* 38, 1583 (1963).
[17] E. W. Radoslovich, *Am. Mineralogist* 48, 76 (1963).

obtained for kaolinite by SERRATOSA *et al.* [18, 19], and NEWNHAM [12] has given a comparable spectrum for a partially oriented dickite preparation. These authors and others [20, 21] have assigned the absorption bands on the assumption that each type of hydroxyl group gives rise to a distinctive absorption band: this is probably an over-simplified approach, as the range of frequencies involved is not much greater than that which can arise from dipole-dipole coupling effects between identical hydroxyl groups—compare, for example, $Mg(OH)_2$, in which the symmetrical and antisymmetrical vibrations differ by 45 cm^{-1} [13]. A detailed X-ray study of dickite has shown that the gibbsite-like layer of hydroxyl groups is involved in weak hydrogen bonding to surface oxygens of the tetrahedral layer of the adjacent sheet, with O(H)—O distances of 3·12, 2·97 and 2·94 Å. Assuming that the hydroxyl groups lie along the O—O directions, they make angles of about 17°, 17° and 14° respectively with the normal to the sheets, and so should absorb more strongly in the randomly oriented specimen than in the oriented. A similar pattern of hydrogen bonding, of which the details have not yet been worked out, occurs in nacrite and kaolinite. The hydroxyl groups of the gibbsite-like sheet are approximately related by three-fold axes passing through the aluminium ions. An exact three-fold symmetry would cause the hydroxyl vibrations of the three groups in the unit cell to couple to give one (symmetrical) vibration with the dipole change along the three-fold axis, i.e. perpendicular to the sheets, and two degenerate vibrations with dipole changes in the plane of the sheets. With this in mind, the pattern of absorption in kaolinite can be explained, by ascribing the 3697 cm^{-1} band to the symmetrical vibration of the gibbsite-like sheet, the bands at 3669 and 3652 cm^{-1} to the in-plane vibrations, with their degeneracy lifted, while the 3620 cm^{-1} absorption arises principally from the hydroxyl group on the side of the tetrahedral sheet. This last assignment is in agreement with the observations on the triphormic dioctahedral minerals, where it was found that their hydroxyl absorption appears strongly in spectra of oriented layers, and also accounts for the relative stability in frequency of this absorption in the different kaolin minerals. In dickite and nacrite it must be concluded that the vibrations of one of the hydroxyl groups of the gibbsite sheet is sufficiently different in frequency from those of the other two to absorb independently, in order to account for the presence of two absorption bands with strong components perpendicular to the sheets. If the hypothesis that marked coupling occurs between the vibrations of different hydroxyl groups is correct, then small amounts of hydroxyl in a synthetic kaolinite containing principally deuteroxyl groups should show a pattern different from, and not simply weaker than, that of kaolinite itself. In fact the one synthetic deuterated kaolinite available to us does show a weak structureless absorption band in the region in which normal kaolinite absorbs, although it is possible that this arises from surface hydroxyl groups, and not from structural hydroxyl.

The different infra-red patterns given by kaolinite, dickite and nacrite permit the

---

[18] J. M. SERRATOSA, A. HIDALGO and J. M. VINAS, *Nature* **195**, 486 (1962).

[19] J. M. SERRATOSA, A. HIDALGO and J. M. VINAS, *Proc. Intern. Clay Conf., Stockholm*, vol. 1. *International Series of Monographs on Earth Sciences*, vol. 14, p. 17. Pergamon Press, London (1963).

[20] H. W. VAN DER MAREL and J. H. L. ZWIERS, *Silicates Ind.* **24**, 359 (1959).

[21] R. J. P. LYON and W. M. TUDDENHAM, *Nature* **185**, 835 (1960).

entification of these minerals, although the infra-red spectra are unlikely to be so nsitive as the X-ray powder pattern in the analysis of mixtures. The infra-red ethod, however, is applicable to kaolin structures with random stacking of the yers, where X-ray methods give less direct information. An example of this is the ugu kaolin characterized as a b-axis disordered structure by X-ray methods [22]. s pattern of hydroxyl absorption (Fig. 3D) is consistent with the presence of acking of both the kaolinite and dickite types, with perhaps a small proportion of icrite-like stacking. In kaolinite successive layers are arranged parallel to each her, but displaced by $-a/3$, to give a triclinic structure; in dickite, the successive yers are also displaced by $-a/3$ but are rotated alternately by $+120°$ and $-120°$ om each other to give a monoclinic structure. The presence of random kaolinite nd dickite stacking in the Pugu kaolin therefore accounts for its pseudomonoclinic -ray pattern; it also accounts for the random $b/3$ shifts, as continuation of the $a/3$ ifts of kaolinite stacking along the new a-axis direction following a dickite-like tation of the layers is equivalent to a combined shift of $-a/3$ and $-b/3$ relative to ne original a-axis direction [12].

rioctahedral minerals

In talc, the hydroxyl group is symmetrically linked to three magnesium ions, and ves a sharp weak band with the dipole change perpendicular to the sheet. As with yrophyllite, the main absorption band has a weak satellite of uncertain origin, hich shows the same polarization (Fig. 4A). Substitution of part of the magnesium y lithium as in hectorite (Fig. 4B) or of Al^{3+} for Si^{4+}, as in saponite (Fig. 4C), leaves ne main absorption unchanged in frequency, although the absorption broadens, and ne low-frequency satellite is lost. The one in eight substitution of Al^{3+} for Si^{4+} in aponite gives rise to a higher-frequency component at 3710 cm^{-1} (Fig. 4C) and this ncreases in strength in phlogopite (Fig. 4D) where the substitution is one in four. he spectra of the phlogopite flake show that the hydroxyl groups giving rise to both omponents are only very slightly inclined, if at all, to the normal to the sheets. If ne replacement of Al-for-Si were a regular one, then three-quarters of the hydroxyl roups in saponite would have one aluminium ion substituted in the six tetrahedra hich surround them, and one-quarter would have none, whereas in phlogopite, half ould have one aluminium and half two aluminium ions in these six tetrahedra. hese considerations suggest that the higher-frequency band must arise from ydroxyl groups having two Al-for-Si substitutions in their immediate vicinity, a tuation which will also occur occasionally in saponite when the aluminium substi- ution is irregular, as it almost certainly is. Of five nearly colourless phlogopites xamined, four showed weak absorption bands, insensitive to the orientation of the ake, at 3622 cm^{-1} and 3600 cm^{-1}. Analysis of one of these showed an Fe content of ·4%. These absorption bands appear more strongly in the spectrum of a green iotite (Fig. 4E) and are clearly associated with Fe-for-Mg substitution. In two very ark brown biotites examined (Fig. 4F) these absorption bands showing no orienta- ion effects lie at still lower frequencies and are much more intense, and the per- endicular band near 3670 cm^{-1} is more diffuse than in phlogopites and biotites of

22] R. H. S. Robertson, G. W. Brindley and R. C. Mackenzie, *Am. Mineralogist* 39, 118 (1954).

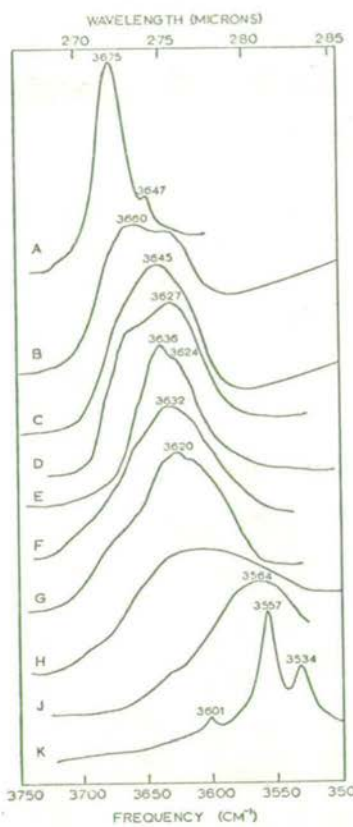

Fig. 2

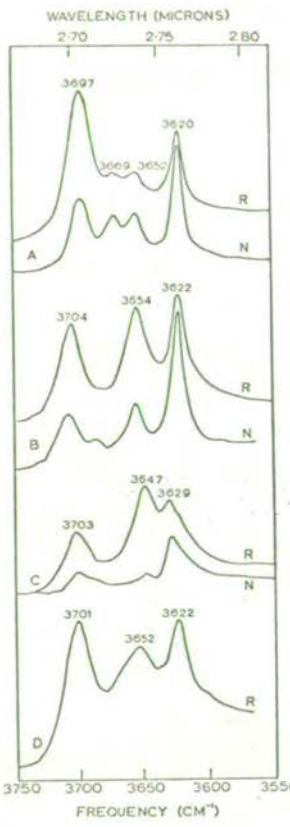

Fig. 3

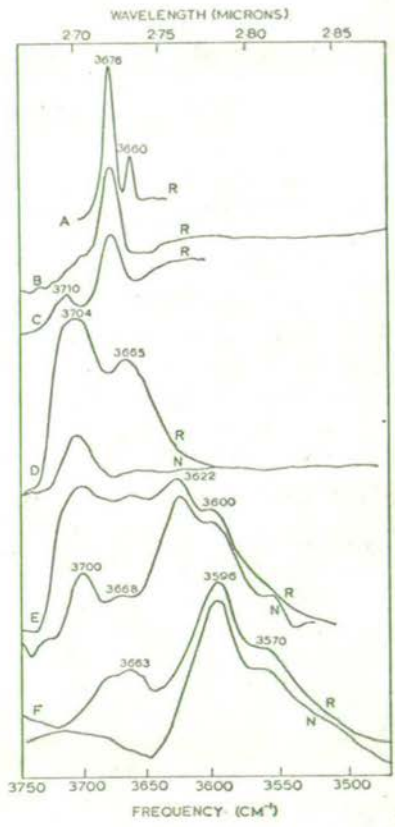

Fig. 4

Fig. 2. Hydroxyl absorption of randomly oriented samples of A—pyrophyllite, B—beidellite, C—rectorite, D—muscovite or paragonite, E—margarite, F—Wyoming montmorillonite, G—Skyrevdalen montmorillonite, H—Woburn montmorillonite, J—nontronite and K—ferric celadonite.

Fig. 3. Hydroxyl absorption of A—kaolinite, B—dickite, C—nacrite, D—Puga kaolin. R indicates randomly oriented specimens, and N films at normal incidence.

Fig. 4. Hydroxyl absorption of A—talc, B—hectorite, C—saponite, D—phlogopite (126 μ), E—green biotite (115 μ), and F—dark brown biotite (25 μ). The mica spectra were obtained from single flakes of the thickness indicated at normal (N) and 45° incidence (R).

lower iron content. The sample giving spectrum 4F contained 4·8% Mg and 24·8% Fe. SERRATOSA and BRADLEY [23] have reasonably suggested that the hydroxyl groups giving the lower frequency absorption bands, which must be inclined at a considerable angle to the normal to the sheet, are associated with sites at which only two of the three possible octahedral positions are filled: such sites appear in increasing amount with increasing substitution of trivalent ions such as Fe^{3+} and Al^{3+} in the

[23] J. M. SERRATOSA and W. F. BRADLEY, *J. Phys. Chem.* **62**, 1164 (1958).

octahedral layer of biotites [24]. BASSETT [25], using lower resolution, has also noted the tendency of hydroxyl absorption in biotites to shift to lower frequencies with increasing iron content.

LATTICE VIBRATIONS

Theoretical considerations

The general features of the infra-red spectrum of talc can be qualitatively interpreted in terms of a silicon–oxygen network of hexagonal symmetry [5], and calculations based on a simple set of force constants are in approximate agreement with these assignments for vibrations with frequencies higher than 600 cm^{-1} [26].

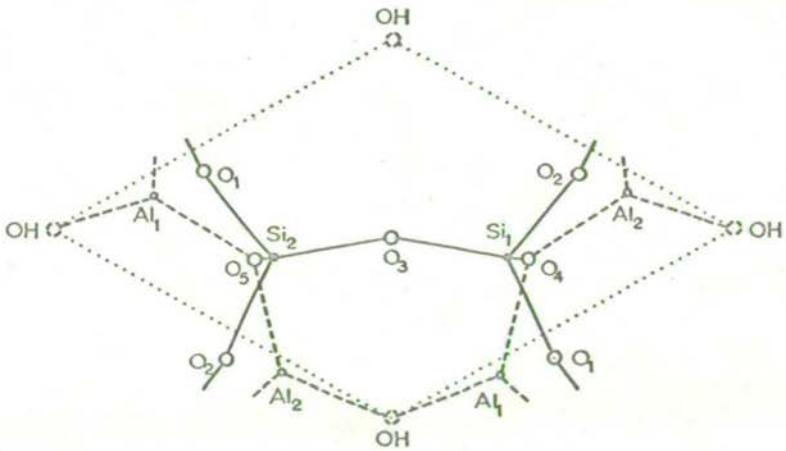

Fig. 5. The unit cell within a single sheet of dickite, omitting the surface layer of hydroxyl groups.

In the dioctahedral minerals, the silicon–oxygen network deviates markedly from ideal hexagonal symmetry, and more complex spectra are obtained. The type of distortion which occurs in dickite [12] is shown in Fig. 5: a similar distortion has been found in muscovite [10]. The principal features are that the silicon tetrahedra are rotated about vertical axes parallel to the sheet, so that the apical oxygens O_4 and O_5, do not lie immediately under silicon ions, and the Si-O_3-Si bond angle is larger (141·8°) than the corresponding angles involving oxygens O_1 and O_2 (128·8° and 131·0°). The resulting structure has only a plane of symmetry perpendicular to the sheet and passing through the hydroxyl groups and O_3 in Fig. 5. The primitive unit cell is of symmetry C_{2h} and all its vibrations are infra-red active. They fall into two classes, nine of symmetry species A' in which the electrical dipole lies in the symmetry plane, and nine of symmetry species A'' in which the dipole is perpendicular to the plane. The kaolin minerals have only one sheet of this type in each layer of the structure, but the triphormic minerals have two, related by a centre of symmetry. The corresponding vibrations of each sheet couple to give two vibrations of the whole

[24] M. D. FOSTER, *Am. Mineralogist* **45**, 383 (1960).
[25] W. A. BASSETT, *Bull. Geol. Soc. Am.* **71**, 449 (1960)
[26] B. D. SAKSENA, *Trans. Faraday Soc.* **57**, 242 (1961)

layer, one infra-red active, and the other Raman active. These pairs will not differ greatly in frequency except for those vibrations which are strongly coupled through vibrations of the octahedral ions linking the two silicon–oxygen networks—that is, some of the lower-frequency vibrations. In actual silicates successive sheets are sometimes stacked parallel to each other, for example in the $1M$ mica structure and the $1T$ kaolinite structure, and these should permit a sharp distinction between the A' and A'' vibrations by the study of single crystals with polarized radiation. More frequently successive layers are rotated relative to each other, as in the $2M$ micas and dickite, so that all vibrations will have components along both the a and b directions in the crystal. The intensities of these components will differ except in stacking with trigonal or hexagonal symmetry. This investigation, however, is concerned principally with bands whose intensities are affected by the angle which the beam makes with the normal to the sheet. The C_s symmetry of the layers does not require any of the absorption bands to be polarized perpendicularly to the sheets, but such bands do occur, and for this reason it is convenient to consider the tetrahedral sheets as having the rather higher point group symmetry C_{2v}. This higher symmetry is obtained by neglecting the rotation of the tetrahedra about their vertical axes: the unit cell has then an additional plane of symmetry perpendicular to the sheet passing through the silicon ions and the oxygen ions O_3, O_4 and O_5, and also a two-fold axis through O_3 (see Fig. 5). The approximate forms of the vibrations expected for this symmetry are shown in Fig. 6: those labelled a_1 develop dipole moments perpendicular to the sheet, those labelled b_1 and b_2 have moments in the plane of the sheet at right angles to each other, while those labelled a_2 develop no dipole moment and are inactive in the infra-red spectrum. With the lower symmetry, C_s, vibrations of type a_1 and b_1 fall into the symmetry species A', and those of type a_2 and b_2 into the species A''. The vibrations drawn in Fig. 6 are formalized, and will not in general correspond to the actual vibrations of the sheet: in particular Si—O stretching vibrations have been separated from Si—O bending vibrations, and while this approximation is often a good one for organic compounds, it is unlikely to be so satisfactory for condensed silicates. In general, this means that the actual vibrations will be some linear combination of the forms shown, and necessary modifications required by the observed spectra will be discussed in the next section.

The infra-red absorption pattern

The infra-red spectra of most of the layer silicates examined here were recorded with samples randomly oriented in potassium bromide disks and also with oriented layers in which the incident beam was perpendicular to the sheet surface. The absorption bands with dipole moments perpendicular to the sheets, or nearly so, were absent or weak in the latter spectra. Their reappearance on turning these oriented layers at an angle to the beam was checked.

Layer silicates in which Al-for-Si substitution was absent or low gave the sharpest spectra and the most clearly defined results and attention will be concentrated on them. These minerals include kaolinite (Fig. 7), nacrite (Fig. 8), pyrophyllite (Fig. 9), montmorillonite (Fig. 10), lepidolite (Fig. 11), and celadonite (Fig. 12): dickite gave a spectrum similar in pattern to that of nacrite, but with significant differences in the frequency of some of the absorption bands. These frequencies are recorded in Table 2,

as are those of Wyoming and Woburn montmorillonites and of nontronite which gave less well defined spectra. The montmorillonite spectra, without polarization observations, have been previously published [8], and the nontronite spectrum is close to that published by STUBIČAN and ROY [4]. Spectra of the rarer minerals, beidellite and rectorite, are shown in Figs. 13 and 14. The beidellite spectrum shows some differences from the published spectra of synthetic preparations [3, 4] particularly in the 650–400 cm^{-1} region.

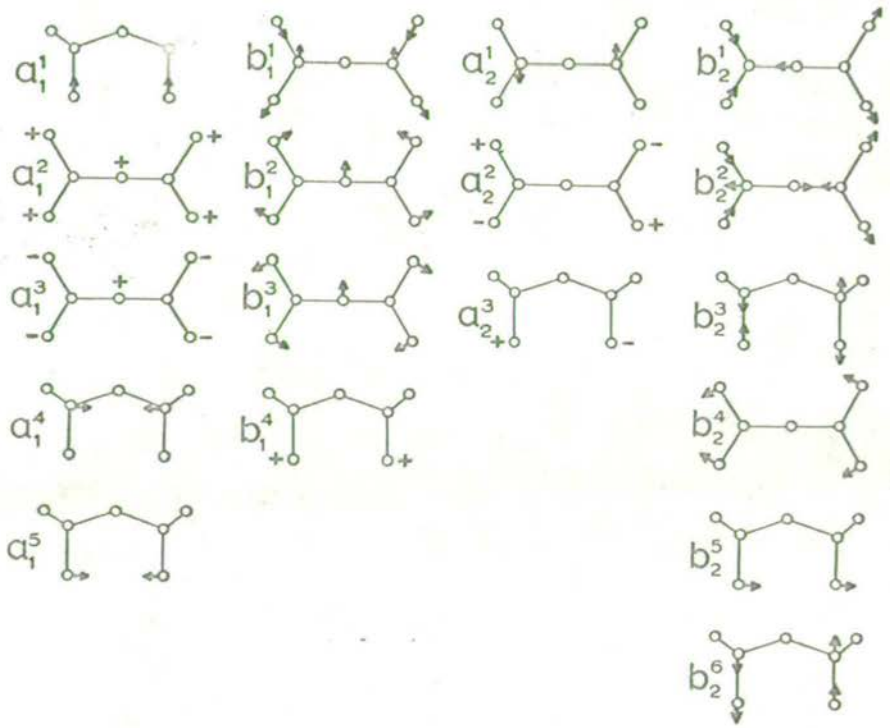

Fig. 6. The vibrations of the unit cell in a tetrahedral layer of symmetry C_{2v}.

Vibrations in the 1150–960 cm^{-1} *region*

The minerals with low Al-for-Si substitution show a broadly similar pattern of absorption in this region, arising from Si—O stretching vibrations. Comparison of the spectra of oriented and random samples show three well-defined medium or strong in-plane vibrations and one perpendicular vibration for each. The perpendicular vibration can be ascribed principally to the Si—O mode a_1^1 (Fig. 6), with some contribution from a_1^2. The position and sharpness of this absorption varies surprisingly with physical state. Thus in the spectra of dickite, nacrite and kaolinite of larger crystal size (equivalent spherical diameter greater than 2 μ) this mode appears as a broad shoulder near 1080 cm^{-1}. The band intensifies, and shifts to higher frequencies in the spectra of smaller crystals until in very finely ground material the band is close to that found for clay kaolinite (1109 cm^{-1}). The nacrite spectrum shown (Fig. 8) has not quite reached this limit. This effect has been noted in dickite,

Fig. 7

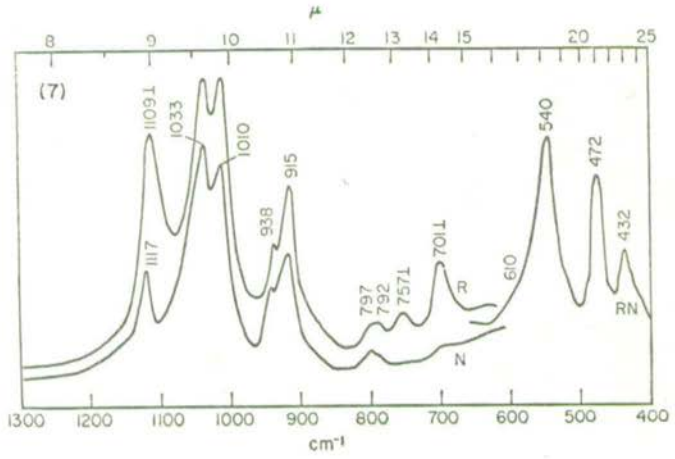

Fig. 9

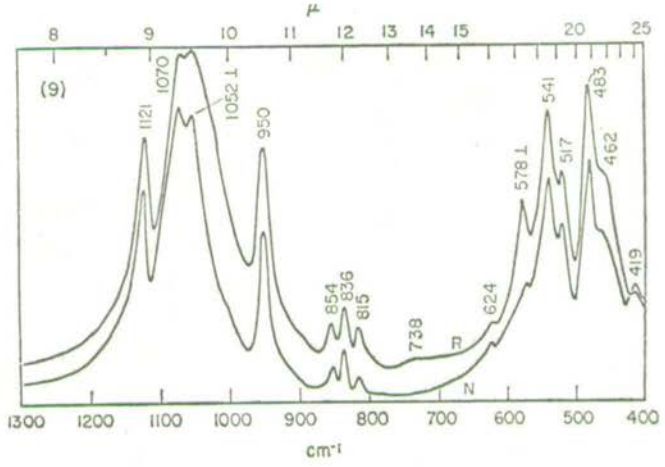

Fig. 8

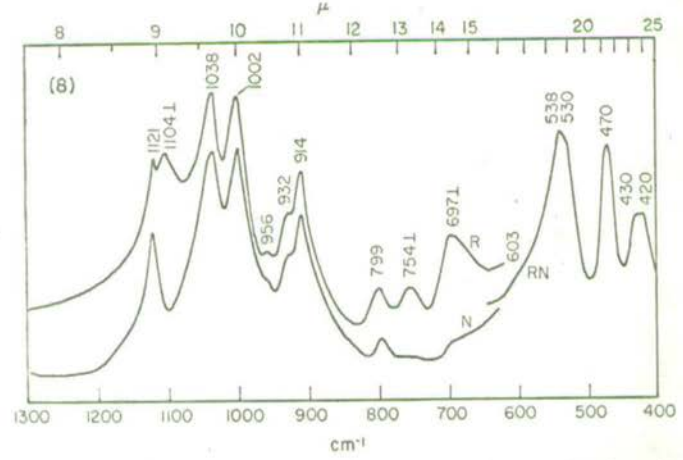

Fig. 10

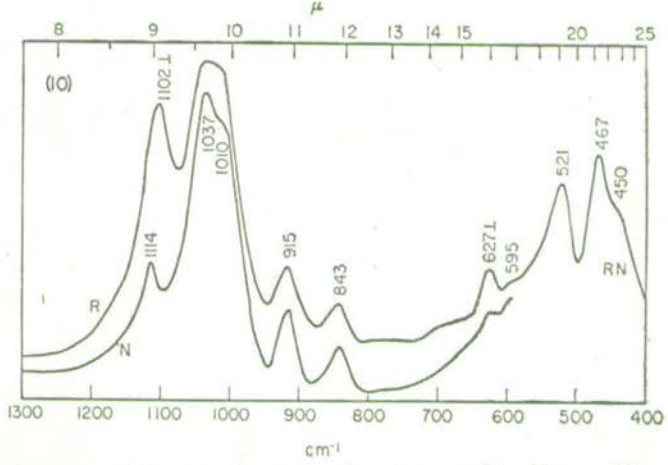

Fig. 7. Infra-red spectrum of kaolinite, using randomly oriented samples (R) and oriented layers at normal incidence (N). RN indicates spectra independent of orientation. Bands showing perpendicular polarization are indicated (P).

Fig. 8. Infra-red spectrum of nacrite.

Fig. 9. Infra-red spectrum of pyrophyllite.

Fig. 10. Infra-red spectrum of Skyrvedalen montmorillonite.

Fig. 11

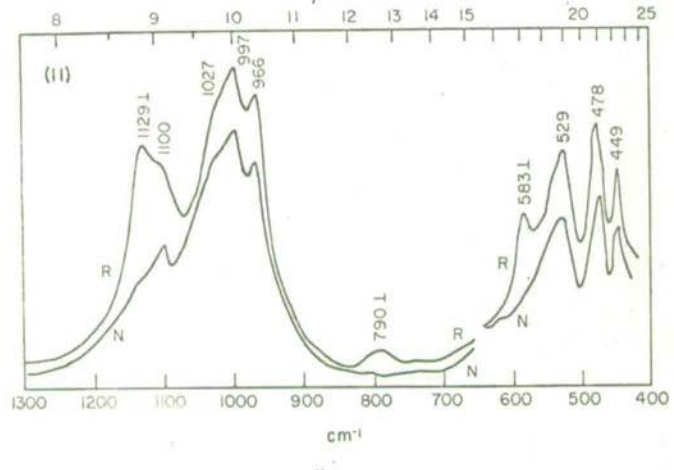

Fig. 12

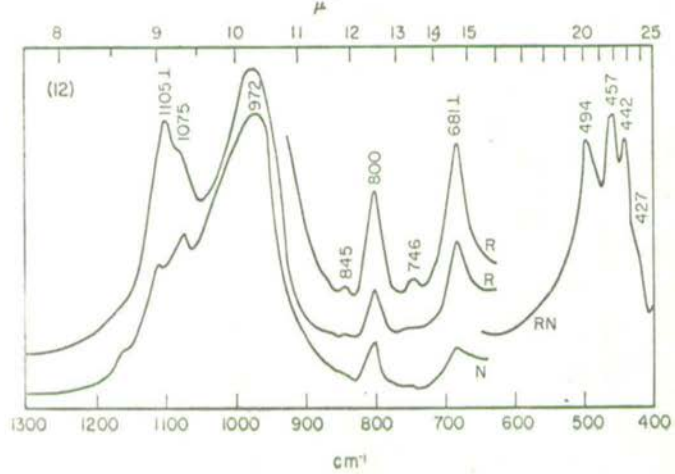

Fig. 11. Infra-red spectrum of lepidolite.

Fig. 12. Infra-red spectrum of ferric celadonite.

Fig. 13

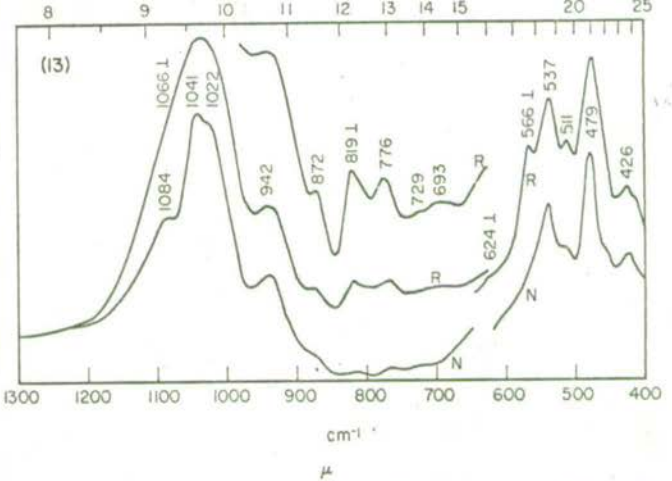

Fig. 14

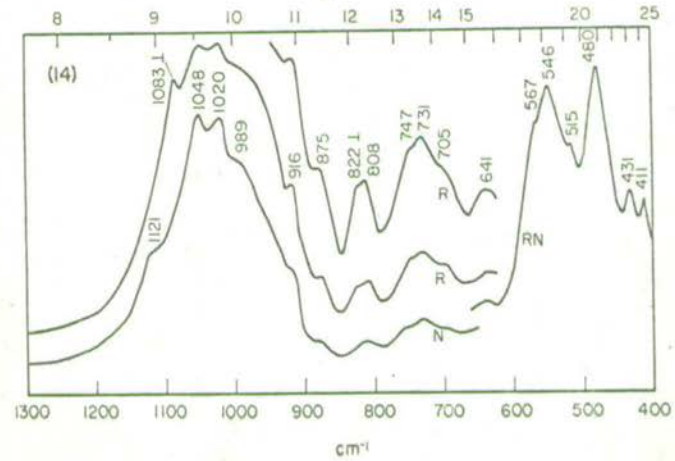

Fig. 13. Infra-red spectrum of beidellite.

Fig. 14. Infra-red spectrum of rectorite.

although differently interpreted, by LYON and TUDDENHAM [27]. Smaller but distinct shifts in frequency together with sharpening and intensification of the bands as particle size decreases also occur with the other less intense perpendicular modes of the kaolin minerals, but absorption of the in-plane modes is not affected. X-ray examination showed that no change in crystal structure occurred under the grinding conditions used. Considerations based on the dipole theory of crystal vibrations [28]

Table 2. Frequency (cm^{-1}) of infra-red absorption bands

	Dickite	Wyoming Montmorillonite	Woburn Montmorillonite	Nontronite
Si—O stretching	1120	1120	1117	1091
	1107 (p)	1080 (sh p)	1074 (p)	1034 (p)
	1034	1048	1038	1017
	1003	1025	1010	
	968			
R—O—H bending	936	920	919	848
	913	890	877	818
	795	849	839	786
	755 (p)	800	790 (p)	753
	699 (p)	622 (p)		680 (p)
	605 (sh)			
Si—O—R^{3+} and R^{3+}—OH	540	523	568	587 (p)
	530 (sh)		521	493
	470	468	473	450
	431		430	430
	422 (sh)			

sh—shoulder; p—perpendicular polarization.

indicate that perpendicular modes of platy crystals, of thickness very much less than the wavelength of the infra-red radiation, should occur at a frequency higher than that of the same vibration in crystals larger than the wavelength, the difference in frequency being a function of the magnitude of the dipole change associated with the vibration, and so with the intensity of absorption. Further work is in progress to determine how well this theory accounts for the present observations.

It has also been noted that the frequency of the perpendicular Si—O mode as determined in inclined oriented layers is about 10 cm^{-1} higher than that found in pressed disk spectra, and reported here, the difference being most clearly seen with montmorillonite, lepidolite and celadonite. Because of this effect, inclining a layer of kaolin to the infra-red beam seemed only to intensify the in-plane band at 1117 cm^{-1} with no indication of the distinct band found at 1109 cm^{-1} in disk spectra. This difference in absorption frequency is presumably an effect of the dielectric constant

[27] R. J. P. LYON and W. M. TUDDENHAM, *11th Pittsburgh Conf. on Anal. Chem. and Appl. Spectroscopy* (1960).

[28] H. FRÖHLICH, *Theory of Dielectrics*. Oxford University Press (1949).

the medium in which the mineral is dispersed, but no detailed explanation can be ven. There is evidence too, that the position and appearance of this absorption nd is very sensitive to the regularity of the structure. Thus it is a broad diffuse nd in halloysite and also in synthetic kaolinite, whether in the normal or deuterated rm [4]. It is a well-defined band in the Skyrvedalen montmorillonite examined re, but this material is unusual in this respect, as the band is not so well defined in ublished spectra of other montmorillonites. Even with this material it has been und that the band broadens markedly after it has been subjected to the usual ocedure involved in saturating montmorillonites with different ions, but still mains sharper than that found for Wyoming montmorillonite where the broad rpendicular band is centered at a lower frequency (1080 cm^{-1} compared with 1102 $^{-1}$). With these fine-grained materials, the particle size effect found in dickite and crite can not affect the results, so that the frequency shifts and band broadening und must be ascribed to irregularity in the structure or to ionic substitution in the ttice.

A striking feature of the results obtained is that the frequency of the perpendicular ode in pyrophyllite, at 1052 cm^{-1}, is so much lower than that found in the kaolin inerals, near 1109 cm^{-1}. This difference can not be related to the fact that pyro-yllite is triphormic whereas the kaolins are diphormic, since montmorillonite is so triphormic, but has an absorption pattern in this region close to that in the olins. It must be concluded, therefore, that the octahedral layers in pyrophyllite have significantly different geometry from those in montmorillonite and the kaolins. the vibration giving rise to this absorption involves the oxygen shared between trahedral and octahedral layers, its frequency might reasonably be expected to be fluenced by the nature of the cations in the octahedral layer. In fact it is found that rtial substitution of magnesium for aluminium, as in montmorillonite, and complete placement of aluminium by ferric, ferrous and magnesium ions as in celadonite uses little change in this frequency from that found in the kaolin minerals. In idolite, which approaches a trioctahedral composition with nearly one aluminium d two lithium ions per unit cell, the perpendicular band at 1129 cm^{-1} is only about cm^{-1} higher in frequency than that of the kaolins but very much higher than that und in the true trioctahedral minerals, talc, saponite, and hectorite (1073 to 1045 $^{-1}$ [5]). On the other hand, nontronite, in which the octahedral sites are occupied incipally by ferric ions, have a very low-frequency perpendicular mode lying at 34 cm^{-1}. It cannot yet be decided whether this low frequency is an effect of the $^{3+}$—O bond forces, or due to some variation of the bond geometry in nontronite. is effect of Fe^{3+} substitution may contribute to the greater diffuseness and lower equency of the perpendicular mode in Wyoming montmorillonite compared with e Swedish montmorillonite, as the former has a significant Fe^{3+} substitution in its tahedral layer.

Of the in-plane vibrations, the two strongest (not resolved in celadonite) can be cribed to the vibrations b_1^1 and b_2^2 (Fig. 6). These form a degenerate pair in the ore symmetrical talc structure, absorbing at 1018 cm^{-1}. The mean frequency of the o bands in the kaolin minerals and the montmorillonites lies close to this frequency the range 1037 to 1018 cm^{-1}, but that of pyrophyllite lies at a much higher fre-ency (mean 1061 cm^{-1}), again suggesting that this mineral differs significantly in

structure from the others. This absorption lies at much lower frequencies in lepidolite (981 cm^{-1}) and celadonite (972 cm^{-1}). A detailed structural analysis of celadonite, based on electron diffraction, has been made by ZVIAGIN [14], but a study of the structure has not yielded a satisfactory reason for its lower frequency. Although both celadonite and lepidolite are micas and so have their interlayer sites fully occupied by potassium ions, this difference from the other minerals examined can not account for their different absorption, since the dioctahedral micas muscovite and phengite both absorb above 1000 cm^{-1} [3], as do lepidolites of lower lithium and higher aluminium contents [6].

The third, higher-frequency, in-plane vibration in this region occurs within the relatively narrow range 1121 to 1100 cm^{-1} in most of the minerals examined. The lowest frequency is given by celadonite where it falls to 1075 cm^{-1}. Like the perpendicular mode, the sharpness and definition of this absorption is very dependent on the degree of order of the structure. In halloysite, synthetic kaolins and synthetic pyrophyllite [3] it is less well-defined than in the more highly crystalline natural minerals examined here, and it is rather ill-defined in beidellite and nontronite, which have higher Al-for-Si substitution than the other minerals. This absorption band has no counterpart in the talc spectrum and must arise from a vibration which is infra-red inactive in that more symmetrical structure. Partial substitution of aluminium for silicon in the tetrahedral layer of the talc structure, as in saponite, does lower the symmetry sufficiently to allow this vibration to appear as a broad shoulder near 1100 cm^{-1} on the high-freqency side of the main Si—O absorption band [5]. This absorption is further enhanced in anhydrous saponite, particularly when magnesium saturated, owing to the disturbing effect of the interlayer ions on the vibration of the silicate sheet. The vibrations b_2^1 and b_2^3 in Fig. 6 or some linear combination of these are the only candidates likely to account for this absorption. SAKSENA's calculations [26] of the vibration frequencies of an Si_2O_5 sheet with hexagonal symmetry, as in talc, do not yield any inactive vibration at such a high frequency. His calculations, however, were based on a simple pattern of force constants which did not take into account interactions between non-bonded atoms, nor the possibly large effects of dipole-dipole interactions on frequencies. A qualitative consideration of nearest-neighbour dipole coupling indicates that the inactive b_2^3 mode would lie at a lower frequency than the related active mode a_1^1, suggesting that it is not an important contributor to this vibration. On the other hand, oxygen–oxygen repulsion forces and dipole-dipole coupling will tend to raise the frequency of the b_2^1 mode, and this absorption band is so assigned.

The frequency of the 1100 cm^{-1} band shows some tendency to follow shifts in frequency of the main infra-red active Si—O in-plane vibrations, but the correlation is not exact, and it has not been possible to correlate these frequency shifts with the limited information available on the geometry of these structures.

Vibrations in the 960–550 cm^{-1} region

In the region below 960 cm^{-1}, vibrations involving the hydroxyl groups and the octahedral cations must be considered as well as those of the silicon–oxygen framework in assigning the absorption bands. Comparison of the spectra of normal kaolinite and nontronite with synthetic materials containing deuterium in place of

drogen has established that the bands near 935 and 914 cm^{-1} in the kaolin minerals, l those at 848 and 819 cm^{-1} in nontronite arise from OH bending vibrations [4]. analogy the same assignment can be given to absorption bands at 950 cm^{-1} in rophyllite, 942 cm^{-1} in beidellite, 915 to 920 cm^{-1} in the montmorillonites, 916 $^{-1}$ in rectorite and possibly 800 cm^{-1} in the ferric celadonite. Lepidolite, in which F es the place of OH, has no corresponding absorption. It is noteworthy that here ain, as in the 1150–960 cm^{-1} region, pyrophyllite is sharply distinguished from the olin and montmorillonite minerals by its higher OH bending frequency. The sorption at 870 cm^{-1} in the Wyoming and Woburn montmorillonite has been ribed to the bending frequency of an OH group shared between Fe^{3+} and Al^{3+} ions the layers of these minerals [8]. This band is absent in the Skyrvedalen montmo-onite, weak in the Wyoming montmorillonite and highest in the Woburn, that is, order of increasing iron content. A correlation between the presence of this sorption band and ferric ion in the octahedral layer is also indicated by spectra own by GRIM and KULBICKI [29]. New evidence has been obtained that this sorption band is associated with ferric ions, as it was been found that it is reduced intensity or eliminated under reducing conditions. This has been achieved by ating Wyoming and Woburn montmorillonite *in vacuo* to 350°, when the reduction effected by the small amounts of organic matter associated with these minerals; e absorption band is unaffected by heating in air to this temperature. Reduction s also been affected by heating hydrazine-saturated samples, in KBr disks in the nge 100°–200°C. Under the latter conditions, the OH bending absorption at 848 $^{-1}$ in nontronite is also eliminated, while the principal band at 819 cm^{-1} is scarcely fected. This indicates that the hydroxyl groups absorbing at 848 cm^{-1} are linked ferric ions which are more readily reduced. Possibly the 848 cm^{-1} band in non-onite like that at 870 cm^{-1} in montmorillonites, arises from hydroxyl groups ared between Fe^{3+} and Al^{3+} ions in the octahedral layer. A bending frequency of droxyl groups shared between Al^{3+} and Mg^{2+} might be expected in the spectra of e montmorillonites, and the band at 850 cm^{-1} may have this assignment, although is also possible that a vibration similar to those in the kaolin minerals near 800 $^{-1}$, or those in pyrophyllite between 854 and 815 cm^{-1} contributes to the 850 cm^{-1} nd of the montmorillonites. The examination of a deuterated montmorillonite ould be necessary to resolve this problem.

As the hydroxyl groups in dioctahedral minerals lie at a small angle to the plane the layers, it might be expected that, in addition to the bending frequencies scussed above whose polarization is in, or nearly in, the plane of the layers, a cond bending frequency with polarization nearly perpendicular to the plane of the eets would appear in the spectra. However, the spectra of normal and deuterated ontronite and kaolinite [4] give no indication of such a band, which would be reduced frequency by a factor of about 1·3 on going from the hydroxyl-containing to the euteroxyl-containing form. Two bands in the kaolinite spectrum do under maller displacements: a weak band showing in-plane polarization at 797 cm^{-1} -kaolinite is displaced to 807 cm^{-1} in *D*-kaolinite, and a medium strength perpe-icular band at 701 cm^{-1} is displaced to 688 cm^{-1}. The displacement of the latter band

9] R. E. GRIM and G. KULBICKI, *Am. Mineralogist* 46, 1329 (1961).

by a frequency factor of 1·02 is close to that expected for a vibration involving the hydroxyl and deuteroxyl groups moving as a whole, for which a factor of 1·028 would be expected. Two bands showing similar displacements on deuteration appear in this region of the spectrum of gibbsite [30], so that the 701 cm^{-1} band of kaolinite and the corresponding bands of dickite and nacrite can with some confidence be ascribed to a vibration in which the gibbsite-like layers of hydroxyl groups in these minerals move in phase, in a direction perpendicular or nearly so to the layers.

Perpendicular vibrations of the octahedral Al^{3+} ions, and of the hydroxyl groups on the side of the tetrahedral layer, would be expected to couple with such a vibration of the gibbsite-like layer, and it is possible that this is the origin of the perpendicular mode at 757 cm^{-1} in the kaolin minerals. If so, it would be expected to undergo some displacement on deuteration, but unfortunately it is not possible to determine its position with sufficient accuracy in the deuterated form, as it is partially obscured by the overlying deuteroxyl bending frequency. The displacement of the weak in-plane vibration at 797 cm^{-1} in *H*-kaolinite to higher frequencies in *D*-kaolinite indicates that this vibration is coupled with the hydroxyl and deuteroxyl bending vibrations possibly it is an out-of-phase vibration of the hydroxyl groups of the gibbsite layer.

Most of the other dioctahedral minerals examined have an absorption band showing marked perpendicular polarization in the 700 to 550 cm^{-1} region: the montmorillonites near 625 cm^{-1}, celadonite at 681 cm^{-1}, nontronite at 680 cm^{-1}, with another at 587 cm^{-1}, pyrophyllite at 578 cm^{-1}, beidellite at 566 cm^{-1} and 622 cm^{-1} and lepidolite at 583 cm^{-1}. In addition lepidolite and the Woburn montmorillonite have perpendicular modes at 790 cm^{-1}, and pyrophyllite has an absorption at 854 cm^{-1} which is slightly weaker in the spectra of oriented films. There are a number of possibilities for the assignment of these bands. Following from the discussion of the 700 cm^{-1} band in the kaolin minerals, they could be ascribed to a vibration of the hydroxyl groups perpendicular to the plane of the layers, or to a vibration of the octahedral ions where these are light (i.e. Al, Mg, or Li). The corresponding band in the trioctahedral layer silicates, talc, saponite and hectorite, occurs near 535 cm^{-1} [5]. Alternatively they may involve vibrations of the tetrahedral layer: the corresponding band in the trioctahedral minerals (a_1^2 in Fig. 6) occurs near 690 cm^{-1}. The persistence of the 677 cm^{-1} band of nontronite after dehydroxylation suggests that it is an Si—O vibration of this type [31]. In the other minerals, the study of synthetic deuterated samples may assist in distinguishing the possibilities.

Talc and its analogues have a well-defined in-plane absorption near 670–650 cm^{-1} (Fig. 16), arising from the degenerate pair b_2^4 and b_1^2 (Fig. 6). In the dioctahedral minerals this degenerate pair may be split to give two separate but weaker absorption bands. In those spectra which give sharp absorption bands, possible assignments are the bands at 836 and 854 cm^{-1} in pyrophyllite, the bands near 800 cm^{-1} in the kaolin minerals, and the bands at 746 and 845 cm^{-1} in celadonite. The displacement to higher frequencies in these dioctahedral minerals compared with the trioctahedral minerals may be due to the greater compression of the silicate layer in the dioctahedral minerals. There are, of course, several other possible assignments for these absorption bands among modes listed in Fig. 6 which are inactive in talc.

[30] V. A. KOLESOVA and Ya. I. RYSKIN, *Opt. i Spektroskopiya* **7**, 261 (1959). Engl. Transl. p. 161.
[31] J. M. SERRATOSA, *Am. Mineralogist* **45**, 1101 (1960).

brations in the 550–400 cm^{-1} region

The strong absorption in the region below 550 cm^{-1} must arise principally from plane vibrations of the octahedral ions and their adjacent oxygen layers. These brations couple to give modes which can equally well be described as metal–ygen stretching or silicon–oxygen bending. Pyrophyllite, which gives the most arply defined absorption bands of all the minerals examined here, has five bands in e region 550 to 400 cm^{-1} (Fig. 9) and two additional bands at 335 and 360 cm^{-1} in e region 400–270 cm^{-1} (TARTE, private communication). This is in good agreement th theory which predicts eight infra-red active low-frequency vibrations composed linear combinations of the four Si—O bending vibrations a_1^5, b_1^4, a_2^3 and b_2^5 in Fig. two in-plane vibrations of the hydroxyl ions, and two mutually perpendicular plane vibrations of the layer of octahedral aluminium ions. The two strongest sorption bands, at 541 and 483 cm^{-1} in pyrophyllite, must arise from mutually rpendicular vibrations, in which the oxygen sheets move in opposition to the tahedral cations. These two strong bands are also striking features of the other inerals containing principally octahedral aluminium, and polarization studies by EDDER and MCDONALD [16] on muscovite indicate that the higher-frequency bration is of symmetry species A', the lower A''. In the kaolin minerals, the bbsite-like layer of hydroxyl groups is also involved in these vibrations, and this is flected in a small displacement (about 5 cm^{-1}) of these absorption bands to lower equency in the synthetic *D*-kaolinite examined.

STUBIČAN and ROY [4] have ascribed the shift of these absorption bands to wer frequencies in nontronite to the increase in ionic radius rather than in mass of e octahedral cation. Further support for this is given by the spectrum of the rric celadonite which contains, in addition to ferric ions, large magnesium and rrous ions in its octahedral sites and whose absorption bands in this region are close frequency to nontronite.

Nontronite and celadonite have strong absorption at 450–430 cm^{-1}; the Woburn ontmorillonite also has much stronger absorption at 430 cm^{-1} than the Skyrvedalen nd Wyoming montmorillonite, and this is no doubt associated with the higher roportion of ferric ions in its octahedral sites.

It is noteworthy that the absorption of lepidolite in this region is similar to pyro-hyllite, although its octahedral composition is very different. Its octahedral sites are most completely filled by one Al and two Li ions; nevertheless its infra-red absorp-on pattern clearly places it in the dioctahedral family, and is quite distinct from that f the trioctahedral minerals. The higher effective symmetry of the latter leaves the i—O bending modes a_1^5 and a_2^3 (Fig. 6) inactive in the infra-red, while the active odes b_1^4 and b_2^5 are nearly degenerate, and couple with the octahedral cations to ive two strong closely spaced absorption bands near 460 cm^{-1} [5]. The lower ymmetry of lepidolite presumably arises from the marked difference in valency etween its octahedral cations, Al^{3+} and Li^+, although it is remarkable that the bsorption pattern in the 550–400 cm^{-1} region apparently remains stable throughout he whole range of Li contents between muscovite and the high-lithium epidolites [6].

Substitution of Al^{3+} for Si^{4+} in the tetrahedral layer, even up to the one-in-two ubstitution of margarite (Fig. 15) does not greatly shift the absorption bands in

this region, and it must be concluded that the pattern of absorption is largely determined by the nature and distribution of the octahedral cations.

Effects of aluminium-for-silicon substitution

Although substitution of aluminium for silicon has been restricted to one in eight in the minerals just discussed, its effect has been pronounced, particularly on the perpendicular and in-plane Si—O frequencies in the 1150—950 cm^{-1} region, which are much more poorly defined in nontronite and beidellite than in the other minerals with lower substitution. These bands are very broad in muscovite and phlogopite.

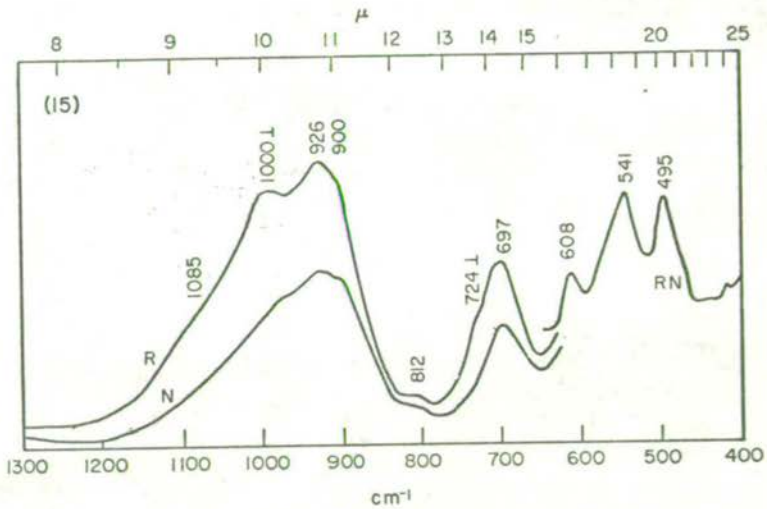

Fig. 15. Infra-red spectrum of margarite.

Similar changes in these absorption bands with increasing Al-for-Si substitution occur in the spectra of lepidolites published by LYON [6] and LYON and TUDDENHAM [32] and these workers have noted similarities in spectra between dioctahedral and trioctahedral layer silicates having similar proportions of Al-for-Si substitution. They note, however, that this similarity does not persist at very low Al contents comparing, for example, talc and pyrophyllite, and the similarity also appears to break down at high Al-for-Si substitution (one in two) where margarite (Fig. 15) shows a displacement of its main Si—O stretching absorption to near 920 cm^{-1} while amesite and aluminium biotite still absorb close to 1000 cm^{-1} [3]. This difference perhaps arises from the very different degrees by which the tetrahedra of these two species are rotated away from the orientation required by hexagonal symmetry: about 21° in margarite, as computed by RADOSLOVICH and NORRISH [33], and only 11·5° in amesite [34]. It is noteworthy, too, that the high-frequency perpendicular Si—O stretching mode is much lower in margarite, at 1000 cm^{-1}, than in the minerals with low aluminium-for-silicon substitution, where it lies near 110

[32] R. J. P. LYON and W. M. TUDDENHAM, *Nature* **185**, 374 (1960).
[33] E. W. RADOSLOVICH and K. NORRISH, *Am. Mineralogist* **47**, 599 (1962).
[34] H. STEINFINCK and G. BRUNTON, *Acta Cryst.* **9**, 487 (1956).

^{1}. It is uncertain to what extent this is due to changes in dipole coupling between Si—O vibrations involved (a_1^1, Fig. 6) or to mechanical coupling between this le and Si—O—Al vibrations of the tetrahedral layer. STUBIČAN and ROY [3] e noted that increasing Al-for-Si substitution gives rise to increased strength of

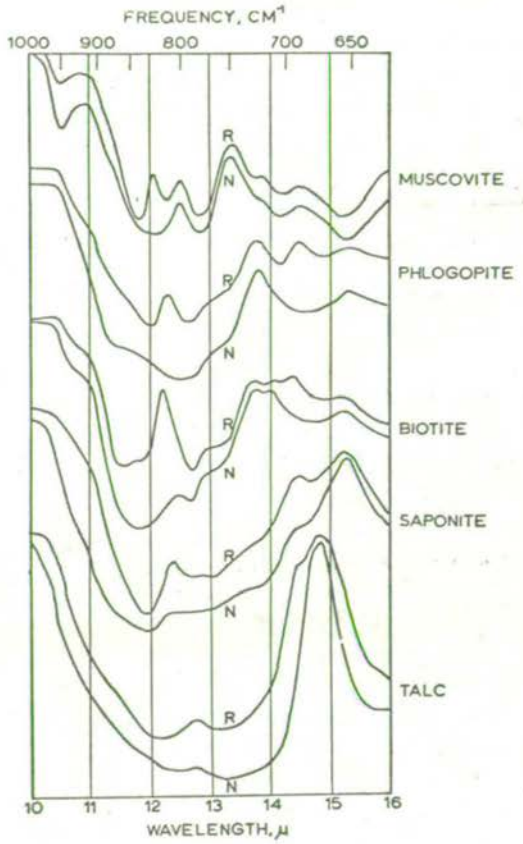

Fig. 16. Infra-red spectra of random specimens and oriented deposits of talc and saponite, and of single crystal flakes of a colourless phlogopite, a green biotite and muscovite, at normal (N) and 45° incidence (R).

sorption in the 600 to 900 cm^{-1} region. Examination of oriented specimens of ponite, phlogopite and muscovite (Fig. 16), and of beidellite (Fig. 13) shows that e absorption band in the 850–800 cm^{-1} region has perpendicular polarization, and esumably involves the a_1^1 mode of AlO_4 tetrahedra. Other absorption bands hich appear to be correlated with tetrahedral aluminium lie at lower frequencies, ar 750 cm^{-1}, and show in-plane polarization. They must arise from Al—O—Si nds. These absorption bands are shifted to lower frequencies in margarite (Fig. 15) hen the perpendicular mode is just detectable at 724 cm^{-1}, on the side of the in-ane absorption at 697 cm^{-1}. In the trioctahedral minerals amesite and aluminium otite, this complex of absorption falls in the 700–600 cm^{-1} region [3].

The spectra of allevardites and rectorites, now known to be the same species [9],

are of interest as half the silicon–oxygen sheets in these minerals are considered to be close in composition to muscovite, and the remainder to montmorillonite having little or no Al-for-Si substitution. The rectorite spectrum (Fig. 14) provides support for this structure, in that the relatively sharp in-plane vibrations at 1121, 1048 and 1020 cm^{-1}, and the perpendicular mode at 1083 cm^{-1} must arise from a network with little Al-for-Si substitution, while the broad absorption around 990 cm^{-1}, the perpendicular mode at 822 cm^{-1} and the in-plane complex of absorption bands around 731 cm^{-1} all point to a moderate degree of Al-for-Si substitution. The absorption pattern is distinctive, and cannot be confused with a simple mixture of muscovite or paragonite with pyrophyllite or montmorillonite. Identical patterns of absorption have been obtained for allevardites from Dagestan, Baluchistan and the type locality, while rectorite from the type locality gives an essentially similar spectrum, differing only slightly in the sharpness and relative intensity of its absorption bands. These observations provide support for the proposal that rectorite and allevardite should be considered as the same species.

CONCLUSIONS

Minerals can be empirically characterized by their infra-red spectra, in the same way as they can by either X-ray diffraction patterns. These methods are often complementary, rather than alternative. Infra-red spectra are of particular value in placing a mineral in its proper position in an isomorphous series without recourse to chemical analyses [6], and the different families of layer silicates examined here provide several examples of such series. Among the dioctahedral smectites, beidellite, nontronite and montmorillonite are readily distinguished, and the results obtained indicate that substitution of ferric ions for octahedral aluminium in montmorillonite can be detected in their spectra. The observations in the phlogopite–biotite series strongly suggest that a study of the hydroxyl absorption of further well-characterized specimens under grating resolution should show a useful correlation with composition of the octahedral layer. Infra-red spectra also serve to distinguish the different kaolin minerals, particularly by their hydroxyl absorption, and to differentiate rectorite from interstratified illite-montmorillonites, which it approaches in composition and structure.

Infra-red spectra also yield information about mineral structure: for example the presence of carbonate in silicates can be readily recognized, and structural hydroxyl groups can be distinguished from water of crystallization. LAUNER [35] noted that there is a tendency for the mean frequency of the absorption due to Si—O stretching to rise with increasing degree of polymerization of the silicon–oxygen tetrahedra. However, the range of Si—O—Si stretching frequencies found in the layer silicates, from 1060 cm^{-1} in pyrophyllite to 972 cm^{-1} in celadonite, shows that factors other than degree of polymerization are important. LAUNER's observation on the effects of degree polymerization might be taken to imply that the stretching frequencies of Si—O—Si linkages are higher than those of Si—O—R linkages, where R is a cation with octahedral or higher co-ordination. That this is not necessarily so is clear from the layer silicates examined here, in which the latter vibrations are

[35] P. J. LAUNER, *Am. Mineralogist*, **37**, 764 (1952).

except in pyrophyllite, higher in frequency than the former, and generally lie near 1100 cm^{-1}.

The infra-red spectra of organic molecules in inert solvents provide valuable information on the presence and environment of individual bonds in the molecules. Minerals, however, must be examined in the solid state, in which the frequencies of vibrations are affected not only by hydrogen bonding, but also by the more subtle influence of charge distributions in their neighbourhood, and by electrical coupling between the oscillating dipoles developed in the bond vibrations. The magnitude of dipole-dipole coupling effects is clear from studies on $NaNO_3$ and $CaCO_3$, where it was found to cause frequency shifts of the order of 100 cm^{-1} [36]. Still greater effects must occur in silicates, whose intense absorption indicates the development of large dipoles in Si—O stretching vibrations. Such effects can reasonably account for the frequency of Si—O—R vibrations being higher than those of Si—O—Si vibrations in the minerals examined here. The dependence of band shape and position on particle size reported here for certain vibrations of the kaolin minerals is also almost certainly a dipole-dipole coupling effect: similar effects must be anticipated with other minerals having strong sharp infra-red absorption bands.

The relationship between structure and spectra is clearly not a simple one, and further work is required to determine those factors which control vibrational frequencies in silicates. A better understanding of these factors must greatly increase the contribution of infra-red spectroscopy to structural studies on silicates. The present study specifies more sharply the outstanding problems to be solved. Of particular interest among these are the many points of divergence between the spectrum of pyrophyllite and those of its close relatives kaolinite and montmorillonite. A full interpretation of these differences must await a detailed X-ray investigation of the pyrophyllite structure.

Acknowledgement—We are indebted to the University of Aberdeen for the use of a Hilger H800 spectrometer for the 700–400 cm^{-1} region.

---

[36] C. Haas and J. A. A. Ketelaar, *Physica* **22**, 1286 (1956).

Clay Min. Bull. (1964), **5**, 443.

INFRA-RED SPECTROSCOPIC STUDY OF THE DEHYDRATION OF MONTMORILLONITE AND SAPONITE

J. D. RUSSELL AND V. C. FARMER

The Macaulay Institute for Soil Research, Craigiebuckler, Aberdeen

Received 7th July 1964

ABSTRACT: The more firmly held water which is directly co-ordinated to the exchangeable cations in smectites is clearly distinguished by infra-red spectroscopy from the more labile water in outer spheres of co-ordination. Li^+, Ca^{2+} and Mg^{2+} retain both types of water to higher temperatures than do K^+, Na^+ and NH_4^+, and the former group give stable monohydrates in saponite which are probably not completely decomposed till 400-600°C. K-, Li- and Na-saponite rehydrate completely after heating, but NH_4-, Mg- and Ca-saponite are irreversibly dehydrated at 600-700°C, by which temperature NH_4^+ is also decomposed. NH_4-, Li- and Mg-montmorillonite fail to rehydrate after heating to 350°C, and changes in their spectra indicate interaction between the exchangeable cations and the lattice. Decomposition of NH_4^+ gives H-montmorillonite, but the products from Li- and Mg-montmorillonite are also acidic, and give spectra similar to that of H-montmorillonite. Na- and Ca-montmorillonite do not rehydrate after heating to 500-550°C, and K-montmorillonite rehydrates only partially in the range 350-550°C. Dehydration of saponite and montmorillonite at low temperatures causes changes in lattice vibrations which are reversed on rehydration. The spectra of the products of dehydroxylation of montmorillonite and saponite are slightly affected by the exchangeable cation originally present.

INTRODUCTION

The value of X-ray diffraction studies of clay minerals is to a considerable extent dependent on a knowledge of the changes in pattern induced by controlled heat treatment, and it is certain that similar techniques will prove valuable in the infra-red study of soil clays. A recent investigation of soil clays containing amorphous material (Mitchell & Farmer, 1962) has shown the need for background information on the spectral changes associated with dehydration and dehydroxylation. This paper aims to provide such information for montmorillonite and saponite saturated with the more common exchangeable cations.

The dehydration of smectites results in a decrease in the basal spacing, which, depending on the particular exchangeable cation present and on the temperature of heating, can become irreversible (Greene-Kelly, 1953; Midgley & Gross, 1956; Rowland, Weiss & Bradley, 1956). This process may be followed in the infra-red spectrum by the changes in intensity and position of water absorption bands near 3430 cm^{-1}, due to OH stretching vibrations, and near 1640 cm^{-1}, due to a vibration involving the H-O-H bond angle. An attempt is made in this investigation to amplify previous studies by Fripiat, Chaussidon & Touillaux (1960). Loss of interlayer water also causes changes in the absorption pattern of the silicate lattice, some of which have been previously noted by Tettenhorst (1962). The significance of these is also discussed.

MATERIALS AND METHODS

The minerals examined were the $< 1{\cdot}2\ \mu$ fraction of Wyoming montmorillonite (*Wilkinite*, from Messrs Bush, Beach and Gent Ltd., Lloyds Avenue, London) and saponite from Allt Ribhein, Skye (Mackenzie, 1957). Na-, K-, Li-, Ca- and Mg-saturated forms of both were prepared by the usual centrifuge technique using N chloride solutions, and NH_4-saturated specimens using N acetate solution (pH 7). Cation-exchange capacities determined by standard methods were, 90 m-eq/100 g for montmorillonite and 124 m-eq/100 g for saponite, on a water-free basis. Samples were moistened with water, ground in a vibratory grinder and allowed to sediment from the aqueous suspensions on to aluminium foil supported on a flat surface. The suspensions were evaporated to dryness overnight and the resulting oriented aggregates were readily peeled from the foil. These aggregates had a surface weight of 1-4 mg/cm^2, were of uniform thickness, and generally did not scatter infra-red radiation. They were examined in an evacuable cell placed in the sample beam of a Grubb Parsons S4 double-beam infra-red spectrometer equipped with a sodium chloride prism covering the range 4000-625 cm^{-1}, and with a 2500 lines per inch diffraction grating giving higher resolution in the 4000-2000 cm^{-1} region (Goulden, 1952). The cell was fitted with sodium chloride windows and a heating coil capable of attaining 350°C. On evacuation, pressures of about 2×10^{-2}mm Hg were achieved with a rotary pump. The films were further heated in an electric furnace in the range 350-900°C. No precaution was taken against rehydration of furnace-heated specimens. The saponites rehydrated very rapidly, but the montmorillonites sufficiently slowly to enable spectra of the anhydrous forms to be obtained by immediately evacuating the furnace-heated samples. Samples were heated for 1 hr at each temperature. For temperatures above 100°C radiation from

the sample became troublesome. It was obviated by heating films under vacuum then cooling to room temperature under vacuum before recording the spectra. Evacuation to 2×10^{-2}mm Hg at temperatures above 100°C causes only a slight decrease in the amount of water retained compared with heating at normal pressure. After heating, the specimens were allowed to rehydrate by exposing them to about 35% relative humidity for 18 hr.

Very thin aggregates (0·1-0·2 mg/cm^2) on AgCl sheets and IRTRAN windows were used to investigate the intense silicate absorption bands near 1000 cm^{-1}. Films were investigated at high relative humidities in a cell fitted with AgCl windows and a detachable well for saturated salt solutions. Thermogravimetric curves (heating rate 4°C/min) and equilibrium weight-loss measurements were obtained on a Stanton TR-01 thermobalance.

RESULTS AND DISCUSSION

Rehydration behaviour following heating

The amount of rehydration after heating smectites to various temperatures for 1 hr was followed by measuring the water absorption at 1640 cm^{-1} (Fig. 1). For the dioctahedral montmorillonite studied here

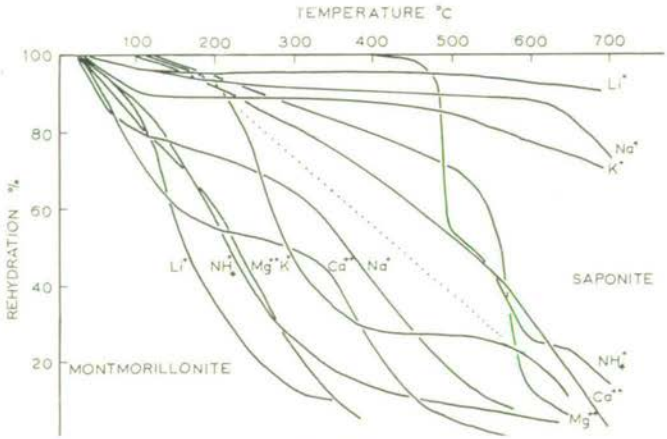

FIG. 1. Percentage recovery of the 1640 cm^{-1} water absorption band in montmorillonite and saponite on exposure to room humidity for 18 hr.

dehydration becomes irreversible at 350°C when the exchange cations are Li^+, Mg^{2+} and NH_4^+. Rehydration of the K-, Na- and Ca-forms decreases gradually with rising temperature to very low values just before dehydroxylation at about 550-600°C. The K-form shows an

almost constant level of rehydration of about 28% over the temperature range 350-550°C. It is uncertain whether this is due to some of the layers continuing to rehydrate fully, or to some water penetrating between layers even in the collapsed state due to the larger layer separation imposed by K^+. The irreversible collapse of Li- and Mg-montmorillonite is generally held to be the result of migration of these cations away from exchange sites into the silicate structure, thus allowing the close approach of adjacent silicate layers. The destination of the migrating cation is claimed by Greene-Kelly (1953) to be vacant sites in the octahedral layer, but from infra-red results Tettenhorst (1962) concludes that suitable ions migrate only into the hexagonal holes in the silicon-oxygen network and do not penetrate further in the temperature

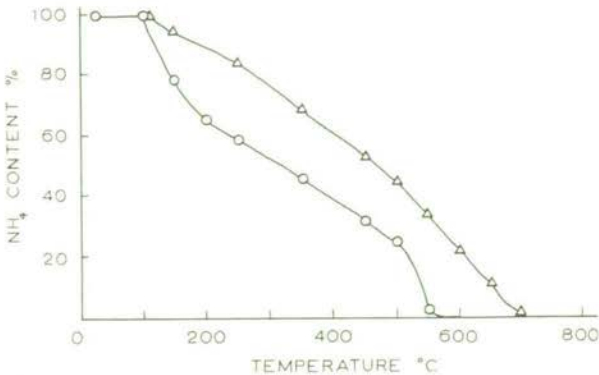

FIG. 2. Percentage NH_4^+ remaining in montmorillonite (O), and saponite (△), after heating to various temperatures, as estimated from the optical density of the NH_4^+ absorption at 1440 cm^{-1}.

range up to 300°C covered in his work. That NH_4-montmorillonite collapses irreversibly after heating to 350°C presumably results from migration of protons from thermal decomposition of NH_4^+ (Cook, 1935; Chaminade, 1962). However, at 350°C just less than half of the original NH_4^+ content still remains (based on the optical density of the infra-red absorption band of NH_4^+ at about 1440 cm^{-1}, Fig. 2). Possibly the interlayer space becomes sealed at the particle edges where decomposition of NH_4^+ has occurred, thereby preventing the re-entry of water into the interlayer space. Fig. 1 also shows that the behaviour of the saponite samples differs from that of the montmorillonite samples. The reversibility of the dehydration of the K-, Li- and Na-saponite bears out the findings of Greene-Kelly, namely that no migration of Li^+ into a trioctahedral lattice occurs, and indicates that this is also true for the larger monovalent cations. Midgley & Gross (1956) found that a

Ca-saturated saponite failed to rehydrate after heating to 650°C. This behaviour was confirmed for Ca-saponite and was also observed for NH_4- and Mg-saponite. Disregarding NH_4^+, which is a special case, it would appear that the valency of the exchange cation, and not its radius, is the factor which determines whether the lattice will collapse irreversibly. In NH_4-saponite, the exchangeable cations are completely decomposed at about 700°C (compare 500-550°C for NH_4-montmorillonite, Fig. 2) but while the protons formed in montmorillonite are accessible, those in NH_4-saponite are not: after exposing the heated clays to the vapour of concentrated aqueous ammonia, the original NH_4^+ content is largely regenerated in montmorillonite, but no NH_4^+ is formed in saponite.

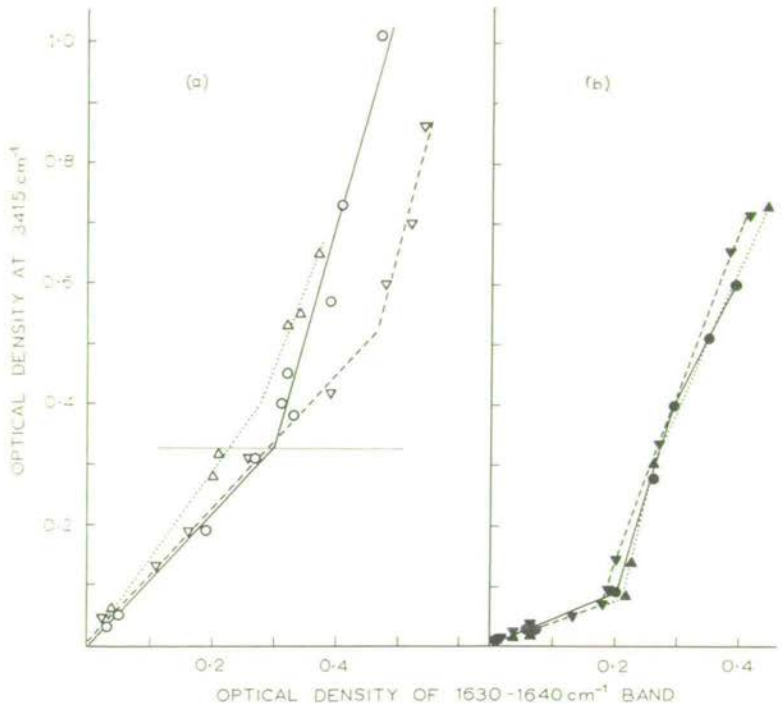

FIG. 3. Variation of the optical density at 3415 cm^{-1} with the optical density of the band maximum at 1630-1640 cm^{-1} in various hydration states of films (2 mg/cm^2) of montmorillonite saturated with different cations:
(*a*) ———, Na^+; ....., K^+; – – –, NH_4^+;
(*b*) ———, Li^+; ....., Ca^{2+}; – – –, Mg^{2+}.

Changes in water absorption bands during dehydration

The temperature range 25-250°C

During dehydration marked changes occur in the relative intensities of the absorption bands due to the OH stretching vibration and the angle deformation of water in smectites. Plots of the optical density at 3415 cm^{-1} against that of the band maximum at 1630-1640 cm^{-1}, at various stages of hydration of montmorillonite and saponite (Figs. 3 and 4) show a marked change in slope, which must correspond to a

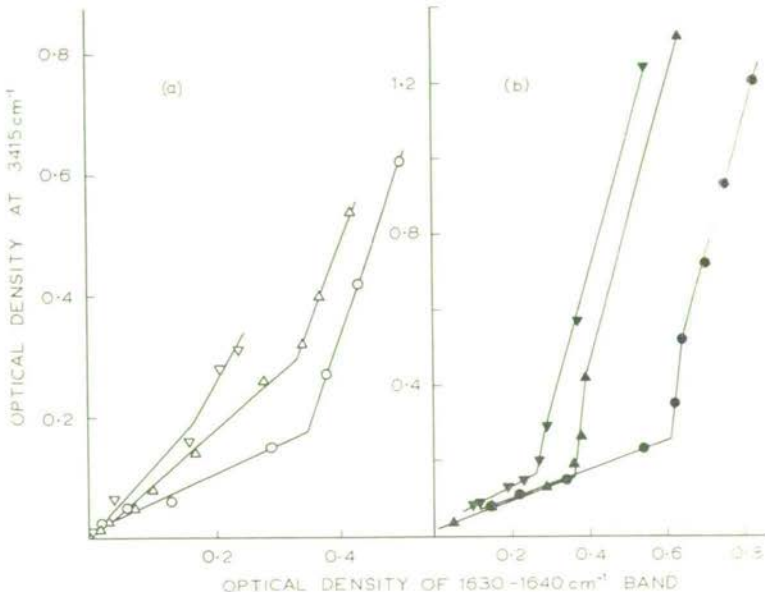

FIG. 4. Variation of the optical density at 3415 cm^{-1} with the optical density of the band maximum at 1630-1640 cm^{-1} in various hydration states of films (2 mg/cm^2) of saponite saturated with various cations:
(*a*) ○, Na^+ △, K^+; ▽, NH_4^+;
(*b*) ●, Li^+; ▲, Ca^{2+}; ▼, Mg^{2+}.

change in the environment of the interlayer water molecules on going from higher to lower hydration states. The curves fall into two types depending on the exchangeable cation present. With Li^+, Mg^{2+} and Ca^{2+} the change in slope occurs near 100°C, but with Na^+, K^+ and NH_4^+, the change occurs at lower temperatures (Figs. 3 and 4, Table 1). For montmorillonite saturated with these larger monovalent ions, a change in slope is only observed above room humidity (about 35%), corresponding to the parts of the curves above the horizontal line in

TABLE 1. Temperatures (in °C) corresponding to complete loss of strongly hydrogen-bonded water from montmorillonite and saponite saturated with various cations. 30-35% Relative humidity (R.H.) was employed except where indicated.

Ion	Montmorillonite	Saponite
Na^+	25; 30% R.H.	45
K^+	25; 30% R.H.	35
NH_4^+	25; 60% R.H.	37
Li^+	100	90
Ca^{2+}	100	105
Mg^{2+}	110	115

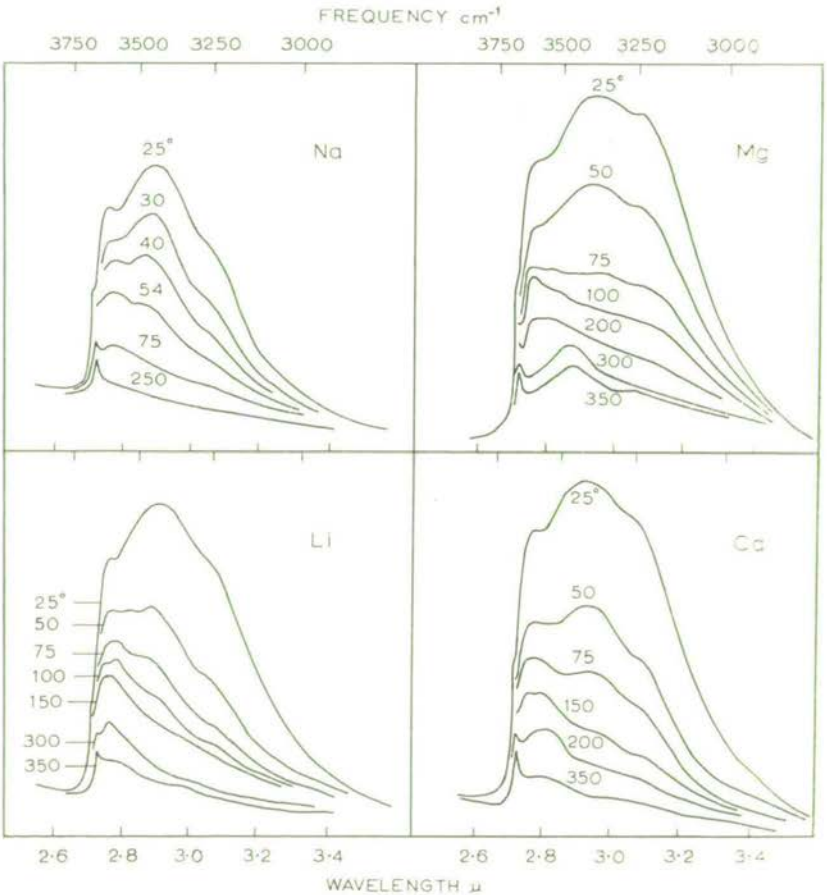

FIG. 5. OH stretching absorption of water in saponite films heated to the indicated temperatures. Film weights: Na^+, 1·6 mg/cm²; Mg^{2+}, 1·8 mg/cm²; Li^+, 1·2 mg/cm²; Ca^{2+}, 1·7 mg/cm².

Fig. 3*a*. The saponite samples were all more highly hydrated than the corresponding montmorillonite samples, owing, probably, to their higher content of exchangeable cations.

The marked changes in slope shown in Figs. 3 and 4 can be correlated with concurrent changes in the appearance of the band due to the OH stretching vibration of water. Thus with Mg-saponite, the water which is more readily lost, corresponding to the steep part of the curve in Fig. 4*b*, is characterized by a broad, strong, OH stretching absorption band with a maximum near 3415 cm^{-1} (Fig. 5) and a much weaker H-O-H bending absorption at 1640 cm^{-1}. These features are similar to those shown by liquid water, so that they can reasonably be ascribed to water molecules involved in hydrogen bonding with other water molecules in the interlayer space. The water which is less readily lost, corresponding to the region of lower slope in Fig. 4*b*, has a maximum at 3610 cm^{-1}, the high frequency indicating the presence of weakly hydrogen-bonded hydroxyl groups. It is close to the highest frequency which has been reported for water in crystalline hydrates (3630 cm^{-1}, by Corbridge & Lowe, 1954). A more unusual feature is its strong H-O-H bending absorption band whose frequency, at 1630 cm^{-1}, is slightly lower than that of the more labile water. This band is stronger than that at 3610 cm^{-1}, a feature which has not been reported for any salt hydrate. It is most closely approached in the absorption of $NaClO_4.H_2O$ and $Mg(ClO_4)_2.6H_2O$, in which absorption at 1630 cm^{-1} is nine-tenths of that at 3560 cm^{-1}. In these salts the water of hydration is co-ordinated to the cation and can form only weak hydrogen bonds with the large anion. It seems likely that a similar situation exists in Mg-saponite, i.e. that the region of low slope in Fig. 4*b* corresponds to water molecules co-ordinated round cations in the interlayer space. Similar results to those described above were obtained with Li- and Ca-saponite, and with the corresponding montmorillonites, although with the latter the changes in the 3600 cm^{-1} region could not be followed owing to overlapping lattice OH absorption: this absorption does not interfere in saponite, where it is a weak band at 3670 cm^{-1}. During dehydration Mg- and Ca-montmorillonite developed a distinctive band near 3500 cm^{-1}, but this was not due to residual water, and will be discussed later.

The high intensity ratio of the 1630 cm^{-1} band to the 3600 cm^{-1} band shown by the more firmly held water in these smectites is due to an enhancement of the 1630 cm^{-1} band for this co-ordinated water. After heating to 100°C the water content of Li-montmorillonite determined from weight-loss curves is reduced to about one-sixth of the original value while the intensity of the 1630-1640 cm^{-1} water absorption band

is only halved. At temperatures immediately below those corresponding to the change in slope in Figs. 3*b* and 4*b*, there is a range in which the intensity of the 1640 cm^{-1} band changes little in Li-, Mg- and Ca-smectites. This gives a marked step in the curves showing the variation of the 1630-1640 cm^{-1} band with temperature (Fig. 6). As equilibrium

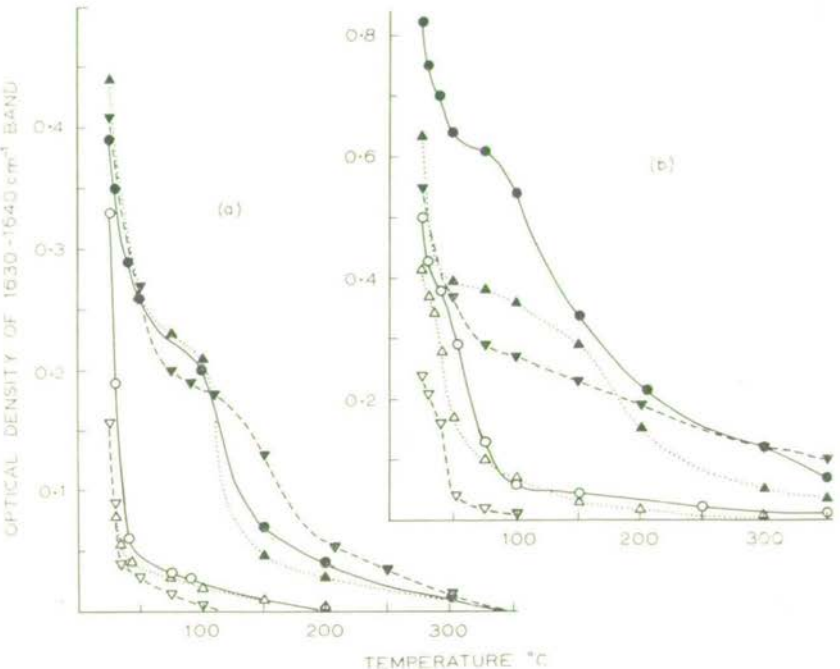

FIG. 6. Variation in the optical density of the 1630-1640 cm^{-1} water absorption band with temperature in (*a*) montmorillonite and (*b*) saponite saturated with the cations:

○, Na^+; △, K^+; ▽, NH_4^+; ●, Li^+; ▲, Ca^{2+}; ▼, Mg^{2+}.

thermogravimetric curves for Li- and Mg-montmorillonite do not show a corresponding step in the water content, this feature must correspond to a region in which the molecular infra-red absorption of the residual water at 1630 cm^{-1} increases. It is uncertain whether this is due to an increasing polarizing effect of the cation as the number of water molecules co-ordinated to it falls, or to the change in environment of the water molecules directly co-ordinated to the cation as water in the outer spheres of co-ordination, to which they are hydrogen bonded, is lost. This effect is also perceptible in the curve for Li- and Ca-smectites in Figs. 3*b* and 4*b* where it gives rise to a very steep part just before the

region of low slope: in this temperature range absorption at 3415 cm^{-1} drops markedly while absorption at 1630-1640 cm^{-1} changes little. This feature is not so marked in the curves for Mg-smectites.

Changes in the layer spacing of smectites with temperature have been examined in some detail (Rowland *et al.*, 1956; Midgley & Gross, 1956) and can be correlated with the infra-red results. Mg- and Ca-smectites have double layers of water molecules in the interlayer space giving 001 spacings of 14-15 Å at room temperature and humidity. They contract to a phase containing single layers of water molecules with a spacing of 11·5-12 Å between 70 and 120°C. Loss of this single layer causes further contraction to 9-9·5 Å between 120 and 300-400°C. Li-montmorillonite, on the other hand, contains only a single water layer at room temperature with a spacing of 12 Å. The spacing slowly contracts to 11·5 Å before breaking down to that of an anhydrous phase in the range 110-400°C. It seems likely, therefore, that the break in the curves in Figs. 3*b* and 4*b* corresponds to an 11·5 Å layer spacing at a stage when all or nearly all the water not directly co-ordinated to cations has been lost. This stage is particularly well defined in vermiculite. In this mineral, an 11·6 Å phase is stable between 80 and 190°C (Rowland *et al.*, 1956). It initially contains 8 molecules of water per Mg^{2+}, but this falls to a stable 3 molecules per cation in the range 120-190°C (Walker, 1956; Walker & Cole, 1957; Keay & Wild, 1961). Thermogravimetric curves for Mg- and Ca-saponite, like that for the natural material (Mackenzie, 1957), show well-defined plateaux in the ranges 130-190°C and 110-150°C, respectively. The weight loss from the centre of these plateaux to 700°C corresponds to 3·8 water molecules per cation. It can be assumed, however, that the weight loss of Na- and K-saponite in this temperature range, amounting to 1·0% of the anhydrous clay, arises from loss of hydroxyl groups at sheet edges and at other lattice imperfections, traces of organic matter, and water adsorbed at other than cation sites, and if the results for Mg- and Ca-saponite are corrected for this, a figure of 3·0 molecules per cation is obtained, in good agreement with Ca- and Mg-vermiculite (Keay & Wild, 1961). The thermogravimetric curve for Li-saponite shows only a weak inflection at about 130°C, so that the degree of hydration of the cation could not be determined with any accuracy but must be at least 2 molecules per cation. Similar weak inflections are present in the curves for Li-, Ca- and Mg-montmorillonite samples. Equilibrium weight-loss measurements on Li- and Mg-montmorillonite show weight-losses between the temperatures at the change in slope in Fig. 3*b* and 400°C which correspond to 1·3 and 4·0 water molecules per cation respectively. Correction of these figures for traces of organic matter and water not associated with

cations gives results close to 1 molecule of water of hydration for Li^+ and 3 for Mg^{2+}. These hydration states are not stable: the water content decreases continuously with temperature rise. The low content in Li-montmorillonite is probably associated with a tendency to tetrahedral co-ordination: Li^+ could be co-ordinated to three oxygens of the silicate lattice on one side and to one water molecule on the other. The very much stronger water absorption in Li-saponite at the change in slope (Fig. 4*b*) indicates that it retains more co-ordinated water than Li-montmorillonite.

It might be anticipated that this residual co-ordinated water in Li-, Mg- and Ca-smectites would be involved in hydrogen bonding to the silicate framework, and such hydrogen-bonded OH groups are probably the origin of the broad diffuse absorption on the low frequency side of the 3610 cm^{-1} maximum. The weakness of this absorption is certainly not due to the orientation of the water molecules in the interlayer space, as this OH absorption band is not affected by tilting the clay films at an angle to the infra-red beam.

The water absorption bands in smectites saturated with Na^+, K^+ and NH_4^+ show changes during dehydration analogous to those shown by smectites saturated with Li^+ and the divalent ions. The changes in absorption pattern given by Na-saponite in the 3000-3600 cm^{-1} region (Fig. 5) are typical of this group. With these larger monovalent ions, strongly hydrogen-bonded water occurs only at much lower temperatures, but it seems likely that here again the change in slope in Figs. 3*a* and 4*a* can be correlated with the loss of interlayer water not directly co-ordinated to the exchangeable cations. Because of the weaker polarizing effect of these ions, the 1630 cm^{-1} band of co-ordinated water is not so strongly enhanced as for Li^+ and the divalent ions, and the gradient of the region of low slope is steeper. Also, the co-ordinated water is lost at lower temperatures (Fig. 6). Direct evidence for co-ordination of water molecules to the cation is given by the spectra of ammonium smectites, which show, in addition to the main NH_4^+ absorption at 3270 cm^{-1}, subsidiary bands at 3045 cm^{-1} and 2855 cm^{-1} due to hydrogen bonding of NH_4^+ to water at room temperature (Mortland *et al.*, 1963). As water is lost, these subsidiary bands weaken and merge into a diffuse residual shoulder, while the 3270 cm^{-1} band sharpens and intensifies. These changes are essentially complete by 75-100°C for NH_4-saponite, and by 50-75°C for NH_4-montmorillonite, by which time residual water is very low.

Na-montmorillonite, however, contains rather more water at room temperature (4·7 molecules per cation) than can reasonably be considered as being co-ordinated to the cation. Although it is possible

that the heating effect of the infra-red radiation is sufficient to drive off all but co-ordinated water in the infra-red studies, retention of water at other than co-ordinated sites cannot be excluded.

The temperature range 250-750°C

After heating in vacuum to 350°C, the temperature limit of the cell used in this work, no residual water absorption could be detected at 1630 cm^{-1} in the various montmorillonites, nor in Na-, K- and NH_4-saponite. Li-, Mg- and Ca-saponite, however, still retain water absorption bands at 1630 cm^{-1} and near 3500 cm^{-1}. In agreement with this, thermogravimetric curves for Na- and K-saponite show in the range 400-700°C only small weight losses of 0·5% and 0·3%, respectively, which could arise from loss of traces of organic matter and of hydroxyl groups from lattice edges and imperfections. Saponite samples saturated with Mg^{2+} and Ca^{2+} show additional weight losses over K-saponite corresponding to 1·0 and 0·8 water molecule per cation, respectively, in this temperature range, while Li-saponite shows an additional weight-loss corresponding to 0·7 water molecule per cation in the range 350-650°C. This weight loss is also shown by the natural saponite (Mackenzie, 1957) which contains 92% Ca^{2+} and 8% Mg^{2+} as exchangeable ions. Thus saponite resembles vermiculite, in which exchangeable Mg^{2+} and Ca^{2+} form monohydrates stable in the ranges 200-300°C and 160-250°C, respectively, before decomposing to anhydrous forms at 500°C (Mg^{2+}) and 400°C (Ca^{2+}) (Keay & Wild, 1961). Under the continuous heating conditions used for thermogravimetric determinations, vermiculite, like saponite, does not become anhydrous till about 650°C (Walker & Cole, 1957).

The monohydrate phase in Mg-vermiculite can be correlated with a stable spacing of 10·3 Å found in the 180-250°C temperature range (Walker & Cole, 1957). Walker (1956) has interpreted this as arising from an approximately regular interstratification of the 11·6 Å phase with an anhydrous 9·02 Å phase. Examination of the water stretching vibrations of Mg-saponite (Fig. 5) shows, however, that the environment of the water retained in the 250-350°C range is different from that in the 11·6 Å phase (the trihydrate) formed at 110°C. The 3610 cm^{-1} band of the trihydrate is lost by 250°C in air, and by 200°C in vacuum, leaving a lower frequency maximum at 3475 cm^{-1}, which must arise from water with both OH groups involved in hydrogen bonding; this absorption weakens but does not change in form between 200 and 350°C. These results are consistent either with a uniform monohydrate phase, or with a dihydrate regularly interstratified with anhydrous layers, the dihydrate decomposing to the anhydrous form without passing through an intermediate monohydrate. A uniform monohydrate is more likely, since

Fig. 1 shows that completely anhydrous layers do not rehydrate, whereas rehydration of the monohydrate amounts to 80-90% in the 250-400°C range, and only falls to 50% at about 580°C (Fig. 1). A regularly interstratified structure would be expected to give only 50% rehydration. If the structure is in fact one with monohydrated ions, its small spacing, 10·3 Å. implies that both Mg^{2+} and its associated water molecule are embedded in hexagonal holes in the silicate layer, probably on opposite sides of the interlayer space. This water molecule would permit a transfer of part of the charge from the divalent Mg^{2+} to a negative site on the opposite silicate sheet.

In Ca- and Li-saponite, residual water absorption at 350°C is weaker than in Mg-saponite, and lies at higher frequencies. In Ca-saponite, the 3610 cm^{-1} band of the trihydrate is lost by 200°C in air leaving a broader band centred on 3565 cm^{-1}, which decreases progressively in intensity to 350°C. In Li-saponite, the 3610 cm^{-1} band moves only slightly to lower frequencies, leaving by 350°C a diffuse shoulder, near 3580 cm^{-1}, on the side of the lattice OH absorption.

The persistence of the 1630 cm^{-1} band of water in these saponites shows that the high-temperature water loss is not due to decomposition of a basic ion formed by a reaction such as

$$Mg^{2+} + H_2O \rightarrow (MgOH)^{+} + H^{+}.$$

Effects of dehydration on lattice vibrations

Removal of interlayer water from smectites induces changes in their lattice vibrations. Results for the two minerals studied will be treated separately.

Montmorillonite

The changes in absorption pattern produced by evacuating Na-montmorillonite at ambient temperature (Fig. 7 and Fig. 8, *a* and *b*) are typical of those occurring with the other ionic species. It is clear that removal of water from the clay structure under very mild conditions affects certain absorption bands. The modifications of the Si-O stretching vibrations near 1047 cm^{-1} and 1120 cm^{-1} are probably caused by distortion of the silicon-oxygen framework when interlayer water is removed, as both vibrations involve the surface layer of oxygen atoms (Farmer & Russell, 1964). In a study of cation migration in a Chetotype montmorillonite, Tettenhorst (1962) did not report these spectral changes, but their occurrence has been confirmed here in a montmorillonite of this type from Skyrvedalen (Rosenqvist, 1959). OH deformation vibrations at 920 cm^{-1} and 890 cm^{-1} are also affected by dehydration, as is a band, possibly of the same origin, at 849 cm^{-1} (Farmer & Russell, 1964).

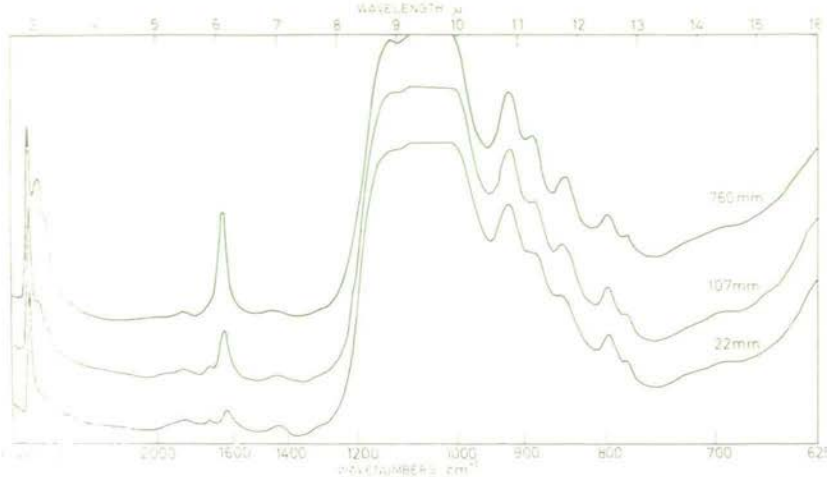

FIG. 7. Infra-red spectrum of Na-montmorillonite film at the air pressures indicated (pressures in mm Hg).

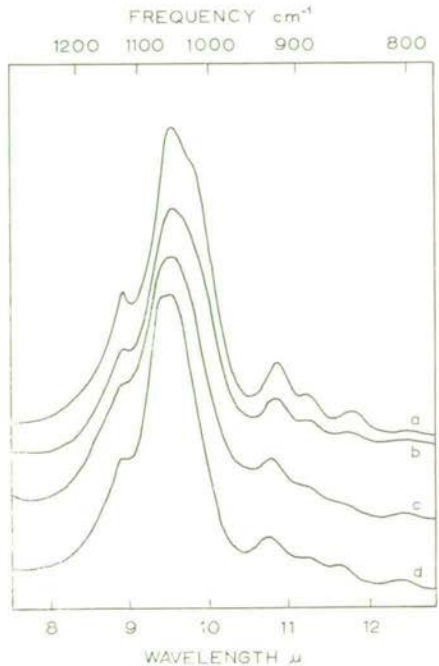

FIG. 8. Effects of denydration and heating on lattice vibrations of montmorillonite: (*a*) Na-saturated, fully hydrated film; (*b*) Na-saturated, evacuated at 25°C; (*c*) Mg-saturated, heated to 350°C; (*d*) Li-saturated, heated to 350°C.

Further major changes occur as a result of heating the various montmorillonite samples at 350-550°C. When the exchange cations are Li^+, Mg^{2+} or NH_4^+ the AlOH deformation vibration at 920 cm^{-1} decreases in intensity and shifts 15-20 cm^{-1} to higher frequency, a weak band develops near 825 cm^{-1} and there are considerable changes in the absorption pattern between 950 and 800 cm^{-1} (Fig. 9). For these ionic

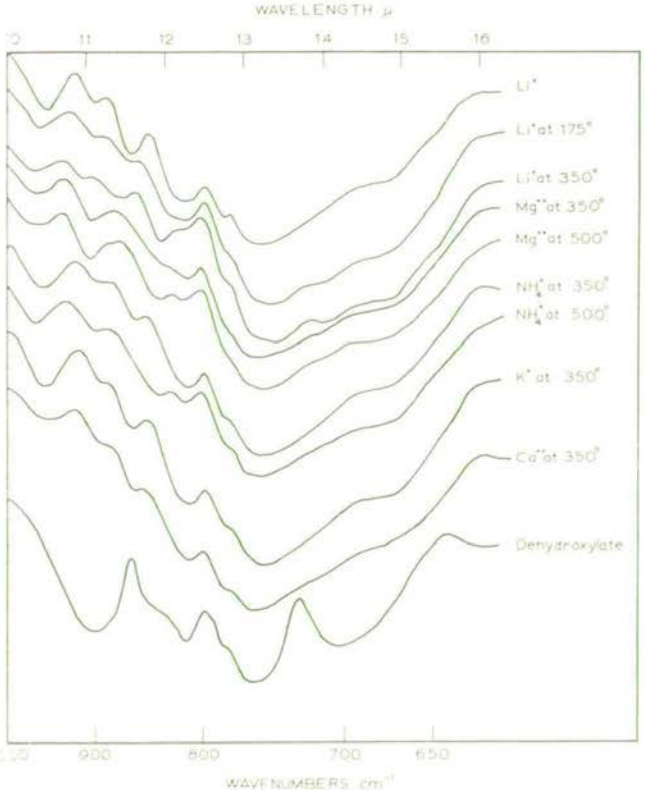

FIG. 9. Effect of heating on the lattice vibrations of montmorillonite samples saturated with the cations shown.

species, heat treatment shifts the main Si-O vibration to higher frequencies (Fig. 8, *c* and *d*), approaching those at which pyrophyllite absorbs. The 920 cm^{-1} band in Ca-montmorillonite behaves like those in the Li-, NH_4- and Mg-forms, although only shifting about 10 cm^{-1} to higher frequency, and the main Si-O band also suffers a high-frequency shift, but no other major change occurs in the pattern between 950 and 800 cm^{-1}. For K- and Na-forms no further change occurs in

this region after the initial decrease in intensities due to removal of water.

Tettenhorst (1962) has observed similar spectral changes and claims that they are consistent with the migration of cations of size up to and including Ca^{2+} into the hexagonal holes in the silicon-oxygen framework but not with their deeper penetration into the octahedral layer. In the Ca-montmorillonite studied here, the decrease in the intensity of the 920 cm^{-1} band was accompanied by the development at 150-200°C of a weak sharp band at 3533 cm^{-1} which persisted until dehydroxylation (Fig. 10). A similar though broader band was observed at 3496 cm^{-1}

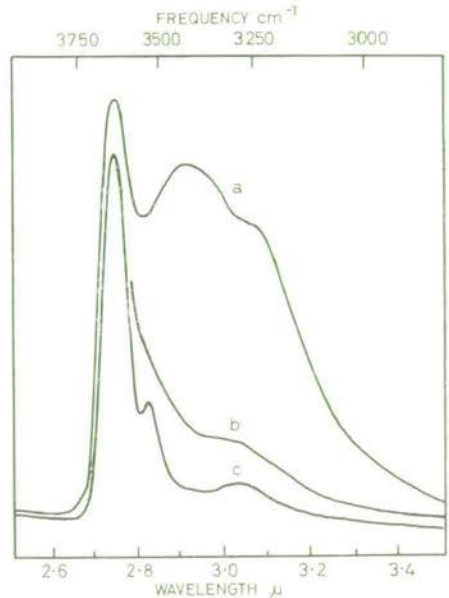

FIG. 10. Lattice OH and water absorption in Ca-montmorillonite: (*a*) fully hydrated, (*b*) evacuated at 25°C and (*c*) heated to 250°C *in vacuo*. Maximum at 3270 cm^{-1} is probably due to NH_4^+.

for the Mg-form, but was lost again at 350-400°C with the development of the features shown in Fig. 9. These bands disappear when the samples are rehydrated and probably arise from perturbed OH vibrations caused by the close approach of Ca^{2+} or Mg^{2+} to the lattice OH groups. Possibly the oxygen of the OH group forms a co-ordinate bond with the cation. The thermal stability of the band in the Ca-form results from the inability of this large ion to penetrate further into the lattice. By contrast, the disappearance of the band in Mg-montmorillonite arises when this small ion migrates into the octahedral layer.

Mortland *et al.* (1963) noted a band at 2632 cm^{-1} in a deuterated Ca-montmorillonite heated to 240°C, which probably corresponds to the 3533 cm^{-1} band found here. They assigned it to a deuteroxyl group formed by previous treatment with ammonia gas, but this assignment seems unlikely, as no corresponding band occurs in Ca-saponite.

The similar spectral features of Li-, NH_4- and Mg-montmorillonite after heating suggest that Li^+ and H^+ also migrate into the octahedral layer: no perturbed lattice OH stretching vibration was observed for these ions, presumably because of their ready penetration into the lattice. Because of its larger ionic radius, K^+ probably does not migrate into the hexagonal hole. Na^+ and Ca^{2+}, of approximately equal ionic radii, should penetrate into the silicon-oxygen network to the same extent. However the AlOH deformation vibration at 920 cm^{-1} is perturbed only for Ca^{2+}. The lower polarizing power of Na^+ would account for its failure to influence the lattice OH groups. Neither K- nor Na-montmorillonite shows the perturbed OH stretching vibration.

An interesting observation is that after heating to 500°C, Li-, NH_4- and Mg-montmorillonite when treated with ethylene glycol and N NaCl solution give acidic solutions, while the reactions of the K-, Na- and Ca-specimens under the same conditions are neutral. The presence of exchangeable protons in the heated NH_4-montmorillonite is readily understood on the basis of decomposition of NH_4^+. Their presence in heated Li- and Mg-samples must be explained by reaction between the exchange cations and either water molecules or lattice OH groups:

(*a*) $Mg^{2+} + H_2O \rightarrow (MgOH)^+ + H^+ \rightarrow MgO + 2H^+$
$Mg^{2+} + 2H_2O \rightarrow Mg(OH)_2 + 2H^+ \rightarrow MgO + 2H^+ + H_2O$

(*b*) $Li^+ + HO\ (lattice) \rightarrow LiO\ (lattice) + H^+$
$Mg^{2+} + HO\ (lattice) \rightarrow Mg^+O\ (lattice) + H^+$

In reaction (*b*) the cation may lie either in the octahedral layer or in the plane of the silicon ions directly above the oxygen. Reaction (*b*), involving a type of dehydroxylation, is supported by the appearance of weak bands near 860 cm^{-1} and 722 cm^{-1} in the heated Li-sample: fully dehydroxylated Li-montmorillonite absorbs at 865 cm^{-1} and 731cm^{-1}. The effect of reaction (*b*) on the intensity of the lattice OH stretching vibration would be expected to be small and indeed no change in the OH band intensity was observed.

A feature of the spectra of these heated montmorillonite samples is that there is little change in the main lattice OH stretching absorption band at 3629 cm^{-1}, apart from a clearer development of subsidiary bands at 3670 and 3650 cm^{-1}, even when the OH deformation band is markedly reduced in intensity and shifted to higher frequency as in Li-, NH_4-, Ca-

and Mg-montmorillonite. However, with the onset of dehydroxylation the lattice OH stretching vibration loses a low-frequency component—possibly as the result of loss of OH groups with Fe^{3+} neighbours (Heller *et al.*, 1962)—and the original vibration at 3629 cm^{-1}, with shoulders at 3700 and 3652 cm^{1-}, becomes a doublet absorbing at 3654 and 3641 cm^{-1}. These frequencies are maintained during dehydroxylation.

Dehydroxylated montmorillonite gives an infra-red absorption pattern (Fig. 9) in which the position of only one weak band varies markedly with the original exchange cation: the band appears at 826 cm^{-1} for Na^+ and K^+ and at 836-833 cm^{-1} for Li^+, NH_4^-, Ca^{2+} and Mg^{2+}. It may have the same significance as that which developed between 830 and 820 cm^{-1} for Li^+, NH_4^+ and Mg^{2+}at lower temperatures, i.e. it may be produced by the migration of a cation into the lattice.

Serratosa (1962) achieved the rehydroxylation of Tidinit montmorillonite by exposing dehydroxylated material to water vapour at 20°C for 30 days. He observed two bands in the dried rehydroxylated material, the original at 3640 cm^{-1} and a weak broad band at about 3260 cm^{-1} which he ascribed to very strongly hydrogen-bonded OH groups. The latter band was lost by 500°C. The montmorillonite used here did not rehydroxylate under the conditions used by Serratosa. However, weak bands near 3270 cm^{-1} and near 1440 cm^{-1} were observed in the spectra of anhydrous samples which had been subjected to heating and cooling cycles. These bands are finally lost from montmorillonite between 500 and 550°C and from saponite at about 700°C, temperatures which are characteristic for loss of NH_4 from these minerals. Contamination of samples by NH_4^+ seems to occur fairly readily during their handling, and several instances of clay spectra showing extraneous absorption bands near 3270 and 1440 cm^{-1} occur in the literature.

Saponite

Fig. 11 illustrates typical changes in the infra-red absorption patterns of the various ionic forms of saponite following dehydration. The curve shown for the Na-form heated to 350°C and cooled in vacuum to room temperature is close to those of Li-, K- and NH_4-specimens. Saponite samples saturated with Li^+, K^+ or Na^+ rehydrate rapidly and completely at all temperatures up to dehydroxylation at 800-900°C, and the spectra of rehydrated samples are identical with those of unheated material. As described above, dehydration of the NH_4-, Ca- and Mg-saponite becomes irreversible after heating to 600-700°C, but unlike the results for montmorillonite, the spectra of the anhydrous forms so obtained are identical with those of materials reversibly dehydrated at

200-350°C. Decomposition of NH_4^+ gives H-saponite with features resembling anhydrous Mg-saponite (Fig. 11). The spectra of all the dehydrated samples show changes which make them closer to the talc spectrum. A broad band develops in the range 780-800 cm^{-1} and the Si-O vibrations at 1000 and 660 cm^{-1} undergo high-frequency shifts to

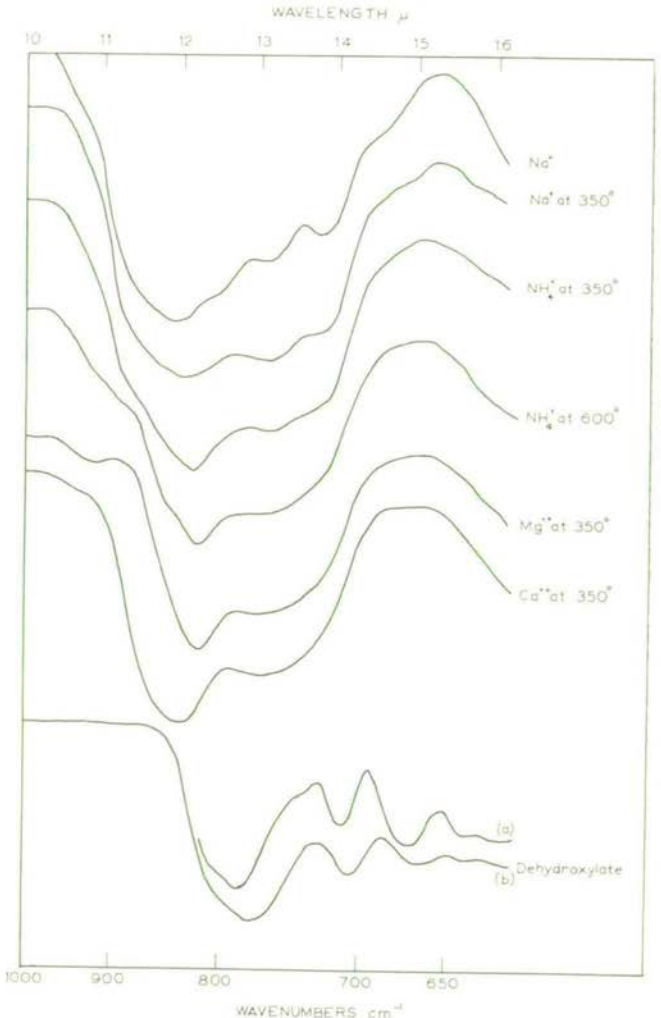

FIG. 11. Effect of heating on the lattice vibrations of saponite samples containing the indicated exchangeable cations. Dehydroxylate pattern (*a*) is that obtained from Na-, K- and Li-saponite, and (*b*) that from NH_4-, Ca- and Mg-saponite.

about 1020 and 668 cm^{-1}. Talc itself absorbs at 1018, 783 and 670 cm^{-1} (Farmer, 1958). Dehydration also causes an enhancement of the 1100 cm^{-1} band of saponite, which is inactive in talc (Farmer & Russell, 1964), and the more strongly polarizing ions, Mg^{2+}, Ca^{2+} and H^+, cause the development of a broad shoulder at 880-910 cm^{-1}, probably arising from some distortion of the silicate lattice. Midgley & Gross (1956) found that the cell dimensions of Ca-saponite after heating to about 650°C agreed well with those of talc. The saponite used in this work derives its cation-exchange capacity almost entirely from Al-for-Si substitutions in the tetrahedral layers and this would favour a situation where relatively strong interlayer links are formed through the divalent exchange cations giving rise to a collapsed structure. This could not occur for monovalent cations. NH_4^+ is anomalous in this respect, but the explanation for its yielding a collapsed structure might be that the very small, highly polarizing hydrogen ions released by the decomposition of NH_4^+ are able to neutralize charge deficiencies at the points of Al-for-Si substitution by settling in the base of each $(AlO_4)^-$ tetrahedron. Dehydroxylation of the saponite structure is complete at about 875°C, and the residue yields an infra-red absorption pattern resembling that of clinoenstatite (Launer, 1952) with some amorphous silica. As with dehydroxylated montmorillonite, there is some variation in pattern depending on the original exchangeable cation. Two types of pattern arise, one given by the K-, Li- and Na-forms (Fig. 11, curve *a*) and the other by the NH_4-, Ca- and Mg-forms (Fig. 11, curve *b*).

CONCLUSIONS

Infra-red spectroscopy shows both similarities and differences in the behaviour of interlayer water in montmorillonite and saponite, the differences arising partly from the readiness with which certain exchangeable cations react with the silicate lattice in montmorillonite. It is possible to distinguish two types of interlayer water in both minerals; the more labile water has an infra-red absorption pattern similar to that of liquid water, and is ascribed to water molecules in outer co-ordination spheres of the exchangeable cations. The more firmly held water is apparently involved in weaker hydrogen bonding, and has unusually strong absorption at 1630 cm^{-1}: it is ascribed to water directly co-ordinated to the cation. Fripiat *et al.* (1960) noted these features of the more firmly held water and ascribed them to water trapped in hexagonal holes in the silicate lattice when the interlayer spacing collapses. The present investigation shows a more marked correlation with the exchangeable cation present. With Na^+, K^+ and NH_4^+, water in the

outer co-ordination sphere is either absent at room temperature or lost by about 40°C, and water directly co-ordinated to the cation is lost by 150-200°C in montmorillonite and by 150-300°C in saponite. With Li^+, Ca^{2+} and Mg^{2+}, water in the outer co-ordination sphere is not lost till about 100°C, leaving trihydrated cations in Ca- and Mg-saponite, and in Mg-montmorillonite, but only a monohydrated cation in Li-montmorillonite. This directly co-ordinated water is not lost till higher temperatures are attained. Fripiat *et al.* (1960) found residual water absorption in thick films (30 mg/cm^2) of montmorillonite and vermiculite even at 400°C for all exchangeable cations studied, but with the thinner films (1-4 mg/cm^2) used in this investigation, only saponite samples saturated with Li^+, Mg^{2+} and Ca^{2+} showed water absorption after heating in vacuum to 350°C. These ions appear to form stable monohydrates in saponite, and so resemble Ca^{2+} and Mg^{2+} in vermiculite (Keay & Wild, 1961).

Like Mg-vermiculite, Ca- and Mg-saponite do not rehydrate after losing their last water molecule near 600°C. Saponite resembles a vermiculite of lower layer charge, in that it does not collapse to a mica-like structure with K^+ and NH_4^+ (Walker, 1961). Indeed K-saponite, like Li- and Na-saponite, continues to rehydrate after heating until dehydroxylation commences, and NH_4-saponite rehydrates until the ion decomposes to give what is presumably H-saponite.

In contrast to saponite, Li-, Mg- and NH_4-montmorillonite fail to rehydrate at room humidity after heating to about 350°C, and onset of irreversibility is associated with a change in the pattern of the lattice vibrations, indicating some interaction between the exchangeable cations and the lattice. This failure to rehydrate is usually ascribed to migration of the exchangeable cation into the vacant octahedral site, giving a pyrophyllite-like structure, but the infra-red pattern obtained does not match that of pyrophyllite (Heller *et al.*, 1962). There are marked similarities between the spectra of the products from Li- and Mg-montmorillonite and that of the H-montmorillonite formed from NH_4-montmorillonite by thermal decomposition. All three products give acidic reactions, indicating that Li^+ and Mg^{2+} must displace protons either from lattice OH groups or from water molecules. The extent to which this occurs has not yet been ascertained.

Ammonium ions decompose at a lower temperature in montmorillonite than in saponite. This may be due to a lower lattice energy of H-montmorillonite compared with that of H-saponite.

The present study has established many features which should prove useful in distinguishing saponites and montmorillonites in soil clays. Absorption of the interlayer water in smectites overlies that of the hydroxyl absorption of hydrated oxides and chlorites, but this inter-

ference can clearly be eliminated if the clays are saturated with Na^+, K^+ or NH_4^+ and heated to 100°C *in vacuo*.

ACKNOWLEDGMENTS

The authors are indebted to Mr B. D. Mitchell for providing the thermogravimetric data, and to Dr L. Heller (Geological Survey of Israel, Jerusalem) and Mr W. A. Mitchell for X-ray examination of some of the samples. Dr R. C. Mackenzie kindly made available the pure saponite used.

REFERENCES

Chaminade R. (1962) *C.R. Acad. Sci., Paris* **254**, 902.
Cook R.L. (1935) *J. Amer. Soc. Agron.* **27**, 297.
Corbridge D.E.C. & Lowe E.J. (1954) *J. chem. Soc.* p. 493.
Farmer V.C. (1958) *Miner. Mag.* **31**, 829.
Farmer V.C. & Russell J.D. (1964) *Spectrochim. Acta* **20**, 1149.
Fripiat J.J., Chaussidon J. & Touillaux R. (1960) *J. phys. Chem.* **64**, 1234.
Goulden J.D.S. (1952) *J. sci. Instrum.* **29**, 215.
Greene-Kelly R. (1953) *Clay Min. Bull.* **2**, 52.
Heller L., Farmer V.C., Mackenzie R.C., Mitchell B.D. & Taylor H.F.W. (1962) *Clay Min. Bull.* **5**, 56.
Keay J. & Wild A. (1961) *Clay Min. Bull.* **4**, 221.
Launer P.J. (1952) *Amer. Min.* **37**, 764.
Mackenzie R.C. (1957) *Miner. Mag.* **31**, 672.
Midgley H.G. & Gross K.A. (1956) *Clay Min. Bull.* **3**, 79.
Mitchell B.D. & Farmer V.C. (1962) *Clay Min. Bull.* **5**, 128.
Mortland M.M., Fripiat J.J., Chaussidon J. & Uytterhoeven J. (1963) *J. phys. Chem.* **67**, 248.
Rosenqvist I.Th. (1959) *Norsk geol. Tidsskr.* **39**, 350.
Rowland R.A., Weiss E.J. & Bradley W.F. (1956) *Clays and Clay Minerals* (A. Swineford, editor). Nat. Acad. Sci.—Nat. Res. Counc., Washington. Publ. 456, 85.
Serratosa J.M. (1962) *Clays and Clay Minerals* (A Swineford, editor), p. 412. Pergamon Press, London.
Tettenhorst R. (1962) *Amer. Min.* **47**, 769.
Walker G.F. (1956) *Clays and Clay Minerals* (A. Swineford, editor). Nat. Acad. Sci.—Nat. Res. Counc., Washington. Publ. 456, 101.
Walker G.F. (1961) *The X-ray Identification and Crystal Structures of Clay Minerals*, 2nd edn (G. Brown, editor), Chap. VII, p. 297. Mineralogical Society, London.
Walker G.F. & Cole W.F. (1957) *The Differential Thermal Investigation of Clays* (R. C. Mackenzie, editor), Chap. VII, p. 191. Mineralogical Society, London.

Biochem. J. (1965) **96**, 1
Printed in Great Britain

Catalpol and Methylcatalpol: Naturally Occurring Glycosides in *Plantago* and *Buddleia* Species

By R. B. DUFF,* J. S. D. BACON, C. M. MUNDIE, V. C. FARMER, J. D. RUSSELL and A. R. FORRESTER
Macaulay Institute for Soil Research, Craigiebuckler, Aberdeen, and Department of Chemistry, University of Aberdeen

(*Received* 9 *November* 1964)

1. A glycoside of the aucubin type has been isolated in crystalline form from *Plantago* and *Buddleia* species, and has been shown to be identical with catalpol (Lunn, Edward & Edward, 1962). Catalpol has not been found in the free state before, but occurs as its *p*-hydroxybenzoyl ester, catalposide, in the genus *Catalpa*. 2. A second glycoside of this type has been obtained in crystalline form from *Buddleia*, and has been shown to be a mono-*O*-methyl derivative of catalpol, for which the name 'methylcatalpol' is proposed. 3. Both *Plantago* and *Buddleia* species are known to contain aucubin. The concentrations of this glycoside and catalpol are comparable in *Plantago*. In *Buddleia* methylcatalpol predominates somewhat over catalpol. Yields of the individual glycosides were about 0·1% of the fresh weight of the leaves. 4. Bobbitt, Spiggle, Mahboob, Philipsborn & Schmid (1962) have suggested structures for catalposide and catalpol based on chemical and physical evidence, in particular on n.m.r. spectra. Reappraisal of this evidence and additional measurements have now confirmed these structures and show that the *Buddleia* glycoside is the 6-*O*-methyl derivative of catalpol.

While seedlings of various species were being examined for their content of soluble sugars it was noticed that aqueous extracts of *Plantago lanceolata* (rib-grass, ribwort plantain) contained two substances that reacted on paper with the benzidine–trichloroacetic acid reagent (Bacon & Edelman, 1951) to give intensely coloured spots with strong fluorescence in ultraviolet light. One, having R_F 0·35–0·40 in butan-1-ol–acetic acid–water (Partridge, 1948; rhamnose taken as R_F 0·37) and giving a grey spot with pink fluorescence, was identified as aucubin (already known to be a constituent of *Plantago*; Bourdier, 1907). The other, which gave a salmon-pink colour with yellow fluorescence and had a somewhat smaller R_F (0·27–0·32), was obtained in crystalline form by partition chromatography on Celite (Lemieux, Bishop & Pelletier, 1956) and has been identified as catalpol (Lunn *et al.* 1962), a product of the alkaline hydrolysis of catalposide, the characteristic glycoside of the fruit of *Catalpa ovata* (Claassen, 1888).

There was no evidence that catalposide itself was present in *Plantago*. Spots with colour reactions similar to those of aucubin and catalpol were usually seen near the solvent front of chromatograms of extracts, but they were very faint in freshly gathered material. It seemed most likely that they were the corresponding aglycones.

A search for catalpol-like substances in plants of related Families (Scrophulariaceae, Lentibulariaceae) and in several species known to contain aucubin or related glycosides was at first unsuccessful. (In this connexion it was noticed, and confirmed by tests with an authentic sample, that asperuloside gives no reaction with the benzidine–trichloroacetic acid spray.) The fresh plant material examined included *Aucuba japonica* and *Garrya elliptica*, which both contained, as expected, large amounts of aucubin. However, extracts of the leaves of *Buddleia globosa* (another known source of aucubin; Trim & Hill, 1952) and of *Buddleia variabilis* contained two such substances, one apparently identical with catalpol, the other having R_F about 0·50, and hence running in front of aucubin. Each was obtained in crystalline form from *B. globosa* by chromatography on charcoal–Celite columns and the first was shown to be identical with catalpol.

The identification of catalpol was helped by a comparison of its infrared spectrum (D.M.S. no. 12902) with that of aucubin (D.M.S. no. 12901), to which it showed a marked similarity. The absence

* Deceased 30 July 1963.

of a carbonyl grouping distinguished it from a number of known glycosides of the aucubin type. The elementary analysis was consistent with the presence of an additional oxygen atom, which would give a relatively small increase in molecular weight. This was confirmed by a somewhat lower glucose content, measured by glucose oxidase after enzymic hydrolysis by a *Plantago* extract. Lunn, Edward & Edward (1961) suggested that catalposide was the *p*-hydroxybenzoyl ester of a hydroxy derivative of aucubin. Hydrolysis of catalposide with 0·1 N-barium hydroxide at room temperature had yielded a substance that they named 'catalpol'. Its infrared spectrum (Lunn *et al.* 1962) was apparently identical with that of our unknown compound, but other properties (m.p. 207·5–209°; $[\alpha]_D^{25}$ −122° in 90% ethanol) differed somewhat from our measurements (m.p. 203–205°; $[\alpha]_D^{25}$ −104° in 90% ethanol, −102° in methanol). Bobbitt *et al.* (1962) later gave m.p. 201–203° and $[\alpha]_D^{25\cdot5}$ −104° in methanol for the product of catalposide hydrolysis by a basic resin, and the acetate prepared from our substance had m.p. $[\alpha]_D$ and infrared spectrum in good agreement with the 'heptaacetyl catalpol' of Lunn *et al.* (1962), which is actually a hexa-acetate (cf. Bobbitt *et al.* 1962).

Treatment with N-sodium hydroxide at 100°, which has no effect on aucubin (Trim & Hill, 1952), converted the plantain glycoside mainly into a substance of smaller R_F (0·12 at 21°). This was isolated by chromatography on charcoal–Celite and yielded a crystalline acetate that resembled the acetate of the alkaline-transformation product reported by Bobbitt *et al.* (1962) in having m.p. 132–133°. Its infrared spectrum had absorption maxima identical with those reported for 'heptaacetyl isocatalpol' by Lunn *et al.* (1962), and in addition the band at 3470 cm.$^{-1}$ (hydroxyl) reported by Bobbitt *et al.* (1962).

Despite the discrepancies noted above there can be little doubt that the glycoside from *Plantago* and *Buddleia* is catalpol, which therefore is accumulated in considerable amounts in the unsubstituted form in these plants, along with the closely related aucubin.

In *Buddleia* species a third glycoside is present. This, although evidently related to both the others, seemed from its infrared spectrum (D.M.S. no. 12903) and its colour reaction with benzidine to be closer to catalpol. On heating in N-sodium hydroxide it was rapidly transformed, giving a product with smaller R_F (0·25), which also indicated a close similarity to catalpol. The replacement of one hydroxyl group in the latter by a methoxyl group would give an empirical formula of $C_{16}H_{24}O_{10}$, which requires C, 51·1; H, 6·4; OMe, 8·2 (Found C, 51·3; H, 6·5; OMe, 8·1%). This would explain the greater R_F value relative to catalpol. Further confirmation of this relationship was obtained from n.m.r. measurements (see below), and by methylating both substances; in each case the same crystalline hexamethyl derivative was formed in good yield. Thus the third *Buddleia* glycoside is a mono-*O*-methyl derivative of catalpol, and might conveniently be named 'methylcatalpol'. Crystallographic evidence was consistent with this formulation. The liberation of glucose by the action of an emulsin preparation showed that the methyl group was located on the aglycone. It then seemed that the location of this methyl group could be settled by a consideration of the n.m.r. spectra of the glycosides and their derivatives.

The n.m.r. spectrum of methylcatalpol (in D_2O) was similar to that of catalpol in the same solvent, showing the vinyl proton as a quartet centred at 3·5 τ with coupling constants $J_1 = 6$ cyc./sec. and $J_2 = 2$ cyc./sec and signals from three protons in the 4·6–5·4 τ region. A sharp signal at 6·4 τ (three protons), not present in the spectrum of catalpol, is attributed to the *O*-methyl group.

From a consideration of the structure of catalpol [Bobbitt *et al.* (1962); (I) in Fig. 1] it should be possible to assign the methoxyl group to either C-6 or C-10 by comparing the spectra of the acetates of the two compounds in the 4·6–5·4 τ region, since protons on carbons bearing secondary, but not

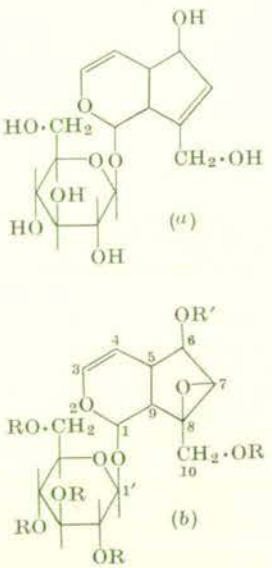

Fig. 1. (*a*) Structural formula of aucubin. (*b*) Formulae based on those proposed by Bobbitt *et al.* (1962) for: (I) catalpol (R = R′ = H); (II) catalpol hexa-acetate (R = R′ = CH_3·CO); (III) catalposide (R = H, R′ = *p*-HO·C_6H_4·CO); (IV) catalposide hexa-acetate (R = CH_3·CO, R′ = *p*-CH_3·CO·O·C_6H_4·CO); (V) methylcatalpol (R = H, R′ = CH_3).

primary, acetylated hydroxyl groups usually appear in this region (Jackman, 1955). The acetyl derivative of methylcatalpol (in $CDCl_3$) is a penta-acetate (two acetate signals corresponding to 15 ± 1 protons based on the vinyl signal centred at $3{\cdot}7\,\tau$) and has signals from seven protons in the $4{\cdot}6$–$5{\cdot}4\,\tau$ region. Catalpol hexa-acetate, however, has eight protons in this region, suggesting that the methyl group is at C-6.

However, each compound has one more proton in the $4{\cdot}6$–$5{\cdot}4\,\tau$ region than would be expected from structures based on (I). Careful measurements of the spectrum of catalposide acetate revealed that it also had eight protons in this region, and not seven as reported by Bobbitt *et al.* (1962). Both integrals were based on their respective vinyl proton signals and on the ratios of their $4{\cdot}6$–$5{\cdot}4\,\tau$ to $5{\cdot}4$–$6{\cdot}6\,\tau$ protons, which were clearly 8:5 and not the expected 7:6. These values did not appear to be consistent with the presence of only one secondary acylated hydroxyl group in the aglycones.

A possible explanation for the discrepancy (proposed by Professor von Philipsborn, personal communication) is that one of the C-10 protons [the C-10 protons are not equivalent in (I) because of the neighbouring asymmetric centre at C-8] has shifted from the $5{\cdot}4$–$6{\cdot}6\,\tau$ region in the glycosides to the $4{\cdot}6$–$5{\cdot}4\,\tau$ region in the acetates, after the introduction of several anisotropic acetyl groups. This has now been confirmed for methylcatalpol by spin-decoupling measurements.

The 60 Mcyc./sec. spectrum of methylcatalpol shows a typical four-line AB-pattern in the $5{\cdot}4$–$6{\cdot}6\,\tau$ region, centred at $\tau = 5{\cdot}68$ and $\tau = 6{\cdot}1$ with $J_{AB} = 13$ cyc./sec., assigned to the coupled C-10 protons. In that of the acetate only one of the doublets ($\tau = 6{\cdot}02$) is easily seen; the other, having shifted to the $4{\cdot}6$–$5{\cdot}4\,\tau$ region, is partly obscured by other signals. The 100 Mcyc./sec. spectrum, however, resolves the multiplet at lower field and shows clearly the presence of the second doublet at $\tau = 5{\cdot}2$ with $J = 13$ cyc./sec. Confirmation of this assignment was obtained by irradiating the sample in the region $\tau = 5{\cdot}2$ (corresponding to the low-field C-10 proton), which caused collapse of the $\tau = 6{\cdot}02$ doublet to a slightly broadened singlet. Hence the seven protons in the $4{\cdot}6$–$5{\cdot}4\,\tau$ region are accounted for, and the position of the methoxyl group on the secondary carbon atom C-6 is established.

The similarity of the spectra of catalpol acetate and catalposide acetate to that of methylcatalpol acetate indicates that their anomalous integrals may be explained in a similar fashion, and a full paper dealing with these substances is soon to be published by Professor von Philipsborn and his colleagues.

The presence of relatively large amounts of aucubin, catalpol and methylcatalpol in *Buddleia* would make this genus a very suitable material for the study of their biosynthesis and interconversion.

There are many reports of the medicinal uses of the plantain (cf. Wren, 1932), including references to its use in wound-healing and as a diuretic. Kimura, Okuda & Takano (1963) have reported on the diuretic properties of the *Catalpa* glycosides. Investigations of this kind should be helped by the knowledge that catalpol can be obtained easily in large amounts from a common weed of temperate regions.

EXPERIMENTAL

Physical methods. The n.m.r. spectra were measured on a Varian A-60 instrument (Varian Associates, Palo Alto, Calif., U.S.A.) at the University of Aberdeen. Infrared spectra were measured in KBr disks with a Grubb–Parsons Double-Beam Spectrometer type S4 equipped with a NaCl prism. Optical rotations were measured in 2 dm. tubes with a sodium light source.

Plant material. Plantago lanceolata L. and *Plantago major* L. were collected on waste ground or grown from seed in the gardens of the Institute. One bush each of *Buddleia globosa* and *Buddleia variabilis* was examined. For most purposes only the leaves were taken and these could be kept at $-15°$ or dried at 50° without appreciable decomposition of the glycosides. Even in plantain leaves that had been heated until they became brown under conditions similar to those of Dijkshoorn (1961) there was little decomposition of the two glycosides.

Isolation of glycosides from P. lanceolata. A typical extraction procedure was as follows.

Fresh leaves (6·5 kg.; 1·4 kg. of dry matter) were chopped into 10 l. of water at 95° containing sufficient $CaCO_3$ (about 200 g.) to prevent the extract from becoming acid. After vigorous stirring for 30 min. the suspension was filtered through cloth and the residue re-extracted for 30 min. with 7 l. of water at 95°. The combined filtrates were reduced in volume to 750 ml. and poured into 4 vol. of ethanol. The precipitate was washed and the filtrate plus washings were reduced in volume to 400 ml. (287 g. of dry matter).

Several procedures were tried for the isolation of the glycosides from this aqueous extract, including adsorption on active carbon (Ultrasorb S.C. 120/240; British Carbo-Norit Union Ltd., Grays, Essex) and clarification with basic lead acetate, but eventually it was found that direct application of the extract to a column of moist Celite (Lemieux *et al.* 1956) and development with butan-1-ol saturated with water effected a considerable purification, and if the appropriate fractions of eluate from this column were applied to a second column both glycosides could be obtained in crystalline form and purified further by recrystallization. Thus the aqueous extract from 9·1 kg. of leaves (500 ml., about 300 g. of dry matter) was applied to a column made from 1·5 kg. of Celite no. 535 (11·5 cm. diam. × 69 cm. high; packed in three sections, 500 g. each). Fractions containing mainly aucubin, the unknown glycoside and glucose were combined (46 g. of dry matter) and applied to a 900 g. Celite column (8 cm. diam × 69 cm. high; packed in five sections). Of the fractions of effluent (each 50 ml.) the first 153 contained no glycosides, the next 43 only

aucubin, 17 a mixture of aucubin and the unknown glycoside, and 25 only the unknown glycoside. From the latter, 8g. of crystalline material was obtained. Similar yields of crystalline aucubin were obtained.

Isolation of glycosides from B. globosa. Leaves (250g.) previously stored at −15° were chopped into boiling water, the pH remaining near neutrality. The whole was blended, again heated to boiling and filtered through cloth. Ethanol (2vol.) was added to the filtrate. The precipitate was removed by centrifuging and the supernatant fluid evaporated to small bulk. This was applied to a column of a mixture of 40g. of British Drug Houses Ltd. Activated Charcoal and 40g. of Celite no. 535 and eluted with a gradient of aqueous ethanol made by dropping ethanol into 1l. of 35% (v/v) ethanol, 5ml. fractions being collected. Fractions 69–80 contained the unknown glycoside with traces of aucubin and catalpol (see below).

Fractions 53–63, which contained catalpol, with smaller amounts of aucubin, the unknown glycoside and sugars (sucrose, oligosaccharide etc.), were combined and evaporated to dryness, the pH being controlled by additions of Bio-Deminrolit resin (The Permutit Co. Ltd.). The residue was applied to a 20g. Celite column, which was developed with aqueous butan-1-ol, 5ml. fractions being collected. Fractions 50–56 were combined, evaporated to small bulk and applied to a further 20g. Celite column. Fractions 61–80 from this column contained almost pure catalpol, which was recrystallized from water (75mg.) and identified by its infrared spectrum.

Enzymic hydrolysis. Dialysed aqueous homogenates of *P. lanceolata* contained a hydrolytic enzyme system or systems that attacked all three glycosides. In each case glucose was liberated and could be estimated by glucose oxidase (Huggett & Nixon, 1957). Analyses of the crystalline glycosides by this method gave a glucose content of 53% for aucubin (calc. 5: %) and 48% for catalpol (calc. 50%).

All three glycosides were also hydrolysed by the crop juice of the snail *Helix pomatia* and by various emulsin preparations.

Identification of aucubin. Aucubin has already been shown to be present in *Plantago* species (Bourdier, 1907). The crystalline material prepared from *P. lanceolata* had m.p. 182°, $[\alpha]_D^{21}$ −171·7° (*c* 1·7 in water) and an infrared spectrum identical with that of an authentic specimen kindly provided by Dr A. R. Trim.

Pharmacological properties. Samples of aucubin and catalpol were supplied to Edinburgh Pharmaceutical Industries Ltd., who reported that tests of anti-bacterial and anti-inflammatory effects were negative.

Identification of catalpol

This glycoside was accompanied by aucubin in extracts of all the samples of *Plantago* spp. and *Buddleia* spp. examined. In butan-1-ol–acetic acid–water at 21° they had R_F values of about 0·25 and 0·35 respectively, calculated from R_F 0·37 for rhamnose. At higher temperatures the R_F of rhamnose in this solvent was unchanged, but those of the glycosides increased, values of 0·37–0·39 being found for aucubin with solvent travel of 30cm. on Whatman no. 1 paper at 25°. Under these conditions the other glycoside had R_F 0·31–0·32, the value given for catalpol by Lunn *et al.* (1962).

Catalpol was prepared from a sample of catalposide kindly provided by Professor J. T. Edward: 1·25g. was dissolved in 40ml. of ethanol, and 100ml. of water and 24g. of De-Acidite FF (OH^- form) were added. The mixture was heated at 50° for 1hr. with occasional shaking; paper chromatograms indicated complete conversion into catalpol and small amounts of material of smaller R_F (possibly isocatalpol). The resin was removed by filtration and the filtrate evaporated to dryness (0·77g.). The material was recrystallized three times from methanol, but still contained some impurity and so was chromatographed on a 20g. Celite column and recrystallized from methanol, yielding 0·26g. of catalpol, m.p. 203–205°, $[\alpha]_D^{22·5}$ −102° [*c* 0·98 in 90% (v/v) ethanol]. This material showed no depression of m.p. when mixed with the plantain glycoside. Additional confirmation of their identity was obtained from their infrared spectra and by the preparation of derivatives.

The glycoside from *Plantago* was acetylated at 25° with acetic anhydride in pyridine. After 24hr. hexane was added (cf. Lunn *et al.* 1962) and crystals appeared. These had properties identifying it with the 'heptaacetyl catalpol' of Lunn *et al.* (1962), namely m.p. 140°, $[\alpha]_D^{22}$ −88° (*c* 1·46 in chloroform); the band maxima found in the infrared spectrum agreed well with those given by Lunn *et al.* (1962), apart from a reported shoulder at 956cm.$^{-1}$ (found at 965cm.$^{-1}$) and a band reported at 699cm.$^{-1}$ (found at 706cm.$^{-1}$).

The glycoside (200mg.) was heated in 5ml. of N-NaOH for 10min., cooled, neutralized with acetic acid and applied to a column (30cm.×2·5cm.) of a mixture of 40g. of British Drug Houses Ltd. Activated Charcoal and 40g. of Celite no. 535. Elution with a gradient produced by dropping ethanol into 1l. of water removed almost the whole of the transformation product before the small residue of the starting material. The product (30mg.) did not crystallize. It was acetylated with acetic anhydride in pyridine, giving a crystalline product (23mg.), m.p. 132–133°, $[\alpha]_D$ −105° (*c* 1·2 in chloroform). Bobbitt *et al.* (1962) give m.p. 131–133° for the hepta-acetyl derivative of the substance produced by opening the epoxide ring. Lunn *et al.* (1962) give m.p. 127–128°, $[\alpha]_D$ −121° (*c* 2·21 in chloroform) for their 'heptaacetyl isocatalpol', and an infrared spectrum in carbon tetrachloride similar to but not identical with that of our acetate.

Unknown glycoside from Buddleia

Fractions from the charcoal–Celite column were evaporated to dryness and the glycoside was recrystallized from water, giving 130mg. of material, m.p. 236–238°, $[\alpha]_D^{22·5}$ −122° [*c* 1·64 in 90% (v/v) methanol]. This material lost the equivalent of 1mol. of water/mol. on drying over P_2O_5 at 15mm. Hg pressure for 4 days at 61°.

Crystallography. The transparent colourless crystals had different habits, depending on the solvent from which they crystallized. From water they formed plates parallel to (001) and elongated parallel to (010), whereas those from propan-2-ol were plates parallel to (010). The refractive indices were $\alpha = 1·533$, $\beta = 1·565$ and $\gamma = 1·569$, with strong negative birefringence. The optic axial plane was parallel to (010) and 2V about 40°.

Single-crystal Weissenberg X-ray-diffraction patterns showed the crystals to be monoclinic with $a = 7·56$ Å, $b = 9·69$Å, $c = 12·07$Å and $\beta = 104°$, and the space group $P2_1/m$.

A density determination gave 1·46g./ml. and this, with the above dimensions, shows the molecular weight to be a submultiple of 748 (twice $C_{16}H_{24}O_{10} = 752$).

Methylation of catalpol. Catalpol (0·98g.) was dissolved in a mixture of 3·0ml. of dimethylformamide and 4·0ml. of methyl iodide, treated with 5g. of Ag_2O at 45° for 5hr. and left overnight at 21°. The Ag_2O was removed by filtration and washed with dry acetone. Filtrate and washings were evaporated to dryness under reduced pressure, the last traces of solvent being removed by prolonged exhaustion (3hr.) by a high-vacuum pump. The residue (1·74g.) crystallized. Treatment with charcoal in hexane gave 0·85g. of crystals that after further recrystallization yielded 0·44g. of *hexamethylcatalpol*, m.p. 79°, $[\alpha]_D^{23.5}$ −91° (*c* 1·96 in chloroform) (Found: C, 57·1; H, 7·7; OMe, 40·6. $C_{21}H_{34}O_{10}$ requires C, 56·6; H, 7·6; OMe, 41·7%). That methylation was complete in one operation was confirmed by the infrared and n.m.r. spectra, which showed the absence of hydroxyl groups and the presence of six methyl groups/mol.

Methylation of Buddleia *glycoside.* The glycoside (55mg.) was dissolved in 0·3ml. of dimethylformamide and 0·4ml. of methyl iodide, 0·5g. of Ag_2O was added, and the mixture was kept for 8hr. at 45° and overnight at 21°. The product was isolated as for hexamethylcatalpol, yielding 42mg. with m.p. 79°, unchanged by admixture with that substance and having an identical infrared spectrum. The two substances were indistinguishable when examined by thin-layer chromatography on Kieselgel G (E. Merck A.-G., Darmstadt, Germany) with chloroform–ether (1:1, v/v) as solvent.

This work was done with the technical assistance of Mrs S. M. Lindsay. We are indebted to Mr A. H. Knight of the Department of Plant Physiology for providing the materials on which the original observations were made. We thank Dr A. R. Trim for very helpful discussions and for gifts of aucubin and asperuloside; also Professor J. T. Edward for a generous sample of catalposide. We are grateful to Professor von Philipsborn of the University of Zürich for help in interpreting the n.m.r. data and for carrying out the crucial spin-decoupling measurements with his Varian HR-100 instrument. We thank Mr K. C. Reid for the biological tests and our colleague Mr W. A. Mitchell for the crystallographic data. The interest and encouragement of Professor Sir Edmund Hirst, F.R.S., did much to bring this research to a satisfactory conclusion.

REFERENCES

Bacon, J. S. D. & Edelman, J. (1951). *Biochem. J.* **48**, 114.
Bobbitt, J. M., Spiggle, D. W., Mahboob, S., Philipsborn, W. von & Schmid, H. (1962). *Tetrahedron Lett.* **8**, 321.
Bourdier, L. (1907). *J. Pharm. Chim., Paris*, **26**, 254.
Claassen, E. (1888). *Amer. chem. J.* **10**, 228.
Dijkshoorn, W. (1961). *Jaarb. Inst. biol. scheik. Onderz. LandbGewass., Wageningen*, p. 99.
Huggett, A. St G. & Nixon, D. A. (1957). *Lancet*, **273**, 368.
Jackman, L. M. (1955). *Applications of Nuclear Magnetic Resonance Spectroscopy in Organic Chemistry*, p. 55. London: Pergamon Press Ltd.
Kimura, K., Okuda, T. & Takano, T. (1963). *J. pharm. Soc. Japan*, **83**, 635. Cited in *Chem. Abstr.* (1963). **59**, 13114f.
Lemieux, R. U., Bishop, C. T., & Pelletier, G. E. (1956). *Canad. J. Chem.* **34**, 1365.
Lunn, W. H., Edward, D. W. & Edward, J. T. (1961). *Chem. & Ind.* p. 1488.
Lunn, W. H., Edward, D. W. & Edward, J. T. (1962). *Canad. J. Chem.* **40**, 104.
Partridge, S. M. (1948). *Biochem. J.* **42**, 238.
Trim, A. R. & Hill, R. (1952). *Biochem. J.* **50**, 310.
Wren, R. C. (1932). *Potter's Cyclopaedia of Botanical Drugs and Preparations*, p. 271. London: Potter and Clarke Ltd.

Offprinted from the *Transactions of The Faraday Society*,
No. 514, Vol. 61, Part 10, October, 1965

INFRA-RED STUDY OF THE REACTIONS OF AMMONIA WITH MONTMORILLONITE AND SAPONITE

Infra-red Study of the Reactions of Ammonia with Montmorillonite and Saponite

By J. D. Russell

The Macaulay Institute for Soil Research, Craigiebuckler, Aberdeen, Scotland

Received 10*th March*, 1965

Three reactions have been distinguished, by infra-red spectroscopy, when the clay minerals montmorillonite and saponite are exposed to a current of gaseous NH_3: (*a*) direct co-ordination of NH_3 by exchange cations on the mineral, (*b*) formation of NH_4 cations and metal hydroxides in the interlayer space from the reaction of NH_3 with hydrated cations, and (*c*) hydrogen bonding of NH_3 to NH_4 cations and to directly co-ordinated NH_3 molecules. The extent to which reactions (*a*) and (*b*) occur depends on the exchange cation. With Li and Na the principal reaction is direct co-ordination of NH_3; the NH_3 is stable to evacuation but is displaced by H_2O. With exchangeable Al, Ca and Mg in montmorillonite, hydroxide and NH_4 formation is the principal reaction and appears to be complete with Al and Mg. There is no evidence for co-ordination of NH_3 to exchangeable Al or Mg in montmorillonite. In Ca- and Mg-saponites, formation of NH_4 is lower and co-ordination of NH_3 higher than in the corresponding montmorillonites. The hydroxides and NH_4 formed with exchangeable Ca and Mg are decomposed by atmospheric H_2O, but are stable with exchangeable Al because of the lower basicity of $Al(OH)_3$. With Cu(II) the principal reaction is co-ordination of NH_3. The complex ions are stable to evacuation but slowly decompose in air giving NH_4 and $Cu(OH)_2$.

Small amounts of NH_4 formed with exchangeable K, Li, Na and NH_4 in montmorillonite and saponite cannot be accounted for by the mechanism proposed for the formation of NH_4 with exchangeable Al, Ca and Mg. Alternative explanations are offered.

Mortland [1] has reviewed studies of ammonia adsorption on montmorillonite, up to 1957; a review of the present position will appear shortly.[2] X-ray diffraction [3, 4] and absorption isotherm studies [3, 5, 8] have shown that NH_3 penetrates into the interlayer space. The amount of NH_3 adsorbed and the final *c*-spacings depend on the exchangeable cations present, and their hydration properties. Both physical and chemical adsorption of NH_3 can occur [5, 7] and there is no sharp delineation between these two processes.[6] Indeed, calorimetric results on heats of adsorption [4] have shown conclusively that there is no break in an energy plot between chemisorption and purely physical adsorption. Mechanisms proposed to account for the retention of ammonia include NH_4^+ formation,[1, 4, 6] co-ordination of NH_3 to the exchangeable cations,[7-9] hydrogen bonding of NH_3 to the clay surfaces,[5, 10] and trapping of NH_3 molecules in the interlayer space.[10] Of these only NH_4^+ formation has been conclusively established by Mortland *et al.*[4] from infra-red studies. These authors found no evidence for adsorbed NH_3 molecules after evacuation. Other mechanisms must, however, be involved to account for all the experimental observations.

In the present investigation the infra-red evidence on the forms in which ammonia is retained by evacuated samples has been re-examined, and information has also been sought on the mechanism which lead to the adsorption of larger amounts of ammonia at higher ammonia pressures. The stability of the different forms of adsorbed ammonia has been assessed.

EXPERIMENTAL

The Wyoming montmorillonite and saponite used and the preparation of thin oriented films of these minerals have been described elsewhere.[11] The minerals were saturated with K, Li, Na, Ca, Cu, Mg, and Al by washing with the appropriate normal chloride solutions; normal ammonium acetate solution pH 7 was used to prepare the NH_4-saturated forms. The procedure involved washing the minerals six times with the appropriate salt solution, twice with water, then a minimum of six times with 80 % v/v aqueous ethanol until washings were free from either chloride or acetate. After further washing with ethanol followed by benzene, the preparations were air-dried. Cation exchange capacities of 90 m equiv. per 100 g for montmorillonite and 124 m equiv. per 100 g for saponite were determined by saturating the original minerals with NH_4^+ then estimation of NH_3 by a microkjeldahl method.

A flat 2 cm diam. specimen of clay film (1-4 mg/cm^2) was mounted in a 0·35 mm path-length cell equipped with 25 mm NaCl windows. Loose-fitting PTFE washers kept the film from contact with the windows. A current of NH_3 gas was passed through the cell for 30 min, then the cell was stoppered and the absorption spectrum of the sample in an atmosphere of NH_3 recorded on a Grubb-Parsons S4 double-beam spectrometer, from 5000-625 cm^{-1} with NaCl optics, and from 4000-2350 cm^{-1} under the higher resolution of a 2500 lines per inch diffraction grating. NH_3 absorption was compensated by a reference cell containing NH_3. Following this, the short-path cell containing the sample in NH_3, and still stoppered, was placed in a 10 cm gas cell which was then evacuated. The short-path cell was not sufficiently gas tight to resist the vacuum and after 1 h at about 0·02 mm Hg pressure, the spectrum of the sample in vacuum was recorded. Spectra of samples allowed to hydrate by exposure to the atmosphere for various periods were also examined.

For chemical determination of total $NH_3+NH_4^+$ contents, films were treated with flowing NH_3 in a Pyrex tube which was then evacuated for 1 h at about 0·02 mm Hg. They were thereafter immersed in 4 % boric acid solution (10 ml), either immediately or following exposure to the atmosphere for varying times. The boric acid suspensions were transferred to a microkjeldahl apparatus and NH_3 determined by the usual procedure.

Ammonium contents of the NH_3-treated minerals were calculated from the optical density of the 1440 cm^{-1} infra-red absorption band of the NH_4 ion using NH_4-saturated montmorillonite and saponite as standards. The films were either weighed or, with montmorillonite, the film weights calculated from the intensity of a silicate absorption band at 800 cm^{-1}. The latter technique was preferable, as it did not assume uniform film thickness. Neither technique was capable of high precision.

RESULTS

MONTMORILLONITE

Infra-red spectra indicated rapid displacement of all water in montmorillonites by ammonia when a stream of ammonia gas was passed over clay films, and the formation of amounts of NH_4^+ which depended on the exchangeable cation. Identical results were obtained when the clay films were first degassed at room temperature before exposure to an atmosphere of ammonia. As the absorption pattern of NH_4^+ is markedly affected by the presence of ammonia in the interlayer space, this effect, as shown by NH_4-montmorillonite, is examined first.

NH_4-MONTMORILLONITE

The infra-red absorption spectrum of NH_4-montmorillonite is shown in fig. 1(*a*) in vacuum, (*b*) in air at about 40 % relative humidity and (*c*) in dry NH_3 gas. Hydrogen bonding to interlayer water causes a broadening of the NH_4^+ stretching absorption, which lies at 3270 cm^{-1} in vacuum, and the development of subsidiary bands at 3045 and 2855 cm^{-1} (fig. 1*a*, *b*). These findings have been discussed by

Mortland *et al.*[4] and Russell and Farmer,[11] but the effects of interlayer NH_3 have not been previously reported. The NH_4^+ stretching vibrations are strongly perturbed by hydrogen bonding to the more basic NH_3 molecules which replace water in the interlayer space of montmorillonite in an atmosphere of ammonia gas. The principal band shifts to 2791 cm^{-1} and submaxima appear at 3353, 3315, 3195, 2980 and 2320 cm^{-1} (fig. 1*c*). The NH_4 deformation frequency shifts from 1430 cm^{-1} in vacuum to 1440 cm^{-1} in air, to 1460 cm^{-1} in NH_3, the band becoming slightly weaker. Other bands due, wholly or in part, to perturbed ammonium ions lie at 2035, 1945 and 1695 cm^{-1}. The last is a bending frequency which is infra-red inactive for full tetrahedral symmetry, and the others are probably combination bands.

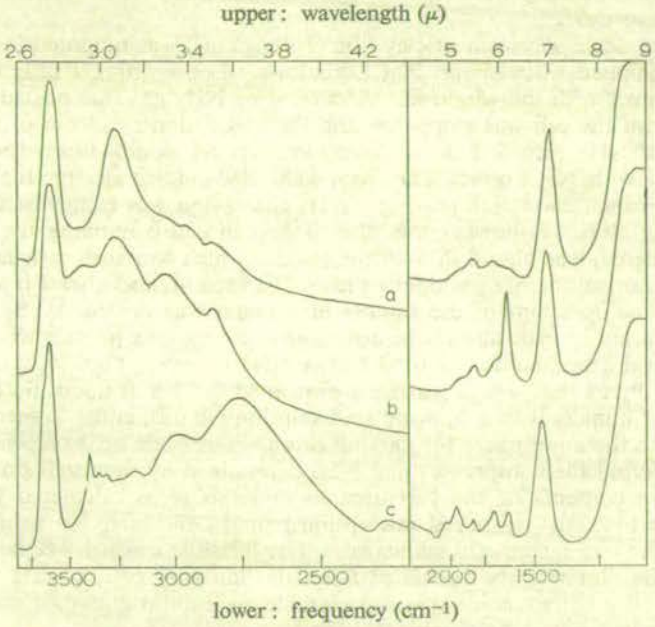

FIG. 1.—Infra-red absorption spectra of NH_4-montmorillonite in vacuum (*a*), hydrated in air at about 40 % relative humidity (*b*), and in dry NH_3 gas (*c*).

Interlayer ammonia gives rise to absorption bands at 3400 cm^{-1} (N—H stretching) and 1623 cm^{-1} (asymmetric deformation) (fig. 1*c*). In the 1100-625 cm^{-1} region (not shown) only a weak band at 714 cm^{-1} could be ascribed to NH_3, probably arising from a librational mode.[12] From the observed perturbation of the NH_4^+ vibrations, it can be concluded that part of this ammonia is held by hydrogen bonding to the ammonium ions, but other sites cannot be excluded.

The lattice vibrations of montmorillonite [13] appear to be less perturbed when NH_3 occupies the interlayer space than in either the anhydrous or hydrated states. Thus, absorption bands due to lattice hydroxyl stretching (3630 cm^{-1}) and bending (920 cm^{-1}) became narrower and more intense as did also the Si—O vibration at 1120 cm^{-1}, and an unassigned band at 849 cm^{-1}. A band at 890 cm^{-1} was, however, depressed. It has been suggested that hydrogen bonding between ammonia and the lattice hydroxyl groups [10] or the oxygens of the silicate sheet [5] contributes to the retention of ammonia by montmorillonite, but these observations indicate that such hydrogen bonding, if present, is weak, since the narrower, more intense absorption bands must arise from more freely vibrating groups.

Removal of the ammonia atmosphere by evacuation at about 0·02 mm Hg for 1 h gave a film whose absorption pattern was close to that of the normal anhydrous material (fig. 1*a*) with, however, an additional weak residual shoulder at 3400 cm^{-1} indicative of the retention against evacuation of a small amount of NH_3, about 20 mmoles NH_3/100 g (table 1). The disappearance of NH_3 bands at 3400, 1623 and 714 cm^{-1} on exposure of the NH_3-treated material to atmospheric water vapour for a few minutes, either before or after evacuation, indicated ready displacement of interlayer NH_3 by water.

Al- Ca-, Mg-, K-, Na- AND Li-MONTMORILLONITE

The spectra in fig. 2 confirm the formation of NH_4^+ in base-saturated montmorillonites after treatment with NH_3 gas,[4] and show that these cations are perturbed by interlayer NH_3 in the same manner as normal exchangeable NH_4^+. In the present study quantitative estimates of the amounts of NH_4^+ formed have been obtained

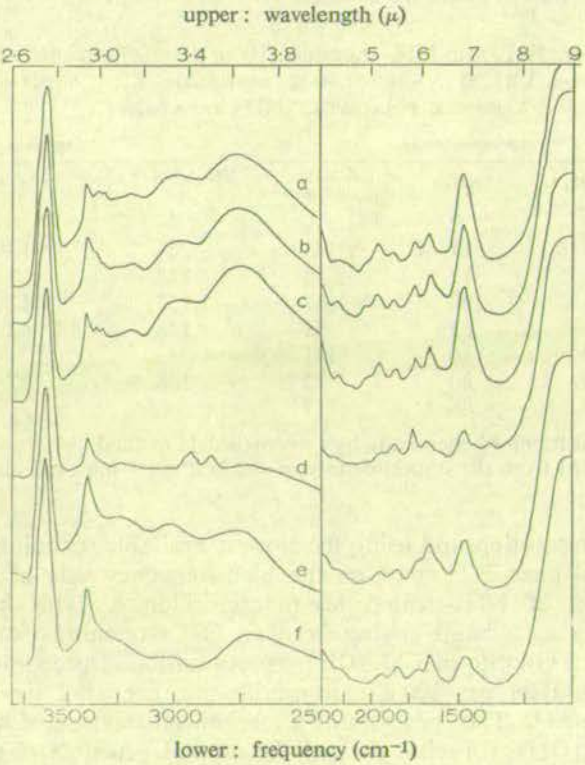

FIG. 2.—Infra-red absorption spectra of montmorillonite, saturated with various cations, in dry NH_3 gas; (*a*) Al^{3+}, (*b*) Ca^{2+}, (*c*) Mg^{2+}, (*d*) K^+, (*e*) Li^+ and (*f*) Na^+.

from the intensity of the 1440 cm^{-1} absorption band. These results (table 1) indicate that with Al^{3+} and Mg^{2+} the amount of NH_4^+ present approaches the cation exchange capacity (90 m equiv./100 g), and with Ca^{2+} it is 75 % of this value following treatment with NH_3, but that much less is formed in montmorillonites saturated with monovalent cations. Li- and Na-montmorillonites show particularly strong bands at 3400 and 1623 cm^{-1} indicating a high proportion of co-ordinated NH_3

round these cations. Ca-montmorillonite contains more NH_3 than montmorillonite saturated with other multivalent cations but not as much as either the Li or Na forms. The shape of the 3400 cm^{-1} absorption band varies with the cation, although its frequency does not: it is a broader band for Li^+, Na^+ and Ca^{2+}, the breadth of the band possibly accounting for the diffuse appearance in Ca-montmorillonite (fig. 2*b*) of the weak but distinct doublet occurring at 3353 and 3315 cm^{-1} with NH_4-, Al- and Mg-montmorillonite (fig. 1*c*, 2*a* and 2*c*). The conclusion that the increased width might reflect a stronger type of NH_3 co-ordination complex with these ions was supported when removal of the NH_3 atmosphere by evacuation left a band of moderate intensity at 3400 cm^{-1}. The band was strongest with Li^+ while that for Ca^{2+} occurred on the side of the much stronger unperturbed NH^+ stretching band at 3270 cm^{-1}. From total nitrogen ($NH_3+NH_4^+$) contents by chemical analysis and NH_4^+ contents estimated from the optical density of the 1440 cm^{-1} ammonium band it can be seen (table 1) that the Li-montmorillonite retains against evacuation 143 mmoles NH_3 per 100 g, Na 75, Ca 58 and K, NH_4, Mg and Al each between 17 and 22 mmoles NH_3 per 100 g.

TABLE 1.—AMOUNTS OF NH_3 AND NH_4 (m equiv./100 g SAMPLE) RETAINED AGAINST EVACUATION (0·02 mm Hg FOR 1 h) BY VARIOUS BASE SATURATIONS OF MONTMORILLONITE AND SAPONITE FOLLOWING NH_3 TREATMENT

	montmorillonite			saponite		
cation	NH_3+NH_4 *	NH_4 †	NH_3 (by difference)	NH_3+NH_4 *	NH_4 †	NH_3 (by difference)
K	28	9	19	44	8	36
Li	160	17	143	264	13	251
Na	102	17	85	128	9	119
NH_4	107	90	17	153	112	41
Ca	123	65	58	148	42	106
Cu	137	16	121			
Mg	102	80	22	138	87	51
Al	103	86	17			

* NH_3+NH_4 was determined chemically by a microkjeldahl method.

† NH_4 was estimated from the optical density of the 1440 cm^{-1} infra-red absorption band of the NH_4 ion.

Under grating resolution and using the slowest available scanning speed, a weak band was observed near 3711 cm^{-1} on the high-frequency side of the lattice OH stretching vibration of NH_3-treated Mg-montmorillonite. This band occurs at the same frequency as a band arising from an OH stretching vibration of interlayer $Mg(OH)_2$ in a chlorite-like $Mg(OH)_2$-montmorillonite preparation containing 1200 m equiv. $Mg(OH)_2$ per 100 g montmorillonite, prepared by the method of Slaughter and Milne.[14] The spectrum of a mechanical mixture of montmorillonite and crystalline $Mg(OH)_2$ (brucite) showed the normal brucite OH stretching band at 3700 cm^{-1}; this band was also observed, in addition to the band at 3711 cm^{-1}, in an interlayer preparation containing 1600 m equiv. $Mg(OH)_2$ per 100 g montmorillonite, signifying $Mg(OH)_2$ as a separate external phase. Thus it appears that $Mg(OH)_2$ is precipitated in the interlayer space of Mg-montmorillonite following NH_3 treatment. A comparison of the intensities of the 3711 cm^{-1} bands in the NH_3-treated material and the 1200 m equiv./100 g interlayer preparation indicated the formation of between 50 and 100 m equiv. $Mg(OH)_2$ per 100 g in the former. This accompanies the formation of 80 m equiv. NH_4^+ per 100 g (table 1). The OH stretching frequency of $Al(OH)_3$ is too weak and diffuse, and that of $Ca(OH)_2$ lies

too close to the lattice OH stretching frequency of montmorillonite to permit their detection in NH_3-treated Al- and Ca-montmorillonites respectively, but it seems likely that these hydroxides are also precipitated in the interlayer space to account for the ammonium formed. The low retention of NH_3 by Al- and Mg-montmorillonite indicates that these hydroxides do not adsorb NH_3.

Exposure of ammonia-treated samples to air for a few minutes brought about a drop in the intensity of the NH_3 stretching band at 3400 cm^{-1}, a rise in water absorption bands, and a sharp decrease in total nitrogen content by analysis: e.g., the 160 mmoles ($NH_3+NH_4^+$) originally present in Li-montmorillonite, fell to 111 after about 6 min, 79 after 15 min and 17 after 2 h. The last figure represented almost entirely NH_4^+ since it agreed well with the 15 m equiv. NH_4^+ per 100 g estimated from the 1440 cm^{-1} band. Similar observations were made for the other ions.

Cu(II)-MONTMORILLONITE

As expected from the ready formation of ammines by copper ions in aqueous solution, Cu-montmorillonite in NH_3 gave a spectrum which showed bands at 3339, 3277, 3185, 1630, 1270 (fig. 3*a*), and also at 715 cm^{-1}, reasonably close to those

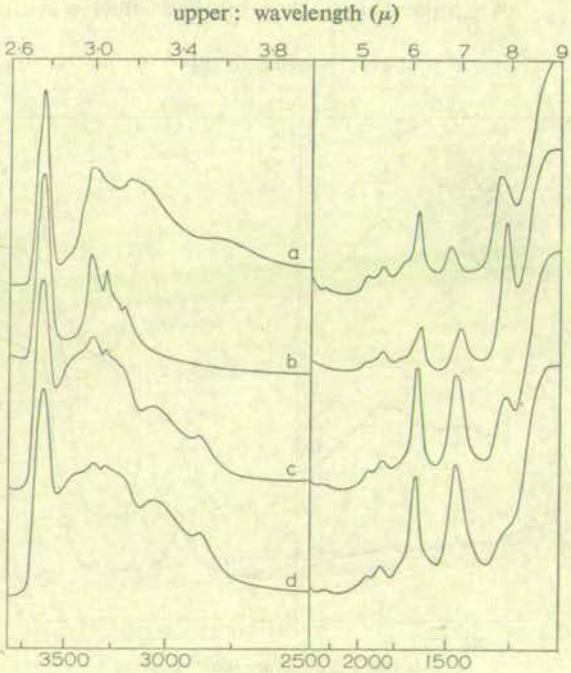

FIG. 3.—Infra-red absorption spectra of Cu(II)-montmorillonite in dry NH_3 gas (*a*), evacuated (*b*), then exposed to air of 40 % relative humidity for 30 min (*c*) and 18 h (*d*).

quoted for ammino-copper(II) salts.[12, 15] A small amount of NH_4^+ was also produced and gave rise to the NH_3-perturbed vibrations at about 2740 and 1464 cm^{-1}. Removal of the NH_3 atmosphere by evacuation at room temperature without exposure to air produced a sharper but not weaker pattern (fig. 3*b*) in which the deformation vibrations at 1630 and 1270 cm^{-1} shifted to 1620 and 1260 cm^{-1}, the

latter having also become more intense. These changes are consistent with the copper-co-ordinated NH_3 molecules having been freed from bonding to interlayer ammonia. The NH_4^+ vibrations are also unperturbed following evacuation. Analysis showed that the copper ions co-ordinated about 184 mmoles NH_3 per 100 g water-free sample (corresponding to 4·1 NH_3 molecules for each Cu) which were stable to evacuation. When the evacuated sample was exposed to air, the spectral changes indicated progressive decomposition of the amminocopper(II) ions and formation of NH_4^+ as the sample hydrated (fig. 3*c* and *d*). A weak inflection near 1270 cm^{-1} was still present after 2 days' exposure of the sample to saturated water vapour, indicating that some of the amminocopper(II) ions were particularly stable. The NH_4^+ content developed after exposure to the atmosphere for several days was close to the cation exchange capacity of the clay.

SAPONITE

On treatment with ammonia, the various substituted forms of saponite showed changes in infra-red absorption pattern similar to those in corresponding montmorillonites. But, whereas in Ca-montmorillonite the amount of NH_4^+ formed was equivalent to 75 % of the cation exchange capacity, in Ca-saponite this figure was only about 34 %. A similar though less marked effect was observed for Mg:

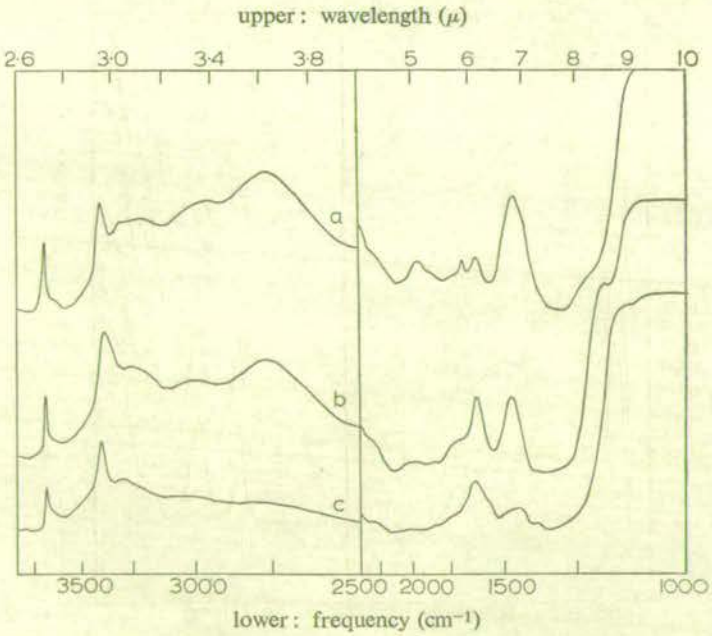

FIG. 4.—Infra-red absorption spectra of saponite, saturated with various cations, in dry NH_3 gas: (*a*) Mg^{2+}, (*b*) Ca^{2+}, (*c*) Li^+.

90 % for montmorillonite, 70 % for saponite. The amounts of NH_4^+ formed in saponite indicate that the exchangeable Ca and Mg ions are only partially converted to hydroxides, and NH_3 determinations (table 1) show that the remaining Ca and Mg ions are co-ordinated by NH_3.

The saponite spectra confirm that NH_3 is co-ordinated to Li, Ca and Mg ions; because of the lower frequency of the principal Si—O vibration of trioctahedral

saponite [16] compared with dioctahedral montmorillonite [13] it proved possible to observe absorption bands at 1127, 1174 and 1218 cm^{-1} with Li, Ca and Mg, respectively (fig. 4). These bands occur in the region expected for the symmetrical deformation vibration of co-ordinated NH_3 and they are consequently assigned to this vibration. Evacuation of Ca-saponite following treatment with ammonia resulted in a marked intensification of the 1174 cm^{-1} band (analogous to the band at 1270 cm^{-1} in NH_3-treated Cu-montmorillonite) and a shift to 1193 cm^{-1}. This frequency shift is in the opposite direction to that observed for Cu-montmorillonite: it is thought to be due to a decrease in the co-ordination number of Ca^{2+} from probably six in the presence of excess NH_3, to two in the evacuated state. The intensification of the band is, as described for Cu-montmorillonite, the result of the unhindered vibration of the co-ordinated ammonia molecules following the removal of NH_3 in outer spheres of co-ordination. While the co-ordinated NH_3 stretching band in all of the montmorillonite samples except that saturated with copper occurred in the range 3400 ± 4 cm^{-1}, the band in the saponites (excluding Ca-saponite) lay at 3391 ± 3 cm^{-1}. With Ca-saponite the band occurred at 3373 cm^{-1} and was much broader than those in the 3390 cm^{-1} region, signifying stronger co-ordination bonds round Ca^{2+}. It can be seen from the intensity of the perturbed NH_4^+ band near 1460 cm^{-1} (fig. 4) that the amount of NH_4^+ formed is highest with Mg^{2+} and lowest with Li^+ and also, from the intensity of the 3400 cm^{-1} band, that interlayer NH_3 is probably highest with Ca^{2+}. Thus, with Ca^{2+} there is considerable competition between formation of NH_4^+ and co-ordination of NH_3; compared with Mg^{2+} the latter is favoured. The amounts of NH_3 retained against evacuation (table 1) follow the same sequence for saponite as for montmorillonite, viz., $Li > Na > Ca > Mg > K$, NH_4, but the absolute values are higher.

The 3711 cm^{-1} band of interlayer $Mg(OH)_2$ was just detectable in NH_3-treated Mg saponite.

STABILITY OF NH_4

Fig. 5 shows the decomposition, on exposure of the samples to air, of the additional NH_4^+ formed in the various NH_3-treated montmorillonites, NH_4^+ being calculated from the intensity of its 1440 cm^{-1} absorption band. For the multivalent ions, as already noted, the amount of NH_4^+ initially formed approaches the cation exchange capacity with Al^{3+} and Mg^{2+} but is somewhat lower with Ca^{2+}, and its decomposition during the first six days is fastest with Ca^{2+} and slowest with Al^{3+}. The further decrease in NH_4^+ was identical for Ca^{2+} and Mg^{2+} while that for Al^{3+} was much slower. The NH_4^+ contents of the samples exposed to air for 14 days were confirmed by analysis.

Decomposition of the NH_4^+ formed on NH_3-treatment of montmorillonite saturated with monovalent cations was rapid with K^+ and NH_4^+ but more gradual with Li^+ and Na^+. The deformation vibration of NH_4^+ formed in montmorillonite saturated with these monovalent cations occurs at the frequency (1430 cm^{-1}) of the anhydrous NH_4 cation, even after long exposure to the atmosphere, and the band has an anomalous shape. The additional NH_4^+ formed in NH_4-montmorillonite is removed by evacuation at 0·02 mm Hg.

When Ca-montmorillonite was exposed to ammonia containing 3 % v/v CO_2, the NH_4^+ formed was stabilized, 70 m equiv. of NH_4^+ remaining after 3 days exposure to the air. CO_2 analyses indicated that equivalent amounts of $CaCO_3$ and NH_4^+ were formed. The presence of CO_2 in the ammonia did not influence the stability of the NH_4^+ formed in Mg-montmorillonite.

DISCUSSION

The present results constitute the first conclusive proof that co-ordination complexes contribute to the chemisorption of ammonia by montmorillonite and saponite, although this mechanism has frequently been postulated.[7-9] Mortland has independently (private communication) detected co-ordinated ammonia in montmorillonite containing the transition metal cations, Cu^{2+} and Co^{2+}; our results give, in addition to evidence for the formation of the tetramminocopper(II) ion, clear evidence for co-ordination of ammonia to alkali and alkaline-earth metal cations. The suggestion of James and Harward [8] that Al^{3+} and Mg^{2+} co-ordinate NH_3 in mont-

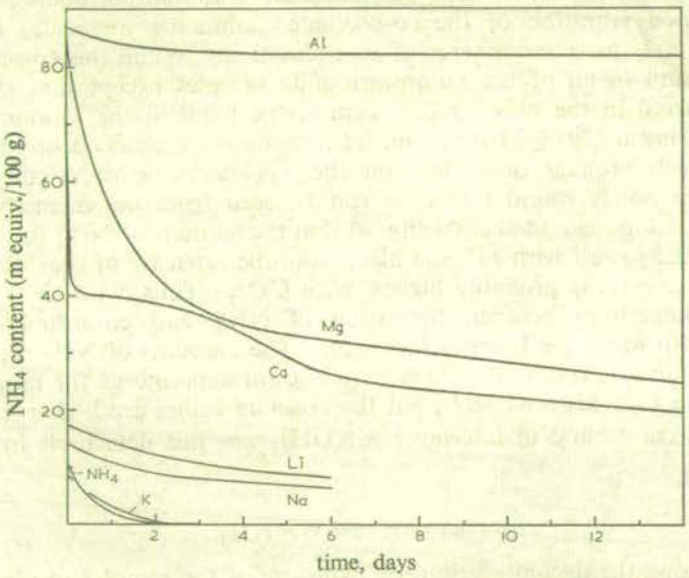

FIG. 5.—Decrease, with exposure to air at about 40 % relative humidity, of the NH_4 formed by NH_3 treatment of montmorillonites containing the following exchangeable cations: (*a*) Al, (*b*) Mg, (*c*) Ca, (*d*) Li, (*e*) Na, (*f*) K, (*g*) NH_4. NH_4 content was estimated from the optical density of the 1440 cm^{-1} infra-red absorption band of the NH_4 cation.

morillonite has, however, been disproved. The infra-red spectrum of NH_3 co-ordinated to alkali or alkaline-earth metal cations has not been previously observed in any environment. The frequency of the NH_3 deformation vibration in these complexes is lower than that found for ammonia co-ordinated to transition metal cations.[12] The high frequency of the N—H stretching vibration observed in montmorillonite (3400 cm^{-1}) is consistent with weak co-ordinate bonds, and weak hydrogen bonding to the silicate lattice. The lower frequencies observed in saponite (3373-3390 cm^{-1}) indicate slightly stronger bonding to the silicate lattice, which can perhaps be correlated with the higher Al-for-Si substitution in saponite.

NH_3 co-ordinated to NH_4^+ and K^+ at NH_3 pressures of 1 atm is lost on evacuation, and the 17-19 mmoles NH_3 retained by K- and NH_4-montmorillonite are thought to be adsorbed at lattice edges and other imperfections, as are the 38 mmoles retained by K- and NH_4-saponite. Correction of the total ($NH_3+NH_4^+$) figures for NH_3 adsorbed on the lattice and for the estimated NH_4^+ contents gives co-ordination numbers, following evacuation at room temperature, of two for Li^+ and one for Na^+ in both minerals, and four for Cu^{2+} in montmorillonite. Estimates of the

amount of NH_3 co-ordinated by Mg^{2+} and Ca^{2+} are necessarily only approximate, as a considerable proportion of these ions are converted to hydroxides. There is clear evidence that $Mg(OH)_2$ does not retain NH_3, and on the assumption that this is also true for $Ca(OH)_2$, co-ordination numbers for Ca^{2+} of four in montmorillonite and two in saponite, and of one for Mg^{2+} in saponite are obtained.

Ammonia occupies the interlayer space in montmorillonite, giving d(001) spacings which are dependent on the cation and the NH_3 pressure.[3, 4] The infra-red spectra of montmorillonite and saponite in NH_3 at a pressure of 1 atm show that water is completely replaced and give information on the mechanisms by which this ammonia is adsorbed. In NH_4-montmorillonite the NH_3 is involved in strong hydrogen-bonding to the cation; in Cu-montmorillonite, additional NH_3 molecules are held by hydrogen bonding round the tetramminocopper(II) cation. This additional NH_3 in outer spheres of co-ordination does not give a sharp band at 3400 cm^{-1} (fig. 3); its absorption bands in this region are presumably rather broad and at lower frequencies, like those of liquid ammonia.[17] The higher intensity of the 3400 cm^{-1} band of co-ordinated ammonia in Na-, Li- and Ca-clays indicates that these cations co-ordinate more ammonia when the gas pressure is higher. A co-ordination number of 3 has been suggested [7] for Na^+ in montmorillonite exposed to NH_3 at a pressure of 45 cm Hg.

Interlayer and co-ordinated ammonia are generally rapidly displaced by water on exposing clay films to the atmosphere. The exception is ammonia co-ordinated to Cu^{2+}: $[Cu(NH_3)_4]^{2+}$ undergoes hydrolysis to give $Cu(OH)_2$ and NH_4^+. This reaction, which also occurs in aqueous solution,[18] must be contrasted with the behaviour of the hexamminocobalt(III) cation in montmorillonite.[19] This cation is stable to water, but decomposes on heating or in vacuum at room temperature, to give NH_4^+. The amminocopper cation is stable in vacuum.

Mortland *et al.*[4] related the amounts of NH_4^+ formed in base-saturated montmorillonite to the amounts of water retained by the different cations after evacuation at various temperatures. They considered that for all the cations they examined (Li, Na, K, Cs and Ca), NH_4^+ was formed by the reaction of NH_3 with this residual water, whose acidity was increased by the polarizing effects of the interlayer cations. They ascribed a band observed at 2632 cm^{-1} in Ca-montmorillonite treated with ND_3 to an adsorbed OD^- group formed by this reaction. The low frequency of its vibration implied that the OD^- group was strongly perturbed by its environment, as a free OD^- group would adsorb near 2710 cm^{-1}. This band has, however, been shown [11] to be more probably due to a lattice OD group, perturbed by the Ca^{2+} ion. In the present investigation the OH vibration of interlayer $Mg(OH)_2$ has been identified, little perturbed by its environment. Under the conditions used here, the water content is not a limiting factor, and the reaction with Al^{3+}, Mg^{2+} and Ca^{2+} can, as suggested by Brown and Bartholomew,[6] be more conventionally considered as the precipitation of these less basic hydroxides in the interlayer space, while ammonium ions replace the exchangeable cations on the exchange sites. Precipitation of $Al(OH)_3$ is quantitative, and the ammonium formed is stable to water vapour. The amounts of Ca^{2+} and Mg^{2+} converted to their hydroxides differ in montmorillonite and saponite, indicating that the environment does play a part. The $Ca(OH)_2$ and $Mg(OH)_2$ initially formed react with the NH_4 ions when atmospheric water displaces excess ammonia from the interlayer space, and the exchange sites are then re-occupied by Ca^{2+} and Mg^{2+}. The soil atmosphere has a higher CO_2 content than the laboratory atmosphere, and evidence presented here suggests that NH_4^+ formed in Ca-saturated soil clays would be stabilized by conversion of the $Ca(OH)_2$ to $CaCO_3$.

The reaction $M^+ + H_2O + NH_3 \rightarrow MOH + NH_4^+$ cannot occur when M^+ is NH_4^+, and seems improbable with the more basic monovalent cations. If it did occur it would be expected to reverse rapidly on admitting water vapour, but in fact Na-, Li- and K-montmorillonites do not show the initial rapid loss of NH_4^+ observed in Ca-montmorillonite, where $Ca(OH)_2$ is certainly formed. Weakly acidic sites [6] can account for the NH_4^+ (about 10 m equiv./100 g) taken up by NH_4- and K-montmorillonite. The higher amounts of NH_4^+ formed in Li- and Na-montmorillonite and its greater stability can be explained if montmorillonite contains some sites like those in vermiculite. NH_4^+ and K^+ in vermiculite are not hydrated and these ions are not readily displaced by other cations. The position of the NH_4^+ deformation vibration in Na- and Li-montmorillonite following ammonia treatment indicates that the NH_4^+ is not hydrated even after long exposure to the atmosphere. Thus, the additional NH_4^+ taken up by these samples (7-10 m equiv./100 g) can be better ascribed to strong adsorption of the NH_4^+, rather than to increased acidity of co-ordinated water molecules.

Although most of the mechanisms established here by which NH_3 is adsorbed by montmorillonite and saponite have been previously postulated, excessive importance has sometimes been ascribed to one or other of them. The present quantitative study places them in perspective, and provides a rational basis for the interpretation of such studies as those of Young and McNeal [10] on the rate of loss of NH_3 from a variety of clay minerals.

The author thanks Dr. V. C. Farmer for his continuous interest in the work and for valuable discussions and advice, also Miss P. Duncan and Messrs. W. J. Scott and J. A. C. Martin for their help in recording spectra and determining NH_3.

1 Mortland, *Adv. Agron.*, 1958, **10**, 325.
2 Mortland and Wolcott, to appear in *Nitrogen* (monograph no. 10 of A.S.A.), ed. Bartholomew (Amer. Soc. of Agron., 1965).
3 Cornet, *J. Chem. Physics*, 1943, **11**, 217.
4 Mortland, Fripiat, Chaussidon and Uytterhoeven, *J. Physic. Chem.*, 1963, **67**, 248.
5 Mortland, *Soil Sci.*, 1955, **80**, 11.
6 Brown and Bartholomew, *Proc. Soil Sci. Soc. Amer.*, 1962, **26**, 258.
7 Barrer and Macleod, *Trans. Faraday Soc.*, 1954, **50**, 980.
8 James and Harward, *Clays Clay Miner.*, 1962, **11**, 301.
9 Slabaugh and Siegel, *J. Physic. Chem.*, 1956, **60**, 1105.
10 Young and McNeal, *Proc. Soil Sci. Soc. Amer.*, 1964, **28**, 334.
11 Russell and Farmer, *Clay Miner. Bull.*, 1964, **5**, 443.
12 Nakamoto, *Infra-red Spectra of Inorganic and Co-ordination Compounds*, (Wiley and Sons, London, 1963), p. 143.
13 Farmer and Russell, *Spectrochim. Acta*, 1964, **20**, 1149.
14 Slaughter and Milne, *Clays Clay Miner*, 1960, **7**, 114.
15 Powell and Sheppard, *J. Chem. Soc.*, 1956, 3108.
16 Farmer, *Miner. Mag.*, 1958, **31**, 829.
17 Demidenkova and Shcherba, *Dokl.* (*Proc.*) *Acad. Sci. U.S.S.R.* (*Phys. Chem. Sect.*), 1958, **22**, 1110.
18 Mellor, *A Comprehensive Treatise on Inorganic and Theoretical Chemistry* (Longmans, London, 1946), vol. 3, p. 190.
19 Chaussidon, Calvet, Helsen and Fripiat, *Nature*, 1962, **196**, 161.

PRINTED IN GREAT BRITAIN AT
THE UNIVERSITY PRESS
ABERDEEN

Spectrochimica Acta, 1966, Vol. 22, pp. 389 to 398. Pergamon Press Ltd. Printed in Northern Ireland

Effects of particle size and structure on the vibrational frequencies of layer silicates

V. C. FARMER and (in part) J. D. RUSSELL
Department of Spectrochemistry, The Macaulay Institute for Soil Research, Craigiebuckler, Aberdeen

(*Received* 17 *June* 1965)

Abstract—The dependence on particle size of the position and shape of certain absorption bands in the spectra of kaolin minerals is ascribed to an effect of the oscillating electric fields induced by the vibrating dipoles. These dipole-induced fields can also account for some discrepancies between calculated and observed frequencies in layer silicate spectra. The effects of dipole coupling between layers and within layers are distinguished. The OH vibration of the mica, phlogopite, is shown to be affected by the electrostatic field due to interlayer potassium ions.

1. INTRODUCTION

SOIL minerals occur in sizes ranging from submicroscopic clays to coarse sands, and in characterizing them by their infra-red spectrum, it is important to recognize those features of the spectra which are purely a function of particle size, so that these can be distinguished from features which reflect variations in composition and structure. The appearance of infra-red spectra is influenced by the well-known Christiansen effect, which is dependent on particle size. Marked changes in the position and appearance of certain absorption bands in the spectra of kaolin minerals have, however, been observed at particle sizes below that at which the Christiansen effect is important [1]. It is the purpose of this paper to show that these effects can, at least qualitatively, be accounted for by consideration of the self-induced fields produced by the oscillating dipoles which give rise to the infra-red absorption bands. That particle size and shape must affect the vibrational frequencies of crystals is clear from FRÖHLICH's discussion of longitudinal and transverse vibrations [2]. FARMER and RUSSELL [1] recognized this effect in the spectra of the kaolin minerals, and BERREMAN [3] has given experimental evidence of the effect in an isotropic crystal. The layer silicates are approximately uniaxial, and in this paper the theory is extended to include crystals of this type. The effect of crystal structure and composition on the vibrational frequencies of layer silicates is also considered.

2. EFFECTS OF PARTICLE SIZE AND SHAPE

Single crystal specimens of the layer silicates can scarcely be obtained thin enough to study the fundamental Si—O stretching frequencies by absorption techniques, although reflection studies can and have been made on micas, most recently by

[1] V. C. FARMER and J. D. RUSSELL, *Spectrochim. Acta* **20**, 1149 (1964).
[2] H. FRÖHLICH, *Theory of Dielectrics*, 2nd Edn., Oxford University Press, 1958.
[3] D. W. BERREMAN, *Phys. Rev.* **130**, 2193 (1963).

VEDDER [4]. Many minerals occur only in microcrystalline form. Absorption studies have therefore been made principally on powders consisting of thin platy particles of dimensions much smaller than the wavelength of the infra-red radiation. Under these conditions, the polarization (P) of the dielectric associated with a crystal vibration produces an effective charge on the crystal surface. When P is perpendicular to the crystal plates [Fig. 1(a)], this surface charge gives rise to a field

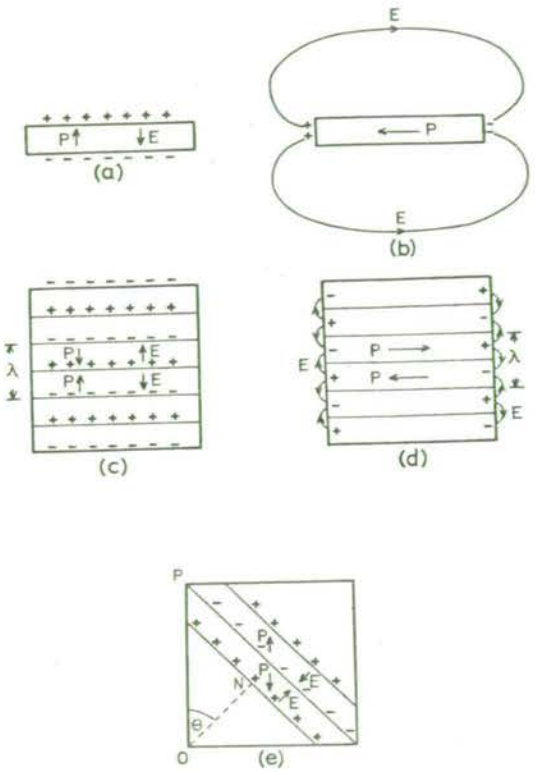

Fig. 1. The dielectric polarization and associated fields produced by vibrations: (a) and (b) in thin platy crystals; (c) in the longitudinal crystal mode and (d) the transverse crystal mode of large isotropic crystals; and (e) in a crystal mode where the wave vector make an angle θ with the optic axis of a uniaxial crystal.

(E) of magnitude $-4\pi P$ which opposes the dipole vibration, and so increases the effective force constant of the vibration. This increased force constant causes a rise in the vibration frequency; the magnitude of this rise is dependent on the magnitude of the dipole moment induced by the vibration. When P is parallel to the crystal plates [Fig. 1(b)], the field is diffuse and does not significantly affect the vibrational frequency. For particles not platy in form, the induced fields will differ: for spheres the field is given by $-4\pi P/3$, and for vibrations perpendicular to the axis of a cylinder, the field is $-2\pi P$.

[4] W. VEDDER, *Am. Mineralogist* **49**, 736 (1964).

For thin platy crystals of isotropic material, the frequency of a vibration perpendicular to the plates corresponds to that of the longitudinal mode (ν_l) in large crystals, whereas the frequency parallel to the plates corresponds to that of the transverse mode (ν_t) in large crystals. In the longitudinal mode, which is inactive in the infra-red, but active in the Raman spectrum [5], polarization waves are set up in the crystal in which the polarization is perpendicular to the wavefronts, and the dipoles are subjected to a self-induced field equal to $-4\pi P$ [Fig. 1(c)] as in the perpendicular vibrations of thin plates [Fig. 1(a)]. In the transverse mode, which is active in both the infra-red and Raman spectrum, the vibrating dipoles are not subjected to this self-induced field [Fig. 1(d)] as in the vibrations parallel to the plane of thin platy crystals [Fig. 1(b)]. BERREMAN [3] has observed the appearance of absorption near the longitudinal frequency (675 cm^{-1}) in the spectrum of a thin layer of lithium fluoride at oblique incidence. At normal incidence, absorption occurred only at the transverse frequency (307 cm^{-1}).

The layer silicates are anisotropic. Although biaxial, they can be treated to a first approximation as uniaxial, with the axis perpendicular to the plates. In uniaxial crystals, large compared with the wavelength of the lattice modes involved, the absorption frequency of a crystal vibration can range between two limits, ν_t and ν_l, depending on the angle, θ, between the optical axis and the normal to the lattice wave [6]. Thus in Fig. 1(e), dipoles oscillating parallel to the axis are subjected to a self-induced field $E = 4\pi P \cos\theta$, which has a component $-4\pi P \cos^2\theta$ opposing the vibration. The square of the vibrational frequency is directly proportional to the effective force constant of the vibration, and the increase in the force constant is directly proportional to the opposing field. Accordingly, the frequency of the vibration is given by

$$\nu_\theta^2 = \nu_t^2 + (\nu_l^2 - \nu_t^2)\cos^2\theta. \tag{1}$$

Similar considerations show that for vibrations perpendicular to the optical axis, and lying in the plane containing this axis and the wave normal, the corresponding formula is

$$\nu_\theta^2 = \nu_t^2 + (\nu_l^2 - \nu_t^2)\sin^2\theta. \tag{2}$$

Vibrations perpendicular to both the axis and the wave normal occur at the limiting transverse frequency, ν_t, for all values of θ. These conclusions have been verified in reflection, absorption and Raman spectra of large uniaxial crystals [6, 7]. However for thin platy uniaxial crystals whose thickness is much less than the wavelength of the lattice waves, the conditions illustrated in Fig. 1(a) obtain when the optical axis is perpendicular to the plates. Vibrations perpendicular to the plates occur at the limiting longitudinal frequency, ν_l, and vibrations in the plane of the plates occur at the limiting transverse frequency, ν_t. These frequencies are independent of the direction of incidence of the infra-red radiation which excites the vibrations.

---

[5] W. VEDDER and D. F. HORNIG, *Advances in spectroscopy* **2**, 189 (1961).
[6] J.-P. MATHIEU, H. POULET and A. TRAMER, *Z. Elektrochem.* **64**, 699 (1960).
[7] J. A. A. KETELAAR, C. HAAS and J. FAHRENFORT, *Physica* **20**, 1259 (1954).

The effects of particle size noted in the kaolin minerals [1] and illustrated for nacrite in Fig. 2, can be interpreted on the basis of the above considerations. The kaolin minerals are layer silicates which contain silicon–oxygen tetrahedra linked to form infinite sheets with a distorted hexagonal structure (Fig. 3). The platy crystal habit of these minerals reflects the structure of the anion sheets. Stretching vibrations involving Si—O—Si bonds accordingly have their dipole oscillation in the plane of the plates, whereas Si—O$^-$ bonds (whose charges are balanced by Al^{3+} in octahedral co-ordination) give a dipole oscillation perpendicular to the plates

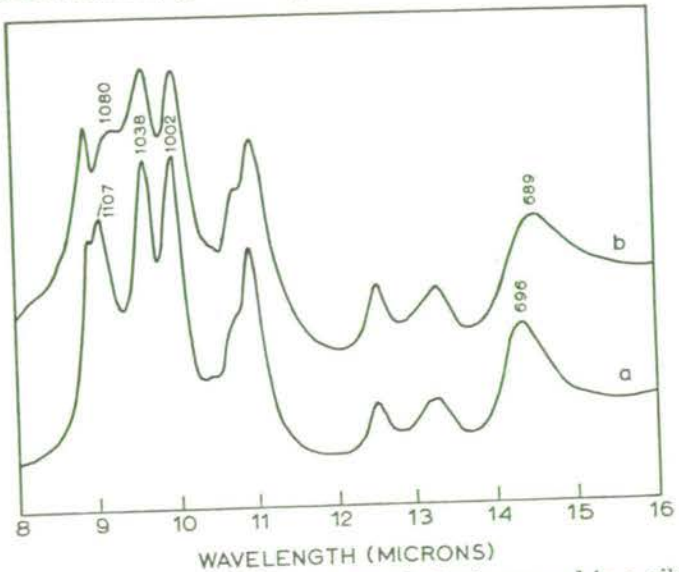

Fig. 2. Infra-red spectra of nacrite: (a) sample finely ground in a vibratory ball mill; (b) coarse material with equivalent spherical diameters between 1·4 and 6 μ.

[1]. For very finely ground nacrite in KBr disks, the perpendicular Si—O$^-$ v
bration appears as a sharp band at 1107 cm^{-1} [Fig. 2(a)], which must correspond t
ν_t. With larger particles, separated by sedimentation, the band appears as a broa
shoulder at 1080 cm^{-1} [Fig. 2(b)]. This broad shoulder corresponds to absorptio
by randomly oriented particles, and so to a range of values of θ in equation 1. Wit
$\theta = 0°$, $\nu_\theta = \nu_t$ but there is no absorption; as θ increases the absorption inte
sifies and the band shifts to lower frequencies. Refraction at the surface of thes
platy crystals can be expected to keep θ well below 90°, so that the transverse fr
quency, ν_t, corresponding to this Si—O$^-$ vibration cannot be estimated from the
results. It will be noted (Fig. 2) that a weaker perpendicular band, at 696 cm^{-1} f
the finely ground material [1], is also displaced to lower frequencies (689 cm^{-1}) f
the larger particle-size fraction.

The in-plane Si—O—Si stretching vibrations at 1038 cm^{-1} and 1002 cm^{-1} a
little affected by particle size (Fig. 2). For the finely ground material, the observ
frequencies correspond to ν_t and this is also the frequency at which larger partic
absorb most strongly, i.e. when $\theta = 0$ in equation 2. Refraction at the crystal su
face must keep θ close to zero within the crystal for the randomly oriented partic
in the KBr disk, so that the frequency does not differ significantly from ν_t.

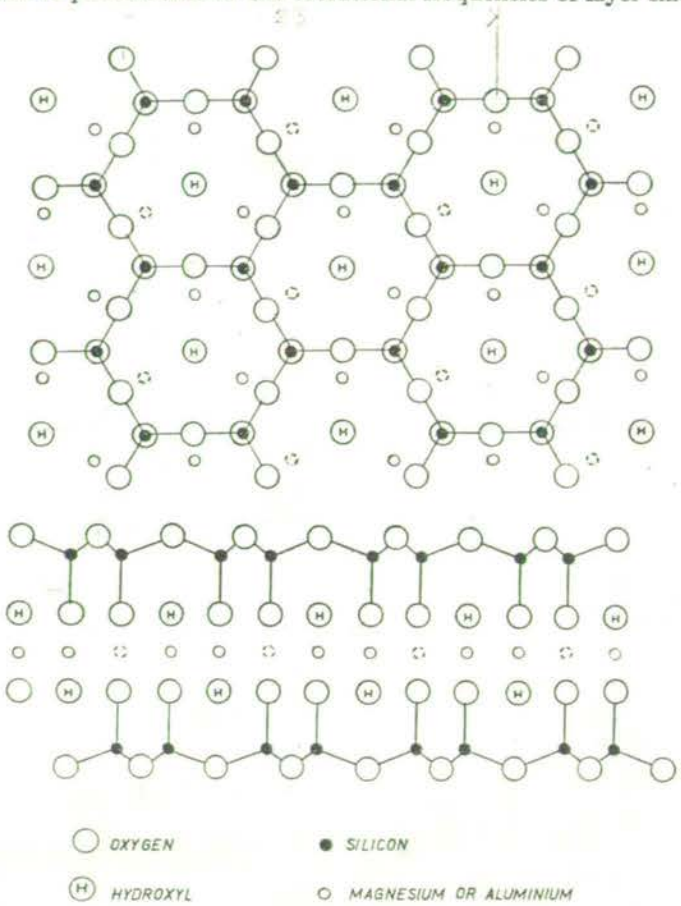

Fig. 3. The structures of the 2:1 layer silicates, talc and pyrophyllite. For clarity only one of the silicate anions is shown in the plan: the other is related to it by centres of symmetry at the dotted sites. In the 1:1 layer silicate, such as the kaolin minerals, one of the two silicate anions is replaced by a layer of hydroxyl groups.

The larger size fraction used for spectrum (b), Fig. 2, was separated by sedimentation, and had equivalent spherical diameters in the range 1·4–6 μ. Examination of this fraction by optical microscopy, following sedimentation on a glass slide and carbon-palladium shadowing, showed it to consist of platy crystals with surface dimensions between 1·3 and 7 μ (mode 2·5 μ) and with thicknesses between 0·2 and 2 μ (mode 0·4 μ). It is remarkable that these particles behave as crystals which are large compared with the wavelength of the lattice modes associated with the perpendicular Si—O^- vibration. This implies a very high refractive index, as the wavelength corresponding to this frequency in air is near 9 μ.

2.1 *Comparison of observed and calculated vibrational frequencies*

Approximate calculations based on reasonable sets of force constants have indicated that the stretching frequency of Si—O^- bonds should be lower than those of Si—O—Si bonds in layer silicates [4]. Powdered material in potassium bromide

disks almost invariably shows the Si—O⁻ vibration at higher frequencies than Si—O—Si vibrations, sometimes over 100 cm^{-1} higher [1, 8]. The only exception is pyrophyllite, where the Si—O⁻ vibration appears to coincide in frequency with a Si—O—Si vibration [1]. The discussion in the previous section has shown, however, that the observed Si—O⁻ frequency corresponds to that of the longitudinal mode, whereas the Si—O—Si frequency corresponds to that of the transverse mode. It seems likely, therefore, that this discrepancy between calculated and observed results would be resolved if the frequencies of corresponding crystal modes were compared. Certainly this appears to be true for talc. In powdered crystals ν_t for Si—O⁻ appears at 1045 cm^{-1}, while ν_t for Si—O—Si is at 1018 cm^{-1} [8]. Some estimate can, however, be made for ν_l for Si—O—Si from the reflection spectrum off the cleavage plane of a large talc crystal, reported by LAZAREV [9]. Strongly infra-red active vibrations are associated with broad regions of nearly total reflection extending between the limits ν_t and ν_l [5]. The talc reflection spectrum shows such a region of high reflectivity between about 1020 cm^{-1} and 1140 cm^{-1}, which can be associated only with the doubly degenerate in-plane Si—O—Si vibrations, so that ν_l for this vibration must lie near 1140 cm^{-1}, that is, considerably higher than ν_l for the perpendicular Si—O⁻ vibration, which is at 1045 cm^{-1}. It should be possible to estimate the transverse frequency for the Si—O⁻ vibration of talc from the reflection spectrum off a face cut perpendicular to the layers. Vedder [4] has reported such a reflection spectrum for muscovite, but it is uncertain, in this case, whether the whole region of strong reflection lying between 900 cm^{-1} and 1050 cm^{-1} can be ascribed to the perpendicular Si—O⁻ vibration, or whether some other vibration, such as an AlOH deformation frequency, contributes to it.

3. THE EFFECT OF CRYSTAL ENVIRONMENT

3.1 *Silicon–oxygen vibrations*

The polarization field which accounts for the difference between transverse and longitudinal frequencies is an average field arising from the separation of charges by distances of the order of 0·1 μ. Superimposed on this average field is a field varying over molecular dimensions, whose calculation requires the summation of the fields of the individual vibrating dipoles. It is therefore relevant to inquire, firstly, how the vibrational frequencies of a single layer of a layer silicate are affected by the layers between which it is sandwiched, and, secondly, how an individual bond vibration within any one layer is affected by neighbouring bond vibrations within that layer.

The first question can be answered by observations on the expanding layer silicates. In these 2:1 layer silicates, the separation of the layers can be varied by the introduction of various polar molecules in the interlayer space. In the course of the present study it has been established that the silicate vibrations are not dependent on whether the silicate layers are separated by a layer of water molecules, giving a d(001) spacing of 11·5 Å, or by a layer of cetylpyridinium bromide, which

[8] V. C. FARMER, *Mineral. Mag.* **31**, 829 (1958).
[9] A. N. LAZAREV, *Optika i Spektroskopiya Akad. Nauk SSSR Otd. Fiz.-Mat. Nauk Sb. Statei* **2**, 286 (1963).

gives [10] a spacing of 42 Å. Even in the anhydrous state when the layers are in Van Der Waals contact, giving a d(001) spacing of 9·5 Å, only minor frequency shifts and changes in band contour occur, some of which are undoubtedly due to the polarizing effect of the exchangeable cations which occupy the interlayer space [11]. These results indicate that there is little coupling between adjacent layers. This is indeed to be expected, as very little electric field will escape from a close-packed planar array of dipoles, no matter whether the dipoles are arranged parallel to the plane as in the Si—O—Si stretching vibrations, or perpendicular to the plane, as in the Si—O^- stretching vibration. It follows that the vibrational frequencies of an individual silicate layer are essentially identical with those of a thin platy crystal whose dimensions are smaller than the wavelength of the lattice vibration excited.

Within any one layer, all the Si—O^- groups are vibrating in phase, and the frequency of vibration of each is affected by the field arising from the vibration of all the others. There are considerable difficulties in the calculation of this field, since it requires a knowledge of the exact form of the vibration, which certainly involves the surface layer of oxygens as well as the inner oxygens of the silicon–oxygen tetrahedral layer. There are uncertainties, too, as to the location of the vibrating dipoles, which involve both nuclear and electronic displacements. Nevertheless, a qualitative picture of the effects can be readily obtained on the simplifying assumption that only Si—O^- bonds are vibrating, and that the field arises from charges (e_0 and e_{si}) residing on the vibrating ions. The vibrations of such a planar array of Si—O^- bonds, in which each bond is normal to the plane, cause no change in oxygen–oxygen forces, or in silicon–silicon forces, since these vibrate in phase. Each oxygen ion, however, is moving in the field produced by the charges residing on the silicon ions, with the result that the effective force constant of the Si—O^- vibration in this environment is higher than that of an isolated Si—O^- bond. The increase in the effective force constant is equal to the force experienced by a charge e_0, residing on the oxygen ion, due to dipoles of magnitude e_{si}, residing on the silicon ions, and pointing in the Si—O^- bond direction. In the summation, the dipole residing on the silicon to which the oxygen is bonded is not considered, as this force must be incorporated in the force constant of an isolated Si—O^- bond. The effect of distant silicon ions can be treated as equivalent to that of a uniform dielectric sheet. The increase in the force constant calculated on this basis is $9{\cdot}0 \times 10^4$ dyn/cm, when e_0 is taken as $-1{\cdot}5$ units, and e_{si} as $+2$ units. Further, a stretching vibration of the Si—O^- bond necessarily involves displacement of the oxygens relative to the sheet of magnesium or aluminium ions to which they are co-ordinated. On the assumption that this displacement is half that of the oxygens relative to silicon, the calculated increase in force constant from this motion is $1{\cdot}0 \times 10^5$ dyn/cm, assuming the Mg—O bond to be purely ionic. The total increase in the force constant ($1{\cdot}9 \times 10^5$ dyn/cm) can be compared with the decrease in the force constant due to the field $4\pi P$ which arises from the polarization of the surrounding dielectric in the transverse mode of large crystals. On the basis of the ionic charges assumed

[10] D. J. Greenland and J. P. Quirk, *Clays and Clay Minerals* **9**, 484 (1962).
[11] J. D. Russell and V. C. Farmer, *Clay Min. Bull.* **5**, 443 (1964).

above, this would be about $2{\cdot}0 \times 10^5$ dyn/cm in the talc structure. This implie that the frequency of an isolated Si—O$^-$ band would be close to, but rather highe than the transverse crystal frequency, but considerably lower than the longitu dinal frequency. A similar calculation made for the in-plane Si—O—Si vibration on the simplifying assumption that the oxygen ion lattice is displaced as a whol relative to the silicon ion lattice, indicates that the force constant of an oxyge undergoing displacement in the plane along the Si—O—Si bond direction is reduce by $4{\cdot}5 \times 10^4$ dyn/cm due to its environment, taking the charge on silicon as $+2$, an that on oxygen as -1. Thus, here too, the effect of the dipole coupling forces is t lower the frequency of the transverse mode below that which would be found i they did not operate.

The considerations presented above allow some predictions to be made abou the frequencies of the Raman active vibrations in layer silicates. In the 2:1 laye silicates, such as talc, pyrophyllite and the micas, there are two sheets of silicon oxygen tetrahedra linked through di- or tri-valent ions to form a composite laye (Fig. 3). The two sheets are related by a centre of symmetry, so that separat Raman active and infra-red active vibrations will appear for each mode of vi bration of a single silicon–oxygen sheet. Little or no dipole or mechanical couplin can occur between the in-plane Si—O—Si vibrations of the two tetrahedral sheets as the silicon ions are separated by about 5·4 Å, so the Raman active mode mus have a frequency close to that of the observed infra-red active mode. On the othe hand the apical oxygens of the two layers are in contact, so that the Raman Si—O stretching frequency could differ from the corresponding infra-red frequency. Th calculated dipole-coupling force acting on any one oxygen due to its motio relative to the other sheet of oxygens is zero in the infra-red-active mode and $-3{\cdot}3 \times 10^4$ dyn/cm in the Raman active mode, lowering the effective Si—O$^-$ force con stant. The Raman frequency of the Si—O$^-$ vibration should therefore be rathe lower than the longitudinal frequency observed in the infra-red spectra of ver small crystals, but considerably higher than the corresponding transverse frequency

3.2 *The hydroxyl stretching vibration* (with J.D.R.)

Substitution of aluminium ions for a quarter of the silicon ions in talc and pyro phyllite (Fig. 3) gives the mica minerals, phlogopite and muscovite. The resultin negative layer charge is compensated by interlayer potassium ions. These sub stitutions shift and broaden the OH stretching absorption band. The 3677 cm band of talc shifts to 3710–3720 cm^{-1} in phlogopite [1, 4], and the 3675 cm^{-1} ban of pyrophyllite is replaced by a very broad band with a maximum at 3627 cm^{-1} an a shoulder at 3660 cm^{-1} [1,12]. FARMER and RUSSELL [1] ascribed these shifts t the layer charge, but VEDDER (private communication) suggested that the fiel exerted by the interlayer potassium ions may be more important. These ions ar positioned directly above the lattice hydroxyl groups (Fig. 3).

Observations now made on the clay minerals saponite and beidellite, which ha lower Al–for–Si substitution, confirm Vedder's suggestion for the talc saponit phlogopite series, but argue against it in the pyrophyllite–beidellite–muscovi

[12] W. VEDDER and R. S. MCDONALD, *J. Chem. Phys.* **38**, 1583 (1963).

series. The clay minerals do not contain sufficient interlayer cations to perturb all the lattice hydroxyls, and these cations can be changed by simple washing with appropriate salt solutions. In the anhydrous state, saponite with interlayer K^+ or Na^+ shows two bands; one at 3678 cm^{-1} corresponding to that of talc, and one at 3710–20 cm^{-1} corresponding to that of phlogopite [1]. The higher frequency component is lost when Na^+ and K^+ become hydrated, showing that it arises from a direct influence of the interlayer cation on the hydroxyl group. In saponite containing interlayer Ca^{2+}, whether hydrated or not, the OH absorption has no high frequency component, indicating that this cation is not positioned above the hydroxyl group.

In contrast to saponite, beidellite in the hydrated state has two broad OH bands of nearly equal intensity at 3660 cm^{-1} and 3635 cm^{-1} [1] which are independent of the exchange cation. Clearly, the 3635 cm^{-1} band, whose frequency is close to that of muscovite, is not due to perturbation of the OH vibration by the interlayer cation. This low-frequency component weakens slightly in anhydrous Na– and K–beidellite; it is very much reduced in intensity in anhydrous Ca–beidellite, and a new band then develops at 3553 cm^{-1}. This band corresponds to one developed in anhydrous Ca–montmorillonite at 3533 cm^{-1}, and like it must be ascribed to a lattice hydroxyl perturbed by Ca^{2+} [11]. The 3660 cm^{-1} band is little affected by the nature of the cation or its hydration state.

These results indicate that there are two different types of lattice hydroxyl groups in beidellite, as previously suggested by FARMER and RUSSELL [1], and show further that as water of hydration is removed from round the interlayer cations these then lie close to the hydroxyl groups which absorb at 3635 cm^{-1} in the hydrated state.

4. GENERAL CONSIDERATIONS

The influence of particle size and shape on vibrational frequencies, reported here for the kaolin minerals, can be expected to be a general effect in crystals which have strong infra-red absorption bands. Thus a marked sharpening of infra-red absorption bands should occur when one or more dimensions of the crystals are reduced below 0·1 μ provided that other factors which lead to band broadening such structural disorder or partial isomorphous substitutions are not operative. Certainly particle size effects should have an important influence on the spectra of amphiboles (chain silicates), which occur in both massive and fibrous forms.

It is clear from the considerations presented here that the frequencies of silicate vibrations can be considerably affected by dipole–dipole coupling forces because of the strong dipoles developed in Si—O vibrations. Such coupling forces must account for the marked differences in frequency and band contour found for the SiO_4 anion in the olivine structure, according to whether it is surrounded by other SiO_4 anions, as in the pure silicates, or surrounded by GeO_4 anions, when it is present in dilute solution in the isomorphous germanates [13]. It is possible, too, that dipole–dipole coupling may contribute to the anomalously high frequencies observed in certain silicate spectra. The calcium silicate, truscottite, has a medium

[13] P. TARTE, *Spectrochim. Acta*, **19**, 25 (1963).

intensity band at 1255 cm^{-1} [14], and the minerals sillimanite [15] and zunyite [16] have strong bands near 1200 cm^{-1}. These frequencies are well above the range (950–1100 cm^{-1}) in which the principal Si—O stretching frequencies of silicates commonly occur.

---

[14] R. A. CHALMERS, V. C. FARMER, R. I. HARKER, S. KELLY and H. F. W. TAYLOR, *Mineral. Mag.* **33**, 821 (1964).
[15] P. TARTE, *Silicates Industr.* **24**, 7 (1959).
[16] H. MOENKE, *Z. Chem.* **4**, 274 (1964).

ISRAEL JOURNAL OF CHEMISTRY
Volume 4, 1966, pp. 201-213

INFRARED STUDY OF THE ADSORPTION OF BENZOIC ACID AND NITROBENZENE IN MONTMORILLONITE

S. Yariv, J.D. Russell and V.C. Farmer

Department of Spectrochemistry, The Macaulay Institute for Soil Research, Aberdeen, Scotland

ABSTRACT

Nitrobenzene and benzoic acid are coordinated through water molecules to the more highly polarizing exchangeable cations in the interlayer space of montmorillonite, but are directly coordinated to NH_4^+ and possibly also K^+. On dehydration of the adsorption complexes the nitrobenzene and benzoic acid become directly coordinated to all of the exchangeable cations investigated. Benzoate ion was also formed in amounts which were dependent on the exchangeable cations.

Introduction

Soil organic matter and synthetic soil conditioners have a high content of carboxylic acid groups, and these groups must play an important part in the formation of clay-organic complexes in the soil. Consequently several workers [1,2,3] have studied the interaction of both simple and polymeric acids with montmorillonite by infrared techniques. The alkali halide pressed disk technique used in previous work is not wholly satisfactory for adsorption studies because of the possibility of interaction with the alkali halide, and the present investigation was undertaken using self-supporting clay films. A greater range of exchangeable cations was also examined, as the cation present has been shown to be the most important factor in determining the mechanism of adsorption of basic molecules in montmorillonite [4,5,6,7,8].

In infrared studies of adsorbed molecules, the maximum amount of information is obtained when these molecules have sharply defined absorption bands, whose vibrational assignment is well established. Accordingly, benzoic acid was selected for the present study, as changes in its spectrum associated with adsorption on alkali halides have been fairly fully characterized [9]. Benzoic acid is a simple analogue of the more complex unsaturated acids which make up humic acid. Further, substituted benzoic

Received: July 24, 1966.

acids are in use as herbicides, and so their fate in the soil is of importance. Adsorption of nitrobenzene was also studied as it is a close structural analogue of benzioc acid, but without the complications arising from the polar, ionizable hydroxyl group in the acid. From X-ray studies Greene-Kelly [10] showed that nitrobenzene is adsorbed in the interlayer space of Na-montmorillonite giving a well defined 15.2 Å complex. His results indicated that benzoic acid also entered the interlayer space, giving a 12.7 Å spacing with non-integral orders in Na-montmorillonite.

Experimental

The methods used to prepare thin clay films of Wyoming bentonite containing the required exchangeable cations have been described, as has the infrared spectrometer and ancillary equipment used [11]. Nitrobenzene was adsorbed by immersion of the clay films in nitrobenzene for 2 days, in watchglasses which were enclosed in a desiccator over P_2O_5. Excess nitrobenzene rapidly evaporated after the films were blotted between filter paper. Benzoic acid was taken up by clay films from boiling saturated solutions of benzoic acid in inert solvents such as cyclohexane, benzene, and carbon tetrachloride. The last was principally used in this work. Similar results were obtained when benzoic acid was adsorbed from the vapour phase at 100°C on montmorillonite, and when an aqueous dispersion of montmorillonite containing dissolved benzoic acid was evaporated to dryness. Layer spacings of the complexes were recorded with a Philips X-ray diffractometer, in the Chemistry Department, University of Aberdeen.

Results

Nitrobenzene-montmorillonite complexes

Nitrobenzene gave regular 15.2 Å complexes with Mg^{2+}, Ca^{2+}, and Cu^{2+}, but gave 15.35 Å complexes with Na^+, Li^+, NH_4^+, and Al^{3+}. K^+ gave a non-integral series with d(001) of 15.2 Å. The infrared spectra showed that water was completely displaced from K- and NH_4- montmorillonite (Figure 1c). Water remaining in montmorillonite containing the other cations was more weakly hydrogen bonded than that present in the normal hydrated state. Thus hydrated Mg-montmorillonite (Figure 1a) has a principal absorption band near 3420 cm^{-1} which can be ascribed to water-water hydrogen bonding. This band is replaced by one at 3500 cm^{-1} in the complex, which must be ascribed to water hydrogen bonded to nitrobenzene, and coordinated to the cation (Figure 1b). The more strongly polarizing cations cause the coordinated water to form stronger hydrogen bonds, absorbing at lower frequencies, so that this band appears at 3480 cm^{-1} with Cu^{2+}, 3500 cm^{-1} with Mg^{2+}, and 3530 cm^{-1} with Ca^{2+}. With Li^+ and Na^+ the maxima of the water absorption bands lay at still higher frequencies, where they were obscured by lattice hydroxyl absorption.

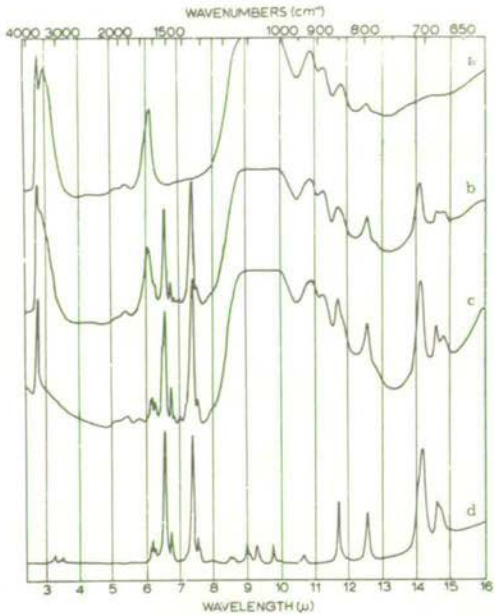

Figure 1

Infrared spectra of, a) hydrated Mg-montmorillonite b) Mg-montmorillonite-nitrobenzene complex, c) K-montmorillonite-nitrobenzene complex, d) liquid nitrobenzene.

The vibrational frequencies of intercalated nitrobenzene were essentially independent of the exchangeable cation, although they differed slightly but significantly from those of liquid nitrobenzene (Table I). In the hydrated complexes of the more polar ions, absorption bands at 856 cm^{-1} and 685cm^{-1} were depressed and broadened relative to the corresponding bands in the anhydrous complexes of K^+ and NH_4^+, and liquid nitrobenzene (Figure 1). The 856 cm^{-1} band involves an in-plane vibration of the NO_2 group [12] and the 685 cm^{-1} band corresponds to an X-sensitive vibration [13] of mono-substitued benzene (C_6H_5X). This observation indicates that the nitrobenzene is involved in hydrogen bonding through the nitro group with water coordinated to the more polar cations. On heating the films under vacuum at 50-100°C, changes in the spectrum indicated that part of the nitrobenzene became directly coordinated to Cu^{2+}, Mg^{2+}, and Ca^{2+}. New absorption bands corresponding to symmetrical stretching of the NO_2 group appeared at 1300 cm^{-1} for Cu^{2+}, at 1315 cm^{-1} for Mg^{2+}, and at 1340 cm^{-1} for Ca^{2+}. The antisymmetrical stretching vibration at 1523 cm^{-1} broadened and shifted 7-10 cm^{-1} to lower frequencies. The original spectrum was obtained when the complexes rehydrated. No significant shifts in frequency were observed with Na^+ or Li^+, although essentially all water was lost from Na^+ montmorillonite at 50°C in vacuum. Probably Na^+ is insufficiently polarizing to perturb the vibrations of the nitro group. The results with Li^+ suggest that nitrobenzene cannot displace coordinated water from this cation. There was some evidence that the anhydrous K^+ and NH_4^+ complexes contained more than one species of nitrobenzene, as a sharp band in the K^+

Table I

Vibrational frequencies (cm^{-1}) and assignments for nitrobenzene and benzoic acid in the free state and when complexed with Ca-montmorillonite

Vibration		Nitrobenzene		Benzoic acid	
Type	Species	Liquid	Ca-complex	Ca-complex	Dimer
NO_2 str.	B_1	1527	1523	1684	1690 C = O
	A_1	1350	1353	1415	1425 C-OH
				1275	1294 C-OH
NO_2 def.	A_1	853.5	856		
Ring vibrations	A_1			1604	1605
	B_1			1584	1585
	A_1	1480	1480	1495	1499
	B_1	1456	1458	1455	1453
	B_1	1318	1320	1320	1326
	A_1	1175	1182	1182	1181 / 1189
	B_2	795	796		
	B_2	704	709	717	708
	A_1	682.5	685	–	668
	B_2	677	675	685	684

complex, and a shoulder in the NH_4^+ complex, appeared at 1535 cm^{-1} on the side of the main 1523 cm^{-1} band. It is noteworthy that both the stretching and bending vibrations of the NH_4^+ ion in the nitrobenzene complex were indistinguishable from those of the anhydrous NH_4^+ cation in montmorillonite in the absence of nitrobenzene [6]. Clearly interaction between the NH_4^+ and nitrobenzene is weak and comparable in character to that with the silicate lattice.

Nitrobenzene was displaced from montmorillonite fairly rapidly by water vapour, at 45% R.H., but the last traces were slowly eliminated, especially with Cu^{2+} and the monovalent cations; the single water layers associated with these cations give lower layer separations than the double layer associated with Ca^{2+} and Mg^{2+}, and this is likely to restrict the rate of diffusion in the interlayer space. Thus all nitrobenzene was eliminated from the Mg^{2+} complex in 4 days, while traces still persisted in the Cu^{2+} complex after 9 days. Changes in the orientation of nitrobenzene were noted as the nitrobenzene was displaced by water from the Ca^{2+} complex. On the basis of observations similar to those made on pyridine in montmorillonite [8], it was found that in the freshly prepared complexes, the nitrobenzene was oriented with its axis of symmetry nearly parallel to the clay sheets, and the plane of the ring at a high angle to the sheets. B_1 absorption bands at 1450 cm^{-1} and 1320 cm^{-1} increased in intensity by 60-80% when the clay film was inclined at 45° to the infrared beam, and the NO_2 antisymmetric stretching band at 1523 cm^{-1} increased by 50%. In films from which the greater part of the interlayer nitrobenzene had been displaced by water, the nitrobenzene molecule took up an orientation with the plane of the ring nearly parallel to the layers. Absorption due to the B_2 vibration at 709 cm^{-1} now doubled in intensity on inclining the film to the beam while other absorption bands due to A_1 and B_1 vibrations showed little change in intensity. This change in orientation of the nitrobenzene is not imposed by a change in layer spacing, as hydrated Ca-montmorillonite also gives a 15 Å spacing.

Benzoic acid complexes

Considerable amounts of benzoic acid (6-20%) were adsorbed by montmorillonite films heated for 10-30 min. in boiling saturated solutions of benzoic acid in CCl_4 or cyclohexane in open vessels. Under these conditions water displaced from the clays was carried off with the solvent vapours. Longer treatment did not increase the amount adsorbed. Examination of the spectra of the films, of which that for Ca-montmorillonite (Figure 2) is typical, showed that the benzoic acid was almost entirely in the form of the molecular acid. Small amounts of benzoate ion, absorbing at 6.35-6.45μ, were detected only in clays containing di- or tri-valent exchangeable cations. Some solvent was also taken up, and only slowly lost on exposure to the atmosphere.

Benzoic acid was adsorbed slowly from cold saturated CCl_4 solution by air-dry clay films. One or two overnight treatments with cold CCl_4 extracted all the adsorbed benzoic acid, leaving only small amounts of benzoate ion in Cu, Al, Mg, and Ca saturated clays, and the amounts of adsorbed benzoic acid were estimated by this means. Atmospheric moisture played an important part in displacing the benzoic acid, as dry CCl_4 did not extract the benzoic acid efficiently.

However, air-dry films retained benzoic acid for long periods when exposed to the atmosphere. The calcium complex, which was particularly stable, still retained benzoic acid after 12 weeks' exposure. Complexes involving monovalent cations were less stable, but benzoic acid was still detectable in Na-montmorillonite after 4 weeks. This implies a considerable reduction in the volatility of benzoic acid in the complexes, as bands associated with excess crystalline benzoic acid in the clay films were lost after one or two days' exposure to the atmosphere.

Table II gives estimates of the amounts of benzoic acid retained by clay films, after brief washing with CCl_4 to remove crystalline benzoic acid, and also the amounts retained after heating in vacuum to 50°C. The large amounts of benzoic acid adsorbed by the clays indicated that the acid must be adsorbed in the interlayer space and this conclusion was supported by the observation that some features of the infrared spectra of the adsorbed molecules were dependent on the interlayer cations and on their hydration state. The spectrum of benzoic acid in Ca-montmorillonite in Figure 2a is largely typical of that given in the air-dry condition by samples containing other exchangeable cations. It is similar in many ways to that observed for benzoic acid monomers adsorbed on the surface of alkali halides [9] in that absorption bands involving the C-O-H group are particularly affected. Thus the shift in the OH stretching vibration of benzoic acid to higher frequencies indicates weaker hydrogen bonding than in the normal crystalline dimeric acid. Shifts to lower frequency of the coupled C-O stretching and OH in-plane bending vibrations, which lie at 1425 cm^{-1} and 1294 cm^{-1} in the dimer (Figure 2d), also indicate weaker hydrogen bonding. A band at 668 cm^{-1} in the dimer, which is known to involve the C-C$\overset{O}{\underset{OH}{<}}$ group [9], is no longer detectable for the adsorbed form in montmorillonite.

The dependence of the C=O stretching frequency on the cation and the hydration state is shown in Table II. In the anhydrous complexes, studied under vacuum at 50-100°C, there is a continuous decrease in the carbonyl frequency in the series Na, Li, NH_4, Ca, Mg, Cu, Al corresponding to increasing perturbation of the C=O vibration by the cation. In air at room temperature, benzoic acid associated with Ca, Mg, Cu, or Al gives a frequency which is independent of the cation and higher than those given in vacuum conditions. The carbonyl frequency of benzoic acid associated with the monovalent ions is unaffected by the hydration state. This difference between the hydrated and the anhydrous state for polyvalent cations is exactly analogous to that found in the nitrobenzene complexes, and could be accounted for by the following mechanism:

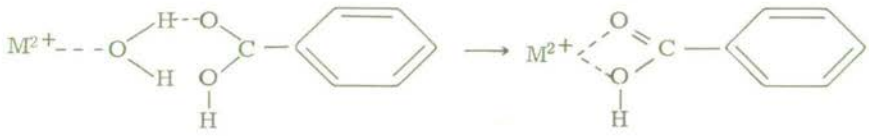

Table II

Carbonyl frequencies (cm^{-1}) and weight per cent of intercalated benzoic acid in montmorillonite previously saturated with various cations

	Na	K	Li	NH_4	Ca	Mg	Cu	Al
Air	1706	1706 1689	1695	1689	1684	1684	1684	1684
Vacuum, 50–100°C	1706	1706	1695 1724 (w.)	1689	1669	1664	1639	1625
Vacuum, 150°C	v.w.	v.w.	v.w.	lost	1739 1667	1740 (w.) 1712 1661	1650	1660 1620 d
Benzoic acid adsorbed, %) a	6.7	10	13.4	12	20	14.6	17	16–17
Benzoic acid adsorbed, %) b	5.3	6	6	7.7	8.6	9.2	9.8	8.7

a: after brief washing in CCl_4
b: retained under vacuum at 50°C

d: diffuse band
w: v.w.; weak, very weak

The OH stretching region is difficult to interpret unambiguously for the benzoic acid complexes, as absorption of interlayer water and of the acid hydroxyl group overlap here. The changes observed in this region were, however, not inconsistent with the above interpretation.

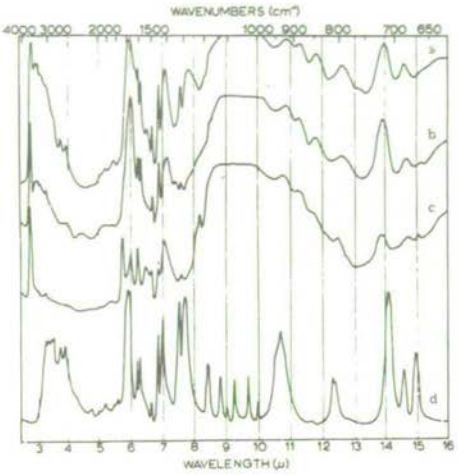

Figure 2

Infrared spectra of Ca-montmorillonite-benzoic acid complex, a) in air, b) in vacuum at 70°C, c) in vacuum at 150°C, and of, d) crystalline benzoic acid (KBr disk).

In addition to the carbonyl vibration, the OH in-plane bending vibration of benzoic acid was markedly affected by dehydration of the clay complexes. This band lies at 1294 cm^{-1} in the dimer [14], and near 1280 cm^{-1} for all complexes in the air-dry state, but on heating and dehydration it shifts to lower frequencies and becomes weak and diffuse. At the same time the benzene ring vibration at 1326 cm^{-1}, which appears to derive its intensity from coupling with this COH vibration, becomes very much weaker. These changes are illustrated for the Ca complex in Figure 2b. Mg^{2+} caused the most change as here the displaced COH deformation could not be detected. With Li^{+} it is shifted to give a diffuse band at 1200 cm^{-1}; with Cu^{2+} and Ca^{2+} a diffuse shoulder extending from 1280 cm^{-1} appeared. With Na^{+} and NH_4^{+}, the COH deformation was least affected. As the different cations have different effects, these results indicate that the cations become coordinated to the oxygen of the COH when interlayer water is removed.

Benzoic acid was lost from NH_4-montmorillonite, and little remained in Na-montmorillonite, in vacuum at 100°C. More benzoic acid was retained by the more polar cations, but that associated with Li was largely lost at 150°C. Benzoic acid associated with the divalent cations underwent further reaction between 100° and 150°C with the loss of all or nearly all hydroxyl absorption, the appearance of one or more higher frequency carbonyl bands between 1650 cm^{-1} and 1740 cm^{-1}, and of one or two sharp

bands near 1230 cm^{-1} (Figure 2c, Table II). These changes indicate the formation of benzoic acid anhydride. The crystalline anhydride has a strong band at 1214 cm^{-1}, and carbonyl frequencies at 1770 cm^{-1} and 1706 cm^{-1}. The low frequency shift of the upper carbonyl frequency shows that the anhydride is coordinated to the cations through its carbonyl groups and the increasing displacement of this band in the series Ca, Mg, and Cu is consistent with their polarizing power. The greater part of the anhydride reverted to the acid when the films rehydrated in air, but a small amount of uncoordinated anhydride persisted as indicated by weak bands near 1770 cm^{-1}, which slowly disappeared on long standing. Vacuum conditions were necessary for the formation of significant amounts of anhydride, as little or none was formed at 200°C in air.

The orientation of benzoic acid in the interlayer space

The benzoic acid complexes generally gave diffuse X-ray patterns indicative of irregular mixed-layer structures. Only Ca^{2+} and Mg^{2+} gave sharp diffraction patterns with nearly integral spacings (Table III). The lower spacings given by Cu^{2+} and the monovalent cations (12.4-12.8 Å) suggest that in these the benzoic acid molecule lies with the plane of the ring nearly parallel to the silicate sheets, and this conclusion was supported by infrared observations on the NH_4^+ complex, in which only the B_2 absorption band at 717 cm^{-1}, which arises from an out-of-plane vibration, increased significantly in intensity when the clay film was placed at 45° to the beam. The increase in intensity (20%) was, however, considerably less than that observed for the corresponding band of the pyridinium ion, which takes up a flat orientation in montmorillonite [8, 15]. This difference indicates that the benzoic acid molecule does not lie strictly parallel to the layers.

Observations on the 14.9 Å Ca^{2+} complex indicated that here the plane of the benzoic acid molecule was inclined at a high angle to the plane of the layers, as the B_1 band at 1455 cm^{-1} increased by 36% on placing the clay film at 45° to the beam, while the B_2 band at 717 cm^{-1} was unaffected. The classification of benzoic acid vibrations into A_1 and B_1 species, shown in Table I, is based on an assumed C_{2v} symmetry which can only be strictly true if there is no coupling between vibrations of the benzene ring and those of the carboxylic acid group, as the latter does not have the two-fold axis required for C_{2v} symmetry. Such coupling does occur, however, [9] and this accounts for the observation that other B_1 bands at 1585 cm^{-1} and 1320 cm^{-1} showed smaller increases in intensity (0 and 15%). As the largest intensity change is observed for a B_1 vibration rather than an A_1 vibration, it seems likely that the benzoic acid molecule is lying with its long axis approximately parallel to the layers.

The formation of benzoate ion in montmorillonite

An absorption band of benzoate ion near 1550 cm^{-1} was present in the spectra of the benzoic acid complexes of the polyvalent cations but of the monovalent cations only lithium showed a weak band due to benzoate. As the frequency, sharpness and intensity of this band was dependent on the interlayer cation, the benzoate ion must be associated primarily with the interlayer cation, and not with the silicate lattice. Further, the position

of the bands were not identical with those of the benzoate salts of the cations, so that the benzoate ion cannot be in the form of a discrete crystalline phase, but presumably lies in the interlayer space. The absorption bands of benzoate ion appeared more strongly in spectra of Cu^{2+} and Al^{3+} complexes, and the intensity of these bands increased when the complexes of the polyvalent cations were examined in vacuum at 100- 150°C (e. g. Figure 2c). This conversion of interlayer benzoic acid to benzoate ion was partially reversed when the complexes rehydrated at room temperature. Benzoic acid was lost from the complexes of the monovalent cations at 100°- 150°C and little or no benzoate ion was then retained. Benzoate ion was completely removed from all complexes by washing with water. As both copper and aluminium benzoate are insoluble in water, the mechanism, at least in these instances, must by hydrolytic.

Benzoate ion is more strongly adsorbed than benzoic acid, and so the ion is the first species formed when montmorillonite is exposed to cold dilute solutions of benzoic acid in carbon tetrachloride. An estimate of the amount of benzoate ion formed was obtained by this means. After equilibration for two weeks in a 0.06% solution, the amounts of benzoic acid adsorbed by montmorillonite saturated with Al^{3+}, Cu^{+2}, Ca^{+2} and Mg^{2+} were, respectively, 2.8, 2.3, 2.2, and 1.5% of the air-dry weight of clay. Examination by infrared spectroscopy confirmed that the benzoic acid was almost entirely in the form of the anion under these conditions. Montmorillonite saturated with Na^{+} and K^{+} adsorbed benzoic acid more slowly under these conditions, but after 2 weeks these also took up about 1.5% benzoic acid; examination by infrared spectroscopy showed the presence of significant amounts of interlayer acid as well as benzoate anion.

Discussion

The present comparative study of interlayer adsorption of nitrobenzene and benzoic acid by montmorillonite shows a common pattern previously found in a study of pyridine adsorption [8]. These three substances can all enter the interlayer space as neutral polar molecules, where they form hydrogen bonds with water molecules which are directly coordinated to the more polar cations, displacing water from outer spheres of coordination in the process. The stability of this configuration is probably related to the greater flexibility of the complex, and to the more efficient packing of the aromatic molecules which can be achieved when a water molecule forms a flexible link between the cation and the polar substituents.

Other workers [16, 17] have concluded that when nitrobenzene is adsorbed on silica gel and on zeolites, hydrogen bonds are formed with the Π electrons of the benzene ring rather than with the nitro group, and have supported this conclusion by the observation that the ultraviolet maximum of nitrobenzene undergoes a red shift in the adsorbed state. This argument does not take into account a fundamental difference between the excited states associated with ultraviolet absorption by nitrobenzene on the one hand and of phenol and aniline on the other [18]. In the excited state of nitrobenzene there is a transfer of electrons from the benzene

ring to the oxygens of the nitro group. Hydrogen bonding to these oxygens therefore stabilizes the excited state, lowers the energy required to excite it and so it must cause a red shift in the ultraviolet absorption. In the excited states of phenol and aniline there is a transfer of electrons from oxygen and nitrogen to the benzene ring. Hydrogen bonding to the lone pair electrons on these atoms therefore stabilizes the ground state, raises the energy required for excitation, and so causes a blue shift in their ultraviolet maxima. It must be concluded that nitrobenzene adsorbed on silica gels and zeolites does form hydrogen bonds through the oxygen of the nitro group. This conclusion was reached for adsorption of nitrobenzene in montmorillonite from infrared evidence.

The cupric cation has a tendency to form strong coordinate bonds with nitrogen, so that pyridine coordinates directly to Cu^{2+}, but nitrobenzene and benzoic acid only become directly coordinated to this cation, as to other polar cations, when water is removed by heating in vacuum. At room temperature nitrobenzene displaces coordinated water round only the least polar cations, K^+ and NH_4^+, and this may be true also for benzoic acid.

Because of its hydroxyl group, benzoic acid can undergo further reactions in the interlayer space. Heating and evacuation gives benzoic anhydride, particularly with the divalent cations, as in these at least two molecules of benzoic acid are associated with each cation, giving a suitable configuration for this reaction. Ionic benzoate (OBz^-) is also formed with polyvalent cations, according to the following reaction:

$$M^{2+}\text{- montmorillonite} + 2HOBz \longrightarrow 2H^+\text{- montmorillonite} + M(OBz)_2$$

Clearly, the equilibrium reached in this reaction depends on the relative stabilities of the phases represented on each side of this equation. Divalent cations must satisfy two negative charges on montmorillonite, and some of these charges may not be sufficiently close to be effectively neutralized by a single cation. It is likely that cations at such sites will react with benzoate ion most readily. That this is not the only factor is clear from the dependence of the amount of benzoate ion formed on the nature of the cation. Al- montmorillonite is known to contain basic cations such as $(AlOH)^{2+}$, and this can obviously react with benzoic acid to give $(AlOBz)^{2+}$ without the formation of hydronium in the exchange sites. This reaction can account for the rather larger amounts of benzoate ion formed in Al- montmorillonite. Cupric cations also have a tendency to form basic salts, but analysis of the Cu- montmorillonite showed an excess of only 4- 5 m equiv. of Cu^{2+} per 100 g air- dry clay, corresponding to about 0.5 % of benzoate ion out of the total 2.3 % formed. There was no evidence for basic cations in Ca- and Mg- montmorillonite, so that the different amounts of benzoate ion formed in these preparations must be related to differences in the stability of the cation- benzoate complex. The slow formation of benzoate ion in montmorillonite containing monovalent cations may be associated with attack on the silicate lattice under the acid conditions.

It is uncertain how far the present results obtained with benzoic acid can be generalized, since the bulk and polarity of the molecule to which the carboxylic acid group is attached must be important in determining whether interlayer penetration can occur. Nevertheless it is likely that the shift in carbonyl frequency observed when acetic acid is adsorbed on montmorillonite [1, 2] is due to hydrogen bonding to water coordinated to cations in

TABLE III

Basal spacings (Å) of variously saturated montmorillonites with interlayer water, and with interlayer benzoic acid

Cation	Hydrated in air	Benzoic acid complexes
Li^+	12.4*,**	12.8
Na^+	11.5	12.1
K^+	11.6	12.6
NH_4^+	12.1**	12.4
Mg^{2+}	14.5**	15.1*,**
Ca^{2+}	15.0*,**	15.1*,**
Cu^{2+}	12.5*,**	12.8
Al^{3+}	14.9**	16.1

* Indicates the presence of integral higher orders of reflection.
** Indicates a sharp peak.

the interlayer space, and this mechanism may operate to lower the carbonyl frequencies of adsorbed polyacrylic acid and polygalacturonic acid [2]. Although Emerson [19, 20] has presented X-ray diffraction evidence to show that polymeric acids do not enter the interlayer space, this was obtained with partially neutralized preparations. Emerson has shown that polymers containing neutral polar substituents, such as dextran and polyvinyl alcohol, do enter the interlayer space, and the present work shows that the unionized carboxylic acid group can behave as such a substituent.

In soil, the formation of interlayer complexes by neutral polar molecules will reduce their volatility, and slow their rate of diffusion through the soil solution. This mechanism of adsorption of unionized acids is only likely to be important where high local concentrations of acid are present, as, at low concentrations, acids will be adsorbed entirely in the anionic form. This form is also a likely product of the interaction of acids with the amorphous oxides of iron and aluminium, which are widely distributed in soils [21].

ACKNOWLEDGEMENT

One author (S. Y.) wishes to thank the Kennedy Leigh Charity Trust and Friends of the Hebrew University of Jerusalem in Great Britain for support while on leave of absence from the Department of Inorganic and Analytical Chemistry, the Hebrew University of Jerusalem.

REFERENCES

1. G.O. LARSON and L.R. SHERMAN, Soil Sci., **98**, 328 (1964)
2. R.A. KOHL and S.A. TAYLOR, Soil Sci., **91**, 223 (1961)
3. R.M. HOLMES and S.J. TOTH, Soil Sci., **84**, 479 (1957)
4. W. BODENHEIMER, L. HELLER, B. KIRSON, and Sh. YARIV, Israel J. Chem., **1**, 391 (1963)
5. W. BODENHEIMER, B. KIRSON, and Sh. YARIV, Israel J. Chem., 1, 69 (1963)
6. J.D. RUSSELL, Trans. Farad. Soc., **61**, 2284 (1965)
7. V.C. FARMER and M.M. MORTLAND, J. phys. Chem., **69**, 683 (1965)
8. V.C. FARMER and M.M. MORTLAND, J. chem. Soc. (A), 344 (1966)
9. V.C. FARMER, Spectrochim. Acta, **8**, 374 (1957)
10. R. GREENE-KELLY, Trans. Farad. Soc., **51**, 412 (1955)
11. J.D. RUSSELL and V.C. FARMER, Clay Miner. Bull., **5**, 443 (1964)
12. S. PINCHAS, D. SAMUEL and B.L. SILVER, Spectrochim. Acta, **20**, 179 (1964)
13. D.H. WHIFFEN, J. chem. Soc., 4221 (1956)
14. V.C. FARMER, Spectrochim. Acta, **15**, 870 (1959)
15. J.M. SERRATOSA Nature, Lond. **208**, 679 (1965)
16. M. OKUDA, J. chem. Soc. Japan, **82**, 1121 (1961)
17. V.N. ABRAMOV, A.V. KISELEV, and V.I. LYGIN, Zh. fiz. Khim., **38**, 1044 (1964)
18. H.H. JAFFE and M. ORCHIN, Theory and Applications of Ultraviolet Spectroscopy, p. 255. John Wiley and Sons, Inc., New York (1962)
19. W.W. EMERSON, Nature, Lond., **176**, 461 (1955)
20. W.W. EMERSON, J. agri. Sci., Camb., **47**, 117 (1956)
21. B.D. MITCHELL, V.C. FARMER, and W.J. McHARDY, Adv. Agron., **16**, 327 (1964)

Reprinted from
CLAYS AND CLAY MINERALS
Proceedings of the Fifteenth Conference
Pittsburgh, Pennsylvania
PERGAMON PRESS – OXFORD & NEW YORK – 1967

INFRARED ABSORPTION SPECTROMETRY IN CLAY STUDIES

by

V. C. FARMER and J. D. RUSSELL

Department of Spectrochemistry,
The Macaulay Institute for Soil Research, Aberdeen, Scotland

ABSTRACT

THE relationships between spectrum and structure in layer-silicates are reviewed, and applied in the study of structural changes occurring during the heating of montmorillonites up to dehydroxylation, and their subsequent rehydroxylation. Information given by infrared spectroscopy on the binding of water in expanding layer silicates is presented, and the physical and chemical processes associated with entry of basic, neutral and acidic molecules into the interlayer space of these minerals are illustrated for ammonia, ethylamine, pyridine, nitrobenzene, and benzoic acid. Problems associated with the study of soil clays, which are often complex mixtures including poorly ordered and amorphous constituents, frequently firmly combined with organic matter, are discussed.

New evidence is presented concerning the environment of the two types of hydroxyl group in beidellite. The thermal stabilities of NH_4^+ and lattice OH in montmorillonite and beidellite, and the properties of their dehydroxylates, are contrasted. The nature of the collapsed phase formed in Li-, Mg-, and NH_4-montmorillonite at 300–500°C is discussed. The presence of weak hydrogen bonds between lattice oxygens and interlayer water is established, although it is shown that the strength of hydrogen bonds formed between NH_4^+ and lattice oxygens is dependent on the sites of substitution in the layer lattice.

INTRODUCTION

INFRARED studies on clays at the Macaulay Institute have been directed towards characterizing the types of clay mineral that occur naturally in soils, and to obtaining information on the surface properties and reactivity of these minerals. As with all physical methods of investigation, the achievement of these aims has required the solution of many problems of technique and interpretation that are raised by the method of investigation itself. On the one hand, infrared methods have the potential to solve many problems in clay studies, if techniques capable of yielding unambiguous results were available. On the other hand, the infrared spectrum has been found to contain a considerable amount of information which cannot yet be fully interpreted.

This paper is concerned with problems of interpretation that have arisen in the course of infrared studies at the Macaulay Institute during the last

ten years and includes some new observations amplifying previously published work. These studies fall naturally into two parts: namely, studies of the vibrations of the hydroxy-silicate structure, and studies of the binding of water and of other molecules and ions in the interlayer space of expanding silicates.

Acknowledgment must be made here to the many collaborators and assistants who have participated in the work, but particularly to Dr. R. L. Mitchell, who recognized so early the potentialities of infrared spectroscopy in soil studies, and who has given the work his continuous support, and to Dr. R. C. Mackenzie, who made his knowledge of clay mineralogy and his collection of well-characterized clay minerals freely available.

THE HYDROXY-SILICATE LATTICE

Vibrations of the Hydroxyl Group

OH stretching.—Vibrations involving the proton, that is, OH stretching and bending vibrations, are very largely independent of the vibrations of silicon and oxygen in the rest of the lattice. These proton vibrations are directly affected by the immediate environment of the proton and can yield information on this environment. The importance of their study was early recognized, but the OH stretching region could not be adequately examined until grating spectrometers giving well resolved spectra such as those in Figs. 1–3 (Farmer and Russell, 1964) became available. Not all the differences in spectra are as yet adequately understood. Perhaps the most striking anomaly is that the OH groups in pyrophyllite absorb at 3675 cm^{-1} whereas the inner OH groups in the kaolin minerals, which apparently have the same environment, absorb at 3620 cm^{-1}. In the dioctahedral series, substitution of Al for Si in the lattice causes a marked broadening in the absorption bands, as in the muscovite and beidellite spectra. The two components in the beidellite spectrum, at 3660 cm^{-1} and 3630 cm^{-1}, must arise from two types of OH, differing, perhaps, with respect to the site of Al-for-Si substitution in neighboring tetrahedra. The lower frequency component weakens considerably when interlayer water is removed from beidellite, indicating that the interlayer cation moves into close proximity with these OH groups. The divalent cation Ca^{2+} has a greater effect than monovalent cations and gives rise to a perturbed OH vibration near 3550 cm^{-1} (Farmer and Russell, 1966). Similar perturbed OH bands appear in the spectra of Ca- and Mg-montmorillonite following dehydration (Russell and Farmer, 1964).

A recent observation made on oriented beidellite films is that the OH group absorbing at 3660 cm^{-1} lies more nearly parallel to the layer sheets than does the OH group absorbing at 3630 cm^{-1}. It may be that the proton of the latter OH is attracted out of the oxygen layer in which it lies, towards an oxygen associated with a site of Al-for-Si substitution in the tetrahedral sheet on the opposite side of the octahedral sandwich. Coordination of the

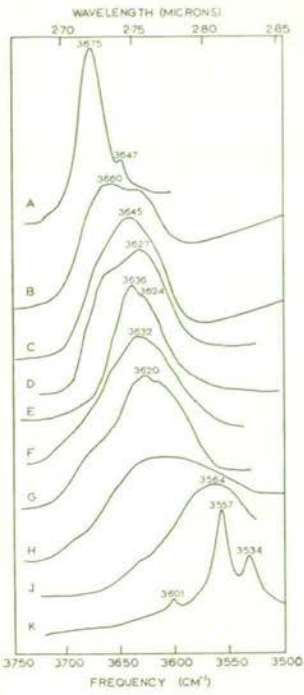

FIG. 1

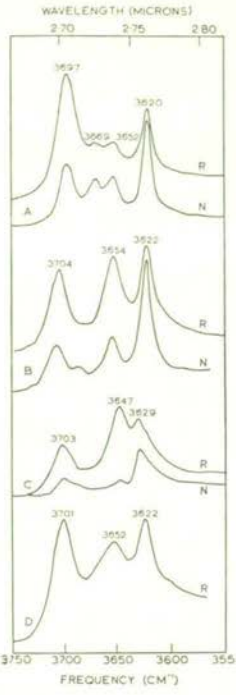

FIG. 2

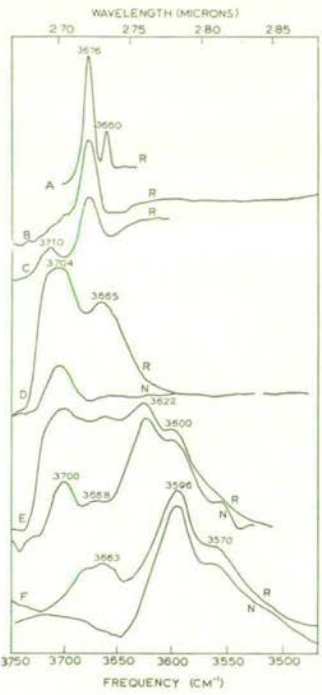

FIG. 3

FIG. 1. Hydroxyl absorption bands of randomly oriented samples of A—pyrophyllite, B—beidellite, C—rectorite, D—muscovite or paragonite, E—margarite, F—Wyoming montmorillonite, G—Skyrvedalen montmorillonite, H—Woburn montmorillonite, J—nontronite and K—ferric celadonite.

FIG. 2. Hydroxyl absorption bands of A—kaolinite, B—dickite, C—nacrite, D—Pugu D kaolinite. R indicates randomly oriented specimens, and N films at normal incidence.

FIG. 3. Hydroxyl absorption bands of A—talc, B—hectorite, C—saponite, D—phlogopite (126 μ), E—green biotite (115 μ), and F—dark brown biotite (25 μ). The mica spectra were obtained from single flakes of the thickness indicated at normal (N) and 45° incidence (R).

exchangeable cation to this OH can then assist in transmitting the cation charge through the silicate lattice when water is removed.

Substitution of Fe^{3+} for octahedral Al^{3+}, as in nontronite and celadonite, causes a striking shift of the OH band to lower frequencies. The extreme sharpness of the OH stretching bands in ferric celadonite can probably be correlated with the absence of Al-for-Si substitution, and with the regularity of the octahedral substitution, as each OH is coordinated to a divalent and a trivalent ion. The two bands at 3557 and 3534 cm^{-1} may arise from OH

groups associated with Fe^{3+}—Mg^{2+} and Fe^{3+}—Fe^{2+}, respectively. Other celadonites and glauconites examined give less sharp spectra, with additional strong OH absorption near 3603 and 3577 cm^{-1}. The additional bands may be correlated with the presence of Al^{3+} in the octahedral layer, and the greater breadth of the bands with Al-for-Si substitution in the lattice. The sharp celadonite spectrum contrasts strikingly with those of montmorillonites, in which substitution is also principally in the octahedral layer. The diffuseness of montmorillonite spectra may be due to the irregularity of the substitution pattern in this mineral.

The spectra of the kaolin minerals (Fig. 2) have provoked a long-continuing discussion, as the problems to be resolved increased with increasing resolving power of the spectrometers used in their study. Considerations based solely on the known lengths of the hydrogen bonds in this mineral lead to the assignment of the highest frequency band to the inner OH group of the kaolinite structure, but Ledoux and White (1964) have conclusively established that the lowest frequency band arises from the inner hydroxyl and that the three higher frequency bands arise from the hydroxyls on the surface of the kaolinite layer. Clearly factors other than hydrogen-bond lengths are important in determining OH stretching frequencies.

Again, the assumption that each absorption band arises from a distinct type of OH implies that there are three different types of surface OH: one type oriented perpendicular to the sheets giving the 3697 cm^{-1} band and two others oriented more nearly parallel to the sheets, giving rise to the 3669 and 3652 cm^{-1} bands. The spectrum can, however, be satisfactorily explained in terms of the structure indicated by X-ray diffraction, in which the surface OH groups are all nearly normal to the layers. Coupling between the three nearly equivalent, surface OH groups in the unit cell can be expected to give one in-phase vibration with strong absorption perpendicular to the layers and two out-of-phase vibrations with weak absorption in the plane of the layers (Farmer and Russell, 1964; Farmer, 1964). Figure 4 illustrates the operation of these coupling forces in the simpler case of two OH groups related by a plane of symmetry and a two-fold axis of symmetry. The symmetric vibration (Fig. 4*a*) has a change in dipole moment along the two-fold axis while the anti-symmetric vibration (Fig. 4*b*) has its dipole change perpendicular to the axis. Because of coupling through the electric fields associated with the vibrating protons the symmetric vibration would have a higher frequency.

The rather different pattern given by nacrite and dickite implies that the surface OH groups in these minerals are less nearly equivalent than those in kaolinite. Small amounts of dickite- and nacrite-type stacking in kaolinite crystals would be expected to give stronger absorption near 3650 cm^{-1} than is found in regularly stacked kaolinites. Such absorption is in fact a common feature of kaolinites from many localities, although the stacking irregularities are not sufficiently numerous to be obvious in the X-ray pattern. This band is strongly developed in Pugu D kaolinite (Fig. 2D) where the stacking

irregularities lead to a *b*-axis disordered type of X-ray diffraction pattern. The infrared spectrum suggests, therefore, that the disorder in this mineral arises from a random sequence of kaolinite-type and either dickite- or nacrite-type stacking.

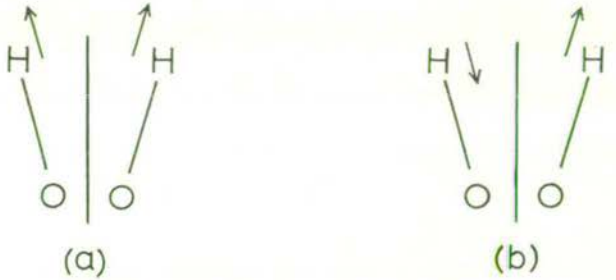

FIG. 4. The symmetrical (*a*) and antisymmetrical (*b*) vibrations of two hydroxyl groups related by a plane of symmetry and a two-fold axis of symmetry, lying in the plane.

In the trioctahedral minerals, Al-for-Si substitution, as in saponite, and Li-for-Mg substitution, as in hectorite, have little apparent effect on the OH stretching frequency. The higher frequency band of saponite at 3710–20 cm^{-1} has been found to appear only when interlayer water is removed from this mineral, and only when it is saturated with the monovalent cations, K^+, Na^+ or NH_4^+ (Farmer and Russell, 1966). It must be ascribed to OH groups whose vibrations are perturbed by the electric field of these monovalent ions, which are positioned directly over OH groups in the anhydrous state. This effect can therefore account for the higher frequency of the principal OH absorption band of phlogopites, near 3704 cm^{-1} (Fig. 3D). Vedder (1964) has suggested that substitution of Fe^{2+} for Mg^{2+} in talc causes a low-frequency shift in the OH vibration, and our study of a series of analysed phlogopites and biotites indicates that a similar effect can be detected in these minerals, so that OH groups associated with ($Mg_2^{2+}Fe^{2+}$) groupings absorb at 3685 cm^{-1}, and those associated with ($Fe_2^{2+}Mg^{2+}$) groupings absorb near 3660 cm^{-1} (see also Jørgensen, 1966). These bands are much broader in biotites than in talc, and so overlap to a considerable extent. This effect cannot, of course, account for the 3665 cm^{-1} band which appears in most phlogopites, where Fe^{2+} is low or absent; this band may arise from ($Al^{3+}Mg_2^{2+}$) groupings (Vedder, 1964).

The group of lower frequency bands in biotites in the 3530–3620 cm^{-1} region are almost certainly associated with vacancies in the octahedral layer, but assignment of the individual components can still not be considered satisfactory. The marked effect of Fe^{3+} on the OH stretching frequencies in the dioctahedral layer silicates suggests that this ion may be associated with the lower frequency bands in biotites, while Al^{3+} is associated with the higher frequency bands.

OH bending.—The OH bending or rocking vibration has not yet been identified in the trioctahedral minerals. In the dioctahedral minerals two OH bending vibrations are to be expected, one with the change in dipole moment in the plane of the sheets, and one nearly perpendicular to this plane, but only the in-plane type has been identified, lying in the 800–950 cm^{-1} region. A band near 400 cm^{-1} has been ascribed to the out-of-plane vibration of the OH group in muscovite (Vedder and McDonald, 1963), but, according to spectra shown in a later publication (Vedder, 1964), this band does not show the appropriate polarization behaviour.

In the montmorillonite group, the bending vibration of OH groups associated with two Al^{3+} ions occurs near 920 cm^{-1}; those associated with two Fe^{3+} ions absorb near 820 cm^{-1}, while vibrations associated with an Al^{3+}—Fe^{3+} pair appear to absorb in the region 845–890 cm^{-1}. This last band is dominant in a montmorillonite (Woburn Fuller's Earth; Heller *et al.*, 1962) which had a particularly high iron content, but is commonly present as a subsidiary band in most published spectra of montmorillonites. Exceptions are montmorillonites from Cheto (Grim and Kulbicki, 1961) and Skyrvedalen (Farmer and Russell, 1964) which are very low in iron. This band is characterized by its ready elimination from the spectrum under reducing conditions (Farmer and Russell, 1964): indeed, simple exposure to hydrazine vapor has been found to be sufficient (Russell, Munsus, and White, unpublished). By this treatment, the spectrum of Wyoming montmorillonite becomes identical with that of Cheto montmorillonite, suggesting that the only difference between these species is the iron content of the former.

Vibrations of the Silicate Anion

The OH stretching and bending vibrations are localized on the proton, but none of the vibrations involving silicon, oxygen, and the octahedral cations can be localized on any one of these atoms. The silicate anion itself gives rise to eighteen vibrations, and the lower frequency vibrations of this structure, especially those of the inner oxygen layer, can be expected to be mechanically coupled with translational vibrations of the octahedral cations and of the OH groups, whose presence contribute another six vibrations. The problem of assignment of the absorption bands is therefore of some complexity (Farmer and Russell, 1964; Vedder, 1964). The high symmetry of the talc structure simplifies the problem, as many of its vibrations are inactive in the infrared. The silicate anion then gives only five absorption bands, two of which have dipole moments perpendicular to the sheets, and three parallel to the sheets. Oriented preparations permit the in-plane vibrations to be distinguished from the perpendicular vibrations (Fig. 5), and a reasonable assignment can be made for trioctahedral layer silicates on this basis (Farmer, 1958). The in-plane Si—O—Si stretching vibrations are degenerate in talc, giving a single band near 1020 cm^{-1}, but are split into two components in the dioctahedral series of layer silicates because of distortion of the tetrahedral layer (Fig. 6, Farmer and Russell, 1964). This distortion

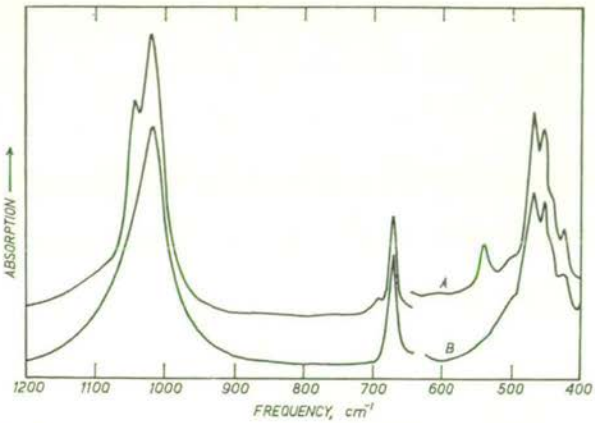

FIG. 5. Infrared spectrum of talc. A—sample in KBr pressed disk; B—oriented film on KBr window.

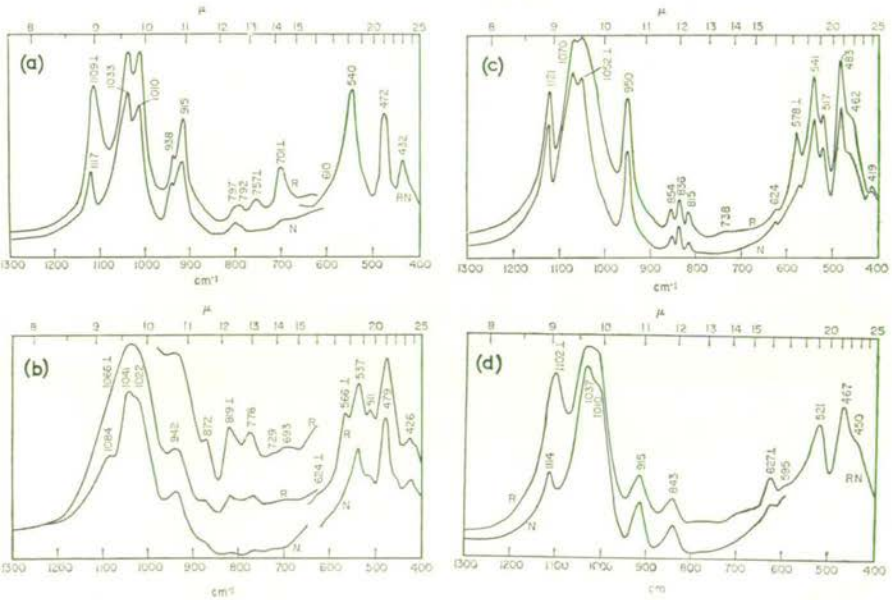

FIG. 6. Infrared spectra of (*a*) kaolinite, (*b*) beidellite, (*c*) pyrophyllite, and (*d*) Skyrvedalen montmorillonite. R indicates randomly oriented samples, N films at normal incidence, and RN spectra independent of orientation.

also causes a band near 1100 cm^{-1} to appear, arising from an in-plane vibration which is inactive in talc. The high frequency of this vibration is rather surprising, as is also that of the perpendicular Si—O^- vibration, which appears in the 1050–1110 cm^{-1} region; they are certainly not accounted for

in terms of the force-constants of the bonds involved. In these vibrations, which are associated with the development of strong dipole moments, account must be taken of the electric fields produced by the oscillating dipoles. Stretching of the Si—O^- bonds causes the thin plates of the layer silicate crystals to become electrically polarized like the dielectric in a parallel-plate condenser. The resultant field, acting on the vibrating ions, can account for the high frequency of the perpendicular Si—O^- stretching vibration. The maximum effect is apparent only for very thin crystals of thickness 0.1 μ or less. With thicknesses of the order of 1 μ, such as occur in crystals of dickite, nacrite, and some kaolinites, the Si—O^- stretching vibration is shifted to a significantly lower frequency (Farmer and Russell, 1966).

The Characterization of Clay Structures and their Reactions

The infrared spectrum is determined by the atomic masses, and by the geometry and force-constants of the interatomic bonds within the individual layers of a layer silicate. It therefore reflects aspects of the structure different from those which determine X-ray diffraction patterns and thermal curves, and gives results largely complementary to these techniques. Thus different types of montmorillonite, such as Cheto, Wyoming, Woburn Fuller's Earth, and beidellite, are readily distinguished by their infrared pattern, although indistinguishable by X-ray diffraction (Farmer and Russell, 1964).

It is illuminating, therefore, to re-examine the thermal reactions of montmorillonites by infrared techniques. Montmorillonite when saturated with Li^+ and Mg^{2+} has been long known to collapse to a 9.5 Å phase after heating at 300–550°C (Greene-Kelly, 1953). This behaviour was ascribed to migration of these small cations into the octahedral layer, giving a pyrophyllite-like structure. The infrared spectrum clearly distinguishes the charged montmorillonite structure from the neutral pyrophyllite structure, and examination of heated montmorillonite samples showed that the pyrophyllite pattern did not develop under these conditions (Russell and Farmer, 1964), but only appeared after montmorillonite had been completely dehydroxylated at 750°C and then rehydroxylated in steam (Heller *et al.*, 1962). The spectra of Li-, Mg-, and NH_4-montmorillonite heated to 350°C did, however, show certain features in common, not shown by Na- or Ca-montmorillonite, and this led to a search for other common properties. As a result it was established that these collapsed montmorillonites all gave strongly acid reactions with indicators in ethylene glycol, and that they could be completely re-expanded by treatment with NH_3 vapor, with the formation of NH_4^+ ions in the interlayer space (Russell and Farmer, 1964).

The development of acidity in NH_4–montmorillonite is clearly due to thermal decomposition of NH_4^+, with loss of NH_3 and liberation of a proton. With Mg- and Li-montmorillonite, protons can only be liberated by reaction of the interlayer cations either with residual water molecules or with lattice OH groups.

Recent results obtained with samples which have been re-expanded with NH_3 (Table 1) indicate that just over half of the original lithium content is no longer exchangeable and has presumably migrated into vacant octahedral sites. There it effectively neutralizes the negative lattice charge and the exchange capacity is correspondingly reduced. Two-thirds of the magnesium ions are no longer exchangeable but the exchange capacity is only reduced by about one-third. Possibly the excess positive charge arising from migration of Mg^{2+} into an octahedral site causes ionization of an overlying lattice OH group. Much of the original acidity indicated by the high NH_4^+ contents immediately after NH_3 treatment is lost after the samples have been equilibrated with ammonium acetate solution.

TABLE 1.—CATION CONTENTS (meq/100 g) OF MONTMORILLONITES, RE-EXPANDED WITH NH_3 FOLLOWING HEATING TO 400°C

Exchangeable cation (a)	NH_4 content after treatment (b)	Exchange capacity (c)	Li and Mg displaced (d)
Li^+	45	45	39
Mg^{2+}	84	54	32
NH_4^+	105	84	

(a) Initial content of 90 meq/100 g.
(b) NH_4^+ content immediately after re-expansion with NH_3.
(c) NH_4^+ content after equilibrating re-expanded samples with neutral ammonium acetate.
(d) Amounts of Li and Mg displaced by ammonium acetate solution.

These results imply, for Li-montmorillonite, that part of the exchangeable Li migrates into the octahedral layer and becomes fixed there, but does not liberate a proton, while the remainder reacts with interlayer water or lattice hydroxyl to yield a proton, but remains in, or close to, the interlayer space. The latter reaction is reversed when the collapsed phase is re-expanded and equilibrated with ammonium acetate, and the lithium ions involved then become exchangeable. A similar process probably proceeds in Mg-montmorillonite although in this instance each Mg^{2+} which migrates into the octahedral layer also liberates a proton.

Beidellite is commonly distinguished from montmorillonite by the fact that Li-beidellite does not collapse after heating to 300°C. Our observations indicate that these minerals are also distinguished by the very different thermal stability of NH_4^+ on the exchange sites. Thermal decomposition of NH_4^+ and loss of lattice OH is readily followed by infrared spectroscopy, and the results (Fig. 7) show that NH_4^+ begins to decompose in montmorillonite at about 150°C, and that decomposition is completed before dehydroxylation of the mineral is complete. In beidellite the NH_4^+ does not begin to decompose until dehydroxylation begins, and is not complete till after dehydroxylation is complete. In montmorillonite the spectrum gives no

indication of the presence of the proton liberated by decomposition of the NH_4^+, but in beidellite an OH doublet develops near 3450 cm^{-1} and persists to over 800°C, although normal lattice OH is eliminated by 650°C. A similar band develops when NH_4-rectorite (Russell and White, 1966) and NH_4-muscovite (White and Burns, 1963) are heated, so its appearance is clearly associated with Al-for-Si substitution in dioctahedral minerals. No such

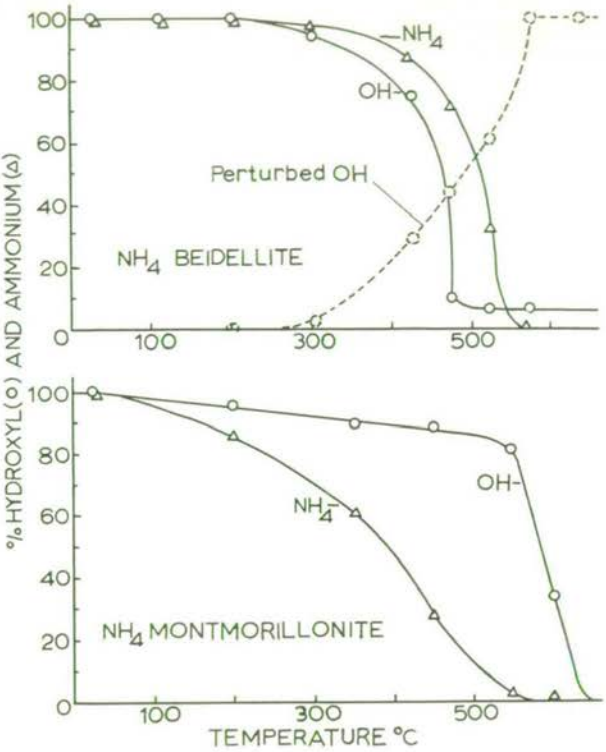

FIG. 7. Loss of (*a*) ammonium and (*b*) lattice hydroxyl groups from montmorillonite and beidellite. Dashed line indicates the development of an OH band near 3450 cm^{-1} in beidellite.

band appears in saponite or hectorite when NH_4^+ in these clays is thermally decomposed. Although the work on rectorite has suggested that the proton liberated by decomposition of NH_4^+ associates with an OH group in the vicinity of tetrahedral Al^{3+} to form an $H^+ \cdots$ OH grouping, the persistence of the OH doublet at temperatures over 800°C is more consistent with an SiOH or AlOH group.

Like the SiOH group formed when NH_4^+ in zeolites is thermally decomposed, the OH group in beidellite reacts with NH_3 to form NH_4^+, and the

3450 cm^{-1} doublet is then eliminated. No NH_4^+ is formed when NH_4-montmorillonite is dehydroxylated and the product is exposed to ammonia, suggesting that the protons liberated in NH_4^+-montmorillonite are eliminated during dehydroxylation. This requires that these protons can migrate through the lattice so that two can associate with a lattice oxygen to form water.

Dehydroxylated montmorillonite has been found to rehydroxylate in steam at 400–500°C to give a neutral pyrophyllite-like structure (Heller *et al.*, 1962). Recent work has shown that dehydroxylated beidellite also partially rehydroxylates under these conditions but the product retains its layer charge. Thus Ca-beidellite is largely regenerated in its original form, while NH_4-beidellite yields a product in which NH_4^+ is formed on treatment with NH_3 gas. The ready rehydroxylation of the 2 : 1 dioctahedral layer silicates indicates strongly that dehydroxylation and rehydroxylation are homogeneous reactions in these minerals.

POLAR MOLECULES IN THE INTERLAYER SPACE OF SMECTITES

Interlayer Water

The typical interlayer molecule of expanding layer silicates is water, and an understanding of the structure of this water layer has been sought by many techniques. The infrared absorption spectrum provides information on the strengths of hydrogen bonds formed in the water layer but the results are complicated by overlapping of the broad absorption bands of water in inner and outer spheres of coordination, and by the band of lattice OH in montmorillonite. There are considerable advantages in working with the trioctahedral minerals, whose lattice OH bands are sharp, weak, and lie at higher frequencies than the water bands. It is then possible to see that water in hectorite containing the non-polar tetramethylammonium ion (Fig. 8) gives two distinct bands at 3630 and 3425 cm^{-1}. Studies with oriented clay films show that the high-frequency band corresponds to a weak hydrogen bond to oxygens of the silicate lattice, and the lower frequency band to water–water hydrogen bonding. A shoulder at 3240 cm^{-1} cannot be taken as evidence for a still stronger hydrogen bond, as it could be the overtone of the HOH angle deformation band at 1630 cm^{-1}. A very similar pattern of absorption (Fig. 8) is given by water in hectorites containing the ammonium and the hexammino-cobalt(III) cation, even though there is clear evidence from the spectra that these cations form hydrogen bonds with water molecules surrounding them (i.e. NH absorption bands of NH_4^+ at 3063 and 2850 cm^{-1}, and of $Co(NH_3)_6^{3+}$ at 3230 cm^{-1}). Accordingly, this pattern of hydrogen bonding can be considered typical of water in outer spheres of coordination round more polar cations. In K-hectorite (Fig. 8) the increased intensity of the 3425 cm^{-1} absorption band indicates that water directly coordinated to the cation forms hydrogen bonds with surrounding water molecules rather

than with the silicate lattice. In Mg- and Cu-hectorite, water coordinated to these more polarizing cations is more acidic and forms stronger hydrogen bonds to water in outer spheres of coordination, as evidenced by the development of strong broad bands in the region below 3300 cm^{-1}. Similar bands which appear both in aqueous solutions of aluminium chloride (Fripiat, Cauwelaert, and Bosmans, 1965) and in Al-montmorillonite must also have the same origin.

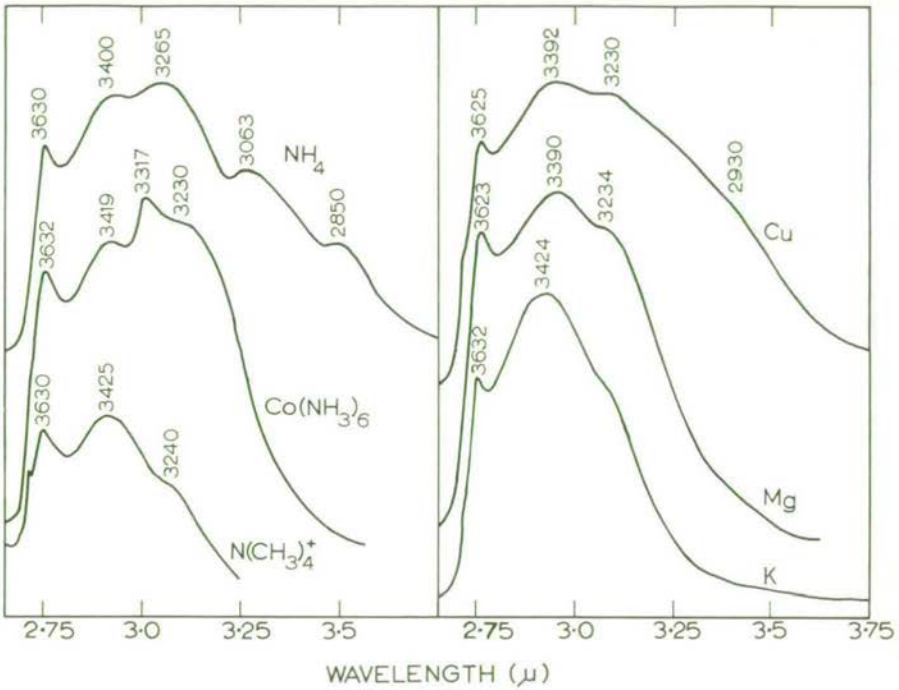

FIG. 8. Stretching vibrations of water in hectorite saturated with various exchangeable cations.

Absorption bands of water directly coordinated to the cation are seen more clearly when water in outer spheres of coordination is removed by heating and evacuation, or displaced by other polar molecules, but the environment of the coordinated water is then very different from that in the normal hydrated state. Thus isolated water molecules remaining in saponite after heating and evacuation can form hydrogen bonds only with the silicate lattice. The strength of hydrogen bonding is again a function of the polarizing power of the cation but the bonds are very much weaker than those formed with water in outer spheres of coordination (Russell and Farmer, 1964). This

investigation showed that the broad absorption near 3200 cm^{-1} in Mg-saponite persists up to at least 200°C, suggesting that a structure of the type

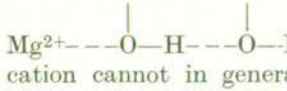

Mg^{2+}---O—H---O—H is particularly stable in this mineral. The divalent cation cannot in general effectively neutralize two negative lattice sites without the assistance of such water bridges, except when chance brings the sites on adjacent silicate layers directly opposite each other.

Polar organic molecules such as pyridine and nitrobenzene readily displace water in outer spheres of coordination round divalent cations and the smaller monovalent cations, where they then form hydrogen bonds with directly coordinated water (Farmer and Mortland, 1966; Yariv, Russell and Farmer, 1966). The strength of hydrogen bonding is then a function of the polarizing power of the cation, the basicity of the organic molecule, and the packing of the organic molecules round the hydrated cation. Thus Mg-hectorite, like Mg-montmorillonite (Farmer and Mortland, 1966), is largely expanded to a 23 Å spacing when freshly removed from pyridine, and in this phase both protons of coordinated water form hydrogen bonds with pyridine, giving a band near 3050 cm^{-1} (Fig. 9). This phase rapidly loses pyridine in air to give a 14.8 Å phase in which packing considerations allow only one proton of each water molecule to form a hydrogen bond to pyridine. The development of a band at 3630 cm^{-1} shows that the other OH group is generally only weakly bonded to the oxygens of the silicate lattice.

It seems likely that hydrogen bonds to those silicate oxygens which carry the negative lattice charge will be rather stronger than hydrogen bonds to uncharged oxygens, and some evidence for this can be seen in the nitrobenzene complex of Mg-hectorite (Fig. 9). Hydrogen-bonding of coordinated water molecules to the oxygens of the nitro group is much weaker than to pyridine, and gives a band near 3500 cm^{-1}. In this complex, the high-frequency band at 3607 cm^{-1} is weakly developed, and is removed simply by evacuation at room temperature. As it seems unlikely that the coordinated water molecules form hydrogen bonds only to nitrobenzene, it is concluded that in this case water hydrogen-bonded to the silicate lattice absorbs below 3600 cm^{-1}.

The negative charge associated with Al-for-Si substitution in the tetrahedral layer should be localized on the three surface oxygens attached to Al^{3+}, whereas the charge associated with substitution in the octahedral layer (Mg for Al, or Li for Mg) can be expected to be more diffusely spread over the surface oxygens. In consequence, stronger hydrogen bonds to surface oxygens associated with Al-for-Si substitution would be anticipated. The infrared spectra of anhydrous smectites containing NH_4^+ do give evidence for this (Table 2). An NH_4 absorption band in the 3025–3050 cm^{-1} region, appearing in the spectra of saponite, vermiculite, and beidellite, indicates hydrogen bonding to surface oxygens, whereas absorption in this region of the spectra of NH_4^+-montmorillonite and hectorite is weaker and more diffuse.

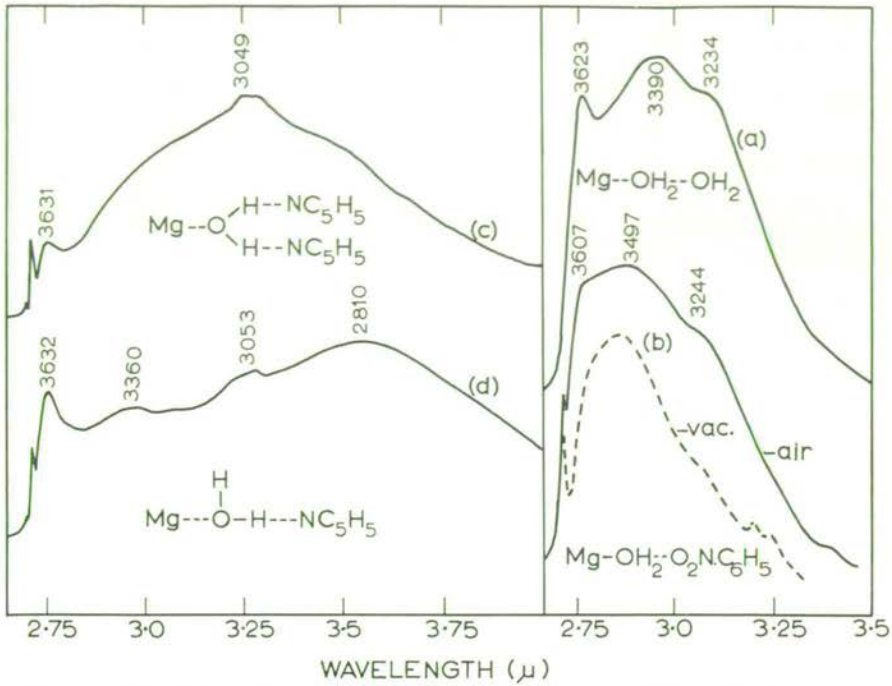

FIG. 9. Water absorption bands in Mg-hectorite, (*a*) normal hydrated state, (*b*) nitrobenzene complex, (*c*) 23 Å pyridine complex, (*d*) 14.8 Å pyridine complex.

TABLE 2.—NH_4^+ ABSORPTION BANDS IN ANHYDROUS LAYER SILICATES

	Frequencies, cm^{-1}
Montmorillonite	3270
Beidellite	3286, 3026
Muscovite*	3300, 3042
Hectorite	3262, (3062 v.w.)
Saponite	3270, 3045
Vermiculite	3255, 3045

* Vedder, 1965; v.w.: very weak.

Interlayer Molecules other than Water

Polar molecules have long been known to substitute for water in the interlayer space of expanding layer silicates, but only by the application of infrared methods has it been possible to get direct evidence of the mechanism of adsorption. In studying the adsorption of ammonia (Russell, 1965), ethylamine (Farmer and Mortland, 1965), pyridine (Farmer and Mortland,

1966), nitrobenzene, and benzoic acid (Yariv, Russell, and Farmer, 1966) several different mechanisms of adsorption have been distinguished, in all of which the exchangeable cation plays a predominant role.

Protonated cations in smectites can form hydrogen bonds with lone-pair electrons in polar molecules. Thus N—H vibrations of ammonium, ethylammonium and pyridinium ions are strongly perturbed by hydrogen bonding to the corresponding free bases. The formation of discrete base–cation dimers of the type (B:H:B) has been postulated for the ethylamine–ethylammonium and pyridine–pyridinium systems. In the former, evidence was obtained for the formation of a symmetrical hydrogen bond, leading to complete suppression of the typical absorption bands of the ethylammonium cation. The weakly polar nitrobenzene molecule, however, leaves the ammonium ion unperturbed and freely rotating in montmorillonite, as it is in the collapsed anhydrous state.

Nitrobenzene and pyridine readily displace water in outer spheres of coordination round Na^+, Ca^{2+}, and Mg^{2+}, and these molecules then form hydrogen bonds with the directly coordinated water molecules (Fig. 9). Benzoic acid enters the interlayer space as the unionized monomer, and its behavior is then similar to that of the structurally analogous nitrobenzene molecule. Pyridine forms a strong coordinate bond with exchangeable Cu^{2+} which is resistant to hydrolysis by water, but part of the pyridine is also indirectly coordinated through a bridging water molecule. Nitrobenzene and benzoic acid do not readily displace coordinated water round Cu^{2+}. Generally, directly coordinated water can be reversibly removed by heating and evacuation, and polar molecules which were in outer spheres of coordination then coordinate directly with the cation. Changes in the spectrum of interlayer benzoic acid indicate that the oxygens of both the carbonyl group and the hydroxyl group become coordinated to the cation. At 150°C in vacuum benzoic acid around divalent cations is converted to benzoic anhydride which is also coordinated with the cation. Attempts to remove directly coordinated water from the magnesium–water–pyridine system leads to ionization of residual water molecules, thus forming pyridinium ions and magnesium hydroxide in the interlayer space.

Ammonia and ethylamine both form tetra-coordination complexes with Cu^{2+}, displacing water entirely; NH_3 readily displaces water round Na^+ and Li^+ and coordinates directly with the cation. Evidence for coordination of NH_3 to Ca^{2+} has also been obtained, but with this cation the principal reaction involves transfer of a proton from coordinated water, giving $Ca(OH)_2$ and NH_4^+ in the interlayer space. Al^{3+} and Mg^{2+} in montmorillonite are quantitatively converted to their hydroxides, and an equivalent amount of NH_4^+ is formed.

Formation of the protonated cations when free bases are adsorbed on montmorillonite has been frequently reported (Mortland *et al.*, 1963; Fripiat, Servais, and Leonard, 1962; Swoboda and Kunze, 1966). In many instances no special role need be ascribed to the montmorillonite environment; for

example, NH_3 will precipitate aluminium and magnesium hydroxides from aqueous solutions of their salts, as well as in Al- and Mg-montmorillonite. Again, the tetra-amminocopper(II) complex readily hydrolyses in neutral solution to give copper hydroxide and ammonium ions: this hydrolysis also occurs in montmorillonite when excess NH_3 is displaced by water.

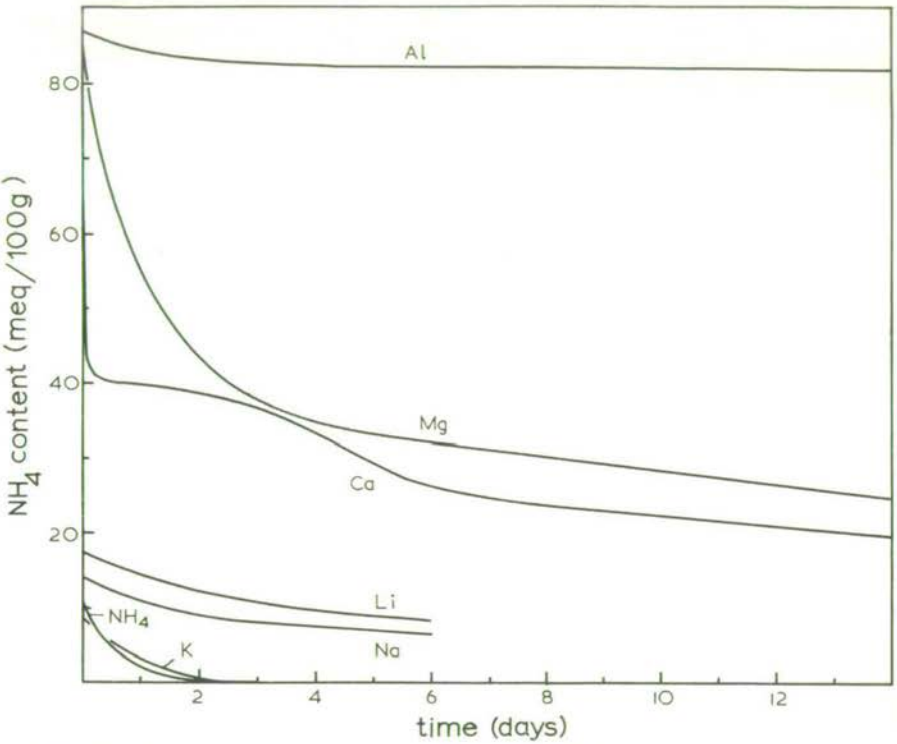

FIG. 10. Decrease, with exposure to air at about 40% relative humidity, of the NH_4 formed by NH_3 treatment of montmorillonites containing the exchangeable cations indicated. NH_4 content estimated from the optical density of the 1440 cm^{-1} infrared absorption band of the NH_4 cation.

On the other hand, the montmorillonite environment must be responsible for the formation of 17 meq NH_4/100 g when Li- and Na-montmorillonite are treated with NH_3, especially as about 10 meq/100 g is retained after long exposure to the atmosphere (Fig. 10). Similarly, the montmorillonite environment must be involved in the formation of pyridinium ion (10 meq/100 g) when pyridine is adsorbed on Na-montmorillonite. The principal cause in both instances appears to be strong preferential adsorption of the protonated cation in the interlayer space of montmorillonite. Inorganic cations do not readily displace pyridinium ion completely from montmorillonite (Farmer

and Mortland, 1966), and montmorillonites have been shown (Alexiades and Jackson, 1966) to have a few sites like those in vermiculite from which NH_4^+ would be displaced only with some difficulty.

A previous discussion of the formation of protonated species when bases are adsorbed on montmorillonite has ascribed the effect to increased acidity of residual water molecules in the interlayer space (Fripiat, 1964), but such increased acidity would not be expected in Na-montmorillonite at normal humidities. The role of preferential adsorption of the protonated cation in the interlayer space should also be considered in other systems.

The formation of ionic species is also possible when acids are adsorbed on smectites, but, in fact, no formation of benzoate anion could be detected in montmorillonite containing monovalent exchangeable cations except after long exposure to the acid. With divalent cations, 13 to 25 meq/100 g of benzoate ion are formed, and the infrared spectra indicated that the anion is associated with the exchangeable cation, rather than with the silicate lattice.

Infrared studies on oriented montmorillonite films also give information on the orientation of interlayer molecules. The results (Farmer and Mortland, 1966; Serratosa, 1966; Yariv, Russell, and Farmer, 1966) confirm Greene-Kelly's conclusion from X-ray studies (1953) that aromatic molecules in their 15 Å complexes lie with the plane of the aromatic ring at a high angle to the silicate layers. There is evidence, however, that the plane of the ring might not be strictly perpendicular to the layers.

THE INFRARED SPECTRA OF SOIL CLAYS

A pure mineral species can often be more quickly and more fully defined in structure and composition by its infrared spectrum than by any other single technique, but few, if any, soil clays are single mineral species. In general, they are complex mixtures which may include several layer silicates (either interstratified or as separate species) feldspars, various forms of silica, oxides and hydroxides of iron and aluminium, carbonates, sulphates, and phosphates. These minerals may be poorly ordered, and associated with varying amounts of amorphous material. As isolated, the clays may contain considerable amounts of organic matter. Infrared spectroscopy can best contribute to the characterization of soil clays if certain precautions are taken in the pre-treatment and preparation of samples.

Soil organic matter has a considerable hydroxyl content, and retains adsorbed water strongly. It also gives rise to strong, broad absorption near 1600 and 1400 cm^{-1} due to carboxylate groups, which are probably the principal site of binding to the inorganic constituents. As these bands overlap those of the mineral component, removal of the organic material is necessary. Hydrogen peroxide, which is commonly used, can leave troublesome oxalate residues (Farmer and Mitchell, 1963). A preliminary treatment with hypochlorite (Anderson, 1963) or hypobromite (Troell, 1931) (which do not leave

oxalate residues but are less effective) followed by hydrogen peroxide is probably the most satisfactory procedure.

Absorption bands of water overlap the OH absorption bands of several mineral species. Water associated with exchangeable cations can be reduced in amount by saturating the exchange complex with potassium ions. Ammonium is an alternative that permits an estimate of the exchange capacity from the intensity of its absorption bands, but these bands complicate the interpretation, as they overlap absorption of other possible components such as goethite and carbonate minerals.

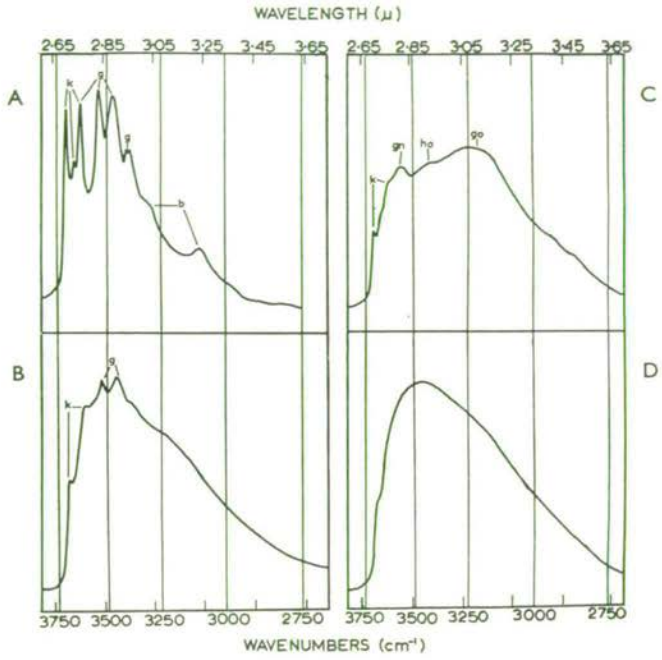

FIG. 11. OH stretching absorption of: A—highly crystalline clay deposit containing kaolinite (k), gibbsite (g) and boehmite (b); B—soil clay containing kaolinite (k), gibbsite (g), and amorphous hydrated oxides; C—soil clay containing kaolinite (k), glauconite–nontronite (gn), goethite (go), and amorphous hydrated oxides (ho); D—soil clay containing principally amorphous hydrated oxides.

The potassium bromide pressed disk technique is a suitable semiquantitative technique for examining clays. It is desirable to use two sample concentrations: 2 mg in a 12.5 mm disk containing 170 mg KBr is generally suitable for examining the OH stretching region and the weaker absorption bands in other regions of the spectrum; but the stronger absorption around 1000 cm^{-1} and 500 cm^{-1} requires only 0.3 mg. Drying the prepared disk at 100°C

reduces to a low level any water adsorbed on the KBr, or held in the interlayer space of smectites containing potassium ions.

Some labeled spectra of soil clays are shown in Figs. 11 and 12. The distinctive bands of kaolin minerals at 3697 and 3620 cm^{-1} can be detected at very low levels. The infrared evidence is of particular value when the 7 Å diffraction line of kaolinite is overlain by second-order diffraction of 14 Å layer silicates. Gibbsite can often be detected at lower levels by its hydroxyl

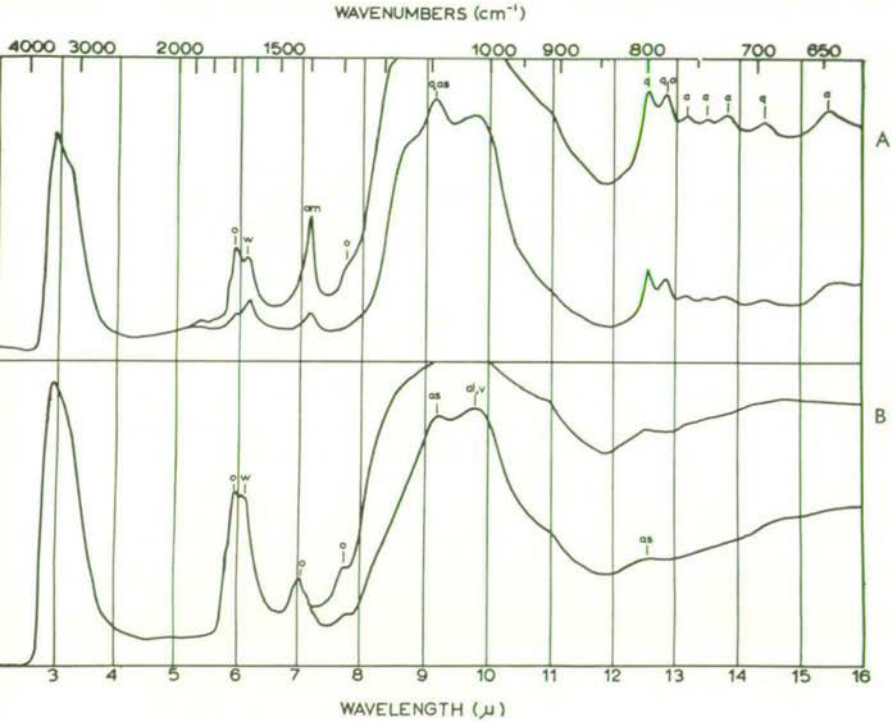

FIG. 12. Infrared spectra of: A—soil clay from sand dunes containing quartz (q), albite (a) and amorphous silica (as); B—soil clay containing amorphous silica (as), vermiculite (v) and allophane (al). Bands of NH_4^+ (am), water (w), and adsorbed oxalate (o) are also indicated.

stretching bands than by X-ray techniques (Wilson, 1966). Nontronite and glauconite have *b*-axis spacings close to those of trioctahedral minerals, but can readily be distinguished in the OH stretching region. Amorphous inorganic materials absorb as strongly in the infrared as do the crystalline species, and their presence in admixture with crystalline components is less readily overlooked in the infrared spectra of soil clays than in X-ray diffraction patterns (Mitchell and Farmer, 1962). Further, the infrared spectrum

clearly distinguishes amorphous silica present as a separate phase from silica in combination with alumina and iron oxides, as in allophanes (Mitchell, Farmer, and McHardy, 1964).

While use of high resolution grating spectrometers has greatly increased the information obtainable in the study of OH groups in clays, there is still a considerable amount of overlapping of the absorption bands of different mineral species. Further clarification of this region can be obtained by progressive thermal decomposition of the hydroxyl-containing components. Mitchell and Farmer (1962) have shown, for example, that allophanes are largely dehydroxylated by heating pressed disks containing them to 300°C. Several other dehydration and dehydroxylation reactions have been followed in alkali-halide pressed disks, but these reactions occur at rather higher temperatures in disks than when the powdered minerals are heated in air (Farmer, 1966).

Looking to the future, it is clearly desirable to develop a convenient technique whereby the spectra of minerals can be followed as the samples are progressively heated. Further assistance in the differentiation of clays can be expected from the accumulating information on the spectral changes associated with adsorption of organic and inorganic compounds on clays. The study of adsorption mechanisms on clay surfaces are also important for an understanding of many reactions which occur in soil. Thus study of the adsorption of NH_3 on clays clarifies the processes occurring when anhydrous NH_3, used as a fertilizer, is injected into soils. Again, the interactions between minerals and organic constituents in soils are illuminated by investigation of the adsorption of simpler organic compounds on pure clay specimens. For example, a recent report by Schnitzer and Kodama (1966) that fulvic acid is preferentially adsorbed in montmorillonite under acid conditions would be anticipated from the work on benzoic acid, which shows that unionized carboxylic acid groups behave like neutral polar substituents. Previous investigations (Emerson, 1955) had indicated that although synthetic polymeric alcohols were adsorbed in the interlayer space of montmorillonite, polymeric acids were not. However, Emerson used partially neutralized preparations of the polymeric acids, and the presence of negatively charged carboxylate ions would tend to inhibit interlayer penetration.

REFERENCES

ALEXIADES, C. A., and JACKSON, M. L. (1966) Quantitative clay mineralogical analysis of soils and sediments: *Clays and Clay Minerals*, Proc. 14th Conf., Pergamon Press, Oxford, 35–52.

ANDERSON, J. U. (1963) An improved pretreatment for mineralogical analysis of samples containing organic matter: *Clays and Clay Minerals*, Proc. 10th Conf., Pergamon Press, Oxford, 380–8.

EMERSON, W. W. (1955) Complex formation between montmorillonite and high polymers: *Nature* **176**, 461.

FARMER, V. C. (1958) The infrared spectra of talc, saponite and hectorite: *Mineral. Mag.* **31**, 829–45.

FARMER, V. C. (1964) Infrared absorption of hydroxyl groups in kaolinite: *Science* **145**, 1189–90.

FARMER, V. C. (1966) Dehydration reactions in alkali-halide pressed disks: *Spectrochim. Acta* **22**, 1053–6.

FARMER, V. C., and MITCHELL, B. D. (1963) Occurrence of oxalates in soil clays following hydrogen peroxide treatment: *Soil Sci.* **96**, 221–9.

FARMER, V. C., and MORTLAND, M. M. (1965) Infrared study of complexes of ethylamine with ethylammonium and copper ions in montmorillonite: *Jour. Phys. Chem.* **69**, 683–6.

FARMER, V. C., and MORTLAND, M. M. (1966) An infrared study of the coordination of pyridine and water to exchangeable cations in montmorillonite: *Jour. Chem. Soc.* 344–51.

FARMER, V. C., and RUSSELL, J. D. (1964) The infrared spectra of layer silicates: *Spectrochim. Acta* **20**, 1149–73.

FARMER, V. C., and RUSSELL, J. D. (1966) Effects of particle size and structure on the vibrational frequencies of layer silicates: *Spectrochim. Acta* **22**, 389–98.

FRIPIAT, J. J. (1964) Surface properties of alumino-silicates: *Clays and Clay Minerals*, Proc. 12th Conf., Pergamon Press, Oxford, 327–57.

FRIPIAT, J. J., CAUWELAERT, F. VAN, and BOSMANS, H. (1965) Structure of aluminium cations in aqueous solutions: *Jour. Phys. Chem.* **69**, 2458–61.

FRIPIAT, J. J., SERVAIS, A., and LEONARD, A. (1962) Study of the adsorption of amines by montmorillonites. III. The nature of the bond amine–montmorillonite: *Bull. Soc. Chim. France* 635–44.

GREENE-KELLY, R. (1953) Irreversible dehydration in montmorillonite. II. *Clay Minerals Bull.* **2**, 52–6.

GRIM, R. E., and KULBICKI, G. (1961) Montmorillonite: high temperature reaction and classification: *Amer. Min.* **46**, 1329–69.

HELLER, L., FARMER, V. C., MACKENZIE, R. C., MITCHELL, B. D., and TAYLOR, H. F. W. (1962) The dehydroxylation and rehydroxylation of triphormic dioctahedral clay minerals: *Clay Minerals Bull.* **5**, 56–72.

JØRGENSEN, P. (1966) Infrared absorption of O—H bonds in some micas and other phyllosilicates: *Clays and Clay Minerals*, Proc. 13th Conf., Pergamon Press, Oxford, 263–73.

LEDOUX, R. L., and WHITE, J. L. (1964) Infrared study of selective deuteration of kaolinite and halloysite at room temperature: *Science* **145**, 47–9.

MITCHELL, B. D., and FARMER, V. C. (1962) Amorphous clay minerals in some Scottish soil profiles: *Clay Minerals Bull.* **5**, 128–44.

MITCHELL, B. D., FARMER, V. C., and MCHARDY, W. J. (1964) Amorphous inorganic materials in soils: *Advances in Agronomy* **15**, 327–83.

MORTLAND, M. M., FRIPIAT, J. J., CHAUSSIDON, J., and UYTTERHOEVEN, J. (1963) Interaction between ammonia and the expanding lattices of montmorillonite and vermiculite: *Jour. Phys. Chem.* **67**, 248–58.

RUSSELL, J. D. (1965) Infrared study of the reactions of ammonia with montmorillonite and saponite: *Trans. Faraday Soc.* **61**, 2284–94.

RUSSELL, J. D., and FARMER, V. C. (1964) Infrared spectroscopic study of the dehydration of montmorillonite and saponite: *Clay Minerals Bull.* **5**, 443–64.

RUSSELL, J. D., and WHITE, J. L. (1966) An infrared study of the thermal decomposition of ammonium rectorite: *Clays and Clay Minerals*, Proc. 14th Conf., Pergamon Press, Oxford, 181–91.

SCHNITZER, M., and KODAMA, H. (1966) Montmorillonite: effect of pH on its adsorption of a soil humic compound: *Science* **153**, 70–1.

SERRATOSA, J. M. (1966) Infrared analysis of the orientation of pyridine molecules in clay complexes: *Clays and Clay Minerals*, Proc. 14th Conf., Pergamon Press, Oxford, 385–91.

SWOBODA, A. R., and KUNZE, G. W. (1966) Infrared study of pyridine adsorbed on montmorillonite surfaces: *Clays and Clay Minerals*, Proc. 13th Conf., Pergamon Press, Oxford, 277–88.

TROELL, E. (1931) The use of sodium hypobromite for the oxidation of organic matter in the mechanical analysis of soils: *Jour. Agr. Sci.* **21**, 476–83.

VEDDER, W. (1964) Correlations between infrared spectrum and chemical composition of mica: *Amer. Min.* **49**, 736–68.

VEDDER, W. (1965) Ammonium in muscovite: *Geochim. Cosmochim. Acta* **29**, 221–8.

VEDDER, W., and MCDONALD, R. S. (1963) Vibrations of the OH ions in muscovite: *Jour. Chem. Phys.* **38**, 1583–90.

WHITE, J. L., and BURNS, A. F. (1963) Infrared spectra of hydronium ion in micaceous minerals: *Science* **141**, 800–1.

WILSON, M. J. (1966) The weathering of biotite in some Aberdeenshire soils: *Mineral. Mag.* **35**, 1080–93.

YARIV, S., RUSSELL, J. D., and FARMER, V. C. (1966) Infrared study of the adsorption of benzoic acid and nitrobenzene in montmorillonite: *Israel Jour. Chem.* **4**, 201–13.

VIBRATIONS DU GROUPE HYDROXYLE DANS LES SILICATES EN COUCHES

V.C. FARMER, J.D. RUSSELL, J.L. AHLRICHS [1] et B. VELDE [2]

Department of Spectrochemistry, the Macaulay Institute for Soil Research, Craigiebuckler, Aberdeen

Sommaire - Au cours des dix dernières années, les études sur des argiles des sols effectuées à l'Institut Macaulay par des méthodes IR ont conduit à des résultats précieux permettant de mieux caractériser leur nature et leurs propriétés. Le présent exposé est consacré à un aspect de ce travail, à savoir aux informations relatives à la structure et à la composition qui résultent de l'étude des vibrations du groupe hydroxyle dans les minéraux argileux cristallins. De nouvelles informations sont également présentées, concernant l'affectation des bandes d'absorption d'hydroxyle dans les céladonites, biotites, phengites, montmorillonites et beidellites.

Summary - Infrared studies of soil clays at the Macaulay Institute have, over the past ten years, made a valuable contribution to characterizing their nature and properties. This paper reviews one aspect of this work, concerning the information on structure and composition which can be derived from study of hydroxyl vibrations in crystalline clay minerals. New information is also presented on the assignment of hydroxyl absorption bands in celadonites, biotites, phengites, montmorillonites, and beidellites.

Les vibrations de valence et de déformation du groupe hydroxyle dans les silicates en couches sont essentiellement localisées sur le proton et pourraient ainsi fournir des renseignements sur le milieu entourant immédiatement le proton. Ceci veut dire que les fréquences des vibrations devraient être en rapport avec la nature des cations octaédriques auxquels le groupe hydroxyle est directement coordonné de même qu'avec les champs électriques provenant des autres ions se trouvant dans son voisinage immédiat. Bien qu'il ne puisse y avoir un couplage mécanique important entre des groupes hydroxyle adjacents, il est possible qu'il se produise un certain couplage par l'action des champs électriques oscillants, dûs aux protons en vibration.

VIBRATIONS DE VALENCE DE OH

La corrélation la mieux définie entre les vibrations de valence de OH et l'occupation octaédrique est trouvée dans le cas des céladonites et des glauconites. L'étude des céladonites synthétiques préparées à la Sorbonne (fig. 1) permet l'identification certaine des fréquences de valence de OH dans les milieux suivants :

Fe^{2+}, Fe^{3+}, OH	= 3 534 cm^{-1}
Mg, Fe^{3+}, OH	= 3 557 cm^{-1}
Mg, Al, OH	= 3 602 cm^{-1}

Ces résultats confirment des conclusions antérieures, moins sûres, basées sur les spectres des céladonites et glauconites naturelles (Farmer et Russell, 1967). Une bande supplémentaire fournie par l'une d'elles à 3 577 cm^{-1} (fig. 1, céladonite A) peut être attribuée, avec une bonne certitude, à Fe^{2+}, Al, OH.

---

(1) Visiting Research Worker, Department of Agronomy, Purdue University, Indiana, U.S.A.

(2) Laboratoire de Pétrographie, Sorbonne.

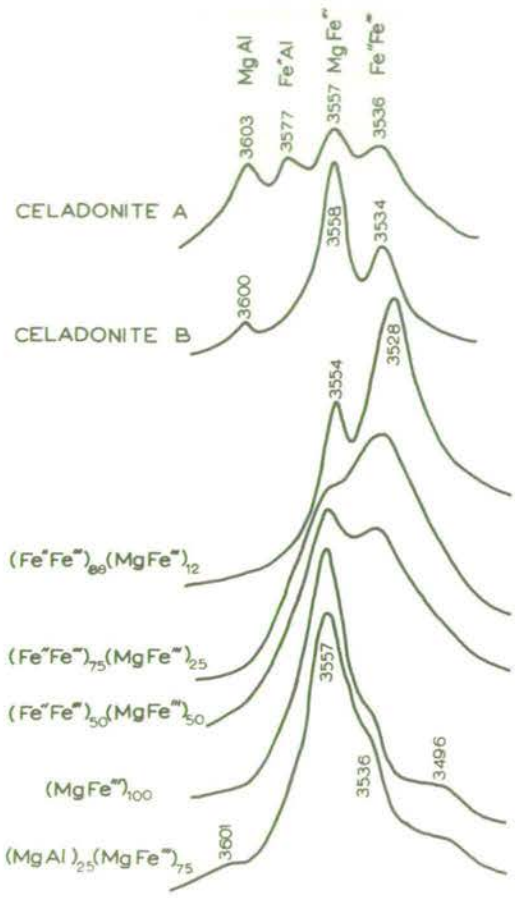

Figure 1 - Vibrations de valence de OH dans des céladonites naturelles (A et B) et synthétiques. L'occupation octaédrique des céladonites synthétiques est calculée à partir de la composition des mélanges utilisés pour la synthèse et peut ne pas représenter exactement la composition de la phase cristalline. Spectres obtenus pour un échantillon de 2 mg dans des disques de KBr de 12 mm.

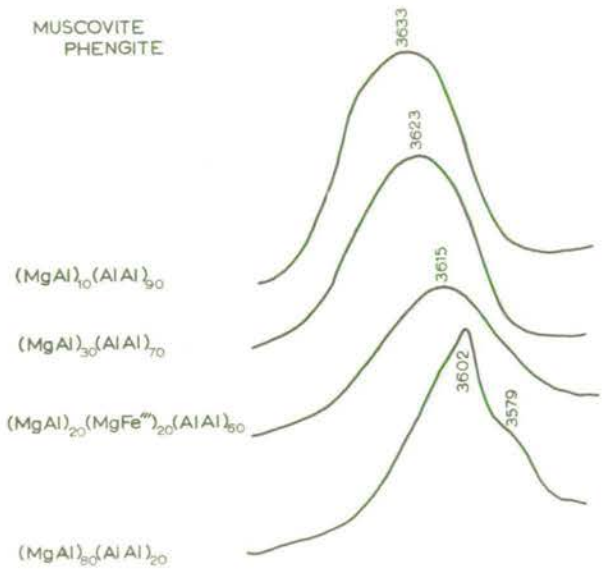

Figure 2 - Vibrations de valence de OH de micas synthétiques de la série muscovite-phengite. L'occupation octaédrique est calculée à partir de la composition des mélanges utilisés pour la synthèse. Spectres obtenus avec un échantillon de 2 mg dans des briques de KBr de 12 mm.

La corrélation directe entre l'occupation octaédrique et la fréquence de valence de OH dans la céladonite est toutefois exceptionnelle dans les silicates à couches dioctaédriques. Ainsi, les fréquences de vibration de différents groupes Al, Al, OH vont pour la kaolinite seule de 3 700 à 3 620 cm^{-1}. On trouve diverses fréquences situées dans cet intervalle pour les pyrophyllite, beidellite, montmorillonite, muscovite et margarite (Farmer et Russell, 1964). Alors que le couplage par l'intermédiaire du champ électrique peut expliquer les trois fréquences de déformation de OH différentes, fournies par les groupes superficiels hydroxyle des couches de kaolinite (Farmer, 1964), une deuteration partielle indique qu'un tel couplage n'influe pas sur les fréquences et contours de bandes trouvées avec la montmorillonite et la beidellite. La largeur considérable de la bande OH dans un grand nombre de ces minéraux reflète probablement un désordre, résultant de substitutions ayant lieu au hasard dans le réseau. Il peut y avoir dans les muscovites et les montmorillonites plus de 30 % de groupes Mg, Al, OH sans qu'une fréquence de valence de OH distincte soit mise en évidence. Par contre dans une muscovite-phengite synthétique contenant

80 % de Mg, Al, OH, la bande 3 602 cm^{-1} de ce groupe devient dominante (fig. 2). Cette distinction entre les groupes Mg, Al, OH dans les céladonites et les montmorillonites permet leur identification sans ambiguïté dans la phase céladonite de mélanges intimes de ces minéraux existant à l'état naturel.

Bien que le remplacement de Fe^{3+} par Al dans la couche octaédrique des montmorillonites et beidellites décale la fréquence de valence de OH de 3 630 cm^{-1} environ, dans les échantillons alumineux purs, à 3 554 cm^{-1} dans la nontronite (Farmer et Russell, 1964), la présence de Fe^{3+} octaédrique dans les montmorillonites est plus facile à déceler dans la région des vibrations de déformation de OH. Il en sera discuté ultérieurement.

Dans le cas des minéraux trioctaédriques, de nettes fréquences de valence reflètant l'occupation octaédrique ont été signalées pour le talc (Vedder, 1964). Dans le talc pur, le groupe Mg, Mg, Mg, OH présente une absoprtion à 3 676 cm^{-1} et le remplacement progressif de Mg^{2+} par Fe^{2+} provoque des décalages sucessifs, de l'ordre de 16 cm^{-1}, vers des fréquences plus basses. Des décalages similaires ont lieu dans les biotites, mais des bandes d'absorption séparées ne peuvent plus être résolues en raison de l'élargissement des bandes d'absorption dû au remplacement de Si par Al (Farmer et Russell, 1967). Le champ électrostatique associé à l'ion potassium de l'inter-couche, dans les phlogopites et les biotites provoque également un décalage des bandes d'absorption de OH vers des fréquences plus élevées que celles des bandes correspondantes du talc (Farmer et Russell, 1966).

Des bandes d'absorption distinctes de groupes hydroxyle, associées avec des vacances dans la couche octaédrique des biotites apparaissent près de 3 620, 3 600 et 3 550 cm^{-1} (Vedder, 1964 ; Farmer et Russell, 1964). Les tentatives d'interprétation fondées sur les spectres des biotites analysées, utilisées dans le travail de Newman et Brown (1966), rapportent la bande 3 550 cm^{-1} à Fe^{3+}, Fe^{2+}, OH et la bande 3 600 cm^{-1} à Al, Fe^{2+}, OH. Ces corrélations sont basées sur les spectres de la figure 3 et sur des observations relatives à douze phlogopites et biotites analysées qui indiquent que les bandes de vacances 3 600 cm^{-1} et 3 550 cm^{-1} existent seulement en présence d'importantes quantités d'ions ferreux et que les deux bandes apparaissent lorsque dans la couche octaédrique il existe aussi bien Al que Fe^{3+}. La seule exception constatée dans le cadre de ces études se rapporte à une phlogopite présentant une bande de vacances peu intense à 3 596 cm^{-1}, pour laquelle l'analyse n'a pas fourni d'aluminium octaédrique ni de vacances. Dans les biotites et vermiculites oxydées existant à l'état naturel ou dans celles oxydées au laboratoire au moyen de H_2O_2 ou de Br_2, il apparaît une bande intense large située à 3 560 cm^{-1} qui peut être associée avec des groupes Fe^{3+}, Fe^{3+}, OH (fig. 4). L'intensité élevée de cette bande indique qu'une augmentation de vacances a lieu pendant l'oxydation. De telles vacances peuvent être prévues lorsque trois ions ferreux adjacents dans la couche octaédrique sont oxydés en ions ferriques. La charge positive se trouvant localement en excès rendrait ce groupement instable et conduirait à la migration d'un ion ferrique, provenant de la couche octaédrique, vers l'espace inter-couche, où il serait emprisonné sous forme d'oxyde ferrique hydraté. Les spectres des biotites atmosphérisées présentent généralement, à côté des bandes hydroxyle du mica, les bandes hydroxyle des minéraux kaoliniques associés (Wilson, 1966).

VIBRATIONS DE DEFORMATION DE OH

Bien que les groupements Al, Al, OH et Mg, Al, OH ne fournissent pas de fréquences de valence de OH nettement définies pour les montmorillonites, ils donnent des vibrations de déformation de OH largement espacées au voisinage de 915 et 845 cm^{-1}, identifiées par le remplacement de l'hydrogène par le deuterium. La deutération met également en évidence deux fréquences de déformation de OH à 949 et à 930 cm^{-1} dans la beidellite, ce qui confirme la présence de deux types différents de groupes OH, fournies entièrement par

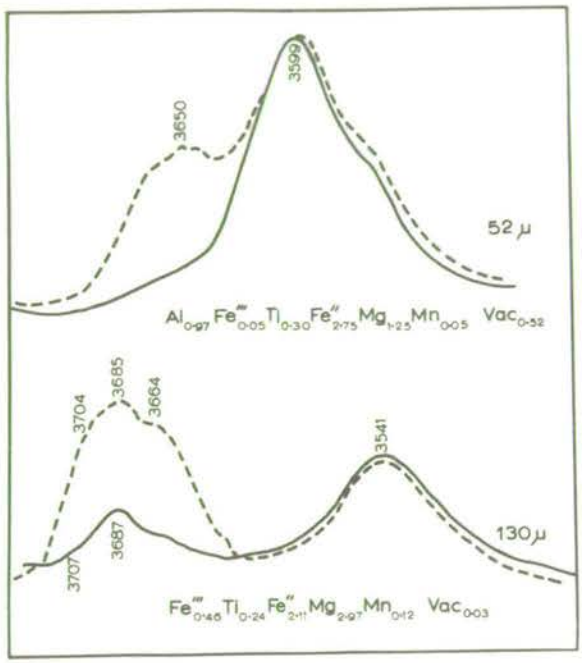

Figure 3 - Vibrations de valence de OH dans des biotites naturelles. Dans un échantillon, Fe^{3+} est le seul cation octaédrique trivalent ; dans l'autre, Al^{3+} est le cation octaédrique trivalent prédominant. L'occupation octaédrique, y compris les vacances (Vac.), est calculée à partir de l'analyse chimique. Spectres obtenus avec des lamelles de clivage de l'épaisseur indiquée ; incidence normale : (tracé plein) et à 45° par rapport à la lamelle : (tracé en tirets).

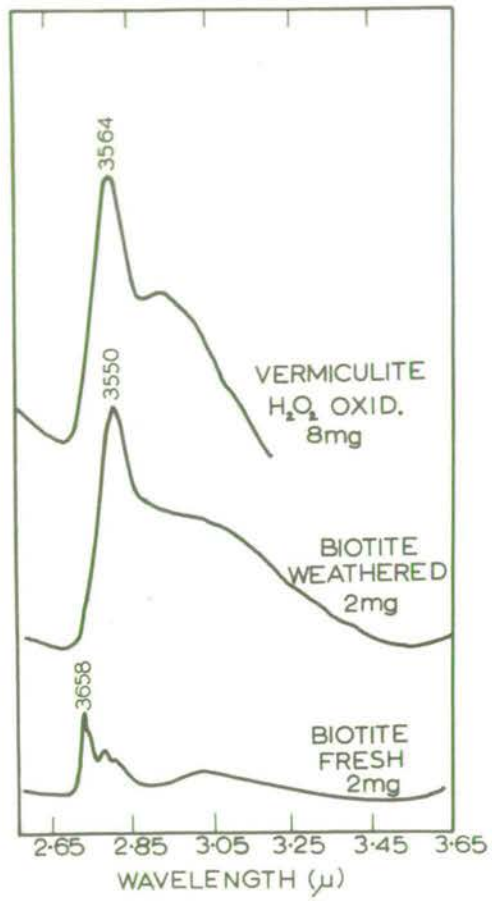

Figure 4 - Vibrations de valence de OH de (a) une biotite verte fraîche, (b) de la forme dorée de la même biotite, produite par oxydation naturelle et (c) d'une vermiculite préparée à partir de la biotite verte par traitement avec des solutions de $BaCl_2$ et oxydation subséquente donnant la forme dorée au moyen de H_2O_2. Spectres obtenus dans les disques de KBr de 12 mm, en utilisant les poids d'échantillon indiqués.

la présence de bandes d'absorption dans la région de valence de OH (Farmer et Russell, 1967). La réduction du Fe^{3+} octaédrique dans la montmorillonite de Wyoming à l'aide d'un traitement par l'hydrazine élimine cette bande et le spectre du produit est alors identique à celui des montmorillonites à faible teneur en fer du type Cheto (fig. 5). Le remplacement de l'hydrogène par le deuterium est plus difficile dans le cas des groupes Fe^{3+}, Al, OH qu'avec celui des groupes Al, Al, OH ou Mg, Al, OH dans la montmorillonite de Wyoming, ce qui est mis en évidence par la persistance de l'absorption à 884 cm^{-1} dans un échantillon deutérisé (fig. 5). Dans la terre à foulons de Woburn la bande correspondante est cependant déplacée plus facilement par la deutération, ce qui confirme qu'il s'agit d'une déformation OH. Dans la nontronite, les groupements Fe^{3+}, Fe^{3+}, OH présentent une absorption à 818 cm^{-1}. Cette bande n'est pas fortement influencée par le traitement à l'hydrazine, mais une bande auxiliaire à 850 cm^{-1}, probablement due à Fe^{3+}, Al, OH se trouve éliminée par un tel traitement. Dans les céladonites et phengites, Mg, Al, OH et Mg, Fe^{3+}, OH présentent une absorption à 836 et à 800 cm^{-1}, respectivement (fig. 6).

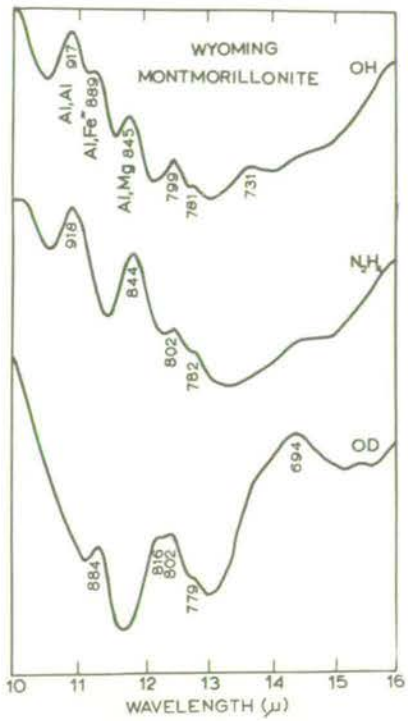

Figure 5 - Spectres IR dans la région de déformation de OH d'une montmorillonite de Wyoming (a) non traitée (OH) ; (b) réduite par de l'hydrazine (N_2H_4) et (c) traitée avec D_2O à 450°C pour transformer les groupes OH en groupes OD (OD). Spectres fournis par les disques de KBr de 12 mm contenant un échantillon de 2 mg.

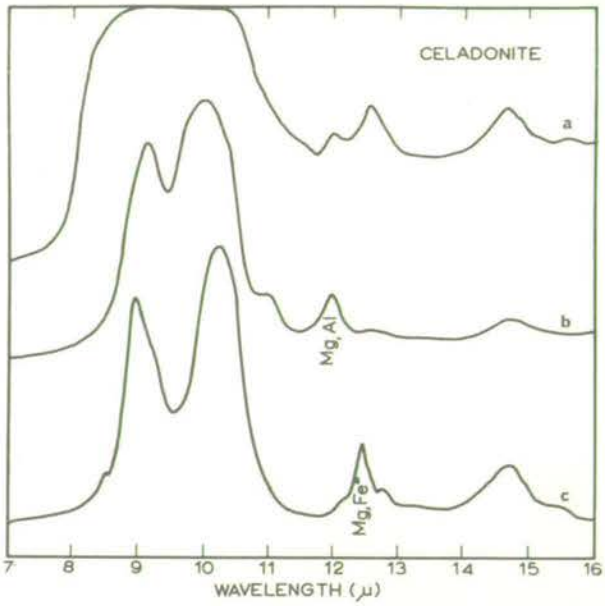

Figure 6 - Spectres IR de : (a) une céladonite naturelle ; (b) une phengite synthétique avec occupation octaédrique $(MgAl)_{80}$ $(AlAl)_{20}$; et (c) une céladonite synthétique avec occupation octaédrique $(MgFe^{3+})_{100}$.

CONCLUSION

L'étude des vibrations du groupe hydroxyle des silicates en couches peut, dans les cas favorables, fournir des informations très intéressantes sur leur structure et leur composition, informations qui ne sont pas faciles à obtenir par d'autres procédés. Parmi les problèmes qui restent à résoudre, signalons celui qui consiste à trouver de façon sûre l'affectation des bandes de toutes les vacances possibles dans les biotites et les vermiculites et également celui relatif à l'effet du Ti^{4+} octaédrique sur les vibrations de OH de ces minéraux. La différence marquée entre les fréquences de valence constatée pour des groupes OH en apparence similaires dans la pyrophyllite (3 675 cm^{-1}) et la kaolinite (3 620 cm^{-1}) appelle encore une explication satisfaisante.

BIBLIOGRAPHIE

FARMER V.C. (1964). - Science 145, 1189 - 90.

FARMER V.C. et RUSSELL J.D. (1964). - Spectrochim. Acta 20, 1149 - 73.

FARMER V.C. et RUSSELL J.D. (1966). - Spectrochim. Acta 22, 389 - 398.

FARMER V.C. et RUSSELL J.D. (1967). - Clays and Clay Minerals, Proc. 15 th Conf., Pergamon Press, Oxford, 121-142.

NEWMAN A.C.D. et BROWN G. (1966). - Clay Minerals 6, 297 - 310.
VEDDER W. (1964). - Amer. Min. 49, 736 - 768.
WILSON M.J. (1966). - Mineralog. Mag. 35, 1080 - 1092.

9th INTERNATIONAL CONGRESS OF SOIL SCIENCE
TRANSACTIONS

VOLUME III PAPER 11

CHARACTERIZATION OF CLAY MINERALS BY INFRARED SPECTROSCOPY

V. C. FARMER, J. D. RUSSELL
AND J. L. AHLRICHS

CHARACTERIZATION OF CLAY MINERALS BY INFRARED SPECTROSCOPY

V. C. FARMER, J. D. RUSSELL, AND J. L. AHLRICHS[1]

Department of Spectrochemistry, The Macaulay Institute for Soil Research, Craigiebuckler, Aberdeen

The infrared spectrum of a clay provides information which is largely complementary to that given by X-ray and thermal methods. A pure mineral species can often be more quickly and more fully defined in structure and composition by its infrared spectrum than by any other single technique; interpretation of features of the spectrum can yield information which cannot readily be obtained by other means. The power of infrared methods in clay studies can, however, be considerably increased by following changes in the spectrum when the clay is subjected to various chemical and physical treatments. Thermal treatment, deuteration, and oxidation-reduction reactions can all contribute to the interpretation of infrared spectra.

Thus changes in spectrum following thermal treatment of clays can identify reactions which give features on differential thermal analysis and thermogravimetric curves. Such studies can differentiate absorption bands of structural *OH* from those of adsorbed water, and can distinguish species of *OH* differing in thermal stability.

Water in clay samples is readily replaced by D_2O on flushing with D_2O vapour at room temperature. Structural *OH* bands and water absorption bands can then be examined free from mutual interference, and information obtained on the accessibility of NH_4^+ in clays. At higher temperatures, structural *OH* can exchange hydrogen atoms for deuterium of D_2O, so that their accessibility and reactivity can be assessed by this means.

The vibrations of *OH* groups coordinated to iron atoms are affected by the valency of iron, and so can serve as an indicator of valency. Thus oxidation-reduction reactions involving iron in octahedral sites of layer silicates can be followed in the infrared spectrum, and the spectral changes induced can assist in characterizing clay species.

The potentiality of these techniques is obvious; their application depends on the availability of suitable apparatus and procedures. It is the purpose of this paper to describe some convenient procedures in use at the Macaulay Institute, and to illustrate their application in clay mineral studies in progress there.

TECHNIQUES

(a) *Sample preparation*

The *KBr* pressed disk technique is perhaps the most generally useful method of sample preparation in clay studies. It is, however, inapplicable in

[1] Visiting Research Worker from Department of Agronomy, Purdue University, Lafayette, Indiana, U.S.A.

investigations concerning the effect of exchangeable cations on clay mineral properties, as exchange between the potassium of the *KBr* and the cation initially on the clay is inevitable. Self-supporting films of smectites (the montmorillonite-saponite group) are ideal subjects for infrared studies. Such films were first used by Serratosa (1960) and Fripiat *et al.* (1960); their potentialities are well illustrated by the work of Mortland *et al.* (1963), Russell and Farmer (1964), Russell (1965) and Farmer and Mortland (1966). The preparation of high quality films is now a routine procedure. Smectites saturated with appropriate cations are best stored as salt-free freeze-dried powders. Such powder (10 mg) is readily dispersed in 1 ml water, and evaporation of this dispersion on to thin polyethylene film, held flat on a glass plate by the capillary action of a drop of water, yields a one-inch diameter film. This film is separated from the polyethylene by drawing the plastic sheet over a sharp edge. Vermiculite films of very high optical quality can be obtained by evaporating dispersions of propylammonium vermiculite prepared as described by Walker and Garrett (1967); such films are sufficiently stable to permit soaking in normal salt solutions to introduce the desired exchangeable cation, and subsequent water washing to remove excess salt. The very high degree of parallelism of the separate vermiculite lamellae which make up these films makes diffusion of gases and liquids into them slow, so that results obtained with them are probably intermediate between those which would be obtained with large single crystals on the one hand, and with separate clay-size crystals on the other. Porous vermiculite films more representative of the properties of clay-size vermiculites can be obtained from dispersions of vermiculite saturated with the common inorganic cations, and these dispersions can be obtained from dispersions of propylammonium vermiculite by washing on the centrifuge with appropriate salt solutions, followed by thorough water washing to remove excess salt. These suspensions require treatment with an ultrasonic probe or a high speed homogenizer to reduce particle size sufficiently to avoid excessive light scattering in the vermiculite films. The Ultra-turrax homogeniser (Janke and Kunkel KG, Staufen, W. Germany) is particularly effective.

The preparation of self-supporting films by evaporation of aqueous suspensions is restricted to minerals of the smectite and vermiculite groups. Films of kaolinite and illite have insufficient cohesion and can only be handled when supported on windows transparent to infrared radiation. Such window materials are often too reactive or too limited in transmission for the purpose in hand. Thus sodium chloride windows are sensitive to high humidities, and will generally convert the clay film to the sodium-saturated form. Silver chloride windows fuse at 450°C, tend to react with base metals, and soon lose transmission after prolonged exposure to light. Zinc sulphide oxidizes on heating in air. The high reflectivity of both silver chloride and zinc sulphide reduces the transmitted radiation. Windows of quartz or thin glass (microscope slides) are suitably unreactive, but limit study to the spectral region (2-5μ) in which *OH* stretching vibrations occur.

Evaporation of aqueous suspensions of hydrated oxide gels and of

allophanes yields films which shrink and crack as they dry. Many soil clays contain these components in amounts sufficient to forbid the formation of satisfactory films. An alternative technique of forming self-supporting films has been found to be applicable to co-precipitated hydrated silica-aluminas. This technique, which involves spreading the finely dispersed freeze-dried powders between two polished steel faces, and pressing them at about 10,000 lb./sq. in., was developed in the study of the surface properties of anhydrous silica, silica-alumina catalysts, and zeolites (McDonald, 1958; Angell and Schaffer, 1965). But films prepared from the highly hydrated oxides of interest in soil studies are not always mechanically stable when heated, and it is difficult to prepare specimens thin enough to study regions of the spectrum where absorption is strong.

(b) *Vacuum cells*

Thermal treatment of clays to remove adsorbed water, or selectively to decompose their components, is a simple procedure; the main problem that arises is the examination of the product under conditions which exclude the readsorption of water. In most commercial infrared spectrometers, it is not permissible to examine samples maintained at temperatures much above 100°C, as thermal radiation from the sample distorts the absorption spectrum. It therefore often becomes necessary to cool and examine the sample in vacuum to prevent exposure to atmospheric moisture. Exclusion of atmospheric moisture is also essential in the examination of reactive deuterated samples.

For both thermal treatment and deuteration studies, the cell described by Angell and Schaffer (1965) has been found particularly convenient. Two or three samples can be treated simultaneously in this cell, so that in comparative studies all samples receive identical treatment. Its sole disadvantage lies in the fact that highly oriented films can be observed only at perpendicular incidence, so that absorption bands associated with dipole oscillations perpendicular to the clay sheets, and so perpendicular to the film surface, can escape detection. In an alternative cell design (Granquist and Kennedy, 1967) sample orientation relative to the incident beam can be adjusted, but this cell has a longer path length, and only one sample can be treated at a time.

(c) *Thermal treatment in KBr pressed disks*

The use of self-supporting films is limited to clays with appropriate physical properties. Powder dispersions on windows require material of small particle size ($< 1\mu$), and a deposition technique which avoids coagulation of these small particles, to give good transmission properties at the shorter wavelengths (near 3μ) where *OH* stretching absorption bands occur. Grinding to achieve a suitable particle size fraction is always a dangerous, if unavoidable, procedure (Farmer, 1964; Tuddenham and Lyon, 1960); quantitative transformation of small samples into a suitable form for study as window-supported dispersions is seldom possible, and always uncertain. For such materials, the *KBr* pressed-disk technique has considerable advantages, as microgram quantities of material can be quan

titatively handled and examined by this means, and particle-size requirements are less stringent because of the good match in refractive index between the minerals and the surrounding *KBr*. Even with minerals which have good film-forming characteristics, the pressed disk technique is often the most convenient way of studying the strongest bands in the spectrum.

Suitably prepared *KBr* pressed disks are sufficiently porous to permit the slow diffusion of water vapour into and out of them (Farmer, 1966). It is therefore possible to drive off adsorbed water by heating the disk overnight in an oven at 100-200°C and to record the spectrum before atmospheric water is readsorbed. Provided the clay complex is saturated with a cation such as ammonium or potassium, and structural hydroxyl absorption is not too weak, 100°C is generally sufficient (Farmer and Russell, 1967). It is also possible to follow thermal decomposition of clay minerals by examining in *KBr* disks a series of samples heated to successively higher temperatures. Where amounts of material are limited, there would clearly be an advantage if thermal decomposition could be followed on a single sample incorporated in a *KBr* disk. This procedure has, in fact, been successfully applied at temperatures up to 300°C (Farmer, 1966) and recent trials have indicated that thermal decompositions generally proceed normally in *KBr* disks at temperatures up to 700°C. Experiments have not been carried out beyond the fusion point of *KBr* (730°C). The pressed disks often become opaque on heating at higher temperatures, but full transparency was readily recovered by repressing the disk. In general, the temperatures of decomposition of clay minerals in disks, following heating for 16 hours, did not differ markedly from those observed when the powdered mineral is heated alone in air.

Selective decomposition of different species of *OH* in a single mineral was observed in a celadonite. It has been established from a study of synthetic and natural celadonites that in this mineral the *OH* stretching frequency is determined solely by the octahedral ions to which the *OH* group is coordinated, provided substitution of aluminium for silicon is low (Farmer, Russell, Ahlrichs, and Velde, 1967). In the celadonite used in the present study, four discrete *OH* stretching frequencies were detectable, corresponding to *OH* coordinated to the following octahedral ion pairs: $Fe^{2+}Fe^{3+}$ — 3534 cm^{-1}; $MgFe^{3+}$ — 3557 cm^{-1}; $Fe^{2+}Al$ — 3577 cm^{-1}; and $MgAl$ — 3602 cm^{-1}. By 400°C, the two lower frequency bands, corresponding to *OH* groups coordinated to a ferric ion, were largely lost, but the two higher frequency bands were not affected. Dehydroxylation was complete for all species of *OH* at 500°C.

In one instance, clear evidence was obtained for interaction between the *KBr* and the mineral. The brucite interlayer of the chlorite, pennine, was found to decompose completely at 500°C in *KBr* disks, but this layer did not begin to decompose till 600°C when the mineral was heated alone. In both instances, *OH* groups of the phlogopite layer were retained up to 700°C, but for the mineral heated alone these absorbed at 3679 cm^{-1}, whereas in the presence of *KBr* they absorbed principally at 3710 cm^{-1}. A frequency near 3679 cm^{-1} is characteristic of *OH* in the talc structure,

whereas a frequency near 3710 cm^{-1} is characteristic of *OH* in phlogopite. The higher frequency of the latter has been shown to be due to the electrostatic field of the potassium ions which are positioned directly above the protons of the lattice *OH* in phlogopite (Farmer and Russell, 1966). The results with the chlorite therefore indicate that potassium ions from the potassium bromide migrate into the interlayer space of the chlorite as the brucite layer decomposes. The infrared spectrum of montmorillonite dehydroxylated in a *KBr* disk showed significant differences from the normal pattern of the dehydroxylate, suggesting that here, too, some interaction with the *KBr* may have occurred.

Applications

Problems in which some of these techniques have found application have frequently arisen in the course of collaborative studies initiated by colleagues at the Macaulay Institute, R. C. Mackenzie, B. D. Mitchell, W. A. Mitchell and M. J. Wilson, as well as by scientists at other centres. Published work involving infrared investigations of clays at this Institute has recently been reviewed (Farmer and Russell, 1967), and it is proposed here to illustrate their application in current investigations which have yielded new and interesting results.

(a) *Deuteration studies*

At room temperature interlayer water in smectites can readily be replaced by D_2O, and exchange can occur between interlayer D_2O and hydrated NH_4^+ to yield ND_4^+. NH_4^+ trapped in the interlayer space of collapsed vermiculites might be expected to be inaccessible to D_2O, and this has been tested with films of vermiculite prepared from the Loch Scye soil vermiculite described by Aitken (1965). These films were prepared in the propylammonium form, and converted to the NH_4^+ form by washing with NH_4Cl solution. Repeated flushing with D_2O at room temperature failed to convert 56% of the NH_4^+ *to* ND_4^+. Warming the film to 350°C in D_2O vapour induced further exchange between D_2O and NH_4^+, but exchange between ND_4^+ and lattice *OH* was then also detectable. It is interesting to compare these results with those obtained by the procedure of Alexiades and Jackson (1966) for estimating the vermiculite content of minerals. This indicated that after potassium saturation and drying at 100°C, 77% of the potassium resisted exchange with ammonium ions. It is clear from this work that estimates of the "vermiculite" content of minerals are dependent on the conditions used and the method of study.

NH_4^+ in beidellite and saponite readily exchanged with D_2O, but a significant proportion of NH_4^+ in Wyoming montmorillonite (12%) and hectorite (23%) resisted exchange with D_2O at room temperature. Alexiades and Jackson (1966) obtained very similar figures for the "vermiculite" content of hectorite and montmorillonite by their procedure. These results support the suggestion that the stable NH_4^+ formed when *Na*-saturated montmorillonite is treated with ammonia gas is strongly adsorbed on inaccessible sites (Russell, 1965).

Exchange between interlayer D_2O and the lattice *OH* of expanding

layer silicates has been mainly studied using ammonium saturated species since the ND_4^+ formed provides a source of deuterium in the interlayer

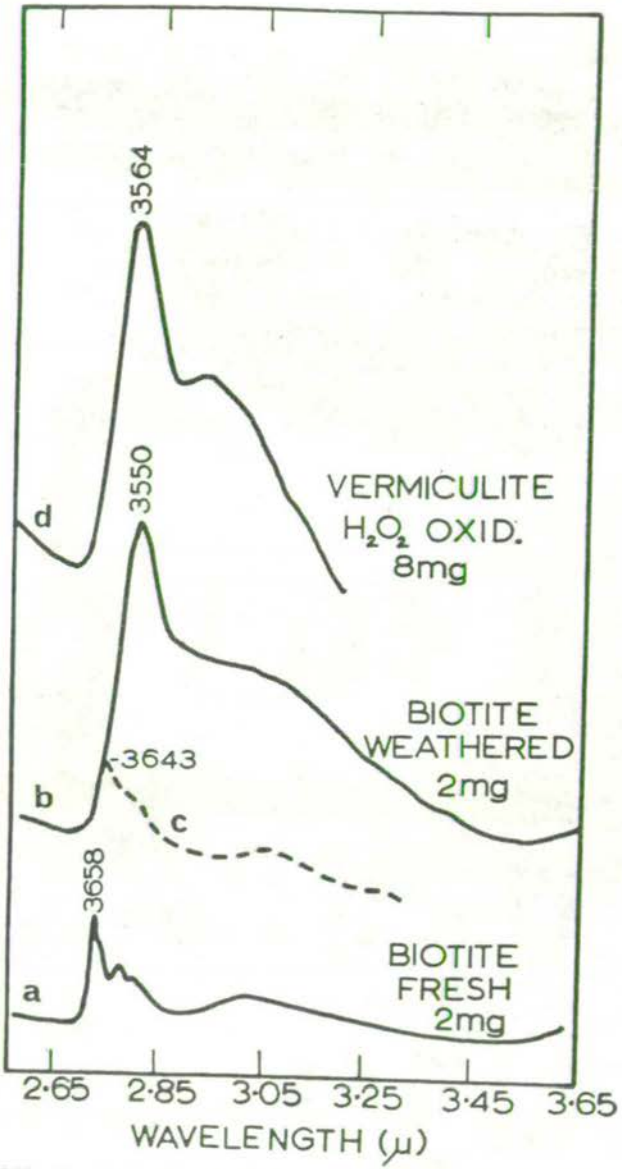

Fig. 1.—OH vibrations of (a) fresh green biotite, (b) weathered, golden biotite, (c) weathered biotite, partially dehydroxylated at 400°C and (d) vermiculite, prepared from fresh green biotite, and oxidized with H_2O_2. Spectra were obtained in 12 mm. *KBr* disks, using the sample weights indicated. For spectra (a), (b) and (d), disks were heated to 200°C to reduce the adsorbed water content, but for spectrum (c), the disk was heated to 400°C to effect dehydroxylation.

space at elevated temperatures, when interlayer D_2O is largely lost, and the mineral collapses to a 10 Å spacing. No exchange with lattice *OH* has been detected at room temperature, but a weak *OD* vibration first appears after treatment at 100°C. In contrast, the hydroxyl of interlayer $Mg(OH)_2$ and $Al(OH)_3$ formed in montmorillonite by the technique of Slaughter and Milne (1960), undergoes essentially complete exchange with D_2O at 100-150°C. On exposing such a preparation to air humidity, interlayer D_2O is replaced by H_2O, and the *OD* vibrations of the interlayer hydroxides can then be observed entirely free from interference by water absorption bands, and relatively free from interference by lattice *OD* absorption. This study has shown that the absorption bands of the interlayers in these synthetic chlorite-like preparations are considerably weaker, and occur at higher frequencies, than the corresponding bands of natural chlorite minerals. The highest frequency observed for the brucite layer in natural chlorites is in pennine, where it gives a strong broad band at 3638 cm^{-1} with a shoulder at 3500 cm^{-1}. In montmorillonite, interlayer $Mg(OH)_2$ gives only the single maximum at 3710 cm^{-1} observed by Russell (1965); interlayer $Al(OH)_3$ has its maximum absorption at 3680 cm^{-1}, with a low frequency shoulder which does not extend much below 3580 cm^{-1}.

Complete or nearly complete replacement of lattice *OH* by *OD* groups in beidellite, montmorillonite, saponite and hectorite is only achieved after repeated treatment at temperatures of 350°C or higher. The temperature of treatment is, however, limited by the tendency of NH_4-saturated smectites to lose their expanding properties (Russell and Farmer, 1964). Comparison of the spectra of the deuterated forms of these minerals with the spectra of the normal proton-containing species permits identification of absorption bands arising from *OH* vibrations. The results (Farmer, Russell, Ahlrichs and Velde, 1967) support previous suggestions (Farmer and Russell, 1964, 1967) that the bending vibrations of *OH* groups coordinated to the octahedral ion pairs *AlAl*, *MgAl*, and $Fe^{3+}Al$ give distinct absorption bands in the 800-950 cm^{-1} region of the spectra of dioctahedral minerals. This assignment is a powerful tool which gives direct information on the octahedral occupancy of montmorillonites, and on the oxidation state of iron in the octahedral layer.

In saponite and hectorite, the study of deuterated samples has indicated that a band at 655 cm^{-1}, previously assigned to an *Si-O* in-plane vibration (Farmer, 1958), is in fact the *OH* bending vibration. This assignment is consistent with the results of neutron scattering studies on these minerals (Naumann *et al.*, 1966).

(b) *Oxidized biotites and vermiculites*

Iron in fresh biotites is predominantly in the ferrous form, but natural weathering processes in soils largely oxidize this iron to the ferric state, with or without accompanying vermiculitization of the biotite (Walker, 1949). Where the ferrous content of the original biotite is high, the valency change must lead to a considerable excess of positive charge in the octahedral layer, and it has been suggested that this is compensated by ejection of ferric ions from the octahedral layer (Walker, 1949). This suggestion is supported

by the common association of goethite (Walker, 1949) and hematite (Rimsaite, 1967a, b) with oxidized biotites, but it is difficult to confirm the hypothesis by chemical analysis, as there are uncertainties in the calculation of structural formulae of biotites (Rimsaite, 1967a), and these uncertainties are further increased by partial vermiculitization and chloritization of oxidized biotites (Rimsaite, 1967b).

Ejection of iron from the octahedral layer leads to an increase in the number of unfilled sites; *OH* groups associated with such vacancies are coordinated to only two octahedral cations, and give distinctive infrared absorption bands, which lie at frequencies lower than the bands of *OH* groups associated with three octahedral cations (Serratosa and Bradley, 1958; Vedder, 1964). Comparison of the spectra of oxidized and unoxidized portions (golden and green respectively) of a single crystal, previously studied by Rimsaite (1967b), confirms the presence of greatly increased numbers of vacancies in the oxidized portion, as indicated by the development of a strong band at 3550 cm^{-1} (Fig. 1a and b). *OH* groups associated with vacancies are lost by dehydroxylation in the *KBr* disk at 400-450°C, and it is then possible to see (Fig. 1c) a weak residual band of *OH* groups associated with filled sites at 3643 cm^{-1}. This frequency can be ascribed to *OH* associated with the grouping Mg_2Fe^{3+}. The principal band of the unoxidized biotite at 3658 cm^{-1} can be ascribed to *OH* associated with Mg_2Fe^{2+}, $MgFe_2^{2+}$ and Fe_3^{2+} groupings, and the loss of this band is consistent with oxidation of ferrous to ferric ions.

Refluxing with $BaCl_2$ solutions proved effective in removing interlayer potassium from the fresh biotite without significant oxidation, as indicated by the infrared spectrum. Air oxidation of the vermiculite formed resulted in partial oxidation (loss of the 3658 cm^{-1} band) without creation of many new vacancies. Oxidation with H_2O_2 or Br_2 caused a marked colour change from green to golden, and in these samples the vacancy band at 3550 cm^{-1} is strongly developed, as in the naturally oxidized biotite (Fig. 1d).

Ferric ions ejected from the octahedral layer of oxidized biotites and vermiculites would be expected to be initially trapped in the interlayer spaces as hydrated ferric oxides or oxy-cations. Treatment of bromine-oxidized vermiculite with hydrazine to reduce these interlayer ferric species to ferrous forms permitted the extraction of 1·6% *Fe* from the vermiculite under mild conditions (*NaCl* solutions containing 1:10 phenanthroline at *pH* 4). The unoxidized vermiculite yielded only one tenth the amount of *Fe* under these conditions.

Infrared study of the thermal behaviour of oxidized biotites and vermiculites (Fig. 1) indicates that considerable loss of lattice *OH* occurs before loss of adsorbed molecular water is complete. Lattice *OH* in altered phlogopites of low iron content is considerably more stable, and infrared studies at this Institute have served to determine the point on thermogravimetric curves at which loss of molecular water is complete and loss of lattice *OH* begins. This information is essential to the calculation of structural formulae for altered phlogopites from the results of chemical analysis (Newman, 1967).

Conclusions

The application of infrared spectroscopy to mineral studies is essentially an empirical science, in which theory guides interpretation and points to profitable fields of investigation, but can seldom predict details of the spectra of novel structures. The development of such a science is necessarily slow, as it is dependent on experience gained from a wide range of minerals and this in turn is dependent on convenient and appropriate apparatus and techniques of study.

The first exploratory investigation of mineral spectra was made over sixty years ago by Coblentz under conditions of intimidating difficulty. Developments in sample handling techniques, infrared spectrometers, and ancillary equipment have now rendered the process of obtaining high quality mineral spectra over an ever-widening range of frequencies a rapid and often routine procedure, and a body of knowledge is being built up which makes the study of such spectra increasingly profitable.

It is hoped that this paper will make some convenient techniques more widely known to soil mineralogists, and suggest possible fields in which they can be employed.

Acknowledgments

The authors are indebted to Dr. J. H. Y. Rimsaite (Geological Survey of Canada) and Dr. A. C. D. Newman (Rothamsted Experimental Station) for samples of well characterized biotites, and to Mrs. K. Law and Mr. A. R. Fraser for able technical assistance.

References

Aitken, W. W. S. (1965)—*Mineralog. Mag.* **35**, 151-164.
Alexiades, C. A. and Jackson, M. L. (1966)—*Clays Clay Miner.* **14**, 35-52.
Angell, C. L. and Schaffer, P. C. (1965)—*J.phys.Chem.* **69**, 3463-3470.
Farmer, V. C. (1958)—*Mineralog. Mag.* **31**, 829-845.
Farmer, V. C. (1964)—In "The chemistry of cements", Taylor, H. F. W. (Ed.). Vol. 2, p. 289. [Academic Press, London.]
Farmer, V. C. (1966)—*Spectrochim. Acta.* **22**, 1053-1056.
Farmer, V. C. and Mortland, M. M. (1966)—*J.chem.Soc.* 344-351.
Farmer, V. C. and J. D. Russell (1964)—*Spectrochim. Acta.* **20**, 1149-1173.
Farmer, V. C. and Russell, J. D. (1966)—*Spectrochim. Acta.* **22**, 389-398.
Farmer, V. C. and Russell, J. D. (1967)—*Clays Clay Miner.* **15**, 121-142.
Farmer, V. C., Russell, J. D., Ahlrichs, J. L. and Velde, B. (1967)—*Bull.Grpe.fr.Argiles.* (In press).
Fripiat, J. J., Chaussidon, J. and Touillaux, R. (1960)—*J.phys.Chem.* **64**, 1234-1241.
Grandquist, W. T. and Kennedy, J. V. (1967)—*Clays Clay Miner.* **15**, 103-117.
McDonald, R. S. (1958)—*J.phys.Chem.* **62**, 1168-1178.
Mortland, M. M., Fripiat, J. J. Chaussidon, J. and Uytterhoeven, J. (1963)—*J.phys.Chem.* **67**, 248-258.
Naumann, A. W., Safford, G. J. and Mumpton, F. A. (1966)—*Clays Clay Miner.* **14**, 367-383.
Newman, A. C. D. (1967)—*Clay Miner.Bull.* **7**, 215-227.
Rimsaite, J. H. Y. (1967a)—"Studies of rock-forming micas". Bulletin **149**, Geological Survey of Canada.
Rimsaite, J. H. Y. (1967b)—*Clays Clay Miner.* **15**, 375-393.
Russell, J. D. (1965)—*Trans.Faraday Soc.* **61**, 2284-2294.
Russell, J. D. and Farmer, V. C. (1964)—*Clay Miner. Bull.* **5**, 443-464.
Serratosa, J. M. (1960)—*Am.Miner.* **45**, 1101-1104.
Serratosa, J. M. and Bradley, W. F. (1958)—*J.phys.Chem.* **62**, 1164-1167.

Slaughter, M. and Milne, I. H. (1960)—*Clays Clay Miner.* **7**, 114-124.
Tuddenham, W. M. and Lyon, R. J. P. (1960)—*Analyt.Chem.* **32**, 1630-1634.
Vedder, W. (1964)—*Am.Miner.* **49**, 736-768.
Walker, G. F. (1949)—*Mineralog.Mag.* **28**, 693-703.
Walker, G. F. and Garrett, W. G. (1967)—*Science,N.Y.* **156**, 385-387.

Summary

The potential contribution of infrared spectroscopy to the characterization of clay minerals is often limited by technical considerations. Recent advances in techniques of sample preparation and handling are described which permit the study of clay mineral spectra under vacuum or controlled-atmosphere conditions after heat treatment at temperatures up to 1000°C. The use of *KBr* pressed disks to follow the thermal behaviour of a single small sample in the range 100 to 700°C is illustrated. Examples of the application of these techniques are given; these include studies of the accessibility and reactivity of ammonium ions and hydroxyl groups in clay minerals, and evidence for the development of octahedral vacancies in biotite and vermiculite consequent upon the oxidation of octahedral ferrous to ferric ions.

Résumé

La contribution potentielle de la spectroscopie infra-rouge à la caractérisation des minéraux des argiles est souvent limitée par des considérations techniques. Des progrès récents dans les techniques de la préparation et du traitement des échantillons sont décrits, qui permettent l'étude des spectres des minéraux d'argiles sous des conditions de vacuum ou d'atmosphère contrôlée, après avoir été soumis à la chaleur jusqu'à 1000°C. L'emploi de disques pressés *KBr* pour observer le comportement d'un seul petit échantillon dans la zone de 100 à 700°C est illustré. Des exemples de l'application de ces techniques sont indiqués; parmi ceux-ci sont inclues des études de l'accessibilité et de la réactivité des ions d'ammonium et des groupes hydroxyles dans les minéraux des argiles, et des évidences du développement de vides dans la biotite et la vermiculite comme suite de l'oxidation des ions octaédriques ferreux en ions ferriques.

Zusammenfassung

Der potentielle Beitrag von infraroter Spektroskopie zu der Kennzeichnung von Tonmineralen, ist oft aus technischen Gründen beschränkt. Jüngste Fortschritte in Methoden der Probebereitung und Handhabung werden beschrieben, welche die Untersuchung von Tonmineral-Spektren unter Vakuum oder kontrollierten atmosphärischen Bedingungen, nach einer Hitze-Behandlung bei Temperaturen bis zu 1000°C, ermöglichen. Die Verwendung von *KBr* gepressten Scheiben, dem Thermalverhalten einer einzelnen kleinen Probe in dem Ausmass von 100° bis zu 700°C folgend, ist beschrieben. Beispiele der Anwendung dieser Methoden werden gegeben; diese enthalten Untersuchungen der Zugänglichkeit und Reaktion von Ammonium-Ionen und Hydroxyl-Gruppen in Tonmineralen, und Beweise für die Entwicklung von oktaedrischen Leeren in Biotit und Vermikulit, welche sich aus der Oxydation von oktaedrischen Eisen- zu Eisenoxyd-Ionen ergeben.

IDENTIFICATION OF INORGANIC PYROPHOSPHATE IN ALKALINE EXTRACTS OF SOIL

By G. ANDERSON and J. D. RUSSELL

An acid-labile phosphate has been detected in alkaline extracts of four acid soils, and has been isolated and purified by ion-exchange and paper chromatography. Its chromatographic properties, its rate of hydrolysis in hydrochloric acid- and the infra-red spectrum of its barium salt show that it is inorganic pyrophosphate.

In three of the soils the amount was in the range 2·1–2·6 ppm P, compared with only 0·5 in the fourth but the investigation was essentially qualitative and losses may have occurred during isolation. The phosphate may occur in the soil in inorganic form or alternatively as an ester which is mineralised during extraction.

Introduction

The phosphorus compounds of natural origin which have so far been identified in soil are inorganic orthophosphate and esters of orthophosphoric acid. Other naturally-occurring compounds of phosphorus, such as pyrophosphate and its esters, have not hitherto been detected in soils although polyphosphates occur in plants and micro-organisms and must reach the soil in decomposing litter.

During investigations in this laboratory on the nature of the phosphates present in sodium hydroxide extracts of soil, fractions have been obtained which do not contain orthophosphate or any of the organic phosphates which have been recognised previously. A substance has been isolated from one of these fractions which releases orthophosphate on treatment with dilute acid and has been identified as inorganic pyrophosphate.

This paper describes the isolation and characterisation of the pyrophosphate.

Experimental

Soil extraction and preliminary fractionation of phosphates

The soil sample (25 g) was pretreated with dilute HCl and extracted with hot NaOH, essentially as described by McKercher & Anderson.[1]. After pH adjustments a fraction containing most of the phosphate was precipitated by the addition of barium acetate and ethanol. This precipitate was shaken for 2 hours with 50 ml of the cation-exchange resin Amberlite IR-120, H^+ form, and the resin was removed by filtration through a filter paper which had been lightly punctured several times with a pointed glass rod. The solution was cleared by centrifuging and passed through a column of Dowex-1 anion-exchange resin (X8; 100–200 mesh; formate form; 160 × 12 mm) at a rate of 0·5 ml/min. The column was eluted at the same rate with 250 ml of 0·24 M and 250 ml 0·40 M ammonium formate, pH 7·0.

The procedure was repeated eight times and 2 l of the 0·40 M formate eluate was reduced in volume to about 250 ml *in vacuo* at 25°. To this was added 200 ml ethanol, a few drops of ammonium hydroxide and 10 ml 30% (wt./vol.) barium acetate. The white precipitate which formed was removed by centrifuging after standing for 16 hours, washed twice with 50% aqueous ethanol, and allowed to drain. The precipitate was dissolved by stirring with 2 ml IR-120 (H) cation-exchange resin and 5 ml water, the solution was decanted, and the resin washed with 5 ml water. The solution and washings were combined.

Ion-exchange chromatography

Phosphates were examined in two different systems, using the chloride and formate forms of Dowex-1 anion-exchange resin (X8; 100–200 mesh).

Chloride form

A solution of the phosphates in the acid form was passed through the column (150 × 10 mm) at a rate of 0·5 ml/min and the column was eluted with 0 to 1 M-KCl at 1 ml/min in an apparatus similar to that described by Parr.[2] The reservoir was a 10 cm diameter glass jar, containing 1 litre M-KCl and the mixing vessel a 12·5 cm beaker with water to the same level (approximately 1·5 l).

Formate form

The phosphate solution was passed through the column (160 × 10 mm) as above. For elution, the mixing vessel consisted of a 250 ml conical filter flask fitted with a funnel containing 1 litre 0·5 M-$HCOONH_4$, pH 7·0, and the column was eluted at 0·5 ml/min.

Gel filtration

The phosphate fractions obtained by ion-exchange chromatography were freed from the eluting salt by gel filtration. The appropriate fractions were bulked, reduced in volume to less than 5 ml *in vacuo* at 25°, and passed through a column of Sephadex G-10 (40–120 μ; 13 × 1 in). The column was eluted with water at a rate of 2 ml/min, and the phosphate content and conductivity of the eluted fractions were measured.

Paper partition chromatography

The solvents were those described by Hanes & Isherwood.[3]

Solvent A

n-Propanol–ammonium hydroxide–water (6 : 3 : 1 by vol.). Descending development for 48 hours.

Solvent B

Iso-propyl ether–90% HCOOH (6 : 4 by vol.). Descending development for 8 hours.

The chromatograms were dried and phosphates located with the ferric chloride–salicylsulphonic acid spray reagent described by Wade & Morgan.[4]

Estimation of phosphate

Orthophosphate was determined by the method of Dickman & Bray as modified by Mehta *et al.*[5] or, in the presence of acid-labile phosphate, by the method of Martin & Doty.[6] Total phosphate was measured as orthophosphate after oxidation of organic matter in the presence of magnesium nitrate followed by treatment with HCl. Acid-labile phosphate was measured as orthophosphate after heating in 1 N-HCl in boiling water for 15 minutes.

Rate of hydrolysis of acid-labile phosphate

Aliquots of an aqueous solution of the phosphate, containing about 10 μg P, were treated with HCl to give a final volume of about 10 ml and a normality of 0·1. The solutions were quickly heated to boiling point over a flame and then placed in boiling water for periods ranging up to 50 minutes. They were immediately cooled and orthophosphate was determined by the method of Martin & Doty.[6] A solution of pyrophosphate of similar concentration was hydrolysed at the same time.

Infra-red analysis

Samples (1 mg) were incorporated in 12 mm diameter KBr pressed discs. Infra-red spectra were recorded on a Grubb Parsons Spectromaster over the range 5000–400 cm^{-1}. Where sample weights were low, a micro-disc technique was employed; 0·1 mg sample was ground with 30 mg KBr and pressed in a 2 mm × 10 mm slot in an aluminium disc.

Results

Soils

The soils examined (Table I) were surface agricultural soils from Wales and Scotland. The Welsh soils were from the National Agricultural Advisory Service reference plots at Trawscoed, Aberystwyth and had received no phosphate fertiliser for twelve years. The Scottish soils had received no phosphate fertiliser other than standard commercial products containing orthophosphate.

Detection of an acid-labile phosphate component

Acid-labile phosphate was first detected in the Trawscoed grass/clover soil. Extraction with alkali and a preliminary fractionation of the phosphates by ion-exchange chromatography yielded two fractions, eluted, respectively, from a column of Dowex-1 with 0·24 M and 0·40 M-$HCOONH_4$. The bulk of the phosphate in the first fraction was inorganic orthophosphate but both fractions contained other phosphates.

Ion-exchange chromatography of the material in the 0·40 M eluate, eluting with a gradient of KCl from Dowex-1, indicated that a number of components were present. Analysis for total phosphate showed several peaks (Fig. 1(a)) while analysis for orthophosphate by the method of Dickman & Bray showed a small peak with a maximum concentration in fraction 24, coinciding with the main component but only constituting a small part of it. Ion-exchange chromatography of orthophosphate under the same conditions gave two peaks, with maxima at fractions 8 and 13 (Fig. 1(b)). It was confirmed that no impurity was present and the peaks were presumably given by different ionic species. Analysis of the main soil peak by the method of Martin & Doty showed that no orthophosphate was in fact present so that the orthophosphate measured by the Dickman & Bray method must have been released by acid hydrolysis. Measurement of acid-labile phosphate showed that about half of the phosphate in the peak was converted to orthophosphate in 15 minutes in 1 N-HCl at 100° (Fig. 1(c). Chromatography of pyrophosphate in the same system gave a peak with maximum at fraction 25 (Fig. 1(d)).

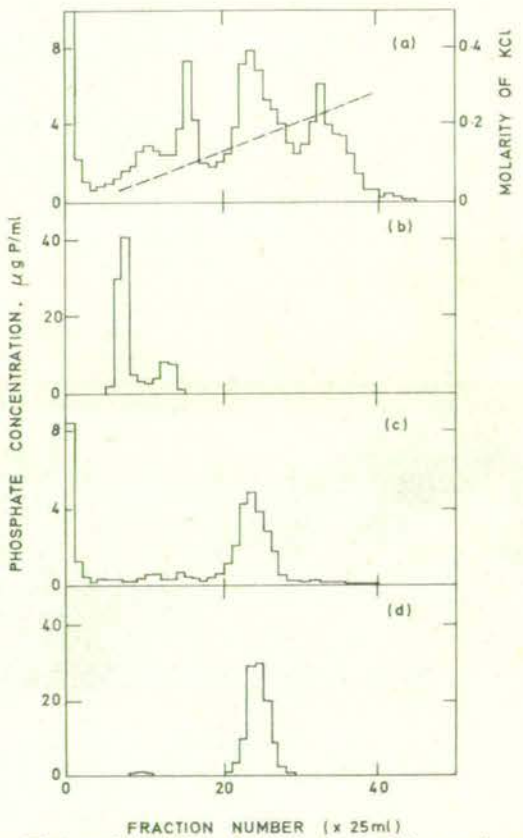

FIG. 1. *Elution of phosphates from Dowex-1 with a gradient of KCl*

Sorbed material: (a) and (c) a phosphate fraction isolated from 200 g soil (total and acid-labile phosphate respectively); (b) 10 mg KH_2PO_4; (d) 10 mg $Na_2H_2P_2O_7$

TABLE I

Soil details

Location	Parent material	Crop	pH	Organic matter %C
Trawscoed, Cardiganshire	Silurian shales	Grass/clover	5·5	3·2
Trawscoed, Cardiganshire	Silurian shales	Potatoes	5·4	2·9
Logie Newton, Aberdeenshire	Slate drift	Grass	6·0	5·7
Greenhall, Aberdeenshire	Granite drift	Grass	5·8	4·8

Characterisation of the acid-labile phosphate

When the fractions containing the acid-labile soil component (21 to 27, Fig. 1(c)) were bulked, concentrated, and passed through Sephadex G-10, phosphate was eluted before KCl. Ion-exchange chromatography of the phosphate, eluting from Dowex-1 with a gradient of $HCOONH_4$, gave peaks with maxima in fractions 24, 51 and 57 (Fig. 2(a)). The first, at 24, was orthophosphate (compare Fig. 2(b)) produced by hydrolysis of the acid-labile component in the period between the two ion-exchange separations. If this time was reduced to the minimum possible, only a trace of orthophosphate was obtained. The second peak, at 51, was the acid-labile component (Fig. 2(c)), incompletely separated from an unidentified component at fraction 57 and its position again corresponded to that of pyrophosphate (Fig. 2(d)). Fractions 45 to 53 were bulked, concentrated, passed through Sephadex G-10 to remove formate and the phosphate solution was concentrated to a volume of about 200 μl *in vacuo* at 25°.

Paper-chromatography of the solution using solvent A showed the presence of three components, one of which, on extraction from the paper with acid, was found to contain acid-labile phosphate. Its position with this solvent was similar to pyrophosphate, inositol diphosphate, and diphosphoglycerate, suggesting that it was a diphosphate (Rpp = 0·97, Table II). A second phosphate, Rpp = 0·56, was probably the component present in the peak at fraction 57 (Fig. 2(a)). A third component, Rpp = 3·60, contained no phosphorus and the fact that it gave a spot with the ferric chloride–sulphosalicylic acid spray reagent indicated it was a complexing agent.

When the solution containing these three components was frozen and allowed to melt, colourless crystals remained undissolved for a short time. The solution was frozen and thawed three times and the crystals removed each time. The material was recrystallised by dissolving in about 100 μl water, adding acetone to precipitate it and heating in water until sufficient acetone had evaporated and the material just dissolved. On cooling, colourless crystals slowly separated. The composition of this substance, its chromatographic properties and its infra-red spectrum confirmed that it was ammonium oxalate.

After removal of most of the oxalate, the phosphate solution was further purified by paper chromatography. It was applied in a band about 12 in long to Whatman No. 1 paper and the chromatogram was developed for 5 days with solvent A. The main (acid-labile) phosphate component was located by spraying strips cut from the edges of the paper, and eluted with water until the volume of eluate was about 200 μl. Chromatography of an aliquot of this solution in solvent B gave a single spot matching pyrophosphate (Table III). The rate of hydrolysis of the phosphate in 0·1 N-HCl at 100° was similar to that of pyrophosphate, with a half-life of about 11 minutes (Fig. 3).

Addition of a few ml of 30% (wt./vol.) barium acetate to the phosphate solution produced a white precipitate which was centrifuged, washed with 50% aqueous ethanol and dried. The infra-red spectrum of the salt confirmed that it was barium pyrophosphate.

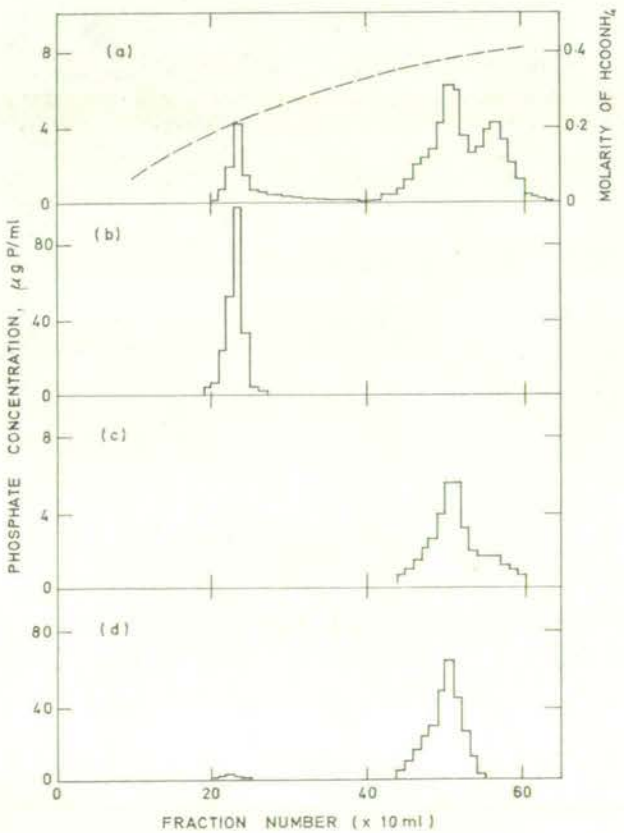

FIG. 2. *Elution of phosphates from Dowex-1 with a gradient of ammonium formate*

Sorbed material: (a) and (c) soil fraction containing acid-labile P (total and acid-labile P respectively); (b) 10mg KH_2PO_4; (d) 10 mg $Na_2H_2P_2O_7$

TABLE II

Paper-chromatography of a phosphate fraction from soil, using solvent A

Distance moved is expressed relative to pyrophosphate (Rpp)

Material	Rpp
Fractions 45 to 53 (Fig. 3(a))	0·56 0·97 3·60
Inositol triphosphate	0·37
Diphosphoglycerate	0·82
Inositol diphosphate	0·90
Pyrophosphate	1·00
Orthophosphate	1·92
Inositol monophosphate	2·25
2-Phosphoglycerate	2·40

TABLE III

Paper-chromatography of an acid-labile phosphate from soil, using solvent B

Distance moved is expressed relative to pyrophosphate (Rpp)

Material	Rpp
Acid-labile P from soil (Rpp = 0·97 in solvent A)	1·00
Inositol diphosphate	0·30
Inositol monophosphate	0·41
Glucose 1 phosphate	0·57
Glucose 1 : 6 diphosphate	0·61
Orthophosphate	1·58

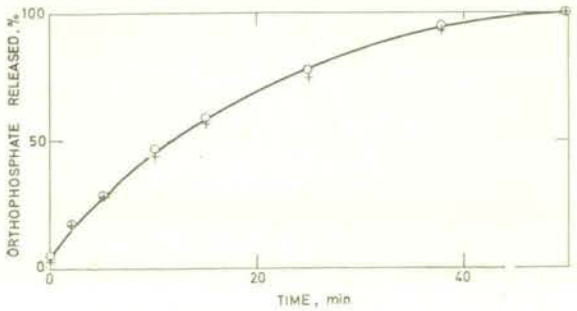

FIG. 3. *Hydrolysis of acid-labile phosphate from soil, and of pyrophosphate, in 0·1* N*-HCl at 100°C*
○ Pyrophosphate; + soil phosphate

The amounts of pyrophosphate-P detected in the eluates from the chloride ion-exchange columns were: Trawscoed (grass), 2·1 ppm in the soil; Trawscoed (potatoes), 2·6 ppm; Logie Newton, 2·1 ppm; and Greenhall, < 0·5 ppm.

Discussion

Fractionation of the phosphates extracted from soils with hot NaOH has yielded an acid-labile phosphate which has been shown to be inorganic pyrophosphate. It was isolated and purified by ion-exchange and paper chromatography and it was characterised by its chromatographic properties, its rate of hydrolysis in HCl and the infra-red spectrum of its Ba salt.

Pyrophosphate is not formed by the action of alkali on orthophosphate in aqueous solution. Even so, the presence of inorganic pyrophosphate in the extract does not necessarily mean that it occurs as such in the soil. If, for example, a pyrophosphate ester is present in which the -C—O—P- linkage is more susceptible to alkaline hydrolysis than the -P—O—P- linkage, then pyrophosphate may be released as an artefact during extraction.

On the other hand, pyrophosphate is present in micro-organisms and plants, and must be added to the soil in decomposing litter. In experiments where a solution of pyrophosphate was added to soils and incubated at laboratory temperature, Sutton & Larsen[7] found that the rate of conversion to orthophosphate varied considerably and was influenced by soil pH and by the level of biological activity. In twelve soils tested, the half life of the added pyrophosphate ranged from 4–100 days. Although their soils adsorbed greater amounts of phosphate as pyrophosphate than as orthophosphate, the former was held with less energy. There was no correlation between soil colloids (clay and organic matter) and pyrophosphate hydrolysis and the authors concluded that where there is a reasonable level of biological activity, added pyrophosphate will quickly disappear.

In the present study no attempt was made to isolate the pyrophosphate quantitatively and the total amount present is not known. Some may have been hydrolysed during acid pretreatment of the soil and loss may have occurred during precipitation of the barium phosphate fraction from the alkali extract. The amounts isolated by ion-exchange chromatography were similar in the Welsh and one of the Scottish soils, ranging from 2·1 to 2·6 ppm P, but the other Scottish soil gave less than 0·5 ppm. Assuming that the pyrophosphate exists in inorganic form in the soil and that the soils tested have considerable biological activity, it would appear that the pyrophosphate is involved in a very active biological cycle.

The occurrence of an acid-labile phosphate in soil, whether it is inorganic or an ester, may account for some of the differences between 'organic' P values given by various extraction methods. In those with a vigorous acid pretreatment it will not survive, but with a short treatment in cold, dilute acid, or with an alkali pretreatment, it may be extracted almost quantitatively. If it escapes hydrolysis during colorimetric estimation of orthophosphate it will be included in the 'organic P' measurement.

Oxalate appeared to be present in considerable quantity in the soil extracts and was eluted from the ion-exchange columns along with several of the phosphate fractions.

The nature of the other phosphates is being investigated.

Acknowledgments

The authors are indebted to the National Agricultural Advisory Service, Trawscoed, Aberystwyth, for providing the Welsh soils; and to Mrs. E. B. Still, Mr. G. S. Sharp and Mr. A. R. Fraser for technical assistance.

Department of Soil Fertility,
The Macaulay Institute for Soil Research,
Aberdeen,
Scotland

Received 19 July, 1968

References

1. McKercher, R. B., & Anderson, G., *J. Soil Sci.*, 1968, **19**, 302
2. Parr, C. W., *Biochem. J.*, 1954, **56**, xxvii
3. Hanes, C. S., & Isherwood, F. A., *Nature, Lond.*, 1949, **164**, 1107
4. Wade, H. E., & Morgan, D. M., *Biochem. J.*, 1955, **60**, 264
5. Mehta, N. C., Legg, J. O., Goring, C. A. I., & Black, C. A., *Proc. Soil Sci. Soc. Am.*, 1954, **18**, 443
6. Martin, J. B., & Doty, D. M., *Analyt. Chem.*, 1949, **21**, 965
7. Sutton, C. D., & Larsen, S., *Soil Sci.*, 1964, **97**, 196

Clay Minerals (1969) **8**, 87.

IMOGOLITE: A UNIQUE ALUMINOSILICATE

J. D. RUSSELL, W. J. McHARDY AND A. R. FRASER

The Macaulay Institute for Soil Research, Craigiebuckler, Aberdeen

(*Received* 7 *January* 1969)

ABSTRACT: The fibrous aluminosilicate imogolite has been studied by electron-optical and infrared absorption methods. Electron diffraction patterns are interpreted in terms of repeat units of 8·4 Å parallel and 23 Å perpendicular to the fibre axis. These spacings can not be reconciled with a continuous silicate chain structure and this conclusion is supported by an Si–O vibration near 930 cm^{-1}. A structure is postulated in which distorted chains of Al–O octahedra are cross-linked through isolated Si_2O_7 groups.

Multiple OH stretching vibrations indicate different types of OH group in the imogolite structure. Absorption bands near 1000, 700 and 600 cm^{-1} are sensitive to sample orientation. This is attributed to the morphology and dimensions of the imogolite fibres.

The Commission on New Minerals and Mineral Names of the International Mineralogical Association (Fleischer, 1963), concluded from the evidence then available, that the soil allopane of low crystallinity and fibrous morphology which Yoshinaga & Aomine (1962) had called imogolite did not warrant classification as a distinct mineral type. Aomine & Miyauchi (1965), Miyauchi & Aomine (1966) and Jaritz (1967) have demonstrated the occurrence of thread-like particles in several volcanic soils, but never succeeded in characterizing the material. That this was probably due to contamination by allophane, with which imogolite invariably co-exists, and amorphous volcanic glass, was shown by Wada (1966) when he succeeded in isolating the fibrous material in a relatively pure form. The infrared absorption spectrum of the fibres suggested a unique structure which chemical analysis showed to contain only SiO_2, Al_2O_3 and H_2O. Deuterium exchange illustrated the presence of hydroxyl groups in the fibre structure (Wada, 1966), and the ease and completeness with which the exchange occurred sugested that the OH groups were all located at the surface of the fibres. Wada (1967) proposed a structural scheme for soil allophanes in general and suggested that the fibrous imogolite was one end-member of a series ranging from imogolite $SiO_2 . Al_2O_3 . 2H_2O$, to allophane $2SiO_2 . Al_2O_3 . 3H_2O$. Recently Yoshinaga, Yotsumoto & Ibe (1968) published an electron diffraction pattern of imogolite.

The aim of this investigation is to provide additional infrared and electron-optical and diffraction data which might help to characterize imogolite and elucidate its structure.

EXPERIMENTAL

Materials

The soil from which imogolite and allophane were isolated is from Uemura, Kumamoto (24–55 cm) and was kindly supplied by Professor Aomine.

Methods

The soil (100 g) was moistened with water, crushed gently, diluted to 2 l, shaken for a short time, then allowed to stand overnight. The supernatant was discarded. This procedure was repeated a further three times on the residue and is essential in eliminating a micaceous fraction.

The wet residue was agitated ultrasonically with 100 W output for 3–4 min producing a jelly-like mass which was diluted with 2 l water, stirred, then allowed to settle overnight. The orange coloured supernatant containing <2 μ particles was separated.

The suspension of <2 μ particles was treated with H_2O_2 followed by citrate-bicarbonate-dithionite (Mehra & Jackson, 1960) to remove organic matter and iron oxides. The resulting suspension of pale grey material was divided into two portions which were treated separately for the isolation of imogolite and allophane,

(*a*) *Separation of imogolite.* Imogolite is more resistant to warm dilute alkali than allophane and was obtained in a relatively pure state by the following procedure; the suspension (10 mg solids/20 ml) was brought to 0·5 N with respect to NaOH and subjected to ultrasonic dispersion at 25 W output for 2–3 min during which time the temperature rose to about 50° C. The grey gelatinous residue was separated and washed five times with water on the centrifuge.

(*b*) *Separation of allophane.* It was found that at slightly acid pH values, allophane was dispersed while imogolite tended to be more coagulated. A fairly good separation was achieved as follows: the suspension was brought to pH 3·5 with HCl and $<0{\cdot}2$ μ material was exhaustively removed and collected by a centrifuge method. This fraction was white and powdery.

Chemical analysis of imogolite and allophane heated to 110° C gave compositions of $3SiO_2 . 2Al_2O_3 . 5H_2O$ and $SiO_2 . Al_2O_3 . 3H_2O$ respectively.

Infrared spectroscopy

Samples were prepared by sedimentation of aqueous suspensions of imogolite and allophane on to AgCl sheet to give films with surface densities of about 1.0, and 0·3 mg/cm^2. Dehydration and deuterium exchange of the samples were carried

out in an evacuable cell similar to that described by Angell & Schaffer (1965). Spectra were recorded over the range 4000–400 cm^{-1} on a Grubb-Parsons Spectromaster grating spectrometer.

Electron microscopy

Specimens were prepared for electron microscopy by ultrasonically dispersing the material in distilled water and drying a drop of the diluted suspension on a carbon-coated support grid. For electron diffraction studies the grids were partly coated with evaporated aluminium.

RESULTS

Electron microscopy

Plate 1 shows electron micrographs of the imogolite and allophane fractions of the Kumamoto soil. As has been reported by numerous Japanese workers, e.g. Yoshinga & Aomine (1962), Wada (1967) and Yoshinga *et al.* (1968) imogolite has a distinctly thread-like morphology (Plate 1(*a*)), each thread consisting of one or more fibre units; the width of these fibre units and the distance between them is variable but is of the order 20–30 Å (Plate 1(*b*)). Thread-like particles can still be seen in the allophane fraction but they are largely swamped by diffuse filmy material (Plate 1(*c*)); where the specimen is more thinly dispersed over the support film (Plate 1(*d*)) thin fibres are more apparent but with numerous small particles of gel adhering to them. The micrographs show that if imogolite is equated with the thread-like particles and allophane with the gel-like material, the imogolite fraction is free of allophane but the allophane is not entirely free of imogolite.

Plate 2(*a*) is a micrograph of a specimen obtained directly from the untreated, moist soil; appoximately 0·2 g of the soil in 3 ml water was subjected to mild ultrasonic treatment for 1 min and, after allowing to settle for a further minute, the supernatant was suitably diluted and the specimen prepared. Although this specimen is largely an intimate mixture of the allophane and imogolite phases there are regions in which the fibres are concentrated in bundles within which there is quite marked parallel alignment (arrowed in Plate 2(*a*)). There are also areas of more randomly oriented fibres which are relatively free from other material (Plate 2(*b*)).

Electron diffraction from a selected area (5 μm^2), including randomly oriented threads, gives a series of reflections ten of which have been assigned to the imogolite phase (Plate 2(*c*)); the others come from a small amount of micaceous material trapped in the threads and are characterized by their spotty nature. The imogolite from the untreated soil and the separated imogolite give identical electron diffraction patterns although the threads in the latter are shorter, wider and more ragged than those from the untreated soil. The *d*-values given in Table 2 have been averaged over several patterns recorded from specimens of both types.

Strong arcing of these reflections (Plate 2(*d*)) is observed in patterns recorded from areas where the fibres are strongly aligned (e.g. arrowed region in Plate 2(*a*)). In such patterns reflections 1, 2, 3 and 4 are reduced to short arcs on an axis normal to the fibre direction. Reflections 5, 9 and 10 become a series of sharply defined arcs on a line parallel to the fibre direction. Reflections 6, 7 and 8 are resolved into two or more pairs of arcs at various angles to the fibre direction. Of these arcs, only those of reflection 6 are sharply defined, falling on lines at an angle of $\pm 30°$ to the fibre axis.

The effect of heating a specimen of imogolite in the electron microscope was studied using a special heating stage described by Agar & Lucas (1962). The morphology of the imogolite remains unchanged up to 700° C, although the electron diffraction pattern fades below this temperature showing loss of internal structure. The allophane fraction is not completely amorphous to electron diffraction; patterns obtained are weaker versions of those recorded for the imogolite fraction (Plate 2(*c*)), the reflections at 4·12 and 1·40 Å being quite strong.

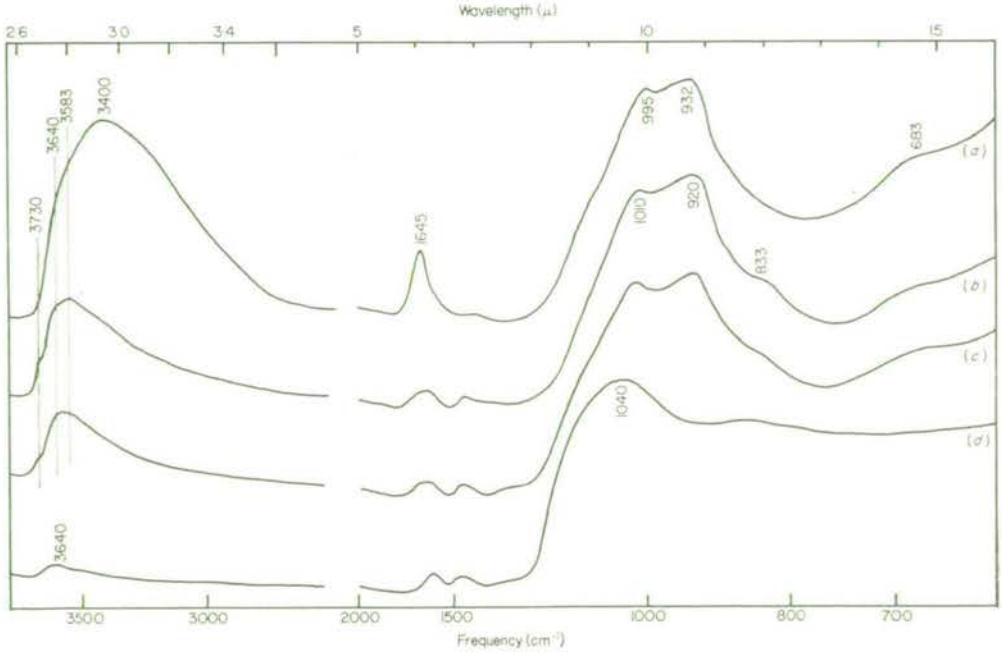

FIG. 1. Infrared absorption patterns of an imogolite film normal to the incident radiation: (*a*) 20° C (*b*) 20° C/10^{-2} mm Hg (*c*) 300° C/10^{-2} mm Hg (*d*) 475° C/10^{-2} mm Hg. The weak OH vibration at 3640 cm^{-1} is due to a trace of a micaceous impurity.

PLATE I

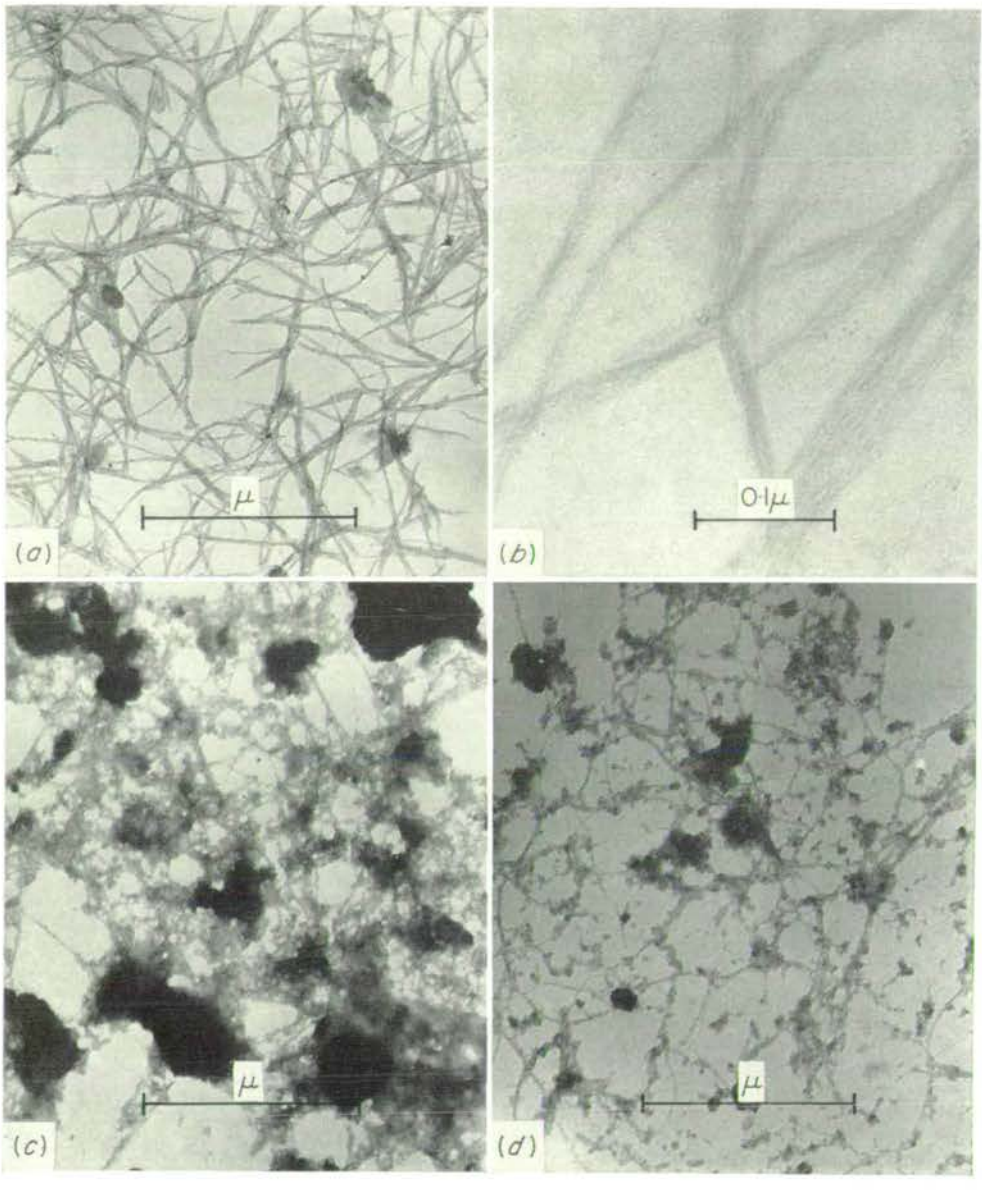

(*a*) Electron micrograph of imogolite after separation procedure.
(*b*) High magnification electron micrograph of imogolite threads.
(*c*) Electron micrograph of allophane after separation procedure.
(*d*) Different field of the same specimen as (*c*).

(*Facing page* 90)

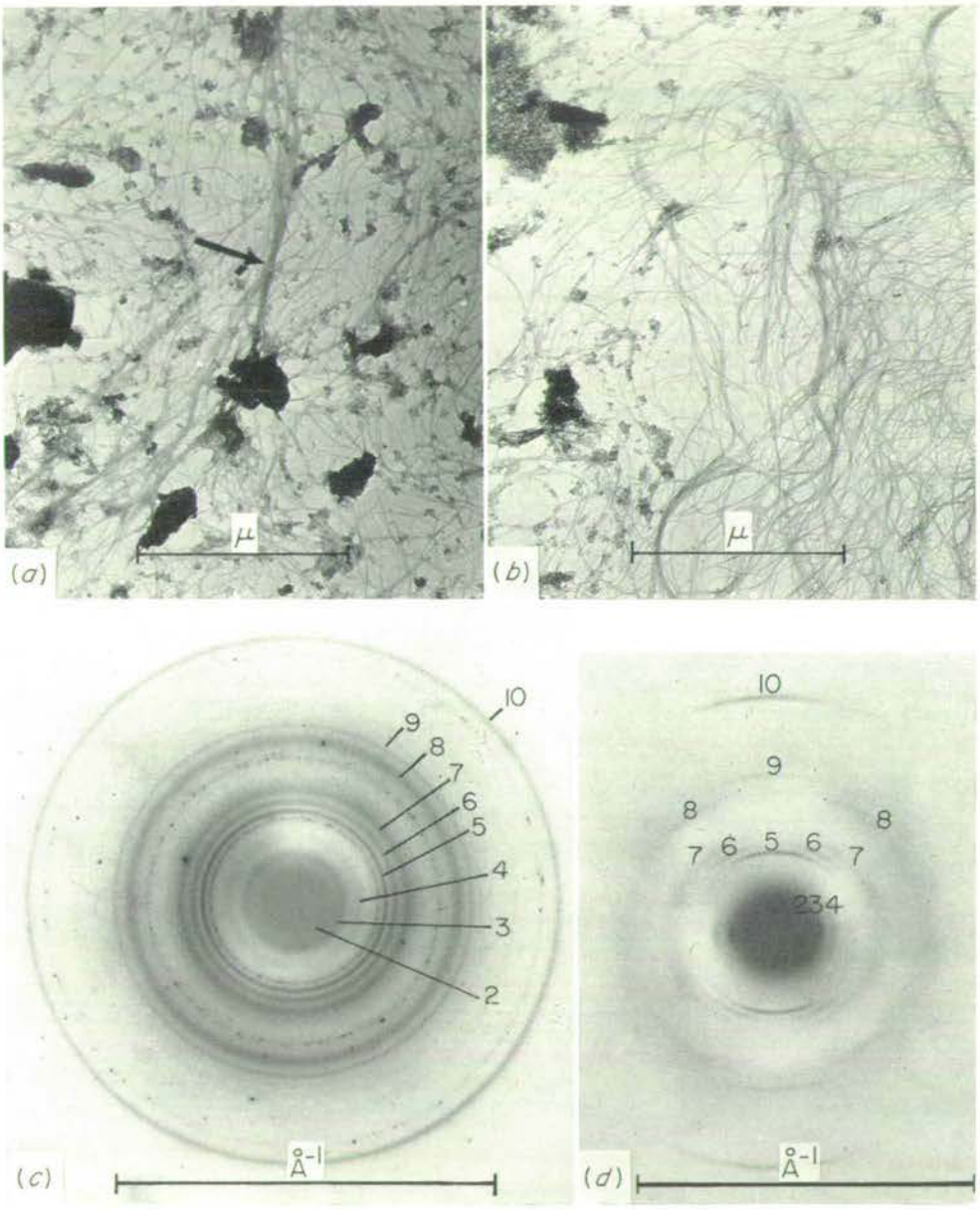

(*a*) and (*b*) Electron micrographs of material obtained by ultrasonic dispersion of the untreated soil.

(*c*) Selected area electron diffraction pattern from randomly oriented imogolite threads.

(*d*) Selected area electron diffraction pattern from a bundle of imogolite threads in parallel alignment.

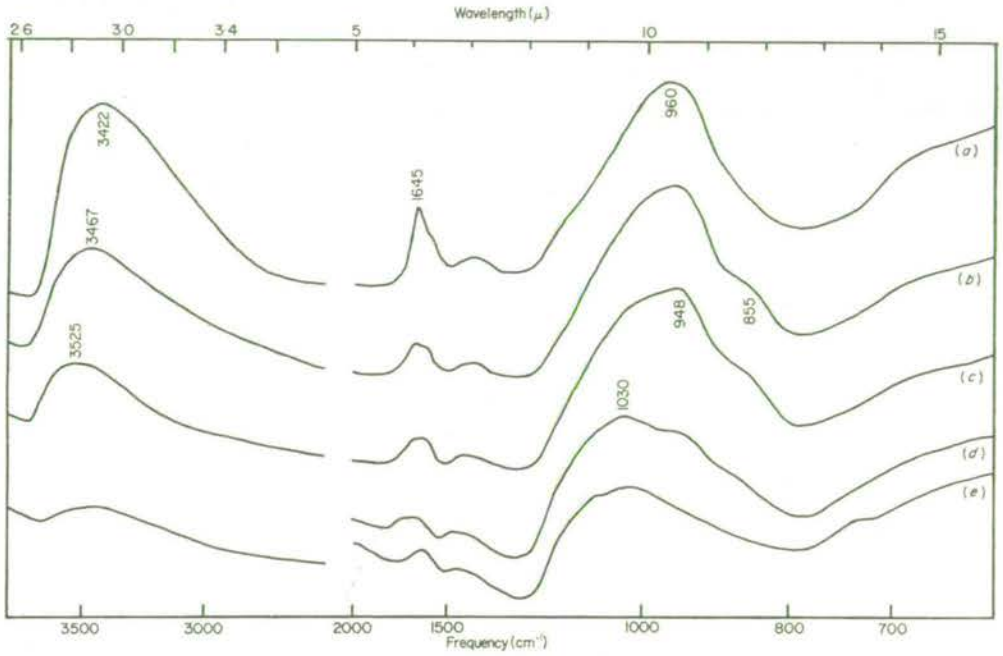

FIG. 2. Infrared absorption patterns of an allophane film normal to the incident radiation: (*a*) 20°C (*b*) 20° C/10^{-2} mm Hg (*c*) 150° C/10^{-2} mm Hg (*d*) 250° C/10^{-2} mm Hg (*e*) 350° C/10^{-2} mm Hg.

Infrared spectroscopy

Dehydration. Physically adsorbed water is almost completely removed from imogolite and allophane by evacuation at room temperature (Figs 1 and 2) as shown by the virtual disappearance of the 1645 cm^{-1} H–O–H angle deformation frequency. The absorption bands remaining in the 3000–4000 cm^{-1} region must belong to stretching vibrations of OH groups.

As a result of dehydration, new bands appear at 833 cm^{-1} in imogolite and 855 cm^{-1} in allophane (Figs 1(*b*), 2(*b*)).

The OH groups remaining in imogolite after removal of adsorbed water are relatively stable up to 200° C, but by 300° C about 40% dehydroxylation has occurred, the principal loss being of OH groups absorbing at 3583 cm^{-1} (Fig. 1(*c*)). Above 300° C, imogolite decomposes rapidly and yields a dehydroxylated phase whose absorption pattern (Fig. 1(*d*)) resembles that of a synthetic silica–alumina co-precipitate with Si : Al = 1 : 1.

Allophane is thermally less stable than imogolite: irreversible structural rearrangements have already commenced at 150° C in vacuum (Fig. 2(*c*)), are more advanced by 250° C (Fig. 2(*d*)) and are essentially complete by 350° C.

The thermal stabilities of OH groups in imogolite and allophane are compared in Fig. 3 where the hydroxyl content as calculated from the optical density of the OH stretching band is plotted against temperature, the samples having been heated in vacuum. Some dehydroxylation of imogolite has probably occurred below 200° C in vacuum.

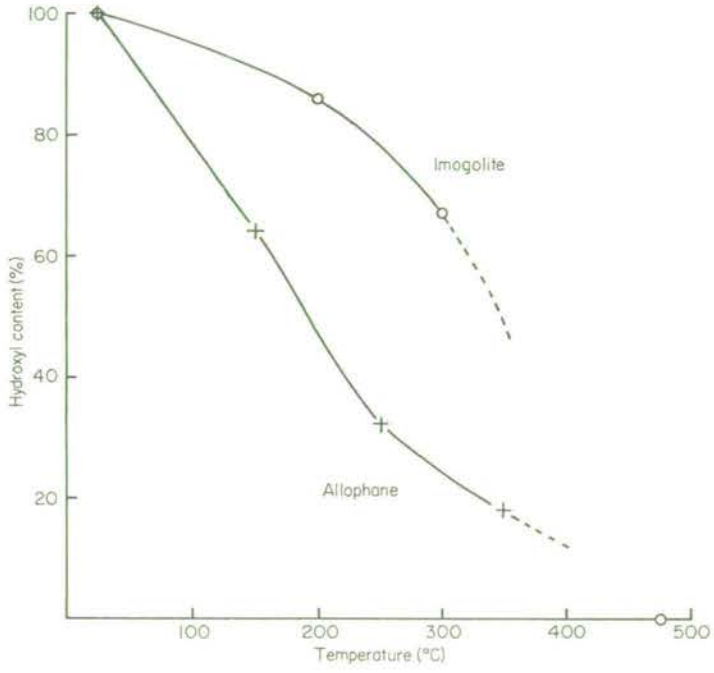

FIG. 3. Variation with temperature of the content of OH groups in imogolite and allophane. Samples were heated for 1 hr at 10^{-2} mm Hg. OH contents estimated from optical densities of OH stretching bands are expressed as a percentage of their optical densities at 20° C/10^{-2} mm Hg.

Deuteration. Exchange with D_2O occurs readily, shifting the bands at 3730, 3640, 3583 and 833 cm^{-1} in imogolite to 2760, 2690, 2640 and 690 cm^{-1} (Fig. 4(*a*), (*b*)), and the bands at 3467 and 855 cm^{-1} in allophane to 2560 and 700 cm^{-1} (Fig. 4(*c*), (*d*)). The ratios of OH/OD frequencies for these bands are shown in Table 1. In imogolite, exchange with D_2O also produces a band at 950 cm^{-1} and a reduction in intensity near 985 cm^{-1}.

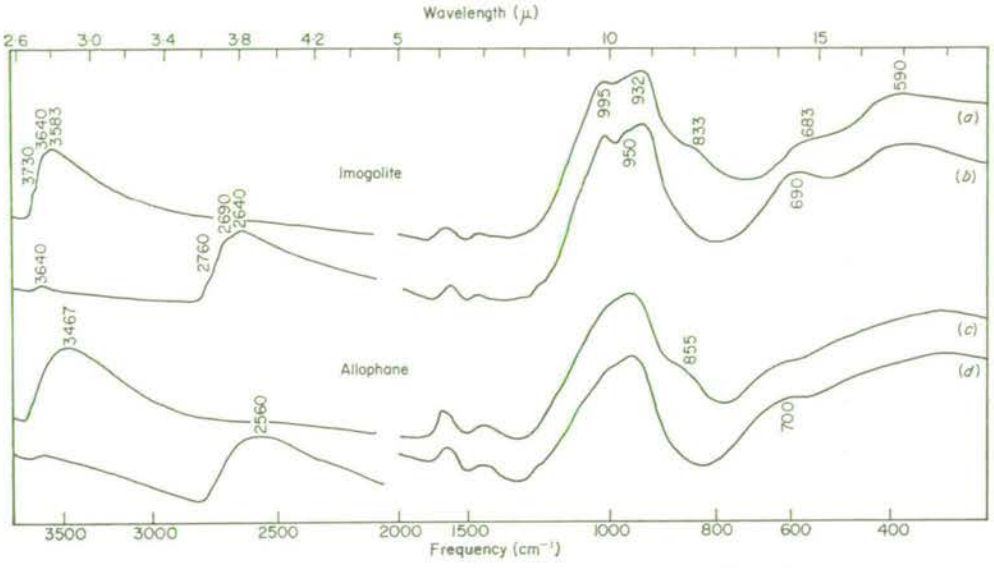

FIG. 4. Normal and deuterated forms of imogolite and allophane following evacuation at 10^{-2} mm Hg. (*a*) OH imogolite (*b*) OD imogolite (*c*) OH allophane (*d*) OD allophane. The weak OH vibration at 3640 cm^{-1} in (*b*) is due to a trace of a micaceous impurity.

TABLE 1. Frequencies (cm^{-1}) of OH and OD vibrations of imogolite and allophane after evacuation at 10^{-2} mm Hg

Imogolite			Allophane		
OH	OD	OH/OD	OH	OD	OH/OD
3730	2760	1·35			
3640	2690	1·35			
3583	2640	1·36	3467	2560	1·36
833	690	1·21	855	700	1·22

Orientation effects. The spectrum of a thin oriented film of imogolite at two angles of incidence to the infrared beam is shown in Fig. 5. Bands near 1000, 680 and 590 cm^{-1} exhibit enhanced intensity at 60° incidence compared with 0°. Sedimented aggregates of allophane show no orientation effects.

Since it seemed possible that the fibrous morphology of imogolite was responsible for the effects observed, a comparison with a sample of similar morphology was made. Fig. 6 shows spectra of an oriented film of crystalline SiC fibres sheathed in amorphous SiO_2 at 0° and 60° incidence to the infrared beam. Bands at 928 and 792 cm^{-1} are of SiC. That at the higher frequency shows an enhancement of its intensity. Bands at 1165, 1080, 490 and 455 cm^{-1} are of the SiO_2 phase. Of these, the 1165 and 490 cm^{-1} almost double their intensities at 60° incidence.

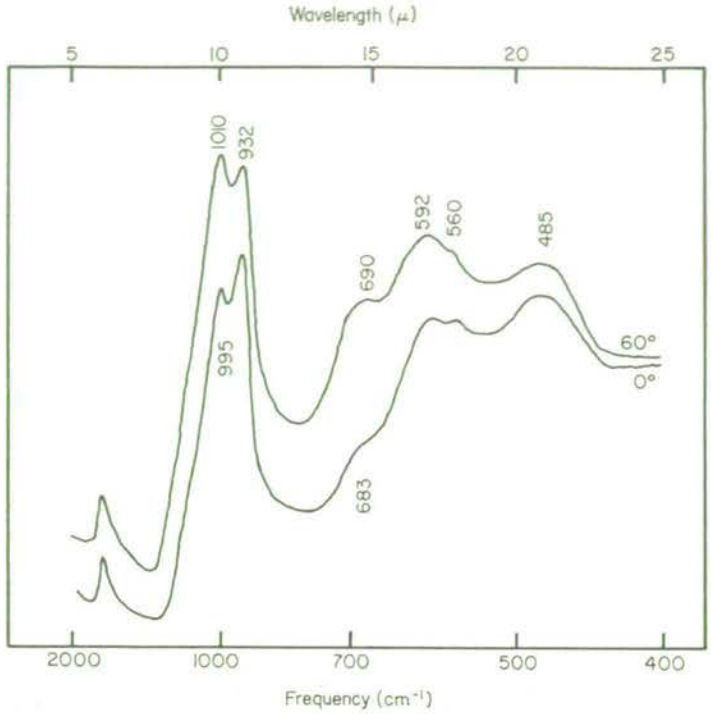

FIG. 5. Infrared absorption spectra of a thin film of imogolite at 0° and 60° incidence to the infrared beam.

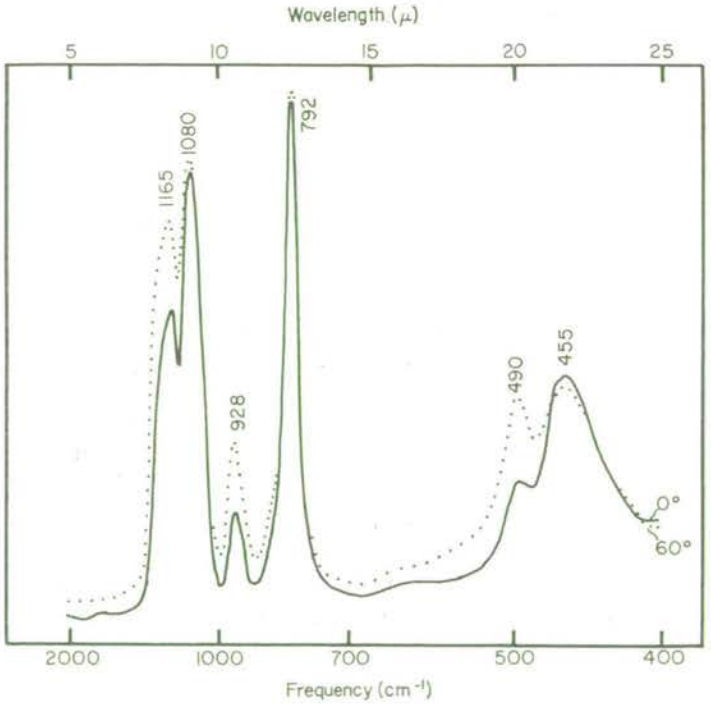

FIG. 6. Infrared absorption spectra of a thin film of fibrous SiO_2–SiC at 0° and 60° incidence to the infrared beam.

DISCUSSION

Electron microscopy

The fibrous morphology of imogolite is its most characteristic property, and is well illustrated in the untreated soil (Plate 2(*b*)). The slightly different appearance of the fibres in the separated imogolite (Plate 1) may be explained by dissolution of the finer threads, which would presumably be more susceptible to attack by the dilute alkali used in the final separation process. Electron diffraction shows however that the threads which survive the alkali treatment are structurally identical to those in the untreated soil.

TABLE 2. Spacings (Å) and proposed indexing of electron diffraction patterns of imogolite

Reflection	*d*(Å)	Intensity	hkl
1	21	very strong; broad	010
2	11·5–11·8	strong; broad	020
3	7·8	strong; broad	030
4	5·7	weak; diffuse	040
5	4·12	very strong; sharp	002
6	3·75	strong; broad	032
7	3·33	weak; diffuse	
8	2·32	strong; broad	
9	2·11	weak; sharp	004
10	1·40	very strong; sharp	006

In the electron diffraction patterns the obvious explanation for reflections 2, 3 and 4 (Table 2) is that they are the 2nd, 3rd and 4th order reflections arising from a repeat unit of 23 Å in a direction normal to the fibre axis. Reflection 1, which is only observed for short exposures, and is difficult to measure accurately, is thought to be the 1st order reflection in this series. The repeat unit of 23 Å may be correlated with the actual distance, observed in Plate 1(*b*), between individual fibre units in an imogolite thread.

Reflections 9 and 10 appear to be the 2nd and 3rd orders of reflection 5 although it may be noted that the *d*-value of 5 is slightly smaller than twice the *d*-value of 9 or three times that of 10; this difference is probably within experimental error but it persists in measurements made over several plates. Since these reflections occur on a line parallel to the fibre axis they indicate a repeat distance of 4·2 or 8·4 Å in this direction; the latter possibility implies that odd orders are absent and that 5, 9 and 10 are the 2nd, 4th and 6th orders of an 8·4 Å repeat unit. It is impossible to say which of the values is correct but in the light of the electron diffraction behaviour of other clay minerals the value of 8·4 Å appears to be the more probable.

From the foregoing interpretation of reflections 1, 2, 3, 4 and 5, 9, 10, an elementary unit cell can be assigned to imogolite taking the fibre direction as the c-axis ($c = 8{\cdot}4$ Å) and the inter-fibre distance as the b-axis ($b = 23$ Å). These seven reflections may then be assigned the following hkl indices 010, 020, 030, 040, 002, 004, 006. Then hkl reflections ($k \neq 0$, $l \neq 0$) may be calculated from simple trigonometry. Such a calculation gives $d_{032} = 3{\cdot}68$ Å and arcs from this reflection would make an angle of $\pm 29°$ with the c-axis. This is in good agreement with the observed d-value for reflection 6 and the angle the arcs from this reflection make with the fibre axis. A similar argument could be applied to reflections 7 and 8 although their less precise arcs and their shorter spacings make attempts at detailed indexing rather meaningless.

The 8·4 Å repeat distance is shorter than the b-parameter of layer silicates (8·9–9·2 Å) and the c-parameter of chain silicates ($2c = 10{\cdot}4$ Å). It cannot therefore be explained by the structure proposed by Wada (1967) which consists of continuous straight chains of Si–O tetrahedra and Al–O octahedra with a repeat along the chains of about 10 Å. A chain structure which satisfies the observed repeat distance along the chain is one based on gibbsite in which every third row of Al atoms is missing. This results in an array of chains with the 8·6 Å gibbsite repeat parallel to the chain axis (Fig. 7). The essential silicon in the structure cannot then be accommodated as a continuous chain. It can exist however as isolated Si_2O_7 groups which link adjacent Al–OH chains. The observed interfibre repeat distance of about 23 Å requires that, in each thread, three of these chains are linked in this manner. This structure also accounts for the off-axis reflections particularly those at $\pm 30°$ to the chain.

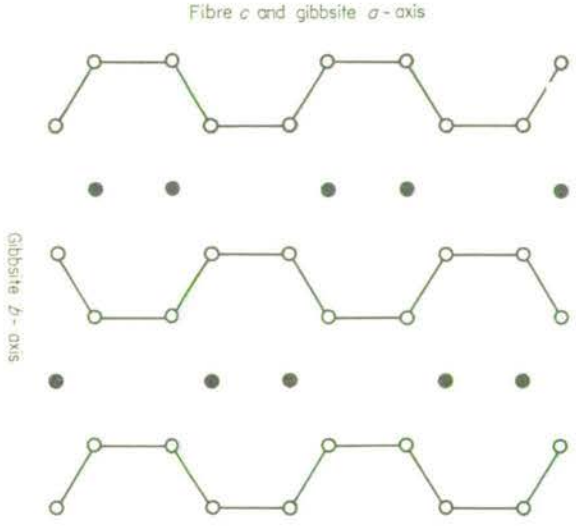

FIG. 7. Possible structure of imogolite. ● — Si; ○ — Al. For clarity, OH. O and H_2O are not shown.

Yoshinaga *et al.* (1968) have published an electron diffraction pattern from a selected area including threads aligned in parallel which shows arcing of reflections identical to that of Plate 2(*d*). The *d*-values of their diffraction lines agree with those given in Table 2 except that reflections 1 and 2 were not recorded by them. The only comment they make is that the *d*-values agree with the X-ray powder data of Yoshinaga & Aomine (1962). However, Wada's indexing of these X-ray data (Wada, 1967) is completely different from the present authors' interpretation of the electron diffraction patterns. The discrepancy arises mainly because Wada based his interpretation on the presence, in X-ray data, of a broad diffraction peak at 13–18 Å. The data were indexed in terms of an ideal average unit cell having $a = 7{\cdot}4$ and $b = 17{\cdot}0$ Å with random orientation along the fibre axis *c*. X-ray examination of imogolite by the present authors has confirmed the presence of a peak in the 13–18 Å region but no 23 Å reflection was observed. This could be explained by the different states of preferred orientation obtaining in X-ray and electron diffraction. For example in electron diffraction the strongest reflections are at 4·12 and 1·40 Å; these reflections are very weak on X-ray diffraction patterns, the 1·40 Å being scarcely detectable.

Infrared spectroscopy

The results of infrared spectroscopy confirm the observations of Wada (1966) on the general appearance of the spectrum of imogolite, the occurrence of OH groups exhibiting OH stretching and bending vibrations (Fig. 1), and on hydrogen–deuterium exchange of these groups (Fig. 4). The ease of complete exchange means that the OH groups are located at the surfaces. The shift of the OH stretching bands to higher frequency on dehydration (Fig. 1) implies that in the hydrated state the OH groups are hydrogen bonded to adsorbed water molecules. The appearance of multiple OH stretching vibrations in dehydrated imogolite suggests that the OH groups occur in discrete environments, in one of which (absorbing at 3730 cm^{-1}) they experience considerable freedom. Dehydrated allophane does not exhibit such discrete OH stretching bands (Fig. 2), the single rather broad band reflecting OH groups involved in a wide range of hydrogen bonds which are generally stronger than those operating in dehydrated imogolite. The reason for the appearance of the OH bending vibrations near 850 cm^{-1} in imogolite and allophane following dehydration must be a low frequency shift brought about by the decrease in strength of hydrogen bonding experienced by the OH groups. While the chemical analysis of allophane and imogolite indicates that only Si–OH and Al–OH groups can be present, it is not yet possible to assign OH vibrations specifically to either of these groups. However, the more discrete OH stretching vibrations (Fig. 1(*b*)) and the higher thermal stability of surface OH groups (Fig. 3) suggest higher ordering of OH groups in imogolite compared with allophane.

The infrared absorption pattern of imogolite in the 900–1100 cm^{-1} region is unusual and quite different from those of allophane on one hand and layer silicates on the other. Wada (1966, 1967) interpreted a strong band at 925 cm^{-1}

as resulting from a high proportion of Si–O–Al linkages relative to Si–O–Si. However, the structure he proposed for imogolite contained a continuous chain of SiO_4 tetrahedra which, unless there was a very high replacement of Si by Al, would be expected to absorb above 925 cm^{-1}. Only when the proportion of Si–O–Al^{VI} is high enough to produce isolated SiO_4 tetrahedra does the Si–O frequency appear near 925 cm^{-1}, e.g. kyanite (Launer, 1952). In the alternative structure proposed above for imogolite silicon appears as Si_2O_7 groups linking adjacent Al–OH chains. While the amount of silicon which can be accommodated in this way falls somewhat below the value found by analysis, the presence of Si_2O_7 groups in imogolite is supported by the band at 935 cm^{-1} (Fig. 5) lying in the range for ortho- and pyrosilicates (900–970 cm^{-1}, Farmer (1964)).

Wada (1966, 1967) did not discuss the absorption band near 1000 cm^{-1} in the imogolite spectrum. The unexepected polarization of this vibration and others near 600 and 700 cm^{-1} (Fig. 5) are analogous to the polarization effects observed for fibrous SiO_2–SiC (Fig. 6) and must be due to the morphology and dimensions of the fibres. Thus, the high frequency bands showing perpendicular polarization at 1163 and 490 cm^{-1} for SiO_2 and 928 cm^{-1} for SiC are due to vibrations perpendicular to the fibre axis. Their frequencies have been considerably raised above those of the corresponding vibrations parallel to the fibre axis at 1080 and 455 cm^{-1} for SiO_2 and 792 cm^{-1} for SiC as a consequence of the small cross-section of the fibres—250 Å—relative to the wavelength of the Si–O and Si–C lattice vibrations. Thus in imogolite the perpendicularly polarized bands at 1010, 690 and 590 cm^{-1} result from high frequency shifts of the parallel vibrations at 932, 560 and 485 cm^{-1} respectively. A similar effect has been demonstrated for thin platy crystals of LiF (Berreman, 1963) and kaolin minerals (Farmer & Russell, 1964, 1966) and was suggested by Summitt (1967) to explain the high frequency band of fibrous SiC (Pultz & Hertl, 1966).

CONCLUSIONS

Electron diffraction has unambiguously identified in imogolite repeat units of 8·4 Å parallel to the fibre axis and 23 Å perpendicular to it. The structure proposed for imogolite by Wada (1967) cannot satisfy these parameters. An alternative structure consists of continuous distorted chains of Al–O octahedra linked through isolated Si_2O_7 groups. This structure also accounts for reflections occurring at definite angles to the fibre axis.

The existence of the Si_2O_7 groups is supported by the infrared absorption band near 930 cm^{-1}. Perpendicularly polarized infrared vibrations are interpreted in terms of the morphology and dimensions of the fibres. Hydroxyl groups on the imogolite surfaces are relatively stable and their multiple OH stretching vibrations suggest that they occur at discrete but as yet unidentified sites.

Aomine & Miyauchi (1965) have classified imogolite into two sub-species, which they called *A* and *B*, on the basis of the behaviour on heating of X-ray spacings in the 13–18 Å region. Imogolite *B* was supposed to be in a more advanced stage of

weathering than *A*. For reasons which are not clear Kanno *et al.* (1968) have further suggested that thread-like particles of volcanic ash soils are not necessarily imogolite. They interpret experimental results as indicating a phase intermediate between allophane and imogolite rather than incomplete separation of the two phases. However, in the present authors' experience the problem is simply one of efficient separation. Indeed it seems unrealistic to suggest that there should exist in the same environment two different phases possessing a similar, unique, morphology.

ACKNOWLEDGMENTS

The authors wish to thank Professor Aomine for the Kumamoto soil and Dr Hertl for the sample of SiC–SiO_2. Thanks are also due to Mr B. F. L. Smith for chemical analyses, Mr A. P. Thompson for X-ray results, and to various colleagues in particular Dr V. C. Farmer, for valuable discussion.

REFERENCES

Agar A.W. & Lucas J.H. (1962) *Proc. 5th int. Congr. Electron Microscopy*, Philadelphia **1**, E2.
Angell C.L. & Schaffer P.C. (1965) *J. phys. Chem.* **69**, 3463.
Aomine S. & Miyauchi N. (1965) *Soil Pl. Fd, Tokyo* **11**, 212.
Berreman D.W. (1963) *Phys. Rev.* **130**, 2193.
Farmer V.C. (1964) *The Chemistry of Cements* (H. F. W. Taylor, editor), Vol. 2, p. 289. Academic Press, London.
Farmer V.C. & Russell J.D. (1964) *Spectrochim. Acta* **20**, 1149.
Farmer V.C. & Russell J.D. (1966) *Spectrochim. Acta* **22**, 389.
Fleischer M. (1963) *Am. Miner.* **48**, 434.
Jaritz G. (1967) *Z. Pfl-Ernähr. Düng. Bodenk.* **117**, 65.
Kanno I., Onikura Y. & Higashi T. (1968) *9th int. Congr. Soil Sci.* **3**, 111.
Launer P.J. (1952) *Am. Miner.* **37**, 764.
Mehra O.P. & Jackson M.L. (1960) *Clays Clay Miner.* **7**, 317.
Miyauchi N. & Aomine S. (1966) *Soil Pl. Fd, Tokyo* **12**, 187.
Pultz W.W. & Hertl W. (1966) *Spectrochim. Acta* **22**, 573.
Summitt R. (1967) *Spectrochim. Acta* **23A**, 2857.
Wada K. (1966) *Soil Pl. Fd, Tokyo* **12**, 176.
Wada K. (1967) *Am. Miner.* **52**, 690.
Yoshinaga N. & Aomine S. (1962) *Soil Pl. Fd, Tokyo* **8**, 114.
Yoshinaga N., Yotsumoto H. & Ibe K. (1968) *Am. Miner.* **53**, 319.

Reprinted from the *Soil Science Society of America Proceedings*
Volume 33, Number 5, September-October 1969
677 South Segoe Road, Madison, Wisconsin 53711 USA

Reactivity of Montmorillonite Surfaces with Weak Organic Bases

Swoboda and Kunze (6) have attempted to compare the surface acidity of montmorillonitic clays, using infrared spectroscopy to distinguish whether various organic bases adsorbed on clay films become protonated. This procedure is, unfortunately, vitiated by the tendency of protonated organic bases, in montmorillonite, to form strongly hydrogen-bonded complexes with excess base. In these complexes the characteristic vibrations of the protonated base are strongly perturbed, and sometimes totally suppressed. The formation of such base-cation complexes in montmorillonite has been established for ammonia (5), ethylamine (1), pyridine (2), urea (4), and various amides (7).

Swoboda and Kunze discounted the occurrence of base-cation complexes in the systems they studied, and questioned the evidence for pyridine-pyridinium complexes. Their interpretation of this evidence is, however, impossible, as it involves hydrogen bonds between pyridine and surface oxygens of the silicate lattice, neither of which have active hydrogen atoms. Further, the formation of hydrogen-bonded complexes between anilinium ions and aniline (one of the other bases used in their study) is readily established. Bands typical of the anilinium ion (Fig. 1*A*), particularly at 1525 cm^{-1}, are displaced or suppressed in the presence of excess aniline (Fig. 1*B*). The marked enhancement of adsorption at 2500–2600 cm^{-1} in the complex is indicative of strong hydrogen bonding. The C–N vibration of aniline, which lies at 1278 cm^{-1} in the liquid, is displaced to 1250 cm^{-1} (Fig. 1*B*) in the complex $R \cdot NH_3^+ — NH_2 \cdot R$, due to hydrogen bonding. A similar, larger displacement occurs when aniline is coordinated to metal cations (3).

The difficulty of detecting anilinium ions by infrared spectroscopy is illustrated for the case of aniline adsorbed on Mg-montmorillonite (Fig. 1*C*). The major part of the aniline appears to be indirectly coordinated to magnesium ions through a bridging water molecule (i.e. $Mg^{2+} \cdot OH_2 — NH_2 \cdot R$), as indicated by the broad OH absorption extending from 3300 cm^{-1} to nearly 2000 cm^{-1} [compare the pyridine-Mg-montmorillonite system (2)]. Nevertheless, comparison of spectra 1*B* and 1*C* indicates that anilinium ion, up to some 20% of the exchange capacity, could well be present as the anilinium-aniline complex, although its presence cannot be positively identified.

The use of infrared spectroscopy to detect protonated organic cations in the presence of excess base is obviously an uncertain procedure. Estimates of the amounts of such cations will depend on the amount of excess base present, and this, in turn, will depend not only on the experimental conditions, but also on the interlamellar space available. Thus, the high exchange capacity of saponite (120 meq/100 g) prevents the uptake of sufficient pyridine to complex with all the pyridinium ions in pyridinium saponite, whereas formation of the pyridine-pyridinium complex in montmorillonite (90 meq/100 g) is more nearly complete (2). It is suggested, therefore, that the conclusions of Swoboda and Kunze on the relative surface acidity of montmorillonitic clays be treated with caution.

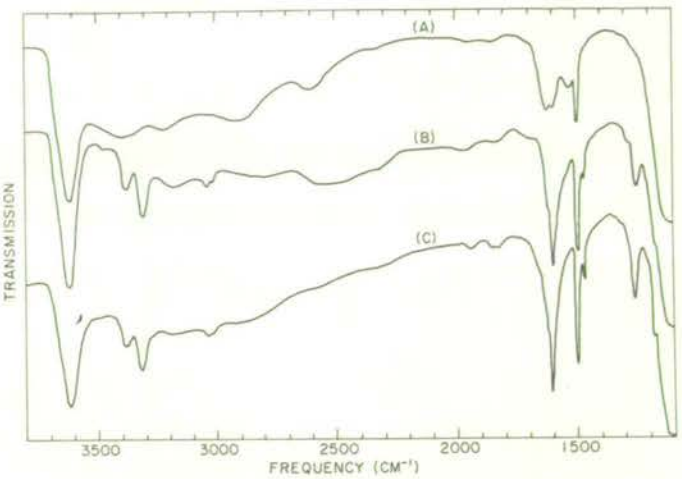

Fig. 1—Infrared spectra of Wyoming montmorillonite films: (*A*) anilinium montmorillonite; (*B*) anilinium montmorillonite after immersion in aniline; (*C*) Mg-montmorillonite after immersion in aniline.

M. M. Mortland

Department of Soil Science
Michigan State University
East Lansing, Michigan 48823

V. C. Farmer and J. D. Russell

Department of Spectrochemistry
Macaulay Institute for Soil Research
Craigiebuckler
Aberdeen, Scotland

References

1. Farmer, V. C., and M. M. Mortland. 1965. An infrared study of complexes of ethylamine with ethylammonium and copper ions in montmorillonite. J. Phys. Chem. 69: 683–686.
2. Farmer, V. C., and M. M. Mortland. 1966. An infrared study of the coordination of pyridine and water to exchangeable cations in montmorillonite and saponite. J. Chem. Soc. (A):344–351.
3. Jungbauer, M. A. J., and C. Curran. 1965. Infrared spectra of complexes of aniline with metal (II) halides. Spectrochemica Acta 21:641–648.
4. Mortland, M. M. 1966. Urea complexes with montmorillonite: an infrared absorption study. Clay Minerals 6: 143–156.
5. Russell, J. D. 1965. Infrared study of the reactions of ammonia with montmorillonite and saponite. Trans. Faraday Soc. 61:2284–2294.
6. Swoboda, A. R., and G. W. Kunze. 1968. Reactivity of montmorillonite surfaces with weak organic bases. Soil Sci. Soc. Amer. Proc. 32:806–811.
7. Tahoun, S., and M. M. Mortland. 1966. Complexes of montmorillonite with primary, secondary and tertiary amides: I. Protonation of amides on the surface of montmorillonite. Soil. Sci. 102:248–254.

Clay Minerals (1969) **8**, 229.

NOTES

A SPECTROPHOTOMETRIC METHOD FOR DETERMINATION OF CATION-EXCHANGE CAPACITY OF CLAY MINERALS

The micro-Kjeldahl method for the determination of cation-exchange capacity of clays (Mackenzie, 1951) is widely used. However, it can be time-consuming and requires considerable experience in estimating the end-point in the acid titration of liberated NH_3. Many alternative methods of determining liberated NH_3 are available, but the photometric method described by Searcy, Reardon & Foreman (1967) for the assay of serum urea as NH_3 is rapid, free from any subjective estimation, and is very sensitive. Its application to the determination of exchange capacities of clay minerals requires the following preliminary procedure: a 5 mg sample of NH_4-saturated clay mineral is digested in 1 ml concentrated HCl for 30 min in a covered vitreosil basin. A blank consisting of the clay mineral in its K-saturated form is run in parallel. The contents of the basin are then transferred to a 100 ml standard flask with NH_3-free distilled water. After addition of 3 ml of 4 N NaOH solution, and dilution to the mark with water the solution is neutral or very slightly alkaline. Clay minerals are not completely dissolved by this procedure, silica gel remaining insoluble. From clays containing iron, hydrated iron oxide gels are also precipitated. These solid phases are readily separated by centrifuging at 300 **g** for 5 min.

In the colorimetric procedure a 2–5 ml aliquot of the clear centrifugate in a 10 ml graduated flask is treated with 2 ml of an aqueous solution containing 8·5% (w/v) sodium salicylate and 0·06% (w/v) sodium nitroprusside, and 2 ml 0·25% (w/v) sodium dichloroisocyanurate in 0·3 N NaOH. The solution is then kept at 37°C for 10 min to ensure complete development of the emerald green colour. Following cooling to room temperature and dilution to the mark with NH_3-free distilled water the absorption is measured in a 10 mm cell over the range 500–1000 mm on a Unicam SP700 recording spectrophotometer, using distilled water in the reference cell. The colour is stable for several days.

For clay minerals of low exchange capacity, e.g. kaolinite, the 5 mg sample is weighed directly into a 10 ml standard flask in which acid digestion, neutralization and colour development are then carried out. After dilution to the mark, the solution is centrifuged and its absorption recorded as described. Aluminium and magnesium, although soluble throughout the digestion and colour development, do not interfere and any possible interference by iron is prevented by centrifuging off the precipitated iron hydroxide.

The absorption maximum occurs at 666·7 nm. Optical densities at this wavelength were measured using a modified base-line technique and converted to concentra-

tions of NH_4 ion by means of a calibration curve prepared from standard $(NH_4)_2SO_4$ solutions. The calibration curve is linear up to a concentration of 0·09 μ-eq NH_4/ml (optical density = 1·1). A useful working range is 0·01–0·04 μ-eq NH_4/ml but reliable measurements can be made down to about 0·005 μ-eq NH_4/ml.

Cation exchange capacities of several clay minerals determined by the micro-Kjeldahl and the photometric method are in good agreement (Table 1). An obvious advantage of the photometric method is the requirement of only 5 mg of sample, compared with 20–120 mg for micro-Kjeldahl determinations.

TABLE 1. Cation-exchange capacities (m-eq/100 g air-dry material) of several clay minerals (<2 μ fractions) by the photometric and micro-Kjeldahl methods

	Mont.*	Verm.	Nont.	Kaol.	$(NH_4)_2SO_4$ standard solution (1·072 μ-eq/ml)
Photometric	84	189	118	2·4	1·063
Kjeldahl	85	190	120	2·9	1·086

* Mont. ≡ Montmorillonite (Wyoming); Verm. ≡ Vermiculite (Loch Scye); Nont. ≡ Nontronite (Koegas); Kaol. ≡ Kaolinite (International).

Acknowledgments

The authors wish to thank Miss C. Bruce of the Department of Pedology for the micro-Kjeldahl determinations.

A. R. FRASER AND J. D. RUSSELL

Macaulay Institute for Soil Research,
Craigiebuckler, Aberdeen.

27 March 1969.

REFERENCES

MACKENZIE R.C. (1951) *J. Colloid Sci.* **6**, 219.
SEARCY R.L., REARDON J.E. & FOREMAN J.A. (1967) *Am. J. med. Technol.* **33**, 1.

REPRINTED FROM
CLAYS AND CLAY MINERALS
Proceedings of the Fourteenth National Conference
on Clays and Clay Minerals, Berkeley, California,
PERGAMON PRESS—OXFORD & NEW YORK— 1966

INFRARED STUDY OF THE THERMAL DECOMPOSITION OF AMMONIUM RECTORITE*

by

J. D. RUSSELL† and J. L. WHITE

Department of Agronomy,
Purdue University, Lafayette, Indiana

ABSTRACT

CHANGES in the infrared absorption spectrum of ammonium-saturated rectorite on heating suggest that the ammonium cations are hydrogen bonded to water molecules when the mineral is hydrated. Further spectral changes above 300°C indicate that lattice OH groups are perturbed by protons liberated from the decomposition of ammonium ions giving rise to an absorption doublet at 3500 and 3476 cm^{-1}. The doublet attains maximal intensity when decomposition of ammonium cations and dehydroxylation of the mineral is complete at about 550°C.

The perturbation effect occurs only for swelling dioctahedral minerals which derive their layer charge from Al-for-Si substitution.

INTRODUCTION

WHILE the existence of hydronium ions in clay minerals has been postulated several times (Brown and Norrish, 1952; Korolev, 1960; Bokii and Arkhipenko, 1962) their presence has never been unambiguously established. In their study of an artificially weathered muscovite White and Burns (1964) concluded from infrared and X-ray data that following hydrogen or ammonium saturation and heating, hydronium ions were produced. The present study is a further investigation of this problem in the mineral rectorite, whose structure has been established most recently (Brown and Weir, 1963) as a regular alternation of mica-like and montmorillonite-like layers. Uchiyama and Onikura (1956) have suggested that rectorite-type minerals are natural weathering products of muscovite and moreover that they may not be of uncommon occurrence.

MATERIALS AND METHODS

The rectorite used was that designated "allevardite-B" by Brown and Weir (1963). It was saturated with H^+, NH_4^+ and Ca^{2+} by treatment with

* This report is journal paper No. 2618 of the Purdue University Agricultural Experimental Station, Lafayette, Indiana. This investigation was supported in part by Public Health Service Research Grant EF-00055, from the Division of Environmental Engineering and Food Protection, and National Science Foundation Grant GP-1219.

† On leave of absence from the Macaulay Institute for Soil Research, Aberdeen, Scotland.

appropriately saturated resin (Dowex 50W-X8) and was examined as films sedimented from aqueous suspension either unmounted or on quartz disks.

Heating of samples up to 700°C in vacuum was carried out in quartz infrared cells using a rotary vacuum pump capable of attaining 10^{-2} mmHg. The cells were cooled under vacuum and infrared absorption spectra were recorded on a Perkin Elmer 421 double-beam spectrometer, with a matching quartz cell in the reference beam. Spectra were recorded over the range 4000–2000 cm^{-1} where the matched cells gave a very flat absorption background and not less than 80% of the radiant energy was available: spectra were also recorded from 4000 cm^{-1} to 500 cm^{-1} with the samples in air.

X-ray diffraction patterns were recorded on a GE XRD5 diffractometer, heated samples being held over P_2O_5 and flushed with dry nitrogen to minimize rehydration. The cation exchange capacity of NH_4^+-rectorite, determined by a conventional microkjeldahl method, was 59 m-equiv./100 g air-dry material.

Samples were deuterated by flushing them six times with the vapor from D_2O (99.7%; General Dynamics Corporation, San Carlos, California).

RESULTS AND DISCUSSION

It can be concluded from Fig. 1 that exchangeable ammonium cations in the expanding layer of ammonium-saturated rectorite are hydrogen bonded to water molecules. The hydrogen bonded NH_4^+ absorption bands at 3190, 3050, 2865, and 1450 cm^{-1} shift to 3280 and 1430 cm^{-1} on heating in vacuum to 200°C. These shifts are consistent with more freely rotating ammonium ions when interlayer water is removed from the sample and are analogous to the shifts observed on dehydrating NH_4^+-montmorillonite (Mortland *et al.*, 1963; Russell and Farmer, 1964). These observations support the conclusion of Brown and Weir (1963) that hydration water and exchangeable cations are associated in the expanding layer of rectorite, and that the expanding layer is montmorillonite-like. However, the lower intensity and greater width of the 1430 cm^{-1} NH_4^+ deformation band in the dehydrated mineral compared with the 1440 cm^{-1} NH_4^+ band in the hydrated mineral are anomalous. They seem to indicate that NH_4 cations participate in a range of strengths of hydrogen bonds to surface oxygens in the dehydrated structure, and these bonds are probably the origin of the residual broad absorption between 3100 and 2800 cm^{-1} (Fig. 1b).

On heating the NH_4^+-rectorite to higher temperatures in vacuum, NH_4 and OH stretching bands decrease in intensity due to decomposition of NH_4 and dehydroxylation of the mineral and a new absorption band develops at 3476 cm^{-1} (Fig. 2). Maximum development of the band occurs at about 550°C when the mineral spectrum shows neither OH nor NH_4 absorption bands.

Scale expansion of the 3476 cm^{-1} band reveals some interesting fine structure (Fig. 3). At 300°C the principal 3476 cm^{-1} band is accompanied by weaker

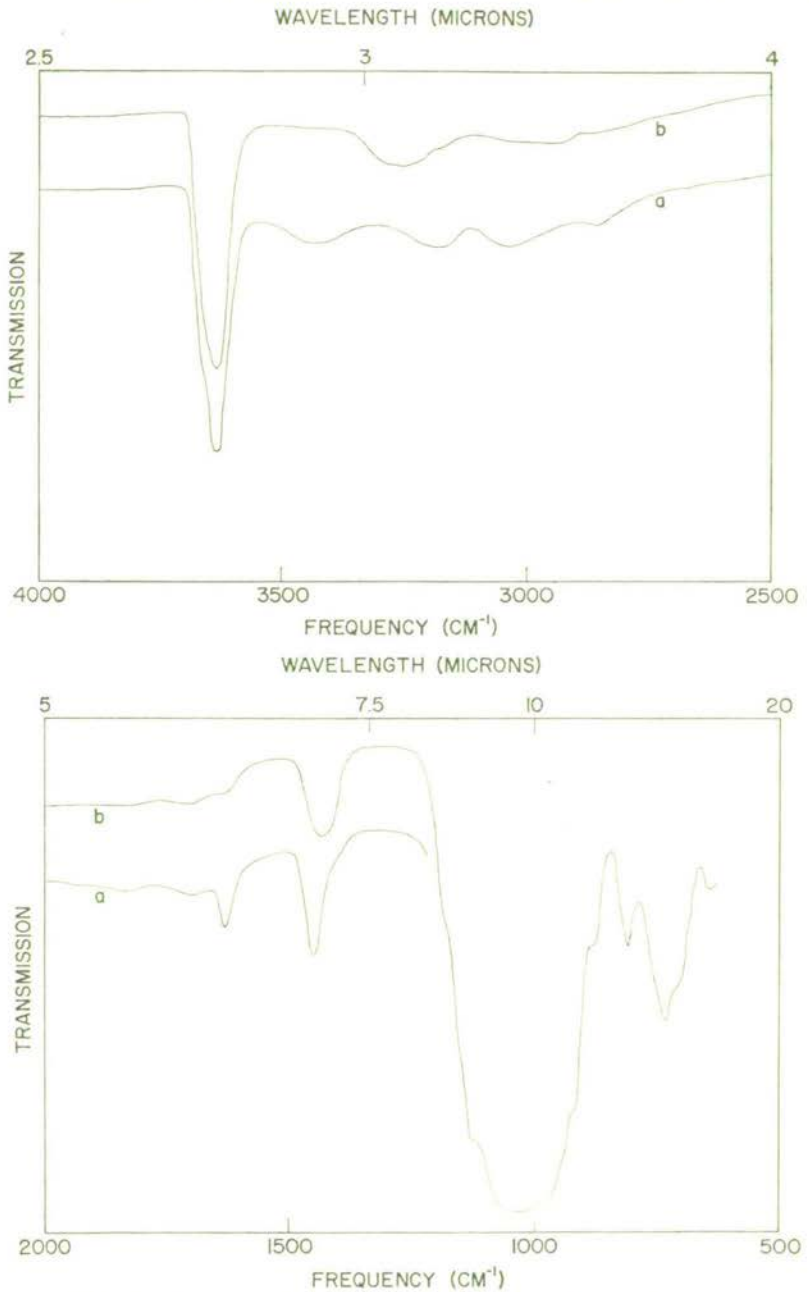

FIG. 1.—Infrared spectra of NH_4^+-rectorite film (a) air-dry, (b) dehydrated by evacuation to 10^{-2} mmHg at room temperature.

deuterated clay systems (Roy and Roy, 1956; Ledoux and White, 1964) and in ordinary and heavy ice (Ockman, 1958) support the assignment.

TABLE 2.—ISOTOPIC RATIOS OF STRETCHING FREQUENCIES OF OH AND OD IN AMMONIUM-SATURATED RECTORITE BEFORE AND AFTER HEATING AND D_2O TREATMENT

Group	νOH	νOD	νOD/νOH
Perturbed lattice	3500	2585	0.739
OH, OD	3476	2565	0.739
Lattice	3650	2720	0.745
OH, OD	3630	2695	0.743
Lattice OH, OD in montmorillonite			0.730*
Lattice OH, OD in kaolinite			0.739†
OH, OD in solid H_2O and D_2O			0.740‡

* Roy and Roy (1956).
† Ledoux and White (1964).
‡ Ockman (1958).

Contrary to the findings of previous investigations (Brindley, 1956) dehydroxylated rectorite can be partially rehydroxylated by exposure to water vapor at room temperature. It was possible then to introduce lattice OD groups into dehydroxylated rectorite by exposure to D_2O vapor. A sample so treated showed a doublet at 2720, 2695 cm^{-1} (Fig. 6). Isotopic ratios of these frequencies with the normal lattice OH frequencies at 3650 (a weak but distinct shoulder), and 3630 cm^{-1} (Fig. 6) are satisfactory (Table 2) and support the assignment of the 2720, 2695 cm^{-1} doublet to unperturbed lattice OD groups.

The doublet nature of the OH and OD stretching bands discussed above indicate that two different types of lattice OH groups exist in the rectorite structure. On the basis of the known structure of the mineral, " . . . a double-layer mineral made up of pairs of 2:1 type alumino-silicate layers. Alternate interlayers are mica-like . . . and montmorillonite-like . . . " (Brown and Weir, 1963), the two types of OH groups would be those adjacent to the mica-like region, and those adjacent to the montmorillonite-like region. Since the higher frequency member of the 3500, 3476 cm^{-1} perturbed OH doublet only developed at high temperatures (Fig. 3) it can be reasonably concluded that the 3500 cm^{-1} band arises from proton perturbation of OH groups adjacent to the mica-like layer: presumably more energy would be required to induce the proton to move into the neighborhood of the mica-like

OH groups. Thus, the higher frequency members of the OH, OD doublets shown in Fig. 6 might arise from vibrations of mica-like OH or OD groups, while the lower frequency vibrations have their origin in montmorillonite-like OH or OD groups. There did not appear to be preferential loss of either of the two types of OH group during dehydroxylation.

The formation of proton-perturbed OH groups was observed only in dioctahedral minerals whose layer charge arises from Al-for-Si substitution in the tetrahedral layer: the effect was not observed in NH_4^+-saturated hectorite, saponite, and Wyoming montmorillonite. It occurred weakly and was of a transient nature in NH_4^+-saturated nontronite. A band at 3472 cm^{-1} was observed by White and Burns (1964) in artificially expanded muscovite following H^+ saturation and heating. The mineral is dioctahedral and has only tetrahedral substitution, and on this basis the band could arise from proton perturbation of lattice OH groups by analogy with H^+-rectorite. Jorgensen (1965) sought a possible explanation of the 3472 cm^{-1} band in the stretching vibration of a lattice OH group with either two Al^{3+} ions and one Li^+ ion or one Al^{3+}, one Li^+ and one Fe^{2+} ions as neighbors by comparison with bands observed in high-lithium micas. However, the 3472 cm^{-1} band was not observed in Li^+ or K^+ saturations of the muscovite following artificial expansion by treatment with molten lithium nitrate.

The proton-perturbed OH group which gives rise to the 3500, 3476 cm^{-1} doublet in heated NH_4^+-rectorite is thermally very stable. The stability of the group can be explained in terms of its environment: the proton is held between a negatively charged apical oxygen and a hydroxyl group on an octahedral Al ion. This can be represented as

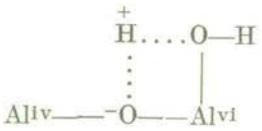

or in the extreme case

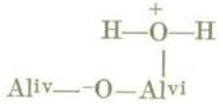

This latter arrangement would be expected to be very stable, final dehydroxylation leaving the charge deficiency on Al^{iv} internally balanced by a positive charge on Al^{vi}. Low stabilities of the proton-perturbed OH group in NH_4^+-nontronite would result from the higher electron affinity of octahedral Fe^{3+} compared with Al^{3+}. Normal dehydroxylation would result leaving the charge deficiency internally compensated by H^+. Another factor in the failure of NH_4^+-nontronite to develop the 3476 cm^{-1} band strongly is that the mineral dehydroxylated at 400°C in vacuum at which temperature only 25% of the NH_4 groups have decomposed. It is to be expected that a stable

proton-perturbed OH group would develop in NH_4^+-beidellite in which both octahedral and tetrahedral Al occur.

Recently it has been suggested from a study of thermal decomposition of ammonium zeolites (Uytterhoeven, *et al.*, 1965) that Si–OH groups absorbing at 3670 and 3585 cm^{-1}, and trigonal Al ions are produced by rearrangement of a Brønsted acid site on the zeolite.

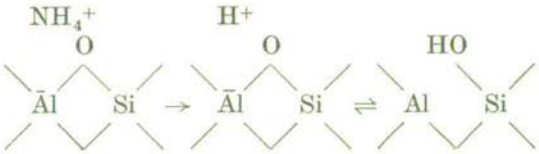

This scheme cannot account for the doublet observed in NH_4^+-rectorite since no regeneration of OH groups could take place on treating the heated sample with NH_3.

The authors would like to thank Dr. M. M. Mortland for helpful discussions.

REFERENCES

BOKII, G. B., and ARKHIPENKO, D. K. (1962) Oxonium ions in vermiculite, *Zh. Strukt. Khim.* **3**, 697–702.

BRINDLEY, G. W. (1956) Allevardite, a swelling double-layer mica mineral, *Amer. Min.* **41**, 91–103.

BROWN, G., and NORRISH, K. (1952) Hydrous micas, *Mineral. Mag.* **29**, 929–32.

BROWN, G., and WEIR, A. H. (1963) The identity of rectorite and allevardite, *Proc. Internat. Clay Conf., Stockholm*, Pergamon Press, New York **1**, 27–35.

JORGENSEN, PER (1965) Infrared absorption of O—H bonds in some micas and other phyllosilicates, *Clays and Clay Minerals*, Proc. 13th Conf., Pergamon Press, New York (in press).

KOROLEV, YU. M. (1960) The structure of allevardite, *Kristallografiya* **5**, 891–5.

LEDOUX, R. L., and WHITE, J. L. (1964) Infrared study of selective deuteration of kaolinite and halloysite at room temperature, *Science* **145**, 47–9.

MORTLAND, M. M., FRIPIAT, J. J., CHAUSSIDON, J., and UYTTERHOEVEN, J. B. (1963) Interaction between ammonia and the expanding lattices of montmorillonite and vermiculite, *Jour. Phys. Chem.* **67**, 248–58.

OCKMAN, N. (1958) The infrared and raman spectra of ice, *Advan. Phys.* **7**, 199–220.

ROY, D. M., and ROY, R. (1956) Hydrogen-deuterium exchange in clays and problems in the assignments of infrared frequencies in the hydroxyl region, *Clays and Clay Minerals*, Proc. 4th Conf., Natl. Acad. Sci.—Natl. Res. Council Pub. 456, pp. 82–4.

RUSSELL, J. D., and FARMER, V. C. (1964) An infrared study of the dehydration of montmorillonite and saponite, *Clay Min. Bull.* **5**, 443–64.

UCHIYAMA, N., and ONIKURA, Y. (1956) Double-layer mica minerals in paddy soil, *Tôhoku Jour. Agr. Res.* **7**, 9–15.

UYTTERHOEVEN, J. B., CHRISTNER, L. G., and HALL, W. K. (1965) Studies of the hydrogen held by solids. VIII. The decationated zeolites, *Jour. Phys. Chem.* **69**, 2117–26.

WHITE, J. L., and BURNS, A. F. (1964) Infrared spectra of hydronium ion in micaceous minerals, *Science* **141**, 800–1.

ISRAEL JOURNAL OF CHEMISTRY
Volume 6, 1968, pp. 315-323
MOKADY MEMORIAL ISSUE

MONTMORILLONITE — S-TRIAZINE INTERACTIONS*

Maribel Cruz, J. L. White

Department of Agronomy, Purdue University, Lafayette, Indiana, U.S.A.

and

J. D. Russell

Department of Spectrochemistry, Macaulay Institute for Soil Research, Aberdeen, Scotland

ABSTRACT

Adsorption of s-triazines on montmorillonite surfaces results in hydrolysis and protonation of the s-triazine compounds. Infrared studies suggest that dissociation of adsorbed water on the clay surface plays a major role in protonation and hydrolysis of the s-triazine herbicides.

Introduction

Increased use of herbicides and pesticides in agriculture has made necessary extensive investigation of the fate of these compounds in soils, particularly the systemic herbicides whose activity depends on uptake by plant roots. Although soil organic matter has been shown to be a major factor in determining movement and fixation of herbicides in soil [1, 2], the importance of the clay fraction is suggested by the adsorption of a range of herbicides by pure clay minerals as has been demonstrated by a number of investigators [3, 4, 5, 6].

Because of its high surface area, montmorillonite has been used in many adsorption studies. It has been demonstrated that s-triazines are adsorbed from aqueous solutions by both Na- and H-montmorillonites [3, 7, 8]. Weber et al. [4] outlined a series of possible reactions by which the triazine herbicide prometone might be adsorbed by montmorillonite. Weber [7] found that the amount of each compound which was adsorbed on the montmorillonite depended on the pH at which the compound became protonated; i.e., the pK_a value, and on the molecular structure of the compound. The postulated adsorption mechanism for prometone was suggested to hold for other triazines. No direct evidence for the state of the adsorbed species was given.

* Journal Paper No. 3287 of the Purdue University Agricultural Experiment Station, Lafayette, Indiana.

Infrared spectroscopy provides a unique method of observing adsorbed species and the present investigation is an attempt at elucidating the mechanism of adsorption of triazines by montmorillonite and the possible effects of exchangeable cations and triazine structure on the adsorption reaction.

Materials and Methods

The montmorillonite used in this study was the $<2\mu$ fraction of Wyoming Bentonite saturated by standard cation exchange resin techniques using Dowex 50W-X8. Montmorillonite was saturated with the following cations: H^+, Na^+, K^+, NH_4^+, Li^+, Mg^{2+}, Ca^{2+}, Cu^{2+}, Ni^{2+}, Co^{2+}, Zn^{2+}, Al^{3+} and Fe^{3+}. Self-supporting films (2-4 mg/cm^2) of these montmorillonites were prepared by sedimentation from aqueous suspension onto thin polyethylene sheets, from which the air-dried films could be readily stripped.

The s-triazine compounds used in this study — propazine, prometone, prometryne, and hydroxypropazine — were high purity compounds obtained from Geigy Chemicals Corporation, Ardsley, New York. Table I gives the structure and chemical name for each of these compounds. The protonated hydroxypropazine was prepared by treatment of hydroxypropazine with HCl followed by successive recrystallizations from water and then from ethanol.

TABLE I. Structure and chemical name of s-triazines [4, 6-bis (isopropylamino) series]

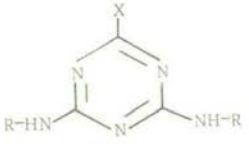

R = C_3H_7 (iso form)

Common Name	Chemical Name	X
propazine	s-triazine, 2-chloro-4,6-bis (isopropylamino)	Cl
hydroxypropazine	s-triazine, 2-hydroxy-4,6-bis (isopropylamino)	OH
prometone	s-triazine, 2-methoxy-4,6-bis (isopropylamino)	OCH_3
prometryne	s-triazine, 2-methylmercapto-4,6-bis (isopropylamino)	SCH_3

The above s-triazines have limited solubility in water. In order to have concentrations of the s-triazines on the montmorillonite surface sufficiently large to be measured by infrared techniques, chloroform and ethanol were used as solvents.

Montmorillonite films were placed in saturated chloroform and ethanol solutions of the above s-triazine compounds and were left in contact with the solutions for varying periods of time at ambient temperature (~22°C). The films were then removed, rinsed twice in solvent, dried, and their infrared spectra recorded on a Perkin-Elmer model 421 infrared spectrophotometer.

Results and Discussion

Adsorption of the s-triazines from chloroform solutions yielded phases whose spectra differed from those of the pure s-triazines in AgCl or KBr disks in showing a relative decrease in intensity of the bands in the 1530-1550 cm^{-1} region (in-plane vibrations of triazine ring and NH in-plane deformation) and a relative intensity increase and slight shift in the band near 1600 cm^{-1} (C = N skeletal vibrations). The general features of the interaction are illustrated for the propazine system in Figure 1. The spectra of propazine and a film of NH_4-montmorillonite reacted with propazine in chloroform solution for varying periods of time are shown in Figure 1a through 1c.

By contrast, the spectra of the species (excluding prometryne) adsorbed from ethanol showed several striking differences from the spectra of the pure compounds in AgCl or KBr disks, notably adsorption bands at 1740 cm^{-1} and 3330 cm^{-1} in the former. The changes observed in the 2000-1500 cm^{-1} region are illustrated in Figure 1e for propazine adsorbed from an ethanol solution by NH_4-montmorillonite. With the exception of prometryne, the phases adsorbed from chloroform initially showed no band at 1740 cm^{-1}, but a weak band developed at this frequency on exposure of the treated films to water vapor (Figure 1d).

That the above reactions are influenced by surface acidity is strongly suggested by the similarities between the infrared spectrum of the reaction between a film of H-montmorillonite and propazine in ethanol (Figure 1f) and the spectra showing reactions between NH_4-montmorillonite and propazine (Figure 1d through 1e). These spectra may be compared with that of protonated hydroxypropazine in a KBr disk (Figure 3e). The latter spectrum has NH stretching bands at 3200 and 3250 cm^{-1}, the C = 0 stretching band at 1765 cm^{-1}, and C = N skeletal vibrations at 1600 cm^{-1}.

Propazine, hydroxypropazine, and prometone gave the same adsorbed phase, the spectra being essentially identical with that of a montmorillonite treated with a dilute HCl solution of any of the s-triazines.

An infrared absorption band in the region of 1750 cm^{-1} is indicative of a carbonyl group. While such a group does not exist in the triazines investigated, hydrolysis could replace the groups at position 2 by OH yielding a common product, hydroxypropazine. Keto-enol tautomerism of

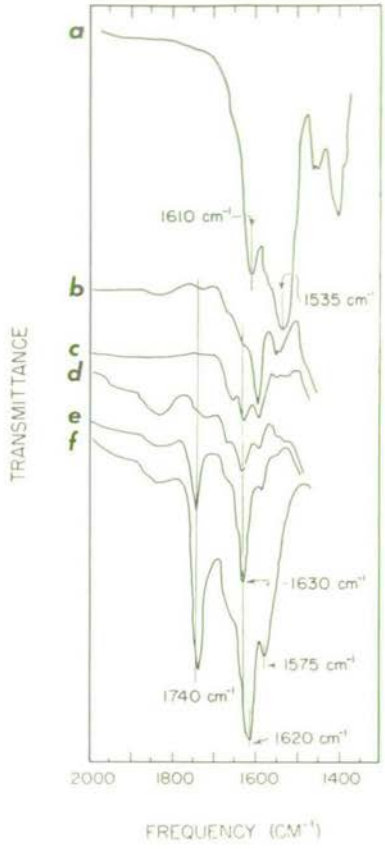

FIGURE 1. Infrared spectra of propazine and propazine-montmorillonite systems. (a) propazine in AgCl disk; (b) NH_4-montmorillonite film treated with chloroform solution of propazine for 3 days; (c) NH_4-montmorillonite film treated with chloroform solution of propazine for 19 days; (d) NH_4-montmorillonite film treated with chloroform solution of propazine for 55 days after exposure to water vapor; (e) NH_4-montmorillonite film treated with ethanol solution of propazine for 3 days; (f) H-montmorillonite film treated with ethanol solution of propazine.

such an OH group would then yield a ring carbonyl group. Since the spectrum of the adsorbed phase is identical with that of the cation-saturated montmorillonite prepared from any of the four triazines, the adsorbed phase must also be a cation.

Hartley [9] has shown that the chloro, methoxy, and thiomethoxy groups of propazine, prometone, and prometryne, respectively, undergo slow hydrolysis in sterile aqueous solution, and the hydrolysis is accelerated by strong acid or alkali. While such extreme conditions are seldom encountered in a normal soil, Hartley and Roe [10] and Low [11] have established that the pH at the surface of a clay particle in suspension is lower than that of the bulk suspension. Recent estimations [8, 9, 12] indicate that the surface of a clay may be 2 to 4 pH units more acid. Gysin and Knüsli [13] have shown that in the absence of a clay surface, the half-life of the acid-catalyzed hydrolysis of simazine can be decreased by a factor of 90 by decreasing the pH from 4 to 2. The protonation of 3-aminotriazole adsorbed on montmorillonite has been reported by Russell, Cruz and White [14]. Protonation in the case of montmorillonite saturated with polyvalent cations was attributed to the highly polarized water molecules in direct coordination to these cations. Thus, the surface of a clay particle might provide sufficiently low pH conditions to promote the acid hydrolysis of propazine and prometone. Such hydrolysis would be expected to give hydroxypropazine.

$$\text{I}\quad \text{P-Cl} \qquad \text{II}\quad \text{P-O-CH}_3 \Big\} \xrightarrow{H_2O/H^+} \text{P-OH} + \text{HCl} \quad \text{P-OH} + \text{CH}_3\text{OH}$$

P =

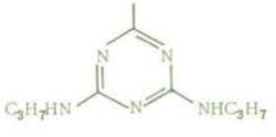

If the surface of the clay is sufficiently acid to promote hydrolysis of the herbicides, such an environment should also induce protonation and tautomerism in these structures. Protonation and tautomeric isomerism involving structures very closely related to hydroxypropazine have been shown to occur in acidic conditions. Thus, Hirt and Schmidt [15], working on the structure and ionization of melamine and its derivatives, showed that ammeline was protonated at pH 4.5.

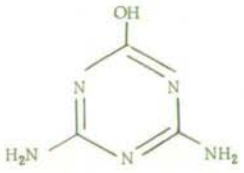

Ammeline

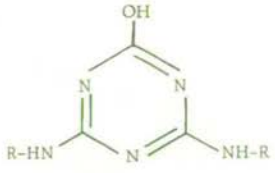

Hydroxypropazine R = C_3H_7 (iso form)

Boitsov and Finkel'shtein [16] working on derivatives of cyanuric acid and melamine, concluded that keto and amino tautomers are favored by low pH, and enol and imino tautomers by high pH. It would seem probable, therefore, that at the clay surface the pH would be low enough to effect, in the adsorbed hydroxypropazine molecule, a sequence of reactions resulting in protonation of hydroxypropazine. Recent NMR studies [17] of the protonated hydroxypropazine indicate that the reactions and structures shown below, together with related structures arising from resonance and tautomerism, are the most probable ones.

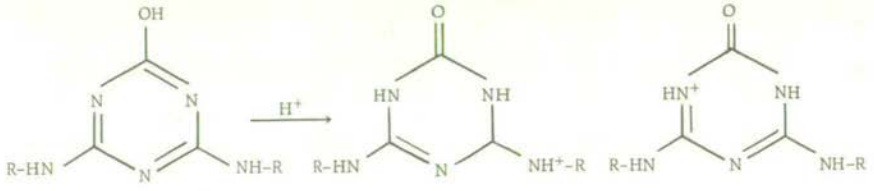

R = C_3H_7 (iso form)

Since adsorption of prometryne by montmorillonite did not produce a phase showing an absorption band at 1740 cm^{-1}, it is concluded that this herbicide failed to undergo hydrolysis at the clay surface. The C-S bond is known to be more stable to scission reactions than is the C-O bond. Scission was achieved by strong acid, but while hydrolysis occurred and produced the same protonated species as found for the other s-triazines, occasionally resinous products were obtained, indicating polymerization reactions.

The s-triazines propazine, prometone, and hydroxypropazine, when adsorbed on the surface of montmorillonite saturated with basic or metallic cations, were not hydrozyled at extremely low levels of moisture, but did

become hydrolyzed upon exposure to water vapor (100% R.H.). The changes in position and intensities of infrared bands in the 1500-1600 cm^{-1} region prior to the appearance of the 1740 cm^{-1} band upon hydrolysis, suggest protonation precedes hydrolysis and may be a prerequisite for adsorption of the s-triazines. These observations indicate that the highly dissociable water on the clay surface may be the source of protons for the protonation and hydrolysis reactions as has been shown in other systems by Mortland et al. [18], Farmer and Mortland [19], Mortland [20], Russell [21], and Fripiat et al. [22].

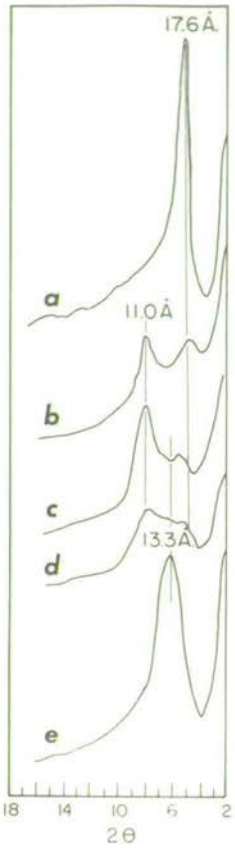

FIGURE 2. X-ray diffractometer tracings of film of montmorillonite. (a) montmorillonite saturated with protonated hydroxypropazine cation; (b) sample (a) after exposure to anhydrous NH_3 gas; (c) sample (b) dried overnight over P_2O_5; (d) sample (c) after exposure to dry HCl gas; (e) sample (d) after exposure to both HCl and H_2O vapors.

The significance of the surface acidity of the montmorillonite may be better appreciated when it is realized that the pH of an HCl solution must be below 3.25 to produce and maintain the protonated from of hydroxypropazine.

The influence of surface acidity on the behavior of adsorbed s-triazines was studied in a qualitative manner through experimentally varying the pH of the clay surface by vapor phase reactions with NH_3 and HCl gases.

In one series of experiments, montmorillonite was saturated with the cationic form of the hydroxypropazine in aqueous solution. The air-dry complex had a basal spacing of 17.6 Å. (Figure 2a); this plus the infrared spectrum (Figure 3a) and unpublished results of infrared pleochroism studies of the complex indicate the presence of two layers of the protonated hydroxypropazine cations between the montmorillonite layers.

The air-dry specimen was then exposed to dry NH_3 gas in a controlled atmosphere sample chamber; the basal spacing shifted to 11.0 Å and only a small peak remained at 17.6 Å (Figure 2b). Infrared spectra (Figure 3b) of the NH_3-treated specimen showed the pattern of hydroxypropazine plus bands at 2350 and 2475 cm^{-1} (not shown in Figure 3). Drying the specimen overnight in a desiccator containing P_2O_5 caused the 17.6 Å spacing to shift to 13.3 Å, probably through loss of water, and a moderately intense x-ray diffraction peak developed at 11.0 Å (Figure 2c). Infrared spectra of the specimen after dehydration over P_2O_5 overnight exhibited a small peak at 1740 cm^{-1}, indicating the formation of a small amount of the protonated form of hydroxypropazine. This is attributed to the higher

degree of dissociation of the residual water on the clay as the water content was decreased [20]. The major portion of the protonated hydroxypropazine was converted to hydroxypropazine external to the interlayer region of the montmorillonite.

Dry HCl vapor was then passed through the specimen chamber. X-ray diffractometer tracings (Figure 2d) of the specimen showed two broad bands at 17.3-16.9 and 12.0-11.3 Å, indicating a mixture of spacings. The infrared spectrum (Figure 3c) of the specimen showed it to be primarily the protonated form of hydroxypropazine with intensities slightly different from those of the protonated hydroxypropazine in a KBr disk (Figure 3e). From the x-ray diffraction and infrared results it is concluded that the hydroxypropazine formed on external surfaces of montmorillonite by the NH_3 treatment was protonated in place by the HCl gas and did not move immediately into interlayer positions in the montmorillonite.

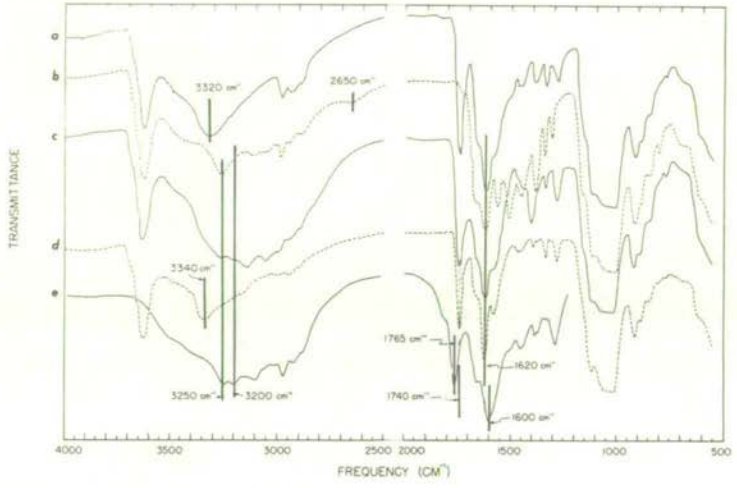

FIGURE 3. Infrared spectra of film of montmorillonite: (a) saturated with protonated hydroxypropazine cation; (b) sample (a) after exposure to anhydrous NH_3 gas; (c) sample (b) after exposure to dry HCl gas; (d) sample (c) after exposure to both HCl and H_2O vapors; (e) protonated hydroxypropazine in KBr disk.

When both HCl and H_2O vapors were passed through the specimen chamber an intense 001 reflection was observed at 13.3 Å (Figure 2e) and the infrared spectrum (Figure 3d) indicated the presence of protonated hydroxypropazine cations in interlayer positions in the montmorillonite. The movement of the protonated hydroxypropazine cation into interlayer positions is accompanied by the shifting of NH stretching bands from 3200 and 3250 cm^{-1} in the crystalline compound (Figure 3e) to 3340 cm^{-1} in the cation-montmorillonite system (Figure 3d). In addition, the C = O stretching band at 1765 cm^{-1} in the crystalline compound shifts to 1740 cm^{-1}

in the cation-montmorillonite system; the C = N skeletal in-plane-vibrations increase from 1600 cm^{-1} in the crystalline compound to 1620 cm^{-1} in the cation-montmorillonite system.

Conclusions

These observations suggest that the s-triazines examined in this study can be adsorbed on interlayer surfaces of montmorillonite and that protonation and hydrolysis of the s-triazines may occur concurrently with or following adsorption.

The infrared studies of the interactions between propazine and montmorillonite in a chloroform system, with and without water, have established the fact that the highly dissociable adsorbed water on the clay surface plays a major role in protonation and hydrolysis of the s-triazine herbicides.

Since the protonated hydroxypropazine, like hydroxypropazine, has no biological activity, the hydrolysis and protonation reactions catalyzed by montmorillonite and similar colloidal surfaces may represent the major mode of degradation of the s-triazines in soils. The protonated hydroxypropazine is water soluble whereas the hydroxypropazine is not; thus, diffusion of the protonated hydroxypropazine as a cation may be an important factor in movement and distribution of the hydroxypropazine in the soil.

ACKNOWLEDGEMENT

This study was supported by Public Health Service research grants ES 00060-5, from the Division of Environmental Sciences, and CC 00248, from the National Communicable Disease Control Center, Atlanta, Georgia.

REFERENCES

1. R.P. UPCHURCH and W.C. PIERCE, Weeds, 6, 24 (1958)
2. T.J. SHEETS, A.S. CRAFTS and H.R. DREVER, J. agric. Fd. Chem., 10, 458 (1962)
3. M.J. FRISSEL, Versl. landbouwk Onderz. Ned. L. 673. Wageningen (1961)
4. J.B. WEBER, P.W. PERRY and R.P. UPCHURCH, Proc. Soil Sci. Soc. Am. 29, 678 (1965)
5. C.I. HARRIS and G.F. WARREN, Weeds, 12, 120 (1964)
6. R.E. TALBERT and O.H. FLETCHALL, Weeds, 13, 46 (1965)
7. J.B. WEBER, Am. Miner., 51, 1657 (1966)
8. G.W. BAILEY, J.L. WHITE and T. ROTHBERG, Proc. Soil Sci. Soc. Am., 32, 222 (1968)
9. G.S. HARTLEY, in: The Physiology and Biochemistry of Herbicides, ed. L.J. Andus, p. 111. Academic Press, New York (1964)
10. G.S. HARTLEY and J.W. ROE, Trans. Faraday Soc., 36, 101 (1940)
11. P.F. LOW, Soil Sci., 77, 29-41 (1954)
12. R.D. HARTER and J.L. AHLRICHS, Proc. Soil Sci. Soc. Am., 31, 30 (1967)
13. H. GYSIN and E. KNÜSLI, Advances in Pest Control Research, Vol. III, p. 302, Interscience, New York (1960)
14. J.D. RUSSELL, M. CRUZ and J.L. WHITE, J. agric. Fd. Chem., 16, 21 (1968)
15. R.C. HIRT and R.G. SCHMIDT, Spectrochim. Acta, 12, 127 (1958).
16. E.N. BOITSOV and A.I. FINKEL'SHTEIN, Optics Spectros., 7, 307 (1959)
17. J.D. RUSSELL, M. CRUZ, J.L. WHITE, G.W. BAILEY, W.R. PAYNE Jr., J.D. POPE, Jr. and J.I. TEASLEY, Science, 159 (1968) (in press)

18. M.M. MORTLAND, J.J. FRIPIAT, J. CHAUSSIDON and J. UYTTERHOEVEN, J. phys. Chem., **67**, 248 (1963)
19. V.C. FARMER and M.M. MORTLAND, J. phys. Chem., **69**, 683 (1965)
20. M.M. MORTLAND, Clay Miner., **6**, 143 (1966)
21. J.D. RUSSELL, Trans. Faraday Soc., **61**, 2284 (1965)
22. J.J. FRIPIAT, A. JELLI, G. PONCELET and J. ANDRE, J. phys. Chem., **69**, 2185 (1965)

The Adsorption of 3-Aminotriazole by Montmorillonite

J. D. Russell,[1] M. I. Cruz, and J. L. White

The 3-aminotriazole molecule is protonated when adsorbed on montmorillonite surfaces to produce the 3-aminotriazolium cation. In the case of montmorillonite saturated with polyvalent cations (Ca^{2+}, Cu^{2+}, Ni^{2+}, Al^{3+}), protonation is believed to be due to the highly polarized water molecules in direct coordination to these cations. The decreasing order of extent of protonation (Ca < Mg < Al) reflects the order of decreasing polarizing power of the cations. Infrared spectra indicate coordination of 3-aminotriazole to Ni^{2+} and Cu^{2+} cations. The infrared absorption band at 1696 $cm.^{-1}$ is assigned to the C=N stretching vibration of the exocyclic $C{=}N\langle^{+H}_{H}$ group. Shifts of the 1696-$cm.^{-1}$ band to 1683 and 1666 $cm.^{-1}$ upon dehydration and deuteration, respectively, suggest that the positive charge on the protonated molecule lies on the exocyclic nitrogen. The protonated molecule undergoes normal exchange reactions with other cations.

Several studies have been made of the fate of 3-amino-1,2,4-triazole in soils (Sund, 1956; Burschel and Freed, 1959; Jordan, 1960; Day *et al.*, 1961; Ashton, 1963; Ercegovich and Frear, 1964). While adsorption of aminotriazole by clay minerals was postulated by Sund (1956) and Ercegovich and Frear (1964), little is known of the interaction with pure clay minerals, particularly of the montmorillonite group. The importance of such reactions cannot be overemphasized in view of their bearing on the persistence of the herbicide in soil.

While the high solubility of aminotriazole in water (28 grams per 100 ml. at 23° C.) suggests ready leaching from whole soil, and this has been demonstrated for Californian soils by Day *et al.* (1961), this investigation indicates that if the soil contains a montmorillonite-type mineral, the aminotriazole might be resistant to leaching as a result of adsorption by the montmorillonite.

EXPERIMENTAL

The interaction between aminotriazole and montmorillonite was investigated by studying the infrared absorption spectra of sedimented montmorillonite films prepared from aqueous suspensions (1% w./v.) of homoionic montmorillonite containing dissolved aminotriazole at four levels—25, 50, 100, and 200% of the cation exchange capacity of the montmorillonite (90 mmoles per 100 grams of clay). The suspensions were slowly evaporated to dryness on thin polyethylene sheet from which the resulting clay films (2.5 to 3 mg. per sq. cm.) could be readily peeled.

DISCUSSION OF RESULTS

It is clear from the identity of the spectra in Figure 1 that the 3-aminotriazole has been converted to the triazolium cation in Mg montmorillonite. While the spectrum shown is qualitatively representative of the complexes of a range of other ionic saturations of montmorillonite (Na, NH_4, Ca, Cu^{2+}, Ni^{2+}, Al^{3+}), the extent to which aminotriazolium cation was formed is dependent on the exchangeable cation (Table I). The 3-aminotriazolium cation is formed, in the case of the polyvalent cations, when 3-aminotriazole becomes protonated by highly polarized water molecules which are in direct coordination to these cations. This type of reaction has been demonstrated previously for other organic bases—ethylamine (Farmer and Mortland, 1965); pyridine (Farmer and Mortland, 1966); and NH_3 (Mortland *et al.*, 1963; Russell, 1965). By contrast, in NH_4 montmorillonite, the triazolium ion is formed by the following reaction:

$$R{-}NH_2 + NH_4^+ \rightarrow R{-}NH_3^+ + NH_3$$

It is not yet clear how the aminotriazolium ion is formed in Na montmorillonite, but it is almost certainly formed by a reaction similar to the one by which NH_4^+ is formed from NH_3 (Russell, 1965), and pyridinium from pyridine (Farmer and Mortland, 1966) in this montmorillonite. Protonation of 3-aminotriazole was maximal in Al montmorillonite where the water molecules coordinated by Al^{3+} are so highly polarized that the clay is acidic. The decreasing order of extent of protonation, Ca < Mg < Al (Table I), reflects the order of decreasing polarizing power of the cations.

In addition to protonation of 3-aminotriazole in both Cu and Ni montmorillonites, spectra indicated coordination of the organic base to these transition metal cations.

Table I. 3-Aminotriazolium Ion Formed in Various Cationic Saturations of Montmorillonite[a]

3-Aminotriazole Added (% Exchange Capacity)	Exchangeable Ion on Montmorillonite						
	Na	NH_4	Ca	Mg	Al	Cu	Ni
	3-Aminotriazolium ion formed						
25	6	17			23	3	22
50	6	28	18	29	47	12	46
100	6	48	23	45	~100	32	42
200	6	49	21	42			

[a] Calculation was based on the absorbance of the 1696-$cm.^{-1}$ band of the 3-aminotriazolium cation using montmorillonite saturated with the cation as the standard. Film weights were standardized either by weight or from the absorbance of a silicate absorption band at 800 $cm.^{-1}$

Department of Agronomy, Purdue University, Lafayette, Ind.

[1] Present address: Department of Spectrochemistry, Macaulay Institute for Soil Research, Aberdeen, Scotland.

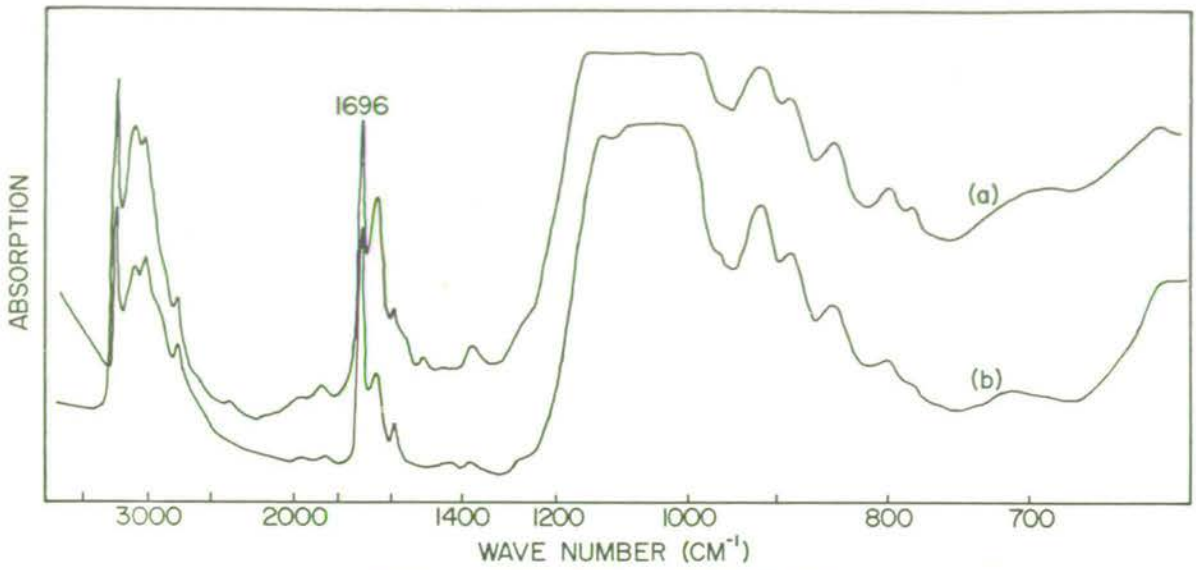

Figure 1. Infrared absorption spectra of films

A. Mg montmorillonite treated with 45 mmoles 3-aminotriazole per 100 grams of clay (3 mg. per sq. cm.)
B. 3-Aminotriazolium saturated montmorillonite (1 mg. per sq. cm.)

Coordination appeared to be the more extensive reaction in the Cu system in which a blue coloration was observed. These findings are in agreement with those of Menoret and Tracez (1957) and Ashton (1963) who demonstrated the formation in solution of stable coordination complexes of 3-aminotriazole with Cu^{2+} and Ni^{2+}, and with the higher stability constants of Cu^{2+} complexes compared with Ni^{2+}.

While Mortland (1966) has observed similar protonation and coordination effects in the adsorption of urea by H and Cu montmorillonites, he found that urea was not protonated in Na, Ca, or Mg clays. This can be explained in terms of the much lower basicity of urea (pK_B = 13.82) compared with 3-aminotriazole (pK_B = 9.83; Schmidt and Gehlen, 1965). The extents of protonation of pyridine (pK_B = 8.77) and aminotriazole in Na, Ca, and Mg montmorillonites agree well in per cent of the exchange capacity—12, 33, and 45 for pyridine (Farmer and Mortland, 1966) and 6, 23, and 45 for aminotriazole (Table I).

Figure 2 shows spectra of the hydrogen and deuterium forms of the Cu montmorillonite complex before and after evacuation, and for comparison analogous spectra of 3-aminotriazolium montmorillonite. Deuteration was effected by flushing samples with D_2O vapor in a cell similar to that described by Angell and Schaffer (1965). The over-all similarity between the spectra of the Cu complex and the triazolium-clay suggests a similar structural form for the organic molecule.

Considering first the spectrum of aminotriazolium montmorillonite (Figure 2*e*) an absorption band near 1700 $cm.^{-1}$ must, in the absence of a carbonyl group in the molecule, arise from a C=N group. Cipens and Grinsteins (1962) have established that while 3-aminotriazole exists in the amino (NH_2) form, its salts are in the imino (C=NH) form. The development of the imino cation is thought to proceed as follows:

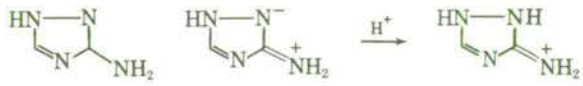

I II III

where structure II is one of the important resonance forms contributing to the true structure of 3-aminotriazole.

Bellamy (1958) has indicated that a grouping of the type 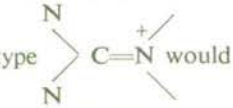 would be expected to absorb near 1700 $cm.^{-1}$ On this basis, the band at 1696 $cm.^{-1}$ is assigned to the C=N stretching vibration of the exocyclic 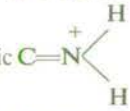 group in structure III; the assumption is made that the low frequency shift caused by conjugation with the double bond in the ring is compensated by the high-frequency shift brought about by the positive charge on the nitrogen, and the bonding of the carbon atom carrying the double bond to a further two nitrogens (Bellamy, 1958).

There are theoretically three further tautomeric variations of structure III in which the positive charge may lie on any of the ring nitrogen atoms. However, these variations tend to be rejected in favor of structure III on considering the behavior of the 1696-$cm.^{-1}$ band. Dehydration by evacuation at room temperature causes a shift from 1696 to 1683 $cm.^{-1}$ (Figure 2*f*) and deuteration a further shift to 1666 $cm.^{-1}$ (Figure 2*h*). Both observations indicate mechanical coupling between the exocyclic C=N and N—H vibrations, but the shift on dehydration has a further significance. The 3-aminotriazolium cation on exchange sites in montmorillonite lies flat in the interlayer space—that is, with the plane of the ring parallel to the cleavage plane. In this position the ion must depend on bonding with water molecules to neutralize effectively

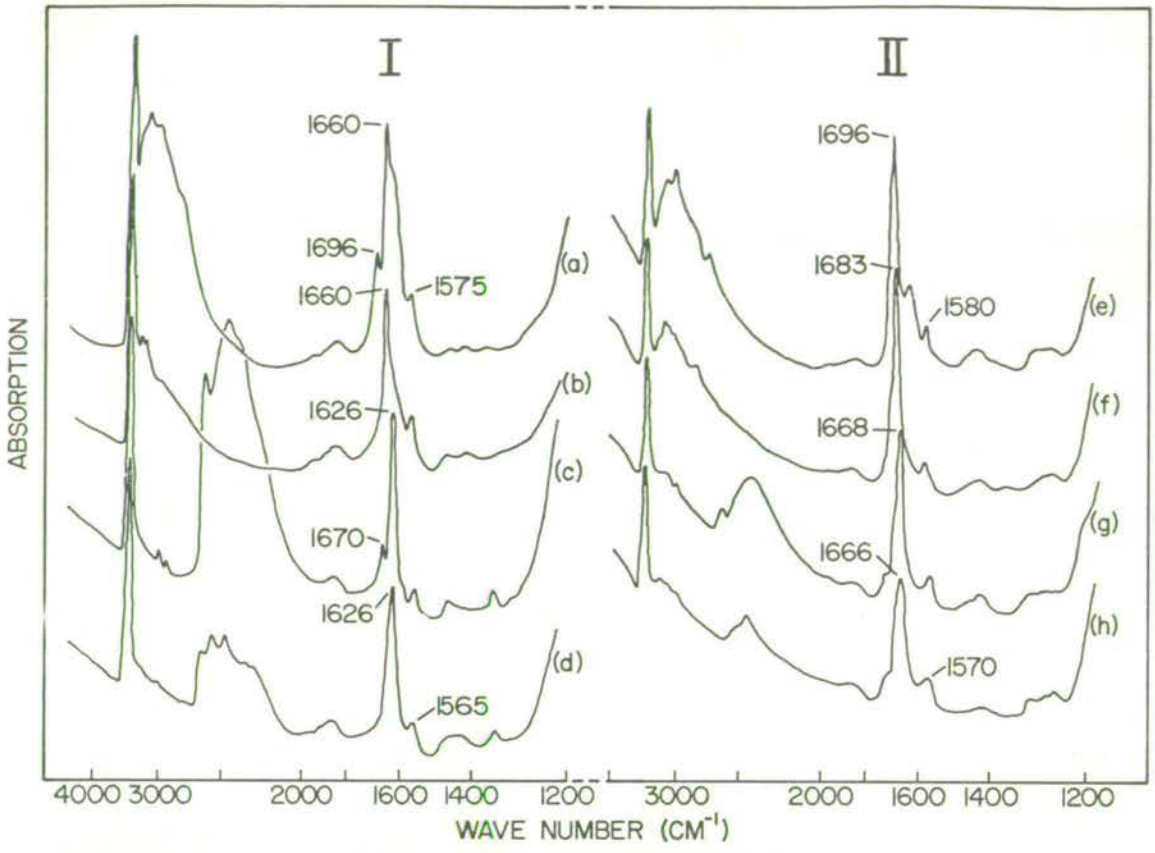

Figure 2. Infrared absorption spectra of films

I. Cu montmorillonite treated with 22.5 mmoles 3-aminotriazole per 100 grams of clay
II. 3-Aminotriazolium montmorillonite under various conditions: (*a*,*e*) at normal hydration; (*b*,*f*) at 0.005 mm. of Hg; (*c*,*g*) treated with D_2O vapor; (*d*,*h*) treated with D_2O vapor then evacuated to 0.005 mm. of Hg

negative charges on the lattice. Removal of interlayer water will result in the group carrying the positive charge being attracted towards the nearest negative lattice charge. If the positive charge resided on any of the ring nitrogen atoms, no appreciable change in the frequency of the exocyclic C=N band would be expected. If, however, the positive charge lies on the exocyclic nitrogen as shown in structure III, removal of water will cause, by the argument above, a lengthening of the exocyclic C=N bond and a shift of the stretching vibration to lower frequencies.

The weak band at 1580 cm.$^{-1}$ (Figure 2*e*) is not appreciably affected by evacuation or deuteration and is assigned to the ring C=N stretching vibration, the somewhat low frequency resulting from conjugation with the exocyclic double bond.

The arguments developed above for the structure of the aminotriazolium ion and the assignments of its absorption bands, also apply to the Cu-aminotriazole complex. The band at 1660 cm.$^{-1}$ is not affected by removal of interlayer water but suffers a shift to 1626 cm.$^{-1}$ on deuteration (Figure 2*d*). This leads to the conclusion that the group giving rise to the vibration is mechanically coupled to N—H, but is uncharged or only weakly so. While addition of a proton to structure II above will completely stabilize structure III, coordination of Cu^{2+} to II will not. The resulting structure of the Cu complex is thought of as one in which the exocyclic C=N bond has partial double bond character,

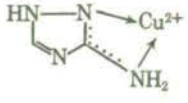

and would give rise to the 1660-cm.$^{-1}$ band. The corresponding band in the Ni aminotriazole complex occurs at 1645 cm.$^{-1}$ which would be anticipated from the lower stability constants of Ni complexes.

Of considerable importance agronomically is the observation that protonation of aminotriazole is dependent on the adequate hydration of the system (except perhaps in the case of the exchange sites being saturated with NH_4) and that in the presence of H_2O, the protonated species is stable on the clay. It can be removed by extraction into ethyl alcohol or similar solvent; presumably dehydration of the clay by the alcohol causes the reaction by which the protonated species was formed to be reversed, producing the neutral aminotriazole molecule which is then dissolved by the alcohol and extracted. While the protonated molecule on the clay is stable to leaching by water, it undergoes normal exchange reactions with other cations, and could thus become available as a herbicide. Thus aminotriazole may persist as an adsorbed cation particularly in an acid soil, and could theoretically be liberated by exchange re-

actions on application of inorganic fertilizers. The magnitude of occurrence of the exchange reactions may be too small to be of practical importance.

LITERATURE CITED

Angell, C. L., Schaffer, P. C., *J. Phys. Chem.* **69,** 3463 (1965).
Ashton, F. M., *Weeds* **11,** 167 (1963).
Bellamy, L. J., "The Infrared Spectra of Complex Molecules," p. 267, Methuen and Co., London, 1958.
Burschel, P., Freed, V. H., *Weeds* **7,** 157 (1959).
Cipens, G., Grinsteins, V., *Latv. PSR Zinat. Akad. Vest. Kim. Ser.* **3,** 401 (1962).
Day, B. E., Jordan, L. S., Hendrixson, R. T., *Weeds* **9,** 443 (1961).
Ercegovich, C. D., Frear, D. E. H., J. AGR. FOOD CHEM. **12,** 26 (1964).
Farmer, V. C., Mortland, M. M., *J. Phys. Chem.* **69,** 683 (1965).
Farmer, V. C., Mortland, M. M., *J. Chem. Soc.* **1966,** p. 344.
Jordan, L. S., *Proc. Ann. Calif. Weed Conf.* **78** (1960).
Menoret, Y., Tracez, J., *Compt. Rend.* **244,** 2827 (1957).
Mortland, M. M., *Clay Minerals* **6,** 143 (1966).
Mortland, M. M., Fripiat, J. J., Chaussidon, J. Uytterhoeven, J., *J. Phys. Chem.* **67,** 248 (1963).
Russell, J. D., *Trans. Faraday Soc.* **61,** 2284 (1965).
Schmidt, J., Gehlen, H., *Z. Chem.* **5,** 304 (1965).
Sund, K. A., J. AGR. FOOD CHEM. **4,** 57 (1956).

Received for review July 24, 1967. Accepted September 19, 1967. Journal paper No. 3128 Purdue University Agricultural Experiment Station, Lafayette, Ind. This study was supported by Public Health Service research grants ES 00060-5, from the Division of Environmental Sciences, and CC 00248, from the National Communicable Disease Control Center, Atlanta, Ga.

A reprint from

Journal of Agricultural and Food Chemistry

Vol. 16, Jan./Feb. 1968, Pages 21–24

Reprinted from
June 21, 1968, Vol. 160, pages 1340-1342

SCIENCE

Mode of Chemical Degradation of s-Triazines by Montmorillonite

J. D. Russell*
Maribel Cruz
J. L. White
G. W. Bailey, W. R. Payne, Jr.
J. D. Pope, Jr., J. I. Teasley

Mode of Chemical Degradation of *s*-Triazines by Montmorillonite

Abstract. *Chemical hydrolysis of the s-triazines after interaction with less than 2-micron (equivalent spherical diameter) montmorillonite clay occurs as a result of protonation at the colloidal surface; protonation occurs even when the exchange sites are occupied by metallic cations. The adsorbed hydrolytic degradation product is not the hydroxy analog, but it is predominantly the keto form of the protonated hydroxy species. This cationic form is held tightly by the clay which may restrict vertical movement and entrance into groundwater. Protonation of the hydroxy analog occurs on the heterocyclic ring nitrogen.*

The *s*-triazines are widely used herbicides, yet their fate in soil and water has not been clearly defined. Metabolism of simazine (*1*, *2*), atrazine (*3*), and ipazine (*4*) by soil microorganisms has been clearly shown. Recent work (*2*, *4*) calls into question the assumption that microbial degradation is a major factor in the detoxification and loss of *s*-triazine herbicides from soil. These authors measured the evolution of CO_2 containing labeled C^{14} and concluded that very little degradation of the 2-chloro *s*-triazine derivatives occurred within a period of 4 to 16 weeks.

Chemical hydrolysis of atrazine produces hydroxyatrazine in strongly acid or basic solutions (*5*). The hydroxy analogs of simazine (*6*, *7*), atrazine (*8*), and propazine (*7*) have been recovered from soils treated with the 2-chloro *s*-triazine derivatives. Thus the hydroxy analog has been proposed as the major degradation product of nonbiological degradation processes. The importance of the inorganic soil constituents in nonbiological degradation has been illustrated by Harris (*7*), who found that formation of the hydroxy analogs of simazine, atrazine, and propazine in five soils was not inhibited by 200 parts per million (ppm) of sodium azide. Atrazine was rapidly detoxified at 95°C in soil, but only slowly detoxified in aqueous solution at the same temperature in the absence of soil.

Direct evidence is not available on whether the degradation product of the *s*-triazine herbicides exists in the adsorbed state and whether the alkylamino functional group significantly affects the degradation reaction. Arm-

strong, Chesters, and Harris (*8*) postulated that the mechanisms proposed (*9*) for the hydrolysis of chlorotriazines would also hold for atrazine. Acid hydrolysis might thus result from protonation of a ring or chain nitrogen atom followed by cleavage of the C-Cl bond by water. We now present spectroscopic evidence on the interaction between *s*-triazines and the silicate surface and the chemical character of the degradation product.

The montmorillonite used in this study was the <2-μ fraction of Wyoming bentonite (Upton, Wyoming). Cation saturation was effected by cation-exchange resin techniques or by repetitive washings with 1*N* chloride salt solutions. Montmorillonite was saturated with the following cations: H^+, Na^+, K^+, NH_4^+, Li^+, Mg^{2+}, Ca^{2+}, Cu^{2+}, Ni^{2+}, Co^{2+}, Zn^{2+}, Al^{3+}, and Fe^{3+}.

Montmorillonite was reacted with the chloro-, methoxy-, and methylmercapto-*s*-triazines in water, methanol, and chloroform for varying periods of time. Aqueous solutions of atrazine and its methoxy and methylmercapto derivatives (containing amounts in excess of the cation-exchange capacity of the montmorillonite) were adjusted to *p*H 3.5 and reacted with a freshly prepared suspension of H-montmorillonite. In the nonaqueous systems, unsupported thin films of montmorillonite were placed in chloroform and methanol solutions of simazine and propazine and their methoxy and methylmercapto derivatives. After the excess *s*-triazine was removed, high-resolution infrared spectra of the clay-organic reaction products were recorded with the use of either unsupported films or micro-KBr techniques. The sample chamber was purged with dry nitrogen.

The *s*-triazines used were of high-purity (*10*). The protonated hydroxypropazine was prepared by treatment of hydroxypropazine with HCl, and then by successive recrystallizations from water and ethanol.

Infrared spectra show that both atrazine (Fig. 1, a and b) and propazine (Fig. 2, a and b) undergo significant changes as a result of interaction with the montmorillonite surface. The most obvious difference between the spectra of pure atrazine and propazine and the *s*-triazine–clay complexes is the appearance in the latter of a strong band at 1740 cm^{-1}. Carbonyl bands usually occur in this region. In addition, bands occur at approximately 1665 and 1630 cm^{-1} in both *s*-triazine–clay complexes.

The current assumption is that degradation of chloro *s*-triazines leads to the formation of the hydroxy analogs as the principal degradation product in soils. Comparison of the infrared spectra of atrazine–clay (Fig. 1b) and propazine–clay (Fig. 2b) with those of the hydroxy analogs (Figs. 1c and 2c, respectively) shows that the adsorbed degraded species are not the hydroxy analogs.

This conclusion is further supported by the changes in the infrared spectra of the hydroxy analogs (Figs. 1c and 2c) which result from interaction with H- and NH_4-montmorillonite (Figs. 1d and 2d). The band positions of the products (Figs. 1e and 2e) resulting from treatment of the hydroxy analogs with HCl to produce the protonated form are essentially identical with those of the product of the *s*-triazine–clay reaction.

The similarity of the spectra of atrazine and propazine (when adsorbed on montmorillonite surfaces) and those of the hydroxy analogs in acidic environment indicates that the adsorbed species have been protonated and hydrolyzed as a result of interaction with the clay surface. Degradation of the chloro *s*-triazines by interaction with the silicate surface results in the formation of the protonated hydroxy analogs of these compounds.

Infrared studies indicate that the chloro *s*-triazines are protonated even though all the exchangeable sites of the clay are occupied by metallic cations. The source of protons in these systems is probably the more highly dissociated water on the clay surface (*11*).

Surface acidity is an important factor in the interaction of montmorillonite systems with herbicides (*12*). The clay-organic interactions suggest that the surface acidity of the clay may be from 3 to 4 *p*H units lower than that

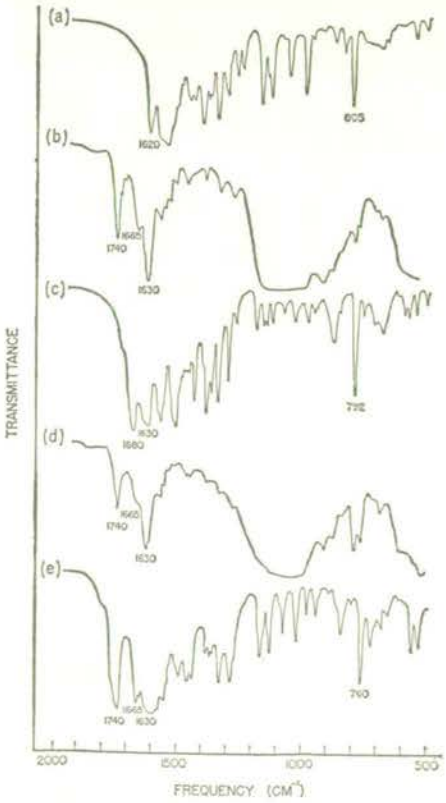

Fig. 1. Infrared spectra from 2000 to 500 cm^{-1} of: (a) atrazine; (b) atrazine–H-montmorillonite clay complex, reaction time 5 days; (c) hydroxyatrazine; (d) hydroxyatrazine–H-montmorillonite clay complex, reaction time 30 minutes; and (e) hydroxyatrazine + 6*N* HCl.

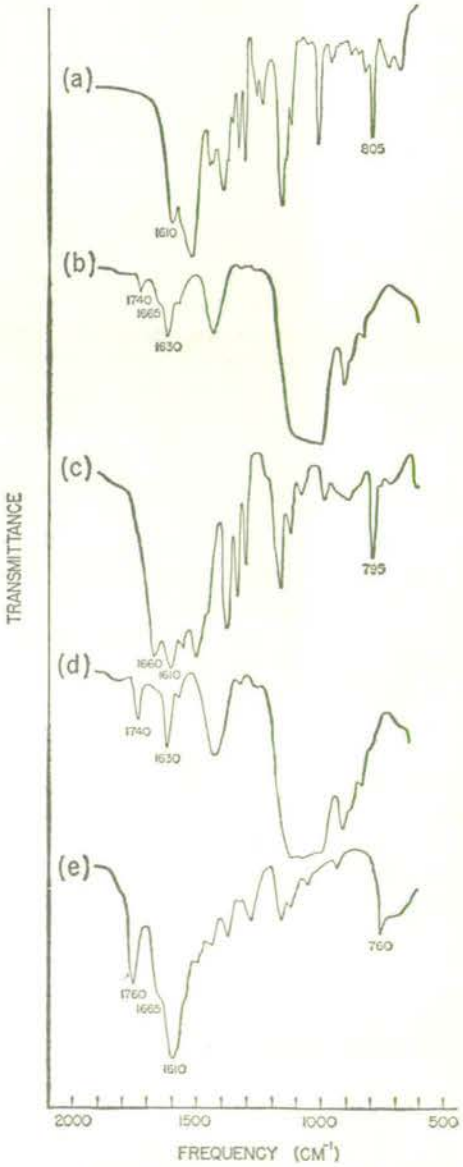

Fig. 2. Infrared spectra from 2000 to 500 cm^{-1} of: (a) propazine; (b) propazine–NH_4-montmorillonite clay complex; (c) hydroxypropazine; (d) hydroxypropazine–NH_4-montmorillonite clay complex; and (e) propazine + HCl.

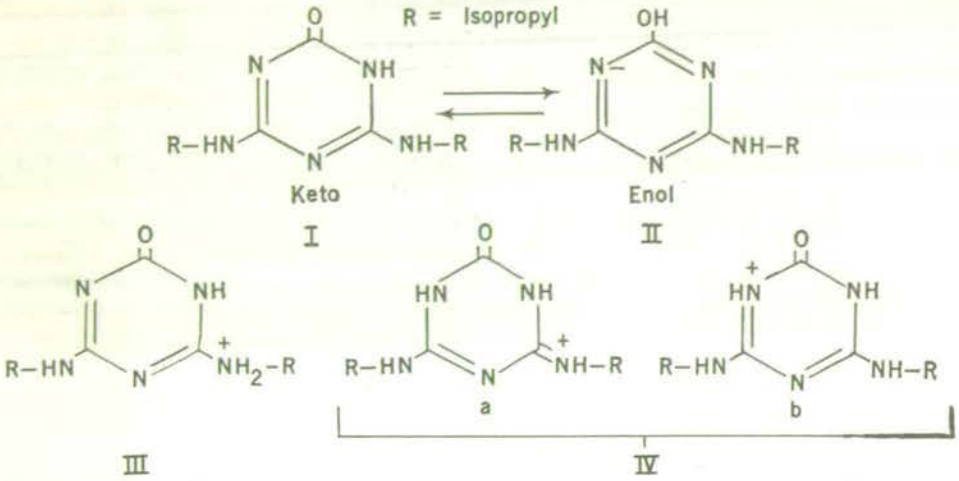

Fig. 3. Tautomeric structures (I and II) of the unprotonated and some possible tautomeric (III) and resonance (IV) structures of protonated hydroxy analogs of chloro *s*-triazines.

measured in the suspension. The fact that no degradation of atrazine was observed in a solution system at a *p*H of 3.5 in the absence of clay illustrates the catalytic function of the clay surface. A similar observation (*8*) has been reported for atrazine in soil studies. In both the low-moisture and high-moisture systems the adsorbed triazine molecules experienced high surface acidity, due in the former case to the highly dissociable water at the clay surface, and in the latter case to the presence of hydrogen as an exchangeable ion.

Two tautomeric forms of the hydroxy analogs are possible (Fig. 3). The appearance of a strong band at 1740 cm^{-1} indicates that the keto form (I) predominates in the protonated hydroxy species. This is supported by the shift of a band at 795 cm^{-1} in the hydroxy analog to 760 cm^{-1} upon protonation (*13*).

Protonation of the hydroxy analog has been postulated to occur either on the ring nitrogens or on the secondary amino groups of the side chains (*14*). Side-chain protonation would yield structure III with an NH_2^+ group, while ring protonation would result in the formation of a structure with either an exocyclic C=N group and the charge on the side chain nitrogen (IVa), or one in which both proton and charge reside on a ring nitrogen (IVb). The positive charge and the proton can reside on any of the three ring nitrogens; by resonance and tautomerism structure IVb will yield five additional isomeric structures. Structure IVa has only one other tautomeric isomer, but will have two more isomers for nonidentical side chains.

Spin decoupling (double resonance) was carried out by irradiating the isopropyl CH_3 groups of protonated hydroxypropazine; this removed the coupling from between the proton of the CH group and the CH_3 groups. As shown in Fig. 4a, the CH resonance changed from a complex multiplet to a doublet upon irradiation of the CH_3 groups. Irradiation of the CH proton caused the signal at 501 cycle/sec to collapse to a singlet (Fig. 4b), confirming the assignment of this absorption to the proton of the alkyl NH group. The doublet of the isopropyl CH_3 groups coalesces to a singlet upon irradiation of the CH proton (Fig. 4c). Structure III, which contains an NH_2^+ group, is ruled out by the NMR spin decoupling experiments. Thus, structure IV and its resonance and tautomeric forms are probably correct.

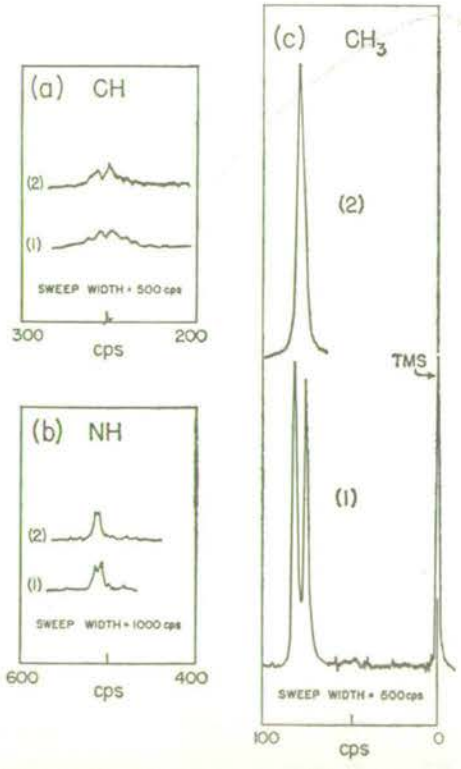

Fig. 4. Double resonance with protonated hydroxypropazine: (a) CH peaks: (1) initial spectrum; (2) CH_3 group irradiated. (b) NH peaks: (1) initial spectrum; (2) CH group irradiated. (c) CH_3 peaks: (1) initial spectrum; (2) CH group irradiated. Solvent: $CHCl_3$; sweep width, 500 cycle/sec.

J. D. Russell*
Maribel Cruz
J. L. White
Department of Agronomy, Purdue University, Lafayette, Indiana
G. W. Bailey, W. R. Payne, Jr.
J. D. Pope, Jr., J. I. Teasley
U.S. Department of the Interior, Federal Water Pollution Control Administration, Southeast Water Laboratory, Athens, Georgia

References and Notes

1. D. D. Kaufman, P. C. Kearney, T. J. Sheets, *Science* **142**, 405 (1963).
2. ———, *J. Agr. Food Chem.* **13**, 238 (1965); P. C. Kearney, D. D. Kaufman, T. J. Sheets, *ibid.*, p. 369; I. C. MacRae and M. Alexander, *ibid.*, p. 72.
3. R. W. Couch, J. V. Gramlich, D. E. Davis, H. H. Funderburk, Jr., *Proc. Southern Weed Control Conf.* **18**, 623 (1965); D. E. David, J. V. Gramlich, H. H. Funderburk, Jr., *Weeds* **13**, 252 (1965).
4. I. C. MacRae and M. Alexander, *J. Agr. Food Chem.* **13**, 72 (1965).
5. H. Gysin and E. Knusli, *Advan. Pest Control Res.* **3**, 289 (1960); D. E. Armstrong, G. Chesters, R. F. Harris, *Soil Sci. Soc. Am. Proc.* **31**, 61 (1967).
6. C. I. Harris, *Weed Res.* **5**, 275 (1965).
7. C. I. Harris, *J. Agr. Food Chem.* **15**, 157 (1967); R. S. Adams, Jr., *Soil Sci. Soc. Am. Proc.* **30**, 689 (1966).
8. D. E. Armstrong, G. Chesters, R. F. Harris, *Soil Sci. Soc. Am. Proc.* **31**, 61 (1967).
9. S. Horrobin, *J. Chem. Soc.* **1963**, 4130 (1963).
10. The *s*-triazines were obtained from Geigy Chemicals Corp., Ardsley, New York.
11. M. M. Mortland, J. J. Fripiat, J. Chaussidon, J. Uytterhoeven, *J. Phys. Chem.* **67**, 248 (1963); M. M. Mortland, *Clay Minerals Bull.* **6**, 143 (1966); V. C. Farmer and M. M. Mortland, *J. Chem. Soc. Ser. A* **1966**, 344 (1966); A. R. Swoboda and G. W. Kunze, *Abstr. 14th North Amer. Clay Mineral Conf., 2nd Mfg. Clay Minerals Soc.* (1965), p. 20.
12. G. W. Bailey, J. L. White, T. Rothberg, *Soil Sci. Soc. Am. Proc.*, in press.
13. N. B. Colthup, L. H. Daly, S. E. Wiberly, *Introduction to Infrared and Raman Spectroscopy* (Academic Press, New York, 1964), p. 235.
14. R. C. Hirt and R. G. Schmitt, *Spectrochim. Acta* **12**, 127 (1958).
15. We thank W. E. Baitinger and J. R. Barnes for interpreting the NMR spectra, and L. H. Keith and A. W. Garrison for helpful suggestions. Mention of products and manufacturer is for identification only and does not imply endorsement by the Federal Water Pollution Control Administration or the U.S. Department of the Interior. Paper No. 3203, Purdue University Agricultural Experiment Station, Lafayette, Ind. Portion of the study performed at Purdue University supported by PHS research grants Nos. ES-00060-5 and CC-00248.
* Present address: Macaulay Institute for Soil Research, Craigiebuckler, Aberdeen, Scotland.

4 March 1968

MINERALOGICAL MAGAZINE

VOLUME 37 NUMBER 292 DECEMBER 1970

Replacement of OH by OD in layer silicates, and identification of the vibrations of these groups in infra-red spectra

J. D. RUSSELL AND V. C. FARMER

The Macaulay Institute for Soil Research, Craigiebuckler, Aberdeen

AND B. VELDE

Laboratoire de Pétrographie, Tours 16–26, Faculté des Sciences de Paris, 9 Quai Saint Bernard, Paris 5ème

SUMMARY. Conditions necessary for exchange between lattice OH groups and D_2O in expanding layer silicates are reported. From spectral changes in the 200–1200 cm^{-1} region resulting from this exchange, in-plane librations of OH co-ordinated to (AlAl), (AlMg), ($AlFe^{3+}$), and (MgMgMg) have been identified in montmorillonite, beidellite, saponite, hectorite, and vermiculite. Both in-plane and out-of-plane librations have been identified for pyrophyllite and celadonite, from comparison of synthetic specimens containing OD with natural or synthetic OH forms. Comparison of hydrogen and deuterium forms of Mg- and Ni-talcs leads to the identification of translational and librational OH vibrations.

TREATMENT of minerals with D_2O at room or higher temperatures leads to conversion of some or all of their OH groups to OD groups. The degree of exchange can be determined from the infra-red spectrum, and this technique has been applied to distinguish different kinds of hydroxyl group in clay minerals (Farmer, Russell, and Ahlrichs, 1968).

Such exchange reactions also serve to identify those infra-red absorption bands that arise from vibrations involving hydroxyl, and by this means Stubican and Roy (1961) established that the in-plane rocking vibration (libration) of hydroxyl linked to two aluminium ions, as in kaolinite and beidellite, lay in the 910–40 cm^{-1} region, whereas libration of hydroxyl linked to two ferric ions, as in nontronite, lay at 827 cm^{-1}. They failed to find a libration of hydroxyl groups in talc or saponite.

In the present paper, the minimum conditions necessary to achieve complete replacement of OH by OD in expanding layer silicates have been investigated, and the deuterated products have been used to identify the librational frequencies of hydroxyl groups in dioctahedral and trioctahedral smectites. Preliminary reports on these

assignments have been published (Farmer, Russell, and Ahlrichs, 1968; Farmer *et al.*, 1967), but these earlier observations in the 1200–650 cm^{-1} region have now been extended to 300 or 200 cm^{-1}, and several vibrations involving hydroxyl have been found. To assist in characterizing these vibrations, OH and OD forms of pyrophyllite, celadonite, and talc have been prepared and examined. OH and OD forms of Ni-talc have also been prepared in an attempt to achieve a complete assignment for the talc spectrum.

Experimental

Replacement of lattice OH groups by OD groups in montmorillonite (Skyrvedalen, Wyoming, and Woburn Fuller's Earth), beidellite (Black Jack Mine, Idaho), saponite (Allt Ribhein, Skye), hectorite (Hector, California), and vermiculite (Loch Scye, Caithness) was readily achieved by heating self-supporting oriented films of NH_4-saturated specimens in D_2O vapour at 300–400 °C in a cell, fitted with AgCl windows, similar to that described by Angell and Schaffer (1965). The cell was successively evacuated to 0·002 mm Hg and filled with D_2O vapour (17·5 mm Hg) six times at room temperature to ensure removal or complete exchange of interlayer water. This procedure also resulted in extensive (80–100 %) exchange of NH_4 ions in all but the vermiculite where about 50 % NH_4 still remained. After heating for 1–16 hours the cell was evacuated, refilled with fresh D_2O vapour, and the heating continued. This procedure was repeated until the infra-red spectrum showed no OH stretching vibrations.

The comparative ease with which H–D exchange took place in the expanding layer silicates is worth noting: 3 one-hour treatments at 350 °C produced virtually complete deuteration of saponite, hectorite, vermiculite, and montmorillonite. Beidellite was slightly more resistant, requiring 4 treatments at 400 °C. Some exchange occurs even at 100 °C—about 7 % in beidellite and up to 25 % in montmorillonite. These results contrast sharply with those of Roy and Roy (1957) who achieved less than 50 % exchange in a hydrothermal treatment of montmorillonite (3 days at 370 °C and about 1·4 kb).

Synthetic deuterated specimens of pyrophyllite, talc, and celadonite were prepared hydrothermally from amorphous gels of the appropriate composition (Luth and Ingamells, 1965) and D_2O. The experimental conditions were: pyrophyllite, 27 days at 447 °C and 2 kb pressure; talc, 7 days at 640 °C and 1 kb; celadonite, 30 days at 360 °C and 1 kb. The composition of the celadonite, which was also prepared in the hydroxyl form, was $KMgFe^{3+}Si_4O_{10}(OH)_2$.

Attempts at hydrothermal synthesis of OD pyrophyllite from either the natural material or its dehydroxylate and D_2O yielded only about 5 and 25 % respectively. The latter is close to the level of rehydroxylation of dehydroxylated pyrophyllite at 500 °C in steam at atmospheric pressure (Heller *et al.*, 1962).

Infra-red absorption spectra were recorded on a Grubb–Parsons Spectromaster over the range 4000–400 cm^{-1} and on a Perkin Elmer 225 down to 300 cm^{-1} or 200 cm^{-1}. Lattice OD groups are stable in air at ambient temperatures. Samples were in the form of oriented separated films, oriented deposits on CsI plates or polyethylene

or AgCl sheet, and were also incorporated in CsBr or CsI pressed discs (0·2–1·5 mg/250 mg, 12 mm diameter). Ishii, Shimanouchi, and Nakahira (1967) have published spectra of randomly oriented talc and pyrophyllite down to about 50 cm^{-1}, and Wilkins and Ito (1967) have studied Ni-talc to 400 cm^{-1}. Our spectra agree well with theirs.

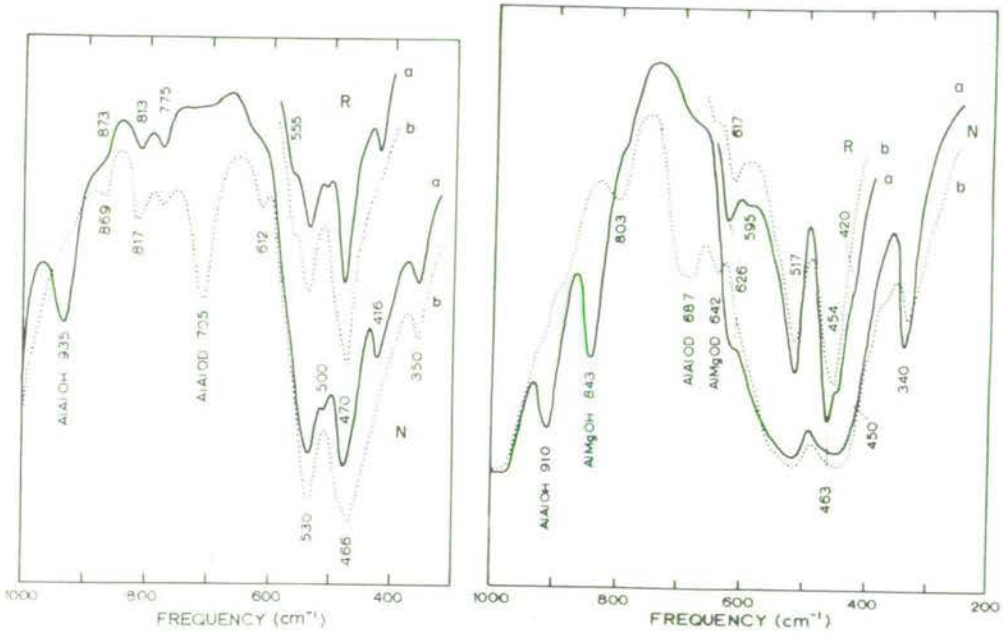

FIGS. 1 and 2: Fig. 1 (left). Infra-red spectrum of beidellite: (*a*) OH form, (*b*) OD form, N: film at normal incidence, R: randomly oriented sample in pressed disc. Fig. 2 (right). Infra-red spectrum of Skyrvedalen montmorillonite: symbols as in fig. 1.

Results and Discussion

The 2:1 dioctahedral layer silicates. When OD groups replace OH groups in dioctahedral layer silicates, the most striking changes in spectra below 1000 cm^{-1} are due to the displacement of the OH in-plane rocking vibration, or libration, to lower frequencies by a factor of 1·30–1·35. Thus the Al_2OH libration, lying at 935 cm^{-1} in OH-beidellite (fig. 1) is replaced by the Al_2OD libration at 705 cm^{-1} in OD-beidellite, as previously noted by Stubican and Roy (1961). Beidellite contains only aluminium ions in its octahedral layer, whereas montmorillonites have hydroxyl groups linked to both Al_2 and AlMg octahedral pairs. In all three montmorillonites (figs. 2, 3, 4) an Al_2OH libration can be identified at 910–20 cm^{-1}, and an AlMgOH libration at 839–48 cm^{-1}, by their displacement to lower frequencies in the OD-forms; these are the only librational frequencies in the iron-free Skyrvedalen montmorillonite (fig. 2).

Absorption bands at 887 cm^{-1} in Wyoming montmorillonite (fig. 3) and at 875 cm^{-1} in Woburn Fuller's Earth (fig. 4) have been ascribed to the libration of hydroxyl

co-ordinated to $AlFe^{3+}$ pairs, on the grounds that their intensity is related to the iron content of the montmorillonites, and that they are readily eliminated from the spectrum under reducing conditions, for example by exposure of clay films to hydrazine vapour (Farmer and Russell, 1964, 1967). The displacement of the 875 cm^{-1} band of Woburn Fuller's Earth to lower frequencies on deuteration (fig. 4) confirms this assignment, but it is noteworthy that at least some of the $AlFe^{3+}OH$ groupings in

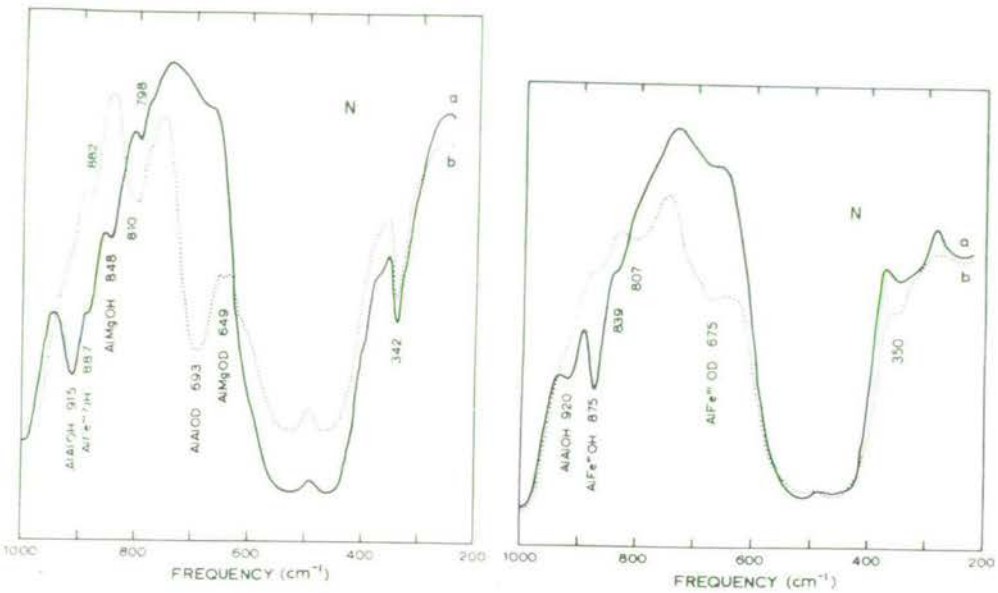

FIGS. 3 and 4: Fig. 3 (left). Infra-red spectrum of Wyoming montmorillonite: symbols as in fig. 1. Fig. 4 (right). Infra-red spectrum of Woburn Fuller's Earth: symbols as in fig. 1.

Wyoming montmorillonite are resistant to deuteration, as the 887 cm^{-1} band persists at 882 cm^{-1} in the deuterated sample (fig. 3). The possibility that the residual 882 cm^{-1} band arises from a different type of vibration was eliminated by the finding that it disappeared when the deuterated mineral was exposed to hydrazine vapour.

Deuteration causes a number of other changes in the spectra, in addition to those associated with the in-plane libration. Thus in montmorillonites, replacement of OH by OD causes the appearance, or the very marked enhancement of a band at 800–10 cm^{-1}, and bands near 620 and 460 cm^{-1} undergo slight shifts. In beidellite, bands at 416 and 500 cm^{-1} are lost, a band appears at 612 cm^{-1}, and bands at 470, 813, and 873 cm^{-1} undergo displacements.

There are two possible causes for these changes in spectra. Firstly, in addition to the in-plane libration of hydroxyl groups in dioctahedral layer silicates, a second, out-of-plane librational frequency should occur, with a dipole oscillation approximately perpendicular to the layer plane. Secondly, coupling between librational and translational vibrations of hydroxyl groups can occur, and so lead to frequency displacements.

In order to distinguish these possibilities under more favourable circumstances than those offered by smectite spectra, spectra of OH- and OD-pyrophyllite, which are sharper and better defined than those of smectites, have been examined (fig. 5). Further assistance in identification was given by comparing the spectra of oriented samples with those of randomly oriented samples; by this means it was possible to identify absorption bands that have a distinct component perpendicular to the layers and therefore appear weaker in the spectra of oriented samples (Farmer, 1958).

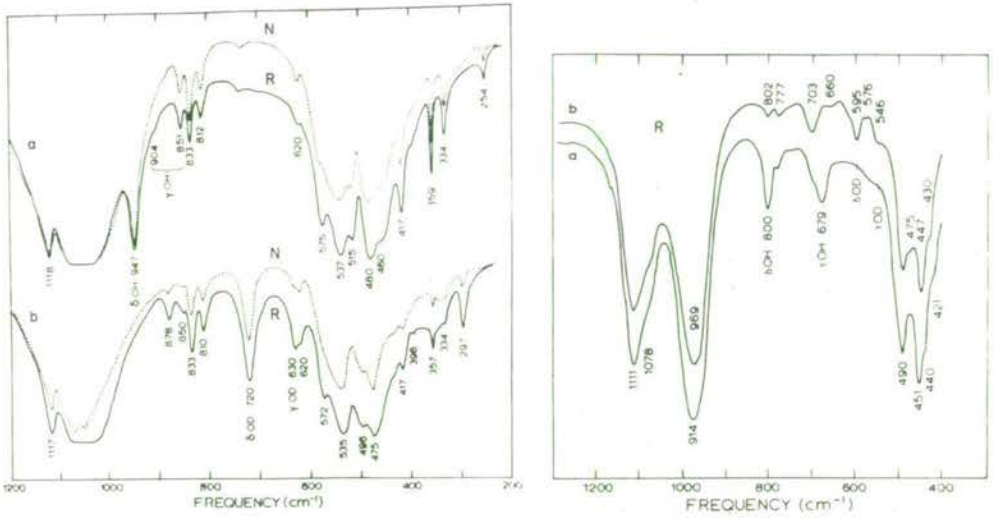

FIGS. 5 and 6: Fig. 5 (left). Infra-red spectrum of pyrophyllite: symbols as in fig. 1. Fig. 6 (right). Infra-red spectrum of celadonite: symbols as in fig. 1.

In the pyrophyllite spectra, the in-plane OH libration at 947 cm^{-1} and the corresponding OD libration at 720 cm^{-1} are readily identified, but the out-of-plane libration is less obvious, as so many changes occur in the spectrum when OD substitutes for OH. Vedder and McDonald (1963) suggested that a band at 405 cm^{-1} in muscovite is the out-of-plane libration of OH, as it was absent from the spectrum of an OD-muscovite. This band of muscovite has clear analogues in beidellite and pyrophyllite, near 417 cm^{-1}, which weaken considerably in the deuterated forms.

A new band appears at 297 cm^{-1} in OD-pyrophyllite that could be interpreted as the out-of-plane libration of OD, corresponding to an OH libration at 417 cm^{-1}. Farmer (1968) has pointed out, however, that the 405 cm^{-1} band of muscovite has no component perpendicular to the layers, and this appears to be true also for the 417 cm^{-1} band of pyrophyllite; thus their assignment as out-of-plane librations is unlikely, and an alternative interpretation of the 297 cm^{-1} band in OD-pyrophyllite must be sought.

A much stronger candidate for the out-of-plane libration of OD-pyrophyllite is a band at 630 cm^{-1}, which has marked perpendicular polarization. The corresponding

OH libration must be considered to couple with a lattice vibration to give a pair of weak bands at 904 and 851 cm^{-1}. In the deuterated form these two bands are replaced by one uncoupled lattice vibration, which appears at the intermediate frequency, 878 cm^{-1}. Taking an estimated value of 880 cm^{-1} for the uncoupled OH-libration, a reasonable value (1·39) is obtained for γ_{OH}/γ_{OD}.

It will be noted that the changes in the 850–900 cm^{-1} region on substituting OD for OH in pyrophyllite cannot be ascribed to coupling between these vibrations and the in-plane libration at 947 cm^{-1}. No such coupling is possible, as the vibrations are of different symmetry species. The unit cell of a single pyrophyllite sheet has symmetry C_{2h}, and its infra-red-active vibrations have dipole oscillations either along the two-fold axis in the plane of the layers (A_u) or at right angles to the axis (B_u). The in-plane libration belongs to symmetry species A_u, whereas both the 851 cm^{-1} band of OH-pyrophyllite and the 878 cm^{-1} band of OD-pyrophyllite have components perpendicular to the layers, and so must belong to the same symmetry species, B_u, as the out-of-plane libration.

The diffuseness of the spectra of the clay minerals makes it impossible to get from them confirmation for the assignment of the OH out-of-plane vibration suggested by the pyrophyllite spectra, but support has been obtained from a comparison of the spectra of synthetic OH- and OD-celadonites (fig. 6) in which each hydroxyl is shared between an Mg^{2+} and an Fe^{3+} octahedral cation. This comparison indicates that the in-plane and out-of-plane librations of OH lie at 800 cm^{-1} and 679 cm^{-1}, and of OD at 595 and 546 cm^{-1}. The 679 cm^{-1} band of OH-celadonite has already been recognized as having a component perpendicular to the layers (Farmer and Russell, 1964), and this is now found to be true also for the 546 cm^{-1} band of OD-celadonite. Thus here again, as in pyrophyllite, the out-of-plane libration is not very much lower in frequency than the in-plane libration.

Returning now to the spectra of beidellite (fig. 1), it can be seen that the spectral changes following deuteration are very similar to those produced in pyrophyllite. The OD out-of-plane libration can be detected at 612 cm^{-1}, and there is also evidence of some band shifts in the 850–900 cm^{-1} region. On the other hand, the striking increase in intensity of absorption near 800 cm^{-1} when montmorillonites are deuterated (figs. 2, 3, 4) has no analogue in either pyrophyllite or celadonite. This absorption is polarized in the plane of the layers, and so cannot be ascribed to the out-of-plane libration of OD. The only alternative is that it is a lattice vibration involving hydroxyl groups, whose intensity and frequency are affected by replacing OH with OD. The presence of lattice vibrations in the 800–900 cm^{-1} region that couple with hydroxyl librations was previously noted in kaolinite spectra (Farmer and Russell, 1964) as well as in the present study of pyrophyllite.

The 2:1 trioctahedral layer silicates. In a previous study of talc, hectorite, and saponite (Farmer, 1958), a medium-intensity band, lying at 670 cm^{-1} in talc and at 655 cm^{-1} in saponite and hectorite, was assigned to an in-plane silicon–oxygen vibration; a possible alternative assignment of this band to an OH librational frequency was discounted, as this vibration in brucite lies near 460 cm^{-1}. However, neutron inelastic scattering

spectra of talc show proton vibrations near 650 and 490 cm^{-1}, which have been correlated with infra-red bands at 670 and 535 cm^{-1} and ascribed to librations of hydroxyl groups by Naumann, Safford, and Mumpton (1966). In addition, neutron scattering indicates a series of vibrations, ascribed to translatory motion of the OH groups, below 400 cm^{-1}.

Neutron inelastic scattering spectra, although they include vibrations that are active in the infra-red spectrum, also reflect all other vibrations of the crystal lattice that involve protons. It is difficult, therefore, to correlate such spectra with infra-red spectra unambiguously, and it seems desirable to search for librational frequencies in the infra-red spectrum of talc by study of a synthetic OD-talc.

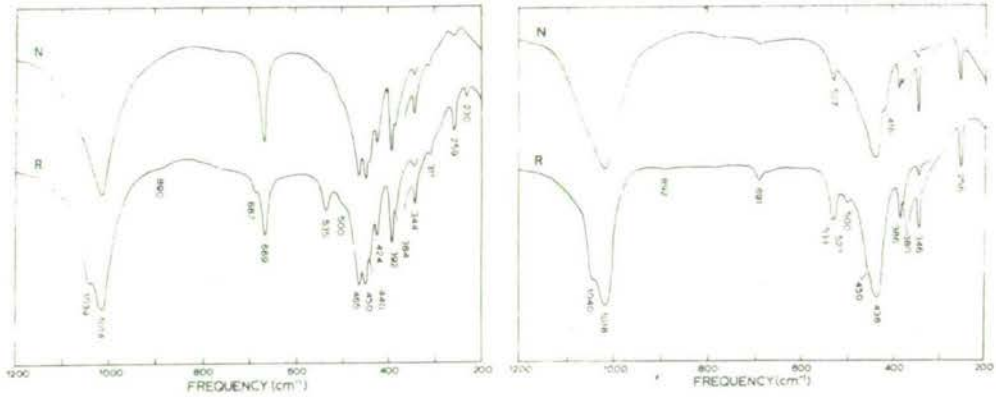

FIGS. 7 and 8: Fig. 7 (left). Infra-red spectrum of MgOH-talc: symbols as in fig. 1. Fig. 8 (right). Infra-red spectrum of MgOD-talc: symbols as in fig. 1.

As the hydroxyl groups in talc are perpendicular to the layers and lie in sites that approximate closely to trigonal symmetry, their two librational motions form a degenerate pair and in the absence of coupling would give a single infra-red absorption band with a dipole change in the plane of the sheets. Comparison of MgOH- and MgOD-talc (figs. 7 and 8) confirms that the 669 cm^{-1} band is the OH libration, as it is replaced in the spectrum of MgOD-talc by the OD libration at 527 cm^{-1}. The ratio ν_{OH}/ν_{OD} (669/527) is 1·27, which is significantly less than the theoretical value (1·37) for a purely librational frequency. This low value is explicable in terms of coupling between librational and translatory vibrations of OH and OD; the effect of this coupling can be seen in displacements of other vibrations, notably that at 465 cm^{-1} in MgOH talc, and also in some marked changes in intensity of absorption bands, when deuterium substitutes for hydrogen. It seems probable that the 465 cm^{-1} band of talc, and not the 535 cm^{-1} band, as suggested by Naumann, Safford, and Mumpton (1966), should be correlated with the neutron scattering peak at 487 ± 23 cm^{-1}, since the 465 cm^{-1} vibration obviously involves hydrogen, whereas the 535 cm^{-1} vibration is little affected by substituting deuterium for hydrogen.

Further guidance in the assignment of the absorption bands of talc can be obtained by comparison of the spectra of NiOH-talc and NiOD-talc with the corresponding

Mg-talcs and by comparison of the spectra of randomly oriented samples in CsBr discs with oriented samples deposited from suspension on CsI plates. On the basis of an approximate treatment of vibrations of the talc lattice, four vibrations with dipole oscillations perpendicular to the plane of the talc layer are expected, and these should be weak or absent in the spectra of oriented samples. Three of these have been identified in MgOH-talc at 1039, 687, and 535 cm^{-1} (Farmer, 1958) and these occur at almost identical frequencies in MgOD-talc (see figs. 7 and 8). In the present study, extension of the spectral range to 200 cm^{-1} indicates that the fourth perpendicular vibration lies at 259 cm^{-1} in MgOH-talc. It is anomalous, however, that the corresponding band of MgOD-talc, at 256 cm^{-1}, does not show obvious perpendicular polarization.

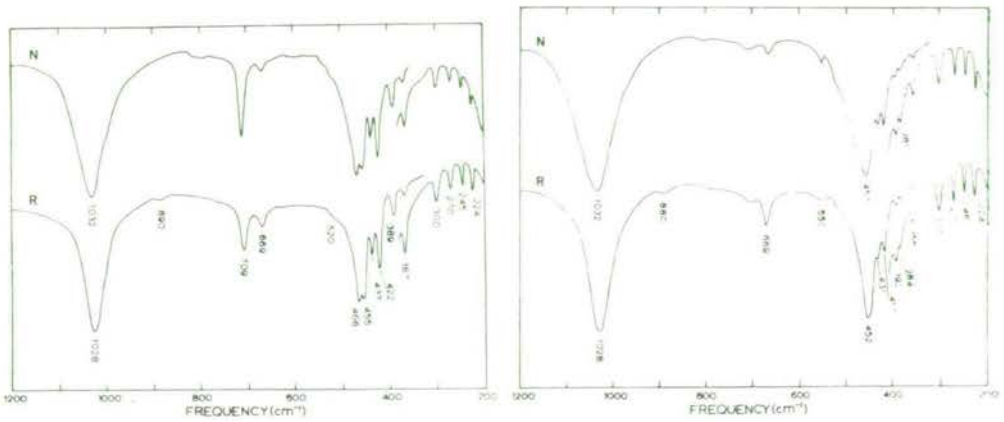

FIGS. 9 and 10: Fig. 9 (left). Infra-red spectrum of NiOH-talc: symbols as in fig. 1. Fig. 10 (right). Infra-red spectrum of NiOD-talc: symbols as in fig. 1.

Of the four perpendicular bands in Mg-talc, the two of higher frequency have been ascribed by Farmer (1958) to Si–O vibrations, and so should not be greatly perturbed by substitution of Ni for Mg in the octahedral layer. The other two perpendicular vibrations involve the octahedral cations and the hydroxyl groups, and these should be profoundly affected by substitution of Ni for Mg. These predictions are confirmed in the spectra of Ni-talc (figs. 9 and 10) although this synthetic material does not give such marked orientation effects as natural talc. The perpendicular band of highest frequency, an Si–O stretching vibration, must lie under the in-plane absorption at 1032 cm^{-1}, and the other perpendicular Si–O vibration can be identified with certainty at 669 cm^{-1}, only a little lower than in Mg-talc. The 535 cm^{-1} band of Mg-talc is totally absent from the spectrum of Ni-talc; its analogue in Ni-talc appears to lie at 455 cm^{-1}, as this band weakens relative to its neighbours in the spectrum of the oriented deposit. The fourth perpendicular band of Ni-talc could not be detected, and may lie below 200 cm^{-1}.

Simplified calculations, which treat the octahedral cations and hydroxyl groups as vibrating between the oxygens of a rigid silicon–oxygen lattice, indicate that the perpendicular vibrations of Mg-talc would lie at 535 and 272 cm^{-1}, while those of

Ni-talc would lie at 437 and 212 cm^{-1}. These rough calculations therefore support the assignments made.

It is more difficult, however, to rationalize the results for the in-plane vibrations of Mg- and Ni-talc. From the approximation that treats the silicate anion as having hexagonal symmetry, and the octahedral layer as trigonal, we expect six degenerate pairs of vibrations. Of these, the Si–O–Si stretch occurs at 1014 and 1032 cm^{-1}, and the OH librations at 669 and 709 cm^{-1}, for Mg- and Ni-talc respectively; for none of these vibrations is any splitting of the degeneracy detectable. Extending the notation used by Farmer (1958), the remaining four, which must all lie below 500 cm^{-1}, include: ν_4, an angle-bending vibration of the Si–O–Si network; ν_5, a vibration in which the octahedral oxygens and hydroxyls move in opposition to the octahedral cations; ν_6, a vibration in which the octahedral cations move in phase with their adjacent oxygen layers, relative to the silicon and surface oxygen layers; and ν_7, a translatory vibration of hydroxyl groups, out of phase with the other oxygens in this layer.

Of these ν_6 is necessarily of low frequency and has been reasonably assigned to a doublet near 170 cm^{-1} by Ishii, Shimanouchi, and Nakahira (1967). This leaves three, possibly degenerate, pairs of vibrations to be identified in the 500 to 200 cm^{-1} region. Examination of the spectra shows that the total number of absorption bands in both Mg- and Ni-talc (some nine or ten) considerably exceeds the number predicted. Thus the approximate treatment that satisfactorily accounts for the absorption pattern above 500 cm^{-1} breaks down for vibrations below 500 cm^{-1}. Nevertheless, some of the stronger bands in the talc spectrum should approximate to the types listed above.

A striking feature of all the talc spectra is the strong absorption near 450 cm^{-1}. Previous attempts to assign the two strong bands of MgOH-talc at 450 and 465 cm^{-1} have assumed that they represent a nearly degenerate pair of vibrations; that is, mutually perpendicular vibrations of the same type. The present spectra disprove this assumption, as the higher frequency band at 465 cm^{-1} in MgOH-talc is displaced to 438 cm^{-1} in MgOD-talc, whereas the 450 cm^{-1} band is not displaced; the two absorption bands therefore represent vibrations that differ in type. On the other hand, the 465 cm^{-1} bands of MgOH- and NiOH-talc are clearly of the same type, since both are displaced in the deuterated forms. The insensitivity of this vibration to the nature of the octahedral cation, and its sensitivity to substitution of deuterium for hydrogen, suggests that it be assigned to ν_7 above. Its relatively high frequency must then be ascribed to strong repulsive forces within the tightly packed oxygen layer in which the hydroxyl group lies.

The persistence of the 450 cm^{-1} vibration of MgOH-talc at 455 cm^{-1} in NiOH-talc has led Stubican and Roy (1961) and Wilkins and Ito (1967) to suggest that it must be an Si–O vibration, presumably ν_4 above. The present results indicate, however, that the 455 cm^{-1} band of NiOH talc either overlies a perpendicular band, or itself has some perpendicular character. If the latter interpretation is correct, then the 450 cm^{-1} band of MgOH-talc can be taken as being ν_5, the in-plane vibration of the magnesium ions, whereas the 455 cm^{-1} band of NiOH-talc must be taken as a perpendicular vibration involving nickel and hydroxyl ions, corresponding to the 535 cm^{-1} band of MgOH-talc. The in-plane motion of the nickel ions probably contributes to the intensity of the

four bands of NiOH- and NiOD-talc in the 200–300 cm^{-1} region. Mg-talc shows only one strong band, at 259 cm^{-1}, in this region, and as this is a perpendicular band it cannot correspond to any of those of Ni-talc.

Conclusions

In the present study some progress has been made in the assignment of the vibrations of layer silicates. The identification of the OH libration in talc, saponite, and vermiculite as lying near 700 cm^{-1} provides a rational explanation for the strong absorption shown by serpentine and chlorites in this region (see, for example, Moenke, 1962), since these minerals have a higher concentration of hydroxyl linked to magnesium. In the dioctahedral minerals, the out-of-plane libration of the hydroxyl group has been plausibly identified in pyrophyllite and celadonite, but it seems that this vibration, unlike the in-plane libration, will be of little diagnostic value in characterizing the octahedral cations to which the hydroxyl group is linked.

TABLE I. *Calculated and experimental vibrational frequencies (cm^{-1}) of talc*

Type of vibration		*Experimental*		*Calculated*	
		Mg-*talc*	Ni-*talc*	*Vedder (1964)*	*Ishii* et al. *(1967)*
Tetrahedral	$A_1\ \nu_1$	1040	*c.* 1025	941	902
	$A_1\ \nu_2$	687	669	554	613
	$E_1\ \nu_3$	1014	1032	1041	1015
	$E_1\ \nu_4$	< 460	< 460	482	543
Octahedral	δ (OH)	669	709		
	trans (OH) ∥	465	466		
	(Mg,Ni) OH ⊥	535	*c.* 455		
	(Mg,Ni) OH ⊥	259	< 200		

The spectra of Ni- and Mg-talc have been assigned with some certainty down to 460 cm^{-1}, and it is now possible to make a comparison in this region between experimental results and the frequencies calculated for the vibrations of the tetrahedral layer (table I). The marked discrepancy between experimental and calculated frequencies for ν_1, the perpendicular Si–O stretching vibration, can be explained by the effect of the coulombic forces that are associated with intense dipole oscillations perpendicular to the plane of a thin platy crystal, and which increase the vibrational frequencies markedly (Farmer and Russell, 1966). The second perpendicular vibration, ν_2, is a much weaker absorber than ν_1, so that here it is unlikely that coulombic forces can account for the discrepancy between observed and calculated frequencies. In calculations, the Si–O–Si stretching-force constant is adjusted to give agreement for ν_3. The calculated frequency for in-plane Si–O–Si bending, ν_4, is too high in the treatment of Ishii and co-workers.

For both talc and pyrophyllite, the region below 460 cm^{-1} is of considerable complexity, and it has not yet proved possible to assign the bands there to particular

vibrations with any certainty. Many bands in this region are affected in intensity an frequency by replacing hydrogen by deuterium in the structures; indeed even th direction of the transition moment of one band in talc appears to change on going fron MgOH- to MgOD-talc. Apparently, the vibrations of the hydroxyl group are strongly coupled with those of other oxygens in the structure, as, indeed, neutron scattering studies have already indicated.

It is noteworthy, however, that the principal differences between the spectra of Mg- and Ni-talc occur in the 400 to 200 cm^{-1} region, confirming the expectation that this region will be of particular value in distinguishing isomorphous minerals.

Acknowledgements. The authors wish to thank Mr. A. R. Fraser for able technical assistance and Dr. D. C. McKean (Department of Chemistry, Aberdeen University) for making available the Perkin Elmer 225 spectrometer.

REFERENCES

ANGELL (C. L.) and SCHAFFER (P. C.), 1965. *Journ. phys. Chem.* **69**, 3463.
FARMER (V. C.), 1958. *Min. Mag.* **32**, 353.
—— 1968. *Clay Minerals*, **7**, 373.
—— and RUSSELL (J. D.), 1964. *Spectrochim. Acta*, **20**, 1149.
—— —— 1967. *Clays and Clay Min.* **15**, 121.
—— —— and AHLRICHS (J. L.), 1968. *Trans. 9th Int. Congr. Soil Sci., Adelaide*, **3**, 101.
—— —— —— and VELDE (B.), 1967. *Bull. Groupe franç. Argiles*, **19** (2), 5.
HELLER (L.), FARMER (V. C.), MACKENZIE (R. C.), MITCHELL (B. D.), and TAYLOR (H. F. W.), 1962. *Clay Min. Bull.* **5**, 56.
ISHII (M.), SHIMANOUCHI (T.), and NAKAHIRA (M.), 1967. *Inorg. Chim. Acta*, **1**, 387.
LUTH (W. C.) and INGAMELLS (C. O.), 1965. *Amer. Min.* **50**, 255.
MOENKE (H.), 1962. *Mineralspektren*, Berlin (Akademie-Verlag).
NAUMANN (A. W.), SAFFORD (G. J.), and MUMPTON (F. A.), 1966. *Clays and Clay Min.* **14**, 367.
ROY (D. M.) and ROY (R.), 1957. *Geochimica Acta*, **11**, 72.
STUBICAN (V.) and ROY (R.), 1961. *Zeits. Krist.* **115**, 200.
VEDDER (W.), 1964. *Amer. Min.* **49**, 736.
—— and MCDONALD (R. S.), 1963. *Journ. chem. Phys.* **38**, 1583.
WILKINS (R. W. T.) and ITO (J.), 1967. *Amer. Min.* **52**, 1649.

[*Manuscript received 24 November 1969*]

Clays and Clay Minerals, 1971, Vol. 19, pp. 55–59. Pergamon Press. Printed in Great Britain

I.R. SPECTROSCOPIC EVIDENCE FOR INTERACTION BETWEEN HYDRONIUM IONS AND LATTICE OH GROUPS IN MONTMORILLONITE

J. D. RUSSELL and A. R. FRASER
The Macaulay Institute for Soil Research, Craigiebuckler, Aberdeen, Scotland

(*Received* 1 *July* 1970)

Abstract—At low levels of hydration, exchangeable D^+ in montmorillonite interacts with lattice OH groups and quantitatively converts AlMgOH groups to AlMgOD. Hydroxyl groups coordinated to two Al ions undergo a slower exchange, the extent of which is restricted by octahedral Fe^{3+} ions.

The OH stretching vibration of AlMgOH groups in montmorillonite is assigned an unusually high frequency (3687 cm^{-1}) compared with that of the same group in phengites (3602 cm^{-1}).

INTRODUCTION

THE IMPORTANCE of the surface acidity of clay minerals in controlling adsorption of both organic and inorganic molecules has been outlined by Mortland (1968). While infrared spectroscopy has demonstrated protonation of species adsorbed on H- or Al-montmorillonite (Russell, 1965; Mortland, 1966; Tahoun and Mortland, 1966) the properties of acid clays themselves have not been investigated by this technique. Mortland (1966) suggested that, on dehydration of protonated urea adsorbed on montmorillonite, H^+ becomes dissociated from the protonated species and can migrate into the clay lattice towards negative charge sites in the structure. A consequence of such migration might be seen in perturbation of the lattice OH groups. This paper describes an investigation by i.r. spectroscopy into this possibility using acid montmorillonites of different octahedral compositions.

EXPERIMENTAL

The resin column method described by Barshad (1969) was used to prepare H-montmorillonites although it was subsequently found that these preparations apparently had no advantage in terms of stability over those prepared by a conventional H-resin method. Al, Mg and Na saturations were carried out either on appropriate resin columns or using salt solutions. Oriented films of the montmorillonites whose compositions and origin are shown in Table 1 were prepared by sedimentation on polyethylene sheet; these films were evacuated to 0·002 mm Hg, flushed with D_2O vapour at about 17 mm Hg, and re-evacuated in an i.r. cell similar to that described by Angell and Schaffer (1965).

RESULTS AND INTERPRETATION

Spectra of air-dry films of all the H-montmorillonites investigated show broad absorption near 2900 cm^{-1}. This is illustrated for the samples from Crook County (Fig. 1a) and Chambers (Fig. 2a). The 2900 cm^{-1} band, which is lost after evacuation at room temperature (Figs. 1b, 2b) and a band at about 1700 cm^{-1} (not shown) are thought to be due to the hydronium ion (Falk and Giguere, 1957). Although the 1700 cm^{-1} band is not appreciably affected when the H-montmorillonite is evacuated or flushed with D_2O vapour, it is removed by treatment with gaseous NH_3. The apparent failure of the 1700 cm^{-1} band to respond to D_2O may be due to its replacement by a deuteronium band of different origin, at the same frequency.

H-montmorillonite loses most of its interlayer water in vacuum at 20°C (Figs. 1b, 2b). Residual molecules, showing absorption bands near 3380 and 3645 cm^{-1} which shift to 2492 and 2703 cm^{-1} after D_2O treatment (Fig. 1), are thought to have one of their OH groups weakly hydrogen-bonded to surface oxygens (Russell and Farmer, 1964; Farmer and Mortland, 1966). The 3382 cm^{-1} water band may indicate replacement of some H by Al in the H-montmorillonite, since Parfitt and Mortland (1968) observed a band near 3400 cm^{-1} in the spectrum of evacuated Al-montmorillonite.

In addition to the bands of residual water, spectra of evacuated H-montmorillonites show a weak absorption band near 3530 cm^{-1}, shifting to about 2610 cm^{-1} after D_2O treatment (Figs. 1 and 2), which may arise from perturbation of some of the

Table 1. Source and composition of montmorillonites investigated

Source	Composition	Ref.
Chambers, Arizona	$0{\cdot}93M^{+}(Si_{7{\cdot}98}Al_{0{\cdot}02})(Al_{2{\cdot}92}Fe^{3+}_{0{\cdot}16}Mg_{0{\cdot}92})O_{20}(OH)_4$	Roberson *et al.* (1968)
Umiat, Alaska	$0{\cdot}92M^{+}(Si_{7{\cdot}84}Al_{0{\cdot}16})(Al_{2{\cdot}96}Fe^{3+}_{0{\cdot}36}Mg_{0{\cdot}84})O_{20}(OH)_4$	Anderson and Reynolds (1967)
Wyoming	$0{\cdot}93M^{+}(Si_{7{\cdot}70}Al_{0{\cdot}30})(Al_{3{\cdot}12}Fe^{3+}_{0{\cdot}37}Mg_{0{\cdot}39})O_{20}(OH)_4$	Heller *et al.* (1962)
Crook County, Wyoming	$0{\cdot}54M^{+}(Si_{7{\cdot}68}Al_{0{\cdot}32})(Al_{2{\cdot}97}Fe^{3+}_{0{\cdot}63}Mg_{0{\cdot}49})O_{20}(OH)_4$	Roberson *et al.* (1968)

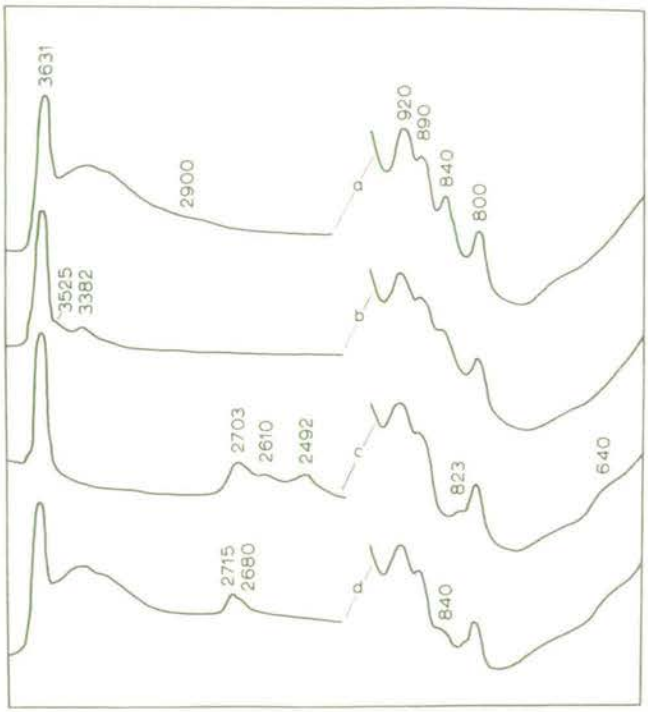

Fig. 1. I.R. spectra of H^{+}-montmorillonite from Crook County, Wyoming: (a) untreated; (b) evacuated to 0·002 mm Hg; (c) flushed with D_2O vapour at 17 mm Hg, then evacuated to 0·002 mm Hg; (d) exposed to air at 20°C and 40% relative humidity following treatment (c).

lattice OH groups by H^{+}. Similar perturbation by Ca and Mg are thought to produce weak bands at 3533 cm^{-1} in Ca- and at 3496 cm^{-1} in Mg-montmorillonite following dehydration (Russell and Farmer, 1964). The band observed by Rosenqvist and Jorgensen (1964) at 3520 cm^{-1} in NH_4-montmorillonite heated above the decomposition temperature of NH_4 ions may also be due to a perturbed lattice OH group.

Although the OH stretching region indicates an interaction between H^{+} and OH groups, there is no evidence of this from the OH librational frequencies. Bands due to AlAlOH at 920 cm^{-1}, $AlFe^{3+}OH$ at 890 cm^{-1} and AlMgOH at 840 cm^{-1} (Russell *et al.*, 1970) show reductions in their intensities (Figs. 1b, 2b) which are not significantly different from those observed for several other cation-saturated montmorillonites (Russell and Farmer, 1964). However, after treatment with D_2O vapour, which in itself produces no change in pattern on the 950–800 cm^{-1} region, evacuation leads to the replacement of the 840 cm^{-1} band of AlMgOH by the AlMgOD frequency at 640 cm^{-1} (Figs. 1c, 2c). Partial regeneration of the 840 cm^{-1} band occurs on exposure of the treated specimens to air humidity and is complete after subsequent

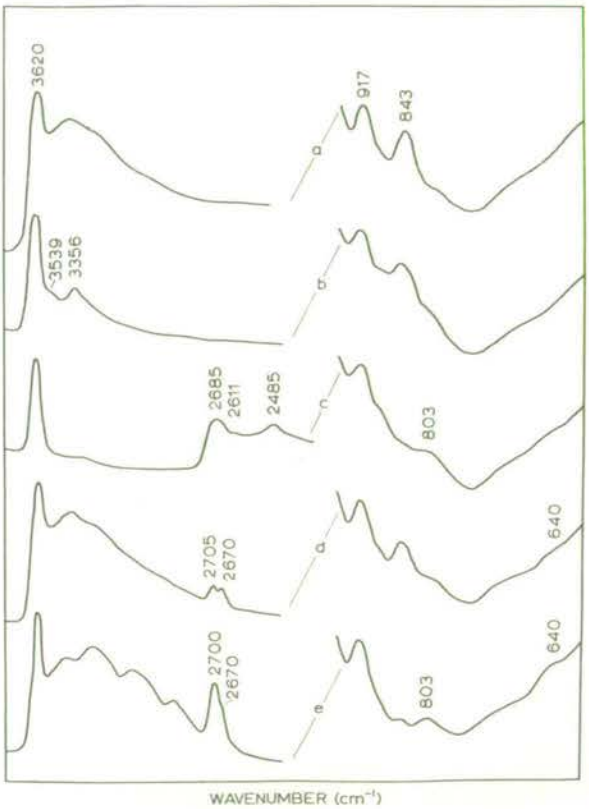

Fig. 2. I.R. spectra of H^+-montmorillonite from Chambers, Arizona: (a) untreated; (b) evacuated to 0·002 mm Hg; (c) flushed with D_2O vapour at 17 mm Hg, then evacuated to 0·002 mm Hg; (d) exposed to air at 20°C and 40% relative humidity following treatment (c); (e) exposed to NH_3 at atmospheric pressure then air following treatment (c).

evacuation. Regeneration in air is greater for the Chambers sample (Fig. 2d) than for the specimen from Crook County (Fig. 1d). The Chambers sample has a lower iron content and less Al-for-Si substitution. Re-exchange of the AlMgOD group in air was minimized when, following D_2O flushing and evacuation, the montmorillonites were treated with gaseous NH_3 without exposure to air. This rapidly converted D^+ to NH_4^+, thereby immobilizing the proton. The spectrum of the Chambers montmorillonite after this D_2O/NH_3 treatment (Fig. 2e) shows a very weak AlMgOH band at 840 cm^{-1}, a well-developed AlMgOD band at 640 cm^{-1} and a pronounced band at 2700 cm^{-1} with an inflexion at 2670 cm^{-1}. From its position and its inverse intensity relationship with the 840 cm^{-1} AlMgOH band, the 2700 cm^{-1} absorption must be due to the stretching vibration of the AlMgOD group. The band of the corresponding AlMgOH vibration, which should occur in the range 3700–3650 cm^{-1}, was found at 3687 cm^{-1} in the montmorillonite from Crook County (Fig. 3) and at 3677 cm^{-1} in that from Chambers. Compared with the frequencies of AlAlOH vibrations, the AlMgOH frequencies in montmorillonite are some 56 cm^{-1} higher, while in phengites they are about 30 cm^{-1} lower (Farmer *et al.*, 1967).

Following D_2O treatment the principal AlAlOH stretching frequency at 3631 cm^{-1} in the Crook County montmorillonite suffers a small (<5 per cent) drop in intensity (Fig. 3) which can be correlated with the appearance of a weak AlAlOD stretching frequency at 2680 cm^{-1} (Fig. 1d). The weak band at 2670 cm^{-1} in spectra of the Chambers montmorillonite is similarly related to the original AlAlOH stretching frequency at 3620 cm^{-1}. The intensity of the 2670–2680 cm^{-1} AlAlOD band increases with the time of exposure of the sample to D^+, more rapidly in the low-iron Chambers sample than in the Crook County specimen.

Spectra of D_2O-treated montmorillonites show, in addition to AlMgOD stretching and librational frequencies, a weak absorption band in the 800–825 cm^{-1} region. Assignment of this band to an OD bending vibration is uncertain since the corresponding OH vibration (assuming an average isotopic shift ratio) would be masked by the intense Si–O stretching vibration near 1050 cm^{-1}. However, the band is clearly due to translatory or librational vibrations of OD linked to Al and Mg, whose frequency appears to be dependent on neighbouring octahedral cations: it occurs at 803 cm^{-1} in the Chambers sample (Fig. 2e), 818 cm^{-1} in the Wyoming and Umiat samples (not shown) and 823 cm^{-1} in the sample from

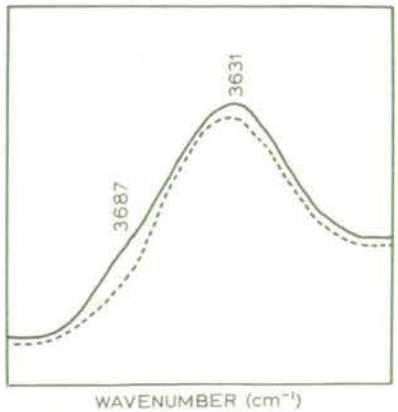

Fig. 3. Hydroxyl stretching vibration of H^+-montmorillonite from Crook County, Wyoming: full line, original; broken line, evacuated, flushed with D_2O vapour, evacuated to 0·002 mm Hg then exposed to air.

Crook County (Fig. 1c), i.e. at frequencies which increase with increasing iron content. Fully deuterated montmorillonites have been found to absorb at 803–805 cm^{-1} with an inflexion on the high-frequency side of the band for the more iron-rich compositions (Russell *et al.*, 1970).

Even though the H-saturated montmorillonites investigated were freshly prepared before use, they will contain exchangeable Al as a result of proton attack on the structure. The presence of exchangeable Al in the montmorillonite does not affect the interpretation of the results of deuteration since it has been found that Al-montmorillonites behave like H-montmorillonites in their ability to undergo deuteration. Consequently, the bands observed at 2704 and 2688 cm^{-1} by Ahlrichs (1968) in Al-montmorillonite treated with D_2O may be re-assigned to AlMgOD and AlAlOD groups respectively.

Deuteration of lattice OH groups is very much slower in Mg-montmorillonites than in the H or Al forms, and can not be detected in Na-montmorillonite. These observations are in accord with the concept of the acidity of water molecules coordinated to exchange cations in montmorillonite (Mortland, 1968).

DISCUSSION

Replacement of Al by Mg in the octahedral layer of the montmorillonite structure results in incomplete neutralization of negative charges on the apical oxygens and OH groups coordinated to Mg. Small, mobile, positively charged ions should be capable of migrating to the vicinity of the negative charge. Although several investigators, among them Rosenqvist and Jorgensen (1964), have postulated that the apical oxygens readily accept protons and generate new lattice OH groups, the present findings do not support this contention.

Direct spectroscopic evidence for the migration of protons in H-montmorillonites may be found in the band near 3530 cm^{-1} which is thought to arise from perturbation of some of the lattice OH groups by protons. More convincing evidence is provided by montmorillonites containing D^+ and D_2O, in that the conversion of AlMgOH groups to AlMgOD must involve migration of D^+ and interaction with OH groups. By implication, interaction and exchange of H^+ with OH groups must also occur.

While protons and deuterons migrate principally to negatively charged AlMgOH groups in montmorillonite, migration to uncharged AlAlOH groups also occurs as shown by the appearance of AlAlOD groups. The latter type of migration appears to be diffusion controlled and may be blocked by octahedral Fe^{3+}: it has been found that $AlFe^{3+}OH$ groups in montmorillonite are not deuterated even at 400°C (Russell *et al.*, 1970).

The mechanism by which protons (and deuterons) migrate from the interlayer to lattice OH groups is linked to the state of hydration of the proton, rapid migration occurring when excess adsorbed H_2O (or D_2O) has been removed. The H^+ (or D^+) species thereby achieve sufficient mobility or a suitably small cross-section to approach the lattice OH groups. Zundel and Metzger (1968) drew similar conclusions from resin systems, claiming that when the number of water molecules coordinated to a proton falls below two, the proton becomes dissociated and migrates to the anion. It is unlikely that the migrating species in the interlayer space of H-montmorillonite is the free proton because the energy of hydration of the proton is very high. The mobile species produced by partial dehydration of the montmorillonite is probably H_3O^+ or $H_5O_2^+$ from which H^+ is transferred to lattice OH by a low-energy mechanism. Two possibilities are: (i) transfer via the surface oxygens and apical oxygens to the OH group; (ii) direct transfer from the hydronium species. Both mechanisms involve large (3·0–3·2Å) oxygen-oxygen separations over which the transfer has to be made, but the second may be more practicable if the hexagonal hole were to expand slightly allowing the hydronium species a closer approach to the OH group.

Although the mechanism is speculative, spectroscopic evidence for migration of protons in H-montmorillonite and interaction and exchange with lattice OH groups is conclusive. Because of the ease with which the exchange reaction with D^+ occurs in montmorillonites saturated with strongly polarizing cations, care is required in interpreting spectra of smectites with synthetic interlayers, for which treatment with D_2O has been used to distinguish the OH absorption bands of the interlayer species from those of the smectites.

REFERENCES

Ahlrichs, J. L. (1968) Hydroxyl stretching frequencies of synthetic Ni–, Al–, and Mg–hydroxy interlayers in expanding clays: *Clays and Clay Minerals* **16**, 63–72.

Anderson, D. M. and Reynolds, R. C. (1967) Umiat bentonite; an unusual montmorillonite from Umiat, Alaska: *Am. Mineralogist* **51**, 1443–1456.

Angell, C. L. and Schaffer, P. C. (1965) Infrared spectroscopic investigations of zeolites and adsorbed molecules: *J. Phys. Chem.* **69**, 3463–3470.

Barshad, I. (1969) Preparation of H-saturated montmorillonites: *Soil Sci.* **108**, 38–42.

Falk, M. and Giguère, P. A. (1957) Infrared spectrum of the H_3O^+ ion in aqueous solutions: *Can. J. Chem.* **35**, 1195–1204.

Farmer, V. C. and Mortland, M. M. (1966) An infrared study of the co-ordination of pyridine and water to exchangeable cations in montmorillonite and saponite: *J. Chem. Soc.* **A**, 344–351.

Farmer, V. C., Russell, J. D., Ahlrichs, J. L. and Velde, B. (1967) Vibration du groupe hydroxyle dans les silicates en couches: *Bull. Grpe Fr. Argiles* **19**, 5–10.

Heller, L., Farmer, V. C., Mackenzie, R. C., Mitchell, B. D. and Taylor, H. F. W. (1962) The dehydroxylation and rehydroxylation of triphormic dioctahedral clay minerals: *Clay Minerals Bull.* **5**, 56–72.

Mortland, M. M. (1966) Urea complexes with montmorillonite: an infrared absorption study: *Clay Miner.* **6**, 143–156.

Mortland, M. M. (1968) Protonation of compounds at clay mineral surfaces: *Trans. 9th Intern. Conf. Soil Sci. Adelaide.* **1**, 691–699.

Parfitt, R. L. and Mortland, M. M. (1968) Ketone absorption on montmorillonite: *Proc. Soil Sci. Soc. Am.* **32**, 355–363.

Roberson, H. E., Weir, A. H. and Woods, R. D. (1968) Morphology of particles in size-fractionated Na-montmorillonites: *Clays and Clay Minerals* **16**, 239–248.

Rosenqvist, I. Th. and Jorgensen, P. (1964) Bonding of hydrogen in hydrogen montmorillonite: *Nature, Lond.* **204**, 176–177.

Russell, J. D. (1965) Infrared study of the reactions of ammonia with montmorillonite and saponite: *Trans. Faraday Soc.* **61**, 2284–2294.

Russell, J. D. and Farmer, V. C. (1964) Infared spectroscopic study of the dehydration of montmorillonite and saponite: *Clay Minerals Bull.* **5**, 443–464.

Russell, J. D., Farmer, V. C. and Velde, B. (1970) Replacement of OH by OD in layer silicates, and identification of the vibrations of these groups in infrared spectra: *Mineral. Mag.* **37**, 869–879.

Tahoun, S. and Mortland, M. M. (1966) Complexes of montmorillonite with primary, secondary, and tertiary amides—I. Protonation of amides on the surface of montmorillonite: *Soil Sci.* **102**, 248–254.

Zundel, G. and Metzger, H. (1968) Energy bands of tunneling excess protons in liquid acids. I.R. spectroscopic study of the nature of $H_5O_2^+$ groups: *Z. Phys. Chem.* Frankf. Ausge. **58**, 225–245.

Résumé—A tous les niveaux d'hydration, le D^+ interchangeable dans la montmorillonite réagit sur les groupes OH croisés et, quantitativement, transforme les groupes AlMgOH en AlMgOD. Les groupes hydroxyles coordonnés aux deux ions Al subissent un échange plus lent, dont l'étendue est restreinte par les ions octahédraux de Fe^{3+}. La vibration tendant à OH des groupes AlMgOH dans montmorillonite a une haute fréquence inhabituelle (3687 cm^{-1}) par comparaison avec celle du même groupe dans les phengites (3602 cm^{-1}).

Kurzreferat—Auf zwei Ebenen der Hydration reagiert austauschbares D^+ in Montmorillonit mit Gitter–OH Gruppen und verwandelt quantitativ AlMgOH Gruppen in AlMgOD Gruppen. Hydroxylgruppen, die mit zwei Al Ionen koordiniert sind erfahren langsameren Austausch, wobei das Ausmass desselben durch oktaedrische Fe^{3+} Ionen begrenzt wird.

Der OH Dehnvibration von AlMgOH Gruppen in Montmorillonit wird eine Frequenz (3687 cm^{-1}) zugeschrieben, die im Vergleich mit der derselben Gruppe in Phengiten (3602 cm^{-1}) ungewöhnlich hoch ist.

Резюме — При низких степенях гидратации обменный ион D^+ в монтмориллоните взаимодействует с группами OH, входящими в кристаллическую решетку, и количественно переводит группы AlMgOH в AlMgOD. Гидроксильные группы, координированные двумя ионами Al, подвергаются более медленному обмену, степень которого ограничена октаэдрическими ионами Fe^{3+}.

Деформационные колебания OH в группах AlMgOH в монтмориллоните имеют необычно высокую частоту (3687 $см^{-1}$) по сравнению с частотой колебания этих групп в фенгитах (3602 $см^{-1}$).

MINERALOGICAL MAGAZINE

VOLUME 38 NUMBER 294 JUNE 1971

Evidence for loss of protons and octahedral iron from oxidized biotites and vermiculites

V. C. FARMER, J. D. RUSSELL, AND W. J. McHARDY
The Macaulay Institute for Soil Research, Craigiebuckler, Aberdeen, Scotland
A. C. D. NEWMAN
Pedology Department, Rothamsted Experimental Station, Harpenden, Herts.
J. L. AHLRICHS
Purdue University, Lafayette, Indiana, U.S.A.
J. Y. H. RIMSAITE
Geology Survey of Canada, Ottawa, Canada

SUMMARY. Infra-red examination of a weathered biotite and of biotites that have been converted to vermiculites and subsequently oxidized, indicates that oxidation of octahedral ferrous ions to ferric ions is associated with a reversible conversion of hydroxyl ions to oxide ions. Subsequently, in high-iron biotites, there is an irreversible loss of ferric ions from the octahedral layer, resulting in an increased number of dioctahedral sites. Electron microscopy and X-ray diffraction indicate that ejected ferric ions form either amorphous interlayer oxides or, when bromine is used as an oxidant, a crystalline external phase of β-FeOOH. The high refractive index of some oxidized vermiculites is shown to be due largely to submicroscopic iron oxides.

IRON in fresh biotites is predominantly in the ferrous form, but natural weathering processes in soils or fractured rocks can largely oxidize this iron to the ferric state, with or without accompanying vermiculitization of the biotite. This change in valency must be compensated by other changes in the biotite, and three possible mechanisms have been postulated, which are formulated below for the ferrous end member (annite) of the phlogopite–biotite series:

loss of interlayer cations

$$(Si_3AlO_{10})Fe^{2+}_3(OH)_2.K+\tfrac{1}{4}O_2+\tfrac{1}{2}H_2O \rightarrow (Si_3AlO_{10})Fe^{2+}_2Fe^{3+}(OH)_2+KOH$$

loss of hydroxyl protons

$$(Si_3AlO_{10})Fe^{2+}_3(OH)_2.K+\tfrac{1}{2}O_2 \rightarrow (Si_3AlO_{10})Fe^{2+}Fe^{3+}_2O_2.K+H_2O$$

loss of octahedral iron

$$(Si_3AlO_{10})Fe^{2+}_3(OH)_2.K+\tfrac{3}{4}O_2+\tfrac{1}{2}H_2O \rightarrow (Si_3AlO_{10})Fe^{3+}_2(OH)_2.K+FeO.OH.$$

The first of these can play at most only a minor role in high-iron biotites, as the amount of iron oxidized during vermiculitization is very much greater than the decrease in layer charge (see, for example, Newman and Brown, 1966).

The second mechanism, involving conversion of hydroxyl to oxide ions, has been well established for thermal oxidation of biotites. Indeed, in an inert atmosphere at 500–900 °C auto-oxidation occurs and hydrogen is liberated (Tsvetkov and Val'yashikhina, 1956). It is less certain that this mechanism is implicated in oxidative weathering, as the excess water always present is difficult to distinguish from constitutional hydroxyl (Rimsaite, 1967, 1970; Newman and Brown, 1966).

The third mechanism, involving formation of iron oxides, was discounted by Wones (1963) in his hydrothermal study of interconversions between annite and oxyannite on the grounds that the oxidation–reduction process was reversible, and no discrete iron oxide phase was detectable. Separation of hematite during hydrothermal oxidation of natural biotites was, however, observed by Hellner and Euler (1957) to begin at 350 °C, without breakdown of the biotite. Loss of octahedral iron has also been postulated as occurring at ambient temperatures in soils to account for the lower iron content of weathered oxidized biotites and vermiculites compared with the fresh biotites from the parent rock (Walker, 1949; Wilson, 1970). Rimsaite (1967), however, has described biotites, high in iron, in which oxidation has occurred without significant change in the total iron content and where no separate iron oxide phase could be detected. Although calculated formulae for these oxidized biotites indicated more octahedral vacancies than in the unoxidized biotites, this was a direct result of the assumption that the total anion charge in the unit cell was unchanged. Since Fe^{2+} is oxidized to Fe^{3+}, fewer cations are required to satisfy the 44 negative charges per unit cell, and the deficit appears as vacancies in the octahedral layer. When the formulae of these oxidized biotites are recalculated on the basis of $44+z$ anionic and cationic charges in the unit cell, where z is the charge difference between the parent and altered micas (Rimsaite, 1970), there is apparently no increase in octahedral vacancies. But these formulae will also be in error if the oxidized biotites contain a submicroscopic iron oxide phase in their interlayer spaces.

In view of the difficulties in interpreting chemical analyses, an infra-red study of biotites, oxidized naturally or in the laboratory, has been undertaken. Infra-red spectra show the vibrations of hydroxyl groups, and should permit observation of loss of hydroxyl, as in the second mechanism above, or change in the co-ordination of hydroxyl, as in the third. Some preliminary results, giving evidence for loss of octahedral iron, have been published (Farmer, Russell, Ahlrichs, and Velde, 1967). Hydroxyl absorption in thermally oxidized biotites has been studied by Vedder and Wilkins (1969).

Materials and methods

Biotites. Several biotites that have been the subject of previous studies have been used in the present work. These included a biotite crystal of which part has been weathered and oxidized, resulting in a change from dark green to gold, from the same locality as biotites 44 and 45 described by Rimsaite (1967, 1970), and also a larger

sample of a similar fresh green biotite (31A), from the same area. Professor Fripiat kindly supplied the Luindi I biotite used in the work of Fripiat, Rouxhet, and Jacobs (1965). The analysed biotites M2 to M5 and their hydrated sodium forms (AM2 to AM5), studied by Newman and Brown (1966), were also examined, together with a biotite (536) of high octahedral aluminium content (Farmer *et al.*, 1967).

Conversion of biotites to vermiculites. Thin flakes of biotite 31A and Luindi biotite were broken down to sub-millimetre size in water suspension in a Waring Blender. Interlayer potassium ions were then replaced by hydrated barium ions by refluxing 5 g of the biotites with 1 l of 0·05 *M* $BaCl_2$ solution, changing the solution each day (Rausell-Colom *et al.*, 1965). Two to three weeks' treatment was necessary to reduce the potassium content to less than 0·5 %. Refluxing the products with 1 *M* NaCl solution (4 treatments of 1 h with fresh solution) replaced the interlayer barium with sodium ions. These hydrated forms, giving 12·1 Å 001 spacings, are here termed vermiculites or altered biotites to distinguish them from the original biotites. Smaller amounts of other biotites were also vermiculitized by this technique.

Oxidation of vermiculites. The dark green or olive-brown vermiculites were oxidized to orange-yellow or golden forms by two techniques: heating on the water-bath for 1 h with H_2O_2, which gave a very bulky product because of exfoliation by liberated oxygen; and immersion in bromine water in a closed vessel, the water being kept saturated by diffusion of vapour from a pool of bromine in a separate beaker. Oxidation to a golden form took one to two weeks, but left the flakes compact.

The oxidized vermiculites were then refluxed with 1 *M* NaCl solutions to ensure that sodium occupied all exchange sites.

Reduction of oxidized vermiculites. Two techniques were used: immersion in hydrazine hydrate in a closed vessel; and repeated treatment with sodium dithionite in citrate buffered solutions, by the method of Mehra and Jackson (1960) for removing iron oxides from clays.

Chemical analysis. 10–25 mg of biotites and vermiculites were dissolved by evaporation with sulphuric and hydrofluoric acids until fuming. Sodium and potassium contents of the solutions were determined by emission flame photometry using an air:acetylene flame, and magnesium similarly, using a nitrous oxide:butane flame; total iron contents were determined colorimetrically using 1,10-phenanthroline, following Sandell (1959). Ferrous iron contents were determined on separate samples (10 mg) brought into solution with sulphuric and hydrofluoric acids, under flowing CO_2, followed by conversion of the hydrofluoric to fluoroboric acid (a micro-modification of the procedure described by Washington, 1930). Ferrous iron was determined colorimetrically following the procedure of Pollock and Miguel (1967) using 4,7-diphenyl-1,10-phenanthroline. Standard curves were prepared from ferrous ammonium sulphate solutions given the same treatment as the samples, including digestion with $HF–H_2SO_4$.

Total iron in dithionite–citrate extracts was determined by the 1,10-phenanthroline

procedure after destroying excess reagents by evaporation of aliquots to dryness with nitric acid, followed by evaporation to dryness with hydrochloric acid to destroy nitrate ion.

Instrumental procedures. Infra-red spectra were recorded on a Grubb–Parsons Spectromaster. Samples were generally dispersed in KBr discs, but films prepared from dispersions of propylammonium-saturated vermiculites were also used (Farmer, Russell, and Ahlrichs, 1968). X-ray diffraction results were obtained with a Philips diffractometer, and electron micrographs with a A.E.I. EM6 instrument.

For electron microscopy small samples of the treated biotites were subjected to 5 min mild ultrasonic treatment in water, and then centrifuged for 30 s or allowed to stand for several hours, when drops of the supernatant fluids had to be diluted to give a suitably dispersed specimen. Platinum carbon replicas of freshly cleaved flakes of the weathered biotite were prepared using a method similar to that described by Roth *et al.* (1967).

Results and interpretation

Fresh biotites

Hydroxyl groups that are co-ordinated to three octahedral cations are oriented nearly perpendicularly to the layers, and give hydroxyl absorption in the range 3640 cm^{-1} to 3705 cm^{-1}, which increases in intensity when biotite flakes are turned at an angle to the infra-red beam (see fig. 1). The vibrational frequency of these hydroxyl groups is determined by the octahedral cations to which they are co-ordinated, by the interlayer cations, and by other factors that are not fully understood (Vedder, 1964; Wilkins, 1967; Vedder and Wilkins, 1969; Farmer and Russell, 1966). The individual components of the absorption band are often unresolved, but the maximum of the composite absorption shifts to lower frequency with increasing octahedral ferrous ion content of the biotite.

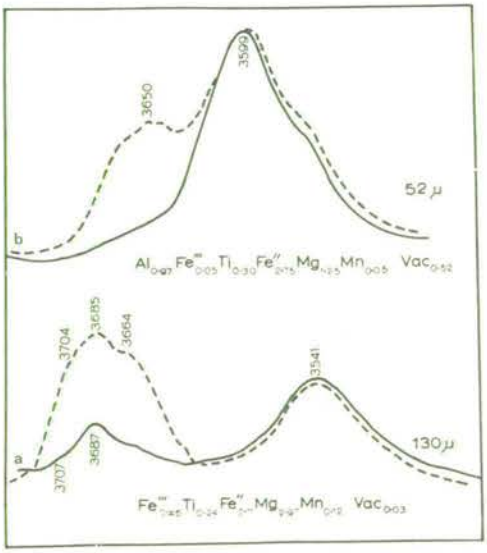

FIG. 1. Hydroxyl absorption of (*a*) biotite M4 and (*b*) biotite 536, with the flake perpendicular to the beam (full line) and at 45° to the beam (dashed line).

Biotites commonly have vacant sites in their octahedral layer, so that some hydroxyl groups are co-ordinated to only two cations. These hydroxyl groups are oriented nearly parallel to the layers and give absorption bands in the region 3620 cm^{-1} to 3540 cm^{-1} (vacancy bands), which are not affected by the orientation of the silicate sheets relative to the beam. Up to three bands may be resolved in this region, at 3620 cm^{-1}, 3600 to 3590 cm^{-1}, and 3560 to 3540 cm^{-1}. Vedder (1964) has suggested

that these bands be ascribed to hydroxyl associated with $R^{2+}R^{2+}$, $R^{2+}R^{3+}$, and $R^{3+}R^{3+}$ octahedral pairs, respectively, where R^{2+} represents Mg^{2+} or Fe^{2+}, and R^{3+} represents Al^{3+} or Fe^{3+}. Such an assignment is inconsistent with the spectrum of biotite M4 (fig. 1), in which only the lowest frequency band appears, but in which the probability of $R^{3+}R^{3+}$ pairs is very low. A more satisfactory assignment (Farmer *et al.*, 1967) arises from the observations (fig. 1) that biotite M4, for which the only vacancy hydroxyl absorption lies at 3541 cm^{-1}, contains octahedral Fe^{3+} but no octahedral Al^{3+}, whereas biotite 536 in which the band at 3599 cm^{-1} predominates, contains considerably more Al^{3+} than Fe^{3+} in its octahedral layer. Since these bands become intense only when the ferrous content is high, they are ascribed to hydroxyl associated with $Fe^{2+}Fe^{3+}$ and $Fe^{2+}Al^{3+}$ pairs, respectively. The vacancy band at 3620 cm^{-1} is never strong, and predominates only in biotites with moderate ferrous contents. As it is always associated with a band at 3590–3600 cm^{-1} it might plausibly be ascribed to hydroxyl co-ordinated to $MgAl^{3+}$. The assignments proposed above are qualitatively consistent with the spectra of fourteen analysed biotites and phlogopites that have been examined.

Oxidized biotites and vermiculites

When biotites were converted to vermiculites by refluxing successively in $BaCl_2$ and NaCl solutions, the hydroxyl absorption pattern did not change, and analyses (table I) showed little oxidation of ferrous ions. Significant oxidation by air does occur during the slower replacement of interlayer potassium by treatment at room temperature with sodium tetraphenyl boron solution (Newman and Brown, 1966) or with frequently changed sodium chloride solutions, and this oxidation affects principally the bands of hydroxyl of filled sites. More vigorous oxidation of these vermiculites with hydrogen peroxide or bromine causes a marked development of hydroxyl absorption in the region of the vacancy bands.

The implications of these changes in absorption of hydroxyl on trioctahedral and dioctahedral sites will be discussed separately.

Hydroxyl on trioctahedral sites. The shift to lower frequencies in the maximum of the trioctahedral hydroxyl absorption that occurs during preparation of the sodium-altered micas from biotites M4 and M5 (figs. 2*b* and 3*b*) can be ascribed to the partial conversion of ferrous ions to ferric ions, and a consequent change in the vibrational frequency of associated hydroxyl groups. This change is almost completely reversed (figs. 2*c* and 3*c*) when these altered micas are reduced with hydrazine, which is known to be effective in reducing octahedral ferric ions in smectites (Farmer *et al.*, 1967). When these biotites are fully oxidized with hydrogen peroxide, the changes in spectra can no longer be completely reversed by hydrazine (fig. 3*d*, *e*); hydroxyl absorption is regenerated but at a lower frequency than in the original biotite, indicating that some of the ferric ions formed in the octahedral layer can no longer be reduced.

These oxidation–reduction reactions might be expected to be associated with changes in the number of hydroxyl groups, according to the equations

$$R^{2+}Fe^{2+}_2(OH)_2 \rightleftharpoons R^{2+}Fe^{3+}_2O_2, \quad \text{and} \quad R^{2+}_2Fe^{2+}(OH)_2 \rightleftharpoons R^{2+}_2Fe^{3+}O(OH)$$

TABLE I. *Characteristics of biotites and vermiculites; exchange capacities and element contents are based on ignited weights*

	Interlayer cations* m. eq./100 g	Fe^{2+}	$Fe^{2+}+Fe^{3+}$	Mg	Refractive index (γ)	d_{001}†	d_{010}†
Biotite 31A	222	20·0 %	23·7 %	1·65 %	1·658	10·07 Å	9·24 Å
Na-form, unoxidized	183	18·9	23·2	1·60	1·621	10·04	9·24
Na-form, Br_2 oxidized	180	< 0·1	24·6	n.d.	~ 1·73	10·24	9·12
Na-form, Br_2 oxidized then reduced	193	3·6	22·0	1·55	1·665	10·20	9·19
Biotite, Luindi	219	16·7	21·7	5·40	1·658	10·05	9·26
Na-form, unoxidized	182	13·5	20·4	5·50	1·620	10·02	9·26
Na-form, Br_2 oxidized	181	< 0·1	20·8	n.d.	~ 1·70	10·08	9·19
Na-form, Br_2 oxidized then reduced	198	3·0	18·5	5·40	1·657	10·08	9·20

* $Na^+ + K^+$, recalculated to correspond to K^+-saturated forms, to allow for the different contributions of Na^+ and K^+ to the formula weights.

† Vermiculites were K^+-saturated and heated to 100° before X-ray examination.

n.d. Not determined.

where R^{2+} represents Mg^{2+} or Fe^{2+}; but quantitative conclusions cannot be drawn from figs. 2 and 3, because of uncertainties about the absorptivity of the different types of hydroxyl group, and difficulties in obtaining quantitative measurements by the pressed-disc technique used. Unambiguous evidence for loss and recovery of hydroxyl was, however, obtained using a film prepared from a dispersion of the high-iron vermiculite 31A (fig. 4). Air oxidation of the suspension had led to almost total

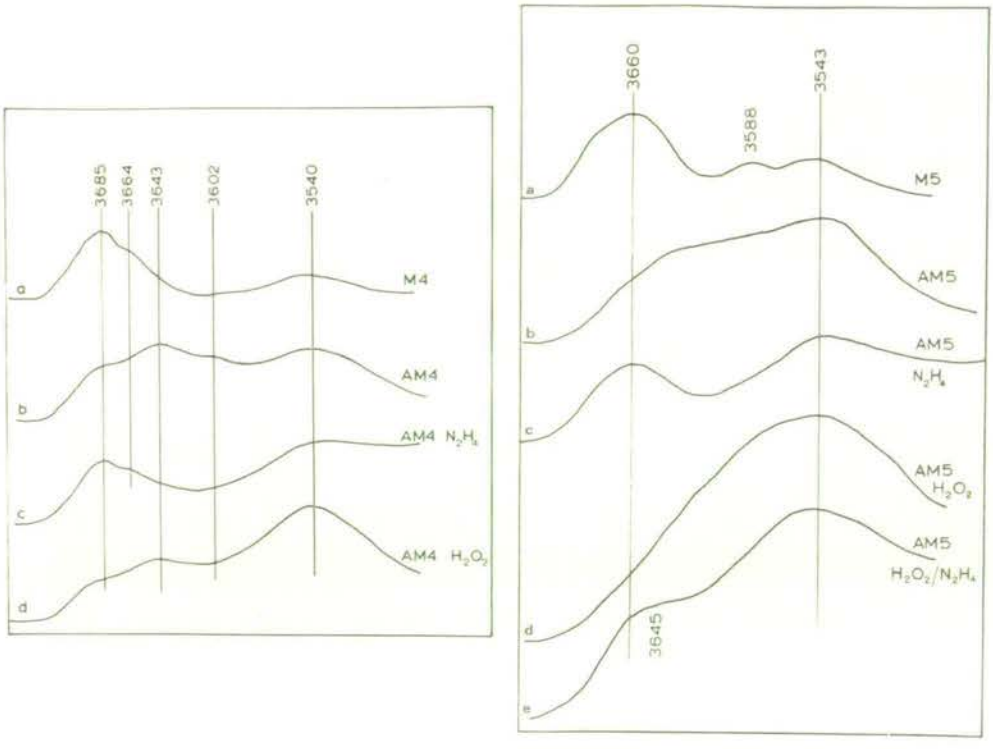

FIGS. 2 and 3: Fig. 2 (left). Hydroxyl absorption of (*a*) biotite M4, (*b*) Na-altered M4 (AM4), (*c*) AM4 treated with hydrazine for 7 days, and (*d*) AM4 oxidized with H_2O_2. 10 mg samples dispersed in KBr discs (12 mm diameter) and discs heated to 200 °C. Fig. 3 (right). Hydroxyl absorption of (*a*) biotite M5, (*b*) Na-altered M5 (AM5), (*c*) AM5 treated with hydrazine for 7 days, (*d*) AM5 oxidized with H_2O_2, and (*e*) AM5 oxidized then treated with hydrazine for 7 days. 10 mg samples dispersed in KBr discs (12 mm diameter), and discs heated to 200 °C.

loss of hydroxyl on trioctahedral sites, and the development of some hydroxyl associated with vacancies, so that the film, in which the vermiculite sheets are in parallel orientation, showed no increase in hydroxyl absorption when turned at 45° to the infra-red beam (fig. 4*b*). After treatment with hydrazine, absorption due to hydroxyl on trioctahedral sites developed (fig. 4*c*), which increased markedly on turning the film at 45° to the beam.

As pointed out by Vedder and Wilkins (1969), trioctahedral sites retaining hydroxyl groups in fully oxidized biotites should be principally of the type Mg_3, Mg_2Al, or

Mg_2Fe^{3+}. The first two are known to absorb near 3700 cm^{-1} and 3660 cm^{-1} respectively (Vedder, 1964) but the third has not yet been positively identified. It should be the only type of hydroxyl to survive on trioctahedral sites in fully oxidized high-iron vermiculites and biotites, but its absorption is obscured by the strong vacancy bands that develop (e.g. fig. 3*d*).

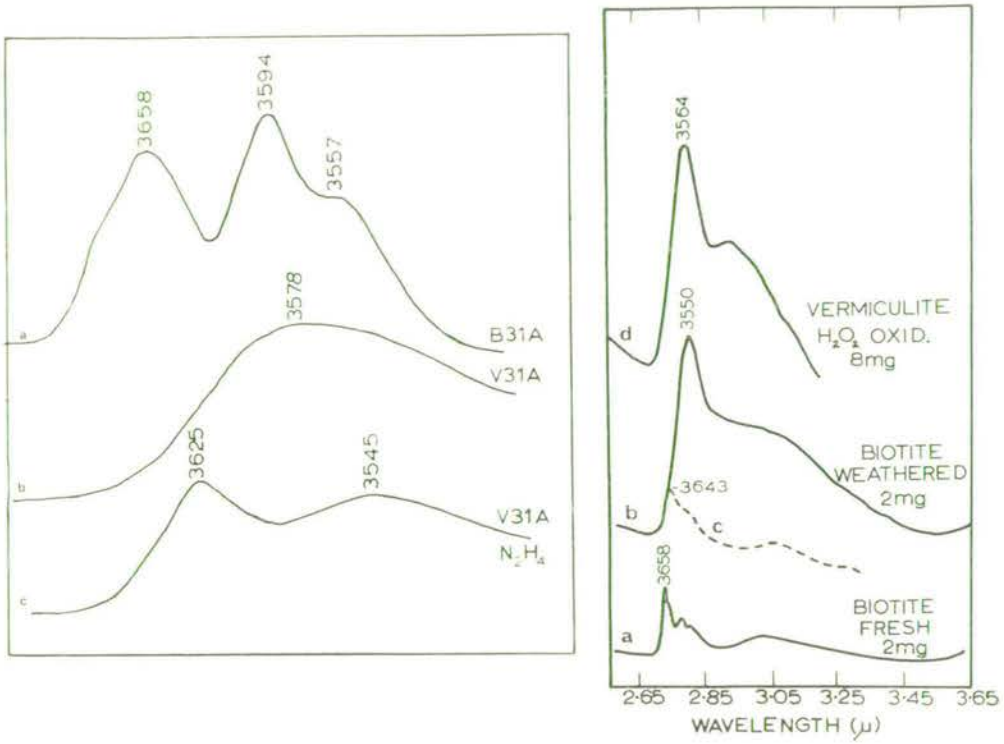

FIGS. 4 and 5: Fig. 4 (left). Hydroxyl absorption of (*a*) flake of biotite 31A, (*b*) Na-saturated film of vermiculite 31A, and (*c*) same film after treatment with hydrazine vapour for 24 hours; all at 45° to beam. Fig. 5 (right). Hydroxyl absorption of (*a*) fresh biotite 44/45F, (*b*) naturally weathered biotite 44/45W, (*c*) weathered biotite, partially dehydroxylated at 400 °C and (*d*) vermiculite 31A oxidized with H_2O_2. Samples in KBr discs heated to 200 °C for *a*, *b*, and *d*, and to 400 °C for spectrum *c*.

Hydroxyls associated with these vacancies were found to begin to dehydroxylate at 300 °C and were generally lost by 400 °C when the samples were heated in pressed KBr discs, i.e. at temperatures considerably lower than those Vedder and Wilkins (1969) found necessary for dehydroxylation in large biotite flakes. The residual band, due to $Mg_2Fe^{3+}OH$, was found at 3640–5 cm^{-1} in all samples studied, including the naturally weathered biotite (fig. 5*c*). In oxidized vermiculites of lower iron content, such as AM2 and AM3, the 3645 cm^{-1} band could be seen superimposed on the absorption of $MgAl^{3+}OH$ at 3660 cm^{-1}, which was present in the fresh biotite, while Mg_3OH was resolved at 3703 cm^{-1}. In oxidized AM4 (fig. 2*d*), Mg_3OH absorption

appears as a weak shoulder at 3680 cm^{-1} on the side of the predominant 3645 cm^{-1} band, confirming the observation of Vedder and Wilkins (1969) that Mg_3OH groups in oxidized biotites absorb at frequencies considerably lower than those given by some phlogopites (3718 cm^{-1}).

The origin of the 3602 cm^{-1} band in vermiculite AM4 (fig. 2*b*) is less certain. This band is also a persistent feature of partially oxidized vermiculite 31A, before it falls to a low level at the stage of oxidation indicated in fig. 4*b*. Possibly it can be ascribed to $MgFe_2^{3+}OH$ groupings, which Vedder and Wilkins (1969) have suggested may persist in oxidized biotites. Certainly, a frequency near 3600 cm^{-1} seems too low to be assigned to, say, an $MgFe^{2+}Fe^{3+}OH$ grouping (Wilkins, 1967).

It should be noted that the frequencies observed for hydroxyl absorption of Na-vermiculites in KBr pressed discs (figs. 2 and 3) are directly comparable with those given by the original biotites, as interlayer Na^+ has an effect on hydroxyl frequencies similar to that of interlayer K^+, and, in any case, much of the interlayer Na^+ is replaced by K^+, by exchange with the KBr.

Hydroxyl on dioctahedral sites. The intensity of the vacancy band near 3560 cm^{-1} that develops in oxidized biotites and vermiculites is a function of the octahedral iron content of the biotites: it was too weak to be detected in the oxidized vermiculite AM3 of Newman and Brown (1966) containing 1·2 iron ions per unit cell of six octahedral sites, but was a pronounced band in oxidized AM4, containing 2·5 iron ions per unit cell (fig. 2*d*). The most intense vacancy bands were given by the naturally weathered biotite (fig. 5*b*) derived from a fresh biotite containing about 4 iron ions per unit cell, and by the laboratory-oxidized vermiculite 31A (fig. 5*d*) of similar iron content.

In these oxidized vermiculites, oxidation of ferrous ions is complete (table I), and the enhancement of the vacancy bands is strong evidence for ejection of octahedral iron to compensate for the change in layer charge. The strong broad vacancy band is similar to, but less intense than that of nontronite, in which $Fe_2^{3+}OH$ groupings absorb at 3564 cm^{-1} (Farmer and Russell, 1964). Some influence of octahedral Al^{3+} can be seen on the frequency of the vacancy band in oxidized vermiculites, which ranges from 3540 cm^{-1} in oxidized AM4, containing no octahedral Al^{3+}, to 3581 cm^{-1} in oxidized vermiculite 536, containing one Al^{3+} per unit cell, which would have hydroxyl groups associated with both Fe_2^{3+} sites and $AlFe^{3+}$ sites.

An estimate of the concentration of dioctahedral sites was made on the assumption that the molar absorptivity of OH on these sites was the same as that in nontronite, using pressed KBr discs of the samples, which were carefully matched to give equal intensity of Si–O absorption near 10 μm. This indicated 1·1 vacancies per six octahedral sites in the naturally weathered biotite, i.e. that over 50 % of the mica was now dioctahedral. Similar estimates for laboratory-oxidized vermiculite 31A indicated 0·95 vacancies for Br_2-oxidized material, and 0·60 vacancies for H_2O_2-oxidized material.

Iron hydroxides, formed by ferric ions ejected from the octahedral layers, are unlikely to contribute to the 3540–80 cm^{-1} vacancy band in oxidized vermiculites

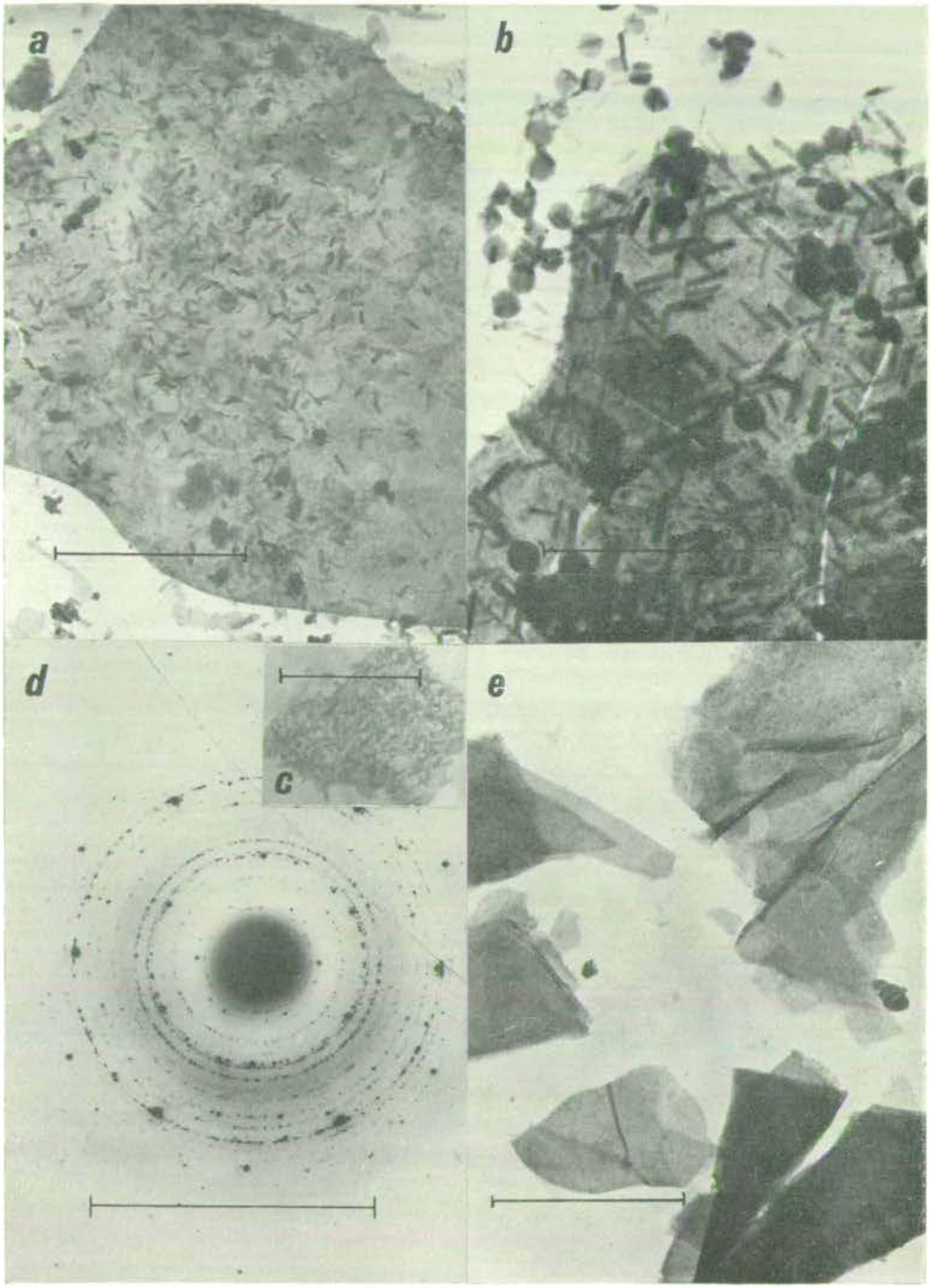

FIG. 6

and biotites. A range of crystalline and amorphous iron hydroxides have been examined, and all have been found to absorb below 3370 cm^{-1}. Thus any iron hydroxides formed in the oxidized micas will probably contribute, together with adsorbed water, to the diffuse absorption on the low frequency side of the 3540 cm^{-1} band in curves *b* and *d* of fig. 5.

Electron microscopy and X-ray examination. To seek confirmation for the loss of octahedral iron, the weathered biotite and the oxidized vermiculites were examined by electron microscopy and by X-ray diffractometry. Under the electron microscope flakes of the vermiculites from biotite 31A and Luindi biotite that had been oxidized by bromine were seen to be covered with fine lath-shaped crystals (fig. 6*a*); on some flakes the crystals show preferred orientation in three directions at 120° to each other, indicating expitaxial growth on the vermiculite surface (fig. 6*b*). Where a large number of these crystals were concentrated within a small flake area as in fig. 6*c* a good polycrystalline electron diffraction pattern was obtained. Measurement of *d*-spacings using the underlying vermiculite pattern as a calibration proved that the laths were crystals of β–FeOOH (akaganéite). This hydroxide is known to crystallize during hydrolysis of ferric chloride solutions, and its appearance here can be ascribed to the hydrolysis of ferric bromide. The bromide ion formed within the interlayers by the reduction of bromine gives the ferric ions that have been ejected from the octahedral layer sufficient mobility to migrate out of the interlayer space, and crystallize as β–FeOOH on the surface of the crystals. Only traces of iron remained in solution following bromine oxidation, and the pH fell only to four.

No β–FeOOH was detected on vermiculites oxidized with H_2O_2; however, the vermiculite flakes had a distinctly mottled aspect indicative of the existence of very finely divided amorphous iron oxide as a separate phase within the vermiculite flake (fig. 6*e*). X-ray diffraction also indicated that the ejected ferric ions formed hydroxides within the interlayer space, increasing the 001 spacing of specimens that had been potassium-saturated and dried at 100 °C from 10 Å for unoxidized vermiculites to 11·13 Å (vermiculite 31A) and 11·42 (Luindi vermiculite) for H_2O_2-oxidized vermiculites. The basal reflections from the K-saturated unoxidized vermiculites were sharp and rational whereas those from H_2O_2-oxidized vermiculites were broad and irrational, indicative of variable interlayer spacing. The vermiculites that had been oxidized with bromine gave lower spacings (table I) than H_2O_2-oxidized material indicating that much but not all of the ejected ferric ions had migrated out of the interlayer space.

FIG. 6. (*a*) Na vermiculite from biotite 31A after bromine oxidation; ultrasonically dispersed. The marker represents 1 μm. (*b*) Na vermiculite from biotite 31A after bromine oxidation; ultrasonically dispersed. Note orientation of laths on the vermiculite flake. The spheres are 880 Å polystyrene latex particles included as magnification check. Marker represents 0·5 μm. (*c*) Mass of lath crystals from bromine-oxidized Na-vermiculite from biotite 31A giving rise to polycrystalline electron diffraction pattern in (*d*). The marker represents 1 μm. (*d*) Selected-area electron-diffraction pattern from the mass of laths in 3*c*. Apart from the 020, 040, and 060 spotty reflections from underlying vermiculite flakes, the *d* spacings agree with published X-ray data for β-FeOOH. The marker represents 1 $Å^{-1}$. (*e*) Na-vermiculite from biotite 31A after H_2O_2 oxidation; ultrasonically dispersed. The marker represents 1 μm.

Rimsaite (1967) reported that the naturally weathered biotite gave spacings nearly identical to those of the unweathered biotite, but that the weathered specimen gave rather diffuse reflections, which suggests the presence of interlayer deposits. Electron micrographs of surface replicas of freshly cleaved faces of weathered mica show that a large proportion of the surface is covered with fine-grained particles (fig. 7*a*). This contrasts strongly with fresh mica, which is typified by a completely smooth surface morphology with occasional sharply defined cleavage steps. At higher magnification two types of deposit can be distinguished. There are clusters of laths or tubes (fig. 7*b*) 0·2–0·4 μm long and 0·02–0·03 μm wide, and clumps of very fine-grained material (fig. 7*c*). Even relatively smooth areas of flake are peppered with fine grains. Some of the weathered mica was crushed lightly and subjected to ultrasonic dispersion so that the laths and the fine-grained material could be examined directly in the electron microscope. Fig. 7*d* shows that the particles in fig. 7*b* are extremely fragile tubes; these gave very weak electron-diffraction patterns, the strongest reflections lying along the axis of the tubes, and corresponding to the 020 and 060 planes of a dioctahedral clay mineral (d_{010} 8·95). The morphology and diffraction pattern of these tubes suggest that they are poorly crystallized halloysite. The grainy electron-dense material in fig. 7*d* corresponds to the material featured in the replica fig. 7*c*. This gave no electron diffraction and is probably amorphous iron oxide.

Selective extraction of iron. In an attempt to measure quantitatively the amount of iron liberated from the octahedral layer, oxidized vermiculites from biotite 31A and Luindi biotite were repeatedly extracted with dithionite–citrate solutions. The amounts of iron extracted from biotite 31A are shown in fig. 8. For bromine-oxidized samples there was an initial rapid solution of iron, which probably corresponds to dissolution of β–FeOOH on the surface of the crystals, followed by a continuous liberation of iron from the mica on successive extractions. Little or no surface hydroxide phase is present on H_2O_2-oxidized specimens; dissolution of iron was slower, and there was no clear break to indicate when interlayer iron hydroxides had been dissolved; nevertheless, a decrease in 001 spacings from over 11 Å to 10·2 Å (K-saturated and dried at 100 °C) does indicate that interlayer hydroxides have been at least partially extracted from H_2O_2-oxidized vermiculites. An estimate of the amount of iron liberated from octahedral sites based on the amount that is rapidly dissolved from the Br_2-oxidized samples indicates 1·8 % Fe from vermiculite 31 A and 1·0 % from Luindi vermiculite. Analysis of the residual material after eight successive extractions with dithionite–citrate (a separate experiment) indicated a loss of about 1·5–2·0 % Fe from both vermiculites (table I). A 2 % loss of iron corresponds to the development of about 0·35 vacancies per six octahedral sites, assuming no other cations are lost. Magnesium analyses indicate little loss of this ion (table I).

Some other features of the oxidized vermiculites are recorded in table I. There is some loss of layer charge during extraction of potassium, but no further change in layer charge occurs on oxidation, although the small increase following subsequent reduction with dithionite solutions is probably significant. There is a considerable increase in refractive index on oxidation of high-iron vermiculites associated with an

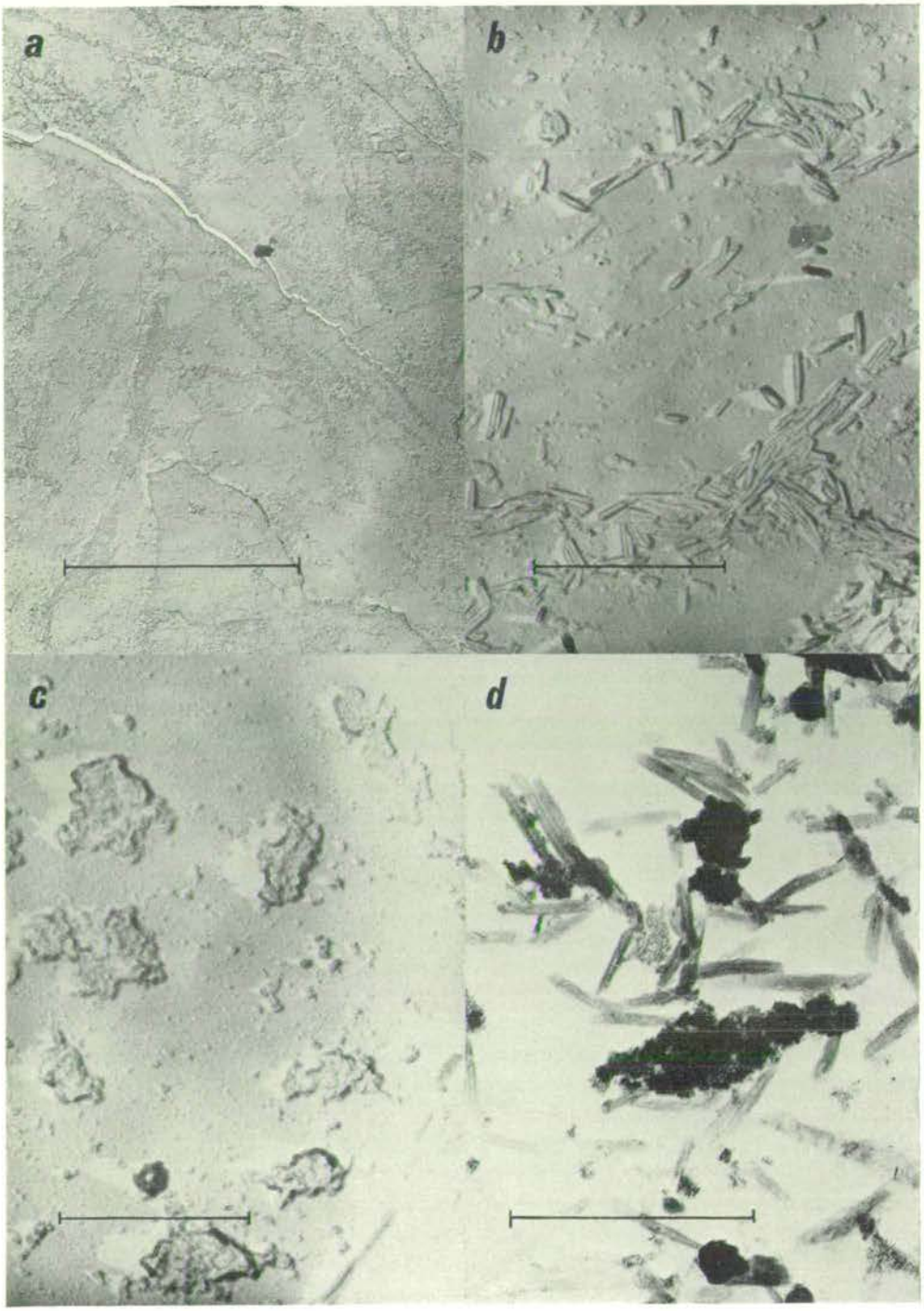

FIG. 7. (*a*) Naturally weathered biotite: carbon replica of freshly cleaved surface, preshadowed with Pt/C at $\tan^{-1}\frac{1}{2}$. The marker represents 10 μm. (*b*) as (*a*). The marker represents 1 μm. (*c*) as (*a*). The marker represents 1 μm. (*d*) Naturally weathered biotite after light grinding and ultrasonic dispersion. The marker represents 1 μm.

increase in 2V from about 8° to 25°, similar to that observed for naturally weathered biotites (Rimsaite, 1967). For biotites of moderate iron content, there is no significant increase of refractive index on oxidation; thus for mica M2 the γ-index of the original mica, its Na-altered form, and the H_2O_2-oxidized Na-altered form are 1·593, 1·584, and 1·582 respectively, and for mica M4 they are 1·617, 1·617, and 1·620, in contrast to M5, for which they are 1·647, 1·646, and 1·685 respectively.

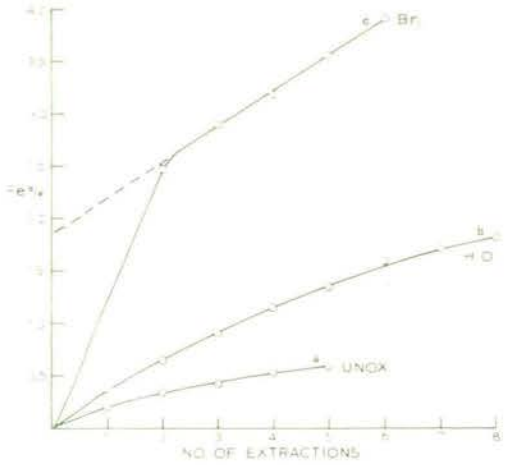

FIG. 8. Accumulated loss of Fe, on successive dithionite–citrate extractions, from vermiculite 31A: (*a*) unoxidized, (*b*) H_2O_2 oxidized, and (*c*) Br_2 oxidized.

It seems likely that the very high refractive indices of the oxidized vermiculites from 31A and Luindi biotites are due largely to the submicroscopic iron oxides present, as the refractive index falls substantially after dithionite extraction (table I), although 2V increases to 35–40°. Re-oxidation of the dithionite-treated vermiculites with bromine did not increase their refractive indices; this is consistent with the expectation that no further separation of iron oxides would occur.

Ignition in air at 650 °C for 20 h increased the refractive index of unoxidized vermiculite 31A to over 1·79, whereas the oxidized vermiculite that had been extracted with dithionite increased only to about 1·76 on ignition.

Oxidation also causes a decrease in the *b* dimension of the vermiculites (table I), as noted by Wones (1963) for synthetic oxybiotites, and also by Rimsaite (1967) for weathered biotites.

Discussion

The present investigation indicates that oxidation of ferrous ions in vermiculitized biotites is compensated first by a reversible loss of protons, and subsequently by an irreversible loss of octahedral iron. Loss of interlayer cations appears to play little part in the compensatory mechanism, as the decrease in layer charge on vermiculitizing the biotites is not much greater than that found by Newman (1967) for his phlogopite P3, and no further change occurs on subsequent oxidation.

In the vermiculitized biotites, the oxidizing agents (bromine, oxygen, or hydrogen peroxide) can enter the interlayer space, where electron transfer from an octahedral ferrous ion to the electron acceptor is probably mediated through a hydroxyl or oxide ion. The initial step probably involves transfer of a hydrogen atom from a hydroxyl group to the oxidant. This type of atom transfer reaction is commonly postulated for oxidation–reduction reactions in aqueous solutions (Basolo and Pearson, 1967).

At a later stage, when the remaining ferrous ions are co-ordinated only to oxide or fluoride ions, electrons may either transfer directly from oxide ions to the oxidant, or indirectly through bridging water molecules, e.g.:

$$Fe^{2+}O^{2-}—HOH—Br_2 \rightarrow Fe^{3+}O^{2-} + OH^- + HBr + Br.$$

By these mechanisms, the grouping $[Fe^{2+}Fe^{3+}_2O^{2-}_2]^{4+}$ is converted to $[Fe^{3+}_3O^{2-}_2]^{5+}$: it is suggested that the resultant local concentration of positive charge is unstable, and that a $[Fe^{3+}O^{2-}]^+$ grouping is ejected through the hexagonal holes in the silicate sheet into the interlayer space. The residual $[Fe^{3+}_2O^{2-}]^{4+}$ grouping could then rehydrate to give $[Fe^{3+}_2(OH)^-_2]^{4+}$. Although ejection of ferric ions appears to proceed more slowly than loss of protons, there is clearly no great energy barrier to this process. The marked optical anisotropy in the (001) plane of oxidized vermiculites indicates that these ions are preferentially ejected from a specific site, probably the unique site that is vacant in dioctahedral micas.

The properties of the naturally weathered biotite examined here closely match those of the laboratory-oxidized vermiculite 31A. Differences in refractive index, 2V, and hydroxyl absorption between the fresh and oxidized forms all agree. Further, changes in infra-red absorption pattern in the 10–15 μm region on weathering, not illustrated here, are closely matched by bromine oxidation of vermiculite 31A, less closely for H_2O_2-oxidized material. There can be no doubt that oxidation in nature and in the laboratory yield very similar products, although there is evidence of a further weathering process yielding small amounts of halloysite-like material in the naturally oxidized biotite. The mechanism of oxidation for the naturally weathered biotite is less obvious, as it retains a 10 Å spacing, suggesting that oxidation has proceeded without expansion of the biotite. It may be, however, that oxidation was a two-stage process, involving initial vermiculitization, followed by readsorption of potassium and collapse to 10 Å. Such a mechanism can be justified by the observation of Barshad and Kishk (1968) that oxidized vermiculites have an increased affinity for potassium. The conversion of hydroxyl to oxide ions, and the development of dioctahedral sites in which the hydroxyl groups are directed away from the interlayer cations, would both tend to increase the strength of binding of K^+ in the interlayer space. If such a process does occur readsorption of K^+ must be highly efficient, as there is little evidence for residual vermiculite layers in the weathered biotite 44W described by Rimsaite (1970). Chloritic material associated with the weathered biotite appears to be a secondary alteration product.

Wilson (1970) has presented infra-red evidence for an increase in octahedral vacancies during oxidative weathering of a biotite to hydrobiotite in soil, associated with a decrease in refractive index, and a considerable loss of iron (from 15·5 % in the fresh mica to about 10·5 % in the weathered mica). Apparently, the complexing and reducing agents present in soils can extract ejected ferric ions from the weathered mica. Walker (1949) also postulated loss of iron during weathering of a biotite in soil to an oxidized 10 Å form, and subsequently to vermiculite. His analyses show, in addition to a loss of 2 % Fe, a substantial loss of MgO (from 9·2 to 5·4 %) in the first weathering product, for which there is no analogy in the present work.

Since ejection of ferric ions from the lattice occurs so readily during oxidation at room temperature it seems highly probable that this will occur also during thermal oxidation of biotites, where blistering and delamination allow access of oxygen. The vacancies that would develop cannot be detected by infra-red spectroscopy, as the dioctahedral sites are dehydroxylated by condensation, forming water (Vedder and Wilkins, 1969). But the high refractive index of thermally oxidized biotites (Rimsaite, 1967) is evidence for interlayer submicroscopic iron oxides, in view of the finding, presented here, that oxidized vermiculites from which the liberated iron oxides have been extracted do not give such high refractive indices on heating. Similarly, it is plausible to suggest that ejection of iron from the octahedral layers occurs also for thermally oxidized amosite, where ferrous ions are oxidized in excess of the hydroxyl content and excess oxygen is taken up (Hodgson, Freeman, and Taylor, 1965*a*). Iron oxides could form in the channel containing the *A* site of amphiboles, and this migration of ferric ions might account for changes in the relative intensity of X-ray diffraction maxima during conversion of amosite to oxyamosite. In thermally oxidized crocidolite, however, there is evidence that the amount of ferrous ion that can be oxidized without breakdown of the amphibole structure is limited to one ferrous ion for each hydroxyl group (Hodgson, Freeman, and Taylor, 1965*b*; Addison, Addison, Neal, and Sharp, 1962).

One unsatisfactory feature of the present investigation is the failure to obtain a consistent estimate for the number of vacant sites that develop in oxidized vermiculites. An estimate based on the intensity of infra-red absorption by hydroxyl on dioctahedral sites indicates nearly one vacancy per six octahedral sites in oxidized vermiculite 31A, whereas the amount of iron that can be extracted by dithionite treatment indicates an increase of at most 0·3 vacancies over the unoxidized material. The number of vacancies originally present in the fresh biotite is uncertain, but appears comparable, from infra-red evidence, with the number in biotite 44F, for which Rimsaite (1970) calculates 0·3 vacancies. Obviously, some aluminium, titanium, and magnesium ions might also be ejected from the octahedral layer, although these are minor components relative to ferrous and ferric ions, and it seems likely that not all the ejected ferric ions were extracted by dithionite treatment. Even allowing for these sources of error, the discrepancy seems significant. The assumptions on which the infra-red estimate is based could well be in error; nevertheless, the higher figures given by this technique agree reasonably with the hypothesis that all $[R^{3+}_3O^{2-}_2]^{5+}$ sites are unstable, and decompose to dioctahedral sites in the oxidized micas. On this basis, and the assumption that the distribution of ions in trioctahedral sites is random, calculation indicates that the number of vacancies that would develop on oxidation of biotites 44F and 45F are 1·3 and 1·0 respectively per six octahedral sites. The infra-red estimate obtained for a weathered biotite from this locality is 1·1 vacancies. Similar calculations indicate the development of only 0·07 vacancies for oxidized AM3 (where no dioctahedral sites could be detected) and 0·25 vacancies for oxidized AM4, which showed a significant vacancy band.

Acknowledgements. The authors are indebted to Mrs. K. Law for able technical assistance, and to Mr. D. Duthie for refractive index measurements.

REFERENCES

ADDISON (C. C.), ADDISON (W. E.), NEAL (G. H.), and SHARP (J. H.), 1962. *Journ. Chem. Soc.* 1468.
BARSHAD (I.) and KISHK (J. M.), 1968. *Science*, **162**, 1401.
BASOLO (F.) and PEARSON (R. G.), 1967. *Mechanisms of Inorganic Reactions*, 2nd edn. New York (Wiley).
FARMER (V. C.) and RUSSELL (J. D.), 1964. *Spectrochim. Acta*, **20**, 1149.
—— —— 1966. Ibid. **22**, 389.
—— —— and AHLRICHS (J. L.), 1968. *9th Int. Congr. Soil Sci., Adelaide, Australia*, **3**, 101.
—— —— —— and VELDE (B.), 1967. *Bull. Groupe franç. Argiles*, **19** (2), 5.
FRIPIAT (J. J.), ROUXHET (P.), and JACOBS (H.), 1965. *Amer. Min.* **50**, 1937.
HELLNER (E.) and EULER (R.), 1957. *Geochim. Acta.* **12**, 47.
HODGSON (A. A.), FREEMAN (A. G.), and TAYLOR (H. F. W.), 1965*a*. *Min. Mag.* **35**, 445.
—— —— —— 1965*b*. Ibid. **35**, 5.
MEHRA (O. P.) and JACKSON (M. L.), 1960. *Clays Clay Min.* **7**, 317.
NEWMAN (A. C. D.), 1967. *Clay Min.* **7**, 215.
—— and BROWN (G.), 1966. Ibid. **6**, 297.
POLLOCK (E. N.) and MIGUEL (A. H.), 1967. *Anal. Chem.* **39**, 272.
RAUSELL-COLOM (J. A.), SWEATMAN (T. R.), WELLS (C. B.), and NORRISH (K.), 1965. In *Experimental Pedology*, eds. E. G. HALLSWORTH and D. V. CRAWFORD, 40. London (Butterworth).
RIMSAITE (J.), 1967. *Clays Clay Min.* **15**, 375.
—— 1970. *Contr. Min. Petr.* **25**, 225.
ROTH (C. B.), JACKSON (M. L.), DE VILLIERS (J. M.), and VOLK (V. V.), 1967. In *Soil Chemistry and Soil Fertility*, ed. G. V. JACKS, p. 217. Trans. Meet. Comm. II & IV, int. Soc. Soil Sci., Aberdeen, 1966.
SANDELL (E. B.), 1959. *Colorimetric Determination of Traces of Metals*, 3rd edn. New York (Interscience).
[TSVETKOV (A. I.) and VAL'YASHIKHINA (E. P.)] Цветков (А. И.) и Вапьяшихина (Е. П.), 1956. Изв. Акад. наук СССР, сер. геол. (*Bull. Acad. Sci. URSS, sér. géol.*), **5**, 74.
VEDDER (W.), 1964. *Amer. Min.* **49**, 736.
—— and WILKINS (R. W. T.), 1969. Ibid. **54**, 482.
WALKER (G. F.), 1949. *Min. Mag.* **28**, 693.
WASHINGTON (H. S.), 1930. *The Chemical Analysis of Rocks*, 4th edn. New York (Wiley).
WILKINS (R. W. T.), 1967. *Min. Mag.* **36**, 325.
WILSON (M. J.), 1970. *Clay Min.* **8**, 291.
WONES (D. R.), 1963. *Amer. Min.* **48**, 1300.

[*Manuscript received 29 April 1970*]

Offprinted from the *Transactions of The Faraday Society*
No. 585, Vol. 67, Part 9, September, 1971

Interlayer Complexes in Layer Silicates

The Structure of Water in Lamellar Ionic Solutions

By V. C. Farmer and J. D. Russell

Dept. of Spectrochemistry, The Macaulay Institute for Soil Research,
Craigiebuckler, Aberdeen

Received 3rd March, 1971

The stretching vibrations of water (H_2O, HDO and D_2O) in montmorillonite, hectorite, saponite and vermiculite are split into two components, similar to those seen in perchlorate solutions. Examination of lower hydrates and pyridine complexes of the layer silicates shows that the higher frequency component corresponds to hydrogen bonds to oxygens of Si—O—Si linkages, the lower frequency component to water-water bonds and hydrogen bonds to oxygens of Al—O—Si linkages. The observations are explained in terms of chains of hydrogen-bonded water molecules which form dielectric links between interlayer cations and oxygens on the silicate anion surface. This concept, together with information obtained on the distribution of charge on the surface oxygens, provides a qualitative explanation of the hydration properties of layer silicates, and is extended to account for the stability of organic complexes of montmorillonite and hectorite. Some analogies between interlayer complexes and ionic solutions are proposed.

The planar anions of the expanding layer silicates are normally separated by one or more layers of water molecules. These water molecules interact with each other, with the surface oxygens of the silicate anions, and with the charge-compensating exchangeable cations, which are incorporated in the structure of the water layers. An understanding of these interactions should not only assist interpretation of the properties of clay-water systems, but also provide a model for the structure of other ionic solutions.

The centres of positive charge deficiency in the silicate anions are associated either with replacements in the tetrahedral layer (e.g., saponite and vermiculite) or with replacements in the octahedral layer (e.g., montmorillonite and hectorite). In the first instance the negative charge is distributed over at least the three surface oxygens coordinated to tetrahedral Al^{3+}, and, in the second, over at least the ten surface oxygens of the four silicon-oxygen tetrahedra whose apices are linked to a site of octahedral substitution. Accordingly, the surface oxygens of montmorillonite and hectorite are weak electron donors, comparable to those of the perchlorate ion, as judged by their effect on the vibrations of ammonium.[1] By the same criterion, surface oxygens of saponite and vermiculite are stronger electron donors than perchlorate, but considerably weaker than nitrate or chloride.

The analogy between the perchlorate and layer silicate anions is reinforced by the observations that water in layer silicates [2] shows a high frequency maximum near 3620 cm^{-1} on the side of the main OH stretching absorption band, similar to that seen in infra-red [3, 4] and Raman [5] spectra of concentrated perchlorate solutions. The origin of this maximum in perchlorate solutions is disputed, but infra-red studies [2] on oriented films of hectorite and montmorillonite have shown that the high frequency maximum in these systems arises from OH groups directed at a high angle to the silicate sheets, indicating that they are involved in weak hydrogen bonding to surface

oxygens. The main water maximum arises from OH groups which lie more nearly in the plane of the sheets, and so thought to be involved in water-to-water hydrogen bonding.

If this picture of the water layers is correct, the strength of hydrogen bonding to the silicate surface should be a function of the electron-donating potential of the surface oxygens and so should be stronger for tetrahedral substitution than for octahedral substitution. Evidence for this is sought here in infra-red spectra of H_2O, HDO, and D_2O in montmorillonite, hectorite, saponite and vermiculite. The effect of the exchangeable cation and of partial replacement of water by pyridine on the water absorption pattern is also examined. Previous studies of HDO in montmorillonite [6] and of H_2O and D_2O in vermiculite [2] gave no information on the orientation of the dipole oscillations associated with the water absorption bands.

EXPERIMENTAL

The exchangeable cation content, water content, and layer spacings of hectorite, montmorillonite, saponite, and vermiculite are given in table 1. Self-supporting, oriented films of these minerals were prepared and their interlayer water replaced by D_2O, or H_2O containing 20 % HDO, in a cell which allowed adjustment of the orientation of the films relative to the infra-red beam.[11] During examination, the films were heated to 30°C by the infra-red radiation, so that the effective humidity, controlled by the presence of free liquid in the system at 20°C, was close to 50 %. At this humidity, films saturated with Cs^+ and Na^+ contained one water layer, and those saturated with Mg^{2+} contained two. When saturated with Cu^{2+}, the montmorillonite contained one water layer, and the vermiculite two. Spectra of less hydrated phases were recorded in the same cell after evacuation and heating.

Spectra were recorded on a Grubb Parsons Spectromaster infra-red spectrometer, generally using radiation polarized with the electric vector perpendicular to the axis of rotation of the films. Sometimes partially polarized radiation was used, and this is indicated in the text.

TABLE 1.—EXCHANGEABLE CATION AND WATER CONTENT (mol) PER UNIT CELL OF COMPOSITION M_n^{z+} $[(Mg, Al, Li)_{2-3}(Si, Al)_4O_{10}(OH)_2]$, xH_2O, AT 50 % R.H.

mineral (source)	M_n^{z+}	xH_2O	H_2O/cation	$d(001)$ Å
montmorillonite [7]	$Na_{0.42}$	2 0	4.7	12.2
	$Mg_{0.21}$	4 4	21.5	14.7
hectorite [8]	$Na_{0.32}$	2.4	7.4	12.1
	$Mg_{0.16}$	3.9	24.3	14.9
saponite [9]	$Na_{0.51}$	3.1	6.0	12.6
	$Mg_{0.26}$	4.6	17.5	14.5
vermiculite [10]	$Na_{0.85}$	3.2	3.7	12.2
	$Mg_{0.43}$	4.6	10.8	14.3

RESULTS

HYDRATES STABLE AT 50 % HUMIDITY

Spectra of HDO in montmorillonite and hectorite at 50 % humidity showed a clearly defined high frequency maximum for all cations (fig. 1). When the films were placed at 45° to the beam, the band in Na-saturated specimens increased by a factor of 4.5-5.5, and that in Mg-saturated specimens by factors of 1.6 (montmorillonite) and 2.4 (hectorite). In saponite this band is less well defined, and in vermiculite it can be distinguished only for the Na-saturated film.

In hectorite, the lattice OH group is perpendicular to the silicate layers and its absorption increased by a factor of 5 in both Na- and Mg-saturated films. This increase is the same as that found for the 2660 cm^{-1} water absorption in Na-hectorite,

so that the OD groups which give rise to this band must lie nearly perpendicular to the layers. The smaller increase of the 2660 cm^{-1} band in Mg-hectorite corresponds to water OD groups which are calculated to lie at about 62° to the plane of the film, and so at a somewhat higher angle to the silicate layers, as these are not perfectly parallel to the film. The principal maximum of the HDO absorption, lying at 2465-2560 cm^{-1}, increases by 5-25 % for all systems except Na-vermiculite, which shows an increase of 45 %. No great weight can be attached to small changes in absolute intensity on inclination, but it can be concluded that in all systems other than Na-vermiculite, most OH groups contributing to the lower frequency maximum lie more nearly parallel to the silicate layers, and are involved in hydrogen bonds between water molecules.

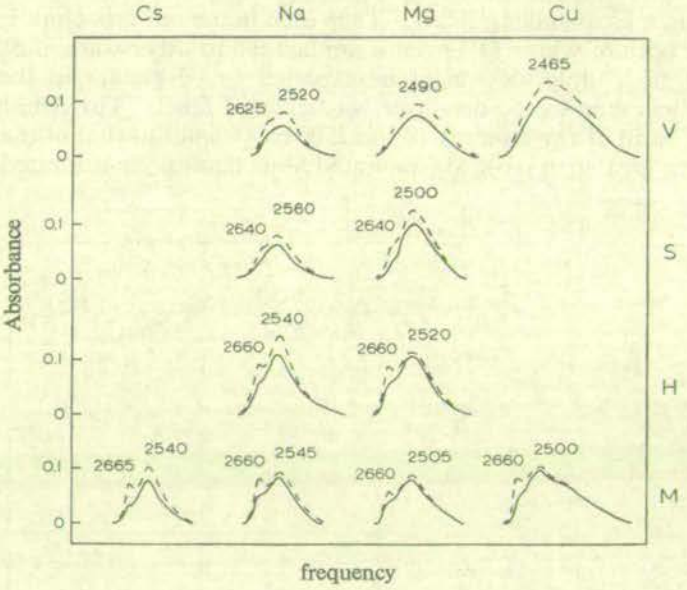

FIG. 1.—OD stretching absorption of HDO in vermiculite (V), saponite (S), hectorite (H) and montmorillonite (M), containing the exchangeable cations indicated. Full line: 0° incidence; broken line: 45° incidence.

Comparison of the absorption of D_2O (fig. 2) with that of HDO (fig. 1) shows that the high frequency band is more intense for D_2O, so that its presence can now be detected even in Mg-vermiculite, although the band is much broader in this system than in the others. With D_2O, the high frequency band does not show such a large increase in intensity on inclining the films to the beam (the increase for Na-saturated films is about 50 %), indicating that the transition moment of this vibration is no longer perpendicular to the layers, although still at a higher angle than that associated with the broad absorption near 2500 cm^{-1}. In all systems, the 2660 cm^{-1} band of HDO is shifted to higher frequency by 20-30 cm^{-1} in D_2O, and a corresponding shift to lower frequencies of the 2500-2560 cm^{-1} band is seen in all systems except Na-vermiculite. These differences between D_2O and HDO, affecting the intensity, frequency, and direction of the transition moments of the vibrations, can all be ascribed to coupling between the two OD vibrations in D_2O molecules that are involved in a weak hydrogen bond through one OD group and a strong hydrogen bond through the other. This suggests a water structure consisting of chains of

hydrogen-bonded water molecules, starting with a water molecule coordinated to a

$$\begin{matrix} & D_a & & D_a & \\ & | & & | & \\ M^{n+}\text{--}O & \text{—} & D_b\text{--}O & \text{—} & D_b\text{--} \end{matrix}$$

cation, i.e., M^{n+}--O—D_b--O—D_b--. The OD_a groups are mostly directed towards the oxygens of the silicate lattice and form weak hydrogen bonds with those surface oxygens which carry little or no charge, so giving rise to the 2660 cm^{-1} band of HDO, while the OD_b groups give rise to the 2520 cm^{-1} band. In saponite and vermiculite the OD_a groups will preferentially associate with oxygens coordinated to Al^{3+} in the tetrahedral layer and so form stronger bonds: this effect can account for the lower intensity of the 2660 cm^{-1} band for HDO in saponite and the further decrease in its intensity in vermiculite. Branching of chains must involve OD_a groups, and cross-linking between chains involve either OD_a groups, or one or more water molecules which form a cross-linking chain, Thus each branch or cross link requires one water molecule both of whose OD groups are bonded to other water molecules, and the number of such molecules might be expected to be greater in the two-layer Mg-saturated films than in the one-layer Na-saturated films. These molecules may account for the ratio of the intensity of the 2500 cm^{-1} band to that of the 2660-2690 cm^{-1} band being greater in most Mg-saturated films than in Na-saturated films.

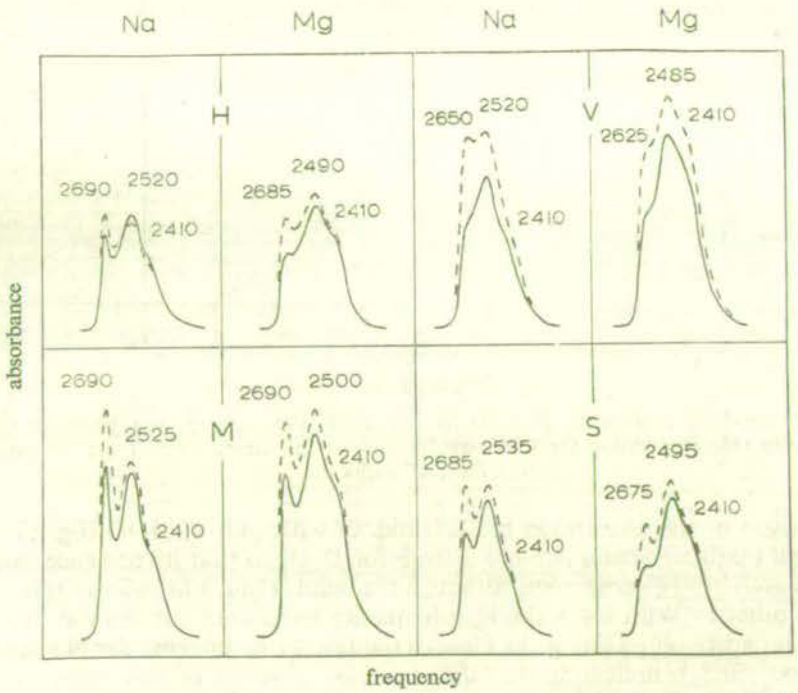

FIG. 2.—OD stretching absorption of D_2O in layer silicates. Symbols as in fig. 1.

Water molecules directly coordinated to small divalent ions will be more strongly polarized than water in outer spheres of coordination, or water coordinated to sodium ions. Accordingly the spectra of HDO in layer silicates (fig. 1) show increasing absorption in the region below 2450 cm^{-1} in the exchangeable cation series Na^+, Mg^{2+} and Cu^{2+} corresponding to stronger water-to-water bonds with increasing polarizing power of the cation. There is, however, little difference between water absorption in Cs- and Na-montmorillonite.

It is impossible to estimate, from the spectra in fig. 1 and 2, the location of OH absorption associated with hydrogen bonds to lattice oxygens coordinated to aluminium. Two approaches have been made to defining its position : one of these involves replacing water in outer spheres of coordination by pyridine; the second involves removing water in outer spheres of coordination by heating specimens in vacuum.

THE Mg-H_2O-PYRIDINE COMPLEX

In the first instance, treatment of Mg-saponite and Mg-hectorite with pyridine displaced almost all the water in outer spheres of coordination, giving an ionic complex which can be formulated [1, 12] as $Mg^{2+}(O—H_b\text{--}NC_5H_5)_6$. The $O—H_b$ group of coordinated water forms a strong hydrogen bond to pyridine, absorbing at 2800-2850 cm^{-1} (fig. 3), and in both systems a sharp absorption due to OH_a groups lies near 3630 cm^{-1}. In saponite, placing the film at 45° to the beam increased

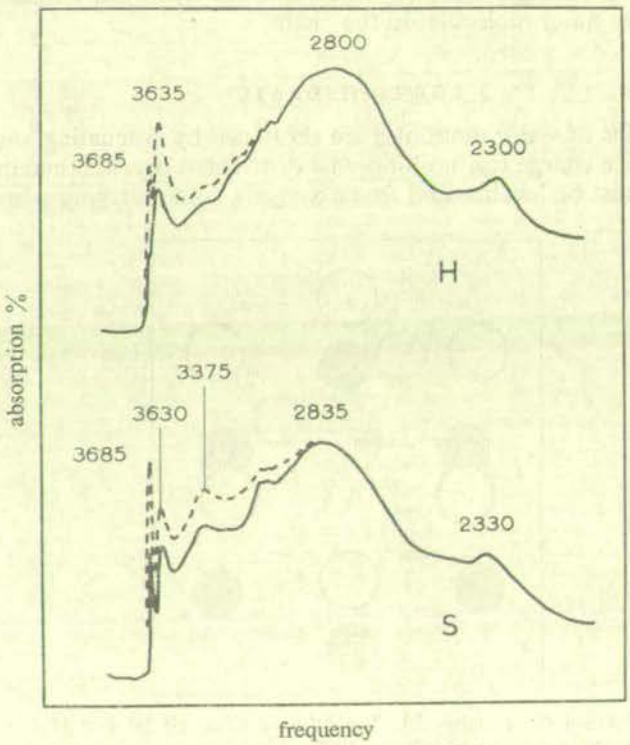

FIG. 3.—OH stretching absorption of H_2O in the Mg—H_2O-pyridine complexes of hectorite (H) and saponite (S). Spectra recorded using partially polarized radiation. Full line : 0° incidence ; broken line : 45° incidence.

the 3630 cm^{-1} band by about 35 %, but also increased absorption in the region 3150-3500 cm^{-1} by 15-30 % (fig. 3S) ; there was no increase below 2900 cm^{-1}. It seems likely that an exchangeable Mg^{2+} cation in saponite will position itself above an Al^{3+} in the tetrahedral layer and form links through directly coordinated water molecules to the three charge-bearing surface oxygens coordinated to Al^{3+}, so that

in these water molecules the OH_a groups absorb at 3150-3500 cm^{-1}. As the substitution of Si by Al is only one in eight, the other three directly coordinated water molecules are unlikely to find charged surface oxygens with which to form hydrogen bonds, so that, in most of these molecules, the OH_a groups can form only weak bonds to uncharged oxygens giving the 3630 cm^{-1} band.

In the pyridine complex of Mg-hectorite, (fig. 3H) the constituent silicate layers were better oriented and the 3635 cm^{-1} band increased by 70 % at 45° to the beam. The increase in the 3350-3500 cm^{-1} region was 17-25 % falling to zero at 3200 cm^{-1}. As at least half the surface oxygens can carry charge in hectorite, at least three-quarters of the water molecules coordinated to Mg^{2+} in this mineral will be able to bond directly to charge-bearing oxygens. Consequently, OH_a groups coordinated to charged and uncharged oxygens must combine to absorb near 3630 cm^{-1} : the weaker orientation effect in the 3350-3500 cm^{-1} region is ascribed to a few stronger bonds to oxygens associated with lattice defects other than the predominant octahedral Li-for-Mg substitution. It has already been established [1] that water in outer spheres of coordination in hectorite absorbs at 3630 cm^{-1}, so it can be concluded that water directly coordinated to Mg^{2+} does not form stronger hydrogen bonds to the lattice oxygens than other water molecules in the chain.

LOWER HYDRATES

When the chains of water molecules are shortened by evacuating and heating the samples, the surface charge can no longer be distributed over the maximum number of oxygens, but must be localized on fewer oxygens, some carrying a higher effective

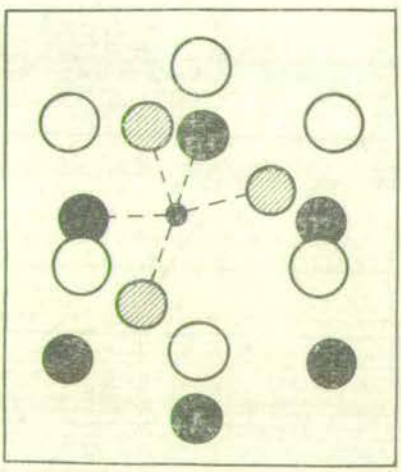

FIG. 4.—Proposed location of exchangeable Mg^{2+} (small filled circle) and H_2O (shaded circles) relative to the upper (open circles) and lower (large filled circles) surface oxygens of the silicate layers. There are four equivalent sites of this type for each opposing pair of hexagonal holes. The hexagons are distorted by rotation of the underlying tetrahedra through ±6°.

charge than in the fully hydrated state. Two distinct phases that are formed in hectorite, saponite, and vermiculite as water is removed from Mg-saturated specimens will be considered here. One of these is an 11.6 Å phase, in which the water content can be reduced to about three molecules per cation, and the second a 10.3 Å phase in which only one H_2O per cation is retained.[13] In hectorite, these phases could be

distinguished by their infra-red spectra, although its thermogravimetric curve did not show such distinct plateaux as did the curves of saponite and vermiculite.

Walker [14] determined the relative position of successive layers in the 11.6 Å phase of vermiculite, but was unable to identify unambiguously the position of interlayer Mg^{2+} and water molecules. He proposed a rather symmetrical structure, in which the Mg^{2+} lies above Al^{3+} in the tetrahedral layer of one sheet and coordinates directly to the three charge-bearing oxygens bound to Al^{3+}. This is a high-energy configuration because of the close approach of Mg^{2+} to Al^{3+}, corresponding to face-sharing between an AlO_4 tetrahedron and an MgO_6 octahedron, a structure which occurs rarely, if at all, in oxides. A more probable configuration is one in which Mg^{2+} coordinates to only two charge-bearing surface oxygens on the lip of a hexagonal hole, and forms links through water to charged sites on the opposing layer. In agreement with this interpretation, a reduction in the effective symmetry of the silicate lattice was indicated by a marked perturbation of the Si—O vibrations of all three minerals when the water content was reduced by evacuation at room temperature, similar to that previously reported for saponite.[13]

Inspection of Walker's structure shows that an Mg^{2+} cation placed so as to co-ordinate to two oxygens on one layer can lie almost directly below the centre of the hexagonal hole in the upper layer (fig. 4). It could then, with three coordinated

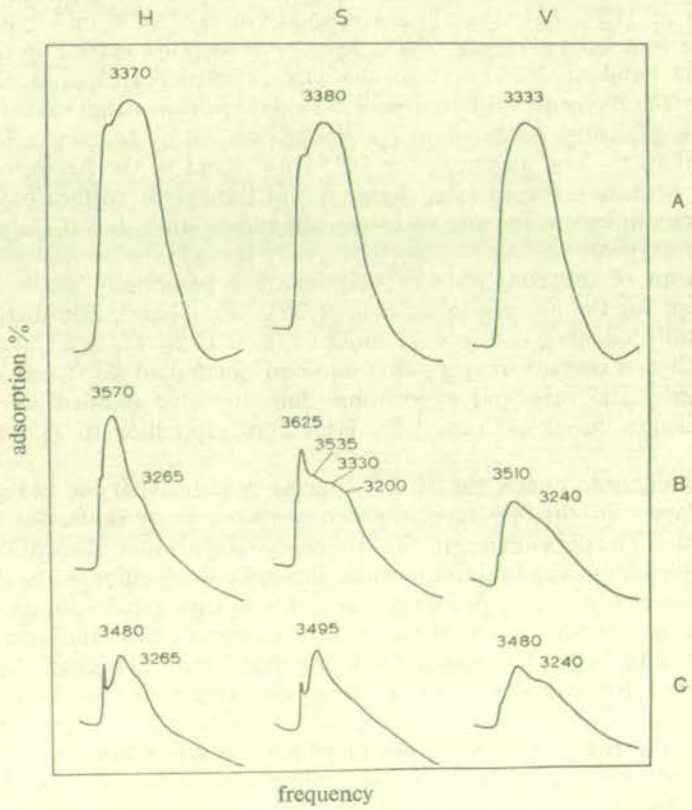

FIG. 5.—OH stretching absorption of H_2O in hectorite (H), saponite (S), and vermiculite (V). A: hydrated at 30 % relative humidity. B: trihydrates formed in vacuum at 30°C for hectorite and saponite, and at 75°C for vermiculite. C: monohydrates formed in vacuum at 150°-220°C. The weak shoulder in hectorite spectra at 3265 cm^{-1} is due to a trace on NH_4^+.

water molecules, form hydrogen bonds to each of the six oxygens round the hexagonal hole in the upper layer.

The infra-red spectra of the trihydrates of hectorite, saponite and vermiculite (fig. 5B) are entirely consistent with this proposed structure. Thus in hectorite, where the charge is widely diffused over the surface oxygens, the hydrogen bonds formed are predominantly weak, giving an OH maximum at 3570 cm^{-1}. A tail to lower frequencies indicates the presence of some stronger hydrogen bonds to oxygens carrying an additional charge. The results are entirely consistent with those obtained from the Mg-hectorite pyridine complex, allowing for the greater localization of charge in the trihydrate.

The trihydrate of Mg-saponite is distinguished from that of hectorite by absorption at both higher (3625 cm^{-1}) and lower (3330 cm^{-1} and 3200 cm^{-1}) frequencies. The latter must be ascribed to hydrogen bonds to oxygens of Al—O—Si linkages: a previous suggestion [1] that they might correspond to bonds between water in inner and outer spheres of coordination is excluded by the present observation that these bands show a pronounced increase in intensity (70 %) when the film is turned at 45° to partially polarized radiation, similar to that shown by the higher frequency absorption at 3535-3625 cm^{-1}. Comparison of these H_2O spectra with corresponding spectra of D_2O and HDO showed that the 3200 cm^{-1} band derived its intensity from the overtone of the 1620 cm^{-1} bending vibration, and that the principal absorption in this region of HDO (2450 cm^{-1}) corresponds to the 3330 cm^{-1} band of H_2O, although there was some evidence of a tail to the absorption extending to lower frequencies. The band at 3625 cm^{-1} of the H_2O system corresponds to bonds to uncharged surface oxygens, and that at 3535 cm^{-1} indicates that some oxygens of Si—O—Si linkages carry a weak negative charge induced by contact with oxygens of Al—O—Si linkages. The absence of a 3625 cm^{-1} band in the hectorite trihydrate indicates that here, too, the surface charge is not limited to surface oxygens which are most directly linked to the site of Li-for-Mg substitution, but is distributed over all the surface oxygens.

The spectrum of the trihydrate of vermiculite is essentially similar to that of saponite, except for the absence of a distinct 3635 cm^{-1} band, due to the very low content of totally uncharged oxygens: most oxygens of Si—O—Si linkages will be in contact with one or two oxygens that are coordinated to Al^{3+} and so carry an induced charge. The principal absorption due to water bonded to oxygens of Al—O—Si linkages lies at 2475 cm^{-1} for HDO, corresponding to 3350 cm^{-1} in the OH region.

In the monohydrate phase, the 10.3 Å spacing requires that the hexagonal holes in successive layers are directly superimposed, with the water molecules lying in the cavities formed. The dependence of the frequency of the water absorption bands on the exchangeable cation shows that the water molecule is coordinated to the cation.[13] When the cation is Mg^{2+}, it is probably more closely associated with one layer than with the other, as the separation of the surface oxygens across the interlayer space would lead to long Mg—O bonds (2.26 Å compared with a normal 2.08 Å) if the cation lay midway between them coordinating two oxygens of each layer. Through the water molecule, Mg^{2+} will be able to establish dielectric links with other surface oxygens round the two hexagonal holes in which the water lies. Only two of the links can involve hydrogen bonds, and these will probably form only with two of the four oxygens most distant from the Mg^{2+}. The usual distortion of the hexagonal holes (fig. 4) will bring two of the four oxygens closer to the water molecule, so that the water will have little or no choice of oxygens with which it can form hydrogen bonds.

This postulated structure is generally consistent with spectra obtained for the monohydrates of hectorite, saponite and vermiculite (fig. 5C). All three show a common feature at 3480-3495 cm^{-1}, which can be interpreted as a hydrogen bond to an oxygen of a Si—O—Si linkage. This appears to represent the maximum strength of hydrogen bond which can be formed to such an oxygen under the most highly polarizing conditions. Saponite and vermiculite, unlike hectorite, have a substantial number of stronger hydrogen bonds absorbing below 3400 cm^{-1}, corresponding to bonds to Si—O—Al linkages. In saponite, the absorption extends well below 3000 cm^{-1}, indicating the presence of particularly strong hydrogen bonds, which probably represent the only links between some tetrahedral Al^{3+} sites and the exchangeable cations. Absorption below 3000 cm^{-1} is less pronounced for vermiculite, as here most tetrahedral Al^{3+} will be able to establish two or three short links with an exchangeable cation. One rather surprising observation was that the 3480-95 cm^{-1} band of saponite and vermiculite had its dipole oscillation more nearly parallel to the plane than the absorption at lower frequencies (intensity increases were 25 % and 40 % respectively, with partially polarized radiation). This difference in orientation suggests that water OH groups involved in stronger hydrogen bonds are directed towards *p*-electron clouds which project from the surface oxygens into the hexagonal holes in the oxygen surface, whereas those involved in weaker hydrogen bonds may have the orientation required for optimum interaction with the Mg^{2+} cation.

OXYGEN-OXYGEN DISTANCES

With the information derived from the trihydrate, it is now possible to make a more detailed interpretation of the spectra of fully hydrated Mg-vermiculite. To simplify the discussion, we have converted OD frequencies to equivalent OH frequencies, using a factor of 1.36, and derived the corresponding O—O distances from the graph of Nakamoto *et al.*[15]. The main absorption at normal incidence of the 14.3 Å phase will be due principally to hydrogen-bonds between water in the first and second spheres of co-ordination. Using the HDO results, this corresponds to an O—O distance of 2.83 Å. Bonds between water and the oxygens of the lattice depend on the charge on these oxygens. Judging from D_2O spectra there is a range of hydrogen bond lengths to oxygens of Si—O—Si linkages in vermiculite from 3.05 Å for uncharged oxygens to 2.93 Å for those carrying an induced charge. Bond lengths to Al—O—Si are probably comparable to those found in the trihydrates of saponite and vermiculite, i.e., about 2.81 Å, and this estimate is consistent with the small shift in the main OD maximum for samples placed at 45° to the beam.

The most detailed X-ray examination [16] of the structure of water in vermiculite places all water molecules close to surface oxygens with O—O distances of 2.77-2.85 Å, which is close to our result for the strongest bonds of this type. The closest distances within a water layer between molecules in the first and second spheres of coordination indicated in the X-ray structure are 2.99 Å, considerably longer than the hydrogen-bond distances indicated by the infra-red results. The X-ray analysis, however, treats water in inner and outer spheres as structurally equivalent, and requires a high temperature factor in the (001) plane, indicating that a significant proportion of the molecules are displaced from the modal position. It seems likely that these displaced molecules lie principally in the second sphere of coordination, and are displaced so as to shorten their contacts with inner-sphere water to about 2.83 Å, while still remaining close to oxygen of the lattice.

No structural information is available for Na-vermiculite, nor for the other mineral species. Our results indicate that both water-to-water and water-to-lattice oxygen bonding is weaker for Na-vermiculite than for Mg-vermiculite. In the

fully hydrated phases, almost all bonds to lattice oxygens in hectorite and montmorillonite are long (3.05 Å), and the majority are long in saponite (2.95-3.05). In these minerals, water-water hydrogen bonds average 2.88 Å for Na-saturated specimens and 2.85 Å for Mg-saturated specimens: these distances are close to those indicated by HDO spectra of perchlorate solutions at comparable ion-water ratios.[4]

DISCUSSION

The results obtained here, which point to chains of hydrogen-bonded water molecules linking cations to negatively charged surface oxygens, can be qualitatively explained in terms of atomic dielectric theory. These concepts also account for many of the known hydration properties of layer silicates.

The polarization in a dielectric between two point charges corresponds on the atomic scale to chains of polarized atoms and bonds linking two ions of opposite charge. The more chains of polarization that can be established between the ions, the lower the electrostatic energy. A gap in a chain, corresponding to an ion not in contact with its immediate neighbour, markedly decreases the polarization in the chain and increases the electrostatic energy. Chains of one or more hydrogen-bonded water molecules provide low-energy links between cations and distant negative sites—substantially lower than alternative links through difficultly polarizable Si—O bonds or O—O contacts. Osmotic swelling pressures will tend to increase the hydration and so the separation of the silicate layer, but this will be opposed by the higher electrostatic energies resulting from the longer dielectric chains involved. For the smaller, more polarizing cations, a single water molecule linking the cation to a negative site can be of lower energy than a direct contact, since by this means a close approach is avoided between the cation and the other polyvalent positive ions associated with the negative site.

As a consequence of these factors, potassium in micas and in vermiculite shows no tendency to hydrate. The potassium ions lie in hexagonal holes in the oxygen surface and are coordinated by twelve oxygens, six of which carry a high negative charge, although all carry some; each oxygen is coordinated to two potassium ions. Hydration could establish no further dielectric links between the cation and the negatively charged surface oxygens. In K-saponite, however, only half the hexagonal holes are filled in the anhydrous state, so that some oxygens are coordinated to only one cation, and some to none. Accordingly K-saponite is hydrated, and will rehydrate [13] even after heating to 700°C, since by this means the potassium ion can establish links with surface oxygens that it could not coordinate directly. For similar reasons, K-montmorillonite and K-hectorite are normally hydrated. But in these minerals the surface charge is very widely and flexibly distributed over the surface oxygens, so that the potassium ion can establish chains of polarization through all its directly coordinated oxygens in the anhydrous state. Consequently, and in contrast to saponite, up to 75 % of the layers in K-montmorillonite fail to rehydrate [13, 17] after heating to 400-500°C. A similar effect would be predicted in hectorite and this has now been confirmed: K-hectorite does not rehydrate in air after heating to 500°C, and some layers remain collapsed after glycerol treatment.

The small sodium ion can not establish contact with surface oxygens as effectively as the potassium ion and is hydrated even in vermiculite. In the single water layer phase, each sodium ion will coordinate to surface oxygens on one side and form water bridges to oxygens on the opposite layer, and also to more distant oxygens on either layer. It has been suggested that each sodium ion sits in a hexagonal hole in one oxygen layer, but observations made in the course of the present study show

that this site is not occupied in saponite or vermiculite, as the perturbation of the lattice hydroxyl vibration [11] which would result from a sodium ion in this position was not found. Presumably the sodium ion is mobile, although generally co-ordinated to two or three surface oxgyens at any one time.

At high humidities, Na-vermiculite expands to a double water layer phase, but will not expand further in water. In this phase the sodium ion must be octahedrally coordinated, and can generally link to four or five charged oxygens through directly coordinated water. If the layers were to separate completely each sodium could form single water links to at most three charged surface oxygens. The layers of montmorillonite do separate completely in water when sodium-saturated.[18] Here the chains of water molecules must in any case be more extended than in vermiculite because of the wide distribution of charge, so that there is little difference in energy between the fully dispersed and the two layer phase.

Unlimited swelling in water also occurs with Li-vermiculite,[19] where the tetrahedral coordination of the lithium ion limits the number of direct water links to opposing surfaces in the double-water layer condition, and with propyl- and butylammonium saturated vermiculite,[19] where the bulk of the alkyl chains restricts the number of water links with surface oxygens. Shorter chain amines can lie flat on the surface, while expansion of longer chain amines is prevented by van der Waals interactions between the interpenetrating alkyl chains which stretch out from opposing layers.

None of the layer silicates show unlimited swelling in water when saturated with divalent cations. Mg-vermiculite does not expand beyond a double-water layer, as in this condition it can generally establish direct links with four or five of the six surface oxygens that it must link to. But in montmorillonite, each magnesium ion must establish links with surface oxygens extending over 4.8 unit cells (29 surface oxygens) requiring six chains each of at least four water molecules in the two-layer phase. The maximum swelling in water corresponds to four water layers,[18] in which each directly coordinated water molecule can form hydrogen bonds to two further water molecules in contact with the surface. Thus in this phase, Mg^{2+} can form two-link water chains with twenty-four surface oxygens, and reaches thirty-six oxygens in no more than three-link chains. Separation of the layers would lead to more extended chains. Unlimited expansion of Mg-vermiculite does occur in concentrated solutions of aminoacids,[20] as the dipolar form of the amino acid permits links of low energy to distant surface oxygens.

The differing distributions of charge over surface oxygens can account not only for differences in the hydration properties of layer silicates, but also for differences in the relative stability of their organic complexes.[2] In montmorillonite and hectorite, the wide distribution of charge allows polarization chains to surface oxygens to be established not only through water chains, but also through pyridine and other polarizable aromatic molecules. These molecules can not transmit high polarizations so readily as water molecules, and so do not easily substitute for water directly coordinated to divalent cations, but they do substitute easily for water in outer spheres of coordination where they take up an orientation with their planes almost perpendicular to the layers,[12, 18] allowing C—H groups to interact with surface oxygens. The 14.7 Å phase which pyridine forms with Mg-montmorillonite and hectorite is stable for several days at moderate humidities, and a 23 Å phase can be formed in which almost all links between Mg^{2+} and surface oxygens are established through water-pyridine chains.[1, 12] Pyridine can not so easily transmit the higher polarizations associated with surface oxygens coordinated to aluminium ions, as in saponite, and this mineral does not give a 23 Å phase with pyridine.[12] Even in the

14.7 Å phase it is uncertain that pyridine plays an essential role in the polarization chains, as a significant number of water chains persist; certainly this phase is less stable than that of montmorillonite or hectorite, losing all its pyridine in one day.

In contrast to pyridine and most other aprotic organic molecules, alcohols readily displace directly coordinated water from divalent cations.[2] Since hydrogen-bonded chains of alcohols can not branch, an octahedrally coordinated magnesium ion can establish only six chains of polarization to surface oxygens through the hydroxyl groups of alcohols. It seems necessary, therefore, that dielectric links to surface oxygens are also established through $—OCH_2$-groupings and this would explain, too, the tendency of coordinated alcohol molecules to form hydrogen bonds to other alcohol molecules, rather than directly to surface oxygens, as indicated in the CD_3OD-montmorillonite system [21] by the usual predominance of the lower frequency OH absorption, near 2500 cm^{-1}, over the higher frequency absorption, near 2660 cm^{-1}.

To conclude, a brief comparison will be made between interlamellar solutions in layer silicates and ionic solutions of simpler salts. The existence of discrete hydration states in layer silicates is a cooperative effect resulting from the possibility of almost regular arrays of cations occupying sites of closely similar energy. This cooperative effect is not possible in simple ionic systems until crystallization occurs, but the concepts developed for layer silicates are equally applicable to solutions. Configurations of cations, water and anions which are stable in layer silicates will also represent minimum energy configurations in ionic solutions at comparable dilution levels: in particular, close analogies might be expected between water in layer silicates and water in perchlorate solutions. In the perchlorate ion, the unit charge is distributed over four surface oxygens; but these oxygens can, because of their exposed position, accept two hydrogen bonds more readily than can the surface oxygens of layer silicates. Thus, their electron-donating potential approaches that of montmorillonite more closely than that of vermiculite. The position of the high frequency band in HDO solutions of perchlorates (2620-2635 cm^{-1}),[4, 5] close to that found in montmorillonite (2660 cm^{-1}) is entirely consistent with the view [3] that it corresponds to water hydroxyls hydrogen-bonded to perchlorate anions.

In the course of the present work, no evidence has been found for broken hydrogen bonds in the water structure of layer silicate, such as Walrafen has postulated for perchlorate solutions.[5] Hydroxyl groups of interlayer water are either involved in water-water bonds, or directed towards oxygens of the silicate lattice, even to uncharged oxygens when the proportion of charge-bearing oxygens is low, as in saponite.

At present there is considerable uncertainty as to whether a water molecule coordinated to a cation can also accept a hydrogen bond from another water molecule. The results presented here for the trihydrate of Mg-hectorite and for the magnesium-water-pyridine complexes show that no such hydrogen bonds exist in the first sphere of coordination round Mg^{2+}. On the other hand, the finding that water-water hydrogen bonds are as strong in Cs-montmorillonite as in Na-montmorillonite shows that the polarization of water in the two systems is similar. It seems necessary, therefore, to assume that water coordinated to Cs^+ can also accept a hydrogen bond, so that it is polarized as much as when coordinated to Na^+.

In addition to analogies between aqueous ionic solutions and hydrated layer silicates, it would be reasonable to expect analogies also for corresponding non-aqueous systems, and for mixed solvent systems. Here we will mention only Mg^{2+}-water-pyridine systems, where pyridine is restricted to the second sphere of coordination both in bulk solution [22, 23] and in layer silicates. The limited ability of directly

coordinated pyridine to transmit high polarizations to molecules in a second sphere of coordination seems a sufficient explanation in both case. In contrast, alcohols, dimethyl sulphoxide, and dimethylformamide can associate strongly in chains, and so readily enter the first coordination shell in competition with water.[24]

The authors thank Mr. A. P. Thomson for X-ray data, and Mr. A. C. Birnie for thermogravimetric data.

[1] V. C. Farmer and J. D. Russell, *Clays Clay Miner.*, 1967, **15**, 121.
[2] V. C. Farmer, *Soil Sci.*, 1971, in press.
[3] K. A. Hartman, *J. Phys. Chem.*, 1966, **70**, 277.
[4] P. Dryjanski and Z. Kecki, *Rocz. Chem.*, 1969, **43**, 1053.
[5] G. E. Walrafen, *J. Chem. Phys.*, 1970, **52**, 4176.
[6] R. A. Leonard, *Soil Sci. Soc. Amer. Proc.*, 1970, **34**, 339.
[7] D. M. Anderson and R. C. Reynolds, *Amer. Mineralogist*, 1967, **51**, 1443.
[8] C. S. Ross and S. B. Hendricks, *Prof. Pap. U.S. Geol. Surv.*, 1945, 205B.
[9] R. C. Mackenzie, *Mineral. Mag.*, 1957, **31**, 672.
[10] W. W. Smith Aitken, *Mineral Mag.*, 1965, **35**, 151.
[11] V. C. Farmer, *Clay Miner.*, 1968, **7**, 373.
[12] V. C. Farmer and M. M. Mortland, *J. Chem. Soc. A*, 1966, 344.
[13] J. D. Russell and V. C. Farmer, *Clay Miner. Bull.*, 1964, **5**, 443.
[14] G. F. Walker, *Clays Clay Miner.*, 1956, **4**, 101.
[15] K. Nakamoto, M. Margoshes and R. E. Rundle, *J. Amer. Chem. Soc.*, 1955, **77**, 6480.
[16] H. Shirozu and S. W. Bailey, *Am. Mineralogist.*, 1966, **51**, 1124.
[17] J. L. Martin Vivaldi, D. M. C. MacEwan and M. Rodriquez Gallego in *International Clay Conf.* 1963, ed. I. T. Rosenqvist and P. Graff-Petersen (Pergamon Press, Oxford, 1963) p. 45.
[18] D. M. C. MacEwan in *The X-ray Identification and Crystal Structures of Clay Minerals*, ed. G. Brown, (Mineralogical Society, London, 1961), p. 143.
[19] W. G. Garrett and G. F. Walker, *Clays Clay Miner.*, 1962, **9**, 557.
[20] G. F. Walker and W. G. Garrett, *Nature*, 1961, **191**, 1389.
[21] Yu. I. Tarasevich and F. D. Ovcharenko, *Dokl. Akad. Nauk. S.S.S.R.*, 1969, **187**. 372.
[22] W. K. Thompson, *J. Chem. Soc.*, 1964, 4028.
[23] A. Fratiello and E. G. Christie, *Trans. Faraday Soc.*, 1965, **61**, 306.
[24] A. D. Pethybridge and J. E. Prue, *Ann. Rep. A*, 1968, **65**. 129.

PRINTED IN GREAT BRITAIN AT
THE UNIVERSITY PRESS
ABERDEEN

(*Reprinted from Nature Physical Science, Vol.* 235, *No.* 53, *pp.* 13–14, *January* 3, 1972)

Reaction of Silica Gel with a Volatile Boron Compound released from Borosilicate Glass

DURING a study of the sorption of *n*-butanol and methanol vapours on silica gels[1] in a vacuum system the formation of a by-product, identified as a silica–boron complex, was observed when the reaction was carried out in 'Pyrex' glassware. This by-product was not formed in a silica vessel and it was therefore concluded that the 'Pyrex' glassware was the source of the boron. Vacuum systems and techniques similar to those employed in this investigation are widely used in studying adsorption on oxide surfaces. It is thus important that workers in this field should be aware of the possible contamination of substrates by a volatile boron compound, and the consequent modification of the surface properties of the oxides.

The vacuum system comprised two interconnected flasks (each 50 cm^3), one for the sample and the other for the alcohol. The flasks had been washed thoroughly with hot distilled water. The gel samples were prepared as films by spreading 7 mg of powder, well ground by hand and heated to 500° C in air, over an area of 1 cm^2 and pressing at 1 t cm^{-2}. The films were contained in an aluminium holder with a 2 mm × 10 mm aperture and were placed in the sample flask in such a way that direct contact of the gel with the glass surface was avoided. The flask was heated to 140° C, evacuated to 10^{-4} torr and then exposed to the vapour from the liquid. The gel was exposed to the vapour overnight at 140° C and the physically adsorbed vapours were removed by evacuating again to 10^{-4} torr.

When films exposed to methanol vapour were analysed spectrographically (arc emission) using boron-free graphite electrodes they were found to contain up to 5,000 p.p.m. boron in the part of the material directly exposed to the vapour. Untreated films showed no detectable boron. The infrared spectrum of the films after exposure to alcohol or water vapour showed a strong band near 7.2 μm (Fig. 1) whose intensity increased in the order water, butanol, methanol (the order of increasing solubility of B_2O_3 in these solvents). The spectra of films treated in a silica reaction vessel did not show the 7.2 μm band. This observation, and the fact that the amount of boron released from the heated sample flask decreased with

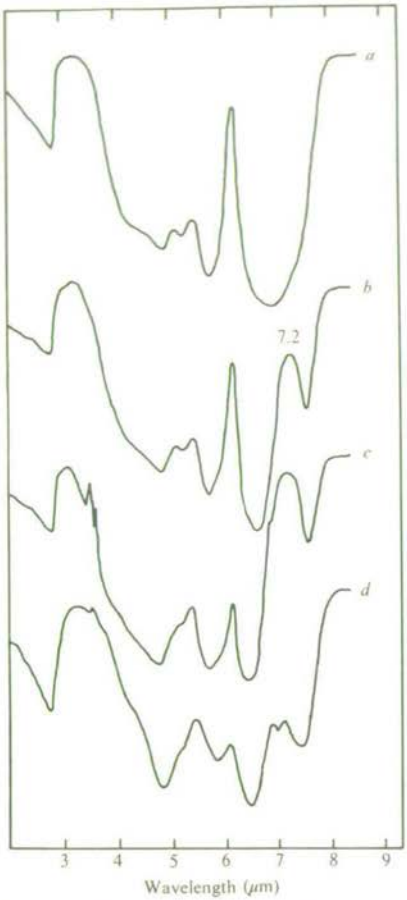

Fig. 1 Infrared spectrum of silica–boron complex. *a*, Fresh silica gel (pressed to a film); *b*, after water vapour treatment; *c*, after methanol vapour treatment; *d*, flushing with dry ammonia gas following methanol vapour treatment.

usage, shows that only the heated 'Pyrex' surface released boron. It is known that the volatility of oxides such as B_2O_3 is increased by the presence of water vapour at elevated temperatures and the species in the vapour phase is probably either metaboric acid BO(OH) or boric acid $B(OH)_3$. In the presence of alcohols, the acid will be esterified forming BO(OR) or $B(OR)_3$.

The 7.2 μm band can be ascribed to a surface group containing boron in three-fold coordination[2], probably resulting from condensation with silanol groups

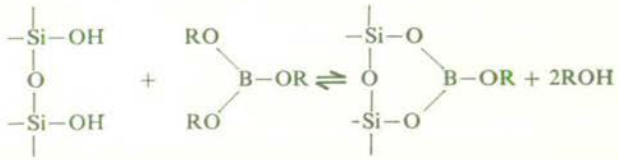

Where R = H, methyl or n-butyl.

The silica–boron complex was unstable in water vapour, being partially hydrolysed at 80% RH and more completely in the presence of HCl gas or liquid water. The extent to which the complex forms, as shown by the intensity of the 7.2 μm band, increases with the specific surface area of the silica gel used (Table 1). The small contents of Na and K in the gels

Table 1 Relative Intensities (RI) of the 7.2 μm Band of Silica Gels with Differing Specific Surface Area

Preparation	Specific surface area ($m^2\ g^{-1}$)	RI	Na (%)	K (%)
Hydrolysis of tetraethyl silicate[3]	663	5	0.006	0.010
Precipitation of Na-silicate	423	4	0.024	0.006
'Aerosil' flame hydrolysis of $SiCl_4$	200	2.9	0.007	0.10

(Table 1) indicate that these ions are not involved in the formation of the complex.

The position of the 7.2 μm band, and therefore also the state of coordination of the boron, remained unchanged when the boron-rich films were heated in air to 1,000° C and the intensity of the band was only slightly reduced. This remarkable thermal stability can be explained by the transformation of the silica–boric acid ester into a borosilicate glass when the temperature is raised[4]. The intensity of the band was considerably reduced after treatment of the boron-containing silica gel with dry NH_3 gas in a cell similar to that described by Angell and Schaffer[5] (Fig. 1). This drop in intensity was presumably the result of a shift of the absorption to lower frequency, brought about by a change in the coordination number of the boron from 3 to 4 following coordination of an NH_3 molecule

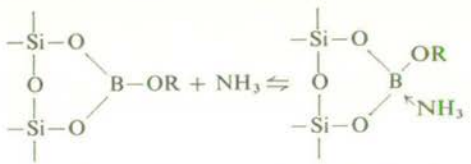

Boron in four-fold coordination[6–8] absorbs between 1,100 and 1,050 cm^{-1}, but no specific band in this region could be

attributed to the complex with NH_3 because of the intense overlying Si—O vibrations.

Mixed silica–alumina gels show almost no reaction with the volatile boric acid, although their surface areas are comparable with those of the silica gels. Their lack of reaction may be ascribed to their lower content of silanol groups[9].

H. HÄNI *
J. D. RUSSELL

The Macaulay Institute for Soil Research,
Craigiebuckler,
Aberdeen

Received October 22; revised December 8, 1971.

* Permanent address: Eidg. Agrikulturchem. Forschungsanstalt, 3097 Liebefeld (BE), Switzerland.

[1] Ballard, C. C., Broge, E. C., Iler, R. K., John, D. S. St, and McWhorther, J. R., *J. Phys. Chem.*, **65**, 20 (1961).
[2] Miller, F. A., and Wilkins, C. H., *Anal. Chem.*, **24**, 1253 (1952).
[3] Leonard, A., Suzuki, Sho, Fripiat, J. J., and De Kimpe, C., *J. Phys. Chem.*, **68**, 2608 (1964).
[4] Plyusnina, I. I., and Kheitonov, Yu. A., *Zh. Strukt. Khim.*, **4**, 555 (1963).
[5] Angell, C. L., and Schaffer, P. C., *J. Phys. Chem.*, **69**, 3463 (1965).
[6] Goulden, J. D. S., *Spectrochim. Acta*, **15**, 657 (1959).
[7] Paterson, W. G., and Onyszchuk, M., *Canad. J. Chem.*, **39**, 986 (1961).
[8] Aknmanova, M. V., and Kurilchikova, G. E., *Optics Spectrosc.*, **8**, 264 (1960).
[9] Fripiat, J. J., *Bull. Grpe. fr. Argiles*, **9**, 23 (1957).

Printed in Great Britain by Flarepath Printers Limited, Watling Street, Colney Street, St. Albans, Herts.

Clay Minerals (1972) **9**, 263.

INTERACTION OF AMMONIA WITH VERMICULITE

J. L. AHLRICHS,* A. R. FRASER AND J. D. RUSSELL

The Macaulay Institute for Soil Research, Craigiebuckler, Aberdeen

(*Received* 5 *September* 1971)

ABSTRACT: The interaction of ammonia with Na−, NH_4−, Ca−, Cu−, and Mg− forms of two vermiculites has been investigated by infrared spectroscopy and chemical analysis. Both NH_4 ions and co-ordinated NH_3 are produced in the interlayer space in amounts which depend on the exchangeable cation and the particle size of the vermiculite. With the exception of that in Cu-vermiculite, the co-ordinated NH_3 is rapidly displaced by atmospheric water vapour. NH_4 ions are slowly decomposed at normal humidity and more rapidly and completely at high humidity. The co-ordinated NH_3 in Cu-vermiculite is converted to NH_4. Relative amounts of NH_4 and co-ordinated NH_3 are influenced by particle size, smaller particles favouring NH_4. The stabilities of both species to water vapour increase with particle size.

INTRODUCTION

The interaction of ammonia with inorganic soil constituents has been the subject of many investigations, reviewed by Mortland (1966). Infrared spectroscopy has been indispensable in identifying the products formed in NH_3-treated clays. Using this technique, both ammonium ion and ammonia co-ordinated to exchangeable cations have been identified in montmorillonite and saponite; the relative amounts and stabilities of these species were shown to be a function of the mineral and the exchangeable cations (Russell, 1965). Since Mortland *et al.* (1963) observed only NH_4 in NH_3-treated vermiculite, and it was postulated (Mortland, 1966) that the NH_4 would be unavailable, it seemed worthwhile to re-investigate the NH_3-vermiculite system, considering also the effect of particle size and physical form of the specimens on the products and their stability.

MATERIALS AND METHODS

The vermiculites used were from Loch Scye, Caithness (Aitken, 1965) and from Llano County, Texas. The latter specimen had a significantly higher Fe content

* Visiting research worker from Department of Agronomy, Purdue University, Lafayette, Indiana, U.S.A.

than material from the same locality characterized by Shirozu & Bailey (1966). The K content was also high and was reduced from about 6 to 0·1% w/w by refluxing for 1 week in 0·2 M $BaCl_2$ with daily replacement of the solution. Aqueous dispersions (about 1% w/v) of the vermiculites were prepared by the alkylammonium method of Walker & Garrett (1967).

The vermiculites were saturated with Na, NH_4, Ca, Cu and Mg by two methods. In one, the alkylammonium-vermiculite suspensions were washed in the centrifuge with 1 M solutions of the appropriate chorides then water, till they were chloride-free. Films were prepared by drying aqueous suspensions of these homoionic vermiculites on polyethylene sheets on a flat surface. The air-dry films, peeled from the polyethylene, were fragile and open in texture, and will be referred to as 'porous'. In the other method, the alkylammonium-vermiculite suspensions were first dried down on polyethylene sheet then saturated with the appropriate cation by washing with chloride salt solutions followed by water. These films were tough, well-oriented and transparent when peeled off, and will be referred to as 'oriented'

Contents of the various exchange cations are shown in Table 1. The c.e.c. of the Loch Scye and Llano vermiculites would appear to be respectively about 172 and 139 me/100 g air-dry sample, corresponding to 215 and 160 me/100 g ignited material (1000°C, Na saturated). The higher exchangeable cation content of the Cu-vermiculites is thought to be due to adsorption of $(CuOH)^+$ ions.

TABLE 1. Exchangeable cation contents (me/100 g air-dry sample) of homoionic saturations of vermiculite from Loch Scye and Llano

Cation	Loch Scye vermiculite	Llano vermiculite
Na*	172	135
NH_4†	180	143
Ca‡	170	137
Cu§	200	179
Mg¶	174	142

*, Flame emission of HF/H_2SO_4 digested mineral; †, Colorimetrically; ‡, Flame emission, Ca replaced by Mg; §, D.C. arc; ¶, Atomic absorption, Mg replaced by Ca.

The vermiculite films (1–2 mg/cm² and of reasonably uniform thickness) were placed in an evacuable pyrex tube through which anhydrous NH_3 gas was passed at a rate of 300–350 ml/min for 2 h (porous films) or 16 h (oriented films or flakes). The films were then transferred from the tube, either immediately or after evacuation at 0·01 mm Hg for 1 h, to flasks containing concentrated HCl for chemical determination of total N (NH_3 + NH_4^+) by the colorimetric method described by Fraser & Russell (1969). Vermiculite films were also treated with NH_3 at the same flow rate, in an evacuable infrared cell similar to that described by Angell & Schaffer (1965). Infrared spectra of the films were recorded successively in an atmosphere of NH_3, in vacuum following the NH_3 treatment, and in air after exposure of the

films to atmospheric water vapour using a Grubb Parsons S4 double-beam spectrometer, from 5000–1000 cm^{-1} with NaCl optics, and from 4000–2350 cm^{-1} under the higher resolution of a 2500 lines per inch diffraction grating.

Ammonium contents of NH_3-treated films of known weight and area were calculated from the absorbance of the NH_4 deformation vibration at 1430 cm^{-1} using the analysed NH_4-vermiculites as standards.

RESULTS AND INTERPRETATION

The investigation of the interaction between NH_3 and vermiculite was carried out on both porous and oriented films of Loch Scye and Llano vermiculites. Results for the porous films were generally more reproducible.

Infrared absorption spectra indicate that flowing NH_3 displaces H_2O from vermiculite interlayers though not so completely as from montmorillonite or saponite (Russell, 1965). Since NH_4 ions are formed in all the samples, it is pertinent to consider the effect of external conditions on NH_4 ions at exchange sites in NH_4-vermiculite. It has previously been shown that the majority of NH_4 ions in vermiculite are inaccessible to D_2O (Farmer, Russell & Ahlrichs, 1968). Consequently the NH_4 bands at 3250, 3060, 2870 and 1430 cm^{-1} in the spectrum of NH_4-vermiculite

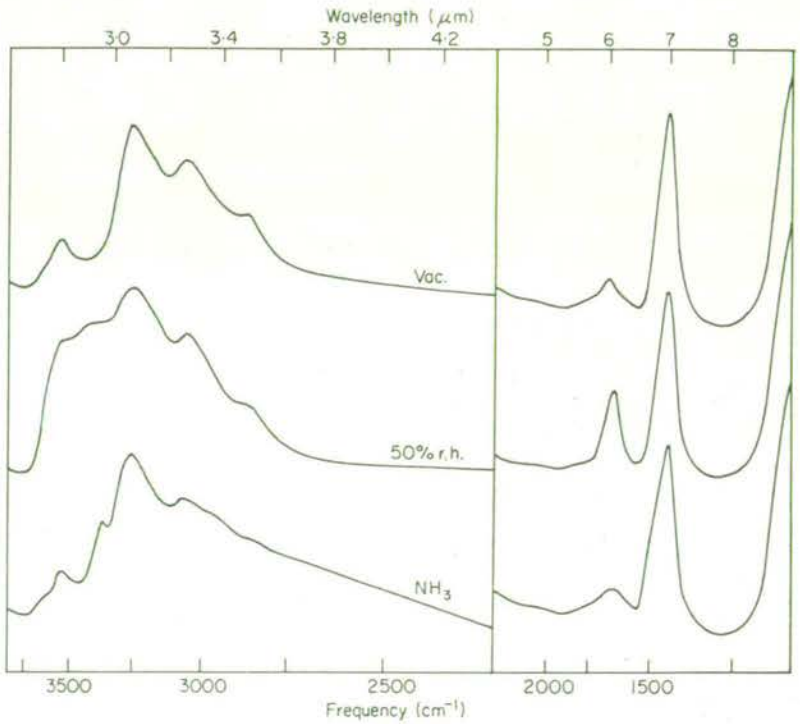

FIG. 1. Infrared absorption spectra of NH_4 – vermiculite (Llano) in vacuum, hydrated in air at about 50% relative humidity, and in dry NH_3 gas.

at 50% r.h., are affected very little on removing under vacuum the water of hydration absorbing at 3400 and 1630 cm^{-1} (Fig. 1). The effect produced by NH_3 on the NH_4 bands although small is more obvious in the spectrum, in the slight weakening of NH_4 bands at 3060 and 2870 cm^{-1}, the appearance of broad absorption below 3000 cm^{-1} and an inflexion near 1500 cm^{-1} (Fig. 1). These new features indicate that in an atmosphere of NH_3 a small proportion of NH_4 ions becomes strongly hydrogen bonded to NH_3 (Russell, 1965; Corset, Huong & Lascombe, 1968b).

Sorption of NH_3

Porous Films. Spectra of Na-, Mg-, Ca- and Cu-vermiculites in NH_3 (broken lines) and in vacuum following NH_3 treatment (full lines Figs. 2 and 3) clearly show that considerable amounts of NH_4 absorbing at 3250, 3080, 2870 and 1430 cm^{-1}

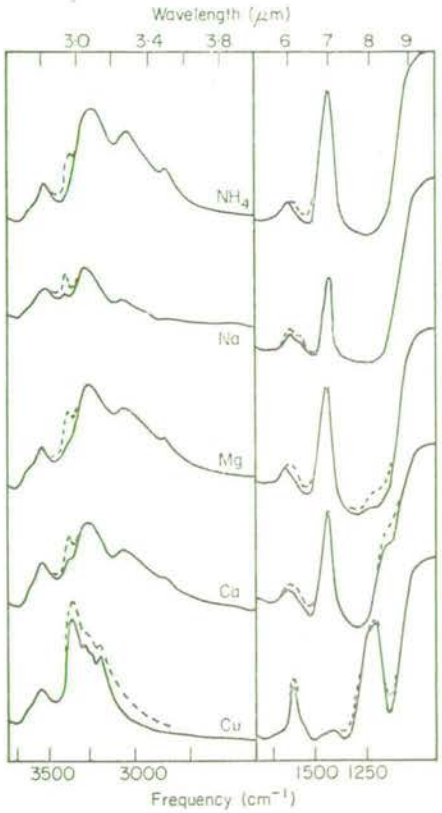

FIG. 2.

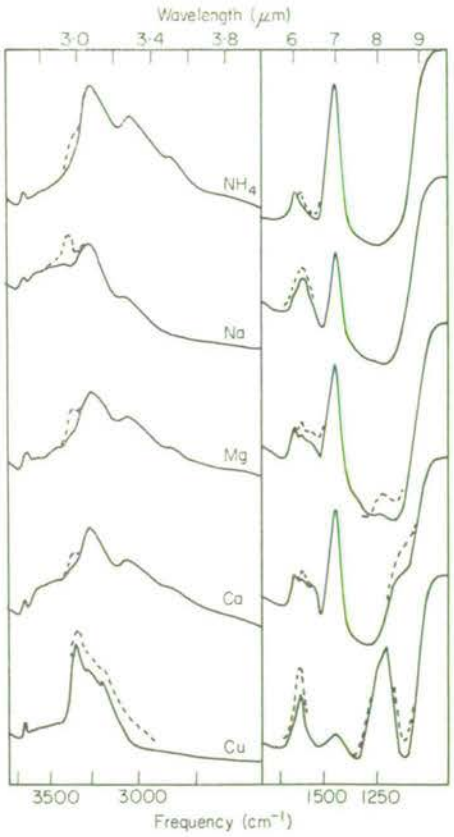

FIG. 3.

FIG. 2. Infrared absorption spectra of Llano vermiculite, saturated with the cations indicated, in dry NH_3 gas (broken curves) and subsequently in vacuum (solid curves).
FIG. 3. Infrared absorption spectra of Loch Scye vermiculite, saturated with the cations indicated, in dry NH_3 gas (broken curves) and subsequently in vacuum (solid curves).

are present in all but the Cu-saturated specimens. The spectrum of NH_4-vermiculite in NH_3 is included for comparison. The amounts of NH_4 formed (Table 2) have been calculated from the absorbance of the 1430 cm^{-1} NH_4 band. Some of the results are similar to those for montmorillonite and saponite (Russell, 1965). With Mg the amount of NH_4 formed approaches the cation exchange capacity, 84% for Loch Scye and 97% for Llano. With Ca, it is about 60% in Loch Scye and 80% in Llano, in agreement more with Ca-montmorillonite (72%) than with Ca-saponite (34%). With Cu the amount of NH_4 formed in vermiculite (6–13 mmol/100 g) is less than that formed in montmorillonite (16 mmol/100 g), but with Na it is up to eight times as high.

In an atmosphere of NH_3, molecular NH_3 co-ordinated to exchangeable metal cations is present in the interlayers for all ion saturations, as shown by the absorption bands near 3370, (3330 for Cu), 1610, and 1150–1230 cm^{-1} (broken lines Figs. 2 and 3). This is substantiated in Cu-vermiculite by the pronounced blue coloration, and by the appearance in the spectrum of bands at 3330, 3270, 3185, 1610 and 1217 cm^{-1}, reasonably close to those quoted for ammino-copper (II) salts (3320, 3250, 3170, 1643, 1287 cm^{-1}; Powell & Sheppard, 1956). In spectra of Mg- and Ca-vermiculites, bands at about 3360–70, 1610, and 1217 cm^{-1} for Mg and 3360–70, 1610, and 1156 cm^{-1} for Ca are assigned to NH_3 co-ordinated to Mg and Ca respectively, in agreement with observations by Russell (1965), and Corset, Huong & Lascombe (1968a). NH_3 is presumably also co-ordinated to Na but the NH_3 band expected at about 1090 cm^{-1} is obscured by intense Si–O vibrations. The considerable decrease in the intensities of 1217 and 1156 cm^{-1} bands on evacuation indicates that much of the ammonia co-ordinated to Mg and Ca is unstable in vacuum. A slight sharpening of the deformation vibration may indicate, as suggested for Ca- and Mg-saponite (Russell, 1965), a decrease in co-ordination number. The stretching band of the NH_3 retained by the Ca- and Mg-vermiculites after evacuation occurs at 3360 cm^{-1} in Loch Scye samples and at 3370 cm^{-1} in Llano samples. These low frequencies suggest that the NH_3 molecules in vermiculite are more strongly hydrogen bonded to surface oxygens than they are in montmorillonite (3400 cm^{-1}) or saponite (3390 cm^{-1}). The increasing strength of hydrogen bonding, montmorillonite $<$ saponite $<$ vermiculite, follows the increasing extent of tetrahedrally-derived negative charge. Ammonia retained by Na-vermiculites absorbs at 3390 cm^{-1}, some 20–30 cm^{-1} higher than the NH_3 retained by Ca and Mg. A similar, though less marked effect was observed in saponite, where, in Na-saponite, NH_3 absorbed at 3395 cm^{-1} compared with 3390 cm^{-1} for Mg. No such effect occurred in montmorillonite.

Less NH_3 is retained against evacuation by Na-vermiculite than by Na-montmorillonite and Na-saponite; in mmol/100 g, 85 for montmorillonite, 119 for saponite, 21 for Loch Scye, and 48 for Llano vermiculite; in mol NH_3/cation, 1 for montmorillonite and saponite but only 0·1–0·4 for the vermiculites. Whereas in montmorillonite and saponite, the amount of NH_3 retained against evacuation follows the sequence Na $>$ Ca $>$ Mg (Russell, 1965), in both vermiculites the order is Ca $>$ Mg $>$ Na.

Oriented Films. Results for oriented films of the various forms of the two

vermiculites are generally similar to those for the porous films, although the replacement of H_2O by NH_3 is much slower in the oriented films. The principal difference between the two types is that generally the oriented films, irrespective of exchangeable cation, retain more NH_3 against evacuation than do the porous ones. This observation includes the NH_4-vermiculites, the absorption band of NH_3 at 3370 cm^{-1} being easily discernible in spectra of evacuated oriented films: ammoniated porous films of the NH_4-vermiculites retain no NH_3 against evacuation. Less NH_4 is produced in the oriented films for all cationic forms, other than the Llano Cu-sample, in which 40 mmol NH_4/100 g is produced compared with only 6 in the porous film (Table 2). This contrasts sharply with the oriented Loch Scye Cu-sample in which no NH_4 could be detected.

The tendency for Llano vermiculite to retain more NH_3 than the Loch Scye sample is more marked for oriented films.

TABLE 2. Maximum N sorbed following NH_3 treatment, and NH_3 and NH_4 (mmol/100 g sample) retained against evacuation (0.02 mm Hg for 1 h), by porous films of Loch Scye and Llano vermiculites saturated with various exchangeable cations

	Loch Scye vermiculite				Llano vermiculite			
		N held against evacuation				N held against evacuation		
Cation	Maximum N*	NH_3+NH_4†	NH_4‡	NH_3§	Maximum N*	NH_3+NH_4†	NH_4‡	NH_3§
Na	124	80	59	21	155	128	80	48
NH_4	248	214	216	—	348	196	189	7
Ca	212	165	120	45	279	204	114	90
Cu	392	348	13	335	425	350	6	344
Mg	233	194	167	27	340	201	139	62

*, Maximum N was determined colorimetrically on samples immediately after removal from the NH_3 stream; †, NH_3+NH_4 was determined colorimetrically; ‡, NH_4 was estimated from the optical density of the 1430 cm^{-1} infrared absorption band of the NH_4 ion; §, NH_3 was obtained by difference.

Decomposition of NH_4 by water vapour

Porous films. Following ammonia treatment and evacuation to remove physically adsorbed NH_3, vermiculite films were exposed to the laboratory atmosphere (50% r.h.) and their infrared spectra were recorded at intervals. The decomposition of the NH_4 formed in the vermiculites is shown in Fig. 4 (Loch Scye) and Fig. 5 (Llano), NH_4 being calculated from the absorbance of its 1430 cm^{-1} absorption band. The NH_4 initially formed in Loch Scye Ca- and Mg-samples (Fig. 4) decomposes rapidly during the first 24 h and then much more gradually thereafter, with Mg showing greater instability. In the Llano Mg-sample (Fig. 5) decomposition is similar to that in the Loch Scye Mg-sample, but in the Llano Ca-sample, it virtually ceases after 24 h. The NH_4-contents of the vermiculites after 12 days' exposure to 50% r.h. were determined by analysis. Estimates from the 1430 cm^{-1} NH_4 band intensity were within $\pm 10\%$ of the analytical values except for the Ca-vermiculites

for which they were 33% higher and the Cu-vermiculites for which they were 39% lower. The high values in Ca-vermiculites suggest that calcium carbonate, which also absorbs near 1430 cm^{-1}, had been formed. This will be discussed more fully in a later section. The low values in the Cu-vermiculites are due to the presence of co-ordinated NH_3. Excellent agreement (within $\pm 4\%$) was obtained between the total N by analysis and the sum of NH_4 estimated from the 1430 cm^{-1} NH_4 band and co-ordinated NH_3 estimated from its 1217 cm^{-1} band. When the NH_3-treated Cu-systems are exposed to air, spectral changes indicate conversion of co-ordinated NH_3 to NH_4^+ ions. This is a slower, more continuous process in the Llano sample (Fig. 5) than in that from Loch Scye (Fig. 4). The additional NH_4 formed in NH_4-saturated vermiculites is lost rapidly and completely in 2–4 days for the Loch Scye sample, resembling the behaviour of NH_4-montmorillonite, but is incompletely lost from the Llano sample. Again decomposition over 2–4 days is rapid, but ceases after 4 days leaving a stable 10–15 mmol of additional NH_4, a value confirmed by analysis. Of the 73 mmol NH_4 formed in Loch Scye Na-vermiculite, 53 mmol are lost rapidly in 2 days, and only a further 7 after 12 days. This behaviour is again similar to montmorillonite. The Llano Na-sample retains a stable 30–40 mmol NH_4 after 2–3 days.

The stability of the NH_4 formed in vermiculite is lower, the higher the relative humidity of the environment to which the vermiculite is exposed: NH_3-treated Mg-saturated Loch Scye vermiculite films containing some 166 mmol NH_4, lose, after 12 days' exposure, 100 mmol NH_4 at 50% r.h., 120 mmol at 80% r.h., and 140 mmol at 98% r.h.

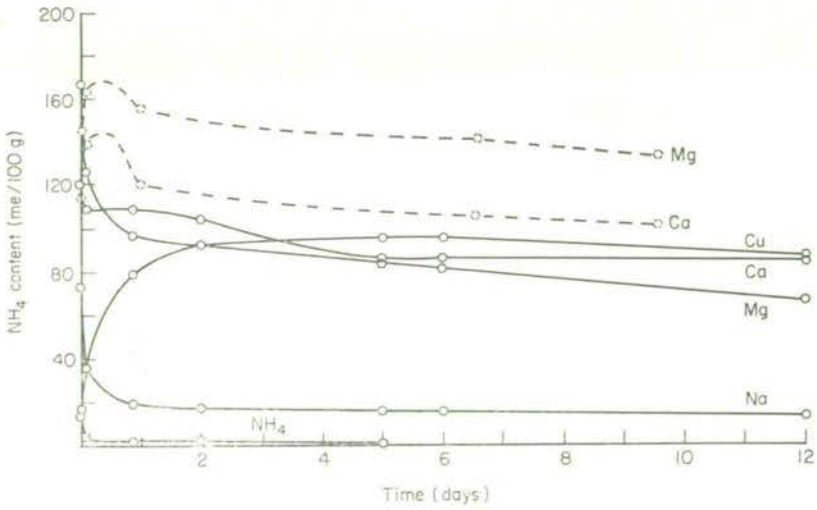

FIG. 4. Decrease, with exposure to air at about 50% relative humidity of the NH_4 formed by NH_3 treatment of porous films (full lines) and oriented films (broken lines) of Loch Scye vermiculite containing the indicated exchange cations. NH_3 content was estimated from the absorbance of the 1430 cm^{-1} infrared absorption band of the NH_4 cation.

Oriented Films. Oriented films of NH_3-treated Ca- and Mg-vermiculites on exposure to air at 50% r.h. show an intitial increase in NH_4 content (broken curves, Figs. 4 and 5). Accompanying changes in the infrared spectrum indicate loss of co-ordinated NH_3 and adsorption of water. Although results were somewhat variable, there is some evidence that the initial increase in NH_4 shown by oriented films of Ca- and Mg-vermiculites only occurs if the flow rate of NH_3 during the initial treatment is high. This produces high levels of co-ordinated NH_3 in preference to NH_4^+. Lower NH_3 flow rates result in higher initial levels of NH_4 which do not increase on exposure to air. The subsequent steady loss of NH_4 from the Ca-vermiculite films after about 1 day's exposure to air is in contrast to the apparent behaviour of the porous films and indicates that very little carbonate is produced. This was substantiated by agreement between NH_4-content from analysis and from the 1430 cm^{-1} band intensity. The stability of the NH_4 formed in Na-vermiculites is greater for oriented than for porous films, presumably due to slower diffusion of molecules and ions in the former.

Effect of CO_2. When porous films of NH_3-treated Ca-vermiculites are exposed to air, NH_4 present is less easily decomposed by water vapour than it is when the films are exposed to CO_2-free air. For example, following NH_3 treatment and evacuation, total $NH_3 + NH_4$ sorbed was 142 mmol/100 g by analysis. After exposure to air at 50% r.h. for 24 h, this value decreased to 107 due mostly to loss of NH_3, but in a CO_2-free atmosphere at the same humidity the NH_4 content fell to 39. Spectra of the films exposed to air show the formation of broad absorption near 1430 cm^{-1} thought to be due to carbonate. No such effects were observed for oriented films of Ca-vermiculite. The reason for this may be linked to the more rapid diffusion of $Ca(OH)_2$ in the porous films to particle edges where reaction

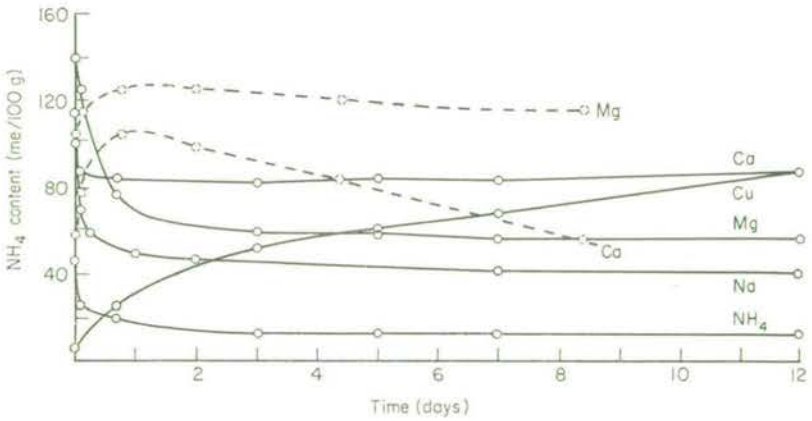

FIG. 5. Decrease, with exposure to air at about 50% relative humidity of the NH_4 formed by NH_3 treatment of porous films (full lines) and oriented films (broken lines) of Llano vermiculite containing the indicated exchange cations. NH_4 content was estimated from the absorbance of the 1430 cm^{-1} infrared absorption band of the NH_4 cation.

with CO_2 can take place. It has previously been shown that the NH_4 formed in Ca-montmorillonite by NH_3 treatment is stabilized when $Ca(OH)_2$ is converted to carbonate in the presence of relatively high levels of CO_2 (Russell, 1965; Du Plessis & Kroontje, 1966).

Effect of particle size on sorption and desorption of NH_3

The infrared spectrum of a large single crystal of hydrobiotite (17 mm diameter disk) following NH_3 treatment is in good qualitative agreement with that of the vermiculite films. Both co-ordinated NH_3 and NH_4 are present, the latter taking about 7 days to reach its maximum value over the whole flake compared with 2–16 h for the films. In contrast, ion exchange was extremely slow when a similar flake was immersed in NH_4Cl solution, the amount of NH_4 introduced even near the edge being substantially less than that formed by NH_3 treatment. The rate of movement of the NH_4 boundary during NH_3 treatment of the large hydrobiotite flake was about 0·4 mm in the first hour.

The NH_4 formed in the large single crystal by NH_3 treatment was stable even after 14 days in water.

A comparison was also made between different forms of Loch Scye Mg-vermiculite. Single crystal flakes (0·15–0·25 mm), oriented and porous films, and <2 μm powder, were treated with flowing NH_3 for 16 h, then the $NH_3 + NH_4$ contents were measured before and after exposure to air at 50% r.h. for 2 h. The flakes and the oriented film contain 200–300 mmol $NH_3 + NH_4$ losing 5% and 30% respectively after 2 h in air. Porous films and powder contain between 150 and 200 mmol $NH_3 + NH_4$ and lose about 30% and 12%. In a separate experiment, flakes were shown to lose over 95% of the $NH_3 + NH_4$ after 15 days at 100% r.h. Although the implications are not absolutely clear, it would appear that oriented films behave like the flakes in sorbing more NH_3 than the porous film or the powder. Comparing the flakes with the powder, it would seem that the sorbed NH_3 is more easily lost from the latter. These observations agree qualitatively with unpublished data (M. H. Stone) on the effect of particle size (1 mm–20 μm) of hydrobiotite on its sorption of NH_3: it was noted that there was a decrease in total NH_3 sorbed (whether as NH_3 or NH_4 or both) with decreasing particle size.

DISCUSSION

The results of the present study establish that NH_4 is formed in vermiculite treated with NH_3 confirming observations by Mortland *et al.* (1963), and that like montmorillonite and saponite (Russell, 1965), vermiculite can absorb NH_3 by co-ordination to exchange cations. The similarity extends to the relative amounts of NH_3 and NH_4 on Ca-, Mg- and Cu-saturated species, but while K- and NH_4-montmorillonite and saponite retain NH_3 against evacuation probably at lattice edges and imperfections, NH_4-vermiculites in the form of porous films do not. The implications are that the vermiculites have fewer structural imperfections or that

the association of NH_3 with such features is weaker than it is in montmorillonite and saponite.

The two vermiculites differ from each other in several respects, but especially in the greater capacity of the Llano specimen to sorb and retain NH_3 (Table 2). The retention appears to have an inverse relationship with cation exchange capacity and, when montmorillonite and saponite are also considered, it attains a maximum value for Ca, Mg, Na and possibly also Li saturations in the c.e.c. range 110–140 me/100 g. This suggests that in this range there may be an optimum balance between the number of interlayer cations and the space available to accommodate NH_3 molecules.

In relation to cation exchange capacity, the levels of formation of NH_4 in Ca-,Mg- and Cu-vermiculites are comparable with those in montmorillonite and slightly higher than those in saponite. But the levels formed in the Na-vermiculites are anomalously high (up to 60% of the c.e.c. in the case of the Llano sample). If the mechanism proposed by Mortland *et al.* (1963), and Mortland & Raman (1968), to account for the formation of NH_4 applies to Na (i.e. $[Na(H_2O)]^+ + NH_3 \rightleftharpoons NaOH + NH_4^+$), the NaOH produced—59 and 80 mmol/100 g for the two vermiculites studied—should migrate to particle edges, and on exposure to air should be converted to Na_2CO_3 which would absorb near 1400 cm^{-1}. There is no spectroscopic evidence for this; the intensity of the 1425 cm^{-1} NH_4 deformation band is consistent with chemical analysis and the band is not broadened; it is difficult to rationalize this with the finding that carbonate is formed in Ca-vermiculite from the less basic $Ca(OH)_2$. High levels of NH_4 and therefore of strong base also, have been reported in Na- and Li-nontronites (Mortland & Raman, 1968), and an explanation was sought in terms of the tetrahedrally derived charge of nontronite producing a stronger polarizing effect on co-ordinated water molecules. But this cannot be the only explanation, since in Na-saponite very low levels of NH_4 are produced.

For the above equilibrium to favour the NH_4 ion, the latter must be effectively removed from the reaction, perhaps by immobilization at sites where it is then inaccessible, due to collapse of the basal spacing on NH_3 treatment. From Figs. 4 and 5 this effect is apparently greater in the Llano specimen, although it is the Loch Scye material which has the greater fixing capacity for K, and also the greater inaccessibility of NH_4 to D_2O. Neither vermiculite contains appreciable F precluding an explanation along the lines proposed by Newman (1969), but it may be that the greater capacity of the Llano vermiculite to trap NH_4 stems from the fact that its NH_4-form is more fully collapsed at normal humidity (d_{001} = 10·5 Å) than is the Loch Scye sample which contains a few layers that are capable of expansion (d_{001} = 11·5 Å).

Contrary to the predictions of Mortland (1966), the additional NH_4 formed in vermiculite is not completely fixed in the interlayers, but undergoes decomposition on exposure to air. At humidities such as might be encountered in soil, the decomposition of NH_4 in porous films of Mg-vermiculite goes almost to completion in about 18 days. The rate of release of NH_4 as NH_3 is approximately 160 mg NH_3

nitrogen/100 g/day, and from oriented films is a more gradual 50 mg/100 g/day over a period of at least 50 days. Small flakes of vermiculite react with NH_3 as completely as clay size material, and in an ammoniated soil could therefore provide a useful reserve of ammonia N for a considerable period. Only in very large flakes does the NH_4 become unavailable, although in this instance the fact that the flakes were of hydrobiotite may explain the increased stability.

ACKNOWLEDGMENTS

The authors would like to thank Dr V. C. Farmer for his continuous interest in the work and M. H. Stone for making his results available.

REFERENCES

AITKEN W.W.S. (1965) *Mineralog. Mag.* **35**, 151.
ANGELL C.L. & SCHAFFER P.C. (1965) *J. phys. Chem., Ithaca*, **69**, 3463.
CORSET J., HUONG P.V. & LASCOMBE J. (1968a) *Spectrochim. Acta*, **24A**, 1385.
CORSET J., HUONG P.V. & LASCOMBE J. (1968b) *Spectrochim. Acta*, **24A**, 2045.
DU PLESSIS M.C.F. & KROONTJE W. (1966) *Proc. Soil Sci. Soc. Am.* **30**, 693.
FARMER V.C., RUSSELL J.D. & AHLRICHS J.L. (1968) *Trans. 9th Int. Conf. Soil Sci., Adelaide*, **3**, 101.
FRASER A.R. & RUSSELL J.D. (1969) *Clay Miner.* **8**, 229.
MORTLAND M.M. (1966) *Agricultural Anhydrous Ammonia*, (M.H. McVickar, W.P. Martin, I.E. Miles and H.H. Tucker, editors), Chap. X, p. 188. Soil Science Society of America. Madison, Wisconsin, U.S.A.
MORTLAND M.M, FRIPIAT J.J., CHAUSSIDON J. & UYTTERHOEVEN J. (1963) *J. phys. Chem., Ithaca*, **67**, 248.
MORTLAND M.M. & RAMAN K.V. (1968) *Clays Clay Miner.* **16**, 393.
NEWMAN A.C.D. (1969) *J. Soil Sci.* **20**, 357.
POWELL D.B. & SHEPPARD N. (1956) *J. chem. Soc.* 3108.
RUSSELL J.D. (1965) *Trans. Faraday Soc.* **61**, 2284.
SHIROZU H. & BAILEY S.W. (1966) *Am. Miner.* **51**, 1124.
WALKER G.F. & GARRETT W.G. (1967) *Science, N.Y.* **156**, 385.

Instrumentation and Techniques

BY

J. D. RUSSELL

Reprinted from THE INFRARED SPECTRA OF MINERALS
Edited by V. C. FARMER (1974) Price £16.00 postage free
ISBN 0 903056 05 4
The Mineralogical Society, 41 Queen's Gate, London, SW7 5HR

Chapter 2

Instrumentation and Techniques

J. D. Russell

It is proposed in this chapter not to list all the available instruments, techniques and procedures used in infrared spectrometry, but to outline, in the light of experience at the Macaulay Institute for Soil Research, what are considered to be the basic instrumental and sample requirements for obtaining meaningful infrared absorption spectra of minerals, and to indicate the type of ancillary equipment which has been found to be most useful in achieving this end. A good extended treatment of the general field of infrared instruments and methods is given in the book edited by Miller and Stace (1972).

INSTRUMENTATION

Commercial infrared spectrometers first became readily available in the mid 1940s and have proliferated greatly since then. The handbook by White (1964), although out of date, contains a good introduction to commercial spectrometers and their capabilities. A more recent listing appears in the book by Stewart (1970). Choice of instrument will always be governed by funds available and specific needs, but in order to obtain good spectra with adequate resolution over a wavelength range capable of giving the best opportunity of characterizing the mineral, the spectrometer should meet certain minimum requirements. These are, that resolution, particularly in the 4000–2000 cm^{-1} region, should be better than 2 cm^{-1} and that the spectra be recorded from 4000 to 400 cm^{-1}, or better still to 200 cm^{-1}. Most spectrometers capable of meeting these requirements employ diffraction gratings as the dispersing elements, and if the coverage is to 200 cm^{-1}, will have facilities for purging the radiation path of water vapour which absorbs strongly below 300 cm^{-1}. For critical work in the range 650–680 cm^{-1} particularly under conditions of low transmission it may be necessary to remove CO_2, which absorbs strongly in this region, from the light path.

It is important that the instrument chosen should have a large and easily accessible sample compartment to accommodate vacuum and high temperature cells, sample holders, attenuators, polarizers and various other attachments necessary in many investigations.

In most spectroscopic investigations, the sample temperature during recording of the spectrum is slightly above ambient (30–40°C). Where it is essential that spectra be recorded with the sample at high temperatures (>200°C), e.g. in phase transition work, interference due to emission by the sample must be overcome. This is achieved by having the radiation-chopping assembly between the sample and the source of radiation, thus ensuring that the unchopped emission from the sample is not amplified by the electronics which are tuned to the chopping frequency.

Conventional grating spectrometers are available to cover the frequency range down to about 20 cm^{-1}. However, with increasing availability of computer facilities, more use is being made of interferometric techniques to scan the frequency range below 700 cm^{-1}. The energy of infrared sources in this region is intrinsically low and in conventional spectrometers is further reduced after dispersion. The interferometric method has the advantage that it is non-dispersive, all of the source energy entering the instrument being available to the detector. As a result, interferometers can more readily achieve higher resolution and undistorted spectra. Ferraro (1971) and Finch *et al.* (1970) outline far infrared instruments available and make some comparisons between interferometers and spectrometers.

The mechanics of recording a spectrum on a modern spectrometer are straightforward but it is essential that the scanning speed is consistent with obtaining photometric and wavenumber accuracy, and that, in regions of the spectrum where sharp absorption bands occur, the scanning speed be slow enough to allow the optimum resolution of the instrument to be realized. For accurate measurement of frequencies of sharp absorption bands, it is necessary to make a point by point scan by hand at regular wavenumber intervals over the maximum, allowing the recording pen time to reach equilibrium at each point, then to interpolate the point of maximum absorption.

In recording spectra and reporting frequencies of absorption bands, it is essential that the instrument is in good optical and electronic condition and that it is calibrated throughout its wavelength range. For most purposes calibration with standard organic substances such as polystyrene film (25 μm thick) and indene containing camphor and cyclohexanone covers most of the wavelength range. For more accurate calibration, water vapour, carbon dioxide, ammonia and other gases can be used. White (1964) makes several recommendations for calibration, some of which have been taken from the I.U.P.A.C. publication "Tables of wavelengths for the calibration of infrared spectrometers" (1961).

TECHNIQUES

Sample preparation

Alkali halide pressed disks. Probably the easiest and most widely used method of preparing a solid sample for IR spectroscopy is that of incorporating it, in a suitable powdered condition, in an alkali halide pressed disk. White (1964) describes the method and its advantages and disadvantages in detail. Fridmann (1967) has recently reviewed and evaluated pelleting techniques generally in infrared spectroscopy. Pressed disks that are formed within a metal sleeve (S_2 in Fig. 2.1) are particularly convenient to handle. Excessive particle size is the major cause of poor-quality spectra and it is of vital importance that the particle size of the sample is reduced to less than about 2 μm otherwise spectra will show distortion of absorption bands and generally low relief. Further detail on the effect of particle size on the absorption spectrum will be found in Chapters 3 and 10. Tuddenham and Lyon (1960) and Farmer and Russell (1966), among others, have discussed the effects of particle

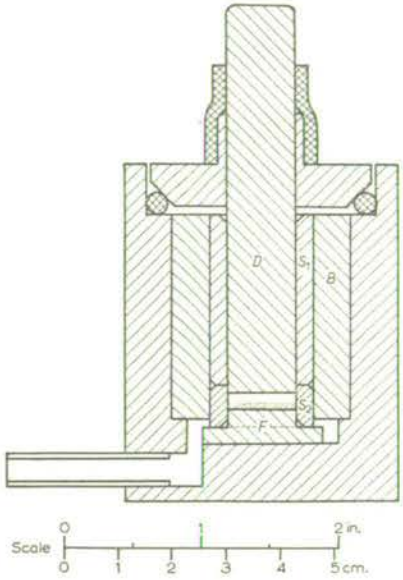

FIG. 2.1. Section of die for preparing pressed disks, from Farmer (1957) by permission.

size on the absorption spectra of minerals. Dry grinding the mineral sample alone can lead to structural modification and, in some cases, to extensive loss of crystallinity (Mackenzie *et al.*, 1956; Farmer, 1958; Dachille and Roy, 1960; Karyakin, 1968; Miller and Oulton, 1970). To overcome this problem the sample is moistened with an inert, volatile, organic liquid such as isopropyl alcohol then ground either by hand or mechanically. Water has also been used successfully and if the sample swells in water (e.g. the smectites) the resultant paste should be freeze-dried to give a product which is ideal for dispersion in an alkali halide disk.

Of the alkali halides, KBr is the most widely used and has proved most generally successful having good transmission down to 250 cm^{-1}. It meets many of the requirements of a good matrix in that it is not too hygroscopic, or soft, has a low sintering pressure and a refractive index that matches those of many minerals. Where a sample has a very low refractive index, KCl might be a more suitable matrix, while for samples of high refractive index, KI or some of the caesium, thallous (Smallwood and Hart, 1963) or silver halides (Spittler and Jaselskis, 1966) would be more suitable. Some of these alternative halides while eminently suitable in terms of refractive index and chemical stability, are difficult to mix and grind, and some difficulty may be experienced in producing good disks.

To prepare a 12 mm diameter KBr pressed disk of a mineral, 0·3–3 mg of the finely particulate sample is added to about 200 mg of the alkali halide in a steel capsule with steel balls and ground and mixed for 2 min on a vibratory grinder. The large excess of halide minimizes structural damage of the sample, and this treatment is usually sufficient to give a uniform mixture which when pressed in an

evacuable die gives a transparent disk. When the disk is of poor quality, either due to inefficient dispersion of the sample or for some other reason, it may be reground by hand, during which the cutting action of halide fragments can aid grinding and sample dispersion, then re-pressed.

White (1964) devotes two sections to sources and pretreatment of KBr for disk preparation and effects of grinding. Our procedure involves selecting a batch of analytical reagent grade KBr which shows minimal IR absorption, apart from that of adsorbed water near 3400 and 1640 cm^{-1} and which contains less than about 0·01% w/w sodium as shown by its failure to form a glucose-NaBr complex when α-D-glucose is incorporated in it (Farmer, 1959). The KBr powder is mechanically ground in an agate mortar for 1·5 h, heated overnight at 550°C, cooled in a desiccator, crushed gently, then stored in a screw-top bottle.

For the routine scanning of the IR spectra of minerals the KBr pressed pellet technique is ideal particularly since the pellets are porous, losing their adsorbed water after heating for several hours at 100°C. It should be pointed out here that the porosity of the KBr disk to H_2O increases with grinding time and that it is intermediate between those of KCl (lower) and KI (higher) (Farmer, 1966). A convenient procedure which we have adopted in work of this kind consists of a rapid check on the intensity of absorption bands, heating disks for 16 h at 100°C followed by cooling in a desiccator then recording the spectrum over the range 4000–2000 cm^{-1}, then 2000–400 cm^{-1}. Re-adsorption by the heated disk of water, whose infrared absorption bands are troublesome round about 3400 cm^{-1}, is sufficiently slow to allow the OH stretching region to be recorded.

Interaction with alkali halide. Disks can be heated to 200°C to remove more strongly held water, but above this temperature, there is a possibility of thermal decomposition of the sample, or interaction between the sample and the alkali halide. The progress of the thermal decomposition of a mineral can be followed very readily in a KBr disk even up to 700°C (Farmer *et al.*, 1968). This is of considerable importance in helping to characterize minerals, from the standpoint of convenience and economy of sample. The transmission of pressed disks is diminished by heating particularly above 200°C but is restored by re-pressing. Some interaction between sample and halide occurs even at room temperature during preparation of disks containing samples which either have exchangeable cations in their structure, e.g. smectites, vermiculites, zeolites, or which are soluble in water, e.g. nitrates and many sulphates. For this latter group of compounds, interaction with the alkali halide can lead to the formation of mixed crystals (Ketelaar and Elsken, 1959; Duyckaerts, 1959), with consequent changes in infrared absorption pattern compared with that of the compound in a mull (see below). White (1964) deals extensively with this and other types of anomalous spectra.

Microdisk methods. In terms of economy of sample the alkali halide pressed disk method is best, requiring only 0·3–3 mg for a normal run and subsequent heating in the disk to elevated temperatures. It is nevertheless possible to obtain adequate spectra of minerals from as little as one tenth of these amounts employing one of the many microdisk techniques available. One that can be used in instruments in

which the sample is mounted at the focus of the infrared beam, and does not require ancillary equipment, involves the incorporation of the mineral (0·1 mg) in KBr and pressing a rectangular pellet whose dimensions are the same as those of the infrared beam at its focus. In this arrangement, all of the sample is irradiated and contributes to the spectrum. Dies which press pellets 5×1 mm^2 are available commercially. Even smaller pellets incorporating a few tens of micrograms of sample can be used in conjunction with beam focusing equipment to yield good spectra.

In the event that interaction between the sample and the alkali halide matrix is suspected and must be avoided, several alternative methods of handling the sample are possible.

Inert pressed disks. An inert disk material such as polyethylene, polytetrafluoroethylene (Teflon), or paraffin wax can, with care, give reasonably transparent disks but they have the disadvantage of having strong absorption bands in the 4000–400 cm^{-1} range. The dehydration of some phosphate minerals was accomplished in Teflon disks. Polyethylene disks are most widely used in the region below 400 cm^{-1}, having only one band at about 70 cm^{-1}. Their preparation requires the sample to be thoroughly preground then simply shaken with polyethylene powder in a steel capsule without balls on a vibratory grinder. A technique involving the cold pressing of samples in a wax disk has been described by Peterkin (1971).

Mulls. An alternative to the disk method of sample preparation, known as the mull technique, was widely used in recording many of the early spectra of minerals and salts (Adler *et al.*, 1951; Miller and Wilkins, 1952) and is essential for hydrated minerals that decompose under vacuum or pressure. It involves grinding the sample thoroughly with an inert oil, such as paraffin oil (nujol), hexachlorobutadiene, or some of the fluorinated hydrocarbon oils such as Fluorolube (Hooker Chem. Corp.). The resultant paste is then squeezed between two alkali halide or other suitable plates. This technique is rapid but is purely qualitative and generally requires more sample than does the KBr disk method. It has the disadvantages of matrix absorption and the inability to subject the sample to thermal treatment. White (1964) gives a well-balanced description of the technique.

Deposits and films. In studies of hydration, dehydration or other reactions involving the surface of a mineral, the limitations of the disk and mull techniques discussed above make it necessary to use alternative methods of sample preparation. One which is frequently used is that of preparing a deposit of the sample as a thin layer on an infrared-transparent window. Minerals with a platy structure like the layer silicates acquire a preferred orientation in such a deposit, having their *c*-axis normal to the plane of the deposit. This gives rise to the possibility of identifying vibrations due to dipole oscillation occurring perpendicular to the plane of the layers, since radiation normal to the layers interacts only with dipoles which have some component of their oscillation parallel to the layers. By tilting the deposit relative to the radiation, vibrations due to dipole oscillations perpendicular to the layers become evident in the spectrum.

Hunt *et al.* (1950) were probably among the first investigators to use this deposit method of sample preparation and applied it with varying degrees of success to a

wide range of minerals and inorganic salts. To prepare deposits of this type, several milligrams of sample are moistened with one or two drops of an alcohol—isopropyl is frequently used—or water, depending on the window material to be used, then thoroughly ground either mechanically or by hand. After dilution to the required concentration, the suspension is pipetted on to the window and, in the case of those in alcohol, stirred with a fine wire until it gels (Farmer, 1958). Evaporation to dryness then gives a deposit of reasonably uniform thickness. Some improvement in uniformity can be achieved by placing a microscope slide on the gel then carefully slipping it off. Deposited films frequently exhibit scattering of infrared radiation. This results in distortion of the background and absorption band contours. Scattering can be reduced dramatically and frequently removed completely by moistening the deposit with a few drops of one of the mulling agents.

When the above method is applied to the expanding layer silicates (smectites and vermiculites) the strong cohesion between particles results in the formation of a deposit which can be peeled from the window to give a self-supporting film which does not scatter infrared radiation. Generally these minerals are very readily dispersed in water and one procedure for making films consists of grinding 5–10 mg of $<2\ \mu$m montmorillonite, for example, with a drop of water in an agate mortar until a smooth paste is obtained. Water is then added up to 1 ml with thorough stirring to give 0·5–1·0% w/v suspensions. A convenient alternative means of efficient dispersion makes use of ultrasonic radiation, treatment for less than 30 s being sufficient for 1 ml of suspension. The suspension is pipetted on to thin polyethylene sheet (100–150 μm) held flat on a glass surface by the capillary action of a drop of water, and allowed to evaporate to dryness overnight at room temperature. This gives a film of about 2·0 to 2·5 cm diameter which can be peeled from the polyethylene by drawing it over a sharp edge. Films of this type, which have been used in IR spectroscopic work for at least 14 years (see for example Serratosa and Bradley, 1958), are strong and easily handled, and when held flat to prevent curling remain whole although brittle even after heating at 700–800°C in air. Serratosa and Bradley (1958) coated heated films with nujol to minimize rehydration. The disadvantage of this procedure is that the coated film cannot be used again. Clay-size vermiculites also respond well to this film-forming procedure, although the films tend to show some scattering of the IR beam. An alternative procedure for this mineral and also for artificially altered micas is that due to Walker and Garrett (1967) using an alkylammonium saturation to achieve dispersion. Films made from such dispersions are of excellent quality and free from scatter, but occasionally may be of such uniform thickness that they display a troublesome interference fringe running through the IR spectrum.

Serratosa and his co-workers (1968, 1970) among others prepare uniform montmorillonite and vermiculite films by filtering a dilute aqueous suspension of the clay through an appropriate micropore filter membrane using a water pump until a deposit of the required thickness, usually 2–5 mg/cm^2, is obtained. When dry, the deposit is removed from the filter membrane to give a self-supporting oriented film. The procedure is a useful one but filtration can be very slow and removal of the film from the membrane is not always easy.

Swoboda and Kunze (1966) sedimented 1% w/v suspensions of montmorillonite on to a fine nylon mesh support for their investigation of the interaction of pyridine with the clay. The mesh support imposes definite limitations on this system from the point of view of possible interaction with the organic vapour present, and instability at high temperatures. Fripiat *et al.* (1960) used a Pt wire mesh as a support for montmorillonite and vermiculite films and also as a heating element.

Pressed pellet. A convenient method frequently used for investigating surface properties of synthetic silica-alumina gels, synthetic zeolites and amorphous silica may also be applicable to natural zeolites and related minerals. It is the method of pelleting the free powder by pressing between polished steel surfaces (McDonald, 1958). The resulting pellets are sufficiently transparent, particularly if the particle size of the powder is about 0·1μm, to enable the OH stretching region to be scanned. They are porous, but less so when compared with the original free powders, as a result of distortion of some sites by the pressure used. This was shown by a lower efficiency of exchange of surface OH groups with D_2O in a pressed pellet of SiO_2 compared with free powder (Hambleton *et al.*, 1965).

Cleaved flakes. Minerals of the mica group which can be cleaved into flakes of suitable thickness can be examined in the IR directly, although such flakes invariably show an interference pattern superimposed on their IR spectrum. Gentle abrasion of one or both surfaces of the flake on a very fine grinding paper is sufficient to destroy the high degree of parallelism of the surfaces of the flake which will then give an interference-free spectrum. In practice, it is not easy to obtain flakes which are sufficiently thin (about 0·1 μm) to allow details of the very intense Si-O vibrations near 1000 cm^{-1} to be observed. Weaker bands such as the OH stretching between 3000 and 3800 cm^{-1} can be studied using flakes of 1–150 μm thickness: for dioctahedral micas, for example, something less than 10 μm would be suitable, whereas for trioctahedral species, anything between 20 and 150μm depending on the number of octahedral vacancies in the structure, would be required. Most of the vibrations below about 500 cm^{-1} should be observable using flakes 1–10 μm thick.

The cleaving of 10–150 μm flakes is relatively simple and is greatly assisted by introducing a drop of water into the partially opened flakes. Flakes 1 to 10 μm thick can be stripped off using adhesive tape. For these very thin flakes, interference fringes are not a problem because of the large frequency interval occupied by one fringe.

Difference spectrometry

A technique occasionally employed in the spectroscopy of minerals is that of recording difference spectra. The general method is described by White (1964) who gives several useful earlier references including one by Willis and Miller (1959). The method consists of cancelling unwanted absorption due to a major phase in the sample by running it against a reference which contains only the major phase. This allows weak absorption due to a minor phase to be observed. Precise cancellation of the major phase is tedious but can be readily achieved using wedge-shaped KBr disks (McCormack *et al.*, 1965).

Wada and Greenland (1970) recorded difference spectra between untreated and variously extracted soil clays in an attempt to characterize the material dissolved during the extraction. They used KBr disks and relied on accurate weighings and good reproducibility in the disk preparation to produce their difference spectra. Weismiller *et al.* (1967) and Ahlrichs (1968) obtained spectra of hydroxyl interlayers by recording difference spectra of montmorillonite films with and without the interlayers. Uncertainties must always exist in these spectra since differences in hydration between the two samples can affect the shape and position of absorption bands. Errors can also arise from changing slit widths, and the low radiation level in regions of intense absorption (Robinson, 1952).

Quantitative spectrometry

The intensity of an absorption band varies with the amount of absorbing material present. Unfortunately this simple statement is complicated by several factors which makes quantitative determination of minerals by infrared spectrometry difficult to achieve in practice. Tuddenham and Lyon (1960) confirmed the findings of Duyckaerts (1959) on the effects of particle size, reproducibility of grinding and disk preparation on the intensity of absorption bands. They also made some important observations on the different degrees of grinding which the component minerals in a mixture undergo depending on their hardness and ease of cleavage. They concluded, that, using carefully controlled methods of sample and disk preparation, they could make reasonably accurate measurements of the amounts of quartz in industrial dusts and of CO_3^{2-} in phosphate rocks. Similarly Flick (1969) obtained good calibration curves for quartz, cristobalite and chrysotile and was able to estimate these minerals in dust samples. As a preliminary to determining the minerals present in coal, Estep *et al.* (1968) made synthetic mixtures of kaolinite, quartz, gypsum, calcite and pyrite and, using bands in the 650–200 cm^{-1} range, were able to determine these minerals with a fair degree of accuracy although, because of overlap of bands, pyrite could not be measured in the presence of high kaolinite contents.

The procedure for quantitative determination of a mineral is relatively simple. An absorption band that is distinctive for the mineral in the system being investigated is selected. Its absorbance is measured by the base-line method which involves drawing a straight line between the points of maximum transmission on each side of the band. A vertical is then erected on this base-line to pass through the point of minimum transmission of the band. The absorbance is then given by the logarithm of the ratio of the transmission of the point on the base line vertically below the peak, to the transmission of the absorption maximum. Uncertainties in the method arise when the base-line is far from horizontal, and when the analytical band is close to another band which is contributing to it. White (1964) devotes a chapter to quantitative work in infrared spectroscopy and deals with many of these problems. To monitor the amount of sample present in the disk it is necessary to weigh sample and KBr accurately, and, after thorough grinding and mixing, then pressing, to reweigh the pressed disk, thus obtaining a measure of the efficiency of transfer of the ground mixture. Alternatively, an inert internal standard (e.g. KCNS) is added to the KBr

to be used in disk preparation, and the ratio of the absorbance of the analytical band to that of the KCNS band at 2125 cm^{-1} is used.

Quantitative work with deposits suffers from all of the shortcomings encountered with disks. For films of reasonably uniform thickness however, it is possible to make some measurements using the weight per unit area of the film or a mineral band as an internal standard to monitor the film. At best, these measurements are only semi-quantitative.

Cells

It is frequently necessary to examine the effect of heating samples in air or in vacuum, or the effect of sorption of gases and vapours in order to obtain information about hydration, thermal stability, surface acidity, etc. Spectral changes arising from the thermal decomposition of a mineral can be of considerable help in the interpretation of reactions observed in differential thermal analysis. For investigations of this type the sample is mounted in some type of vacuum cell. While there are numerous designs available for such a cell, that suggested by Angell and Schaffer (1965) has proved very successful (Fig. 2.2). The sample in the form of a film, either self-supporting or on some IR-transparent substrate, is mounted in a steel ring, placed in the cell, then manoeuvred with the aid of an external bar magnet. With the sample in the side-arm of the cell carrying the windows, spectra can be recorded. The sample can then be transferred to the other arm which is placed in a small tube furnace. This arm can be made of quartz, permitting the sample to be heated to 1000°C. Heating can be combined with evacuation where it is desirable that the sample should not undergo oxidation, or where rehydration is to be avoided. Samples after heating are normally allowed to cool to less than 100°C before transferring them into the side-arm to record spectra. Of considerable advantage is the capacity of this type of cell to accommodate up to five samples simultaneously and still allow them to be fairly easily manipulated. A slight disadvantage of the cell is that the samples are at normal incidence only to the infrared beam. This problem can be overcome using a cell of the design of Uytterhoeven (illustrated by Granquist and Kennedy, 1967) (Fig. 2.3). The sample film is carried on a slider which slots into a groove in a quick-fit stopper. Rotation of the stopper allows the film to be placed at any angle to the radiation. Again, the sample is heated at the end of the cell remote from that carrying the windows; the slider is piston-like and moves gently under gravity in the body of the cell. Only one sample at a time can be examined.

The technique of recording spectra of samples at low temperatures, down to that of liquid nitrogen (−196°C) at least, has become routine with the availability of commercial variable-temperature cells which are easy to operate. One of the most widely used, made by Beckman-RIIC, can give temperatures over the range +250 to −196°C and control them to better than 1°. Low-temperature spectra of several minerals (Schroeder *et al.*, 1962; Ishii *et al.*, 1967) and synthetic aluminate hydrates (Henning and Kaesner, 1968) have been recorded with some surprising results; these include increased intensities, splitting of many bands and a general increase in sharpness. These effects, which occur for systems which are hydrated or contain

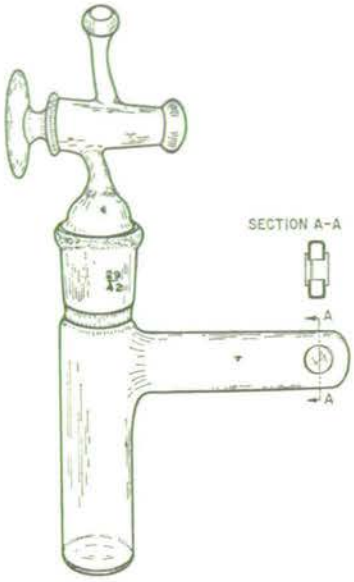

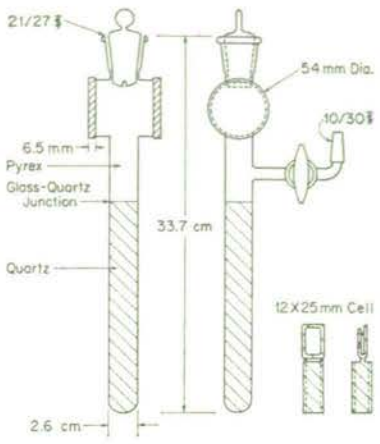

FIG. 2.2 (left). Glass infrared vacuum cell, from Angell and Schaffer (1965) by permission.
FIG. 2.3 (right). Glass/quartz infrared vacuum cell permitting variation in angle of incidence of infrared beam on sample film, from Granquist and Kennedy (1967) by permission.

other hydrogen-bonded hydroxyl groups, may assist in complete vibrational analysis and, equally importantly, they may lead to more positive identification of minerals and types of isomorphous substitution.

Surface studies by IR spectroscopic methods currently form a large part of the literature. A very useful survey of such work has been made by Little (1966). Studies of adsorbed species increasingly involve minerals, particularly clay minerals, such as kaolinites, vermiculites and smectites, and zeolites, but also oxides, e.g. Al_2O_3, TiO_2, SiO_2, and hydroxides. The adsorption of organic and inorganic vapours and gases on such substrates can be carried out in vacuum cells of the type described and the adsorption complex characterized by monitoring spectral changes which result from evacuation, heating, or flushing with another gas or vapour. From observations of this kind, it is possible to establish, for example, the acidity of the mineral surface in terms of its ability to protonate organic or inorganic bases, the existence of Lewis acid sites, coordination to surface cations, etc.

One of the most important contributions that IR spectroscopy can make in mineral studies is in distinguishing ionic hydroxyl groups from molecular water. Both species exhibit OH stretching frequencies in the range 3750–3000 cm^{-1} but only the latter possesses an angle deformation frequency in the 1600 cm^{-1} region. The existence of one or both species can be ascertained quite rapidly after evacuation and heating in one of the cells described. In addition, much useful information on the same topic can be obtained from what has become an almost routine procedure, that of exchange with heavy water (D_2O). Once again, this operation is readily carried out with the

sample (film, deposit or pellet) in one of these cells fitted with water-insoluble windows such as AgCl or one of the series of Irtran windows. After several alternate evacuations and filling with D_2O vapour at room temperature, the spectrum should show complete conversion of accessible hydration water to the D analogue with corresponding low-frequency shifts in OH stretching and angle deformation vibrations. This also makes it possible to differentiate water which for steric or structural reasons is inaccessible to D_2O. In systems in which all of the hydration water is accessible this procedure should result in a spectrum in which ionic OH stretching bands are clearly visible. In the absence of molecular water in or on the mineral structure, it is possible to distinguish ionic OH groups occupying different sites in the structure by their relative ease of exchange with D_2O carried out at successively higher temperatures. Surface OH groups will invariably undergo exchange under relatively mild conditions, whereas internal ionic OH groups may require heating at several hundred degrees centigrade in D_2O vapour for several hours. This procedure has been used to establish the vibrational frequencies of inner and outer OH groups in kaolinite (Ledoux and White, 1964; Wada, 1967), and to identify OH vibrations in a range of smectites (Russell *et al.*, 1970) and in micas (Vedder and Wilkins, 1969; Rouxhet, 1970).

The degree of sophistication in infrared cells for absorption work can be very high and a good example is that illustrated by Little (1966), for the gravimetric determination of the amount of adsorption on to a sample whose IR spectrum can be scanned simultaneously. A similar cell was used by White *et al.* (1967) for the sorption of rare gases on zeolites.

Reflectance methods

While the vast majority of the infrared spectroscopic investigations of minerals use absorption methods, other techniques are available. These measure reflection and emission of IR radiation by the sample. The latter method, although not widely used in mineralogy, has been discussed by Lyon (1962). Reflection methods are of three types, diffuse reflectance, specular reflectance and internal reflectance. In the first, reflectance is from powdered material but results are difficult to interpret because they are partly due to transmission and partly due to reflection, and are also dependent on particle size (Lyon, 1964). In the second type the intensity of the reflectance of IR radiation from a highly polished surface of the specimen is measured. Physicists use this method to obtain refractive indices and absorption coefficients by subjecting the reflectance measurements to mathematical analysis. Spectra, although broadly similar to conventional absorption spectra, differ markedly in many respects particularly for samples whose refractive index, in the vicinity of a strong absorption band, varies widely with wavelength. In spite of problems associated with interpretation Hidalgo and Serratosa (1961) concluded that clay minerals could be readily recognized from their reflection spectra in the 200–650 cm^{-1} region. Lyon (1962) also showed that it was possible to use specular reflection spectra to broadly classify rocks and minerals. His results from powdered specimens pelleted in polymethyl methacrylate were not too encouraging although Aronson *et al.* (1966) obtained a satisfactory

far-IR spectrum of fayalite (Fe_2SiO_4) provided the signal to noise ratio was adequate and the particles were well compacted. Powdered specimens always give reduced spectral contrast and occasionally also give spurious bands. Whether these bands are due to some real effect of particle size or to impurities has not been resolved, but the former cause would seem more likely (see Chapter 3).

The third reflectance technique involves internal reflection or attenuated total reflection (ATR), and evidence from organic samples indicates that ATR spectra are very similar to true absorption spectra. An excellent text on the subject is that by Harrick (1967). The method was originally devised for obtaining spectra of intractable substances but has also proved highly successful with liquids and powders. Good ATR spectra of a quartz-kaolinite mixture (Harrick and Riederman, 1965) and several rocks and minerals including albite and augite (Harrick and Bloxsom, 1966) have been obtained, the samples all being in powder form. From the paucity of ATR spectra of polished surfaces of bulk minerals, or of large single crystals such as mica, it might be inferred that the method does not work well for them and therefore must be considered of limited value. If samples are already in powdered form a straightforward absorption spectrum would be recorded in preference to one by ATR.

Spurious absorption bands

Infrared spectroscopic techniques can be highly sensitive and impurities may be very readily detected. The interpretation of a spectrum must always take account of the possible presence of spurious bands from contaminants picked up during sample preparation and handling. A fairly comprehensive list of such bands and their sources was compiled by Launer (1965) but it is by no means exhaustive: clay minerals, for example, with their large, highly reactive surfaces are prone to adsorption of organic compounds from the vapour phase and can show bands of low to moderate intensity in the regions of 2900 and 1400 cm^{-1} due to C–H stretching and deformation vibrations respectively. Such bands are most frequently observed in spectra of samples subjected to evacuation by rotary pump, and have been interpreted wrongly as arising from strongly hydrogen-bonded water molecules (Jorgensen and Rosenqvist, 1963). Clays containing exchangeable cations or acidic hydroxyl groups readily react with ammonia from the atmosphere, forming ammonium ion which absorbs near 3270 and 1430 cm^{-1}. This kind of contamination can be troublesome and quite widespread since aqueous ammoniacal bases are used in many commercial preparations including floor polish.

A common source of spurious bands is atmospheric water vapour. The bands occur mostly at low transmission due to imbalance between sample and reference beams or to excessively high stray light. The bands appear as weak sharp satellites, either positive or negative, superimposed on absorption bands in the region 3700–3600 cm^{-1}, where lattice OH stretching vibrations of layer silicates occur. Saksena (1964) wrongly interpreted weak bands of this type superimposed on the much broader OH stretching vibration of muscovite as being OH vibrations arising from imperfect crystallinity. Similarly Chukhrov *et al.* (1964, 1965) recorded weak sharp bands in

this area in spectra of allophanes and inferred that they were due to allophane hydroxyls. This problem can be minimized by purging the radiation path, particularly in the monochromator, with water-free air or nitrogen. Bands due to water vapour also occur between 1400 and 1800 cm^{-1}, where they might give rise to inflexions on the 1640 cm^{-1} angle-bending vibration of H_2O or on the CO_3^{2-} or NH_4^+ bands between 1400 and 1500 cm^{-1}.

A band at about 1360 cm^{-1} in the spectrum of a plate of NaCl was ascribed (Launer, 1965) to $NaNO_3$ resulting from interaction between NaCl and N_2O formed at the Nernst filament. The author has observed the occurrence of such a contaminant on the NaCl entrance window of a monochromator. This results in a reduction of available energy at 1360 cm^{-1}, giving rise, in a double-beam instrument, to spectral distortion in this region. Regular examination of the window (perhaps twice a year) is desirable. Gentle lapping with alcohol on velvet is sufficient to remove the contaminant.

REFERENCES

ADLER H.H., KERR P.F., BRAY E.E., STEVENS N.P., HUNT J.M., KELLER W.D. & PICKETT E.E. (1951) Infrared spectra of reference clay minerals. *Am. Petrol. Inst. Research Project 49.*

AHLRICHS J.L. (1968) Hydroxyl stretching frequencies of synthetic Ni-, Al-, and Mg-hydroxy interlayers in expanding clays. *Clays Clay Miner.* **16**, 63–71.

ANGELL C.L. & SCHAFFER P.C. (1965) Infrared spectroscopic investigations of zeolites and adsorbed molecules. *J. phys. Chem.* **69**, 3463–3470.

ARONSON J.R., EMSLIE A.G. & MCLINDEN H.G. (1966) Infrared spectra from fine particulate surfaces. *Science, N.Y.* **152**, 345–346.

CHUKHROV F.V., BERKHIN S.I., ERMILOVA L.P., MOLEVA V.A. & RUDNITSKAYA E.S. (1964) On the problem of allophanes. *Izvest. Akad. Nauk SSSR Ser. Geol.* **29** (4), 3–19.

CHUKHROV F.V., RUDNITSKAYA E.S., MOLEVA V.A. & YERMILOVA L.P. (1965) Phosphate allophanes. *Izvest. Akad. Nauk SSSR Ser. Geol.* **30** (3), 51–57.

DACHILLE F. & ROY R. (1960) High pressure phase transformations in laboratory mechanical mixers and mortars. *Nature, Lond.* **186**, 34 and 71.

DUYCKAERTS G. (1959) The infrared analysis of solid substances—a review. *Analyst, Lond.* **84**, 201–214.

ESTEP P.A., KOVACH J.J. & KARR JR., C. (1968) Quantitative infrared multicomponent determination of minerals occurring in coal. *Analyt. Chem.* **40**, 358–363.

FARMER V.C. (1957) Effects of grinding during the preparation of alkali halide disks. *Spectrochim. Acta* **8**, 374–389.

FARMER V.C. (1958) The infrared spectra of talc, saponite and hectorite. *Miner. Mag.* **31**, 829–845.

FARMER V.C. (1959) Interaction between sugars and alkali halides in pressed disks. *Chemy Ind.* 1306–1307.

FARMER V.C. (1966) Dehydration reactions in alkali halide pressed disks. *Spectrochim. Acta* **22**, 1053–1056.

FARMER V.C. & RUSSELL J.D. (1966) Effects of particle size and structure on the vibrational frequencies of layer silicates. *Spectrochim. Acta* **22**, 389–398.

FARMER V.C., RUSSELL J.D. & AHLRICHS J.L. (1968) Characterization of clay minerals by infrared spectroscopy. *Trans. IX int. Cong. Soil Sci.*, Adelaide, Australia, 1968 **3**, 101–110.

FERRARO J.R. (1971) *Low Frequency Vibrations of Inorganic and Coordination Compounds.* Plenum Press, New York.

FINCH A., GATES P.N., RADCLIFFE K., DICKSON F.N. & BENTLEY F.F. (1970) *Chemical Applications of Far Infrared Spectroscopy.* Academic Press, London.

FLICK K. (1969) Infrared spectrophotometric study of silicotic and asbestos-containing dusts. *Arbeitsschultz, Cologne* **7**, 161–167.

FRIDMANN S.A. (1967) Pelleting techniques in infrared analysis. A review and evaluation. *Prog. Infrared Spectrosc.* **3**, 1–23.

FRIPIAT J.J., CHAUSSIDON J. & TOUILLAUX R. (1960) Study of dehydration of montmorillonite and vermiculite by infrared spectroscopy. *J. phys. Chem.* **64**, 1234–1241.

GRANQUIST W.T. & KENNEDY J.V. (1967) Sorption of water at high temperatures on certain clay mineral surfaces. Correlation with lattice fluoride. *Clays Clay Miner.* **15**, 103–117.

HAMBLETON F.H., HOCKEY J.A. & TAYLOR J.A.G. (1965) An infrared investigation of the effect of pressure on silica powders as revealed by deuterium oxide exchange. *Nature, Lond.* **208**, 138–139.

HARRICK N.J. (1967) *Internal Reflection Spectroscopy*. Interscience Publishers.

HARRICK N.J. & BLOXSOM J.T. (1966) Study programme to obtain the infrared internal reflection spectra of powdered rocks. NASA contract CR-92572.

HARRICK N.J. & RIEDERMAN N.H. (1965) Infrared spectra of powders by means of internal reflection spectrometry. *Spectrochim. Acta* **21**, 2135–2139.

HENNING O. & KAESNER B. (1968) Low-temperature infrared spectra of aluminate hydrates. *Silikattechnik* **19**, 24.

HIDALGO A. & SERRATOSA J.M. (1961) Infrared reflection spectra of clay minerals. *An. R. Soc. esp. Fis. Quim.* **57A**, 225–230.

HUNT J.M., WISHERD M.P. & BONHAM L.C. (1950) Infrared absorption spectra of minerals and other inorganic compounds. *Analyt. Chem.* **22**, 1478–1497.

INT. UNION PURE APPL. CHEM., Commission on molecular structure and spectroscopy (1961) *Tables of Wavenumbers for the Calibration of Infrared Spectrometers*. Butterworths, London.

ISHII M., SHIMANOUCHI T. & NAKAHIRA M. (1967) Far infrared absorption spectra of layer silicates. *Inorg. Chim. Acta* **1**, 387–392.

JORGENSEN P. & ROSENQVIST I.T. (1963) Replacement and bonding conditions for alkali ions and hydrogen in dioctahedral and trioctahedral micas. *Norsk. geol. Tidsskr.* **43**, 497–536.

KARYAKIN A.V. (1968) Methods for preparing samples of inorganic substances for studying various forms of water. *Z. Prikl. Spektrosk.* **8**, 260–262.

KETELAAR J.A.A. & VAN DER ELSKEN J. (1959) Frequency shifts in the infrared absorption spectrum of complex ions in solid solution. *J. chem. Phys.* **30**, 336–337.

LAUNER P.J. (1965) Tracking down spurious bands in infrared analysis. In *Laboratory Methods in Infrared Spectroscopy* (R. G. J. Miller, ed.), pp. 13–17. Heyden, London.

LEDOUX R.L. & WHITE J.L. (1964) Infrared study of selective deuteration of kaolinite and halloysite at room temperature. *Science, N.Y.* **145**, 47–49.

LITTLE L.H. (1966) *Infrared Spectra of Adsorbed Molecules*. Academic Press, London.

LYON R.J.P. (1962) *Evaluation of Infrared Spectrophotometry for Compositional Analysis of Lunar and Planetary Soils*. Stanford Research Institute, California.

LYON R.J.P. (1964) Ibid., *Part II: Rough and Powdered Surfaces*, NASA CR-100.

MACKENZIE R.C., MELDAU R. & FARMER V.C. (1956) Effect of grinding on the crystal structure of micas. *Ber. dt. keram. Ges.* **33**, 222–229.

MCCORMACK H., DEELEY E.L. & TADAYON J. (1965) Compensating infrared spectroscopy. *Nature, Lond.* **207**, 474–476.

MCDONALD R.S. (1958) Surface functionality of amorphous silica by infrared spectroscopy. *J. phys Chem* **62**, 1168–1178.

MILLER F.A. & WILKINS C.H. (1952) Infrared spectra and characteristic frequencies of inorganic ions. *Analyt. Chem.* **24**, 1253–1294.

MILLER J.G. & OULTON T.D. (1970) Prototropy in kaolinite during percussive grinding. *Clays Clay Miner.* **18**, 313–323.

MILLER R.G.T. & STACE B.C. (1972) *Laboratory Methods in Infrared Spectroscopy*, 2nd edn. Heyden, London.

PETERKIN M.E. (1971) Cold pressing solid samples in a wax disk for far infrared analysis. *Appl. Spectrosc.* **25**, 502.

ROBINSON D.Z. (1952) Quantitative analysis with infrared spectrophotometers. Differential analysis. *Analyt. Chem.* **24**, 619–622.

ROUXHET P.G. (1970) Kinetics of dehydroxylation and of OH–OD exchange in macrocrystalline micas. *Am. Miner.* **55**, 841–853.

RUSSELL J.D., FARMER V.C. & VELDE B. (1970) Replacement of OH by OD in layer silicates, and identification of the vibrations of these groups in infrared spectra. *Miner. Mag.* **37**, 869–879.

SAKSENA B.D. (1964) Infrared hydroxyl frequencies of muscovite, phlogopite and biotite micas in relation to their structure. *Trans. Faraday Soc.* **60**, 1715–1725.

SCHROEDER D.A., WEIR C.E. & LIPPINCOTT E.R. (1962) Lattice frequencies and rotational barriers for inorganic carbonates and nitrates from low-temperature infrared spectroscopy. *J. Res. natn. Bur. Stand.* **66A**, 407–434.

SERRATOSA J.M. (1968) Infrared study of benzonitrile–montmorillonite complexes. *Am. Miner.* **53**, 1244–1251.

SERRATOSA J.M. & BRADLEY W.F. (1958) Determination of the orientation of OH bond axes in layer silicates by infrared absorption. *J. phys. Chem.* **62**, 1164–1167.

SERRATOSA J.M., JOHNS W.D. & SHIMOYAMA A. (1970) Infrared study of alkyl-ammonium vermiculite complexes. *Clays Clay Miner.* **18**, 107–113.

SMALLWOOD S.E.F. & HART P.B. (1963) Thallous bromide as a disk material in infrared absorption spectroscopy. *Spectrochim. Acta* **19**, 285–291.

SPITTLER T.M. & JASELSKIS B. (1966) Preparation and use of powdered silver chloride as infrared matrix. *Appl. Spectrosc.* **20**, 251.

STEWART J.E. (1970) *Infrared Spectroscopy: Experimental Methods and Techniques.* Marcel Dekker, New York.

SWOBODA A.R. & KUNZE G.W. (1966) Infrared studies of pyridine adsorbed on montmorillonite surfaces. *Clays Clay Miner.* **13**, 277–288.

TUDDENHAM W.M. & LYON R.J.P. (1960) Infrared techniques in the identification of and measurement of minerals. *Analyt. Chem.* **32**, 1630–1634.

VEDDER W. & WILKINS R.W.T. (1969) Dehydroxylation and rehydroxylation, oxidation and reduction of micas. *Am. Miner.* **54**, 482–509.

WADA K. (1967) A study of hydroxyl groups in kaolin minerals utilizing selective deuteration and infrared spectroscopy. *Clay Miner.* **7**, 51–61.

WADA K. & GREENLAND D.J. (1970) Selective dissolution and differential infrared spectroscopy for characterization of amorphous constituents in soil clays. *Clay Miner.* **8**, 241–254.

WALKER G.F. & GARRETT W.G. (1967) Chemical exfoliation of vermiculite and the production of colloidal dispersions. *Science, N.Y.* **156**, 385–387.

WEISMILLER R.A., AHLRICHS J.L. & WHITE J.L. (1967) Infrared studies of hydroxy-aluminium interlayer material. *Proc. Soil Sci. Soc. Am.* **31**, 459–463.

WHITE J.L., JELLI A.N., ANDRÉ J.M. & FRIPIAT J.J. (1967) Perturbation of OH groups in decationated Y-zeolites by physically adsorbed gases. *Trans. Faraday Soc.* **63**, 461–475.

WHITE R.G. (1964) *Handbook of Industrial Infrared Analysis.* Plenum Press, New York.

WILLIS H.A. & MILLER R.G.J. (1959) Difference spectroscopy in the near infrared. *Spectrochim. Acta* **14**, 119–126.

THE INFRARED SPECTRA OF MINERALS

CONTENTS

Chapter	*Page*
Vibrational Spectroscopy in Mineral Chemistry *By* V. C. FARMER	1
Instrumentation and Techniques *By* J. D. RUSSELL	11
The Interaction of Infrared Radiation with Crystals *By* A. HADNI	27
Symmetry and Crystal Vibrations *By* V. C. FARMER and A. N. LAZAREV	51
The Dynamics of Crystal Lattices *By* A. N. LAZAREV	69
Order-disorder Effects *By* W. B. WHITE	87
Vibrational Spectra and the Crystal-chemical Classification of Minerals *By* H. H. W. MOENKE	111
Raman Spectroscopy of Minerals *By* W. P. GRIFFITH	119
The Vibrations of Protons in Minerals: Hydroxyl, Water and Ammonium *By* YA. I. RYSKIN	137
The Anhydrous Oxide Minerals *By* V. C. FARMER	183
Borates *By* S. D. ROSS	205
The Carbonate Minerals *By* W. B. WHITE	227
Orthosilicates, Pyrosilicates, and other Finite-chain Silicates *By* V. C. FARMER	285
The Common Chain, Ribbon, and Ring Silicates *By* R. G. J. STRENS	305
The Layer Silicates *By* V. C. FARMER	331
Silica, the Three-dimensional Silicates, Borosilicates and Beryllium Silicates *By* H. H. W. MOENKE	365
Phosphates and other Oxy-anions of Group V *By* S. D. ROSS	383
Sulphates and other Oxy-anions of Group VI *By* S. D. ROSS	423
Cements: The Hydrated Silicates and Aluminates *By* O. HENNING	445
Ceramics and Thermal Transformation of Minerals *By* F. FREUND	465
Glasses *By* S. PARKE	483
Appendix : Site Group to Factor Group Correlation Tables *By* V. C. FARMER	515
Indexes	527

Printed in Great Britain by Adlard & Son Ltd.
at the Bartholomew Press, Dorking

(*Reprinted from Nature Physical Science, Vol.* 240, *No.* 104, *pp.* 187–189
December 25, 1972)

Imogolite, a Hydrated Aluminium Silicate of Tubular Structure

IMOGOLITE, a gel-like hydrous aluminium silicate identified in several volcanic ash soils and other weathered pyroclastic deposits, has been shown by electron microscopy[1] to consist of bundles of fine tubes, each about 20 Å in diameter. Electron diffraction patterns[2,3] indicate a repeat distance along the tube axis of 8.4 Å, and a repeat distance perpendicular to this axis of 22 to 23 Å, corresponding to centre-to-centre tube separations. X-ray diffraction patterns are more diffuse, and differ principally in that the highest spacing observed for desiccated material is 18.4 Å. Two empirical formulae have been proposed: $1.5SiO_2 \cdot Al_2O_3 \cdot 2.5H_2O$ (ref. 2) and $1.1SiO_2 \cdot Al_2O_3 \cdot 2.3–2.8H_2O$ (ref. 3); these two papers also advance tentative structures which assign the 8.4 Å repeat distance to a gibbsite-like chain or ribbon, although they differ in the nature of the postulated silicate anion. Neither accounts for the cylindrical structure later established.

In our work, advantage has been taken of a chemical procedure for differentiating silicate anions of low degrees of polymerization, which is based on conversion of the anion to a trimethylsilyl ether and subsequent identification of the volatile ether by gas chromatography[4,5]. Application of this technique to imogolite gave a high yield of volatile products of which 95% was the orthosilicate ether and 5% the pyrosilicate ether; no other ethers were detected. This ratio of ortho to pyrosilicate was higher than that obtained from olivine and other orthosilicates[5]. Application of the

Table 1 Relative Yields of Trimethylsilyl Ethers from Silica-Aluminas

Sample	Ethers derived from			
	SiO_4	Si_2O_7	Si_3O_{10}	Si_4O_{12}
Imogolite	95*	5	0	0
Allophane[11] $0.73\ SiO_2 \cdot 1Al_2O_3 \cdot xH_2O$	120	17	4	2
Silica–alumina precipitate $0.86\ SiO_2 \cdot 1Al_2O_3 \cdot xH_2O$	30	12	5	4
Silica–alumina precipitate $2\ SiO_2 \cdot 1Al_2O_3 \cdot xH_2O$	16	9	5	2

* Areas of gas chromatographic peaks generated from samples, containing equal amounts of silica.

same procedure to two synthetic and one natural hydrated aluminium silicate (allophane) gave higher proportions of di, tri, and tetrasilicate ethers (Table 1). The evidence for an orthosilicate group in imogolite is therefore strong.

Consideration of how an orthosilicate anion might be associated with a gibbsite sheet suggests that one such anion could displace hydrogen from the three hydroxyl groups surrounding a vacant octahedral site (Fig. 1*a*). The fourth Si–O bond would then point away from the sheet and be neutralized by a proton to form SiOH. This structure requires a considerable shortening of the O–O distances round the vacant octahedral site, from about 3.2 Å in gibbsite to less than 3 Å, appropriate to the edges of an SiO_4 tetrahedron. This contraction could account both for the shortening of the repeat distance from 8.6 Å in gibbsite to 8.4 Å in imogolite and also for the curling of the gibbsite sheet to form a tube (Fig. 1*b*). The resulting structure would have a composition $(OH)_3Al_2O_3SiOH$, close to that given by Wada and Yoshinaga[8].

Accordingly three trial structures were constructed on this basis. The resulting cylinders had circumferences of ten, eleven, and twelve gibbsite unit cells, with gibbsite *b* along the circumference and gibbsite *a* parallel to the cylinder axis. The symmetry elements of the cylinders, ignoring translations along their axes, are identical with those of the point groups C_{2nh}, with $n=10$, 11 and 12. The cylinder axes are simultaneously n fold rotation axes, $2n$ fold screw axes with displacement $c/2$, and S_{2n} rotation-reflexion axes: there are mirror planes and reflexion-rotation planes perpendicular to the axes at the levels indicated in Fig. 1. The atomic coordinates for the C_{20h} and C_{24h} structures (Table 2) both give reasonable values for interatomic distances (Table

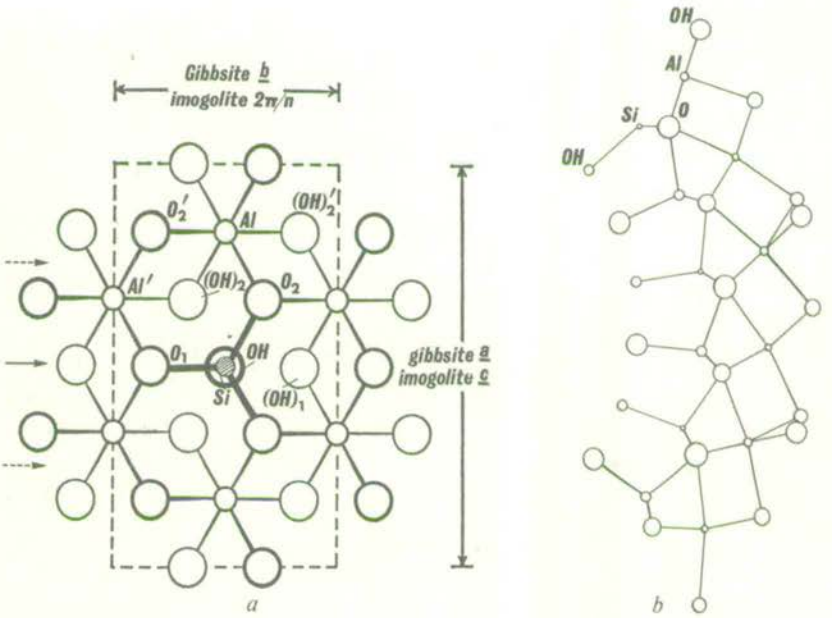

Fig. 1 *a*, Postulated relationship between the structural unit of imogolite and that of gibbsite. SiOH groups which would lie at the cell corners in imogolite have been omitted from the diagram. A reflexion plane (solid arrow, left) and rotation-reflexion planes (broken arrows) are indicated. The atoms are labelled as in Table 2. *b*, Curling of the gibbsite sheet induced by contraction of one surface to accommodate SiO_3OH tetrahedra: projection along the axis (imogolite *c*).

3); the corresponding values for the C_{22h} structure are close to the mean of these. The outside diameters of the cylinders (OH–OH) range from 18.3 Å to 20.2 Å, consistent with interaxial separations of 21 to 23 Å for an aligned array of cylinders.

Table 2 Atomic Cylindrical Coordinates of Tubes with C_{2nh} Symmetry ($n=10$ and 12)

Atom	r (Å)		ψ degree		z (Å)	Symmetry operations for $360°/n$ unit
	C_{20h}	C_{24h}	C_{20h}	C_{24h}		
OH(Si)	4.78	5.74	−1.94	−1.62	0	*a*
Si	6.40	7.36	−1.94	−1.62	0	*a*
O_1	6.97	7.93	11.98	9.99	0	*a*
O_2	6.97	7.93	−6.01	−5.00	1.40	*a*, *b*
Al	8.05	9.01	0.00	0.00	2.70	*a*, *b*
$(OH)_1$	9.13	10.09	−13.73	−11.44	0	*a*
$(OH)_2$	9.13	10.09	7.08	5.92	1.67	*a*, *b*

a: $r'=r;\ \psi'=\psi+180°/n;\ z'=4.2-z$. *b*: $r''=r;\ \psi''=\psi;\ z''=-z$. Operations required to generate cylindrical unit cell: $r'''=r;\ \psi'''=\psi+360°/n;\ z'''=z$. Origin on mirror plane. Centre of symmetry at $r=0$, $z=0$ (n even); $r=0$, $z=\pm 2.10$ (n odd).

Table 3 Interatomic Spacings (Å) in Tubes of C_{20h} and C_{24h} Symmetry

	Atoms	C_{20h}	C_{24h}
SiO_4H	Si-OH	1.62	1.62
	Si-O	1.72; 2 × 1.58	1.65; 2 × 1.58
	O-O	2.80; 2 × 2.59	2.80; 2 × 2.50
	O-OH	2.60; 2 × 2.63	2.58; 2 × 2.63
	OH-OH	3.00	3.00
Gibbsite sheet	Al-O	1.86; 1.90; 2.00	1.83; 1.84; 1.99
	Al-OH	1.83; 1.96; 1.96	1.79; 1.86; 1.94
	O-O *	2.59; 2.59; 2.80	2.50; 2.50; 2.80
	OH-OH *	2.57; 2.93; 2.98	2.57; 2.77; 2.78
	OH-OH †	3.33; 2 × 3.69	3.33; 2 × 3.47
	O-OH ‡	2.59; 2 × 2.53	2.54; 2 × 2.52
	O-OH §	2.79; 2.81; 2.84	2.76; 2.76; 2.80

* Round Al; † round vacancy; ‡ shared edge; § unshared edge.

Fourier transforms of the three structures projected perpendicular to the cylinder axes indicated very similar patterns of scattering intensity. The best overall agreement with a new electron diffraction pattern of imogolite that shows more detail than any previously published (Fig. 2) was obtained for the C_{20h} structure with a b spacing (inter-axial distance) of 23 Å. It will be seen (Fig. 3) that the following salient features of the diffraction pattern are accounted for: first, the intensities of $0k0$ reflexions fall off sharply after $k=5$; second, 071 is the strongest of the $0k1$ reflexions; third, the 002 and 022 reflexions are very weak; fourth, 063 is the strongest of the $0k3$ reflexions; and fifth, 006 is strong.

Fig. 3 represents a projection along the radius with $\Psi=0$.

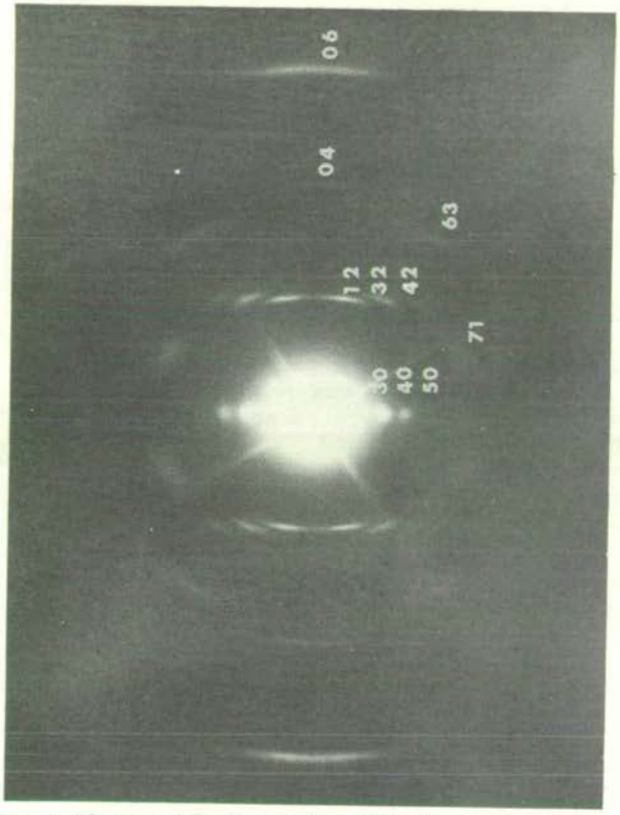

Fig. 2 Electron diffraction pattern (kl indices indicated) from well-oriented imogolite fibres, from the Kitakami pumice bed[3].

Projections along radii with $\Psi=3n^0$ ($n=1$ to 12) gave almost identical predictions for $0kl$ reflexions with l even, but not with l odd; the magnitude of 071 was found to oscillate sinusoidally between ± 150 units and that of 063 between ± 180 units. One additional region of strong scattering not shown in Fig. 3 appeared near 083 (maximum intensity 150 units) where weak diffraction can be seen in the original photograph.

Fourier transforms of projections of the C_{22h} and C_{24h} models gave equally satisfactory agreement with the electron diffraction patterns for all but the 050 and 022 reflexions for interaxial spacings of 22 Å and 23 Å respectively. For both models the predicted intensity of 050 was too low (3 to 12 units) and 022 too high (about 45 units). An increase of the r coordinates in the C_{22h} structure to increase 050 intensity also increased 022 intensity.

Although the structure of C_{20h} symmetry gave the best fit with diffraction data, no claim can be made that it is a closer approach to the true structure than the other two possibilities examined. One apparently unsatisfactory feature of the C_{20h} structure is that the high interaxial spacing (23 Å) requires an OH-OH spacing between cylinders of 5 Å; such a separation is not unreasonable for the hydrated condition, but would be surprising for material dehydrated in the electron microscope. It should be possible to modify the coordinates of any of the three structures considered to be consistent with the diffraction pattern and with direct inter-cylinder contacts, but the limited diffraction data available did not appear to justify further attempts at refinement of the coordinates. The measure of agreement achieved suggests that these structures are correct in principle.

There is also a fair measure of agreement between infrared observations on imogolite and features expected from the proposed structures. Thus the position of the chief Si-O stretching absorption in imogolite, at 930 cm^{-1}, is entirely consistent with the presence of orthosilicate, and the higher frequency peak near 1,000 cm^{-1} is accounted for by the fibrous morphology[2]. The accessibility of all OH groups accounts for their ready exchange with D_2O (refs. 2, 6), and bands which shift on deuteration, near 833 cm^{-1} and 960 cm^{-1}, can be ascribed to bending vibrations of AlOH (ref. 7) and stretching vibrations of Si-OH respectively (compare silica gel[8] where Si-OH lies at 950 cm^{-1}). The position of the chief OH stretching maximum[2] at 3,580 to 3,640 cm^{-1} is consistent both with free AlOH groups on the surface of cylinders (compare the kaolin minerals absorbing at 3,620 to 3,670 cm^{-1}) and also with SiOH groups with O-O separations of about 3 Å (following the correlation of

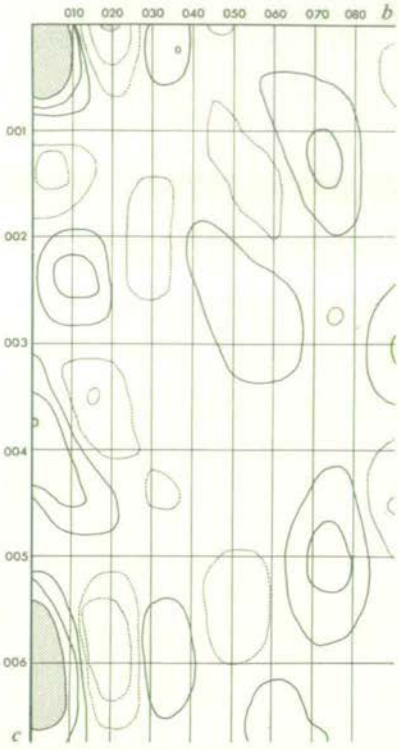

Fig. 3 Fourier transform of a projection of the C_{20h} structure on an $0kl$ reciprocal lattice net drawn for $b=23$ Å, $c=8.4$ Å. Contours at 50, 150 and 300 arbitrary units (>300 shaded); - - -, negative regions; intensity at 000=1,000.

Nakamoto, Margoshes and Rundle[9]). A weak sharp OH absorption at 3,730 cm^{-1} given by the imogolite examined by Russell *et al.*[2] may arise from a silica gel impurity, and this could account for the higher silica content of their material. There is, however, no marked feature near 1,100 cm^{-1} which would be expected if silica gel were present. If this absorption at 3,730 cm^{-1} arises from the SiOH groups of the imogolite, these must be essentially free, and so separated by more than the 3 Å assumed in the trial structures. This could be achieved by expanding the radii of the C_{20h} and C_{22h} structures.

Some support for such expanded structures comes from estimates of the pore volume of imogolite by Wada and Henmi[10]. From absorption studies using quaternary ammonium chlorides, they estimate a central pore diameter

of 9 to 11 Å, and from water absorption data they estimate the volume of this pore to be 0.13 ml. g^{-1} anhydrous clay. If an Si(OH)--H_2O contact of 2.84 Å is assumed, the effective diameter of the central pore in the C_{24h} structure defined in Table 2 is 11.2 Å, and the pore volume 0.10 ml. g^{-1}. Expansion of the C_{20h} structure to the same r coordinates as the C_{24h} structure gives a pore volume of 0.13 ml. g^{-1}. In such a structure, the (Si)OH-OH separation is 3.6 Å, consistent with an (Si)OH stretching frequency of 3,730 cm^{-1}.

P. D. G. Cradwick
V. C. Farmer
J. D. Russell

Macaulay Institute for Soil Research,
Craigiebuckler,
Aberdeen

C. R. Masson

Atlantic Regional Laboratory,
National Research Council of Canada,
Halifax,
Nova Scotia

K. Wada

Faculty of Agriculture,
Kyushu University,
Fukuoka

N. Yoshinaga

Faculty of Agriculture,
Ehime University,
Matsuyama

Received September 25; revised November 13, 1972.

[1] Wada, K., Yoshinaga, N., Yotsumoto, H., Ibe, K., and Aida, S., *Clay Min.*, **8**, 487 (1970).
[2] Russell, J. D., McHardy, W. J., and Fraser, A. R., *Clay Min.*, **8**, 87 (1969).
[3] Wada, K., and Yoshinaga, N., *Amer. Min.*, **54**, 50 (1969).
[4] Götz, J., and Masson, C. R., *J. Chem. Soc. A*, 2683 (1970).
[5] Götz, J., and Masson, C. R., *J. Chem. Soc. A*, 686 (1971).
[6] Wada, K., *Amer. Min.*, **52**, 690 (1967).
[7] Farmer, V. C., *Clay Min.*, **7**, 373 (1968).
[8] Hino, M., and Sato, T., *Bull. Chem. Soc. Japan*, **44**, 33 (1971).
[9] Nakamoto, K., Margoshes, M., and Rundle, R. E., *J. Amer. Chem. Soc.*, **77**, 6480 (1955).
[10] Wada, K., and Henmi, T., *Clay Sci.*, **4**, 127 (1972).
[11] MacKenzie, K. J. D., *Clay Min.*, **8**, 349 (1970).

Printed in Great Britain by Flarepath Printers Ltd., St. Albans, Herts.

Geoderma, 11(1974) 63—66

THERMAL DECOMPOSITION OF PROTEIN IN SOIL ORGANIC MATTER

J.D. RUSSELL[1], A.R. FRASER[1], J.R. WATSON[2,3] and J.W. PARSONS[2]

[1] *Macaulay Institute for Soil Research, Aberdeen (Great Britain)*
[2] *Department of Soil Science, University of Aberdeen (Great Britain)*
[3] *Department of Soil Science and Plant Nutrition, University of Western Australia, Nedlands, W.A. (Australia)*

(Accepted for publication October 25, 1973)

ABSTRACT

Russell, J.D., Fraser, A.R., Watson, J.R. and Parsons, J.W., 1974. Thermal decomposition of protein in soil organic matter. Geoderma, 11: 63—66.

Infrared spectroscopy and nitrogen analyses suggest that secondary amide groups in protein-like components of soil clay-organic complexes and extracted organic matter decompose above 100°C to yield ammonia which is retained as NH_4^+ by acid-washed clay-organic complexes. Above about 400°C, other volatile nitrogenous decomposition products are released. Clay surfaces in the clay-organic complexes may catalyse the decomposition.

During investigations using infrared absorption spectroscopy of soil clay-organic complexes and soil organic matter from surface horizons of several agricultural soils developed on a variety of parent materials, it was observed that absorption bands due to peptide at 1550 cm^{-1} and 1650 cm^{-1} decreased after heating alkali-halide pressed disks of the samples to 200°C (Fig.1). This can be readily interpreted as arising from decomposition of secondary amide linkages in the organic component of the clay-organic complex. With acid-washed complexes the disappearance of secondary amide absorption bands was accompanied by the appearance of NH_4^+ absorbing near 1410 and 3250 cm^{-1} (Fig.1b,c). No ammonia was retained (as NH_4^+) by K^+-saturated clay-organic complexes (Fig.1a), but ammonia was evolved. This was shown when the K^+-saturated complexes were heated for 16 h in a stream of NH_3-free air, ammonia evolved being trapped in 1.5*M* H_2SO_4 and determined by the colorimetric method of Fraser and Russell (1969). Organic matter extracted by formic acid (Watson and Parsons, 1974) behaves similarly to the acid-washed clay-organic complexes on heating (Fig.1d) demonstrating that the clay fraction of the complex, consisting mainly of illite, montmorillonite and kaolinite, was not essential in the decomposition reaction.

Ammonia released by the K^+-saturated clay-organic complex increased rapidly with temperature up to about 230°C, then began to level off at a maximum value about 400°C (Table I). A plot of these data suggests a maximum release

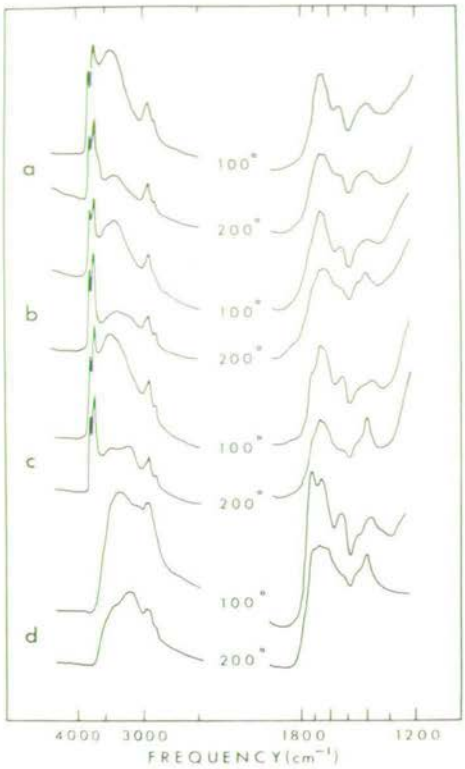

Fig.1. Infrared spectra of KBr disks containing Reading Meadow soil clay (<2 μm) and the organic matter extracted from it by formic acid. Disks heated to 100° and 200°C contained: (a) soil clay — K^+ saturated; (b) soil clay — HF extracted; (c) soil clay — HF/H.COOH extracted; (d) soil organic matter — H.COOH soluble.

TABLE I

Nitrogen liberated from K^+-saturated soil organo-clay complex on heating to various temperatures

Temperature (°C)	N liberated (mequiv./100 g)	
	Total*	NH_3-N**
25	—	—
100	N.D.	3
150	3	5
200	12	11
230	29	28
400	64	33

*Determined on CHN analyser by difference.
**Determined colorimetrically.
N.D. = not determined.

of about 34 mequiv. NH_3/100 g air-dried clay, or 0.48 g N/100 g clay. The reasonable agreement between this value and the content of amino-acid nitrogen in the complex (0.52 g N/100 g: Watson and Parsons, 1974) supports the observations from infrared spectroscopy that the amino-acid residues in protein-like structures decomposed to yield NH_3, and further, that virtually all of this NH_3 was released at 300—400°C. The N remaining in the sample after heating to 400°C was 24 % of that originally present, compared with the residual 15 % found by Schnitzer and Hoffman (1964) in podzolic B_h horizon organic matter after heating at 540°C. These authors made no comment on the type of nitrogenous compounds undergoing decomposition during heating or on the decomposition products. It is clear from Table I that up to 230°C ammonia was virtually the sole nitrogenous decomposition product, but at 400°C about half of the nitrogen was released as other volatile products.

The pattern of NH_3 release described here agrees with that outlined by Kasarda and Black (1968) from mass spectrometry of protein pyrolysis products. These authors considered the appearance of NH_3 as being indicative of protein decomposition and noted that it was detectable above the background at 130—150°C. Ammonia was not identifiable by mass spectrometry in the products of pyrolysis of soils at 600°C (Bracewell, 1971) due presumably to interference by water, and was not observed by gas chromatography of pyrolysed soil organic matter (Wershaw and Bohner, 1969; Kimber and Searle, 1970) as a result of its strong adsorption on the columns. In the present study, ammonia was detected after heating soil clay-organic complexes at 100°C (Table I) suggesting either that the analytical technique used was more sensitive than those described by other authors or that the peptide linkages in the clay-organic complexes were more thermally labile. This instability might be due to catalysis by either silicate surfaces or other inorganic constituents present in the complexes. Although none refers specifically to protein-like components of soil organic matter, there have been several reports on the catalytic effects of clay surfaces (see, e.g., references cited by Mortland, 1970; Arpino and Ourisson, 1971; Durand et al., 1972; Galwey, 1972); however, it has been shown (Juste and Dureau, 1967) that the thermal stabilities of several amino-acids were lower when mixed with the clay fraction of a soil than when mixed with quartz. These authors also found that decomposition of amino-acids by heating was accompanied by a large increase in exchangeable NH_4^+ on the clays.

The determination of NH_3 produced by thermal decomposition of clay-organic complexes may provide a simple means for studying protein-like components in soil organic matter. The formation of ammonia at relatively low temperature may contribute to the increased availability of nitrogen following, for example, steam sterilization of soil or the burning of vegetation or crop residues, many examples of which occur in the literature (see for example Commonw. Bur. Soils Annot. Bibliogr., Nos.794, 804, 825).

REFERENCES

Arpino, P. and Ourisson, G., 1971. Interactions between rock and organic matter. Esterification and transesterification induced in sediments by methanol and ethanol. Anal. Chem., 43: 1656—1657.

Bracewell, J.M., 1971. Characterisation of soils by pyrolysis combined with mass spectrometry. Geoderma, 6: 163—168.

Durand, B., Pelet, R. and Fripiat, J.J., 1972. Alkylammonium decomposition on montmorillonite surfaces in an inert atmosphere. Clays Clay Miner., 20: 21—35.

Fraser, A.R. and Russell, J.D., 1969. A spectrophotometric method for determination of cation-exchange capacity of clay minerals. Clay Miner.,8: 229—230.

Galwey, A.K., 1972. The rate of hydrocarbon desorption from mineral surfaces and the contribution of heterogeneous catalytic-type processes to petroleum genesis. Geochim. Cosmochim. Acta, 36:1115—1130.

Juste, C. and Dureau, P., 1967. Production of ammonia nitrogen by thermal decomposition of amino-acids with a clay-loam soil. C.R. Acad. Sci., Paris, Sér. D, 265: 1167—1169.

Kasarda, D.D. and Black, D.R., 1968. Thermal degradation of proteins studied by mass spectrometry. Biopolymers, 6:1001—1004.

Kimber, R.W.L. and Searle, P.L., 1970. Pyrolysis gas chromatography of soil organic matter. Geoderma, 4:47—71.

Mortland, M.M., 1970. Clay-organic complexes and interactions. Adv. Agron., 22: 75—117.

Schnitzer, M. and Hoffman, I., 1964. Pyrolysis of soil organic matter. Soil Sci. Soc. Am. Proc., 28: 520—525.

Watson, J.R. and Parsons, J.W., 1974. Studies of soil organomineral fractions, II. J. Soil Sci. (in press).

Wershaw, R.L. and Bohner, G.E., 1969. Pyrolysis of humic and fulvic acids. Geochim. Cosmochim. Acta, 33: 757—762.

(Reprinted from Nature, Vol. 248, No. 5445, pp. 220–221, March 15. 1974)

Surface structures of gibbsite goethite and phosphated goethite

INFRARED studies of surface hydroxyls on solids of high area have been limited to almost anhydrous materials prepared at elevated temperatures. These studies have made an important contribution to the understanding of surface catalysis, but have little relevance to adsorption processes that occur on moist surfaces at ambient temperatures. Such processes contribute to a wide range of everyday phenomena, including the retention of fertilisers and pesticides in soils.

Here we establish that the surfaces of the crystalline hydroxides gibbsite (γ-$Al(OH)_3$) and goethite (α-FeOOH), both common soil components, are accessible to infrared study, and that their surface structures are well defined and closely related to their bulk structures. The observation of

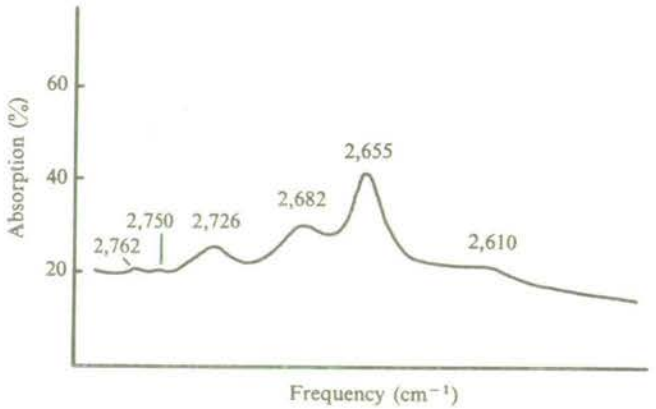

FIG. 1 Infrared absorption of surface Al-OD groups on the (001) face of gibbsite in the form of a polycrystalline film (6.2 mg cm^{-2}). Weak bands at 2,762 and 2,750 cm^{-1} may arise from Si-OD of adsorbed silicic acid; the band at 2,610 cm^{-1} is due to bulk OD.

these surface hydroxyls opens the way to the study of their involvement in surface reactions.

Electron microscope analysis shows the synthetic gibbsite[1] was in the form of thin hexagonal plates of diameter about 250 nm and thickness 9 nm. Their surface consisted principally of (001) faces with a calculated area of 96 $m^2\ g^{-1}$, whereas edge faces represented only 8 $m^2\ g^{-1}$. On evaporation from suspension, this material formed excellent self-supporting films with the crystal plates parallel to the film plane.

The infrared spectrum of this gibbsite is dominated in the 3,000 to 4,000 cm^{-1} region by absorption due to the stretching vibrations of bulk hydroxyl groups, which give bands at 3,622 cm^{-1} and 3,529 cm^{-1} polarised in the (001) plane, and a third at 3,460 cm^{-1} polarised perpendicularly to that plane. Gibbsite consists of infinite planes of close-packed hydroxyl groups parallel to (001), the planes being bound together in pairs by aluminium ions to form a layer structure. Thus the perpendicular 3,460 cm^{-1} band can be correlated with hydrogen bonds between layers (2.82 to 2.87 Å long[2]) and the 3,622 cm^{-1} and 3,529 cm^{-1} bands correspond to longer hydrogen bonds between hydroxyls within the same plane (3.29 Å and 3.13 Å long according to ref. 2; a longer in-plane OH-OH separation of about 3.38 Å probably involves no interaction).

Absorption by these bulk hydroxyls largely obscures the absorption bands of surface Al-OH groups, but a brief (10 s) treatment of a gibbsite film with D_2O followed by evacuation revealed surface Al-OD groups absorbing at 2,726 cm^{-1}, 2,682 cm^{-1} and 2,655 cm^{-1} (Fig. 1), which were lost again immediately on exposing the films to water vapour. The corresponding frequencies of surface Al-OH groups would be

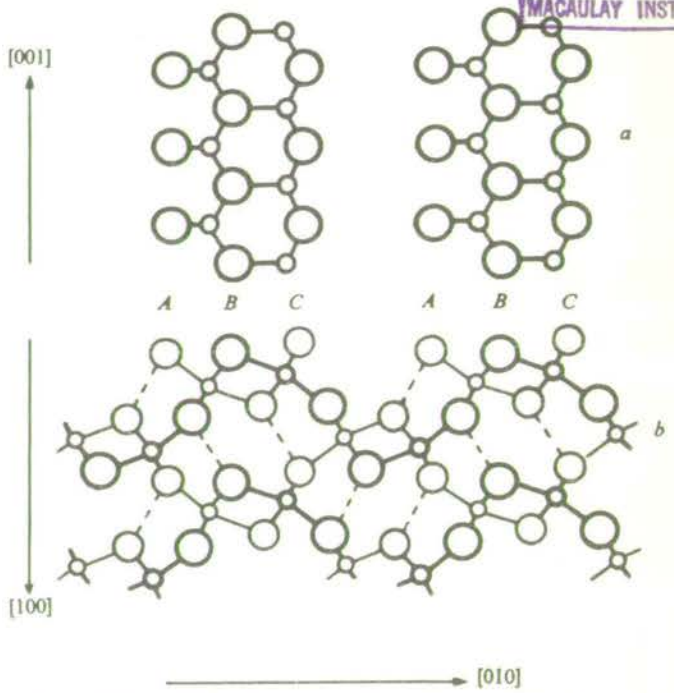

FIG. 2 Plan (*a*) and section (*b*) of the (100) face of goethite (after Bragg and Claringbull[5]).

3,690 cm^{-1}, 3,629 cm^{-1} and 3,588 cm^{-1} but only the first can be seen in evacuated films because of the strong absorption by bulk hydroxyl groups. All three surface absorption bands are polarized in the plane of the layers, so the OH groups that were involved in interlayer bonding within the crystal (absorbing at 3,460 cm^{-1}) must link OH groups within the surface plane, and probably absorb at 3,690 cm^{-1}. This weak interaction leads to a lengthening of other in-plane OH-OH separations, so that hydroxyls that absorb at 3,529 cm^{-1} and 3,622 cm^{-1} within the crystal absorb at 3,588 cm^{-1} and 3,629 cm^{-1} on the surface.

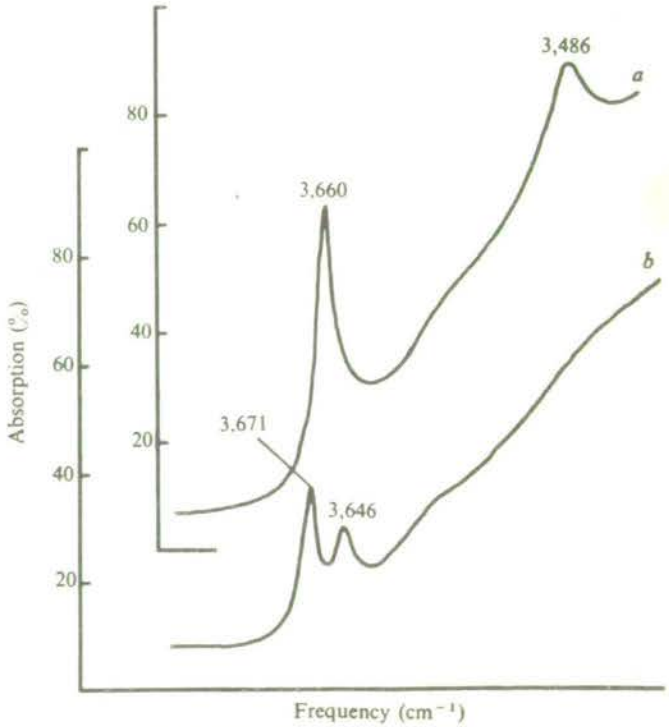

FIG. 3 Infrared absorption of surface OH on: *a*, Goethite; *b*, phosphated goethite. Both in the form of polycrystalline deposits (5.4 mg cm^{-2}).

The synthetic goethite used was prepared as was specimen 1(c) of ref. 3, and, like that specimen, consisted of thin laths with the (100) faces predominant, typically measuring 150 nm in the [001] direction, 30 nm wide and 10 nm thick. The calculated area of the (100) faces is 45 $m^2\ g^{-1}$, with edge planes contributing about 15 $m^2\ g^{-1}$.

The goethite structure (Fig. 2) can be regarded as being built from strips of condensed Fe(O, OH) octahedra, each strip being two octahedra wide. The strips, which are seen in plan in Fig. 2*a*, and in section in Fig. 2*b*, share O^{2-} ions along their edges to give an open structure in which the gaps between the strips are bridged by hydrogen bonds (dashes in Fig. 2*b*) involving OH groups shared between three Fe^{3+} ions. These bulk hydroxyls absorb at 3,145 cm^{-1}. The same hydroxyls (labelled *B* in Fig. 2) are also exposed on the (100) surface together with two new types of hydroxyls (labelled *A* and *C*) which arise from protonation of the oxide ions along the edges of the strips. Of these surface hydroxyls, types *B* and *C* cannot form hydrogen bonds within the surface, since all adjacent hydroxyls are coordinated to a common Fe^{3+} ion, but type *A* hydroxyls, each coordinated to only one Fe^{3+}, can form bonds 3Å long with each other.

In the spectra of films of goethite examined *in vaeuo* (Fig. 3*a*) type *A* hydroxyls absorb at 3,486 cm^{-1} and the non-bonded hydroxyls absorb at 3,660 cm^{-1}. These surface hydroxyls are readily converted to OD, absorbing at 2,700 cm^{-1} and 2,581 cm^{-1}, by brief (1 min) treatment with D_2O, and they interact with adsorbed water when the films are exposed to air, as shown by broadening and displacement of the absorption bands.

Goethite that had been treated with 200 μmol per g H_3PO_4 or NaH_2PO_4 before preparing films showed no absorption due to type *A* hydroxyls (Fig. 3*b*), thus confirming the hypothesis of Atkinson *et al.*[4] that phosphate replaces these hydroxyls, forming bridges between adjacent Fe^{3+}. The spectra also demonstrate an interaction between phosphate and *B* or *C* type hydroxyls, resulting in new bands appearing at 3,671 cm^{-1} and 3,646 cm^{-1}. This could represent the effect of a hydrogen bond between surface $(FeO)_2PO{\cdot}OH$ groups, acting as proton donors, and type *C* hydroxyls. These and other reactions of surface hydroxyl groups on hydroxides are being actively investigated.

We thank Dr W. J. McHardy for electron microscopy and Dr P. D. G. Cradwick for calculating OH-OH separations in gibbsite.

J. D. Russell
R. L. Parfitt*
A. R. Fraser
V. C. Farmer

Department of Spectrochemistry
Macaulay Institute for Soil Research,
Craigiebuckler, Aberdeen

Received December 3, 1973; revised January 28, 1974.

* On study leave from the University of Papua New Guinea, Boroko, Papua New Guinea.

1 Gastuche, M. C., and Herbillon, A., *Bull. Soc. Chim. Fr.*, 1404 (1962).
2 Saalfeld, N., *Neues Jb. Miner. Abh.*, **95**, 1 (1960).
3 Atkinson, R. J., Posner, A. M., and Quirk, J. P., *J. inorg. nucl. Chem.*, **30**, 2371 (1968).
4 Atkinson, R. J., Posner, A. M., and Quirk, J. P., *J. inorg. nucl. Chem.*, **34**, 2201 (1972).
5 Bragg, L., and Claringbull, G. F., *The Crystal Structures of Minerals*. (Bell, London, 1965).

Printed in Great Britain by Henry Ling Ltd., at the Dorset Press, Dorchester, Dorset

Contrib. Mineral. Petrol. 47, 1—6 (1974)

A New Interpretation of the Structure of Disordered α-Cristobalite

M. J. Wilson, J. D. Russell, and J. M. Tait

The Macaulay Institute for Soil Research, Craigiebuckler, Aberdeen, AB9 2QJ

Received May 13, 1974

Abstract. Disordered α-cristobalite which occurs extensively in bentonites, opals and particularly deep-sea cherts, has been previously interpreted in terms of a unidimensionally disordered structure in which cristobalite is interstratified with two-layer tridymite-like sheets. An alternative interpretation is that the structure is essentially tridymitic but that the sheets are stacked with random transverse displacement normal to the *c* axis, an arrangement similar to the translational, turbostratic stacking postulated for smectites. This interpretation was arrived at after a comparitive study of a silica phase in an Italian bentonite and a deep-sea chert, material which yielded an X-ray powder pattern almost identical with that of disordered α-cristobalite, but electron diffraction patterns and infrared spectra more consistent with tridymite. It is suggested that this type of silica, which has been described almost universally as cristobalite, is more appropriately referred to as disordered α-tridymite.

Introduction

Disordered α-cristobalite has been reported as a minor phase in bentonites (Flörke, 1955) and as a major constituent of certain opals (Jones and Segnit, 1971); more recently it has been found extensively in deep-sea cherts (Rex, 1969; Calvert, 1971a and b). The mineral is usually characterized by a simple X-ray powder pattern consisting of a strong, broad reflection at approximately 4.1 Å and a medium reflection at 2.5 Å. The 4.1 Å reflection is often accompanied by a fairly strong peak or shoulder at 4.3 Å. Flörke (1955) explained this diffraction pattern in terms of a unidimensionally disordered α-cristobalite structure in which the layers of SiO_4 tetrahedra, although well ordered, are irregularly stacked in the [111] direction normal to the layers. The three-layer cristobalite structure was thought to contain two-layer tridymite-like sequences, variation in this type of disorder resulting in the broadening and shifting of the strong reflections and in the elimination of the weak ones. On this basis the peaks at 4.1 Å and 2.5 Å in the powder pattern correspond to the 101 and 200 reflections, respectively, of α-cristobalite, whilst the peak at 4.3 Å is attributed to tridymitic domains within the structure. This interpretation seems to have been generally accepted. The object of the present study is to present an alternative interpretation based on the supposition that the structure is, in fact, dominated by tridymitic two-layer sheets which are stacked with random transverse displacement normal to the *c* axis.

Materials and Methods

The two specimens studied in detail were a bentonite and a deep-sea cristobalite chert. The bentonite is from an unknown source in Italy and contains approximately 14 per cent of a

silica phase, which could not be physically separated from the bulk of the montmorillonitic clay. The chert was recovered during the Deep Sea Drilling Project from the Kerguelen Plateau in the Southern Ocean (Eltanin core 47–15) and has been previously extensively studied (Wise *et al.*, 1972; Weaver and Wise, 1972). It is essentially monomineralic and in its morphological and X-ray characteristics is apparently quite typical of deep-sea cristobalite cherts.

The samples were examined by X-ray powder diffraction, electron microscopy and infrared spectroscopy. For X-ray diffraction the samples were mounted in an aluminium holder, powder patterns being recorded by a Philips 2kW diffractometer using iron filtered CoKα radiation. Transmission electron microscope observations and electron-diffraction studies were made using an AEI EM6 instrument, the samples having been ultrasonically dispersed in water and dried down on a carbon-coated copper grid. Infrared spectra (1400–400 cm^{-1}) were recorded on a Grubb-Parsons Spectromaster. Samples were either incorporated in KBr pressed disks (0.3 mg of 1 mg in 170 mg KBr) or sedimented from aqueous suspension and air dried to give self-supporting films (approximately 2 mg/cm^2).

Results

Both samples yield X-ray powder patterns similar to that described above, the most characteristic feature being the broad intense reflection at 4.1 Å. The X-ray diffractometer trace of the chert has been previously illustrated by Wise *et al.* (1972). Under the electron microscope a platy, well-shaped, hexagonal morphology was revealed with individual particles ranging from 0.1 μm to 1 μm in diameter. The flakes in the chert were larger and better formed than those from the bentonite, which were generally clustered together and associated with montmorillonite. A scanning electron microscope study (Weaver and Wise, 1972) has shown that the chert is actually made up of distinctive bladed spherules, individual blades or plates being from 300 to 500 Å thick. Similar spherules have been synthesized by Oehler (1973) who pointed out that the basic platy morphology is characteristic of tridymite and is distinctly different from the octahedral crystal habit of cristobalite.

Electron Diffraction. In both samples the platy particles yield a hexagonal diffraction pattern consistent with tridymite. Diffraction from the plates in the bentonite gives a d-spacing of 8.64 Å (Fig. 1 A) — measured with respect to the diffraction rings of montmorillonite — corresponding to $a_{hex} = 9.98$ Å, in general agreement with the a dimension of low tridymite. In fact, the true cell of α-tridynite is orthorhombic although dimensionally it is pseudohexagonal with $b_0 = a_0\sqrt{3}$. This gives orthorhombic cell parameters of $a = 9.98$ Å and $b = 17.28$ Å, in agreement with the values listed by Frondel (1962). A hexagonal lattice giving a d-spacing of 4.32 Å is shown by the plates from the chert (Fig. 1 B) but additional weaker reflections again indicate doubling to 8.64 Å. It should be noted that cristobalite with (111) parallel to the electron beam would also give a hexagonal diffraction pattern, but when the patterns are interpreted in this way, the calculated cubic cell edge is 6.11 Å which is irreconcilable with either pseudocubic α-cristobalite ($a = 4.97\sqrt{2} = 7.03$ Å) or cubic β-cristobalite ($a = 7.13$ Å). A prominent feature of both diffraction patterns is the streaking between the reflections along the three principal directions in the (001) plane. This streaking can be accounted for by a stacking disorder although in beidellite it has been interpreted as an expression of deformation within the tetrahedral layers (Gatineau *et al.*, 1972).

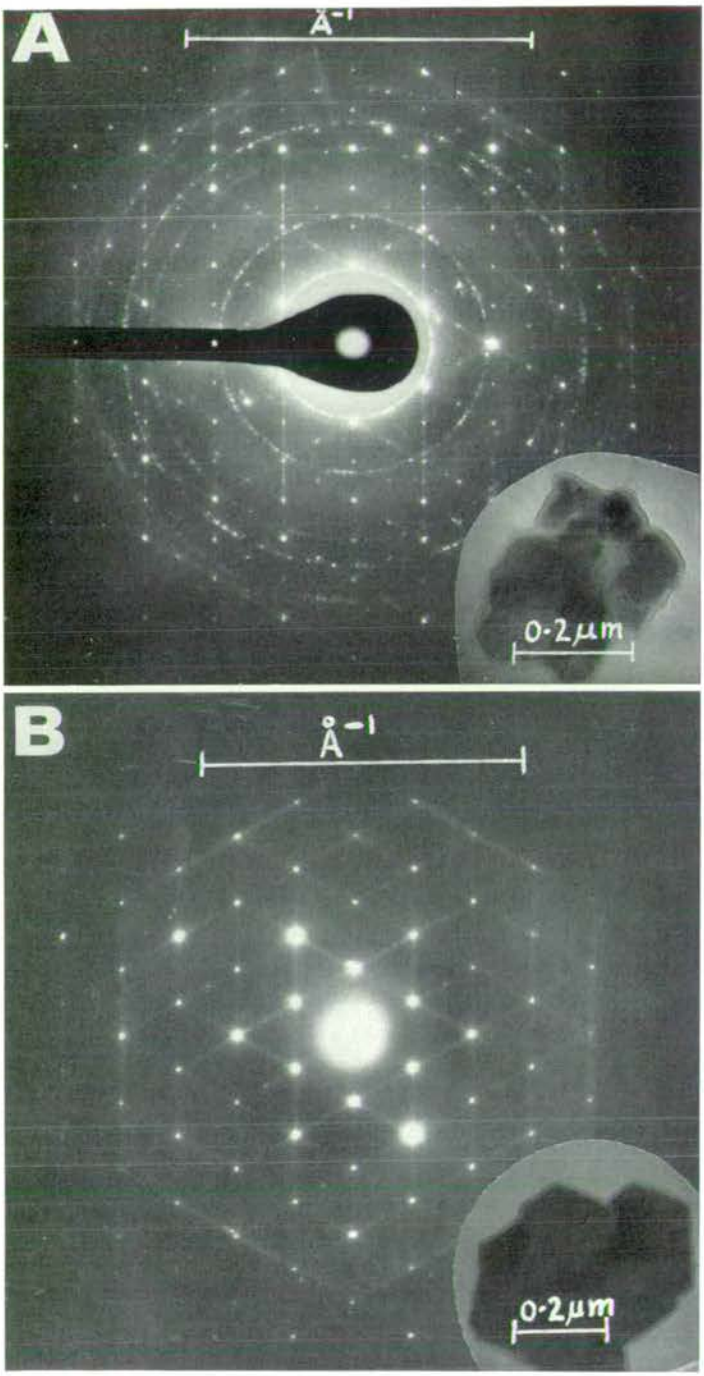

Fig. 1 A and B. Electron diffraction patterns from the silica phase in (A) bentonite and (B) deep-sea chert. In pattern A the inner ring is the 4.49 Å reflection from montmorillonite used as calibration. Streaking between reflections in both patterns is evident

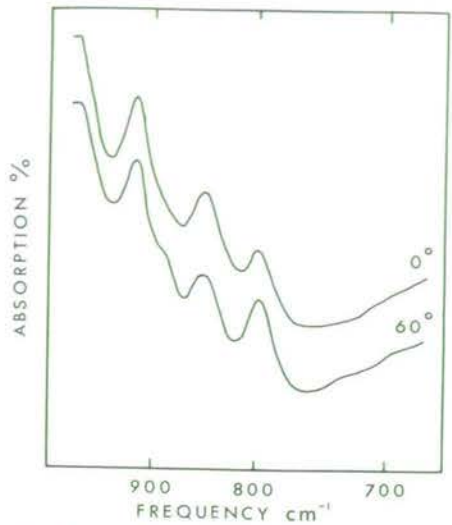

Fig. 2. Infrared absorption spectra of oriented film of Italian bentonite at different angles of incidence

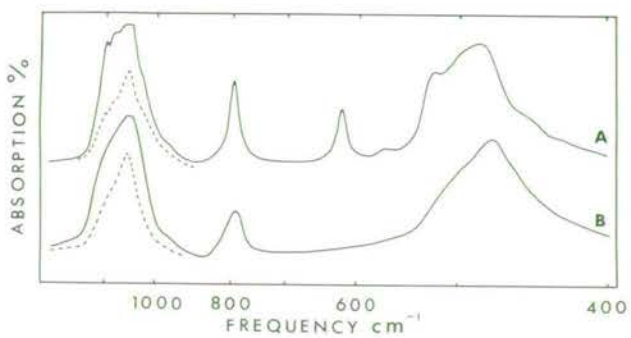

Fig. 3 A and B. Infrared absorption spectra of KBr pressed disks of A) cristobalite B) deep-sea chert (full lines 1 mg/170 mg KBr, dashed lines 0.3 mg/170 mg KBr)

Infrared Spectroscopy. The infrared spectra of both samples failed to reveal any of the diagnostic α-cristobalite absorption bands at 620, 520, 300 and 145 cm^{-1}. That of the bentonite is typical of Cheto-type (low iron) montmorillonite with an additional medium intensity band near 790 cm^{-1} suggestive of a silica phase. That this band is due to a separate phase is indicated by the fact that it is absent from the spectrum of the bentonite treated with 0.5 M NaOH, a treatment which leaves the montmorillonite unaffected. Spectra of an oriented film of the bentonite recorded at angles of incidence of 0° and 60° (Fig. 2) show that the 790 cm^{-1} band is strongly pleochroic and must therefore arise from particles with platy morphology. The band found at this frequency in tridymite and other SiO_2 polymorphs (Lippincott *et al.*, 1958) has been attributed to a Si-Si stretching vibration in

which the oxygen atoms move comparatively little. The deep-sea chert yields a spectrum (Fig. 3 B) showing bands characteristic of tridymite (or a glass) at 1104, 790 and 474 cm^{-1}. It also includes a broad low-frequency band near 183^{-1} but lacks a band at 560^{-1}. The latter band has been assumed to be characteristic of tridymite (Plyusnina *et al.*, 1970) although it is not always present even in synthetic specimens (Lippincott *et al.*, 1958) and is probably due to an impurity. The 790 cm^{-1} band is not pleochroic in the chert because the silica phase could be examined only in the spherular form. It has been previously noted (Jones and Segnit; Calvert, 1971 a) that the infrared spectrum of disordered α-cristobalite is similar to tridymite rather than cristobalite, but this has been attributed to the effect of the one-dimensional stacking disorder postulated by Flörke (1955). However, there seems no clear reason why such a disorder should necessarily result in the suppression of the cristobalite bands.

Discussion and Conclusions

It appears that the morphology, electron diffraction pattern and infrared spectrum of the silica phase in both bentonite and deep-sea chert are consistent with tridymite rather than cristobalite. It remains to consider how this can be reconciled with the X-ray powder pattern. Firstly, it should be noted that the spacings at 4.3, 4.1 and 2.5 Å can be quite reasonably considered as h00, 00l and hk0 reflections, respectively, of α-tridymite. Certainly, in most highly crystalline samples of α-tridymite the 4.3 Å reflection is stronger than that at 4.1 Å but in the present case the effect of disorder should also be considered. It is suggested that disorder in the silica phase does not result from an irregular stacking sequence of cristobalite and tridymite layers as envisaged by Flörke (1955), but is due to the layers being affected by random transverse displacement normal to the *c* axis, as observed in single crystals of type M low tridymite by Sato (1964). Such disordering is analogous to the translational turbostratic stacking postulated for smectites (Méring and Oberlin, 1971), where the lack of coherent diffraction is a statistical effect. Thus, although diffraction does occur in individual particles — as evidenced by electron diffraction — the superposition of many particles where the layers are laterally displaced at random results in the absence of a normal powder diffraction pattern. Turbostratically disordered smectites are characterized by X-ray powder patterns with strong 00l Bragg reflections, and weaker and broader diffraction bands arising from what is essentially a two-dimensional lattice; it seems likely that in similarly disordered tridymite the 4.1 Å repeat distance between the linked silica sheets would yield the most intense reflection. In addition to stacking disorder there is also the possibility of deformation within the tetrahedral sheets In fact, according to Gatineau *et al.* (1972) such deformation may actually cause the stacking disorder.

Calvert (1971 a) has drawn attention to the fact that silica with the X-ray powder pattern discussed above occurs extensively in geologically young formations. With few exceptions (Buurman and Van der Plas, 1971) this material has been described as cristobalitic; it is now suggested that it is more appropriately referred to as disordered α-tridymite.

Thanks are due to Mr R. H. S. Robertson, Pitlochry for the sample of bentonite and Mr D. S. Cassidy, Associate Curator, Antarctic Research Facility, Florida State University, U.S.A. for the sample of deep-sea chert.

References

Buurman, P., Van der Plas, L.: The genesis of Belgian and Dutch flints and cherts. Geol. Mijnbouw **50**, 9–28 (1971)

Calvert, S. E.: Nature of silica phases in deep sea cherts of the North Atlantic. Nature phys. Sci. **224**, 133–134 (1971a)

Calvert, S. E.: Composition and origin of North Atlantic deep sea cherts. Contr. Mineral. and Petrol. **33**, 273–288 (1971b)

Flörke, O. W.: Zur Frage des „hoch" Cristobalit in Opalen, Bentoniten und Gläsern. Neues Jahr b. Mineral. Monatsh. **1955**, 217–233

Frondel, C.: The system of Mineralogy, vol. III. Silica minerals. New York and London: Wiley 1962

Gatineau, L., Tchoubar, D., Méring, J.: Structures lamellaires: méthodes d'études de leurs imperfections. Bull. Soc. Franç. Mineral. Crist. **95**, 713–721 (1972)

Jones, J. B., Segnit, E. R.: The nature of opal. I. Nomenclature and constituent phases. J. Geol. Soc. Australia **18**, 57–68 (1971)

Lippincott, E. R., Van Valkenburg, A., Weir, C. E., Buntin, E. N.: Infra-red studies on polymorphs of silicon dioxide and germanium dioxide. J. Res. Nat. Bur. Std. **61**, 61–70 (1958)

Méring, J., Oberlin, A.: The smectites. In: Electron optical investigation of clays (Gard, J. A., ed.), p. 193–229. London: Mineralogical Society, 1971

Oehler, J. H.: Tridymite-like crystals in cristobalitic "cherts". Nature phys. Sci. **241**, 64 (1973)

Plyusnina, M. N., Maleyev, G. A., Yefimova, G. A.: Infra-red spectroscopic study of cryptocrystalline varieties of silica (Russian). Izv. Akad. Nauk SSSR, Geol. No. 9, 78 (1970). *Translated in*: Intern. Geol. Rev. **13**, 1750 (1971)

Rex, R. W.: X-ray mineralogy studies-Leg 1. In: Initial reports deep sea drilling project, vol. 1 (Ewing, M. *et al.* eds.), p. 354–367. Washington: U.S. Government Printing Office

Sato, M.: X-ray study of low tridymite (2). Structure of low tridymite, type M. Mineral. J. (Tokyo) **4**, 131–146 (1964)

Weaver, F. M., Wise, S. W.: Ultramorphology of deep sea cristobalitic chert. Nature phys. Sci. **237**, 56–57 (1972)

Wise, S. W., Buie, B. F., Weaver, F. M.: Chemically precipitated sedimentary cristobalite and the origin of chert. Eclogae Geol. Helv. **65**, 157–163 (1972)

Dr. M. J. Wilson
The Macaulay Institute for Soil Research
Craigiebuckler
Aberdeen, AB9 2QJ
Great Britain

Plant and Soil **41**, 695–696 (1974) Ms. 2566

SHORT COMMUNICATION

Comment on 'Spectroscopie infra-rouge de quelques acides humiques' by J. R. Bailly

Summary

In the authors' opinion the I.R. spectra of humic acids may have been erroneously interpretated by Bailly owing to contamination by inorganic salts.

Bailly [1] has recently presented I.R. spectra of fraction III from a separation on Sephadex of humic acids from various soil types, and gives an interpretation of most of the absorption bands. The author has failed to appreciate that the humic material present is in the form of carboxylate salt and that the majority of his samples contain silica gel, as well as sulphate and bicarbonate. The bicarbonate, probably present as the potassium salt since samples were incorporated in KBr disks (*cf* Spectrum No. 55, Nyquist and Kagel [4]), is responsible for absorption bands at 2600, 1640, 1400, 840 and 700 cm^{-1} and its presence invalidates the conclusions made by the author concerning bands in these regions. Silica gel, present in greatest amount in samples giving curves V and VII, is responsible for absorption bands at 1100 and 800 cm^{-1}, but the intensity of absorption near 1150 cm^{-1} suggests that sulphate must also be present. As a consequence of this contamination, the measurement of ratios of absorption band intensities (Table 2) would appear to be of no value. These observations on contamination by inorganic salts are substantiated by evidence (to be published) that during fractionation of humic acid on Sephadex, inorganic salts are eluted simultaneously with the material giving peaks 3 and 4 (on the numbering system used by Bailly and Margulis [2]) and that peak 3 particulary contains these salts. Since the humic acid was precipitated by H_2SO_4 and was then applied to the Sephadex in a dilute NaOH solution, sulphate and bicarbonate are likely to occur in fraction III, obtained from peak 3 on drying.

Another instance of contamination by bicarbonate can be seen in spectra of hymatomelanic acid fractions shown by Clark and Tan [3], who did not recognize that the samples were contaminated and interpreted their spectra as substantiating the presence of a polysaccharide-ester linkage in humic acid; in addition, they erroneously identified absorption bands due to silica gel as arising from polysaccharide.

Considerable care has clearly to be taken to avoid inclusion of inorganic

salts during isolation of fractions of soil organic matter and the interpretation and conclusions of Bailly [1] and Clark and Tan [3] must be largely discounted.

J. D. Russell and H. A. Anderson

The Macaulay Institute for Soil Research,
Craigiebuckler, Aberdeen, AB9 2QJ, Scotland

Received July 17, 1974

References

1 Bailly, J. R., Plant and Soil **40**, 285–302 (1974).
2 Bailly, J. R. and Margulis, H., Plant and Soil **29**, 343–361 (1968).
3 Clark, F. E. and Tan, K. H., Soil Biol. Biochem. **1**, 75–81 (1969).
4 Nyquist, R. A. and Kagel, R. O., Infrared Spectra of Inorganic Compounds. Academic Press, London. p. 75 (1971).

Soil Biol. Biochem. Vol. 7, pp. 35–38. Pergamon Press 1975. Printed in Great Britain.

THE OCCURRENCE OF APHID WAX IN PEAT

R. E. WHEATLEY, M. P. GREAVES and J. D. RUSSELL

The Macaulay Institute for Soil Research, Craigiebuckler, Aberdeen AB9 2QJ, Scotland

(*Accepted* 1 *July* 1974)

Summary—Small white aggregates frequently observed in peat have been studied using scanning electron microscopy and infrared absorption spectrometry. It has been shown that they are fibrous, consisting of paraffin wax and associated carbohydrate and secondary amide, and are secreted by the aphid *Colopha compressa*, which colonizes the roots of *Eriophorum* spp. growing on peat. This is the first report of the occurrence of this aphid species in Scotland.

INTRODUCTION

During surveys of peat deposits in Scotland small white aggregates up to 3 mm in diameter have frequently been observed in the peat (Mr. P. C. Jowsey, personal communication). We thought that these aggregates might be either fungal or bacterial colonies, but we could find no information on their nature and origin. This paper reports an investigation into the origin of these aggregates.

MATERIALS AND METHODS

Distribution of the aggregates in the peat was determined by taking a series of samples using a peat sampler (Jowsey, 1966) to a depth of 6 m in a basin bog at Lyne of Skene, Aberdeenshire.

Larger samples for examination and comparison were taken from two horizons in the peat, one near to the surface containing live roots of *Eriophorum* spp. (Fig. 1) and the other at a depth of about 1 m below the surface (Fig. 2). The sample from 1 m was obtained by digging a trench and removing about 10 l. of peat from the appropriate level. In the laboratory the sample was mixed with 5 vol of water and the suspension allowed to settle. The aggregates floated to the surface and were transferred individually by suction, using a vacuum pump, into a Buchner flask. Aggregates from the roots of an *Eriophorum* tussock were picked off with fine forceps. For infra-red (i.r.) examination samples of the aggregates (1 mg) were mixed with KBr (170 mg) and pressed into 12 mm dia discs. After drying the discs at 100°C for 16 h their i.r. absorption spectra were recorded on a Grubb Parsons S4 double beam spectrometer.

Aggregates were also removed aseptically for plating out on Oxoid nutrient agar, and for examination with the light and the S4 scanning electron microscopes (Cambridge Scientific Instruments Ltd.). For examination with the light microscope aggregates were stained for 2 min with aqueous aniline blue (1% w/v). For study under the scanning electron microscope they were mounted on stubs using double sided adhesive tape and freeze-dried.

Aphids were prefixed in osmium tetroxide vapour at room temperature for 7 days, dried for 72 h at −60°C and 1.33 N m^{-2} in an Edwards–Pearse Tissue Drier (Edwards High Vacuum) and then mounted on stubs which had been lightly sprayed with 101 protective coating (Letraset International Ltd.). The specimen stubs were precoated with carbon followed by a Ag–Pd (4:1) alloy, to a coating thickness of 20 nm.

RESULTS

The aggregates were found to be distributed throughout the depth of the peat, but high concentrations were observed in certain horizons.

Aggregates from within the peat were observed by light microscopy to contain fungal hyphae and bacteria. On plating out on nutrient agar media the hyphae failed to grow, and were assumed to be dead. The bacteria, however, grew well.

The scanning electron micrographs show that the aggregates have a fibrous structure (Fig. 3) and that the surface aggregates contain one or more apterous aphids [Fig. 4(a)] which secrete the fibres from rows of dorsally situated glands [Fig. 4(b)]. A comparison between micrographs of aggregates from the surface peat and from peat from a depth of 1 m (shown by pollen analysis to be approximately 4000 yr old) show significant differences. The fibres in aggregates from the surface (Figs 5 and 6) appear as interlinked solid structures. Very few linkages can be seen between fibres of aggregates from 1 m depth (Figs 7 and 8). These latter fibres appear as bundles of fibrils and consequently have a less coherent structure.

Both types of aggregates showed some staining with aqueous aniline blue. Aggregates from the roots showed little surface staining but were densely stained at the broken ends of the fibres. Fibres from aggregates sampled at 1 m showed surface staining but only between the fibrils.

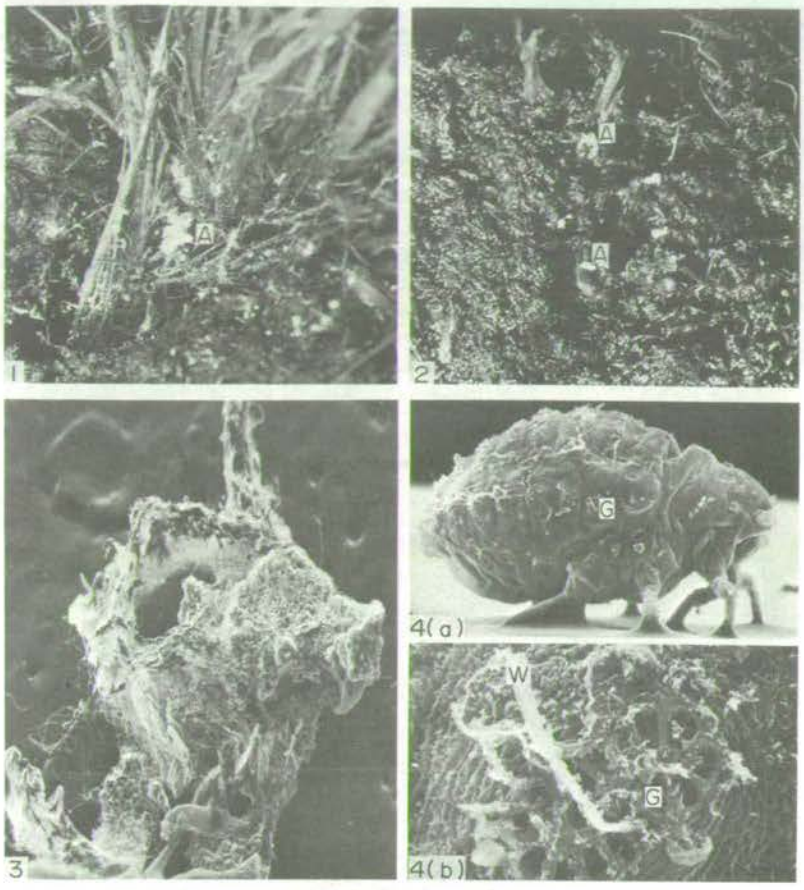

Fig. 1. Aggregates (A) on the live roots of *Eriophorum* sp. (× 2).

Fig. 2. Aggregates (A) in peat from a depth of 1 m (× 2).

Fig. 3. Fibrous aggregate from the roots of *Eriophorum* (× 15), aphid removed.

Fig. 4(a). The aphid *Colopha compressa* (Koch) (× 40), showing the dorsal wax glands (G).

Fig. 4(b). Dorsal gland (G) and wax (W) (× 400).

The i.r. absorption spectrum of aggregates from the plant roots (Fig. 9(a)) is consistent with the presence of long saturated paraffinic chains in the structure. Absorption bands are also present at 1737 and 1188 cm^{-1}, both characteristic of ester groups, while those at 1708 and 1208 cm^{-1} are characteristic of ketone groups. Weak absorption near 1360 and 1170 cm^{-1} suggests the presence of methyl ketones (Colthup, Daly and Wibberly, 1964). The spectrum also shows broad absorption underlying the 1050 cm^{-1} region and at about 3430 cm^{-1}, indicative of carbohydrate; bands at about 1645 and 1525 cm^{-1} are characteristic of secondary amide linkages. Comparison of this spectrum with that obtained for aggregates from 1 m in the peat profile [Fig. 9(b)] shows no difference in the paraffinic or waxy material. Absorption bands due to carbohydrate and secondary amide, however, are very much weaker in the latter spectrum [Fig. 9(b)].

A survey of several peat bogs in Aberdeenshire and Banffshire during April 1973 showed that the aphid was present at all sites where *Eriophorum* spp. were growing. It was usually found amongst the decaying leaf sheaths and new roots at the base of *Eriophorum* tussocks, although in a few isolated instances it occurred in appreciable numbers on or near older roots, some 10–15 cm from tussocks. The aphid was not found associated with any other plant genus.

Specimens of the aphid forwarded to the British Museum (Natural History) were identified as *Colopha compressa* (Koch).

DISCUSSION

The small white aggregates found in some Scottish peat bogs consist of flocculent wax threads produced by the aphid *Colopha compressa* (Koch). This aphid has previously been reported from only two sites in the

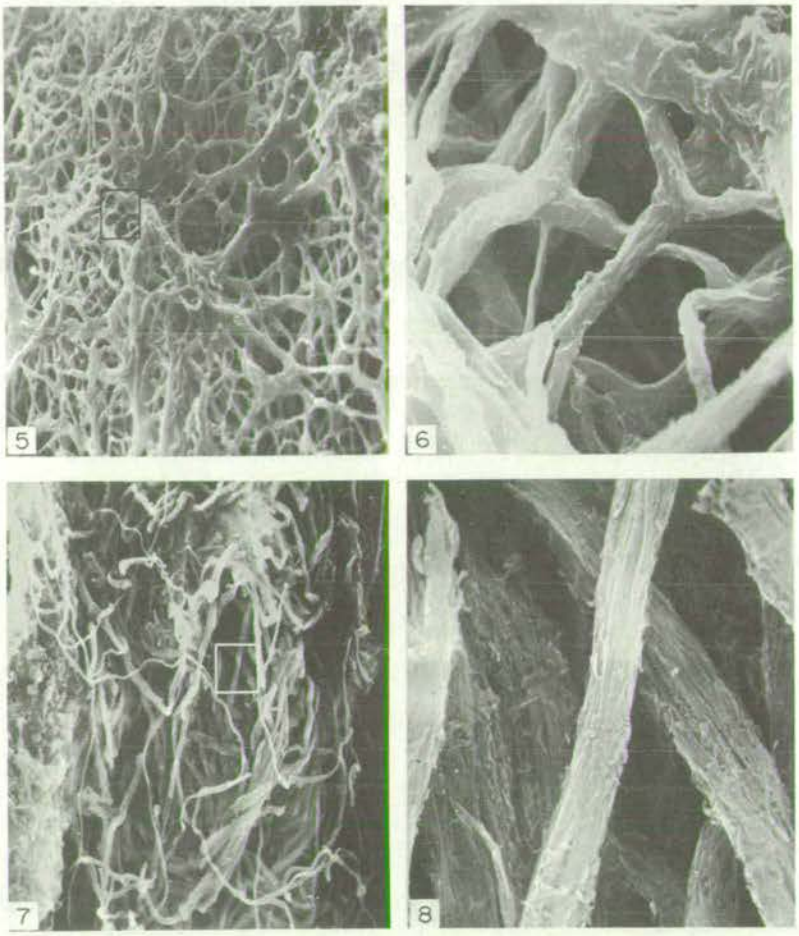

Fig. 5. As Fig. 3 showing the linkages between fibres and the ridged surface appearance (× 150).

Fig. 6. Inset of Fig. 5 (× 1,500).

Fig. 7. Fibres from an aggregate at 1 m depth showing lack of linkages between fibres and the numerous fibrils in each fibre (× 150).

Fig. 8. Inset of Fig. 7 (× 1,500).

United Kingdom; on *Carex ovalis* roots at Camberley, Surrey by E. E. Green, and on *Eriophorum angustifolium* roots at Moscar Cross, Sheffield, Yorkshire by G. Jackson (Dr. V. G. Eastop, personal communication).

Normally *C. compressa* overwinters in galls on the aerial parts of its primary host, *Ulmus* spp., and colonizes the roots of *Eriophorum* only during the summer. At all the Scottish sites examined, however, *Ulmus* spp. were absent and the presence of aphids on the roots of *Eriophorum* during the winter months suggests that the aphid has adapted to a new life cycle in which the parthenogenetically produced forms overwinter on *Eriophorum* roots. The occurrence of the aggregates in every horizon sampled suggests that the aphid has been present throughout the period of peat formation, a span of about 10,000 yr. The main reason for the secretion of wax by the aphid is probably to void excess carbohydrate ingested in its diet of plant juices. The wax also protects the aphid from predators and from bog water (Phillipson, 1971).

Observations on the chemical nature of the aggregates by i.r. absorption spectrometry are comparable with those obtained chemically on aphid cornicle wax by Chibnall, Latner, Williams and Ayre (1934) who found that it resembled a C_{30} keto-acid and a corresponding keto-alcohol. The spectra show that the aggregates consist of long, saturated paraffinic chains, carbohydrate and secondary amides. The spectra obtained from both types of aggregates are similar, except for the more intense absorption bands for carbohydrate and secondary amide for aggregates from the roots, suggesting that although the paraffinic contents of the two aggregates are similar, the carbohydrate and secondary amide content is much greater in the aggregates from the roots. Furthermore the fibres of aggregates from the roots are solid in appear-

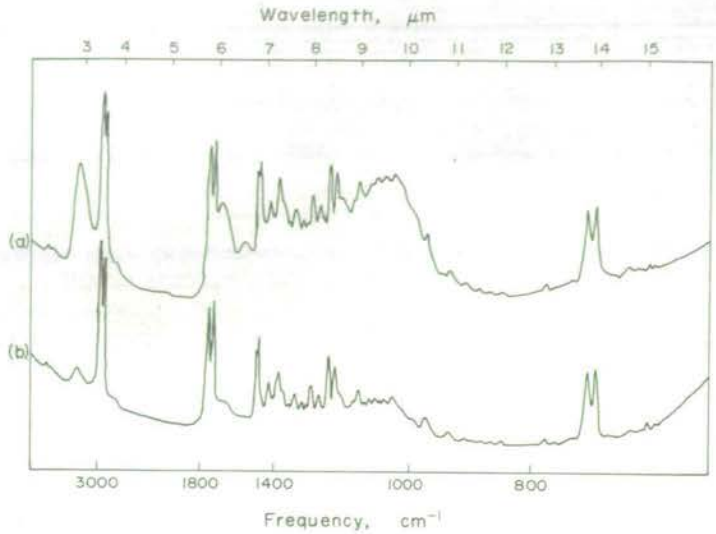

Fig. 9. Infra-red absorption spectra of aphid wax from (a) *Eriophorum* sp. root. (b) peat at 1 m depth.

ance and have a wrinkled surface reminiscent of distortion caused by freeze-drying, whereas the fibres of aggregates from 1 m depth appear as bundles of fibrils without a surface coating. These facts, together with the way in which the aggregates stain with aniline blue, suggest that when secreted by the aphid the wax fibres consist of fibrils held together in a matrix of carbohydrate and secondary amide.

Although at a later stage the matrix appears to disintegrate (Fig. 7) the spectrum of the aggregates from 1 m depth shows that they still contain some carbohydrate and secondary amide. Since this peat has been shown by pollen analysis to be 4000 yr old the rate of degradation of these two groups of readily metabolized compounds must be slow in peat. Examination of the aggregates by microscopy and plating out on agar showed that viable bacteria are present within them, and these microorganisms might normally be expected to utilize rapidly any carbohydrate or secondary amide source that was available. The survival of these two groups of compounds in the peat, over a period of thousands of years, indicates the hostile environment which a peat bog offers to the microbial population.

Acknowledgements—The authors wish to thank Dr. V. F. Eastop of the British Museum (Natural History) South Kensington, London, for identifying the aphid and providing information about its life cycle.

REFERENCES

CHIBNALL A. C., LATNER A. L., WILLIAMS E. F. and AYRE C. A. (1934) The constitution of coccerin. *Biochem. J.* **28,** 313–325.

COLTHUP N. B., DALY L. H. and WIBBERLEY S. E. (1964) *Introduction to Infrared and Raman Spectroscopy* p. 243. Academic Press, New York.

JOWSEY P. C. (1966) An improved peat sampler. *New Phytol.* **65,** 245–248.

PHILLIPSON J. (1971) *Methods of Study in Quantitative Soil Ecology*, pp. 233–246. Blackwell Scientific Publications, Oxford.

Offprinted from the *Journal of The Chemical Society, Faraday Transactions I*, 1975, vol. 71.

Adsorption of Carbon Dioxide on Goethite (α-FeOOH) Surfaces, and its Implications for Anion Adsorption

By J. D. Russell,* E. Paterson, A. R. Fraser and Victor C. Farmer

The Macaulay Institute for Soil Research, Craigiebuckler, Aberdeen AB9 2QJ

Received 7th December, 1974

Carbon dioxide is strongly adsorbed as CO_3^{2-} on moist goethite surfaces, but as both CO_3^{2-} and HCO_3^- on dry surfaces. On the basis of a model of the surface, sites for the adsorption of the carbonate species are suggested where these ions would play a role in redistributing surface charge. A similar role is proposed for strongly adsorbed anions such as phosphate.

Russell *et al.*[1] reported that the vibrations of surface hydroxyl groups, absorbing at 3 486 cm^{-1} and 3 660 cm^{-1}, can be seen in infrared spectra of films prepared from synthetic goethite and examined in vacuum. On the basis of a model of the predominant (100) face of these goethite preparations, they suggested that the 3 486 cm^{-1} band can be assigned to singly coordinated surface hydroxyl groups (A-type, see fig. 4), which can form hydrogen bonds with each other, and the 3 660 cm^{-1} band to the two-coordinated (C-type) or three-coordinated (B-type) surface hydroxyl groups, neither of which can form hydrogen bonds.

When goethite films are examined in air, the absorption bands of surface hydroxyl are suppressed, and there appear bands that can be assigned to adsorbed water and to a carbonate species that derive from adsorbed atmospheric carbon dioxide. This paper explores the energetics and mechanism of adsorption of CO_2 on goethite under anhydrous and moist conditions. No previous studies of this reaction are known to the authors, although Aylmore [2] has noted that the adsorption isotherm of CO_2 on goethite shows anomalous features, which he ascribed to physical sorption into microporous regions.

Since goethite occurs widely in soils and sediments, often as surface coatings on other minerals, its adsorption characteristics are of considerable geochemical and pedological interest.

EXPERIMENTAL

Synthetic goethite was prepared by the method of Atkinson *et al.*[3] Ferric nitrate solutions were partially neutralized and kept at room temperature for 50 h, then adjusted to pH 11.8 and maintained at 60°C for 4 days. After washing free from salt on the centrifuge the preparations were stored as suspensions containing 10-20 mg cm^{-3}. The size of the goethite crystals obtained depended on the ratio of added OH^- to Fe^{3+} present in solution during the preliminary aging period; the predominant (100) face of a typical thin lath, as seen in the electron microscope, varied from about 500 by 40 nm for OH/Fe = 0 to about 130 by 20 nm for OH/Fe = 2. A parallel variation occurred in their phosphate sorption capacity, the plateaux of phosphate adsorption isotherms at pH 3 to 4 ranging from 120 to 240 μmol g^{-1}: this corresponds to surface areas of 48-96 m^2 g^{-1} according to the correlation established by Atkinson *et al.*[4] The phosphate sorption capacity changed most rapidly between OH/Fe ratios of 0.75 and 1.0.

The adsorption of CO_2 by goethite in aqueous suspension was measured using a Warburg manometric apparatus. The goethite suspensions (2.5 cm^3 containing 25-50 mg) were placed

in the Warburg flasks, and equilibrated with flowing atmospheres of CO_2+N_2 gas mixtures containing 0.08, 1.08, 10.2 or 100 % CO_2 (supplied by British Oxygen Company). After one hour, the manometer was closed and the adsorbed CO_2 liberated by adding from a sidearm 0.2 cm^3 of a solution containing 0.36 mmol H_2SO_4. Standard Warburg practice was followed.[5]

The adsorption of CO_2 on approximately 1 g freeze-dried goethite was measured using a standard high vacuum volumetric system [6] after the sample had been outgassed for 18 h at 10^{-2} N m^{-2}. The pressure measurements were made using a mercury manometer read to 0.1 mm with a cathetometer. The isotherms were determined at 0°C and room temperature (normally 22-23°C) and the reversibility of the temperature dependence of the amount adsorbed was checked at a number of points on the isotherm.

For infrared absorption studies, films prepared by drying 0.6 cm^3 of goethite suspension on 1 mm thick AgCl sheet of area 2.5 × 1.2 cm were examined in a cell through which were passed CO_2+N_2 gas mixtures each at 0 % and 58 % relative humidity (controlled by P_2O_5 and saturated NaBr solution, respectively), and also in pure dry CO_2 following evacuation and deuteration in a vacuum cell. Because of heating by the infrared beam, the absorption features observed probably corresponded to a temperature of 30°C.

RESULTS AND INTERPRETATION

CO_2 ADSORPTION ON DRY SURFACES

The pattern of carbonate absorption bands seen in the 1 700–1 000 cm^{-1} region of spectra of goethite films exposed to CO_2 was found to be critically dependent on the humidity of the atmosphere. Under strictly anhydrous conditions, the principal absorption bands lay near 1 620, 1 410 and 1 240 cm^{-1} (fig. 1b,c), superimposed on goethite combination bands at 1 786 cm^{-1} and 1 652 cm^{-1} (fig. 1a). The bands of the adsorbed phase must in part arise from a bicarbonate species, since the band

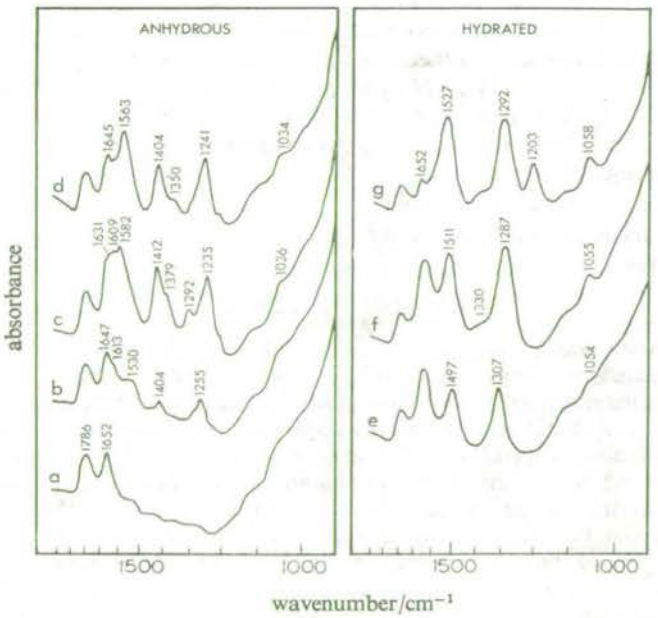

FIG. 1.—Infrared spectra of goethite aged at OH/Fe = 1.5 : (a) in vacuum, (b) in 0.08 % CO_2 in N_2, (c) in 100 % CO_2, (d) deuterated, in 100 % CO_2, (e) in moist 0.08 % CO_2, (f) in moist 100 % CO_2, (g) deuterated, in moist 100 % CO_2. The percentage CO_2 is numerically equal to its partial pressure in kN m^{-2}.

positions and contours were modified when the goethite surface was deuterated before adsorption of CO_2 (fig. 1d). Bicarbonate on oxide surfaces [7] commonly absorbs near 1 650, 1 400 and 1 230 cm^{-1}, but the 1 230 cm^{-1} band of HCO_3^- arises from a δ(COH) vibration and is absent from the spectra of DCO_3^-. The persistence of absorption at 1 240 cm^{-1} in the spectrum of carbonate on deuterated goethite (fig. 1d) indicates that a distorted CO_3^{2-} ion is also present : the other member of the ν_3 CO_3^{2-} doublet appears to lie in the complex of bands in the 1 600 cm^{-1} region. Even at the lowest CO_2 pressure studied (0.08 % CO_2, corresponding to a partial pressure of 0.08 kN m^{-2}, illustrated in fig. 1b, bands due to both HCO_3^- (1 404 cm^{-1}) and CO_3^{2-} (1 255 cm^{-1}) were present and both increased in intensity with small shifts in frequency up to 10 kN m^{-2} CO_2. Between 10 and 100 kN m^{-2} CO_2, the band of HCO_3^- now at 1 412 cm^{-1} ceased to increase, but CO_3^{2-} bands at 1 235 cm^{-1} and 1 582 cm^{-1} continued to increase slightly in intensity. At pressures above 1 kN m^{-2}, physically adsorbed CO_2 on the surface could be detected at 2 345 cm^{-1}, a position close to that of the gas (2 349 cm^{-1}). The intensity of this band increased five-fold as the CO_2 pressure increased from 10 to 100 kN m^{-2}.

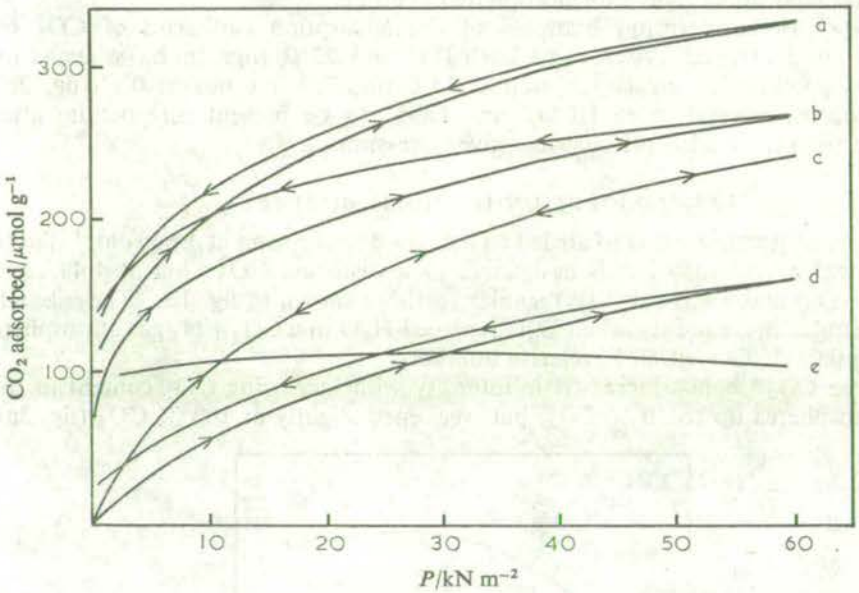

FIG. 2.—Adsorption/desorption isotherms of CO_2 on goethite aged at OH/Fe = 1.5: (a) at 0°C on untreated sample, (b) at 22°C on untreated sample, (c) at 0°C on phosphated sample, (d) at 22°C on phosphated sample. (e) Difference between adsorption curves at 22°C on goethite and phosphated goethite.

The formation of carbonate on the goethite surface also led to changes in the OH stretching region. Surface hydroxyl on goethite absorbs at 3 660 cm^{-1} and 3 486 cm^{-1}, but in the presence of 1 kN m^{-2} CO_2 the 3 660 cm^{-1} band weakened and shifted to 3 650 cm^{-1}, new features appeared at 3 677 and 3 600 cm^{-1}, and the 3 486 cm^{-1} band was replaced by one at 3 425 cm^{-1} (calculated from the corresponding OD band at 2 528 cm^{-1}). At higher CO_2 pressures the 3 650 and 3 677 cm^{-1} bands were largely displaced to 3 590 cm^{-1} probably by interaction of these surface OH with physically adsorbed CO_2.

A goethite preparation which had been exposed to excess phosphate ion at pH 3.5

to give a phosphate-saturated surface showed only physically sorbed CO_2 and very weak carbonate bands when exposed to 100 kN m^{-2} CO_2.

Adsorption isotherms of CO_2 on goethite exhibited a steeply rising portion at low pressure (fig. 2a, b), followed by a more gradual increase at pressures above 1 kN m^{-2}. The initial region of strong adsorption was absent from the adsorption isotherms of a fully phosphated goethite (fig. 2c, d), but above 3 kN m^{-2} the isotherms followed a course similar to those of the unphosphated sample. In this region, the difference between the amounts of CO_2 adsorbed on the phosphated and unphosphated surface was almost constant at 110 μmol g^{-1} (fig. 2e), corresponding to half the measured phosphate sorption capacity. In the absence of the infrared observations, which show that chemisorption on goethite proceeds progressively throughout the whole pressure range, one might conclude from the isotherms that chemisorption is complete at 3 kN m^{-2}, and that only physical adsorption occurs above that pressure. Isosteric heats of adsorption derived from isotherms at 0°C and 22°C (fig. 2) also gave no indication of chemisorption on goethite in the pressure range 10–50 kN m^{-2}. These heats lay between 8 and 16 kJ mol^{-1} for unphosphated goethite and near 30 kJ mol^{-1} for phosphated goethite.

The desorption-adsorption branches of the adsorption isotherms of CO_2 on goethite showed marked hysteresis at both 0°C and 22°C (fig. 2a, b), whereas on phosphated goethite hysteresis was seen at 22°C (fig. 2d) but not at 0°C (fig. 2c). Infrared spectra showed more HCO_3^- and CO_3^{2-} to be present on goethite after desorption than after adsorption at any given pressure.

CO_2 ADSORPTION ON MOIST SURFACES

Exposure of goethite films to air led to increased absorption at 1 645 cm^{-1} due to adsorbed water, and also bands assignable to a distorted CO_3^{2-} ion at 1 497 and 1 307 cm^{-1} (ν_3) and 1 054 cm^{-1} (ν_1) similar to those shown in fig. 1e. These bands were unchanged in frequency when D_2O replaced H_2O in a $CO_2 + N_2$ gas atmosphere containing 0.08 % CO_2 at 58 % relative humidity.

All three CO_3^{2-} bands increased in intensity with increasing CO_2 content in the moist atmospheres up to 10 % CO_2, but weakened slightly at 100 % CO_2 (fig. 3a),

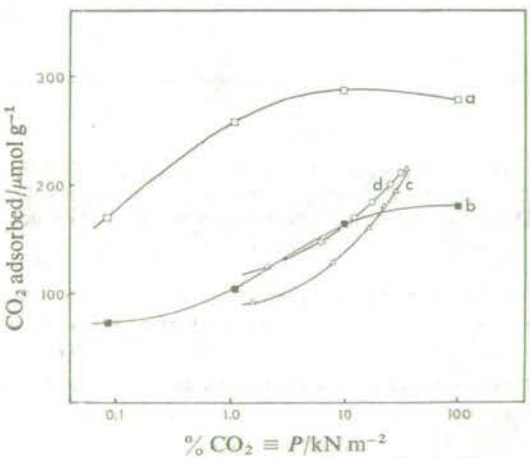

FIG. 3.—Variation with CO_2 pressure of infrared band intensities (arbitrary units) and adsorbed CO_2 on goethite aged at OH/Fe = 2. (a) 1500 cm^{-1} band of CO_3^{2-} on moist goethite, (b) CO_2 adsorbed on goethite in suspension at 25°C, (c) adsorption and (d) desorption isotherms of CO_2 on anhydrous goethite.

and a new broad band appeared near 1 330 cm^{-1} (fig. 1f). Replacement of H_2O by D_2O in the CO_2 atmosphere modified the 1 330 cm^{-1} band and caused increased absorption at 1 527 cm^{-1} (fig. 1g) analogous to the increased absorption at 1 563 cm^{-1} in the dry deuterated system (fig. 1d). These results suggest that in the moist system, as in the dry system, CO_2 is in part adsorbed as HCO_3^- in the 100 % CO_2 atmosphere, and that some of the CO_3^{2-} present at low CO_2 pressures is converted to HCO_3^- at high CO_2 pressures.

As measured in the Warburg apparatus, the amount of CO_2 adsorbed by goethite suspensions increased continuously with increasing CO_2 content in the atmosphere (fig. 3b). Between 1 % and 10 % CO_2 in the atmosphere, the amounts adsorbed on goethite in suspension (fig. 3b) are similar to those retained by dry goethite on the desorption branch (fig. 3d). The amount of CO_2 adsorbed in 100 % CO_2 was directly proportional to the phosphate sorption capacity of the goethite; 0.70 ± 0.02 mol CO_2 were adsorbed per mol PO_4^{3-} for seven different preparations with phosphate sorption capacities ranging from 120 to 240 μmol g^{-1}.

DISCUSSION

The infrared results show that progressive chemisorption of CO_2 occurs on dry and moist goethite surfaces at all pressures up to atmospheric, at a temperature near 30°C. On moist surfaces, adsorption occurs predominantly as CO_3^{2-}, although there is evidence of partial conversion of carbonate to bicarbonate at atmospheric pressure, indicating that these species are adsorbed on closely related sites. On dry surfaces, both CO_3^{2-} and HCO_3^- are present at all pressures, and a substantial amount of physical adsorption occurs at higher pressures. Physical adsorption is the predominant mode on phosphated goethite. Surface carbonate interacts strongly with A-type hydroxyl, which is also involved in phosphate adsorption.

Without the infrared evidence, the finding that all adsorbed CO_2 can be pumped off at low pressures had previously [2] been taken to imply that only physical adsorption occurred.

THE LOCATION OF THE CARBONATE ION ON THE GOETHITE SURFACE

Adsorption of CO_2 as CO_3^{2-} is most directly interpreted as implying a reaction between CO_2 and an O^{2-} ion on the surface, whereas adsorption as HCO_3^- requires a reaction involving a surface hydroxyl group. Examination of the postulated structure of the predominant (100) face of goethite shows that such reactions are structurally and energetically plausible.

The (100) face is thought to consist principally of three types of hydroxyl groups labelled A, B and C in fig. 4, and there is only one accessible oxide ion, labelled C′, lying in the groove that runs in the [001] direction. This oxide ion carries an unbalanced negative charge ($-2+\frac{3}{2}$), as it forms three bonds each of formal value a half with the three Fe^{3+} ions to which it is coordinated, insufficient to neutralize completely its two negative charges. Within the body of the goethite crystal, the excess charge on such oxide ions is neutralized by hydrogen bonds (dotted in fig. 4) donated by hydroxyl ions, which carry an unsatisfied positive charge ($-1+\frac{3}{2}$) according to an approximate calculation of the type illustrated above for the oxide ions. In the actual structure, the Fe—O^{2-} bonds are shortened and the Fe—OH^- bonds are lengthened so that the unbalanced charges are less than $-\frac{1}{2}$ and $+\frac{1}{2}$ respectively. The charge transfer involved in the hydrogen bond is also less than $+\frac{1}{2}$, since the bond is not symmetrical.

Carbonate ion formed on the goethite surface could play a similar role to hydrogen

bonding within the crystal in redistributing the excess negative charge on the C′-type oxide ions. The reaction $O^{2-}+CO_2 \rightarrow CO_3^{2-}$ leads to a redistribution of the excess charge on a single oxide ion over the three oxygens of the carbonate ion; in addition, hydrogen bonds formed between A-type surface hydroxyl groups and the CO_3^{2-} ion (fig. 4, left) permit a further transfer of negative charge to the Fe(OH, O) surface octahedra bearing A-type hydroxyl groups. On the assumption that the C′ oxide ion and the A-hydroxyl have the same relative position on the surface as they have in the body of the crystal, geometrical calculations indicate that the hydroxyl-to-carbonate hydrogen bond would be about 2.83 Å long, which is in fair agreement with the distance of 2.86 Å calculated from the observed OH stretching frequency (3 425 cm^{-1}) using the correlation of Nakamoto *et al.*[8]

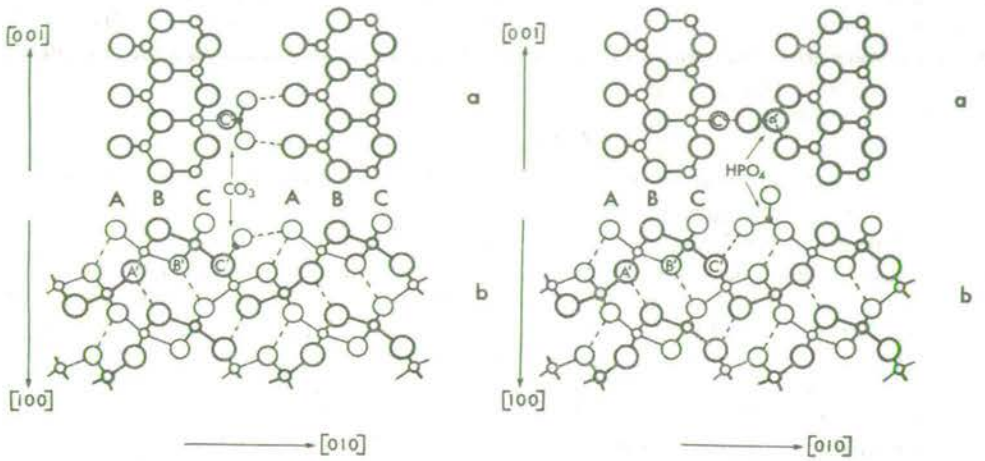

FIG. 4.—Left: site of adsorption of CO_2 on the (100) face of goethite, seen in plan in (a) and in section in (b), Right: site of adsorption of HPO_4^{2-} on goethite.

It is not, perhaps, immediately obvious that the surface octahedra carrying A-type hydroxyl groups should have an excess positive charge to be distributed through hydrogen bonds. However, approximate calculations that assign the full formal charges to Fe^{3+}, O_3^{2-} and OH^-, and assume that hydrogen bonds between OH^- and O^{2-} transfer a charge of $+\frac{1}{3}$, indicate that both types of surface octahedra (those involving A-type and those involving C-type hydroxyl groups) would carry an excess positive charge of $+\frac{1}{9}$. The excess positive charge on the surface octahedra carrying C-type hydroxyl groups can be transferred directly to the C′-type oxide ions which are shared with these octahedra, but hydrogen-bonding to carbonate ion is the most direct route for charge redistribution from surface octahedra carrying A-type hydroxyl groups.

Formation of CO_3^{2-} is not the only mechanism available in these systems to transfer positive charge from A-type OH^- to C′-type O^{2-}. For example, a water molecule can accept a hydrogen bond from an A-type OH, and donate hydrogen bonds to two C′-type O_3^{2-}, in contrast to CO_3^{2-} which links two OH groups to one oxide ion. Consequently, an adsorption pattern in which water molecules and CO_3^{2-} alternate along the grooves in the (100) face would provide links involving every A-type OH and every C′-type O^{2-}. At saturation, on this basis, one carbonate ion would be expected for every three A-type hydroxyl groups, a prediction that is in excellent agreement with the finding of 0.7 mol CO_3^{2-} per mol PO_4^{3-} adsorbed, since

there appears to be one phosphate ion adsorbed for every two A-type hydroxyl groups.[4]

Bicarbonate ion replacing an A-type hydroxyl by the reaction $OH^- + CO_2 \rightarrow OCOOH^-$ could also transfer charge by forming a hydrogen bond to an O^{2-}. Packing considerations prevent every hydroxyl being replaced by bicarbonate, and it appears that a mixture of carbonate and bicarbonate links gives the lowest surface energy under anhydrous conditions although some uncompensated oxide ions are unavoidable. Because of the less satisfactory charge compensation, carbonate on anhydrous surfaces is more highly strained than on moist surfaces, as shown by the greater splitting of the two components of the ν_3 stretching vibration (350 cm^{-1} compared with 190 cm^{-1}).

THE ROLE OF ADSORBED ANIONS ON THE GOETHITE SURFACES

The suggestion made above that adsorption of CO_2 leads to a substantial reduction in surface energy by providing a route for charge redistribution over the surface raises the question whether other strongly adsorbed species, such as phosphate, arsenate and selenite studied by Hingston *et al.*,[9] play a similar role. It is immediately obvious that the HPO_4^{2-} ion could function as a bridge for charge redistribution if it displaces two A-type OH^- ions, and forms a hydrogen bond to C′-type oxide ions (see fig. 4, right).

It has already been proposed [4] that adsorbed phosphate does replace A-type hydroxyl groups and it has been shown that the absorption band of these hydroxyl groups is absent from spectra of phosphated goethite.[1] Examination of the infrared absorption of phosphated goethite which had been briefly exposed to D_2O showed a surface OD band at 2 515 cm^{-1} which can be ascribed to the bonded POD—O^{2-} groups. This OD wavenumber corresponds to an OH wavenumber of 3405 cm^{-1}, implying an O—O separation in the hydrogen bond of 2.85 Å, which is consistent with the structure sketched in fig. 4. Moreover, the P—O stretching frequencies seen in the 1 000-1 190 cm^{-1} region are displaced by deuteration, as could only occur for an acid phosphate group.

The proposed mechanism for phosphate adsorption is directly applicable to arsenate, but selenite, also strongly adsorbed, must be present as the monofunctional $HSeO_3^-$ ion if it is to serve as a channel for charge transfer. Steric considerations prevent the pyramidal hydrogen selenite ion from replacing every A-type hydroxyl group, so that only ten mole per cent more selenite than phosphate is adsorbed in the pH range 3-7. However, when phosphate and selenite are both present on the goethite surface, it may again become possible to replace every A-type hydroxyl group by alternating HPO_4 and $HSeO_3$ ions; examination of molecular models suggests that such packing is sterically possible. Should this happen, the total number of moles of HPO_4^{2-} plus $HSeO_3^-$ would be greater for mixed adsorption than for either alone, and this has in fact been found. Indeed for the particular case of phosphate and selenite adsorbed on goethite at pH 7 [fig. 2 of ref. (9)], the model sketched above is consistent with the observation that on 1 g of a goethite preparation 85 μmol $HSeO_3^-$ can be adsorbed along with 150 μmol HPO_4^{2-} (displacing 385 μmol of A-type OH), on a surface which retains only 183 μmol of HPO_4^{2-} alone, or 206 μmol of $HSeO_3$ alone, on the reasonable assumptions that the total number of A-type hydroxyl groups amounts to something over 400 μmol g^{-1} and that phosphate when adsorbed alone leaves a proportion of isolated A-type hydroxyl groups along the row.

It may be necessary to propose other mechanisms of adsorption to account for the additional uptake of selenite and phosphate observed in mixed solutions at low pH

and at high concentrations of phosphate in solution [9] but the scheme outlined here indicates that many of the features of mixed adsorption can be explained without the assumption of the three different types of site (common sites, and sites on which only one or other of the anions can be adsorbed) proposed by Hingston *et al.*[9]

Dr. I. R. MacDonald kindly carried out the Warburg volumetric measurements.

[1] J. D. Russell, R. L. Parfitt, A. R. Fraser and V. C. Farmer, *Nature*, 1974, **248**, 220.
[2] L. A. G. Aylmore, *Clays Clay Miner.*, 1974, **22**, 175.
[3] R. J. Atkinson, A. M. Posner and J. P. Quirk, *J. Inorg. Nuclear Chem.*, 1968, **30**, 2371.
[4] R. J. Atkinson, A. M. Posner and J. P. Quirk, *J. Inorg. Nuclear Chem.*, 1972, **34**, 2201.
[5] W. M. Umbreit, R. H. Burris and J. F. Stauffer, *Manometric Techniques* (Burgess, Minneapolis, 1957).
[6] P. H. Emmett, *Adv. Colloid Sci.* 1942, **1**, 1.
[7] Ya. M. Grigor'ev, D. V. Pozdnyakov, and V. N. Filimonov, *Zhur. fiz. Khim.*, 1972, **46**, 316.
[8] K. Nakamoto, M. Margoshes and R. E. Rundle, *J. Amer. Chem. Soc.*, 1955, **77**, 6480.
[9] F. J. Hingston, A. M. Posner and J. P. Quirk, *Disc. Faraday Soc.*, 1971, **52**, 334.

PRINTED IN GREAT BRITAIN AT
THE UNIVERSITY PRESS
ABERDEEN

Geoderma, 14 (1975) 125—138

IRON OXIDE AND CLAY MINERALS AND THEIR RELATION TO COLOURS OF RED AND YELLOW PODZOLIC SOILS NEAR SYDNEY, AUSTRALIA

B.G. DAVEY[1], J.D. RUSSELL and M.J. WILSON

The Macaulay Institute for Soil Research, Craigiebuckler, Aberdeen (Great Britain)

(Received June 26, 1974; Revised version accepted February 18, 1975)

ABSTRACT

Davey, B.G., Russell, J.D. and Wilson, M.J., 1975. Iron oxide and clay minerals and their relation to colours of red and yellow podzolic soils near Sydney, Australia. Geoderma, 14: 125—138.

The iron oxide and clay minerals in some typical red and yellow podzolic soils from New South Wales have been investigated by X-ray diffraction and infra-red spectroscopy. The dominant iron oxide mineral is goethite containing about 13—14 mol % AlOOH, this being the mineral which gives the yellow soils their characteristic colour. The red soils also contain finely divided hematite which masks the colour of the goethite. Lepidocrocite was not detected in any of the soils examined. The dominant clay minerals are kaolinite and dioctahedral interstratified illite—smectite, the latter being more concentrated in the finer clay fractions, especially in soils developed on calcareous greywacke. In the red podzolic soil developed on Ashfield shale, illite—smectite is strongly interlayered with well-ordered aluminous material. Dickite occurs in this soil.

INTRODUCTION

The investigation by Walker (1960) of the soils of the County of Cumberland, N.S.W., showed that the podzolic soils developed on shales and sandstones of the Wianamatta series and their erosion products are coloured red on the hills and yellow in the valleys and along some of the stream terraces. The cause of this colour difference has never been established. The traditional viewpoint, that red soils owed their colour to hematite, orange soils to lepidocrocite and yellow soils to goethite, was dispelled by Schwertmann and Lentze (1966), who concluded that soil colour is not a reliable guide in this respect. A similar conclusion was reached by Ségalen (1969) for some tropical red and yellow soils, and again for some American red and yellow podzolic soils by Soileau and McCracken (1967). The present study attempts to characterize the iron oxide and clay minerals in the red and yellow podzolic soils in the County of Cumberland and to seek a relationship between mineralogy and colour.

[1] Permanent address: Department of Soil Science, University of Sydney, N.S.W., Australia.

the Wheat Industry Research Committee of New South Wales and the provision of laboratory facilities by the Council and Director of the Macaulay Institute for Soil Research.

REFERENCES

Bayliss, P., Loughnan, F.C. and Standard, J.C., 1965. Dickite in the Hawkesbury sandstone of the Sydney Basin, Australia. Am. Miner., 50: 418—426.

Berner, R.A., 1969. Goethite stability and the origin of red beds. Geochim. Cosmochim. Acta, 33: 267—273.

Edwards, A.P. and Bremner, J.M., 1967. Dispersion of soil particles by sonic vibration. J. Soil Sci., 18: 43—47.

Farmer, V.C. and Russell, J.D., 1964. The infrared spectra of layer silicates. Spectrochim. Acta, 20: 1149—1173.

Farmer, V.C. and Russell, J.D., 1967. Infrared absorption spectrometry in clay studies. Clays Clay Miner., 15: 121—142.

Jonas, K. and Solymar, K., 1970. Preparation, X-ray derivatographic and infrared study of aluminium substituted goethites. Acta Chim. Acad. Sci. Hung., 66: 383—394.

Loughnan, F.C., Koko, M. and Bayliss, P., 1964. The red beds of the Triassic Narrabeen Group. J. Geol. Soc. Aust., 11: 65—78.

Lovering, J.F., 1956. The stratigraphy of the Wianamatta Group, Triassic System, Sydney Basin. Rec. Aust. Museum, 23: 169—201.

Norrish, K. and Taylor, R.M., 1961. Isomorphous replacement of iron by aluminium in soil goethites. J. Soil Sci., 12: 294—306.

Northcote, K.H., 1971. A factual key for the recognition of Australian Soils. Rellim Tech. Publ. South Australia.

Oinuma, K. and Hayashi, H;, 1968. Infrared spectra of clay minerals. J. Toyo Univ. Gen. Educ. (Nat. Sci.), 9: 57—98.

Reynolds, R.C. and Hower, J., 1970. The nature of interlayering in mixed layer illite—montmorillonites. Clays Clay Miner., 18: 25—36.

Schwertmann, U., 1971. Transformation of hematite to goethite in soils. Nature (Lond.), 232: 624—625.

Schwertmann, U. and Lentze, W., 1966. Bodenfarbe und Eisenoxidform. Z. Pflanzenernähr. Düng. Bodenkd., 115: 209—214.

Ségalen, P., 1969. Contribution à la connaissance de la couleur des sols à sesquioxides de la zone intertropicale: sols jaunes et sols rouges. Cah. O.R.S.T.O.M. Pédologie, 7: 113—236.

Soileau, J.M. and McCracken, R.J., 1967. Free iron and coloration in certain well-drained coastal plain soils in relation to their properties and classification. Soil Sci. Soc. Am. Proc., 31: 248—255.

Thiel, R., 1963. Zum system αFeOOH-αAlOOH. Z. Anorg. Allg. Chem., 326: 70—78.

Van Houten, F.B., 1973. Origin of red beds — A review 1961—1972. Ann. Rev. Earth Planet. Sci., 1: 39—61.

Van Der Marel, H.W. and Krohmer, P., 1969. OH stretching vibrations in kaolinite and related minerals. Contrib. Miner. Petrol., 22: 73—82.

Walker, G.F., 1958. Reactions of expanding lattice clay minerals with glycerol and ethylene glycol. Clay Min. Bull., 3: 302—313.

Walker, P.H., 1960. A soil survey of the County of Cumberland, Sydney Region, New South Wales. N.S.W. Dep. Agric. Soil Survey Bull., No.2. Govt. Printer, N.S.W.

Walker, P,H. and Hawkins, C.A., 1957. A study of river terraces and soil development on the Nepean River, N.S.W. J. R. Soc. N.S.W., 91: 67—73.

Walker, T.R., 1967. Formation of red beds in modern and ancient deserts. Bull. Geol. Soc. Am., 78: 353—368.

Walker, T.R., 1974. Formation of red beds in moist tropical climates. — A hypothesis. Bull. Geol. Soc. Am., 85: 633—648.

Offprinted from the *Journal of The Chemical Society, Faraday Transactions 1*, 1976, Vol. 72.

CONFIRMATION OF THE SURFACE STRUCTURES OF GOETHITE (α-FeOOH) AND PHOSPHATED GOETHITE BY INFRARED SPECTROSCOPY

PO_2 group.[3] Compared with HPO_4^{2-} in alkali and alkaline earth phosphates (table 1), the in-plane and out-of-plane POH deformations of adsorbed phosphate are at markedly lower frequencies, but this is consistent with its involvement in weaker hydrogen bonds [νOH = 3 405 cm^{-1} ; νOD = 2 515 cm^{-1}, see fig. 4(*c*)] than are encountered with HPO_4^{2-} in crystalline salts (νOH = 2 400-2 900 cm^{-1}).

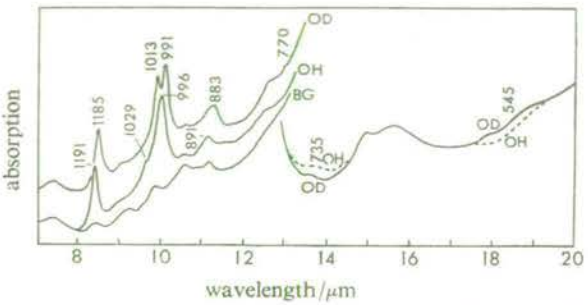

FIG. 2.—Infrared absorption of surface phosphate at saturation levels on a α-FeOOD (7-13 μm) and on α-FeOOH (13-20 μm) with surface OH and surface OD ; all samples in vacuum. Curve BG shows the background absorption of α-FeOOD with surface OH. Band positions are in wavenumbers/cm^{-1}.

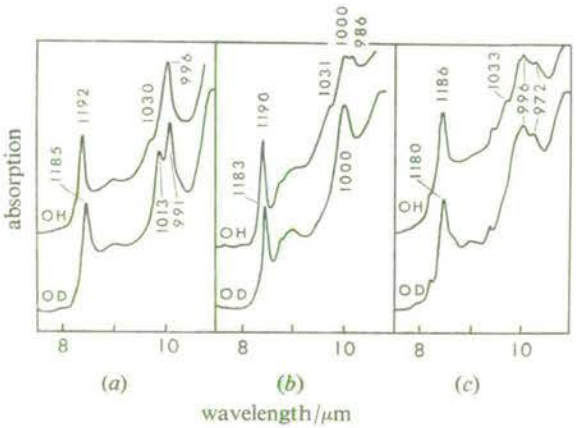

FIG. 3.—Infrared spectra of phosphated α-FeOOH with surface OH and OD, in vacuum. (*a*) 200 μmol g^{-1} phosphate ; (*b*) 50 μmol g^{-1} phosphate ; (*c*) 200 μmol g^{-1} phosphate after exposure to pyridine and brief evacuation. Band positions are in wavenumbers/cm^{-1}.

A previous infrared study [4] of phosphate adsorbed on goethite assigned a shoulder near 1 100 cm^{-1} to the phosphate, but this feature is a goethite combination vibration, whose intensity varies relative to the phosphate bands as a function of coverage and surface area.

Addition of 200 μmol g^{-1} of $(NH_4)H_2PO_4$ to α-FeOOH gives films showing phosphate absorption bands identical with those obtained using H_3PO_4, even when the films are only air-dry. Little ammonium absorption is detectable at 1 400 cm^{-1} in the air-dry condition, and none after evacuation. A slightly modified spectrum is obtained when goethite is equilibrated with K_2HPO_4 solution (pH 10) and then briefly washed with dilute KOH solution of pH 10. Under these conditions the surface is not saturated with phosphate, and the spectrum is matched exactly by evaporating 25-50 μmol g^{-1} H_3PO_4 with goethite [fig. 3(*b*)]. Clearly, the adsorbed acid phosphate groups have little affinity for potassium or ammonium ions.

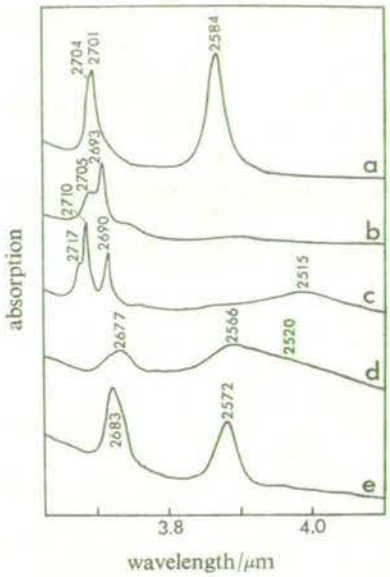

FIG. 4.—Infrared spectra of surface OD groups on goethite preparations in vacuum: (*a*) untreated; (*b*) fluoridated; (*c*) phosphated; (*d*) with adsorbed pyridine; (*e*) with hydrocarbon oil. Band positions are in wavenumbers/cm^{-1}.

HYDROXYL VIBRATIONS

Although the proposed model of the goethite (100) surface includes three different types of hydroxyl group, only two OH stretching frequencies can be confidently identified, at 3 660 and 3 486 cm^{-1}. Some deuterated goethite preparations clearly show two unresolved components at 2 701 and 2 704 cm^{-1} in the OD band of higher frequency [fig. 4(*a*)]. The two components are clearly resolved when the goethite is treated with 700 μmol g^{-1} of HF [fig. 4(*b*)]. Fluoride completely replaces A-type OD groups at 2 584 cm^{-1}, but little or no replacement of B- or C-type OD occurs even when the concentration of HF is increased to 1 000 μmol g^{-1}: apparently, excess HF is lost on evaporation. Possibly the broader component at 2 704 cm^{-1} can be assigned to B-type OD groups, as these are more likely to be perturbed by adjacent fluoride ions.

The region of B- and C-type OD absorption is resolved into three sharp components when the surface is saturated with phosphate [fig. 4(*c*)]. This is predictable on the basis of the structure shown in fig. 1. When all A-type OD groups are replaced by phosphate, all C-type OD groups have identical environments, but B-type OD groups fall into two classes, one directly opposite to an O–P–O bridge, the other lying between unbridged A-type oxygens. Accordingly, the higher frequency doublet is assigned to B-type OD, and the lower frequency singlet to C-type OD.

LEWIS SITES ON GOETHITE AND PHOSPHATED GOETHITE

Adsorption of pyridine on deuterated goethite, followed by brief evacuation, strongly perturbs the absorption bands of surface OD groups. The spectrum is broad [fig. 4(*d*)] but seems to include A-type OD both hydrogen-bonded to pyridine (a shoulder near 2 520 cm^{-1}) and involved in van der Waals interactions (2 566 cm^{-1}); B- and C-type OD are involved only in van der Waals interactions (2 677 cm^{-1}).

The effect of van der Waals interactions alone can be seen when the goethite surface is covered with mineral oil [fig. 4(*e*)].

In the 1 400 to 1 700 cm^{-1} region (not shown), bands at 1 608 cm^{-1} and 1 592 cm^{-1} indicate the presence of two forms of pyridine. Following accepted assignments,[5] the first can be ascribed to pyridine held on Lewis acid sites, which in this case must be ferric ions, and the second can be ascribed to pyridine held by hydrogen bonding. No band near 1 540 cm^{-1} corresponding to pyridinium ion is present, indicating the absence of Brönsted acidity. Removal of the hydrogen-bonded pyridine by prolonged pumping at 0.002 Torr allows the unperturbed vibrations of the surface OD on (100) faces to reappear in the spectrum, although the coordinated pyridine absorbing at 1 608 cm^{-1} resists evacuation. This establishes that the coordinated pyridine is held by Fe^{3+} on edge faces of the crystals, whereas hydrogen-bonded pyridine is held on (100) faces.

The coordinated pyridine is readily displaced by water vapour, which in turn is firmly held on the Lewis acid sites and resists prolonged evacuation: its bending vibration is detectable super-imposed on a goethite overtone vibration at 1 652 cm^{-1} by the slight decrease in absorption at this point when pyridine is adsorbed, or when D_2O replaces H_2O. Examination of models of the goethite structure suggests two possible schemes for the (010) edge face, depending on the section chosen; one of these consists of hydroxyl groups only, while the other consists of equal numbers of hydroxyl groups and water molecules coordinated to underlying ferric ions. The second structure would lead to some 220 $\mu mol\ g^{-1}$ of Lewis sites in the preparation studied here, but steric considerations would prevent more than one in three sites (about 70 $\mu mol\ g^{-1}$) from being occupied by pyridine. This is in fair agreement with the 60 $\mu mol\ g^{-1}$ of strongly adsorbed pyridine that was found in a dilute acid extract by ultraviolet absorption.

No pyridinium ion is formed when pyridine is adsorbed on phosphated goethite, and, again, two forms of pyridine are indicated by bands at 1 608 and 1 592 cm^{-1}. Modification of the phosphate absorption bands [fig. 3(*c*)] suggests that pyridine is now hydrogen-bonded to some of the POH(D) groups, although the position of the (P)O–D stretch at 2 505 cm^{-1} (not shown) is almost unchanged, indicating that the hydrogen bond is little stronger than that formed with the surface. Here again, as for goethite itself, perturbation of B- and C-type OD by van der Waals interactions is indicated by displacement of their absorption bands. The hydrogen-bonded pyridine is released more slowly on pumping from phosphated goethite than from goethite, but finally only pyridine coordinated to edge site, absorbing at 1 608 cm^{-1}, remains.

CONCLUSIONS

The results presented here, together with evidence for surface oxide ions based on CO_2 adsorption,[2] strongly support the structures proposed (fig. 1) for the (100) face of goethite and phosphated goethite. These surfaces are now probably more convincingly defined than is any other oxide surface. The sharpness of the absorption bands of surface groups shows that the (100) surface constitutes a highly regular crystalline array, although small amounts of surface contaminants, such as vacuum pump oil or salts, cause a loss of band resolution, and some goethite preparations do not give optimum surface spectra. Such preparations often have crystals of irregular or anomalous shape.

The dimensions and structure of the HPO_4^{2-} ion appear to be specially appropriate for reaction with the goethite surface. A survey of a number of goethite complexes involving other acids, to be published elsewhere, has revealed that none shows such

sharp infrared absorption features as does phosphated goethite. Even fluoride, which appears to replace all A-type hydroxyl, gives a slightly irregular surface as judged by the breadth of the absorption band of remaining B-type hydroxyl groups.

[1] J. D. Russell, R. L. Parfitt, A. R. Fraser and V. C. Farmer, *Nature*, 1974, **248**, 220.
[2] J. D. Russell, E. Patterson, A. R. Fraser and V. C. Farmer, *J.C.S. Faraday I*, 1975, **71**, 1623.
[3] S. D. Ross in *The Infrared Spectra of Minerals*, ed. V. C. Farmer (Mineralogical Society, London, 1974), p. 383.
[4] R. J. Atkinson, R. L. Parfitt and R. St. C. Smart, *J.C.S. Faraday I*, 1974, **70**, 1472.
[5] F. P. Parry, *J. Catalysis*, 1963, **2**, 371.

(PAPER 5/1514)

PRINTED IN GREAT BRITAIN AT
THE UNIVERSITY PRESS
ABERDEEN

MINERALOGICAL MAGAZINE, MARCH 1976, VOL. 40, PP. 447–51

Nickeloan pyroaurite from Leslie, Aberdeenshire

M. J. WILSON, P. D. CRADWICK, M. L. BERROW, W. J. McHARDY, AND J. D. RUSSELL

The Macaulay Institute for Soil Research, Craigiebuckler, Aberdeen AB9 2QJ

SUMMARY. A nickel-bearing mineral belonging to the pyroaurite–sjögrenite group has been found in a serpentinite rock near the village of Leslie, Aberdeenshire. X-ray powder diffraction data and electron-probe microanalysis indicate that the mineral has a three-layer rhombohedral structure with a probable formula near $Mg_4^{2+}Ni_2^{2+}Fe_2^{3+}(OH)_{13}CO_3.4H_2O$. The mineral can therefore be described as nickeloan pyroaurite. It decomposes readily in mildly acid conditions and if inherited by serpentinite-derived soils could well be an important source of plant-available nickel.

THE pyroaurite–sjögrenite group of minerals has recently been reviewed by Taylor (1973). The group has the general formula $M_6^{2+}M_2^{3+}(OH)_{16}CO_3.4H_2O$, with a structure consisting of brucite-like layers alternating with layers of water and carbonate groups (Ingram and Taylor, 1967); it also has two isostructural sub-groups which have been characterized as three-layer rhombohedral (3R) and two-layer hexagonal (2H) polytypes. Most of the minerals belonging to the group show a divalent to trivalent metal cation ratio of 3:1, the best characterized polymorphs being pyroaurite and sjögrenite with Mg^{2+} and Fe^{3+}, hydrotalcite and manasseïte with Mg^{2+} and Al^{3+}, and stichtite and barbertonite with Mg^{2+} and Cr^{3+}. Two other varieties have also been reported in which Ni^{2+} replaces Mg^{2+}, namely reevesite with Ni^{2+} and Fe^{3+} (White *et al.*, 1967; De Waal and Viljoen, 1971) and eardleyite with Ni^{2+} and Al^{3+} (Taylor, 1973). Several related nickeliferous hydroxide minerals with X-ray powder patterns similar to the pyroaurite–sjögrenite group are also known (Jambor and Boyle, 1964; Lapham, 1965).

The mineral reported in this paper is a previously undescribed nickel-bearing variety belonging to the pyroaurite–sjögrenite group. It appears to be a 3R polytype with approximately one out of every three Mg^{2+} replaced by Ni^{2+} and it can, therefore, be described as nickeloan pyroaurite. The occurrence of this type of mineral in serpentinite suggests that it may act as a source of available nickel in some serpentinite-derived soils.

Experimental. The mineral occurs in serpentinite rock exposed in a roadside quarry approximately 1 km west of the village of Leslie, Aberdeenshire (NJ/585247). It is disseminated sporadically through the rock and is also found along fracture surfaces where it occurs as soft, pale, grass-green encrustations. The mineral is intimately associated with fibrous chrysotile from which it could not be entirely separated. The serpentinite does not appear to have been affected by weathering to any great extent and the mineral probably formed during a period of hydrothermal alteration, the occurrence of which is indicated by conspicuous veining.

The mineral was hand-picked from the rock under a binocular microscope and characterized by X-ray diffraction, infrared spectroscopy, transmission and electron microscopy, and electron-probe microanalysis.

Results

X-ray powder pattern. The mineral was first detected during a preliminary X-ray powder diffraction survey of the mineralogy of the serpentinites in north-east Scotland.

TABLE I. *d-spacings,* intensities, observed and calculated structure factors, and indexing of lines of the mineral from Leslie, Aberdeenshire, referred to 3R (pyroaurite) and 2H (sjögrenite) unit cells.*

1			2				3			
d	*I*	F_{obs}	*hkl*	d_{calc}	F_{calc}	F_{obs}	*hkl*	d_{calc}	F_{calc}	F_{obs}
7·68 Å	not measured		0003	7·68 Å	—	—	0002	7·68 Å	—	—
3·83	0·7803	0·1460	0006	3·84	60·79	62·87	0004	3·84	41·67	24·36
2·65	not measured		10$\bar{1}$1	2·667	—	—	10$\bar{1}$1	2·645	—	—
2·611	0·2263	0·1152	01$\bar{1}$2	2·615	57·58	49·61	0006	2·56	2·35	19·22
2·435	0·0555	0·0573	10$\bar{1}$4	2·433	18·89	24·68	10$\bar{1}$3	2·534	16·87	9·56
2·316	0·2036	0·1231	01$\bar{1}$5	2·320	58·40	53·01	?		—	—
2·100	0·0590	0·0730	10$\bar{1}$7	2·080	14·41	31·44	?		—	—
1·961	0·1793	0·1362	01$\bar{1}$8	1·964	73·98	58·65	10$\bar{1}$5	2·022	19·01	22·72
1·920	not measured		0.0.0.12	1·920	—	—	0008	1·920	—	—
1·746	0·0885	0·1071	1.0.$\bar{1}$.10	1·748	49·60	46·17	0009	1·707	0·0	17·89
1·649	0·0700	0·1008	0.1.$\bar{1}$.11	1·651	37·69	43·41	10$\bar{1}$7	1·699	3·01	16·82
1·548	0·0794	0·1140	1.1.$\bar{2}$.0	1·550	56·61	49·09	1.1.$\bar{2}$.0	1·549	38·30	19·02
1·503	0·893	0·1243	1.1.$\bar{2}$.3	1·519	44·51	53·53	1.1.$\bar{2}$.2	1·519	29·12	20·74

1. *d* spacings and intensities of X-ray powder pattern. The line at 7·68 Å is too intense and those at 2·65 and 1·92 Å too weak for accurate measurement.

2. Indexing of lines and calculated structure factors referred to the 3R (pyroaurite) unit cell with $a = 3{\cdot}1$, $c = 23{\cdot}04$ Å. The F_{obs} values are those of column 1 scaled by the factor $K = \Sigma F_{calc}/\Sigma F_{obs}$.

3. As in column 2 referred to the 2H (sjögrenite) unit cell with $a = 3{\cdot}1$, $c = 15{\cdot}36$ Å.

* Philips camera of 57·3 mm radius, Co-$K\alpha$ radiation.

It yields a strong reflection at about 7·7 Å, which can easily be distinguished from the strong, first order basal reflection of the serpentine minerals at 7·3 to 7·4 Å and, after deletion of the chrysotile reflections, the powder pattern (see Table I) agrees well with those of pyroaurite, of the nickeliferous mineral described by Lapham (1965), and of reevesite (White *et al.*, 1967). The mineral appears to be thermally unstable, as heating at 300 °C results in the elimination of the entire powder pattern.

In order to determine the polytype, the powder pattern was indexed using unit cells of 3R and 2H types (Table I). Indexing of the powder lines suggests that the mineral is a 3R polytype, a conclusion that is supported by the average values of the discrepancies between calculated and observed *d* spacings.

To confirm this designation and to test the hypothesis that the mineral has the same structure as pyroaurite with nickel (which is later shown to be an important constituent) replacing some magnesium, the intensities of the strong lines of the powder pattern were measured on two microphotometers and compared with calculated data.

Intensities were converted to structure factors, F_{obs}, using Lorentz and polarization factors for a randomly oriented powder. Structure factors F_{calc} were calculated for the reflections assuming that Ni replaces one-third of the Mg atoms. The observed structure factors were then scaled to those calculated using the scale factor $K = \Sigma F_{calc}/\Sigma F_{obs}$. The resulting values for the two polytypes are shown in Table I. Using indexed lines only, the R factors, where $R = \sum\{|F_{obs}|-|F_{calc}|\}/\sum|F_{obs}|$, for the 3R and 2H models are 0·168 and 0·70 respectively. The structure factor agreement is thus sufficiently good to confirm that the mineral is a 3R rather than a 2H polytype.

The *infrared spectrum* of the mineral is similar to those of related minerals such as sjögrenite and hydrotalcite (Mumpton *et al.*, 1965) and also resembles that of reevesite (De Waal and Viljoen, 1971). It is characterized by intense absorption near 3440 cm^{-1} indicating relatively strongly hydrogen-bonded OH. There are also moderately strong bands at 1355 cm^{-1} and 1626 cm^{-1}, which are associated with hydrated basic carbonate. Spectral changes brought about by heating the sample are similar to those described by Mumpton *et al.* (1965) for coalingite and may be interpreted in terms of loss of hydration water and structural modification of the basic carbonate at 100 °C, followed by progressive loss of structural OH up to 300 °C to give an anhydrous carbonate phase. Other features of the infrared spectrum were obscured by bands associated with admixed chrysotile.

Electron diffraction. Hand-picked fragments were dispersed ultrasonically in distilled water and a drop of the resulting suspension dried on a carbon support film on a transmission-electron-microscope grid. Electron microscopy revealed that the bulk of the sample consists of fibres giving a typical chrysotile electron-diffraction pattern. Although many large electron-dense particles were aggregates of fibres, some had a platy morphology (fig. 1a) and yielded a hexagonal electron diffraction pattern (fig. 1b) very similar to that given by brucite crystals with (0001) normal to the beam. The pattern can be interpreted, therefore, as a section of the reciprocal lattice normal to c consisting of *hki*0 reflections only. Accurate measurement of the d spacings in patterns from two crystals gave d_{110} 1·555 ± 0·0015 Å for one and 1·545 ± 0·004 Å for the other, corresponding to a 3·11 ± 0·01 Å and 3·09 ± 0·01 Å, respectively. This overall variation in a is rather greater than would be expected from errors in measurement and may indicate some variation in chemical composition between crystals. Electron diffraction measurements are in good agreement with X-ray results except that the $10\bar{1}0$ reflection was absent on the X-ray pattern, an observation consistent with rhombohedral structure. Its appearance on the electron diffraction pattern can be accounted for by super-lattice effects arising from cation ordering—as proposed for sjögrenite and pyroaurite by Taylor (1969). These effects may also explain the presence of additional weak spots on some patterns (arrowed in fig. 1c), which together with the stronger ones lie on a hexagonal lattice of a parameter $\sqrt{3}\times 3{\cdot}1$.

Electron-probe microanalysis. The Stereoscan stage was modified so that transmission-electron-microscope specimen grids could be examined in scanning transmission mode with simultaneous X-ray analysis. In practice only particles $> 2\ \mu m$ gave a reasonable X-ray count and analysis can only be approximate. The platy

particles that yield the hexagonal electron-diffraction patterns mentioned above contain magnesium, nickel, and iron, with a small amount of silicon due to some adhering chrysotile. Two platy particles gave counts indicating Mg:Ni:Fe ratios of 1·0:2·5:4·9 and 1·0:3·6:5·0. The fibrous chrysotile contains little or no nickel but there appears to be a little iron. As the amount of X-rays generated depends greatly on

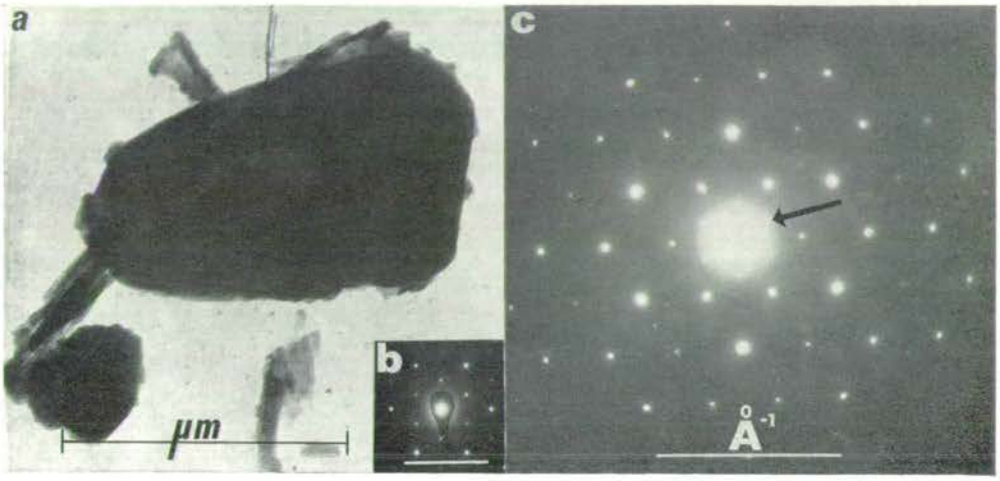

FIG. 1a. Electron micrograph of pyroaurite-like mineral showing platy morphology. b. Electron-diffraction pattern from particle in fig. 1a. c. Electron-diffraction pattern of a pyroaurite-like particle showing additional weak spots, one of which is arrowed.

TABLE II. *Metallic ions extracted at different pH values from serpentinite rock containing pyroaurite-like mineral (expressed as ppm in* $<$ *2 mm crushed rock).*

	Ni	Fe	Co	Cr	Mg
Total content	2400	46000	170	1960	220000
2·5% acetic acid (pH 2·5)	1950	2400	42	21	5500
1*N* ammonium acetate/acetic acid (pH 4·5)	1690	2300	22	5·5	3600
1*N* ammonium acetate (pH 7·0)	30	29	0·54	0·13	560

particle thickness, quantitative analysis is not possible but comparison of the count rates of magnesium, nickel, and iron with those for appropriate standards indicates that these elements are present in the platy mineral in the approximate atomic proportion 2:1:1.

Acid extraction of serpentinite rock. The serpentinite rock was crushed to fragments less than 2 mm in diameter and extracted with acetic acid (pH 2·5), ammonium acetate/acetic acid (pH 4·5), and ammonium acetate (pH 7·0). Over 80 % of the total nickel of the rock is mobilized by a single acetic acid treatment (Table II), and significant amounts of iron and cobalt are also released. Extraction at pH 4·5 removes 70 % of the total nickel but at pH 7·0 only a minor amount is extracted. X-ray diffraction

traces of $< 0{\cdot}5$ mm fraction of the crushed serpentinite demonstrate that the nickel-bearing pyroaurite-like mineral is completely decomposed at pH 2·5 and 4·5 and it seems reasonable to conclude that most, if not all, of the nickel extracted in these relatively mild conditions is associated with this phase. It may be noted that although the ratio of nickel to iron is 1:20 in the rock the three different extractants always remove these metals in an approximate 1:1 ratio. This suggests that there is a similar nickel:iron ratio in the mineral decomposed—which is consistent with the results obtained by electron-probe microanalysis. It is clear that should this type of mineral occur in serpentinite-derived soils it would quickly break down under acid pedogenic conditions to release appreciable amounts of mobile nickel and iron.

Conclusions. The X-ray powder data and the infrared spectrum indicate that the mineral has a pyroaurite-type structure, although its composition differs from that of pyroaurite in that it contains nickel as well as magnesium and iron. In view of the fact that most minerals in the pyroaurite–sjögrenite group have a divalent to trivalent metal : cation ratio of 3:1, the most likely structural formula of the mineral is $Mg_4^{2+}Ni_2^{2+}Fe_3^{2+}(OH)_{16}CO_3{\cdot}4H_2O$. The mineral can therefore be best described as nickeloan pyroaurite.

REFERENCES

De Waal (S. A.) and Viljoen (E. A.), 1971. *Amer. Min.* **56**, 1077.
Ingram (L.) and Taylor (H. F. W.), 1967. *Min. Mag.* **36**, 465.
Jambor (J. L.) and Boyle (R. W.), 1964. *Canad. Min.* **8**, 116.
Lapham (D. L.), 1965. *Amer. Min.* **50**, 1708.
Mumpton (F. A.), Jaffe (H. W.), and Thompson (C. S.), 1965. Ibid. **50**, 1893.
Taylor (H. F. W.), 1969. *Min. Mag.* **37**, 338.
—— 1973. Ibid. **39**, 377.
White (J. S.), Henderson (E. P.), and Mason (B.), 1967. *Amer. Min.* **52**, 1190.

[*Manuscript received 1 April 1975, revised 21 April 1975*]

Plant and Soil **47**, 263–264 (1977) Ms. 3277

SHORT COMMUNICATION

Comment on 'Contamination of humic acid by silica gel and sodium bicarbonate' by K. H. Tan

Summary

Although Tan[9] has demonstrated that soil humic acid fractions can be prepared free from contaminants, nevertheless, such contaminants have occurred in earlier work and have led to erroneous conclusions based on incorrect interpretation of infrared spectra.

Tan[9] has clearly and unambiguously shown in his recent article that the infrared spectra contained therein are of humic, hymatomelanic and fulvic fractions free from the carbonate–bicarbonate contaminants discussed by Russell and Anderson[8]. He did not, however, comment on the fact that some of the I.R. spectra of hymatomelanic fractions published by Clark and Tan[2] – *e.g.* those in Fig. 4, (2), (3) and (4) – show absorption characteristics consistent with weak to strong contamination by carbonate and/or bicarbonate, and that these authors had erroneously interpreted spectral changes between 1600 and 1750 cm^{-1}, a region where bicarbonate absorbs strongly (Fig. 2 (2) of Ref.[9]), as evidence of carboxyl groups arising from the hydrolysis of a polysaccharide ester linkage in humic acid. Moreover, spectra published by Bailly[1] also show evidence for the presence of bicarbonate in several humic acid preparations and bicarbonate absorption bands have been wrongly assigned to β-keto-enol structures. Both occurrences of bicarbonate point to faulty experimental procedure during pH adjustment and/or dialysis.

Although spectra reproduced in the article by Tan[9] show no absorption bands due to silica gel, the original criticism[8], that the spectra of polysaccharide fractions from hymatomelanic acid (Fig. 6 (1), (2) and (3) of Ref.[2]) showed a pattern of absorption bands consistent with contamination by silica gel (*cf.* Fig. 17 of Ref.[4]), is still valid. It should also be pointed out that the majority of the spectra published by Tan and Clark in Ref.[10] purporting to be of fulvic acids and fulvic acid fractions, are of samples grossly contaminated by silica gel (Figs. 1, 2, 3 of Ref.[10]) or by carbonate and/or bicarbonate (Figs. 4D and 5D of Ref.[10]). The failure of the authors to recognize the presence of these components in their fractions led them to the erroneous assignment of silica gel bands to polysaccharide.

In our previous criticism[8] it was not disputed, as Tan[9] has stated, that the procedures of extraction and dialysis used in the isolation of humic and fulvic

acids usually yield products considered to be free of contaminants. Rather, the plea was made that care needs to be taken in meticulously carrying out these procedures to ensure minimum contamination. It is essential in interpreting infrared spectra of soil organic fractions to make judicious reference to reputable compilations of spectra of inorganic salts[6] and minerals[3 5] in order to avoid assigning to the organic matter, absorption bands arising from contaminants. The authors feel that where misleading results have been wrongly interpreted and published, they should be identified as such for the benefit of other workers in the field. It should be noted that failure to make such identification has resulted in the appearance, in a textbook[7], of an erroneous statement concerning the structure of soil organic matter based on the incorrect conclusions of Clark and Tan[2].

J. D. Russell and H. A. Anderson
The Macaulay Institute for Soil Research,
Craigiebuckler, Aberdeen, AB9 2QJ, Scotland

Received 14 September 1976

References

1 Bailly, J.-R., Plant and Soil **40**, 285–302 (1974).
2 Clark, F. E. and Tan, K. H., Soil Biol. Biochem. **1**, 75–81 (1969).
3 Farmer, V. C., The Infrared Spectra of Minerals. Mineralogical Society, London (1974).
4 Hunt, J. M. *et al.*, Anal. Chem. **22**, 1478–1497 (1950).
5 Moenke, H., Mineralspektren, I. Akademie-Verlag, Berlin (1962).
6 Nyquist, R. A. and Kagel, R. O., Infrared Spectra of Inorganic Compounds. Academic Press, London (1971).
7 Russell, E. W., Soil Conditions and Plant Growth (10th Ed.) Longman, London (1973).
8 Russell, J. D. and Anderson, H. A., Plant and Soil **41**, 695–696 (1974).
9 Tan, K. H., Plant and Soil **44**, 691–695 (1976).
10 Tan, K. H. and Clark, F. E., Geoderma **2**, 245–255 (1969).

(Reprinted from Nature, Vol. 260, No. 5552, p. 597, April 15, 1976)

Possible relationship between soil fulvic acid and polymaleic acid

In the course of structural investigations into the organic matter component of soil, it became clear that the fulvic acid solutions[1] (the alkali-soluble fractions of humus not precipitated by acid) contained a high proportion of their soluble organic matter as a polymer, consisting of a carbon skeleton highly substituted by carboxyl groups. The solutions also normally contained peptide and polysaccharide mixtures or complexes which could be removed almost entirely by fractionation on charcoal[2], a technique which allowed the isolation of the polycarboxylic acid. Brown acidic polymers virtually identical with those found in the fulvic acid solution were recovered from podzol B_h horizon humus by extraction of the soil with dilute mineral acid or trisodium citrate solutions (*p*H 7.0) followed by dialysis.

Infrared spectroscopy, elemental analysis and a study of the degradation products of these polymers and their derivatives suggested that the polymers had an aliphatic or alicyclic backbone substituted predominantly by vicinal carboxyl groups. The soil polymers still contained polysaccharide, phenolic derivatives and nitrogen, but in low amounts, the last being accountable as amino acid residues and the ammonium ion. The product arising from the hydrolysis of pyridine-catalysed homopolymerised maleic anhydride[3] was found to be chemically and structurally related to the natural polymers, as shown by the similarities between their infrared absorption spectra (Fig. 1), their analysis (polymaleic acid: C 48.76, H 3.30, N 0.82%; B_h citrate-soluble humus: C 47.62, H 3.39, N 0.86%; for comparison, fulvic acid polymer: C 46.18, H 2.68, N 0.95%) and certain of their acid-hydrolysis products (Fig. 2). The dissimilar hydrolysis products, levulinic acid and the phenolic acids, could arise from species adsorbed on to or incorporated into the natural polymer, and this was demonstrated with the synthetic polymer. Slight differences between the potentiometric titration curve of the polymaleic acid[4] and that of the soil polymer were similarly explicable, while the solution-*p*H visible absorption spectra relationships were identical.

Although the complete structure of polymaleic acid has yet to be elucidated, certain aspects of the structure are known, for example, the existence of vicinal carboxyl groups readily dehydrating to yield anhydride, a property shown spectroscopically by fulvic acid, and unsaturation which accounts for an absorption band near 1,620 cm^{-1} in the infrared spectrum of fulvic acid. It is these features that make this polymer attractive as a model for fulvic acid.

Fig. 1 Infrared spectra of *a*, polymaleic acid, *b*, fulvic acid in KBr pressed disks (1-mg sample and 170-mg KBr in a 12-mm diameter disk). Absorption in (*b*) near 1,000–1,100 cm^{-1} is from carbohydrate.

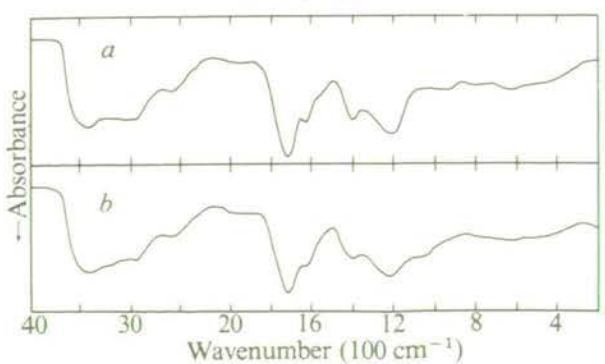

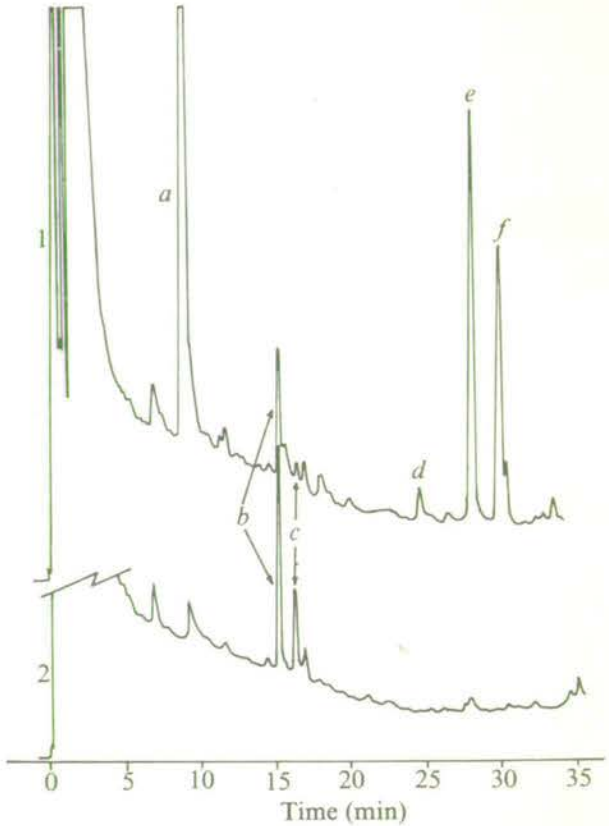

Fig. 2 Gas chromatography curves of trimethylsilyl derivatives of ether-soluble products from 6 M HCl hydrolysis of (1) Humus podzol Bh citrate-soluble humus, (2) Polymaleic acid. Products identified by gas chromatography–mass spectrometry: *a*, Levulinic acid TMS; *b*, Succinic acid di-TMS; *c*, Fumaric acid di-TMS; *d*, 4-Hydroxybenzoic acid di-TMS; *e*, Vanillic acid di-TMS; *f*, 3,4-Dihydroxybenzoic acid tri-TMS. GC conditions: 3% OV-1 on AW silanised Diatomite C (1.5 × 0.006 m); 15 cm^3 min^{-1} nitrogen carrier gas; temperature programme 100 °C isothermal for 5 min, 4 °C min^{-1} to 250 °C, isothermal at 250 °C for 10 min.

Structures already proposed[5] for fulvic acid are based on aromatic residues that have been assumed to arise partly from lignin- and/or tannin-derived material. Previous unpublished work by H.A.A. and A. Hepburn has shown that the yields of aromatic molecules from degradations are sufficiently low for these compounds to be considered of minor importance in the structure. Further structural investigations of fulvic and polymaleic acids are in progress.

H. A. Anderson
J. D. Russell

The Macaulay Institute for Soil Research,
Craigiebuckler,
Aberdeen, UK

Received November 22, 1975; accepted March 11, 1976.

1 Oden, S., *Ber. dt. chem. Ges.*, **35**, 651 (1912).
2 Forsyth, W. G. C., *Biochem. J.*, **41**, 176 (1947).
3 Braun, D., and Pomakis, J., *Makromol. Chem.*, **175**, 1411 (1974).
4 Barone, G., and Rizzo, E., *Gazz. chim. ital.*, **103**, 401 (1973).
5 Schnitzer, M., *Agron. Abstr.*, 77 (1971).

Printed in Great Britain by Henry Ling Ltd., at the Dorset Press, Dorchester, Dorset

Clay Minerals (1977) **12**, 55.

RECOGNITION OF IMOGOLITE STRUCTURES IN ALLOPHANIC CLAYS BY INFRARED SPECTROSCOPY

V. C. FARMER, A. R. FRASER, J. D. RUSSELL AND N. YOSHINAGA*

*Department of Spectrochemistry, The Macaulay Institute for Soil Research, Craigiebuckler, Aberdeen, Scotland, and * Department of Agricultural Chemistry, Ehime University, Matsuyama, Japan*

(*Received* 18 *May* 1976)

ABSTRACT: Imogolite structures in allophanic clays can be recognized and semi-quantitatively estimated by an absorption band at 348 cm^{-1}. Allowance can be made for interference by aluminous dioctahedral layer silicates present in small amounts.

Although the tubular aluminium silicate hydrate, imogolite, is known to be frequently associated with allophane in soils and other weathering environments (Wada & Harward, 1974), there has been no simple method for recognizing its presence in allophanic clays or any satisfactory procedure for estimating its amount. Its weak X-ray and electron diffraction patterns require the presence of bundles of aligned tubes, and the endotherm present on DTA curves of pure samples appears to be rapidly suppressed when the imogolite tubes are dispersed in a matrix of allophane. The most sensitive technique involves electron microscopy of the highest resolution, capable of showing the characteristic railway-track appearance of individual tubes (Wada & Harward, 1974), but this procedure is technically demanding, time-consuming, and cannot be made quantitative.

Infrared spectra of imogolite in the 4000–400 cm^{-1} region (Russell, McHardy & Fraser, 1969) are not sufficiently distinctive to allow its recognition in the presence of allophane, but extension of the spectrum to lower frequencies has now revealed a distinctive absorption band at 348 cm^{-1} (Fig. 1A). This band is totally absent from spectra of synthetic hydrated silica–alumina precipitates, and appears only weakly in spectra of natural allophanes from a variety of sources (Fig. 1B and Table 1), including samples from a volcanic ash soil from Okamoto (Yoshinaga & Aomine, 1962), a pumice bed from Kakino (N. Yoshinaga, unpublished), an encrustation on limestone from Derbyshire (MacKenzie, 1970) and a phosphatic allophane from Sta Creu Alorde, Barcelona (Scott Williams Co.). Careful examination of these allophanes by high resolution microscopy could not detect any imogolite in the European samples, and only rare and isolated tubes in the Japanese samples.

Semi-quantitative estimates of the imogolite content of allophanic clays can be made on the basis of the absorbance of the 348 cm^{-1} band (Table 1) measured from the steeply sloping background shown as broken lines in Fig. 1A and B. A correction might be applied for a contribution from accompanying allophane to the 348 cm^{-1} band, but it is

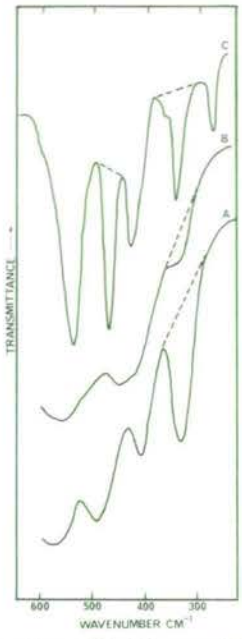

FIG. 1. Infrared spectra of (A) 1 mg imogolite (Kurayoshi), (B) 1 mg allophane (Okamoto), (C) 0·33 mg kaolinite. All samples ground 5 min with 170 mg KBr and pressed to give a 12-mm disk which was dehydrated by heating for 16 h at 150°C. Spectra recorded on a Perkin Elmer 577 spectrometer. The dashed lines indicate the baselines from which band absorbances are measured.

at present considered likely that the weak bands shown by allophane samples arise from imogolite or local structures related to imogolite, as the intensity of the 348 cm^{-1} band is correlated with that of a shoulder near 430 cm^{-1}, which lies close to a band of pure imogolite at 425 cm^{-1}. Admittedly, an estimate of 17–33% imogolite (as calculated from the 348 cm^{-1} band intensity) in the allophanes listed in Table 1 apparently conflicts with the almost complete absence of long tubes recognizable in the electron microscope, but there could well be short tubes less than 10 nm long present, which would not be recognizable among the agglomeration of 5 nm diameter spheres that make up much of

TABLE 1. Absorption bands near 350 cm^{-1} in possible clay components, and their absorbance for 1 mg clay in a 12 mm KBr disk, heated to 150°C overnight

Mineral	Wavenumber (cm^{-1})	Absorbance	Mineral	Wavenumber (cm^{-1})	Absorbance
Imogolite (Kurayoshi)	348	0·27	Montmorillonite	345	0·18
Allophane (Kakino)	348	0·06	(Wyoming)		
Allophane (Okamoto)	348	0·065	Illite (Ballater)	342	0·11
Allophane (Barcelona)	348	0·045	Diaspore	350	1·38
Allophane (Derbyshire)	348	0·09		370	0·65
Kaolinite (St. Austel)	348	0·67	Boehmite	325	0·40
Halloysite (Wagon Wheel)	348	0·52		370	0·45
			Gibbsite	370	1·20

the Japanese and Derbyshire allophanes. In support of this hypothesis, it was noted that the electron diffraction pattern from the Derbyshire allophane showed a series of four diffuse rings, three of which corresponded in position to the (06), (63) and (42)+(71) reflexions of imogolite (Cradwick *et al.*, 1972). The fourth corresponded to a diffraction ring of imogolite at 1·17 Å, but was relatively stronger in the allophane. None of these rings was obvious in the diffraction of Barcelona allophane, which has the weakest absorption at 348 cm^{-1} of those listed in Table 1. In our present state of knowledge, however, it seems wise to report estimates based on the 348 cm^{-1} band as 'imogolite structures' rather than as imogolite in the strict mineralogical sense.

Aluminous dioctahedral layer-silicate clays such as montmorillonite, illite, and the kaolinite group interfere with the infrared estimation of imogolite, since they also have an absorption band near 350 cm^{-1} (Table 1). Their presence can be recognized by a band at 470 cm^{-1} and its intensity can be used to make an allowance for their contribution to the 348 cm^{-1} band. For the kaolin minerals, whose presence is easily recognized in the 3600–3700 cm^{-1} region (Farmer, 1974), this contribution does not exceed 40% of the absorbance of the 470 cm^{-1} band, measured from the background shown in Fig. 1C. The corresponding contributions of montmorillonite and illite are less than 10%. Nontronite, glauconite and trioctahedral layer silicates such as saponite, vermiculite, and chlorite do not interfere. Of the aluminium hydroxides, only diaspore interferes (Table 1), but its presence is improbable in soil clays, and can be recognized in other regions of the spectrum. The iron oxides, goethite, lepidocrocite and hematite, do not absorb near 350 cm^{-1}, nor do felspars and quartz. In case of doubt, the possible presence of interfering minerals can always be checked in samples heated to 350°C to decompose allophane and imogolite.

This infrared procedure for estimating imogolite structures can be applied to size fractions unsuitable for electron microscopy, and should greatly facilitate exploration of their distribution in soils.

REFERENCES

Cradwick P.D.G., Farmer V.C., Russell J.D., Masson C.R., Wada K. & Yoshinaga N. (1972) *Nature phys. Sci.* **240,** 187.

Farmer V.C. (1964) *The Infrared Spectra of Minerals.* The Mineralogical Society, London.

MacKenzie K.J.D. (1970) *Clay Miner.* **8,** 349.

Russell J.D., McHardy W.J. & Fraser A.R. (1969) *Clay Miner.* **8,** 87.

Wada K. & Harward M.E. (1974) *Adv. Agron.* **26,** 211.

Yoshinaga N. & Aomine A. (1962) *Soil Sci. Pl. Nutr.* **8**(2), 6.

SOMMAIRE: Il est possible de reconnaître les structures imogolites dans les argiles allophaniques et de les estimer semi-quantitativement par une bande d'absorption à 348 cm^{-1}. Une tolérance peut être envisagée pour l'interférence par des silicates à strate dioctaédrique alumineuse présente en petites quantités.

KURZREFERAT: Imogolitstrukturen in Allophanton können unter Anwendung eines Absorptionsbandes von 348 cm^{-1} identifiziert und halbquantitativ abgeschätzt werden. Durch von in kleinen Mengen vorhandenen tonerdehaltigen Silikaten (dioktaedrische Schicht) bedingte Interferenz kann berücksichtigt werden.

RESUMEN: Las estructuras de imogolita en las arcillas alofánicas pueden reconocerse y calcularse semicuantitativamente por una banda de absorción de 348 cm^{-1}. Puede dejarse un margen de tolerancia para compensar la interferencia por los silicatos aluminosos de la capa dioctaédrica presentes en pequeñas cantidades.

Clays and Clay Minerals, Vol. 24, pp. 53–59. Pergamon Press 1976. Printed in Great Britain

A MÖSSBAUER AND I.R. SPECTROSCOPIC STUDY OF THE STRUCTURE OF NONTRONITE

B. A. GOODMAN, J. D. RUSSELL and A. R. FRASER

The Macaulay Institute for Soil Research, Craigiebuckler, Aberdeen AB9 2QJ, U.K.

and

F. W. D. WOODHAMS

Department of Natural Philosophy, University of Aberdeen, Aberdeen, U.K.

(*Received* 18 *January* 1976; *and in final form* 3 *March* 1976)

Abstract—Mössbauer and i.r. spectra of a series of nontronites show that Fe^{3+} and Al^{3+} are distributed between tetrahedral and octahedral sites. The Mössbauer results have reaffirmed the occupation by Fe^{3+} of octahedral sites at which these ions are coordinated to pairs of OH groups in both *cis* and *trans* configurations. The distribution of Fe^{3+} between these two sites varies considerably but in all of the nontronites some Fe^{3+} occurs in the *trans* site in contrast to the all *cis* occupancy of the centro-symmetric structure proposed by Mering and Oberlin (1967). In one of the nontronites the distribution of Fe^{3+} between these two sites approaches that in the ideal non-centrosymmetric structure proposed for montmorillonite.

INTRODUCTION

Ferruginous smectites are of widespread occurrence in rocks and soils, but have been investigated much less closely than their aluminum analogues. Nontronite, an end-member of the dioctahedral iron smectites is defined as an iron-rich analogue of beidellite, deriving its layer charge almost exclusively from Al-for-Si substitution (Brown, 1961). The ideal formula, $M^{+}_{0.67}$ $(Si_{7.33}$ $Al_{0.67})$ Fe_4 O_{20} $(OH)_4$ shows only this type of substitution, in agreement with the limitations placed by Ross and Hendricks (1945) on the compositional range of high-iron montmorillonites. In the beidellite–nontronite series, however, complete isomorphous replacement of Al^{3+} by Fe^{3+} should be possible, giving rise to Fe^{3+} in tetrahedral sites. Therefore there should be three possible sites for iron in nontronite, one tetrahedral and two octahedral, the two octahedral sites corresponding to *cis* and *trans* arrangements of the hydroxyl groups, respectively.

Although indirect evidence of tetrahedral occupancy has come from chemical analysis (e.g. Osthaus, 1954), Mössbauer spectroscopy has the potential for directly probing the coordination of iron in minerals, as for example in the investigations of many iron-containing minerals by Bancroft *et al.* (1967). Mössbauer spectra of nontronites have been reported by several workers (Weaver *et al.*, 1967; Taylor *et al.*, 1968; Bischoff, 1972; Brunot, 1973) but only Brunot has attempted to analyze well-defined spectra in terms of both octahedrally- and tetrahedrally-coordinated iron.

I.r. spectroscopy is also sensitive to the structure and composition of layer silicates, although the field of nontronites has not yet been well explored (Serratosa, 1960, 1962; Stubican and Roy, 1961; Farmer and Russell, 1964). Here, both i.r. and Mössbauer techniques are applied in studying a variety of nontronite samples covering a wide range of composition.

EXPERIMENTAL

Materials

The nontronites were purified by saturation with Na^{+} (Li^{+} for the Californian specimen), dispersion in water, then separation of < 1.4 μm and < 0.2 μm fractions by centrifuging. These fractions were resaturated with Na^{+} using conventional centrifuge procedures, then freeze dried. Si, Fe, Al, Mg, Ca, Na and K were determined using electron microprobe analysis, and cation exchange capacities were measured on NH_4^{+}-saturated specimens using the colorimetric method of Fraser and Russell (1969). Sources, approximate chemical compositions and cation exchange capacities (C.E.C.) are shown in Table 1. The high C.E.C. of the Californian specimen is consistent with the need to use a Li-saturated sample to achieve efficient dispersion in water, in agreement with observations made on the dispersion of vermiculite of comparable C.E.C. (Walker and Garrett, 1967).

Instrumental techniques

Mössbauer. Spectra were recorded in 512 channels of a spectrometer (Harwell Scientific Services, Didcot, Berks.), incorporating an Ortec Model 6200 analyzer. A ^{57}Co in Pd source of nominal strength 25 mCi was used with an argon-methane proportional counter as γ-ray detector. Velocity calibration was carried out with a high purity metallic iron foil using

Table 1. Composition and cation exchange capacities (m-equiv./100 g air-dry clay) of nontronites from various sources

Source		C.E.C.	Composition per $O_{20}(OH)_4$
Washington, U.S.A. (Source clay minerals repository)†	(WAS)	103	$(Si_{7.30}Al_{0.70})(Al_{1.06}Fe_{2.73}Mg_{0.26})$
Garfield, Washington, U.S.A. (A.P. 1. H33b)	(GAR)	117	$(Si_{6.84}Al_{1.05}Fe_{0.11})(Fe_{3.96}Mg_{0.04})$
Clausthal, Zellerfeld, Germany	(CLA)	115	$(Si_{6.81}Al_{0.13}Fe_{1.06})(Fe_{4.01}Mg_{0.07})$
A crocidolite deposit, Koegas, Cape Province, South Africa	(CRO)	137	$(Si_{6.75}Al_{0.06}Fe_{1.19})(Fe_{3.90}Mg_{0.24})$
Koegas, Cape Province, S.A.	(KOE)	134	$(Si_{6.61}Al_{0.08}Fe_{1.31})(Fe_{4.06}Mg_{0.10})$
An amosite deposit, Penge, Cape Province, S.A.	(AMO)	115	$(Si_{6.84}Al_{0.04}Fe_{1.12})(Fe_{4.04}Mg_{0.15})$
Panamint Valley, California, U.S.A.	(CAL)	155	$(Si_{6.21}Al_{0.14}Fe_{1.65})(Fe_{4.04}Mg_{0.21})$

All nontronites contain traces of Ca, K and Ti.
† Selected, purified sample, Source Clay Minerals Project (*Clays & Clay Minerals* (1973) **21**, 71).

the data of Preston *et al.* (1962). To minimize thickness effects the absorbers contained 3 mg iron/cm^2 freeze-dried nontronites. They were prepared, either by direct weighing of the sample into a perspex holder and sealing with the minimum of pressure, or by grinding the sample thoroughly with five times its weight of alumina, then sealing in a perspex holder. Identical spectra were obtained from absorbers prepared by both methods and in most of the later experiments they were prepared by the former method.

The spectra were fitted to a sum of doublets having Lorentzian peak shapes using a least squares computer program. The peaks of each doublet were constrained to have equal areas and widths. A parabolic baseline was assumed and χ^2 was used as a goodness-of-fit parameter. For statistically acceptable fits χ^2 is required to lie between the 1% and 99% limits of the χ^2 distribution i.e. between about 416 and 561 for 486 *d.f.*, where the number of degrees of freedom is equal to the number of channels fitted minus the number of variables in the fit.

I.r. spectroscopy. Spectra were recorded from 4000–400 cm^{-1} on a Grubb Parsons Spectromaster and from 500–40 cm^{-1} on a Beckmann-RIIC FS 720 interferometer. The nontronites were in the form of either self-supporting films (2 mg/cm^2), prepared by evaporating aqueous suspensions on to polyethylene sheet from which they were peeled when air-dry, or thinner, supported films (0.3 mg/cm^2) prepared by evaporation on to 1 mm AgCl or polyethylene plates.

RESULTS AND INTERPRETATION

Mössbauer spectroscopy

The isomer shift, δ, is sensitive not only to the oxidation state of high spin ions, but also to the coordination number of these ions. For Fe^{3+}, δ decreases with a decrease in coordination number as a result of an increase in the covalent character of the bonding. As an example ferriphlogopite, which contains tetrahedrally-coordinated Fe^{3+}, has $\delta = 0.17$ mm/sec relative to iron metal (Annersten *et al.*, 1971), whereas in montmorillonite, which contains octahedrally-coordinated Fe^{3+}, $\delta = 0.35$ mm/sec (Tennakoon *et al.*, 1974), both values being obtained with absorbers at room temperature. The quadrupole splitting, Δ, is a measure of the electric field gradient at the ^{57}Fe nucleus and in the case of high spin Fe^{3+} is predominantly determined by the distortion from cubic symmetry of the lattice surrounding the iron atom. Thus a simple point charge model predicts that the *trans* arrangement of the OH groups in the octahedral complex $Fe^{3+}(OH)_2O_4$ will produce an electric field gradient of twice the magnitude of, but opposite sign to, the corresponding *cis* grouping.

The Mössbauer spectrum of the nontronite *ex* crocidolite (CRO) at 77°K which is typical of all the nontronite spectra, (Fig. 1) appears to consist of two peaks of unequal intensity. Identical spectra were obtained when the absorber was rotated through 30° and 45°, thus demonstrating the absence of texture effects (Gonser and Pfannes, 1974). Very similar spectra were also obtained at room temperature, thus eliminating the possibility of any significant anisotropy of the recoil-free fraction (Goldan'skii *et al.*, 1963). It would appear, therefore, that the asymmetry in the spectra must arise from the presence of more than one component.

The results of fitting the spectrum to one, two and three doublets are shown in Fig. 1. From the isomer shifts it is clear that all of the iron is in the ferric form (Bancroft *et al.*, 1967). The fits illustrated in Fig. 1(ii) and (iii) correspond to different models assumed when making initial estimates of the parameters for the least squares program. Figure 1(ii) illustrates the results of assuming two octahedral environments with similar isomer shifts for Fe^{3+}, while Fig. 1(iii) shows the results of assuming one octahedral and one tetrahedral site, the isomer shift for the tetrahedral site being markedly lower than that of the octahedral site. In both cases the χ^2 values were too high to be acceptable. The use of three doublets, Fig. 1(iv), with initial values based on a combination of those shown in Fig. 1(ii) and (iii), produced a fit having a significantly lower χ^2 value. Similar results were also obtained with the other nontronites studied, with the exceptions of those from Garfield and Washington, which produced fairly good fits with Fe^{3+} in two

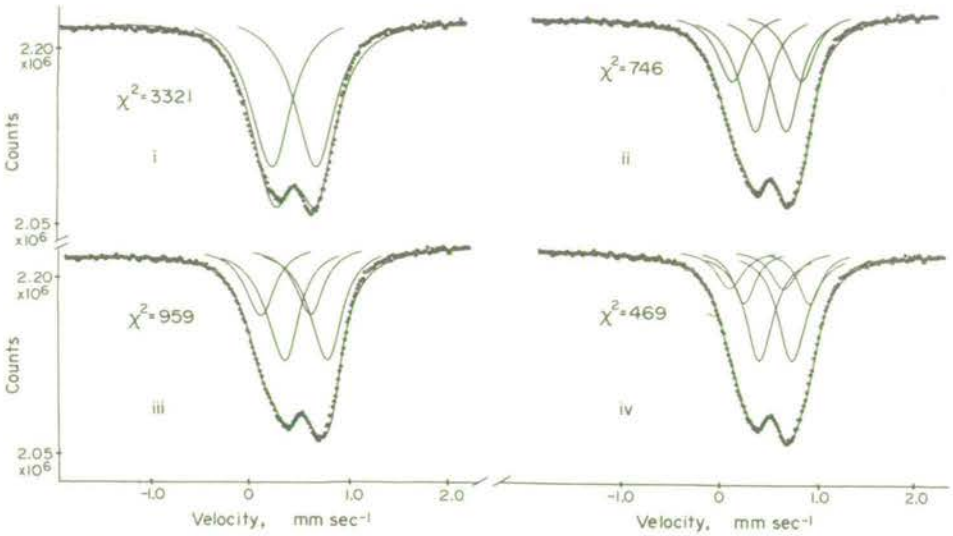

Fig. 1. Mössbauer spectrum at 77°K of nontronite *ex* crocidolite (CRO) fitted to (i) one octahedral doublet, (ii) two octahedral doublets, (iii) one octahedral and one tetrahedral doublet, (iv) two octahedral and one tetrahedral doublets.

octrahedral sites only. The three-doublet fits to the spectra of these nontronites showed a small amount of the tetrahedral doublet and these results are shown in Table 2 together with those for the other nontronites. If a constant recoil-free fraction can be assumed for iron in the three types of structural site then the % columns in Table 2 are a measure of the percentage of the total iron in each site. The computed standard deviations quoted in Table 2 are minimum errors because the effects of finite sample thickness, non-linearity of the waveform and calibration errors have been ignored, although these are all likely to be small. However, in this work six peaks with a total of fourteen variables have been fitted to two slightly asymmetric peaks. The necessity of using such a large number of variables has been adequately demonstrated and the model adopted is justified by the fact that there are only three possible sites for Fe^{3+} in nontronite and the Mössbauer parameters are similar to those expected for Fe^{3+} in such sites.

A somewhat different interpretation of a nontronite Mössbauer spectrum has been presented by Brunot (1973) who studied a hydrothermal and a sedimentary nontronite at room temperature. The spectrum of the hydrothermal nontronite was analyzed in terms of two doublets with parameters similar to those obtained from the two-doublet fit to the sample from Garfield (Table 2) when account is taken of the effects of the different temperature used on the isomer shifts, δ. For this sample Brunot's assignment of the com-

Table 2. Computed results from the Mössbauer spectra of nontronites

	$Fe^{3+}_{(oct)}$								$Fe^{3+}_{(tet)}$				
	cis OH				*trans* OH								
Nontronite	Δ	δ	Γ	%	Δ	δ	Γ	%	Δ	δ	Γ	%	χ^2
WAS	0.29	0.48	0.37	70	0.62	0.48	0.35	24	0.60	0.29	0.26	6	485
	(0.02)	(0.01)	(0.02)	(11)	(0.02)	(0.01)	(0.02)	(8)	(0.02)	(0.01)	(0.02)	(3)	
WAS	0.27	0.47	0.35	52	0.62	0.45	0.41	48					675
(2 doublets)	(0.01)	(0.01)	(0.01)	(4)	(0.01)	(0.01)	(0.01)	(4)					
GAR	0.27	0.50	0.32	54	0.62	0.50	0.29	37	0.47	0.30	0.22	9	437
	(0.01)	(0.01)	(0.01)	(4)	(0.01)	(0.01)	(0.01)	(3)	(0.01)	(0.01)	(0.01)	(2)	
GAR	0.25	0.48	0.34	59	0.65	0.47	0.31	41					567
(2 doublets)	(0.01)	(0.01)	(0.01)	(3)	(0.01)	(0.01)	(0.01)	(3)					
CLA	0.33	0.50	0.38	64	0.67	0.50	0.27	21	0.61	0.30	0.31	15	636
	(0.01)	(0.01)	(0.01)	(5)	(0.01)	(0.01)	(0.02)	(4)	(0.01)	(0.01)	(0.01)	(2)	
CRO	0.34	0.49	0.36	59	0.67	0.49	0.28	22	0.56	0.29	0.32	19	469
	(0.01)	(0.01)	(0.01)	(4)	(0.01)	(0.01)	(0.01)	(3)	(0.01)	(0.01)	(0.01)	(2)	
KOE	0.32	0.50	0.36	54	0.62	0.51	0.25	19	0.53	0.31	0.29	27	541
	(0.01)	(0.01)	(0.01)	(5)	(0.01)	(0.01)	(0.02)	(3)	(0.01)	(0.01)	(0.01)	(2)	
AMO	0.34	0.49	0.34	51	0.64	0.50	0.27	21	0.54	0.31	0.35	28	556
	(0.01)	(0.01)	(0.01)	(4)	(0.01)	(0.01)	(0.01)	(3)	(0.01)	(0.01)	(0.01)	(3)	
CAL	0.33	0.50	0.33	44	0.60	0.50	0.28	24	0.48	0.31	0.31	32	475
	(0.01)	(0.01)	(0.01)	(4)	(0.01)	(0.01)	(0.01)	(4)	(0.01)	(0.01)	(0.01)	(3)	

Quadrupole splittings, Δ, isomer shifts, δ, and peak widths, Γ, all in mm/sec with δ relative to iron metal. Figures in brackets indicate one S.D.

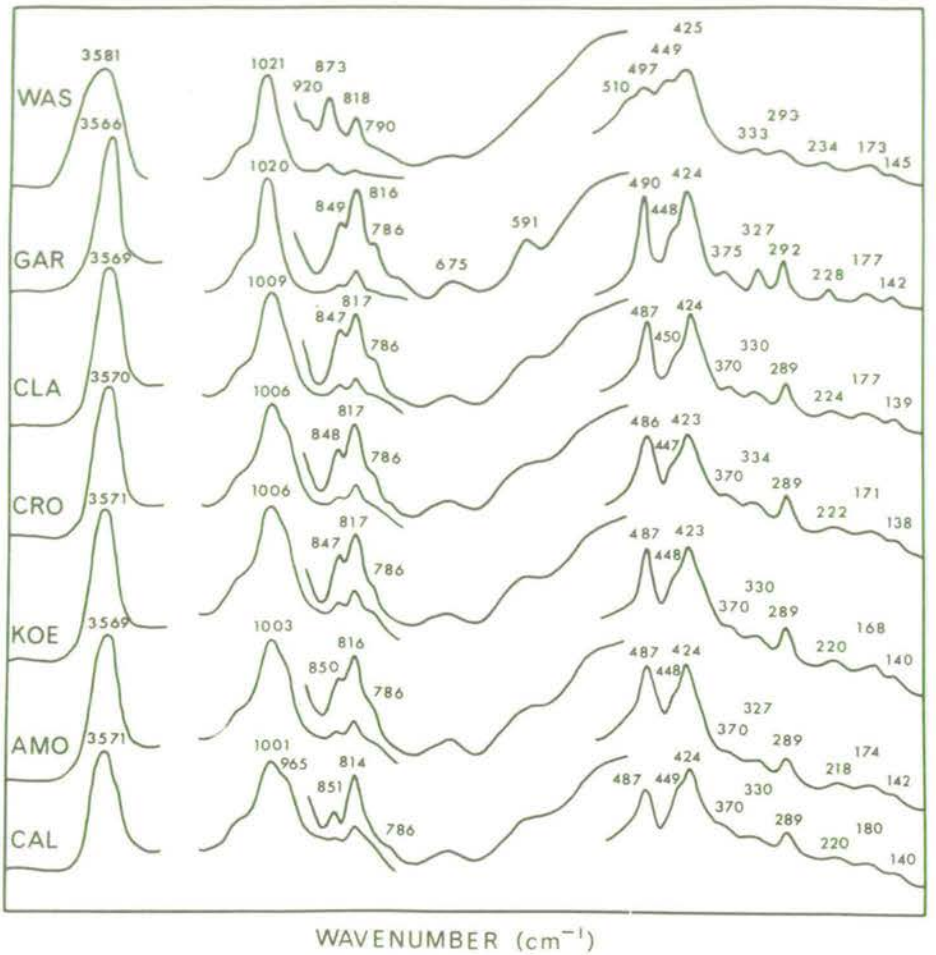

Fig. 2. I.r. absorption spectra of nontronites from various sources (See Table 1).

ponents to octahedral sites with *cis* and *trans* hydroxyl groups was analogous to the assignments in the present work. The nontronite of sedimentary origin however had an additional doublet with $\Delta = 1.22$ mm/sec and $\delta = 0.40$ mm/sec (relative to iron metal) and this was assigned to Fe^{3+} in tetrahedral sites. For reasons mentioned earlier this value of δ is higher than expected for tetrahedral iron which would be expected to have parameters similar to the iron in ferriphlogopite ($\Delta = 0.50$ mm/sec, $\delta = 0.17$ mm/sec, relative to iron metal, Annersten *et al.*, 1971) and it is similar to that observed for Fe^{3+} in octahedral coordination. Although the value of Δ for Brunot's additional doublet is higher than is usually expected for octahedral Fe^{3+}, such values have been observed in microcrystals of iron oxide minerals (e.g. Schroeer, 1968). In another investigation the spectrum of a natural ferric gel from a fresh water lake was analyzed in terms of a range of quadrupole splittings, a value of $\Delta = 1.05$ being obtained at the half height of the distribution function (Coey and Readman, 1973). It is therefore possible that the additional doublet is caused by the presence of a microcrystalline ferric oxide or gel ferric hydroxide impurity, a conclusion that is supported by Brunot's observation that this doublet is lost preferentially by treatment with sodium dithionite solution, an established method for the removal of poorly crystalline iron oxides from mineralogical specimens (Mitchell and Mackenzie, 1954; Mehra and Jackson, 1960).

I.r. spectroscopy

The i.r. spectra of six of the seven nontronites (Fig. 2) are generally similar with only small spectral variations, but that of the Washington sample is obviously different over the entire spectral range shown. This difference is reflected in its chemical composition (Table 1), having more Al^{3+} and less Fe^{3+} than the others. The variations in spectra occur in several well defined regions and these will be dealt with in turn, beginning with that centred on 850 cm^{-1}.

760–960 cm^{-1} *region.* Librational vibrations of OH groups in dioctahedral layer silicates occur in this frequency range in which the nontronites generally show three absorption bands. The strong band at 814–818 cm^{-1} arises from OH groups coordinated to two

Fe^{3+} ions, an assignment which is now well established (Serratosa, 1960; Stubican and Roy, 1961). The weaker band at 847–851 cm^{-1} (873 cm^{-1} for the Washington sample) has a less certain assignment, but it is thought to be the libration of the $AlFe^{3+}OH$ group in agreement with the proposal of Serratosa (1960) and Heller *et al.* (1962). This assignment, however, requires that the analytical compositions (Table 1) be altered. They are conventionally calculated on the assumption that the tetrahedral deficit of Si is made up by Al^{3+} as far as possible, then by Fe^{3+} as required. This results in most of the nontronites having no octahedral Al^{3+}. The alterations would be such that Al^{3+} and therefore Fe^{3+} are distributed between octrahedral and tetrahedral sites. The Mössbauer results indicate the distribution of Fe^{3+} between these sites (Table 2), but no direct information is available on how Al^{3+} is distributed. Some idea of the abundance of Al in octahedral sites can be obtained from the intensity of the AlFeOH libration which varies considerably within the group of nontronites. Using a nontronite band near 675 cm^{-1} as an internal standard, the order of absorbances, and therefore of octahedral Al^{3+}, is WAS > CLA > KOE > CRO > GAR > AMO > CAL. The position of the absorption maximum of the AlFeOH libration varies within the group of nontronites. It shifts from 847–851 cm^{-1} in six of the nontronites containing relatively small amounts of Al to 873 cm^{-1} in the Washington sample, of highest total Al^{3+}, and therefore highest octahedral Al content. This upward shift in frequency of the AlFeOH libration continues in the more aluminous smectites, rising to 877 cm^{-1} for Woburn Fuller's Earth and 890 cm^{-1} for Wyoming montmorillonite (Farmer and Russell, 1964). From this it would appear that the AlFeOH librational vibration occurs at higher frequencies when the neighbouring cations are aluminium and at lower frequencies when they are iron.

The possibility of assigning the 816 cm^{-1} and 850 cm^{-1} absorption bands to librations of OH groups in *trans* and *cis* octahedral configurations was considered. This was rejected, however, because the relative intensities of the two bands did not agree with the octahedral site occupancies indicated by the Mössbauer results (Table 2), and also because of the unrealistically large frequency difference between vibrations of the two types of OH group. Apart from the slightly different stereochemistry round Fe^{3+} ions, these OH groups have identical relationships to the oxygen ions in the silicon–oxygen framework of the tetrahedral layers, and would be expected to exhibit essentially the same librational frequencies.

All of the nontronites contain octahedral Mg^{2+} (Table 1), which, because of the high content of Fe^{3+}, is almost certain to have three Fe^{3+} neighbours in the octahedral layer and therefore to be involved in a $Fe^{3+}MgOH$ grouping. By analogy with AlMgOH which in montmorillonites absorbs at 843 cm^{-1} compared with 915 cm^{-1} for AlAlOH (Farmer and Russell, 1964) $Fe^{3+}MgOH$ in nontronite should absorb at a lower frequency than the 817 cm^{-1} for $Fe^{3+}Fe^{3+}OH$. The inflection near 785 cm^{-1} in all of the nontronite spectra (Fig. 2) has been found to shift to 585 cm^{-1} on deuteration and is therefore tentatively assigned to the libration of $Fe^{3+}MgOH$. Its frequency is in fair agreement with the value of 800 cm^{-1} found for this vibration in a synthetic $Fe^{3+}Mg$ celadonite (Farmer *et al.*, 1967), considering that the frequency will vary with the composition of the octahedral layer.

975–1200 cm^{-1} *region.* The position of the intense Si-O stretching absorption band shifts from 1021 cm^{-1} in the Washington and Garfield samples, to 1009 cm^{-1} in Clausthal, to 1006 cm^{-1} in Crocidolite and Koegas, to 1003 cm^{-1} in Amosite, to 1001 cm^{-1} in the California sample (Fig. 2). This progressive shift to lower frequencies correlates well with the increasing content of Fe^{3+} in tetrahedral sites calculated from chemical compositions and from Mössbauer results (Table 3) and must be due to increasing Fe-for-Si substitution. In an analogous manner, replacement of Si by Al causes the Si–O stretching band to shift from 1014 cm^{-1} in talc, to 1005 cm^{-1} in saponite, to 994 cm^{-1} in a synthetic phlogopite (Farmer, 1974), and from 1070 cm^{-1} in pyrophyllite, to 1041 cm^{-1} in beidellite, to 1022 cm^{-1} in muscovite (Farmer and Russell, 1964). A band near 965 cm^{-1} in the nontronite spectra also intensifies with increasing tetrahedral Fe^{3+} content. It is strongest in the spectrum of the California sample in which about 1 in 5 Si^{4+} ions is replaced by Fe^{3+} and may be analogous to the band at 958 cm^{-1} in the spectrum of ferriphlogophite in which the replacement of Si by Fe^{3+} is 1 in 4 (Farmer, 1974).

3550–3650 cm^{-1} *region.* The absorption bands due to the OH stretching vibration of six of the nontronites show little variation in position, occurring in the frequency range 3566–3571 cm^{-1}. This is consistent with $Fe^{3+}Fe^{3+}OH$ being the predominant grouping in these nontronites. The corresponding band in the spectrum of the Washington sample is centred on 3581 cm^{-1} with broader absorption on the high-frequency side of the band. This is indicative of considerable replacement of octahedral Fe^{3+} by Al giving rise to $AlFe^{3+}OH$ and AlAlOH groups which absorb in the range 3600–3630 cm^{-1} (Farmer and Russell, 1964). These conclusions are substantiated by the presence in the spectrum of the Washington sample of the $AlFe^{3+}OH$ libration frequency at 873 cm^{-1} discussed above, and a weak band near 915 cm^{-1} due to hydroxyl libration of the AlAlOH group.

100–700 cm^{-1} *region.* Absorption patterns of the nontronites in this region are included mainly for completeness and to supplement the spectrum shown by Larson *et al.* (1972) covering the range 400–200 cm^{-1}. The nontronites generally show the same pattern of absorption bands, but that of the Washington sample is more diffuse. Additional strong bands near

Table 3. Relationship between the Si–O stretching frequencies of various nontronites and their tetrahedral Fe^{3+} contents calculated from Mössbauer results and chemical compositions

Nontronite	Fe on tetrahedral sites (% of total Fe) Mössbauer	Microprobe analysis	Si–O (cm^{-1})
CAL	32 ± 3	29	1001
AMO	28 ± 3	22	1003
KOE	27 ± 2	24	1006
CRO	19 ± 2	23	1006
CLA	15 ± 2	21	1009
GAR	9 ± 2	3	1020
WAS	6 ± 3	0	1021

450 cm^{-1} and 510 cm^{-1} in the spectrum of the latter testify to its more aluminous composition (compare for example 467 and 521 cm^{-1} in montmorillonite and 479 and 537 cm^{-1} in beidellite, Farmer and Russell, 1964). The spectrum of the Garfield sample is notable for the good definition and sharpness of its absorption bands. With increasing tetrahedral iron content in the series Garfield to California (Table 3) bands become progressively broader, weaker and less well defined but remain relatively constant in position. The diffuseness of the Washington spectrum in this region must be due to the presence of considerable octahedral Al.

DISCUSSION

The Mössbauer spectra, using the new interpretations described earlier, indicate the presence of tetrahedral iron in most if not all of the nontronites.

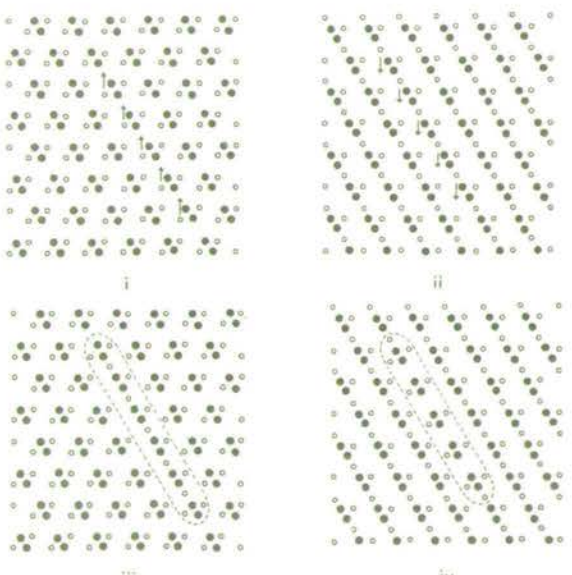

Fig. 3. Dioctahedral arrangements of Fe^{3+} ions (●) and OH groups (○). (i) centrosymmetric (all *cis*) (ii) non-centrosymmetric (*cis*/*trans* = 1/1). Arrows indicate movement of Fe^{3+} ions generating (iii) a *cis*/*trans* region in an all *cis* array and (iv) an all *cis* region in a *cis*/*trans* array.

The order of tetrahedral iron content is WAS < GAR < CLA < CRO < KOE < AMO < CAL, which is similar to that deduced from the analytical results and Si–O frequencies (Table 3). The main discrepancies between the Mössbauer and analytical results occur with the Washington and Garfield samples where 0 and 3%, respectively, of the iron is required in tetrahedral sites to satisfy the analytical results, but appreciably higher amounts are indicated by the Mössbauer experiments. The i.r. spectra show the presence of a peak consistent with an AlFeOH libration indicating octahedral Al contents in the order WAS > CLA > KOE > CRO > GAR > AMO > CAL. The presence of such a peak in spectra of these samples provides further evidence that the distribution of iron and aluminium is more random than is usually assumed. Unfortunately the Mössbauer estimations are subject to appriciable errors because of the high degree of overlap of the peaks, so that accurate estimates of tetrahedral iron contents are unobtainable. A similar problem exists with quantitative estimation using the AlFeOH libration in the i.r. spectra, thus making a reliable recalculation of the structural formulae impossible at present.

The Mössbauer results have also indicated a distribution of octahedral cations over the two types of site, the one with *trans* hydroxyl accounting for between 25 and 41% of the octahedral cations. These conclusions contrast sharply with those of Mering and Oberlin (1967), from their work on selected area electron diffraction of a nontronite from Pfaffenreuth, that a centrosymmetric structure existed (i.e. one in which all the octahedral cations are bound with *cis* hydroxyl groups). Similar work by these authors indicated the presence of a non-centrosymmetric structure for Wyoming montmorillonite (i.e. equal numbers of octahedral cations with *cis* and *trans* hydroxyl groups). These two structures are illustrated in Fig. 3(i) and (ii) which for simplicity shows only the positions of the octahedral cations and the hydroxyl groups. The Garfield nontronite with 41% of its octahedral iron in sites with *trans* hydroxyl groups (calculated from Table 2) would appear to have a structure similar to that of Wyoming montmorillonite. The

remaining samples with between 25 and 35% of their octahedral iron in such sites have structures intermediate between the centro- and non-centrosymmetric types. None of the samples shows any tendency to approach the structure proposed for the Pfaffenreuth nontronite.

The Mössbauer results give only averages for the relative proportions of the two types of octahedral site throughout the structure. Figure 3(iii) and (iv) illustrates ways in which local defects in the ideal structures could produce mixtures of the two types of site within one sheet. At the intersection of two phases a hydroxyl group is produced which is bound either to three cations or less likely to one cation and two vacancies. Trioctahedral sites are almost certain to occur but while they were not detectable in infrared spectra, their presence was indicated by the overfilling of the octahedral layers in all but one of the nontronites.

Acknowledgements—We wish to thank Dr. W. J. McHardy for performing the microprobe analyses and Professor J. L. Post, California State University, for the California nontronite.

REFERENCES

Annersten, H., Devanarayanan, S., Häggström, L. and Wäppling, R. (1971) Mössbauer study of synthetic ferriphlogopite: *Phys. Status Solidi* (B), **48**, K137–K138.

Bancroft, G. M., Maddock, A. G. and Burns, R. G. (1967) Applications of the Mössbauer effect to silicate mineralogy—I. Iron silicates of known crystal structure: *Geochim. Cosmochim. Acta* **31**, 2219–2246.

Bischoff, J. L. (1972) A ferroan nontronite from the Red Sea geothermal system: *Clays & Clay Minerals* **20**, 217–223.

Brown, G. (1961) *The X-ray Identification and Crystal Structures of Clay Minerals*, 544 pp. Mineralogical Society, London.

Brunot, B. (1973) Application of the Mössbauer effect to the study of clay minerals. Hydrothermal nontronite and a nontronite from Lake Malawi: *Neues Jahrb. Mineral., Monatsh.* 452–461.

Coey, J. M. D. and Readman, P. W. (1973) Characterization and magnetic properties of natural ferric gel: *Earth Planet. Sci. Lett.* **21**, 45–51.

Farmer, V. C. (1974) *The i.r. Spectra of Minerals*, 539 pp. Mineralogical Society, London.

Farmer, V. C., Russell, J. D., Ahlrichs, J. L. and Velde, B. (1967) Vibrations du groupe hydroxyle dans les silicates en couches: *Bull. Groupe Fr. Argiles* **19**, 5–10.

Farmer, V. C. and Russell, J. D. (1964) The i.r. spectra of layer silicates: *Spectrochim. Acta* **20**, 1149–1173.

Fraser, A. R. and Russell, J. D. (1969) A spectrophotometric method for determination of cation-exchange capacity of clay minerals: *Clay Miner.* **8**, 229–230.

Goldan'skii, V. I., Makarov, E. F. and Krapov, V. V. (1963) Difference in two peaks of quadrupole splitting in Mössbauer spectra: *Phys. Lett.* **3**, 344–346.

Gonser, U. and Pfannes, H. D. (1974) Texture Problems: *J. Phys.*, Paris Colloq. **6**, 113–120.

Heller, L., Farmer, V. C., Mackenzie, R. C., Mitchell, B. D. and Taylor, H. F. W. (1962) The dehydroxylation and rehydroxylation of triphormic dioctahedral clay minerals: *Clay Miner. Bull.* **5**, 56–72.

Larson, S. J., Pardoe, G. W. F., Gebbie, H. A. and Larson, E. E. (1972) The use of far infrared interferometric spectroscopy for mineral identification: *Am. Miner.* **57**, 998–1002.

Mehra, O. P. and Jackson, M. L. (1960) Iron oxide removal from soils and clays by a dithionite–citrate system buffered with sodium bicarbonate: *Clays & Clay Minerals* **7**, 317–327.

Mering, J. and Oberlin, A. (1967) Electron-optical study of smectites: *Clays & Clay Minerals* **15**, 3–25.

Mitchell, B. D. and Mackenzie, R. C. (1954) Removal of free iron oxide from clays: *Soil Sci.* **77**, 173–184.

Osthaus, B. B. (1954) Chemical determination of tetrahedral ions in nontronite and montmorillonite: *Clays & Clay Minerals. Proc. 2nd Nat. Conf. Nat. Acad. Sci. Nat. Research Council Publ.* **327**, 404–416.

Preston, R. S., Hanna, S. S. and Heberle, J. (1962) Mössbauer effect in metallic iron: *Phys. Rev.* **128**, 2207–2218.

Ross, C. S. and Hendricks, S. B. (1945) Minerals of the montmorillonite group: *Prof. Pap. U.S. Geol. Surv.* **205B**, 23–79.

Schroeer, D. (1968) Quadrupole interaction in α-ferric oxide microcrystals: *Phys. Lett* **A27**, 507–508.

Serratosa, J. M. (1960) Dehydration studies by i.r. spectroscopy: *Am. Miner.* **45**, 1101–1104.

Serratosa, J. M. (1962) Dehydration and rehydration studies of clay minerals by i.r. absorption spectra: *Clays & Clay Minerals* **9**, 412–418.

Stubican, V. and Roy, R. (1961) A new approach to the assignment of i.r. absorption bands in layer silicates: *Z. Krist.* **115**, 200–214.

Taylor, G. L., Ruotsala, A. P. and Keeling, R. O. (1968) Analysis of iron in layer silicates by Mössbauer spectroscopy: *Clays & Clay Minerals* **16**, 381–391.

Tennakoon, D. T. B., Thomas, J. M. and Tricker, M. J. (1974) The surface and intercalate chemistry of layered silicates—II: A ^{57}Fe Mössbauer study of the role of lattice-substituted iron in the benzidine-blue reaction of montmorillonite: *J. Chem. Soc. Dalton* pp. 2211–2215.

Walker, G. F. and Garrett, W. G. (1967) Chemical exfoliation of vermiculite and the production of colloidal dispersions: *Science* **156**, 385–387.

Weaver, C. E., Wampler, J. M. and Pecuil, T. E. (1967) Mössbauer analysis of iron in clay minerals: *Science* **156**, 504–508.

ADSORPTION ON HYDROUS OXIDES
I. OXALATE AND BENZOATE ON GOETHITE

R. L. PARFITT[1], V. C. FARMER and J. D. RUSSELL
(Department of Spectrochemistry, The Macaulay Institute for Soil Research, Aberdeen)

Summary

The adsorption of oxalic acid on synthetic goethite (α-FeOOH) was studied using adsorption isotherms. Infrared spectra were obtained for goethite-oxalate complexes at several points on the isotherms. On a goethite preparation with a phosphate sorption capacity of 200 μmol g^{-1} the amounts of oxalate strongly adsorbed varied from near zero at pH 8 to about 100 μmol g^{-1} at pH 4 and below. At pH 3.4, the first 100 μmol g^{-1} of oxalic acid added was strongly adsorbed as a binuclear complex (FeOOC–COOFe), replacing two singly-coordinated OH groups by ligand exchange. At higher concentrations a further 200 μmol g^{-1} of oxalic acid formed a monodentate complex (FeOOC–COOH) so that more oxalate could be accommodated.

Benzoic acid was weakly adsorbed on goethite with one benzoate oxygen replacing one singly-coordinated OH. The other oxygen of the COO group fitted into the goethite surface so that the benzene ring was at a high angle to the (100) face.

Introduction

IT is now widely believed that hydrous oxides of aluminium and iron in soils can provide many more sites for adsorption of acidic organic substances than can clays and smectites, but a recent review by Greenland (1971) has revealed little more than circumstantial evidence in support.

Hingston *et al.* (1968, 1972) have studied the adsorption of several inorganic anions on goethite and gibbsite and have postulated that ligand exchange (specific adsorption) takes place whereby OH coordinated to iron or aluminium ions in the surface are replaced by the anions, but it has not yet been established whether organic acids are adsorbed by this mechanism, although work of Watson *et al.* (1973) suggests it is likely. This question is explored here in a study of the adsorption of oxalate and benzoate on goethite, correlating the infrared spectra of adsorbed species with adsorption isotherms.

Infrared studies have previously provided evidence for a model of the (100) face of goethite in which equal amounts of one-, two- and three-coordinated hydroxyls (A, C, and B types) are exposed, and have shown that only the A-type hydroxyls are displaced by phosphate ions which bridge adjacent oxygens to form binuclear complexes: FeO(PO.OH)OFe (Atkinson *et al.*, 1974; Russell *et al.*, 1975; Parfitt *et al.*, 1976).

[1] On leave from Department of Agriculture, University of Papua New Guinea.

Journal of Soil Science, 1977, 28, 29–39

Materials and methods

Goethite preparation

The sample was prepared by the method of Atkinson *et al.* (1968). Sodium hydroxide was added to ferric nitrate solution at a OH/Fe ratio of 1.5 and aged initially for 50 h before adjusting the pH to 11.8 and maintaining at 60 °C for four days. The goethite crystals seen under the electron microscope were lath-shaped with the (100) face predominating. The average dimensions were 160 x 26 x 6.5 nm which gives a calculated surface area of 90 $m^2\ g^{-1}$. Such crystals would have approximately 400 $\mu mol\ g^{-1}$ of each of the A, B, and C-type hydroxyls exposed on (100) faces and this is consistent with a measured phosphate adsorption capacity of 204 $\mu mol\ g^{-1}$ at pH 3.4.

The ^{14}C-labelled oxalic acid used for adsorption isotherms was obtained from the Radiochemical Centre, Amersham, England.

Adsorption isotherms

Oxalic acid Preliminary experiments showed that equilibrium was attained after two hours shaking. Oxalic acid solutions were adjusted to the required pH with NaOH and 5 cm^3 aliquots were mixed with 10 cm^3 of 0.2 M NaCl and 0.1 cm^3 of ^{14}C-labelled oxalic acid (1 μCi) in centrifuge tubes. Goethite suspension (5 cm^3 containing 0.11 g) was added and the tubes were shaken at 20 °C for 16 h. The tubes were centrifuged for 15 min at 2000 rpm and 0.2 cm^3 of each supernatant was dried on a fibre glass pad for counting in a Packard Liquid Scintillation Spectrometer. The amount of oxalate adsorbed was calculated by difference between the initial and final solution concentrations.

Benzoic acid Preliminary experiments showed that equilibrium was reached after shaking for one week. It was found that the presence of 0.001 M KCl reduced benzoate adsorption by at least 20 per cent, and so the isotherms were determined in the absence of added electrolytes. Equal volumes of oxide suspensions and benzoic acid solutions (adjusted if necessary to the required pH with NaOH) were mixed and shaken for one week at 20 °C. The tubes were centrifuged at 9,000 rpm for 20 min and benzoate in the supernatant was determined by measuring absorbance at 267 nm using a Unicam SP 700 Spectrophotometer. Blanks were treated and analysed in the same way.

Infrared studies

The goethite complexes were prepared by mixing calculated amounts of goethite and solutions of the acids, shaking and drying onto AgCl plates. Evacuation and D_2O treatment were carried out in a vacuum cell. Spectra were recorded on a Grubb Parsons Spectromaster.

Results

Oxalate adsorption

Adsorption isotherm

Fig. 1 shows three regions for the adsorption of oxalate on goethite at pH 3.4. Initially, about 100 μmol g^{-1} of oxalate was adsorbed very strongly, similar to the strong adsorption of phosphate on goethite as a binuclear (bridged bidentate) complex (Atkinson *et al.*, 1974; Parfitt *et al.*, 1976). An additional 200 μmol g^{-1} of oxalate was adsorbed more weakly in a second region (II) of the isotherm, where the curve resembled isotherms obtained with benzoic acid (Fig. 1) and with 2,4-D on goethite (Watson *et al.*, 1973). In the third region (III) small additional amounts of oxalate were adsorbed above 300 μmol g^{-1} but the slope of the isotherm indicated low adsorption energy.

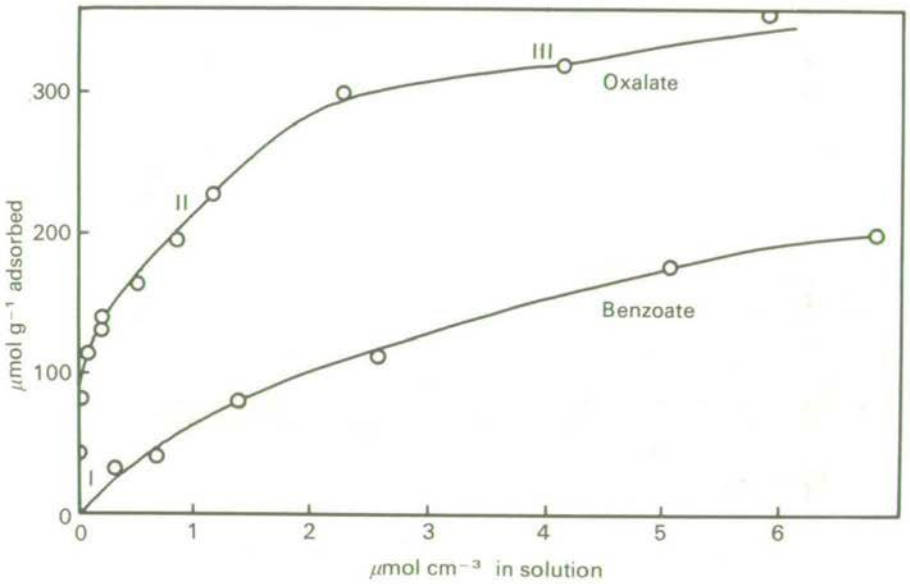

FIG. 1. Adsorption isotherms of oxalate on goethite at pH 3.4 in 0.1 M NaCl, and benzoate on goethite at pH 3.3.

Adsorption envelope The effect of pH on the adsorption of oxalate was measured at the beginning of the second region (about 0.1 μmol cm^{-3} in solution). Adsorption increased from near zero at pH 8.0 to 110 μmol g^{-1} at pH 4.2, then remained at this level down to pH 2.5. Thus the adsorption envelope of oxalic acid, like that of other polyprotic acids (Hingston *et al.*, 1972), showed a marked change in slope at a pH equal to the pK_2 value (4.2) for the acid.

Ionic strength effect The effect of different concentrations of NaCl on oxalate adsorption was measured at pH 3 using an initial concentration of 1 mM oxalate. Adsorption was found to decrease from 160 μmol g^{-1} in 0.01 M NaCl to 120 μmol g^{-1} in 1 M NaCl. A similar but larger effect has been found for 2,4-D adsorption (Watson *et al.*, 1973).

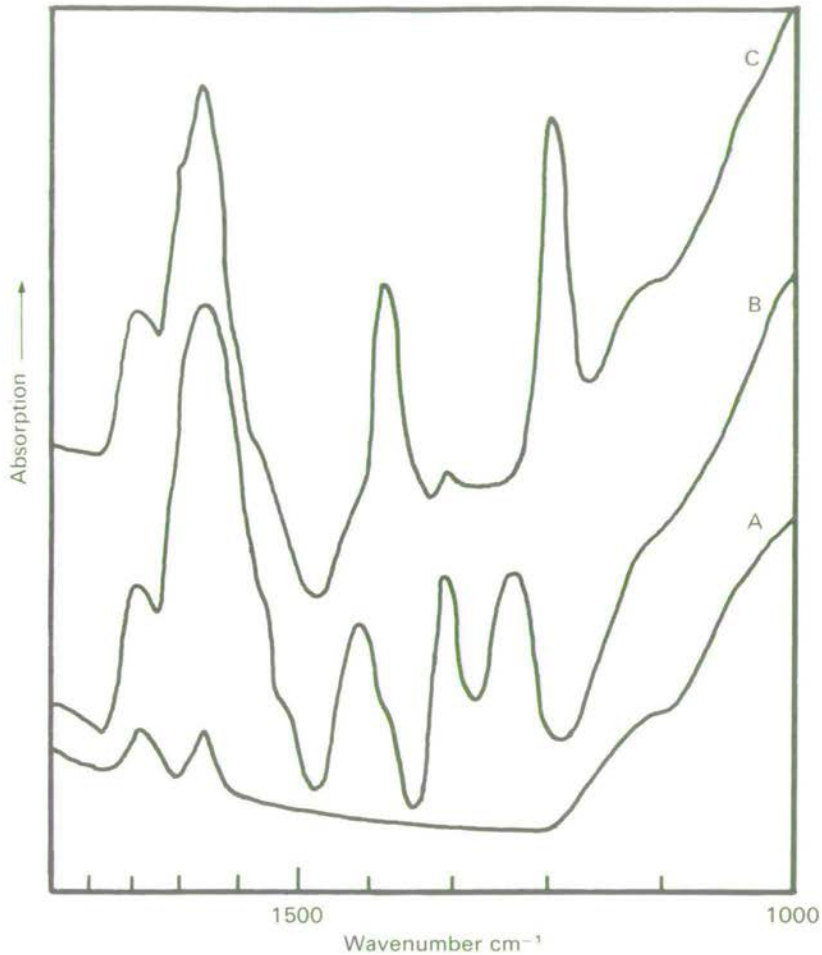

FIG. 2. Infrared spectra of goethite films with: (A) no oxalic acid, in vacuum; (B) 100 μmol g^{-1} oxalic acid, air dry; (C) 100 μmol g^{-1} in vacuum.

Infrared spectra

When oxalic acid was adsorbed onto goethite the infrared spectra indicated that the acid had reacted to form a complex oxalate. The infrared absorption differed for surface loadings corresponding to regions I and II of the isotherm, and will be considered separately.

Region I When 50 and 100 μmol g^{-1} of oxalic acid were adsorbed, bands were observed at 1660, 1520, 1408, 1304 and 1232 cm^{-1} in air-dry films (Fig. 2b). On evacuating for 10 min at 1 N m^{-2} the 1520 and 1304 cm^{-1} bands disappeared (Fig. 2c). These bands were due to surface CO_3^{2-} which could be removed on evacution (Russell *et al.*, 1975). The CO_3^{2-} bands decreased in intensity as more oxalic acid was adsorbed and were absent when 200 μmol g^{-1} oxalate was present, an amount sufficient to block all the sites of CO_2 adsorption.

After evacuation, the oxalate bands at 1408 and 1302 cm^{-1} shifted to 1374 and 1193 cm^{-1} respectively and a shoulder was seen on the 1660 cm^{-1} band at 1710 cm^{-1}. The bands at 1660 and 1710 cm^{-1} were similar to the $C{=}O_{II}$ bands of the $[Fe(C_2O_4)_3]^{3-}$ complex but the 1374 and 1193 cm^{-1} bands corresponded more closely to the $C{-}O_I$ stretching bands in dimethyl oxalate (Table 1). This suggests that oxalic acid reacted with two Fe^{3+} ions to form a binuclear complex rather than with one Fe^{3+} ion to form a bidentate chelate.

TABLE 1

Absorption bands (cm^{-1}) of oxalate on goethite and in model compounds

$(COOH)_2$ adsorbed (μmol g^{-1})		*Assignment*	*Model compounds*		
100	*200*		*cis-dimethyl oxalate**	*bidentate complex† $K_3[Fe(Ox)_3]3H_2O$*	*$(COONa)_2$ on goethite*
1710	1710	$\nu C{=}O_{II}$	1776	1712	
1660	1660	$\nu C{=}O_{II}$	1770	1667,1649	1665($\nu_a COO^-$)
1374	1364	$\nu C{-}O_I$	1325	1390	1307($\nu_s COO^-$)
1193	1174	$\nu C{-}O_I$	1165	1270,1255	

*Schmeltz *et al.* (1957).
†Nakamoto (1963).

Parfitt *et al.* (1976) have shown that surface hydroxyls which are coordinated to one Fe^{3+} ion (A-type OH) absorb at 3486 cm^{-1} (2584 cm^{-1} OD) in goethite and that this band is absent when 200 μmol g^{-1} phosphate is adsorbed since A-type OH are replaced by phosphate ions. When increasing amounts of oxalate were adsorbed on goethite and the surface converted to the OD form by exchange with D_2O, the intensity of the 2584 cm^{-1} OD band decreased progressively (Fig. 3) indicating that A-type OD were also replaced by oxalate oxygen. The $O_I{-}O_I$ distance in the oxalate ion is 0.27–0.28 nm so there will be little strain on the oxalate or the goethite surface in replacing two A-type OH or OD separated by 0.30 nm (Fig. 4). The shortening of the O–O distance across the oxygens bridged by oxalate will, however, lengthen the hydrogen bond between these oxygens and

adjacent A-type hydroxyl to 0.31 nm: this longer hydrogen bond is thought to explain the appearance of a band at 3560 cm^{-1} (2635 cm^{-1} OD; Fig. 3b, c) when oxalate partially replaces A-type hydroxyl. In support of this assignment, a similar band at a slightly higher frequency (3584 cm^{-1}) was found when 50 or 100 $\mu mol\ g^{-1}$ of phosphate partially replaced the 400 $\mu mol\ g^{-1}$ of A-type hydroxyl; the higher

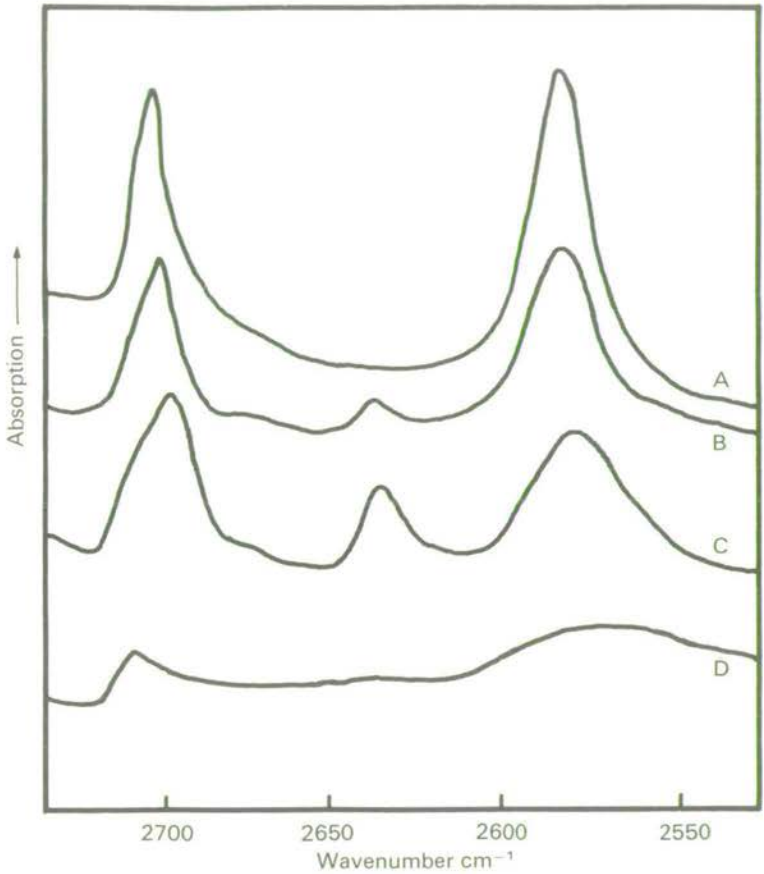

FIG. 3. Infrared spectra of surface OD on goethite with: (A) no oxalate; (B) 50 $\mu mol\ g^{-1}$ oxalic acid; (C) 100 $\mu mol\ g^{-1}$ (D) 200 $\mu mol\ g^{-1}$ (all D_2O treated and evacuated).

frequency reflects a longer hydrogen bond (0.325 nm) than with oxalate, consequent on the closer spacing (0.25 nm) of oxygens bridged by phosphate.

The presence of 50–100 $\mu mol\ g^{-1}$ oxalate caused only a minor perturbation of adjacent B- and C-type hydroxyl groups, leading to a broadening and a slight displacement of the corresponding infrared

absorption band, which lies at 3660 cm^{-1} (2702 cm^{-1} OD; Fig. 3) on the clean surface. From the model of the (100) surface, a hydrogen bond is possible between C-type hydroxyl and the O_{II} oxygen of oxalate, but there is no evidence from the spectra of such an interaction, suggesting that these oxygens are directed away from the surface.

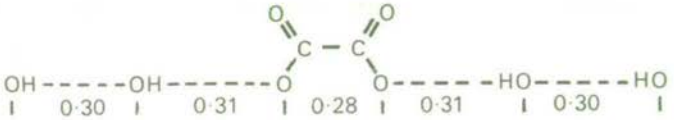

FIG. 4. Distortion of the regular O – – – O separations (nm) caused by oxalate substitution in the row of A-type hydroxyl groups.

Region II When a film of goethite treated with 200 $\mu mol\ g^{-1}$ of oxalic acid was examined in vacuum, bands at 1710, 1660, 1364, 1300 and 1174 cm^{-1} were observed (Fig. 5 and Table 1). The 1364 and 1174 cm^{-1} bands correspond closely with those of *cis*-dimethyl oxalate, indicating that oxalate was again present as the binuclear complex. These two bands were at a lower frequency than when 100 $\mu mol\ g^{-1}$ of oxalate was adsorbed. The 1300 cm^{-1} band, unchanged on evacuation (Fig. 5b), probably arose from the presence of a little ionic oxalate which absorbs at this frequency (Table 1).

On brief exposure (10 sec) to D_2O followed by evacuation, a new band appeared at 1260 cm^{-1} assignable to a δ (OD) deformation, and a shoulder at 1775 cm^{-1}, assignable to C=O, was seen more clearly (Fig. 5c): this indicated the presence of COOD. These acid bands were still more strongly developed when 300 $\mu mol\ g^{-1}$ was adsorbed (Fig. 6b, c). The δ (OH) band which gave rise to the δ (OD) band at 1260 cm^{-1} was probably obscured by the C–O stretching vibration at 1364 cm^{-1}. The position of these COOH bands indicated that the C=O and OH were not involved in strong hydrogen bonds. Therefore, it was likely that some oxalate was adsorbed as a monodentate complex FeOOC · COOH. Oxalate adsorbed in this form would be less strongly adsorbed than the binuclear complex and this is consistent with Region II of the isotherm which resembles curves obtained for monobasic acids.

The isotherm can, therefore, be taken to indicate that 100 $\mu mol\ g^{-1}$ of oxalate was adsorbed as the binuclear complex replacing 200 $\mu mol\ g^{-1}$ A-type OH and that a further 200 $\mu mol\ g^{-1}$ was adsorbed as the monodentate complex replacing a further 200 $\mu mol\ g^{-1}$ A-type OH: most of the A-type OH would be replaced in this way. Since the amount of oxalate strongly adsorbed varies with pH, the proportions of bidentate and monodentate species must also vary.

Oxalate adsorbed in Region III may be due to the adsorption of iron oxalate complexes formed by attack on the goethite at high oxalate concentrations; such complexes could give rise to the shoulder at 1408 cm^{-1} in Fig. 6c (cf. Table 1).

The OD stretching bands were modified further when 200 $\mu mol\ g^{-1}$ of oxalate was adsorbed. The bands near 2707 and 2570 cm^{-1} were broad and weak and the 2635 cm^{-1} band was absent (Fig. 3d). At the 300 $\mu mol\ g^{-1}$ level a broad feature was observed between 2515 and

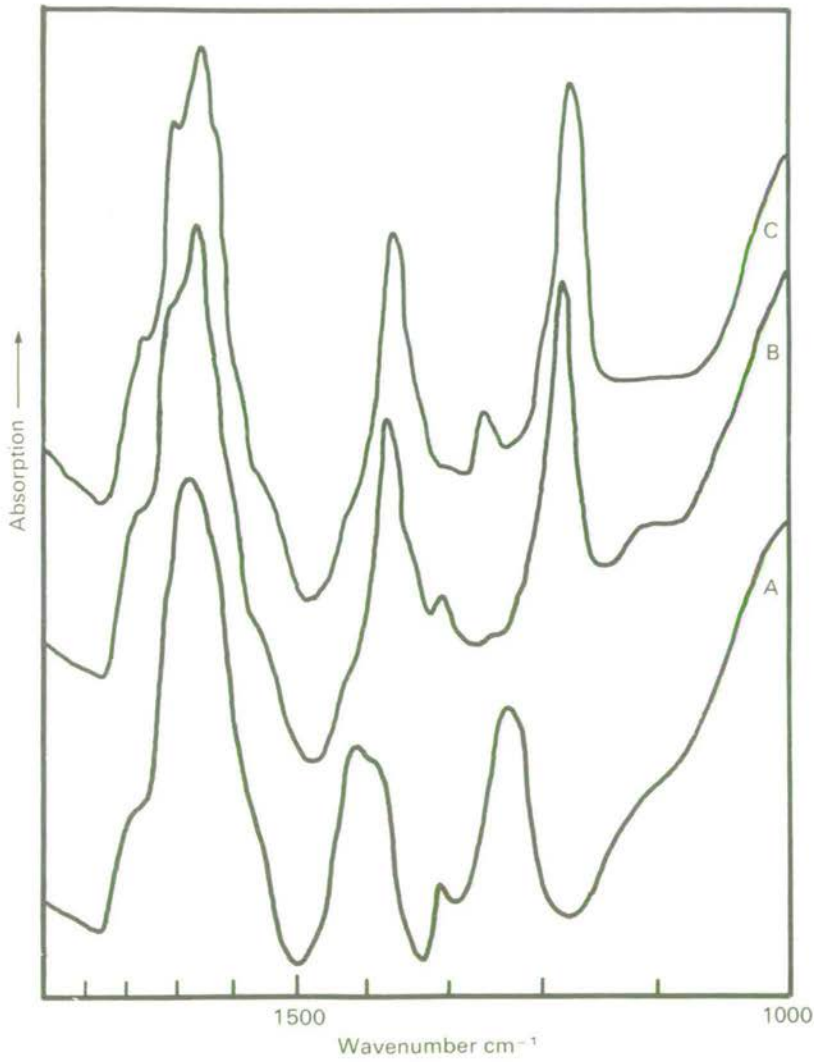

FIG. 5. Infrared spectra of goethite with 200 $\mu mol\ g^{-1}$ oxalic acid: (A) air dry; (B) evacuated; (C) D_2O treated and evacuated.

2600 cm^{-1} which probably arises partly from the OD stretching vibration of the COOD of monodentate oxalate. The other OD stretching bands were not observed since most A-type groups were now replaced and B and C-type groups could interact with the COOD of adsorbed monodentate oxalate by hydrogen bonding.

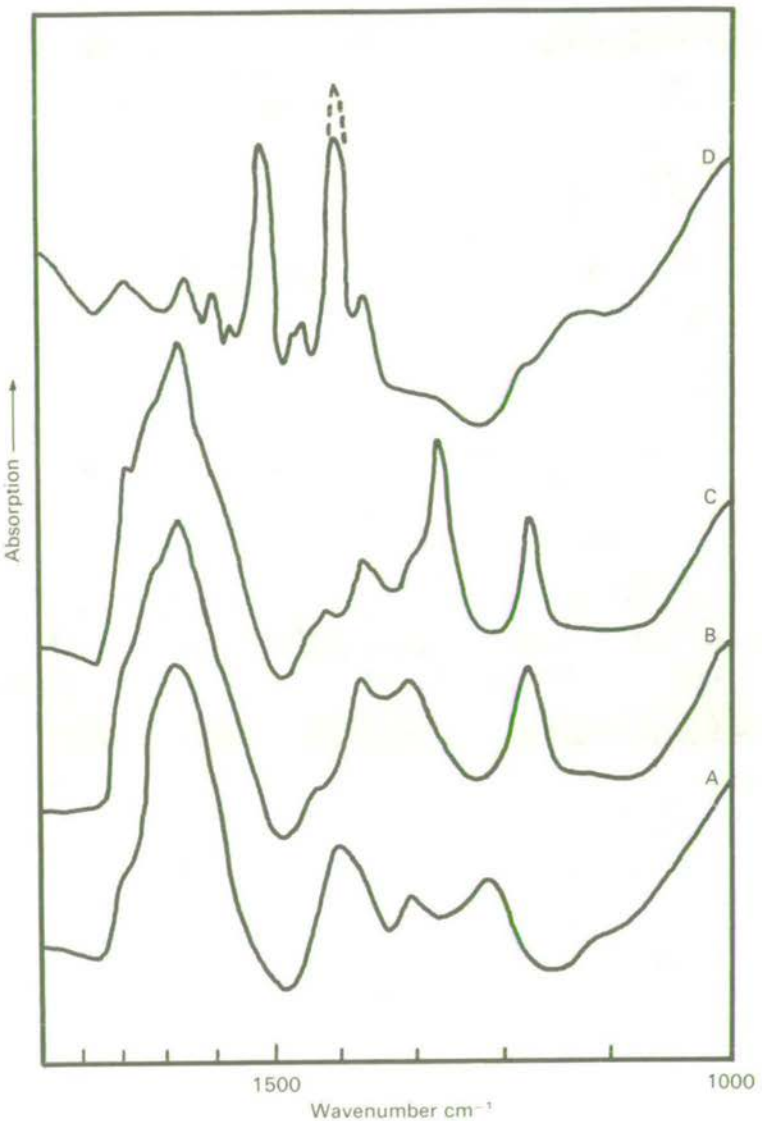

FIG. 6. Infrared spectra of goethite with 300 μmol g^{-1} oxalic acid: (A) air dry; (B) evacuated; (C) D_2O treated and evacuated; (D) Spectrum of goethite with 150 μmol g^{-1} benzoic acid in vacuum (broken line, film at 45° to beam).

Benzoate adsorption

The adsorption isotherm for benzoic acid on goethite (Fig. 1) was similar to that for 2,4-D on goethite (Watson *et al.*, 1973) and indicative of weak adsorption. The infrared spectrum of 150 μmol g^{-1} benzoic acid on goethite (Fig. 6d) was similar to that of iron benzoate, but the COO^- antisymmetric and symmetric stretch vibrations at 1515 and 1400 cm^{-1} were intensified relative to other benzoate absorption bands. No bands assignable to benzoic acid were present. A pleochroic effect noted on the COO^- symmetric stretch band at 1400 cm^{-1} indicated that the aromatic ring is at a high angle to the goethite (100) face. This can be explained if one benzoate ion replaced one A-type OH ion (Fig. 7) and the COO^- group fitted into the adjacent surface groove (Parfitt *et al.*, 1976). In agreement with this proposal, the 3486 cm^{-1} band of the A-type OH ions was reduced in intensity indicating replacement of these OH ions by benzoate. The intensity of the

FIG. 7. Proposed orientation of benzoate ions substituting for A-type hydroxyl groups.

absorption band of the B- and C-type OH ions at 3660 cm^{-1} was also reduced and a shoulder appeared at 3620 cm^{-1}. This is ascribed to a van der Waals interaction between aromatic C–H groups on the benzoate and these adjacent hydroxyls. A similar effect was seen when paraffin oil covered the goethite surface.

Discussion

Although both phosphate and oxalate can be adsorbed on goethite in a binuclear form, bridging adjacent Fe^{3+} on the surface, there was a striking difference between the amounts of the two species so adsorbed. With phosphate all A-type hydroxyls could be displaced by the same binuclear species, whereas with oxalate only part of the A-type hydroxyls were replaced by the binuclear species, the remainder being replaced by a more weakly adsorbed monodentate acid oxalate anion. This difference in behaviour may be explained by phosphate being adsorbed as $(FeO)_2PO \cdot OH$, which can redistribute charge over the goethite surface by forming hydrogen bonds through its POH group with adjacent surface oxide ions carrying an excess negative charge (Russell *et al.*, 1975). Binuclear oxalate cannot do this, nor is the acid

oxalate ion likely to be effective. Steric interaction between adjacent adsorbed species must also be important, for oxalate is broader than phosphate (0.28 nm compared with 0.25 nm), and the projecting C=O groups of adjacent anions would lie only 0.32 nm apart, close to the minimum acceptable van der Waals separation.

Benzoate was also weakly adsorbed as a monodentate species, with its benzene ring at a high angle to the (100) face. It, too, cannot transfer charge effectively.

REFERENCES

ATKINSON, R. J., PARFITT, R. L., and SMART, R. St. C. 1974. Infrared study of phosphate adsorption on goethite. J. Chem. Soc. Faraday Trans. I **70**, 1472–9.

—— POSNER, A. M., and QUIRK, J. P. 1968. Crystal nucleation in Fe (III) solutions and hydroxide gels. J. inorg. nucl. Chem. **30**, 2371–81.

GREENLAND, D. J. 1971. Interactions between humic and fulvic acids and clays. Soil Sci. **111**, 34–41.

HINGSTON, F. J., ATKINSON, R. J., POSNER, A. M., and QUIRK, J. P. 1968. Specific adsorption of anions on goethite. Trans. 9th int. Congr. Soil Sci., Adelaide **1**, 669–78.

—— POSNER, A. M., and QUIRK, J. P. 1972. Anion adsorption by gibbsite and goethite. 1. The role of the proton in determining the adsorption envelopes. J. Soil Sci. **23**, 177–92.

NAKAMOTO, K. 1963. *Infrared spectra of inorganic and coordination compounds.* New York: Wiley.

PARFITT, R. L., RUSSELL, J. D., and FARMER, V. C. 1976. Confirmation of the surface structures of goethite (α-FeOOH) and phosphated goethite. J. Chem. Soc. Faraday Trans. I **72**, 1082–87.

RUSSELL, J. D., PATERSON, E., FRASER, A. R., and FARMER, V. C. 1975. Adsorption of carbon dioxide on goethite (α-FeOOH) surfaces and its implications for anion adsorption. Ibid. **71**, 1623–30.

SCHMELTZ, M. J., MIYAZAWA, T., MIZUSHIMA, S., LANE, T. J., and QUAGLIANO, J. V. 1957. Infrared absorption spectra of inorganic coordination complexes. IX. Infrared spectra of oxalate complexes. Spectrochim. Acta **9**, 51–8.

WATSON, J. R., POSNER, A. M., and QUIRK, J. P. 1973. Adsorption of the herbicide 2,4-D on goethite. J. Soil Sci. **24**, 503–11.

(Received 31 March 1976)

ADSORPTION ON HYDROUS OXIDES
II. OXALATE, BENZOATE AND PHOSPHATE ON GIBBSITE

R. L. PARFITT,[1] A. R. FRASER, J. D. RUSSELL and V. C. FARMER
(Department of Spectrochemistry, The Macaulay Institute for Soil Research, Aberdeen)

Summary

Adsorption isotherms, the infrared spectra of adsorbed species, and the amount of hydroxyl released when oxalate is adsorbed, all indicate that adsorption of oxalate, benzoate and phosphate at low solution concentrations occurs only on $Al(OH)(H_2O)$ sites exposed on edge faces of the platy gibbsite crystals studied. This is confirmed by the finding that the vibrations of surface hydroxyl groups on the principal plate faces are unaffected when excess oxalate is present, and further supported by the low affinity for oxalate of imogolite, a tubular mineral with a very large gibbsite-like surface, but with a very low concentration of edge sites.

Infrared spectra indicate that oxalate is adsorbed in bidentate form. Near neutrality and at low solution concentrations, gibbsite adsorbs more oxalate than does goethite of comparable surface area.

Introduction

IN part I (Parfitt *et al.*, 1977) the adsorption of oxalate and benzoate on goethite was contrasted with that of phosphate, on the basis of adsorption isotherms and the infrared spectra of the adsorbed species. A similar comparative study is made here for adsorption on gibbsite, and the behaviour of gibbsite and imogolite, which are thought to have similar surfaces, are also compared.

Gibbsite, goethite and imogolite are widely distributed in soils, and their surface reactions are likely to be similar to those of the many other types of iron and aluminium hydroxide surfaces that can also be present. Oxalic acid is a common plant acid that persists in soil, and its presence is known to reduce phosphate adsorption on goethite and gibbsite (Nagarajah *et al.*, 1970) and to interfere with adsorption of humified material on imogolite (Inoue and Wada, 1971).

Infrared studies have established that only singly coordinated hydroxyl groups on the goethite surface are displaced by anions (Parfitt *et al.*, 1976), but the reactive sites on gibbsite have not yet been identified. Hydroxyl groups on the (001) surface of gibbsite are accessible to infrared study (Russell *et al.*, 1974), and evidence for their involvement in adsorption reactions was sought in the present investigation.

[1] On leave from Department of Agriculture, University of Papua New Guinea.

Journal of Soil Science, 1977, 28 40–47

Materials and methods

Gibbsite The synthetic gibbsite was prepared by the method of Gastuche and Herbillon (1962), and stored as a suspension containing 12 mg cm^{-3}. The crystals were seen in the electron microscope to consist of thin 6-sided plates with diameters mostly around 200 nm. Crystal thicknesses were more variable, as shown by shadowing. None exceeded 18 nm, and most were less than 4 nm. The total area per gram of edge faces is controlled only by the plate diameter, and so can be calculated to lie around 9 $m^2\ g^{-1}$. The total area of pseudohexagonal (001) faces depends on crystal thickness, and so clearly exceeds 50 $m^2\ g^{-1}$ (corresponding to the maximum thickness of 18 nm), and probably lies around 100 $m^2\ g^{-1}$. The measured BET surface area, using nitrogen adsorption, was only 45 $m^2 g^{-1}$, probably due to face-to-face contacts in the freeze-dried specimens used.

Imogolite A purified freeze-dried sample from the Kitakami pumice bed, kindly supplied by Prof. N. Yoshinaga, was dispersed in HCl at pH 2.5. After dialysis till chloride-free, the suspension contained 5 mg cm^{-3}, based on dry (100 °C) weight.

Adsorption isotherms and hydroxyl release Oxalate adsorption was measured in 0.1 M NaCl using a ^{14}C tracer. Benzoate adsorption was determined without added electrolyte, using ultraviolet absorption at 267 nm to monitor solution concentrations. Full details are given in Part I. Phosphate adsorption from solutions containing 0.1 M NaCl was followed by colorimetric analysis of the supernatant solution. Hydroxyl ion released by oxalate adsorption was determined during step-wise addition of $Na_2(COO)_2$ solution (initially 5 mM and later 50 mM) to gibbsite suspension (400 mg in 50 ml), through which nitrogen was bubbled. Solutions and suspension were initially at pH 6, and the suspension was readjusted to pH 6 with 5 mM HCl after each addition. Equilibration was rapid, and the pH was stable after 1 min. At each step, the amount of oxalate adsorbed was obtained by reference to an adsorption isotherm.

Infrared spectroscopy Surface complexes on gibbsite were prepared by adding appropriate amounts of the acids or salts to gibbsite suspensions which were then evaporated in shallow dishes to give self-supporting films of 3–5 mg cm^{-2}. Evacuation and D_2O treatment were carried out in a vacuum cell. Spectra were recorded on a Grubb Parsons Spectromaster.

Results

Adsorption isotherms

Oxalate was almost totally adsorbed by gibbsite at pH 4 and pH 6.5 up to 20 $\mu mol\ g^{-1}$ (Fig. 1A). Thereafter, adsorption increased continuously with solution concentration, but the isotherm at pH 6.5

showed a marked change in slope after 70 μmol g^{-1} was adsorbed (dashed curve, Fig. 1A). At low solution concentrations, adsorption was independent of pH between 3.5 and 6, but fell off at higher pH values (Fig. 1B). At higher solution concentrations (>0.5 μmol cm^{-3}), more oxalate was adsorbed at pH 4 than at pH 6.5 (dashed curves, Fig. 1A), but here aluminium was found in the solution, and the adsorbed species may be an aluminium oxalate complex. Titration of hydroxyl released by oxalate adsorption at pH 6 showed (Fig. 2) a progressive release up to 40 μmol g^{-1}, when just over 30 μmol g^{-1} oxalate was adsorbed. Further adsorption of oxalate up to 80 μmol g^{-1} released little more hydroxyl.

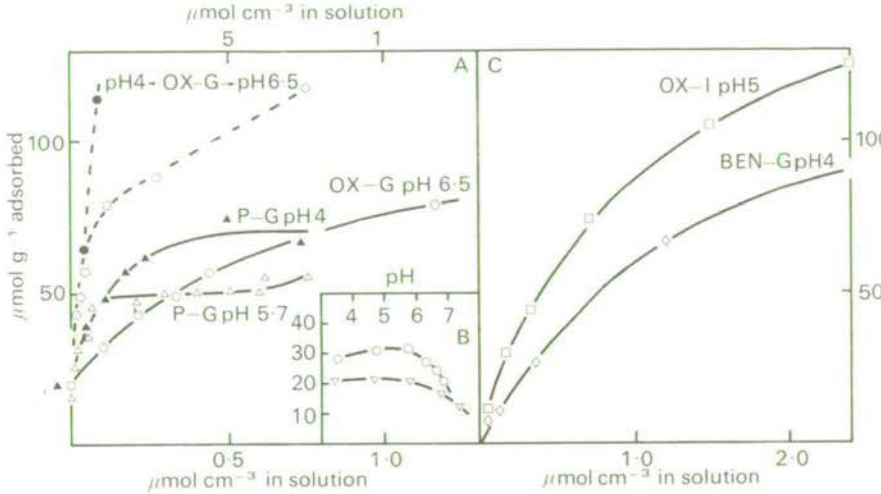

FIG. 1. (A) Adsorption isotherms for oxalate (OX) and phosphate (P), on gibbsite (G). The upper concentration scale refers to the dashed curves only. Oxalate on gibbsite at pH 6.5 is plotted on both concentration scales.
(B) Adsorption envelope for oxalate adsorbed on gibbsite with 50 μmol g^{-1} added (circles) and 25 μmol g^{-1} added (triangles).
(C) Adsorption isotherms for benzoate (BEN) on gibbsite (G) and oxalate (OX) on imogolite (I), calculated on anhydrous weight.

Unlike gibbsite, imogolite showed no region of strong adsorption of oxalate (Fig. 1C).

Adsorption isotherms of phosphate on gibbsite (Fig. 1A) like those of oxalate, showed almost total adsorption up to 25 μmol g^{-1}, but, unlike oxalate, gave fairly well defined plateaux of 50 μmol g^{-1} at pH 5.7, rising to 70 μmol g^{-1} at pH 4. Benzoate showed no region of strong adsorption on gibbsite. (Fig. 1C).

Infrared Spectroscopy

From the hydroxyl release curve (Fig. 2), it can be concluded that oxalate is adsorbed largely as NaOOC . COOH up to about 40 μmol g^{-1}, but that further oxalate is adsorbed as neutral salt. Accordingly, gibbsite films containing 20, 40, 80 and 160 μmol g^{-1} of oxalate were prepared by adding the monohydrogen salt up to the 40 μmol g^{-1} level, and the disodium salt above that level.

The absorption bands of free $Na_2(COO)_2$ first became detectable at 80 μmol g^{-1}, and were clearly evident in the spectrum at 160 μmol g^{-1} (Fig. 3) as strong or medium absorption bands at 1630, 1326 and 1304 cm^{-1}, close to those reported for crystalline sodium oxalate at 1640, 1338 and 1320 cm^{-1} (Schmeltz *et al.*, 1957). At 80 μmol g^{-1}

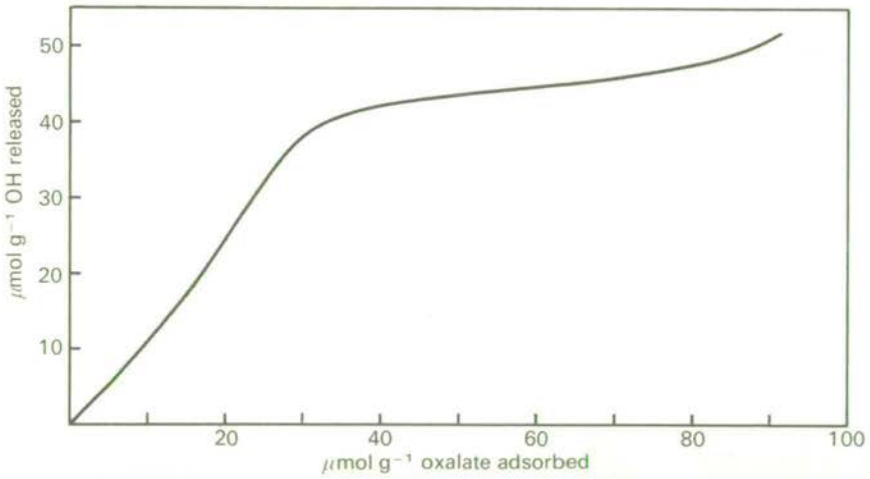

FIG. 2. Relationship between hydroxyl released from gibbsite and oxalate adsorbed at pH 6.

the absorption bands of adsorbed oxalate lay at 1721, 1686 and 1414 cm^{-1}, close to those of crystalline trioxalatoaluminate complexes (1722, 1683 and 1405 cm^{-1}; Nakamoto, 1963). Similar but slightly different frequencies were given by adsorbed oxalate at 20 μmol g^{-1} (Fig. 3). It is concluded that oxalate is chemisorbed on gibbsite up to about 80 μmol g^{-1}, and that the form or environment of the adsorbed species changes above 20 μmol g^{-1}, where the oxalate band at 1383 cm^{-1} begins to be replaced by one at 1414 cm^{-1} (Fig. 3). Even at 160 μmol g^{-1} of oxalate, the absorption bands of surface hydroxyl on the (001) face of gibbsite (Russell *et al.*, 1974) were not modified.

The infrared spectrum of 50 μmol g^{-1} benzoic acid on gibbsite showed bands at 1600, 1540 and 1460 cm^{-1}, which are close to the

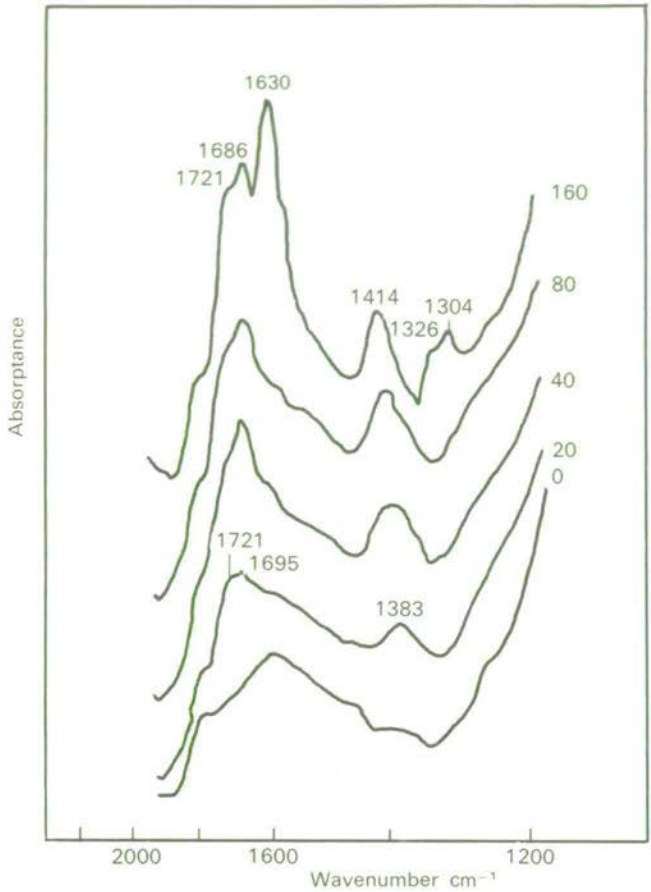

FIG. 3. Infrared absorption of gibbsite films with increasing amounts of added oxalate: 0, 20, 40, 80, and 160 μmol g^{-1}.

bands of aluminium benzoate. With 100 μmol g^{-1} benzoic acid, additional bands corresponding to the unionized acid appeared at 1695, 1315, and 1280 cm^{-1}. The 1315 cm^{-1} and 1280 cm^{-1} bands both showed pleochroic effects when the gibbsite film was inclined to the infrared beam. As these bands have transition moments that lie in the plane of the benzene ring, perpendicular to the long axis of the molecule, it can be concluded that the molecules of benzoic acid lie with their long axis parallel to the (001) faces, but with the plane of the ring perpendicular to the face.

Discussion

Gibbsite has a layer structure, so cleavage of the crystals along (001) planes breaks only hydrogen bonds, and the (001) faces must have

essentially the same structure as that found by X-ray diffraction analyses within the crystal. That is, they must consist of a close-packed pseudo-hexagonal array of hydroxyl groups, each linked to two underlying Al^{3+} ions. The estimated area of these faces in the sample used here indicates that some 2,000 μmol g^{-1} of hydroxyl must be exposed on them.

The edge faces carry broken bonds, but examination of the crystal structure indicates that the (100) and (110) faces, which are almost identical, will carry equal numbers of hydroxyl and water molecules for electrical neutrality, one of each being coordinated to one underlying Al^{3+} (Fig. 4). The separation of OH and H_2O coordinated to the same Al^{3+} will be about 0.27 nm, and there are hydrogen-bonded contacts between successive layers involving oxygen-to-oxygen distances of 0.28–0.29 nm. The gibbsite used should carry around 60 μmol g^{-1} of $Al(OH)(OH_2)$ groupings exposed on edges at electrical neutrality, as estimated from the crystal dimensions.

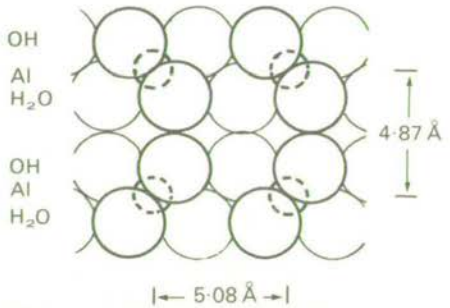

FIG. 4. Probable structure of the edge faces, (100) and (110), of a gibbsite crystal, after Bragg and Claringbull (1965).

Comparison of these calculations with the results of the adsorption studies clearly indicates that chemisorption of oxalate, phosphate and benzoate occurs only on the edge sites of the gibbsite crystals. The amount of hydroxyl released when oxalate is adsorbed (45 μmol g^{-1} from Fig. 2) must be adjusted for the positive charge carried by gibbsite crystals at pH 6 (25 μmol g^{-1}, as found by Hingston *et al.* (1972) for a similar preparation) giving a total of 70 μmol g^{-1} of reactive $Al(OH)(OH_2)$ sites, close to the 60 μmol g^{-1} calculated for edge faces. Strong adsorption of oxalate and phosphate occurs only up to just over 20 μmol g^{-1} (Fig. 1A and B), presumably due to steric interference between adjacent adsorbed ions, but the maximum capacity for these ions is around 70 μmol g^{-1}, as indicated by the adsorption plateau for phosphate at pH 4, and the change in slope of the oxalate isotherm at pH 6.5. Infrared spectra also indicate that gibbsite can only hold about 80 μmol g^{-1} of oxalate in bidentate form and show, moreover, that no

reaction occurs with hydroxyl groups on (001) surfaces, even when excess oxalate is present.

Two modes of adsorption of a bidentate oxalate group on edge faces can be postulated, either chelated to a single Al^{3+} cation, or bridging between two cations in adjacent layers, since in both cases the O–O separation within the $OH–H_2O$ pair replaced (Fig. 4) is similar to that of the oxygens of the oxalate group (0.28 nm). The 1383 cm^{-1} band of adsorbed oxalate on gibbsite at 20 $\mu mol\ g^{-1}$ has a frequency close to that of the bridging oxalate group on the goethite surface (1374 cm^{-1}, Part I), but the higher frequency observed (1414 cm^{-1}) at 80 $\mu mol\ g^{-1}$ is close to that of chelating oxalate in oxalatoaluminate complexes.

Infrared spectra also indicate that benzoic acid is chemisorbed at 50 $\mu mol\ g^{-1}$, but that part is physically adsorbed at 100 $\mu mol\ g^{-1}$. This is consistent with adsorption on edge sites, since benzoate can act as a bidentate ligand up to 70 $\mu mol\ g^{-1}$, replacing a hydroxyl and a water molecule, whilst additional benzoic acid can be adsorbed by van der Waals or Π–Π interactions between the aromatic rings of the acid molecules and those of the benzoate ions already adsorbed. This would cause the carboxylic acid groups to be directed away from the surface, and would give an orientation of the benzoic acid entirely consistent with the observed infrared pleochroism. A similar two-layer mode of adsorption has been propsed for 2,4-D on goethite to account for flotation effects which reverse at higher adsorbate levels (Watson *et al.*, 1973).

Further evidence for the lack of reactivity of the hydroxyl groups on the (001) face of gibbsite comes from the absence of a region of strong adsorption for oxalate on imogolite. This clay mineral consists of tubes of 2 nm diameter whose outer surface is thought to have the same structure as that of the (001) face of gibbsite (Cradwick *et al.*, 1972). The tube surface has a calculated area of 900 $m^2\ g^{-1}$ and carries 15 $mmol\ g^{-1}$ of doubly coordinated hydroxyl groups, whereas edge sites of $Al(OH)(H_2O)$ structure, exposed at tube ends, amount to only 4 $\mu mol\ g^{-1}$. Clearly, the outer surfaces of the tubes do not provide any regular adsorption site for oxalate.

The results of this investigation therefore support the view of Muljadi *et al.*, (1966) that only edge sites in gibbsite crystals are involved in ligand exchange adsorption processes. They also establish that, at low solution concentrations near neutrality, oxalate is more strongly adsorbed on gibbsite than on goethite (Part I) of comparable surface area. Similar sites to those exposed on gibbsite crystal edges probably occur in higher concentration on poorly crystalline aluminium hydroxides and allophanes, and could also be present on the edges of layer silicate clay minerals. On the other hand, the surface of imogolite resembles that of the (001) surface of gibbsite and both are unreactive

at low solution concentrations. The hydroxyl surface of the kaolin minerals also has this structure and so is probably unreactive.

REFERENCES

BRAGG, L., and CLARINGBULL, G. F. 1965. *The crystal structure of minerals.* London: Bell.

CRADWICK, P. D. G., FARMER, V. C., RUSSELL, J. D., MASSON, C. R., WADA, K., and YOSHINAGA, N. 1972. Imogolite, a hydrated aluminium silicate of tubular structure. Nature, Lond. **240**, 187–9.

GASTUCHE, M.-C., and HERBILLON, A. 1962. Alumina gels: crystallization in a de-ionized medium. Bull. Soc. Chim. Fr. 1404–12.

HINGSTON, F. J., POSNER, A. M., and QUIRK, J. P. 1972. Anion adsorption by goethite and gibbsite: I. J. Soil Sci. **23**, 177–92.

INOUE, T., and WADA, K. 1971. Reactions between a humified clover extract and imogolite as a model of humus-clay interaction: Part I. Clay Sci. **4**, 61–70.

NAGARAJAH, S., POSNER, A. M., and QUIRK, J. P. 1970. Competetive adsorption of phosphate with polygalacturonate and other organic anions. Nature, Lond. **228**, 83–4.

MULJADI, D., POSNER, A. M., and QUIRK, J. P. 1966. The mechanism of phosphate adsorption by kaolinite, gibbsite and pseudoboehmite. J. Soil. Sci. **17**, 212–47.

NAKAMOTO, K. 1963. *Infrared spectra of inorganic and coordination compounds.* New York: Wiley.

PARFITT, R. L., RUSSELL, J. D., and FARMER, V. C. 1976. Confirmation of the surface structure of goethite and phosphated goethite. J. Chem. Soc. Faraday Trans. I **72**, 1082–87.

—— FARMER, V. C. and RUSSELL, J. D. 1977. Adsorption on hydrous oxides: I. Oxalate and benzoate on goethite. J. Soil Sci. **28**, 29–39.

RUSSELL, J. D., PARFITT, R. L., FRASER, A. R. and FARMER, V. C. 1974. Surface structures of gibbsite, goethite and phosphated goethite, Nature, Lond. **248**, 220–1.

SCHMELTZ, M. J., MIYAZAWA, T., MIZUSHIMA, S., LANE, T. J., and QUAGLIANO, J. V. 1957. Infrared absorption spectra of inorganic coordination complexes. IX. Infrared spectra of oxalate complexes. Spectrochim. Acta **9**, 51–8.

WATSON, J. R., POSNER, A. M. and QUIRK, J. P. 1973. Adsorption of the herbicide 2,4-D on goethite. J. Soil Sci. **24**, 503–11.

(*Received 31 March 1976*),

ADSORPTION ON HYDROUS OXIDES. IV. MECHANISMS OF ADSORPTION OF VARIOUS IONS ON GOETHITE

R. L. PARFITT[1] AND J. D. RUSSELL

(Department of Spectrochemistry, The Macaulay Institute for Soil Research, Craigiebuckler, Aberdeen)

Summary

Infrared spectroscopy has been used to investigate the complexes that are formed when acids are evaporated onto goethite. It is probable that, like HPO_4^{2-}, the anions SO_4^{2-}, SeO_3^{2-}, and oxalate are adsorbed by ligand exchange and form binuclear bridging complexes where two singly coordinated A-type OH groups are replaced by two oxygen atoms of one ligand. There is evidence that HPO_4^{2-} and oxalate are likely to be present in this form in wet environments, and this is probably also true for SO_4^{2-} and SeO_3^{2-}.

Fluoride ions can completely replace the singly coordinated A-type OH groups but do not replace C- or B-type OH groups that are coordinated, respectively, to two and three Fe^{3+} ions. The other halides, nitrate, and benzoate partially replace the A-type OH groups, benzoate being adsorbed as a monodentate ligand.

Copper ions do not appear to react with A-type OH but zinc ions are probably adsorbed on the goethite (100) face in conjunction with carbonate or bicarbonate.

Introduction

TROPICAL soils and volcanic ash soils that have been weathered for long periods contain large amounts of hydrous oxides of iron and aluminium, such as goethite and gibbsite. In Parts I and II it has been shown that the most reactive OH groups on the surface of these oxides are singly coordinated; OH groups shared between two or three cations appear to be relatively inert (Parfitt *et al.*, 1977*a*,*b*). Hydroxyl groups coordinated to Al and Fe are also present on the edges of layer silicate minerals, so that their reactions are important in most soils.

Posner, Quirk and co-workers have suggested that anions such as phosphate, sulphate, selenite and molybdate are adsorbed on gibbsite and goethite by ligand exchange (Bowden *et al.*, 1973). This mechanism has been confirmed, and the binuclear form of the adsorbed species has been established by infrared spectroscopy for the adsorption of phosphate and oxalate on goethite (Parfitt *et al.*, 1976, 1977*a*), and for phosphate on other iron oxides (Parfitt *et al.*, 1975). IR spectroscopy has also established that benzoate is adsorbed on goethite as a monodentate species (Parfitt *et al.*, 1977*a*) but the mechanism of adsorption of most nutrient anions is not known.

Hingston *et al.* (1972) suggested that chloride and nitrate are adsorbed on these surfaces by non-specific adsorption where the anions

[1] On leave from Department of Agriculture, University of Papua New Guinea.

Journal of Soil Science, 1977, 28, 297–305.

balance the charge developed by the adsorption of H^+. However Parfitt *et al.* (1977*a*) have shown that adsorption of benzoate and oxalate is reduced in the presence of chloride which may compete for the adsorption sites.

The mechanisms of adsorption on goethite of these and other anions, and also of the cations zinc (which is thought to be specifically adsorbed (Bowden *et al.*, 1974)) and copper are investigated in this study.

Materials and methods

The method of preparation of the synthetic goethite has been described by Parfitt *et al.* (1977*a*). The goethite was stored at a suspension concentration of 22 mg cm^{-3}.

The acids used were of analytical reagent grade. They were made up as approximately 0.01 M solutions and their concentration was determined accurately by titration with sodium carbonate solution.

The complexes were prepared by pipetting calculated volumes of acid (or $CuCl_2$ or $ZnCl_2$ solution) and goethite suspension into a tube where they were mixed by shaking briefly. The complexes were dried on 1 mm AgCl plates to give thin films (3 to 5 mg cm^{-2}) which were examined by infrared spectroscopy in a vacuum cell. D_2O treatment consisted of exposure to D_2O vapour for 10 s followed by evacuation. Four treatments were necessary for complete exchange of surface OH. Hydroxyl groups within the crystal (absorbing at 3150 cm^{-1}) were not exchanged with D_2O during these treatments.

Results

Binuclear complexes

The spectrum of goethite treated only with D_2O and then evacuated (Fig. 2) shows the bands that arise from the A, B and C types of surface OD groups (Fig. 1): A-type at 2584 cm^{-1}, B- and C-type at 2701 cm^{-1} with a shoulder at 2704 cm^{-1} (Parfitt *et al.*, 1976).

The spectra of surface OD groups were considerably modified for goethite carrying 100 and 200 μmol g^{-1} (Fig. 2b–e) of $(COOH)_2$, H_2SeO_3, H_3PO_4 and H_2SO_4. For H_2SeO_3, H_3PO_4 and H_2SO_4 at 200 μmol g^{-1}, the 2584 cm^{-1} band of A-type OD groups was absent or very weak (Fig. 2) suggesting virtually complete replacement of these surface groups which amount, by calculation from crystal dimensions, to 400 μmol g^{-1} (Parfitt *et al.*, 1976). This result agreed well with the measured phosphate sorption capacity of goethite at pH 3.4 (204 μmol g^{-1}), as each phosphate replaces two OH groups to form the binuclear FeOPO(OH)OFe species (Parfitt *et al.*, 1976). It is probable that, like phosphate, selenite and sulphate were adsorbed as binuclear species FeOSe(O)OFe and $FeOS(O_2)OFe$ on the goethite surface.

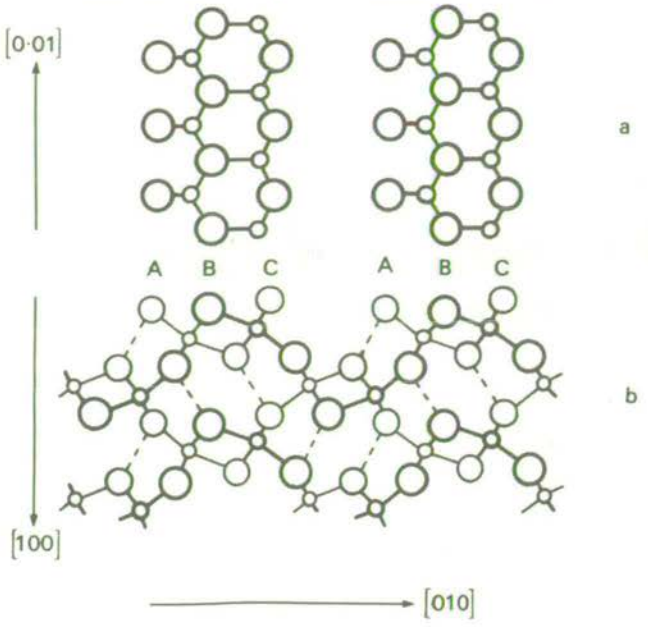

FIG. 1. Plan (a) and section (b) of the (100) face of goethite. A, C and B are respectively 1-, 2- and 3-coordinated OH groups.

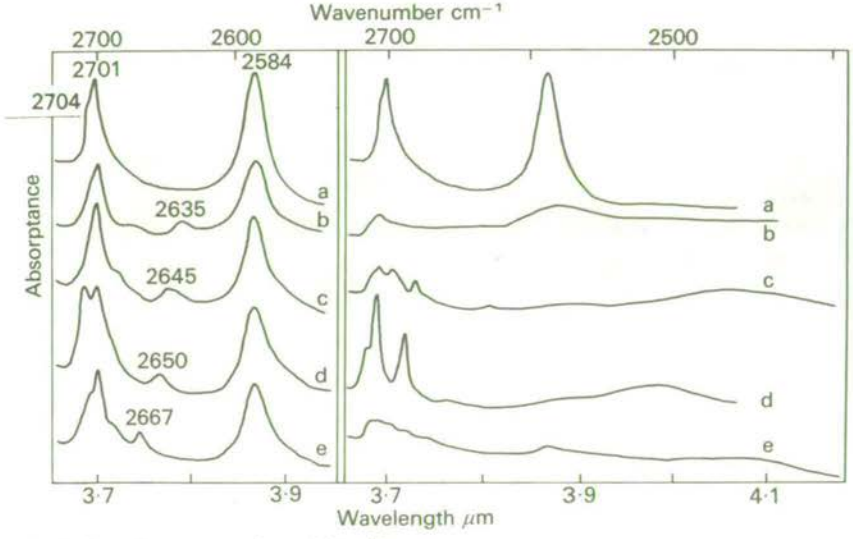

Fig. 2. Infrared spectra of goethite films.

On left: (a) untreated, (b) with 100 μmol oxalic acid g^{-1}, (c) 100 μmol selenious acid g^{-1}, (d) 100 μmol phosphoric acid g^{-1}, (e) 100 μmol sulphuric acid g^{-1}

On right: (a) untreated, (b) with 200 μmol oxalic acid g^{-1}, (c) 200 μmol selenious acid g^{-1}, (d) 200 μmol phosphoric acid g^{-1}, (e) 200 μmol sulphuric acid g^{-1}.

All films treated with D_2O then evacuated.

The spectrum of goethite with 200 μmol g^{-1} oxalic acid showed a broad band at 2580 cm^{-1} (Fig. 2) suggesting that, unlike the above mineral acids at this level, oxalic did not completely replace A-type OH. This is in agreement with previous conclusions (Parfitt *et al.*, 1977*a*) that approximately 100 μmol g^{-1} was adsorbed as a binuclear complex, FeOOC–COOFe, and 100 μmol g^{-1} as a monodentate complex, FeOOC·COOH, leaving about 100 μmol g^{-1} of A-type OD unreacted.

Spectra of goethite carrying 100 μmol g^{-1} of all of these acids (Fig. 2) showed a weak band between 2630 and 2670 cm^{-1}. The origin of this band is thought to be the A-type hydroxyl groups that are adjacent to adsorbed anions and so form hydrogen bonds to the oxygens of the anions as follows;

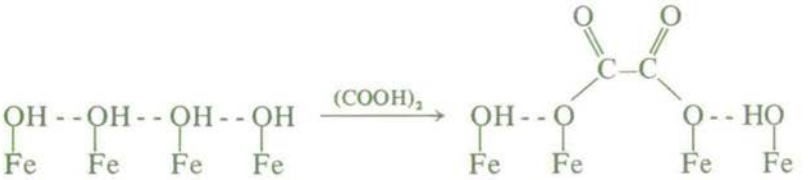

As the O–O separation within the anion decreases, the length of this hydrogen bond will increase and Table 1 shows the expected increase in OH frequency. These results are therefore consistent with acids forming binuclear complexes on the goethite surface.

The adsorbed ligands can be expected to interact in various ways with the different surface hydroxyl and oxide groups. Russell *et al.* (1975) have suggested that oxide ions on the goethite surface accept a hydrogen bond from the POH of adsorbed phosphate which gives the band at 2525 cm^{-1} (Fig. 2d, right). Adsorbed selenite and sulphate form stronger hydrogen bonds with the goethite surface than does phosphate, as indicated by OD stretching absorption near 2460 cm^{-1} (Fig. 2c,e, right) equivalent to an OH stretching frequency of 3320 cm^{-1} and a bond length of 0.28 nm (Nakamoto *et al.*, 1955). Since

TABLE 1

OH–O (anion) bond lengths calculated from O–O anion dimensions and stretching frequencies of A type OH(OD) *groups in goethite complexed with various anionic binuclear ligands.*

Ligand or anion	*O–O separation within anion* nm	*Expected length of* OH_A*-anion bond nm*	νOH cm^{-1}	νOD cm^{-1}
OH	–	0.30	3486	2584
oxalate	0.28	0.31	3560	2635
SeO_3^{2-}	0.27	0.315	3576	2645
PO_4^{3-}	0.25	0.325	3584	2650
SO_4^{2-}	0.24	0.33	3613	2667

these ligands have only S=O and Se=O oxygens available, the hydrogen bond must form between these oxygens and adjacent B-type OD groups; bonds to C-type OD groups would be longer than 0.30 nm. The pyramidal selenite ligand is likely to be oriented with three oxygens at the surface and the Se atom directed away from the surface. The tetrahedral sulphate ligand is probably in a similar orientation with one S=O directed away from the surface.

The spectra of surface OD groups of goethite with different additions of borate, molybdate and silicate suggested that these ions were adsorbed on the goethite surface by ligand exchange with A-type OD groups but the forms of the adsorbed anions are not known.

Monodentate ligands

When monobasic acids were evaporated onto goethite they reacted to form products with well-defined spectra (Fig. 3a–i).

Benzoic acid (200 μmol g^{-1}) was adsorbed as benzoate in the monodentate form (Parfitt *et al.*, 1977*a*), and this resulted in generally lower intensities of bands in the spectrum of surface OD groups (Fig. 3a). The breadth of the A-type OD band suggested that these groups were perturbed by the presence of benzoate. The broad shoulder at 2680 cm^{-1} has been ascribed to OH groups of types B and C involved in a van der Waals interaction with CH groups of the benzoate ion (Parfitt *et al.*, 1977*a*).

The spectrum of 150 μmol g^{-1} HNO_3 on goethite indicated that nitrate was formed. The absorption pattern of the surface OD groups did not show the 2680 cm^{-1} band due to the van der Waals interaction discussed above for adsorbed benzoate, but was otherwise similar to that of goethite with adsorbed benzoate (Fig. 3a,b) suggesting that nitrate was probably present as a monodentate species.

The spectrum of goethite carrying 100 μmol g^{-1} HF (Fig. 3c) showed a lower intensity of the A-type OD band at 2584 cm^{-1} (cf. Fig. 2a) consistent with replacement of these groups by F^- which slightly perturb neighbouring OD groups. This pattern of replacement was continued through 300 μmol g^{-1} (Fig. 3d) and was completed when more than 400 μmol g^{-1} HF was added, the spectrum showing that only the A-type OD groups were replaced by F^- (Fig. 3e). The B- and C-type OD groups were perturbed and resolved into two bands at 2694 and 2705 cm^{-1}. When large amounts of HF (up to 1000 μmol g^{-1}) were evaporated onto goethite the same spectrum was obtained showing that B- and C-type OH groups do not exchange with fluoride and that excess HF is lost by volatilization.

Virtually identical spectra were obtained with 100 μmol g^{-1} of HCl, HBr and HI on goethite (that for HCl is shown in Fig. 3f) but at 200 μmol g^{-1} spectra differed for the three halogen acids (Fig. 3g,h,i). The

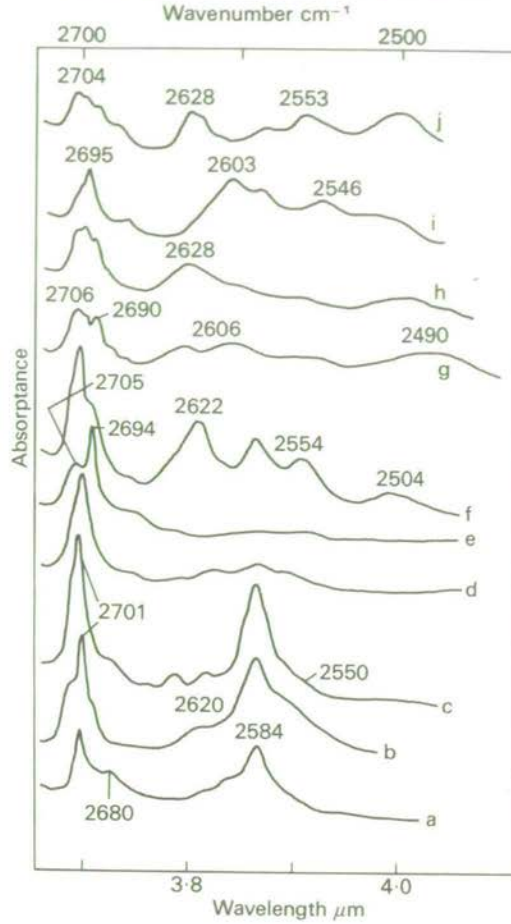

FIG. 3. Infrared spectra of goethite films treated with (a) 200 μmol benzoic acid g^{-1}, (b) 100 μmol HNO_3 g^{-1}, (c) 100 μmol HF g^{-1}, (d) 300 μmol HF g^{-1}, (e) >400 μmol HF g^{-1}, (f) 100 μmol HCl g^{-1}, (g) 200 μmol HCl g^{-1}, (h) 200 μmol HBr g^{-1}, (i) 300 μmol HI g^{-1}, (j) 50 μmol $ZnCl_2$ pH 7 g^{-1}.
All films treated with D_2O then evacuated.

spectrum of goethite with these halides at the 100 μmol g^{-1} level showed bands at 2504, 2554, 2584 and 2622 cm^{-1} (Fig. 3f), a pattern quite different from that with HF adsorbed at this level (Fig. 3c). Nevertheless, the lower intensity of the band at 2584 cm^{-1} due to A-type OD compared with that in untreated goethite (Fig. 2a) indicated that chloride, bromide and iodide, like fluoride, reacted with and replaced A-type OD groups. When these halogens replace OD (OH) groups their greater size will cause considerable distortion in the array of surface OH groups, and could force a shortening of some O . . . . . O separations. One possible assignment for the band at 2554 cm^{-1} therefore is to hydrogen-bonded OD groups involved in shortened O–O

approaches i.e. 0.29 nm. The 2622 cm^{-1} band must then be assigned to an OD group hydrogen-bonded to an adjacent halide group.

Among several possible assignments for the 2504 cm^{-1} band the most convincing is a hydrogen bond between the proton of sorbed HCl and the C oxide ion in the surface groove. The band was very weak in spectra of goethite with less than 100 $\mu mol\ g^{-1}$ halogen acid, but its intensity increased with increasing acid and became strong for HCl at 200 $\mu mol\ g^{-1}$ when it occurred at a slightly lower frequency (2490 cm^{-1}, Fig. 3g). At these higher levels, the absorption band of B- and C-type OD groups, at about 2700 cm^{-1} in the untreated goethite, became very complex due to interactions with the sorbed halogen acid. This assignment was supported by the observation that prolonged evacuation of goethite with 200 $\mu mol\ g^{-1}$ HBr simultaneously reduced the intensity of the 2504 cm^{-1} band and increased that of the band due to unperturbed B, C-type OD groups near 2700 cm^{-1}. With 200 $\mu mol\ g^{-1}$ HCl (Fig. 3g), however, the absorption pattern given by goethite was stable to evacuation implying that the HCl molecule was more strongly held on the goethite surface than was the larger HBr. The much larger HI molecule did not give the 2504 cm^{-1} band even at 300 $\mu mol\ g^{-1}$, due presumably to its weaker adsorption and loss on drying.

Cu and Zn

When 50 $\mu mol\ g^{-1}$ of $CuCl_2$ was added to goethite, and the suspension then adjusted to pH 7 with NaOH and dried, the spectrum of the product was identical to that of goethite with 50 $\mu mol\ g^{-1}$ HCl. It appeared that there was no direct interaction between copper ions and surface OH groups.

The spectrum of goethite with 50 $\mu mol\ g^{-1}$ $ZnCl_2$ was quite different. Absorption bands in the 1000 to 1600 cm^{-1} region were consistent with the presence of a complex carbonate. The carbonate bands were not removed on evacuation but they were modified after exposure to D_2O indicating that bicarbonate or OH groups were present, although the spectrum did not agree with that of hydrozincite (Moenke, 1962), a naturally occurring zinc hydroxycarbonate of formula $Zn_5(OH)_6(CO_3)_2$. Hydroxyl groups of A, B and C type were all strongly perturbed (Fig. 3j).

CO_2 adsorption

Air-dry films of goethite have been shown to react with atmospheric CO_2 to give a surface carbonate species with infrared bands at 1054, 1307 and 1497 cm^{-1} (Russell *et al.*, 1975). However, when more than 100 $\mu mol\ g^{-1}$ of phosphate, sulphate, selenite or oxalate were adsorbed no carbonate was formed, presumably due to blocking of the adsorption sites by these anions. At levels of adsorbed ligand less than 100 $\mu mol\ g^{-1}$ the usual carbonate bands were seen, but the band at

1497 cm^{-1} had reduced intensity relative to that of the band at 1307 cm^{-1}.

Additions of 200 μmol g^{-1} of HCl, HBr or HI completely prevented CO_2 adsorption but a little carbonate (<10% calculated from intensities of carbonate bands near 1500 and 1300 cm^{-1} was still adsorbed when 300 μmol g^{-1} of fluoride was adsorbed. The carbonate was usually lost immediately on evacuation, but it was held more strongly in the presence of adsorbed fluoride, and during evacuation the carbonate bands at 1515 and 1307 cm^{-1} shifted to 1530 and 1290 cm^{-1}. When more than 400 μmol g^{-1} of fluoride was added no CO_2 adsorption took place.

Discussion

Adsorption isotherms and isotope exchange studies of phosphate on goethite in aqueous suspension have shown that the anion is adsorbed as a binuclear species (Atkinson *et al.*, 1972). This conclusion was also reached from an infrared study of the phosphate-goethite system in the air-dry state (Atkinson *et al.*, 1974). Similarly, observations on the strong adsorption of oxalic acid by goethite, supported by infrared evidence (Parfitt *et al.*, 1977*b*), indicated that the oxalate group was present on the surface partly as a binuclear species.

Because its effect on the infrared spectrum of surface OD groups is analogous to that of adsorbed phosphate, selenite is probably also adsorbed as a binuclear species on the goethite surface in the air-dry state. This conclusion is supported by the observation of Hingston *et al.*, (1968, 1974) on adsorption and desorption studies in aqueous suspension, but runs counter to the proposal of Russell *et al.* (1975) who suggested a monodentate form.

There are no results available for sulphate adsorption on goethite in suspension although adsorption on hematite, which has been shown to have a hydroxylated surface related to goethite, is not reversible (Aylmore *et al.*, 1967). Sulphate is retained at low pH by tropical soils containing hydrous iron or aluminium oxides but less strongly than is phosphate which can be used to extract sulphate (Haque and Walmsley, 1973). These observations and the results presented in Table 1, in which sulphate is grouped with phosphate, selenite and oxalate, support the conclusion that sulphate is adsorbed as a binuclear ligand.

Benzoate and 2,4-D are adsorbed on goethite as monodentate species, replacing A-type OH groups as does fluoride. This explains the reversible adsorption and the lower binding constant for these anions (Watson *et al.*, 1973; Hingston *et al.*, 1974; Parfitt *et al.*, 1977*a*,*b*), compared with phosphate which is binuclear and has a much higher binding constant (Bowden *et al.*, 1974).

The binding constant for zinc on goethite is large and shows that it is strongly adsorbed (Bowden *et al.*, 1974), infrared data indicating that it

may be held as a hydroxycarbonate on the (100) face. Copper does not react directly with the (100) face but it may react with $FeOH_2$ and $FeOH^-$ on the (010) face.

In contrast to the conclusions drawn from isotherm studies that adsorption of NO_3^- and Cl^- is non-specific (Hingston *et al.*, 1972), it is reasonably certain from their effect on infrared spectra that NO_3^-, Cl^-, Br^{-1} and I^- react with, and replace, surface OH groups when their corresponding acids are evaporated onto goethite. The results show that the reactions occur even in the air-dry state since sites for CO_2 adsorption are seen to be blocked. This situation also arises when NaCl, but not $NaNO_3$, is evaporated onto goethite. With $NaNO_3$, no reaction occurs and CO_2 is able to form carbonate on the surface. The order of adsorption is probably $Cl^- > HCO_3^- > NO_3^-$.

REFERENCES

ATKINSON, R. J., PARFITT, R. L., and SMART, R. St. C. 1974. Infrared study of phosphate adsorption on goethite. J. Chem. Soc. Faraday Trans. I **70**, 1472–9.

—— POSNER, A. M., and QUIRK, J P. 1972. Kinetics of isotopic exchange of phosphate at the α–FeOOH (goethite) – aqueous solution interface. J. inorg. nuclear Chem. **34**, 2201–11.

AYLMORE, L. A. G., KARIM, M., and QUIRK, J. P. 1967. Adsorption and desorption of sulphate ions by soil constituents. Soil Sci. **103**, 10–5.

BOWDEN, J. W., BOLLAND, M. D. A., POSNER, A. M., and QUIRK, J. P. 1973. Generalized model for anion and cation adsorption at oxide surfaces. Nature, Phys. Sci. **245**, 81–3.

—— POSNER, A. M., and QUIRK, J. P. 1974. A model for ion adsorption on variable charge surfaces. Trans. 10th int. Cong. Soil Sci. Moscow, Vol II 29–36.

HAQUE, I., and WALMSLEY, D. 1973. Adsorption and desorption of sulphate in some soils of the West Indies. Geoderma **9**, 269–78.

HINGSTON, F. J., POSNER, A. M., and QUIRK, J. P. 1968. Adsorption of selenite by goethite. Adv. Chem. **79**, 82–90.

—— —— —— 1972. Anion adsorption by goethite and gibbsite. I The role of the proton in determining adsorption envelopes. J. Soil Sci. 23, 177–92.

—— —— —— 1974. Anion adsorption by goethite and gibbsite. II Desorption from hydrous oxide surfaces. Ibid. **25**, 16–26.

MOENKE, H. 1962. *Mineralspektren*, I Berlin: Akademie-Verlag.

NAKAMOTO, K., MARGOSHES, M., and RUNDLE, R. E. 1955. Stretching frequencies as a function of distances in hydrogen bonds. J. Am. Chem. Soc. **77**, 6480–6.

PARFITT, R. L., ATKINSON, R. J., and SMART, R. St. C. 1975. The mechanism of phosphate fixation by iron oxides. Proc. Soil Sci. Soc. Am. **39**, 837–41.

—— FARMER, V. C., and RUSSELL, J. D. 1977*a*. Adsorption on hydrous oxides: I Oxalate and benzoate on goethite. J. Soil Sci. **28**, 24–39.

—— FRAZER, A. R., RUSSELL, J. D., and FARMER, V. C. 1977*b*. Adsorption on hydrous oxides: II Oxalate, benzoate and phosphate on gibbsite. J. Soil Sci. **28**, 40–7.

——, RUSSELL, J. D., and FARMER, V. C. 1976. Confirmation of the surface structures of goethite (α–FeOOH) and phosphated goethite by infrared spectroscopy. J. Chem. Soc. Faraday Trans. I **72**, 1082–7.

RUSSELL, J. D., PATERSON, E., FRASER, A. R. and FARMER, V. C. 1975, Adsorption of carbon dioxide on goethite surfaces and its implication for anion adsorption. J. Chem. Soc. Faraday Trans. I **71**, 1623–30.

WATSON, J. R., POSNER, A. M., and QUIRK, J. P. 1973. Adsorption of the herbicide 2,4-D on goethite. J. Soil Sci., **24**, 503–11.

(Received 25 May 1976)

J. Sci. Fd Agric. 1977, **28**, 852–854

Ammonia-treated Vermiculite—a Possible Controlled-release N-fertiliser

James D. Russell and Anthony R. Fraser

Department of Spectrochemistry, The Macaulay Institute for Soil Research, Craigiebuckler, Aberdeen AB9 2QJ

(*Manuscript received 14 February 1977*)

The preparation of ammonium-treated vermiculite containing almost 1.3% ammonium-N is described. The product is relatively stable on storage in air for 3 years, but during leaching with water for 20 weeks, 2.8–4.0 mm flakes released 30% of their N and 0.25–0.5 mm flakes 90%. Its potential as a controlled-release nitrogen fertiliser is briefly discussed.

1. Introduction

Anhydrous ammonia gas depends for its efficient use as a nitrogenous fertiliser on being trapped by soil and then slowly released to be used by microorganisms and plants. Clay minerals are among the more important soil constituents involved in the initial trapping and to gain a better understanding of this reaction, Russell[1] and Ahlrichs *et al.*[2] investigated the adsorption of anhydrous ammonia by montmorillonite, saponite and vermiculite. Using infrared spectroscopy it was shown that the ammonia is adsorbed in three forms: (a) ammonium ions, produced when ammonia reacts with water molecules coordinated to exchangeable cations,

$$M^{2+}(H_2O)_n + 2NH_3 \rightleftharpoons M(OH)_2 + 2NH_4^+ + (H_2O)_{n-2};$$

(b) ammonia directly coordinated to exchangeable cations; (c) ammonia hydrogen bonded to ammonium ions and to coordinated ammonia.

Ammonia in forms (b) and (c) is readily displaced by water vapour but ammonium ions [form (a)] are more stable, particularly those in ammonia-treated vermiculite, their stability increasing with increase in vermiculite particle size.[2] These authors also observed that the ammonium formed in large (10–20 mm) flakes of hydrobiotite, which is a regular interstratification of vermiculite layers and inert non-expanding biotite layers, appeared to be stable to immersion in water, suggesting that in large flakes it may be relatively stable in soil. Hydrobiotite is readily available commercially usually under the name vermiculite. This name will be adopted in the present communication, the purpose of which is to describe the preparation and properties of ammonia-treated vermiculite (hydrobiotite)—ATV—and its possible role as a controlled-release N-fertiliser.

2. Experimental

The preparation of ATV consisted of passing anhydrous ammonia gas vertically upwards through vermiculite (Mandoval Limited, Surrey) loosely packed in a pyrex glass column 100 × 2.5 cm diam. at a flow rate of 5–10 cm^3/s. The ammonia displaced hydration water from the flakes which then became wet. The flow of ammonia was continued until the flakes were dry and, to complete the treatment in a reasonable time, the column was heated gently in the latter stages with heating tapes. Using this procedure, the treatment took 8 h. The flakes were washed on a Buchner funnel until the washings were neutral to test paper, then air-dried overnight at 35°C to give a product free of the smell of ammonia. The intense NH_4^+ deformation band at 1430 cm^{-1} in the infrared absorption

Table 1. Amino acid analysis of Cappelle-Desprez β-gliadin (residues per molecule)

	Experimental	Nearest integers
Asx	10.3	10
Thr	5.54	6
Ser	20.3	20
Glx	115.2	115
Pro	61.3	61
Gly	9.8	10
Ala	10.2	10
Val	15.0	15
Cys	7.6	8
Met	2.2	2
Ile	12.1	12
Leu	22.0	22
Tyr	10.9	11
Phe	14.0	14
Lys	1.0	1
His	6.1	6
Arg	5.7	6
Trp	0.48	1
Total	329.7	330

Calc. mol. wt. assuming complete amidation = 37 792.

Average wt. of anhydro amino acid = 114.5.

Calc.[4] molar extinction coefficient = 2.3×10^4 litre mol^{-1} cm^{-1}.

$\frac{\text{Ionic} + \text{polar}}{\text{Non-polar}} = 1.13$.

Protein/N ratio (assuming complete amidation) = 5.54.

Acknowledgements

The financial support of the Ministry of Agriculture, Fisheries and Food is gratefully acknowledged by the Research Association. The author thanks Mr C. H. Groves for the photography, Miss W. A. Keddie for experimental assistance and Mr D. Smith for running the analyser.

References

1. Booth, M. R. *J. Sci. Fd Agric.* 1970, **21**, 185.
2. Ewart, J. A. D. *J. Sci. Fd Agric.* 1973, **24**, 685.
3. Ewart, J. A. D. *J. Sci. Fd Agric.* 1975, **26**, 1021.
4. Ewart, J. A. D. *J. Sci. Fd Agric.* 1975, **26**, 5.
5. Ewart, J. A. D. *Lab. Pract.* 1976, **25**, 769.
6. Ewart, J. A. D. *J. appl. Chem. Biotechnol.* 1976, **26**, 239.
7. Liu, T.-Y. *Meth. Enzymol.* 1972, **25**, 44.
8. Simpson, R. J.; Neuberger, M. R.; Liu, T.-Y. *J. biol. Chem.* 1976, **251**, 1936.
9. Goodwin, T. W.; Morton, R. A. *Biochem. J.* 1946, **40**, 628.

spectrum of these flakes (≯25 μm thick for optimum transmission) confirmed that they contained only ammonium ions and that NH_3 coordinated to Mg^{2+}, the principal exchange cation in hydrobiotite and vermiculite, was not present as no band in the 1220 cm^{-1} region[1] was detectable even in spectra of flakes up to 100 μm thick. Ammonium ions in the flakes were determined quantitatively by decomposition in 12 M-HCl at 80°C (three 1 h treatments with 3 ml acid per g ATV) and measuring NH_4^+ in solution either colorimetrically[3] or using a NH_3 electrode, the latter method being preferred because it is rapid, more convenient, and equally sensitive. Two fractions of vermiculite flakes (c.e.c. 90–100 mEq/100 g), 0.25–0.5 mm, and 2.8–4.0 mm, treated with ammonia as described, contained respectively 88 and 90 mEq NH_4^+/100 g indicating that reaction (a) had gone virtually to completion. Flakes containing less NH_4^+ were obtained when other methods of preparation were employed. For example a shorter flow time of 1 h, when the flakes in the column first became completely wet, gave flakes containing 30–40 mEq/100 g. A leaching procedure using saturated aqueous ammonia solution introduced a maximum of about 40 mEq/100 g into the flakes. Thermally, the ammonium ions in ATV are as stable as those on exchange sites in NH_4^+-saturated vermiculite, decomposing above 600°C.

3. Results and discussion

The reaction by which ammonia is converted to ammonium ions in vermiculite is reversed by water vapour, but it is particularly noteworthy that after 3 years' storage in a loosely stoppered container the ammonium content of the larger flakes was unchanged and that of the smaller size fraction had decreased only from 88 to 70 mEq/100 g. The ammonium ions in ATV were less stable to continuous leaching by distilled water. When 0.5 litre/day was passed through 6 g flakes in a 20 cm vertical column, the NH_4^+ content of the 0.25–0.5 mm flakes decreased much more rapidly than did that of the 2.8–4.0 mm flakes (Figure 1). The sharp decrease shown by the larger size fraction during the first week probably represents release of NH_4^+ from the more accessible flake edges. The subsequent release over the next 19 weeks, equivalent to a full growing season, is much slower, two-thirds of the original NH_4^+ still remaining in these larger flakes. Over the same period, the 0.25–0.5 mm flakes released 90% of their ammonium ions. Although these leaching conditions are extreme compared with those likely to be encountered in the field in the absence of vegetation, they are probably not too dissimilar from those to be found in the presence of a growing crop which, like the flowing leach water, will continuously remove the displaced ammonium ions. This would suggest that after harvest of a crop grown on larger size ATV flakes, a substantial proportion of the original NH_4^+ content of the flakes could still be available for uptake by a crop in the following year. These results indicate a possible application of ATV as a controlled-release nitrogen fertiliser for which the rate of release depends to some extent on the particle size of the flakes, although plan

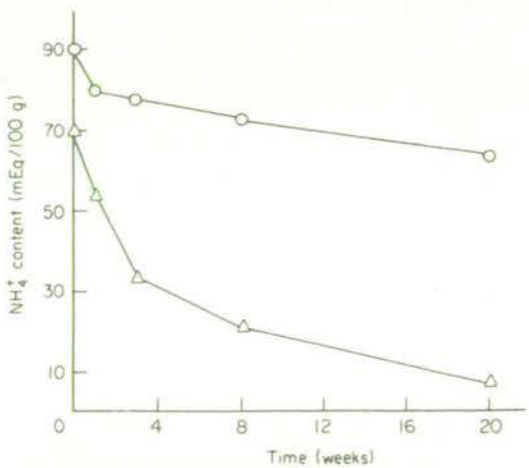

Figure 1. Changes in NH_4^+ content (mEq/100 g) of two particle size fractions of ammonia-treated vermiculite flakes during leaching at 20 C with distilled water at a rate of 0.5 litre/day. ○, Coarse, 2.8–4.0 mm; △, fine, 0.25–0.50 mm.

roots may play some part in actively removing NH_4^+ from the flakes by a mechanism similar to that operating when K^+ is extracted from biotite by wheat seedlings.[4] Preliminary pot trials using two particle sizes of ATV as the sole nitrogen source for a variety of crops of different seasonal nitrogen demand support this conclusion. Detailed results of these trials will be published at a later date.

Further control of the rate of release of ammonium ions from ATV may be possible using exfoliated material produced by brief heat treatment at 500°C. Exfoliated flakes, since they contain very little water, adsorb only small amounts of ammonia; similarly, completely ammoniated flakes, because they contain little adsorbed water, do not undergo exfoliation. However ammoniated flakes, containing 70 mEq NH_4^+/100 g and, therefore, also some hydration water, exfoliate partially and still contain 56 mEq NH_4^+/100 g. Macroscopically, this material has a much larger surface area and might exhibit a more rapid release of ammonia under moist conditions.

4. Conclusions

The most important properties in considering ATV as a viable nitrogenous fertiliser are its long-term stability in storage and the slowness of its release of NH_3 in the field. Since the rate of release is primarily controlled by the particle size of the ATV flakes, it should be possible to select a mixture of sizes of exfoliated and/or unexfoliated flakes whose release pattern over the duration of the growing season would match closely the seasonal nitrogen demand of a particular crop. Clearly, this would give ATV considerable advantage over most other N-fertilisers in that losses due to leaching and denitrification should be minimised resulting in more efficient use by the crop of the N supplied, and in less pollution of drainage water. Set against this is the low N content of ATV, 1% compared with 20–50% for other pure N fertilisers. As a bonus however, ATV contains about 5% K, most of which might be available to crops.[4] Material similar to ATV is likely to be formed *in situ*, on direct injection of anhydrous ammonia fertiliser, in soils that contain hydrobiotite or vermiculitic weathering products.

References

1. Russell, J. D. *Trans. Faraday Soc.* 1965, **61**, 2284.
2. Ahlrichs, J. L.; Fraser, A. R.; Russell, J. D. *Clay Minerals* 1972, **9**, 263.
3. Fraser, A. R.; Russell, J. D. *Clay Minerals* 1969, **8**, 229.
4. Mortland, M. M.; Lawton, K.; Uehara, G. *Soil Sci.* 1956, **82**, 477.

CHEMICAL AND INFRARED SPECTROSCOPIC STUDIES OF FULVIC ACID FRACTIONS FROM A PODZOL

H. A. ANDERSON, A. R. FRASER, A. HEPBURN, and J. D. RUSSELL
(The Macaulay Institute for Soil Research, Craigiebuckler, Aberdeen, AB9 2QJ)

Summary

Infrared spectroscopy and chemical degradation indicated several fulvic acid fractions from an iron-humus podzol capable of complexing and translocating metals. Acidic polysaccharides, some of them resembling pectic acid, were isolated in appreciable quantities. These are able to bind metals through carboxyl groups, but peptide components present in the polysaccharide fraction may provide alternative metal complexing centres. The high yield of acid-extractable organic matter from the illuvial humus, together with its high content of carboxylic acid groups, make it likely that this fraction plays a major role in the translocation of metals. Phenolic compounds allegedly associated with this process were present in the fulvic acid solution in low amounts, and only in the extracts from the organic horizons.

Introduction

THE term 'podzol' originally implied the occurrence of a bleached A_2 layer below the surface horizons of the soil profile (Muir, 1961). Wider definitions of the term include features which may be more obvious in the field, for example the existence of an ochreous B horizon containing translocated humus (*cf.* Romans, 1970). The accumulation of humus in the B horizon, accompanied by relatively high concentrations of aluminium and iron, has been held to indicate an organic complexation and translocation of mineral cations. Indeed, laboratory experiments involving leaf leachates (Bloomfield, 1970), and field studies on the composition of canopy drip and the movement of sub-surface soil water (Davies, 1970) have demonstrated the feasibility of such hypotheses.

Soil organic matter is also likely to be important in this type of translocation, particularly the more soluble, lower molecular weight, fulvic acid fraction. Forsyth (1947) introduced a method of fractionating fulvic acid solutions based on adsorption of the mixtures on charcoal and the subsequent elution (by various solvents) of fractions A, B, C and D. The aim of the present study is to characterize these Forsyth fulvic acid fractions from a podzol under natural vegetation, using infrared spectroscopy and chemical degradation, and to deduce whether they are capable of complexing and translocating metal ions. A preliminary account of this work has already been given (Anderson, 1970).

Journal of Soil Science, 1977, 28, 623–633

Materials and methods

Soil profile

The soil examined was a freely-drained iron-humus podzol, of the Countesswells series, Countesswells Association, from Glentanar, Aberdeenshire. It is a stony sandy loam derived from granite, and has been formed under the natural Caledonian pine forest, which is considered to have been extant for at least seven thousand years. The pit was dug at O.S. map reference NJ 484917, and the profile consisted of L, F_1 and F_2 layers, with $A_{2/1}$, $A_{2/2}$, B_{2h}, $B_{2/3}$, B_3 and B_3/C horizons, all of which were sampled.

Extraction

Air-dried soil samples (200 g from organic layers, 1000 g from mineral horizons) were extracted with 1:1 ethanol-benzene (Soxhlet) until the extract was colourless. The soil was air-dried and repeatedly extracted with 0.1 M hydrochloric acid (10 litres) for 15 h at room temperature, the solution being removed by centrifugation, until the extract was colourless. The residual soil was further extracted exhaustively with 0.5 M sodium hydroxide in a similar manner, the dark solution being clarified by passage through a centrifugal separator. Acidification of the combined alkali-extracted solutions to pH 1 precipitated humic acid (HA) which was isolated by conventional procedures (Farmer and Morrison, 1960).

The hydrochloric acid extract and the supernatant solution from the HA precipitation were regarded as fulvic acid (FA) solutions and were termed F(1) and F(2) respectively. Fractions A–D were then isolated by adsorption on charcoal and elution with A) 0.1 M hydrochloric acid, B) 90 per cent acetone, C) water and D) 0.1 M sodium hydroxide, as described by Forsyth (1947), except that fraction D was neutralized with hydrochloric acid, evaporated to about 500 cm^3 and dialysed in Visking tubing against distilled water (5 x 5 litres), then freeze-dried. The high ash contents of the F(2)D fractions were lowered on further dialysis against 0.1 M hydrochloric acid, followed by water. The material which precipitated on acid dialysis {F(2)Dp} was collected by centrifugation and was freeze-dried, as was the soluble fraction {F(2)Da}.

Infrared spectroscopy

Spectra of samples (1 mg in 12 mm diameter KBr pressed discs), were recorded on a Grubb-Parson S4 double beam spectrometer over the range 2–16 μm.

Quantitative analysis

Neutral sugars Samples were hydrolysed and analysed for individual sugars as described by Cheshire *et al.* (1971).

Uronic acids Samples (5 mg) were hydrolysed in 1 ml 0.5 M sulphuric acid for 4 h at 110 °C in sealed tubes. The hydrolysates were centrifuged and the combined supernatant solutions and washings were diluted to 2 ml before analysis by an automated carbazole method (Balazs *et al.*, 1965) Estimations were corrected for background colour and neutral sugar content.

Elemental analysis Samples were analysed using a Hewlett-Packard 185 CHN Analyzer. In the case of the isolated organic matter, only the HA's, the F(1)B and D, and the F(2)C and D fractions were analysed; possible contamination of the F(2)B fractions is discussed below.

Qualitative chromatographic analysis

Polysaccharide Samples (5 mg) were hydrolysed as under 'Uronic acids'; the hydrolysates were neutralized with 1 M sodium hydroxide, then evaporated to dryness. The residues were extracted thrice with 2 ml of ethyl alcohol-acetic acid-water (2:1:1), the combined extracts were filtered and evaporated to dryness, then dissolved in 500 µl 80 per cent ethyl alcohol. Aliquots (30 µl) were chromatographed on Whatman No. 1 paper in n-butyl alcohol-acetic acid-water (150:30:70; upper layer) for 72 h, then sprayed with *p*-anisidine reagent (Hough *et al.*, 1950).

Amino acids Samples were hydrolysed in 6 M hydrochloric acid, chromatographed in two dimensions (Piper and Posner, 1968), sprayed with ninhydrin and estimated visually against standard chromatograms.

Phenols Samples were chromatographed on thin layers of Kieselgel G (Merck) in methyl alcohol-benzene-acetic acid (8:45:4), phenols were located by spraying with diazotized sulphanilamide (Stahl, 1965), and estimated as above.

Results

Yields

Fulvic fractions A contained only traces of organic matter and were discarded. The yields of other organic fractions (Table 1) are consistent with those expected from an iron-humus podzol, a high yield of HA in the organic horizons decreasing sharply on passing into the mineral soil horizons. This was followed by a slight increase in HA content and a dramatic increase in the FA content, particularly the acid-soluble F(1) fractions, in the B_2h and $B_{2/3}$ (illuvial) horizons. As previously observed in a Canadian podzol (Schnitzer and Wright, 1957), the coloured FA components in the B horizons are readily extracted by dilute mineral acids, whereas the FA humus of the F and H lavers is not

TABLE 1

Yields of ash-free products as per cent air dried soil

Sample		*Humic*	*F(2) Fulvic acid fractions*			*Fulvic B and D*	*Soil*
horizon	*depth (cm)*	*acid*	*B*	*C*	*D*	*carbon*	*carbon %*
L	30–26	16.5	0.03	0.3	1.7	1.5	44.5
F_1	25–18	14.0	0.3	0.3	1.2	1.1	45.1
F_2(H)	18–10	22.5	0.5	0.1	0.7	1.1	47.4
F_2(H)	8– 0	33.0	0.5	0.2	0.5	1.0	44.2
$A_{2/1}$	0–10	5.0	0.1	0.02	0.4	4.0	4.9
$A_{2/2}$	13–25	1.0	0.02	0.02	0.2	12.2	0.8
B_{2h}	33–38	2.5	0.1 (2.3)	0.02	0.2 (2.7)	55.2	4.6
$B_{2/3}$	38–50	1.3	0.02 (1.8)	0.005	0.2 (1.9)	65.9	2.8
B_3	60–70	0.5	0.003	0.001	0.3	14.2	1.0
B_3/C	78–88	0.2	0.001	<0.001	0.3	21.5	0.6

The yields in parenthesis are for F(1)B and F(1)D; yields of these fractions in other horizons were <0.001 per cent. The column under "Fulvic B and D carbon" expresses the total carbon extracted in the F(1) and F(2)B and D fractions as per cent soil carbon.

appreciably soluble under these conditions. It was observed that the coloured FA fractions (B and D) from the B horizons were also partly extracted by ethanol-benzene; yields of these fractions increased when the organic solvent extraction was omitted. Forsyth's fractionation of the mineral acid extracts of the B horizons resulted in elution of organic matter predominantly in the B and D fractions, with only negligible amounts in the A and C fractions.

Elemental analysis

Table 2 shows the C, H and N contents of the HA's and the F(2)C

TABLE 2

Elemental analyses of Glentanar humic and fulvic fractions; 1 HA; 2 F(2)C; 3 F(2)D; 4 F(2)Da; 5 F(2)Dp

Layer or horizon	C%					H%					N%				
	1	2	3	4	5	1	2	3	4	5	1	2	3	4	5
L	54.1	40.5	56.1	38.9	47.7	5.7	6.8	5.5	4.7	4.2	2.6	0.5	0.9	0.5	0.9
F_1	53.8	39.5	37.5	39.8	45.9	5.6	6.8	4.5	5.1	4.2	2.6	0.5	0.6	0.6	0.9
F_2(H)	50.7	41.3	44.9	42.0	45.7	5.1	6.9	4.6	5.0	4.0	1.8	0.5	0.8	0.7	0.9
F_2(H)	53.3	40.3	46.9	42.0	46.9	5.0	6.7	4.5	4.6	4.6	1.6	0.8	0.8	0.7	0.9
$A_{2/1}$	51.5	39.6	46.3	39.2	47.6	4.2	6.6	4.9	5.7	4.5	1.8	1.4	1.4	1.4	1.2
$A_{2/2}$	53.6	36.4	44.0	44.5	47.5	5.0	6.3	3.8	4.8	4.2	2.4	1.6	0.7	0.9	0.8
B_{2h}	50.8	39.0	41.8	47.9	48.6	4.8	6.6	3.9	4.9	4.7	3.2	6.0	0.9	1.2	1.3
$B_{2/3}$	52.1	36.1	46.7	47.1	47.6	4.8	6.3	3.8	5.0	4.1	3.0	5.5	1.1	1.3	1.3
B_3	54.8	35.0	27.2	34.0	47.4	5.6	6.1	3.7	5.8	5.5	3.6	2.9	0.8	1.4	2.0
B_3/C	54.2	34.2	40.5	42.9	46.5	5.3	6.5	4.1	6.0	4.2	3.9	3.3	1.5	1.9	1.4

Note: the values, for air-dried material, are corrected for ash contents, which were 1–4% except in the F(2)D fractions (10–50%).

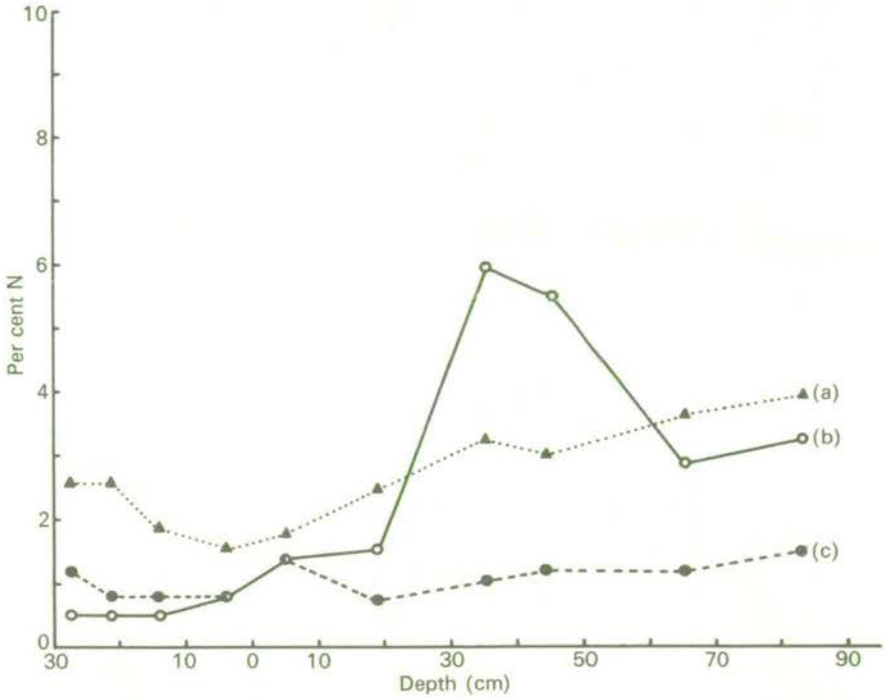

FIG. 1. Nitrogen contents (expressed on an ash-free basis) of, a) humic acids, b) F(2)C fractions, c) F(2)D fractions.

and F(2)D fractions. The nitrogen contents show an interesting series of relationships (Fig. 1); both the HA and F(2)D values initially decrease before rising gradually with increasing depth in the profile. The F(2)C nitrogen content, initially lower than that of either of these fractions, shows a remarkable increase in the B_2h horizon before returning to follow closely that of the HA in the lower horizons. The pattern of increasing nitrogen contents closely resembles that for the amounts of amino acids liberated on acid hydrolysis.

The analysis (C 46.9 ± 0.5, H 3.1 ± 0.2, N 0.9 ± 0.1%) of the non-diffusible F(1)B and F(1)D fractions from the $B_{2/h}$ and $B_{2/3}$ horizons are the same as those of their F(2)B counterparts, although the F(2)D fractions have appreciably higher C, H and N contents.

Fulvic acid fractions

Fraction B Low amounts (<0.05%) of free *p*-hydroxybenzoic, vanillic, 3,4-dihydroxybenzoic and syringic acids were present in all F(2)B fractions down to the $A_{2/2}$ horizon. Below the A horizons, polymeric material eluted in this fraction masked the possible presence of the last two compounds; the concentration of phenols in the B_{2h}

horizon must be less than 2%, since aromatic bands were not detected in the infrared spectrum. Because the phenolic acids were more abundant from the organic horizons, it was concluded that these acids were lignin degradation products. Dilute sulphuric acid hydrolysis released high amounts of monosaccharides, but the phenolic acid content decreased, and no other phenolic products were seen in the chromatograms.

The infrared spectra of the F(2)B fractions were consistent with a polycarboxylic acid containing low amounts of amide and polysaccharide. No degradation studies were made of the crude F(2)B fractions because of their probable contamination by artifacts. The initial acetone eluate from the Forsyth procedure contains hydrochloric acid, and this leads to aldol condensation of the ketonic solvent. Indeed, 'blank' replication of the charcoal fractionation led to low yields of diacetone alcohol, mesityl oxide and phorone in the B fraction. In an attempt to remove these low molecular weight artifacts, the B fractions were dialysed. Those from the samples above the $A_{2/2}$ yielded diffusible acidic brown gums as the major products, the greater part of the amide-polysaccharide being retained by the membrane. The B_{2h} and $B_{2/3}$ horizons, however, gave higher molecular weight non-diffusible fractions free from the acetone-derived contaminants. This was also true of the F(1)B products, the soluble non-diffusible fraction of which yielded infrared spectra (Fig. 4c), indicating a polycarboxylic acid similar to that isolated from F(2)B. A preliminary account of the similarity between these natural polycarboxylic acids and a synthetic model compound has already been published (Anderson and Russell, 1976).

Hydrolysis of all non-diffusible F(1)B and F(2)B fractions yielded low amounts of amino acids and sugars, consistent with the very weak absorption bands in the infrared spectra. These spectra were virtually identical to those of the diffusible B fractions, suggesting that the contaminants made little or no contribution to the infrared spectra. This similarity further suggested that the major difference between the diffusible and non-diffusible B fractions was one of molecular size.

Fraction C Appreciable yields of material were recovered in this fraction only after the alkaline extraction (*i.e.* in F(2)C). Infrared spectra of the products (Fig. 2) showed both their predominantly polysaccharide nature and a variable amide contribution increasing with depth. These features give rise respectively to (a) intense absorption bands centred between 9.0 and 9.5 μm, and (b) an amide II band at 6.45 μm (Bellamy, 1975). The amide I band is obscured by carboxylate and water absorption near 6 μm. The intensity of the amide II band parallels the nitrogen content of the samples, increasing to the B_{2h} (Fig. 2c) and thereafter decreasing (Fig. 2d). Yields of amino acids on

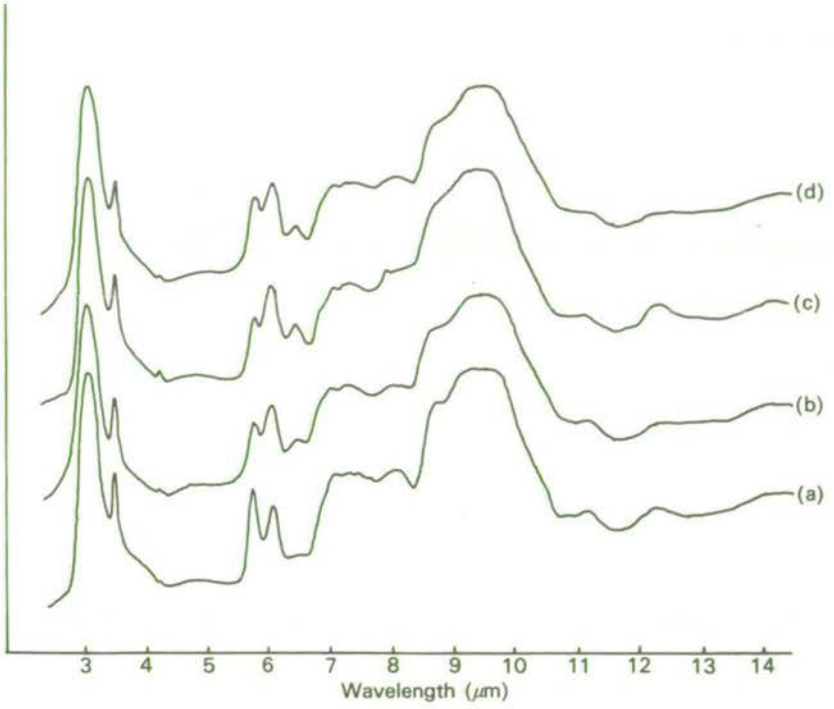

FIG. 2. Infrared spectra of fulvic acid (F(2)C) fractions from the following samples: a) L (30 – 26 cm), b) F_2(H) (8 – 0 cm), c) B_{2h} (33 – 38 cm), d) $B_{2/3}$ (38 – 50 cm).

TABLE 3

Contents of neutral sugars and uronic acids in hydrolysates, as per cent ash-free samples

	F(2)C							*F(2)D*
Layer or horizon	*Ara*	*Gal*	*Glu*	*Man*	*Rha*	*Xyl*	*uronic acid*	*uronic acid*
L	1.8	10.4	12.1	18.2	0.6	8.2	6.2	17.0
F_1	2.0	16.9	11.5	33.6	0.7	7.6	7.1	26.9
F_2(H)	1.9	23.0	11.1	19.5	4.5	7.9	8.5	9.1
F_2(H)	0.9	23.1	11.2	15.1	2.6	3.3	7.3	10.9
$A_{2/1}$	2.0	23.5	11.0	19.6	3.4	6.6	7.5	8.0
$A_{2/2}$	3.9	28.9	7.8	23.8	1.3	9.1	6.8	3.8
B_{2h}	2.3	18.5	8.6	15.9	1.0	5.0	6.4	7.1
$B_{2/3}$	3.2	16.0	6.4	15.3	3.8	4.8	5.9	2.8
B_3	3.0	7.6	5.9	9.0	0.9	4.1	4.6	4.8
B_3/C	*	*	*	*	*	*	5.0	6.7

Ara: arabinose, Gal: galactose, Glu: glucose, Man: mannose, Rha: rhamnose, Xyl: xylose.
*insufficient sample for hydrolysis.

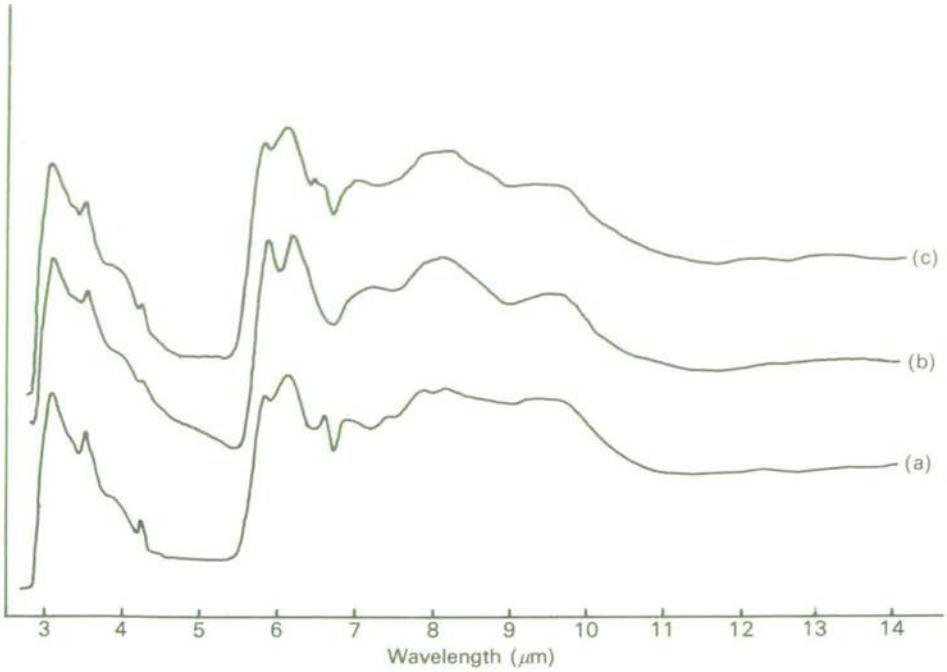

FIG. 3. Infrared spectra of humic acids from the following samples: a) F_1 (25 – 18 cm), b) $A_{2/2}$ (13 – 25 cm), c) B_{2h} (33 – 38 cm). Absorption at 4.22 μm is due to carbon dioxide, caused by spectrophotometer imbalance.

hydrolysis showed a similar trend; very low from the litter, F and H horizons, but increasing sharply with depth, the B_{2h} and $B_{2/3}$ samples having higher contents than the others. A similar, but less spectacular, increase in amide is seen in spectra of the HA's from these horizons (Fig. 3). The HA spectra also show lignin absorption at 6.62 μm (cf. Farmer and Morrison, 1960), but only in the samples from the litter and F layers. Hydrolysis showed a general decrease of neutral sugars, particularly galactose and mannose with depth (Table 3).

Fraction D The majority of these fractions contained silica gel, recognized by its characteristic infrared spectrum, and generally had higher ash contents than any of the others. Dialysis in an acid medium yielded a non-diffusible soluble fraction, F(2)Da, and a precipitate, F(2)Dp, both of which had much lower ash contents.

The infrared spectrum of the F(2)Da fraction from the F_1 horizon strongly resembled that of pectic acid (Fig. 4); this was also true of the litter layer fraction but spectra became more diffuse for fractions from greater depth. The uronic acid contents of these fractions (Table 3) support these observations, those from the litter and F_1 horizons being about four times those from the mineral layers. Amide absorption in

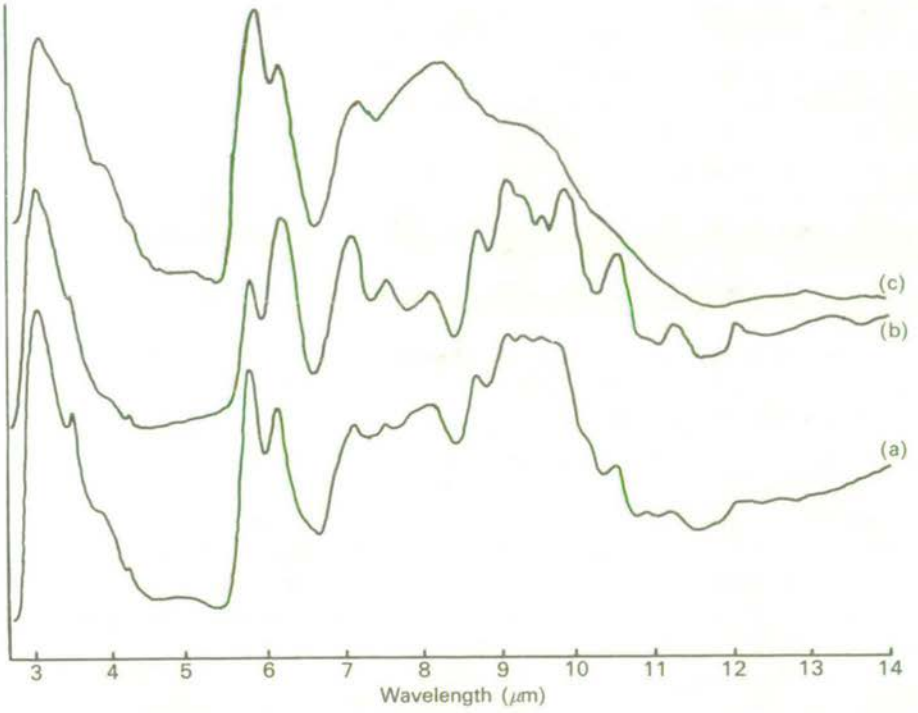

FIG. 4. Infrared spectra of a) F(2)Da fraction from F_1 layer, b) pectic acid (from Italian rye-grass), c) F(1)Ba fraction from B_{2h} horizon.

the spectra of the F(2)D fractions was weak or absent. The soluble, non-diffusible F(1)D fractions from the B_{2h} and $B_{2/3}$ horizons had infrared spectra very similar to those of the F(1)B, F(2)B and F(2)D fractions.

Discussion

The development of a bleached A_2 horizon involves the leaching of mineral cations, supposedly by soluble organic compounds and it has been shown that leaf leachates contain compounds including organic acids and amino acids, and particularly phenols, which can dissolve iron oxide with varying degrees of success (Muir *et al.*, 1964; Bloomfield, 1970; Davies, 1970). The present study of the Glentanar profile has identified small amounts of phenolic compounds in the fulvic acid B fractions from the organic horizons only. The source of the phenols may have been lignin residues since lignin-like absorption was observed in the co-extracted humic acids. The relatively low yields of phenols from the organic layers suggest that these compounds could play only a minor role in metal translocation in this iron-humus podzol profile. The importance of phenols in the process may have been over-emphasized by other authors because of their abundance in other podzolic profiles.

Of the phenols isolated from soil organic fractions some may be artifacts. The production of phenols by degradation of humic acids is well documented (Schnitzer and Khan, 1972) but observations of the derivation of phenols from non-aromatic precursors are equally well known. Both 3,4- and 3,5-dihydroxybenzoic acid have been produced in the caustic fusion of furfural polymers (Cheshire *et al.*, 1968) and furfural is produced from polysaccharides under similar conditions; less severe treatment with dilute acid is sufficient to convert sugar residues into catechol derivatives (Popoff and Theander, 1970, 1976).

In agreement with the conclusions drawn by Wright and Schnitzer (1960) from a study of the podzolized Armadale profile, it is thought that the coloured fulvic acid polymers isolated from the Glentanar illuvial humus, in many respects similar to those isolated from the Canadian soil (Schnitzer and Desjardins, 1962), are probably responsible for the major part of the podzolization process. The abundance of carboxylic acid groups in these polymers makes them obvious complexers of metal cations, and their ease of extraction lends credence to the concept of their existence in the soil as metal-organic complexes of the type that would result from the postulated podzolization process.

Other fractions capable of involvement in this process have been isolated from the Glentanar profile. They have high contents of uronic acids and bear considerable resemblances to pectic acid isolated from plant sources. Forsyth's 'polysaccharide' fractions, corresponding to F(2)C in the present work, also contained uronic acid residues, but he concluded that these were mainly glucuronic acid present as an aldobionic acid group, linked to glucose (Forsyth, 1950). In the present study, infrared spectroscopy and chemical analysis show that the uronic acids appear mainly in the F(2)D fractions and to a lesser degree in the F(2)C products. Although the polyuronides isolated from the L, F and H layers possibly arose from non-humified plant tissue, the isolation of such compounds from a podzol is of major interest in view of the known chelating ability of these compounds (Grasdalen *et al.*, 1975). Their survival can be explained by cation chelation affording protection from microbial attack, as has been observed for neutral polysaccharides (Martin *et al.*, 1966), and such complexes would effect transport of the cations. The increase in amino acid content with depth in the F(2)C fractions provides evidence for alternative sources of sites capable of metal-binding and transport.

REFERENCES

ANDERSON, H. A. 1970. Some aspects of the chemistry of the Glentanar podzol profile. Welsh Soils Disc. Grp. Rpt. No. 11, 124–32.

—— and RUSSELL, J. D. 1976. Possible relationship between soil fulvic acid and polymaleic acid. Nature, Lond. **260**, 597.

BALAZS, E. A., BERNSTON, K. O., KAROSSA, J., and SWAN, D. A. 1965. An automated method for the determination of hexuronic acids. Analyt. Biochem. **12**, 547–58.

BELLAMY, L. J. 1975. *The infrared spectra of complex molecules*, 3rd ed. vol. I, London: Chapman and Hall.

BLOOMFIELD, C. 1970. The mechanism of podzolization. Welsh Soils Disc. Grp. Rpt. No. 11, 112–23.

CHESHIRE, M. V. C., CRANWELL, P. A., and HAWORTH, R. D. 1968. Humic acid-III. Tetrahedron **24**, 5155–67.

—— MUNDIE, C. M., and SHEPHERD, H. 1971. The pentose fraction of soil polysaccharide. J. Soil Sci. **22**, 222–36.

DAVIES, R. I. 1970. The podzol process. Welsh Soils Disc. Grp. Rpt. No. 11, 133–42.

FARMER, V. C., and MORRISON, R. I. 1960. Chemical and infrared studies on phragmites peat and its humic acids. Scient. Proc. R. Dubl. Soc. Ser. A. 1, 85–104.

FORSYTH, W. G. C. 1947. Studies on the more soluble complexes of soil organic matter. I. A method of fractionation. Biochem. J. **41**, 176–81.

—— 1950. Studies on the more soluble complexes of soil organic matter. 2. The composition of the soluble polysaccharide fraction. Ibid. **46**, 141–6.

GRASDALEN, H., ANTHONSEN, T., LARSON, B., and SMIDSROD, O. 1975. NMR studies of the interaction of metal ions with poly(1,4-hexuronates). Acta chem. scand. **B29**, 99–108.

HOUGH, L., JONES, J. K. N., and WADMAN, W. H. 1950. Quantitative analysis of mixtures of sugars by the method of partition chromatography. J. chem. Soc. 1702–6.

MARTIN, J. P., ERVIN, J. O., and SHEPHERD, R. A. 1966. Decomposition of the iron, aluminium, zinc and copper salts or complexes of some microbial and plant polysaccharides in soil. Proc. Soil Sci. Soc. Am. **30**, 196–200.

MUIR, A. 1961. The podzol and podzolic soil. Adv. Agron. **13**, 1–56.

MUIR, J. W., MORRISON, R. I., BOWN, C. J., and LOGAN, J. 1964. The mobilization of iron by aqueous extracts of plants. J. Soil Sci. **15**, 220–5.

PIPER, T. J., and POSNER, A. M. 1968. On the amino acids found in humic acid. Soil Sci. **106**, 188–92.

POPOFF, T., and THEANDER, O. 1970. Formation of aromatic compounds from D-glucuronic acid and D-xylose under slightly acid conditions. Chem. Communs 1576.

—— —— 1976. Formation of aromatic compounds from carbohydrates. Part III. Reaction of D-glucose and D-fructose in slightly acidic, aqueous solution. Acta chem. scand. **B30**, 397–402.

ROMANS, J. C. C. 1970. Podzolization in zonal and altitudinal context in Scotland. Welsh Soils Disc. Grp. Rpt. No. 11, 88–101.

SCHNITZER, M., and DESJARDINS, J. G. 1962. Molecular and equivalent weights of the organic matter of a podzol. Proc. Soil Sci. Soc. Am. **26**, 362–5. and references therein.

—— and KHAN, S. V. 1972. *Humic substances in the environment* New York: Marcel Dekker, Inc.

—— and WRIGHT, J. R. 1957. Extractions of organic matter from podzolic soils by means of dilute inorganic acids. Canad. J. Soil Sci. **37**, 89–95.

STAHL, E. 1965. *Thin layer chromatography*. London: Academic Press Inc.

WRIGHT, J. R., and SCHNITZER, M. 1960. Oxygen-containing functional groups in the organic matter of the A_o and B_h horizons of a podzol. Proc. 7th int. Congr. Soil Sci., Madison, II 17, 120–127.

(Received 10 December 1976)

Plant and Soil **48**, 547–548 (1977) Ms. 3383

SHORT COMMUNICATION

Comment on 'Spectroscopie infra-rouge de quelques fractions d'acides humiques obtenues sur Sephadex'

Summary

It is suggested that, in IR spectra of fractions of soil organic matter eluted from Sephadex, absorption bands ascribed to aromatic ethers, epoxide rings and alcoholic or phenolic hydroxyl groups by Bailly[1] are more consistent with a conventional humic material in its carboxylate form and an associated soil clay mineral such as illite.

Bailly[1] has interpreted various absorption bands in the infrared spectra of humic acid fractions eluted from Sephadex as arising from aromatic ethers, epoxide rings and free alcoholic or phenolic hydroxyl groups and has related these fractions to para-humic substances synthesized microbially from simple phenolic acids. We suggest that Bailly's interpretations based on the frequencies of individual absorption bands are unrealistic, and that a wider, more balanced appraisal of the spectra should be made. A more reasonable interpretation of his spectra (*e.g.* Fig. 1a) is that they arise from a humic fraction in the carboxylate form (Fig. 1c) and an associated clay mineral such as illite (Fig. 1b). All of the spectral features in fraction B (Fig. 1a) can be accounted for by a mixture of these two components thereby invalidating all of Bailly's conclusions.

Clay minerals are common components in soil organic matter fractions, particularly from podzols, and their absorption patterns have appeared in spectra of humic fractions in the literature on several occasions. Bailly dismissed the possibility that 'Si-O-Si' was present in substantial amounts in his fractions on the basis of comparison with a spectrum of silica gel (Ref. 2 p401, No. 480 – incorrectly quoted by Bailly as No. 478). His conclusion that silica gel is absent from his fractions is probably correct but he failed to consider that layer silicates with maximum absorption for the Si-O stretching vibration in the range 970–1100 cm^{-1} might be present[3].

Bailly's observation that aromatic and aliphatic residues are present in his samples may be correct, but his conclusion that these residues rather than carboxylate are principally responsible for the broad absorption bands near 1600 and 1400 cm^{-1} is not. His conclusion was based on the incorrect assumption that because the organic fraction could be eluted from Sephadex ahead of simple Na salts, the organic fraction could not be in the form of the

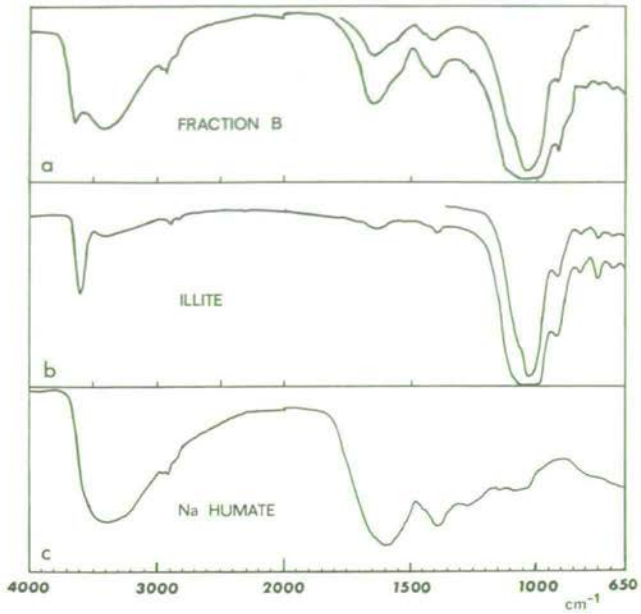

Fig. 1. Infrared spectra of KBr pressed disks of: –
(a) Fraction B (Ref. 1 Fig. 4),
(b) Ballater illite,
(c) Na humate from a podzol B horizon.

sodium carboxylate salt. If an organic acid is applied to Sephadex in the form of a sodium carboxylate salt it *must* be eluted by neutral distilled water in this form.

It should be pointed out that minor amounts of more esoteric organic functional groups could be present in Bailly's, or any other, fractions of soil organic matter, but the presence of intense overlapping absorption bands of humate and clay minerals as major components precludes the positive identification of such functional groups from infrared spectra.

J. D. Russell and H. A. Anderson
Macaulay Institute for Soil Research,
Craigiebuckler, Aberdeen, AB9 2QJ

Received 4 February 1977

References

1 Bailly, J. R., Plant and Soil **45**, 95–112 (1976).
2 Colthup, N. B., *et al.*, Introduction to infrared and Raman spectroscopy. Academic Press (1965).
3 Farmer, V. C., The infrared spectra of minerals. Mineralogical Society, London (1974).

Clay Minerals (1978) **13**, 133.

THE EFFECT OF Fe-FOR-Si SUBSTITUTION ON THE *b*-DIMENSION OF NONTRONITE

J. D. RUSSELL AND D. R. CLARK

The Macaulay Institute for Soil Research, Craigiebuckler, Aberdeen, Scotland

(*Received* 27 *September* 1977)

ABSTRACT: A survey of 060 spacings of dioctahedral smectites has shown that for nontronites with only iron on octahedral sites, a linear relationship exists between the *b*-axial dimension and the number of atoms of tetrahedrally coordinated Fe^{3+} per unit cell containing $O_{20}(OH)_4$. The slope, 0·0497 Å/Fe^{3+}, is steeper than that for the increase in *b* resulting from Fe^{3+} on octahedral sites, 0·0377 Å/Fe^{3+}, demonstrating the greater importance of tetrahedral substitution in influencing *b*. Factors that take account of the number of Fe^{3+} atoms on tetrahedral sites have been incorporated in existing formulae for calculating *b*-axis cell dimensions for smectites, but these are usually less successful in predicting *b* than a new formula involving only tetrahedral and octahedral iron contents.

It has been known for many years that cell dimensions are related to isomorphous substitution and cation radii. Several formulae have been devised for calculating *b* parameters of layer silicates from their unit cell compositions, among them those of Brindley & MacEwan (1953) and Radoslovich (1962), and frequent use is made of the value of the 060 (complex reflection) spacing in predicting octahedral composition. This spacing usually lies between about 1·48 and 1·56 Å; values less than about 1·51 Å are taken to indicate dioctahedral structures, and those greater than 1·51 Å trioctahedral. The distinction between the two types of structure on this basis is not sharp, as a nontronite has been reported to give a spacing of 1·522 Å (MacEwan, 1961). The iron contained in this specimen occurs in octahedral sites only, but Goodman *et al.* (1976) have shown that in addition to complete octahedral filling by Fe^{3+}, extensive Fe^{3+}-for-Si substitution can occur in nontronite. This suggested the possibility that the *b* dimension might be influenced by this type of substitution and prompted a survey of the 060 spacings of ferruginous dioctahedral smectites. The smectites included a group of dioctahedral montmorillonites of low iron content, the nontronites studied by Goodman *et al.*, and two additional nontronites from El Pao, Venezuela, and Pfaffenreuth, Bavaria. The latter two nontronites were purified as described by Goodman *et al.* (1976) to give $<1{\cdot}4$ μm fractions of the following compositions as indicated by electron microprobe analysis:

El Pao $(Si_{7\cdot33}Al_{0\cdot11}Fe^{3+}_{0\cdot56})\ (Fe^{3+}_{3\cdot90}Mg_{0\cdot11})O_{20}(OH)_4Na_{0\cdot66}$ (cf. Isphording, 1975)
Pfaffenreuth $(Si_{6\cdot83}Al_{0\cdot93}Fe^{3+}_{0\cdot24})\ (Fe^{3+}_{4\cdot00}Mg_{0\cdot05})O_{20}(OH)_4Na_{1\cdot03}$

The 060 spacings were measured on X-ray powder photographs obtained using filtered CoKα radiation and a 114·83 mm Debye-Sherrer powder camera. They are shown in Table 1 with iron contents as $\%Fe_2O_3$ and as Fe^{3+} on tetrahedral and octahedral sites,

TABLE 1. Iron contents and b dimensions of smectites

	Fe_2O_3 (%)	$Fe^{3+}/O_{20}(OH)_4$		d(060) (Å)	b (Å)			
		Tet.	Oct.		Obs.†	Calc. 1‡	Calc. 2	Calc. 3
1 Nontronite (California)	44	1·65	4·04	1·535	9·210	9·240	9·218	9·215
2 Nontronite (Crocidolite-deposit, Koegas)	43	1·19	3·90	1·534	9·204	9·202	9·193	9·187
3 Nontronite (Koegas)	42	1·31	4·06	1·533	9·198	9·206	9·199	9·199
4 Nontronite (Amosite-deposit, Penge)	42	1·12	4·04	1·532	9·192	9·195	9·192	9·189
5 Nontronite (Clausthal)	43	1·06	4·01	1·530	9·180	9·185	9·186	9·185
6 Nontronite (El Pao)	34	0·56	3·90	1·527	9·162	9·148	9·161	9·156
7 Nontronite (Pfaffenreuth)	33	0·24	4·00	1·524	9·144	9·149	9·165	9·144
8 Nontronite (Garfield)	33	0·11	3·96	1·523	9·138*	9·141	9·160	9·136
9 Nontronite (Washington)	27	0·0	2·73	1·512	9·072	9·087	9·100	9·084
10 Fullers' earth (Woburn)	6·6	0·07	0·72	1·504	9·024	9·035	9·019	9·012
11 Montmorillonite (Otay)	1·2	0·0	0·11	1·499	8·994	9·034	9·008	8·986
12 Montmorillonite (Chambers)	2·2	0·0	0·25	1·498	8·988	9·006	8·996	8·991
13 Montmorillonite (Wyoming)	3·5	0·0	0·37	1·498	8·988	8·989	8·986	8·996
14 Montmorillonite/beidellite (Unterrupsroth)	0·05	0·0	0·005	1·496	8·976	8·984	8·980	8·982
Correlation coefficient						0·984§	0·990§	0·996§

* Kerr *et al.* (1950) quote 9·175 Å using CoKα radiation and a 19 cm dia. camera for a Garfield nontronite with an essentially identical composition.

† b(Obs.) = $6 \times d$(060).

‡ Values in columns headed Calc. 1, 2, 3 are obtained from equations 1, 2 and 3 in the text.

§ $P < 0{\cdot}001$.

Mössbauer spectroscopy having shown that all iron is in the ferric form. Values of 1·523–1·535 Å for samples 1–8 with Fe_2O_3 contents of 33–44% occur in the range usually associated with trioctahedral filling, whereas those for the smectites of lower iron contents (samples 9–14) were more normal for dioctahedral minerals. MacEwan (1961) showed that the *b* dimension increased linearly with the number of Fe^{3+} atoms in octahedral coordination up to the maximum of four. In agreement with this relationship, a plot of *b* versus octahedral Fe^{3+} content is linear up to the maximum, with a slope of 0·0377 Å per Fe^{3+} (Fig. 1a) but rises more steeply with a slope of 0·0497 Å per Fe^{3+} for the higher-iron specimens (Fig. 1b) in which the additional iron goes into tetrahedral sites (samples 1–7, Table 1). None of the earlier investigators had access to nontronite with this type of substitution, which consequently was seldom considered, but the excellent linear relationship between the *b* dimension and the number of Fe^{3+} atoms on tetrahedral sites clearly demonstrates the effect of substitution of Si by Fe^{3+}. Such an effect of tetrahedral Fe^{3+} is to be expected in view of the substantial terms for tetrahedral Al in the *b*-axis formulae of Brindley & MacEwan (1953) and Radoslovich (1962) for smectites, but contrasts sharply with the assumption by the latter author that neither Al nor Fe^{3+} in tetrahedral sites in antigorite or in cronstedtite contributes to their *b* dimensions.

To obtain a measure of the effect of tetrahedral Fe^{3+} on the *b* dimension of smectites, the data for samples 1–6 (Table 1) and the two above-mentioned *b*-axis formulae were

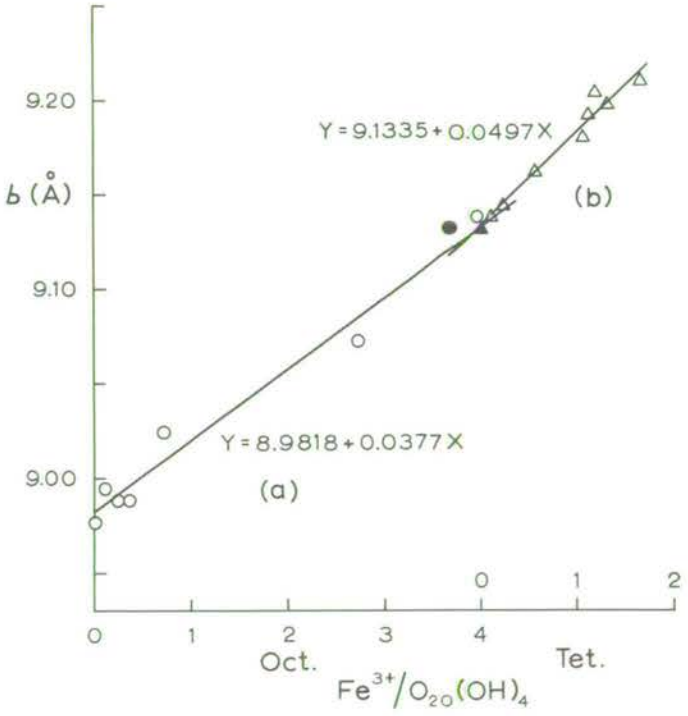

FIG. 1. Relationship between observed *b* dimension ($= 6 \times d(060)$) and the number of Fe^{3+} ions per unit cell on octahedral (circles) and tetrahedral (triangles) sites for a series of dioctahedral smectites. Probabilities for regression equations are $P < 0{\cdot}001$. Solid symbols refer to the nontronite composition reported by MacEwan (1961).

used to calculate factors for tetrahedral Fe^{3+} of 0·14 in the Brindley & MacEwan (1953) formula which now becomes

$$b(\text{Å}) = 8{\cdot}92 + 0{\cdot}06x + 0{\cdot}14y + 0{\cdot}09q + 0{\cdot}18r + 0{\cdot}27s \quad (1)$$

and 0·082 in the Radoslovich (1962) formula which now becomes

$$b(\text{Å}) = 8{\cdot}944 + 0{\cdot}037x + 0{\cdot}082y + 0{\cdot}096q + 0{\cdot}096r \quad (2)$$

For both formulae, x and y are the numbers of Al^{3+} and Fe^{3+} ions in tetrahedral coordination, and q, r and s are the numbers of Fe^{3+}, Mg^{2+} and Fe^{2+} ions in octahedral coordination in the half unit cell.

The linearity of the plots in Fig. 1 suggests that the b dimension might be determinable from the unit cell contents of Fe^{3+} only. Using the regression equations, the relationship

$$b(\text{Å}) = 8{\cdot}982 + 0{\cdot}099y + 0{\cdot}075q \quad (3)$$

is obtained, y and q having the same significance as in the formulae above. The correlation coefficient between calculated values of b from formula (3) and the observed values was 0·996 compared with 0·984 and 0·990 for those obtained from (1) and (2) respectively (Table 1), indicating that formula (3) is generally better at predicting b, and that tetrahedral and octahedral Fe^{3+} exert a major effect on the b dimension.

ACKNOWLEDGMENTS

We wish to thank Dr R. Glaeser and Professor W. C. Isphording for the specimens of nontronite from Pfaffenreuth and El Pao respectively, Dr W. J. McHardy for the electron microprobe analyses, and Mr R. H. E. Inkson for statistical calculations.

REFERENCES

Brindley G.W. & MacEwan D.M.C. (1953) *Ceramics—A Symposium*, p. 15. The British Ceramic Society, Stoke-on-Trent.

Goodman B.A., Russell J.D., Fraser A.R. & Woodhams F.W.D. (1976) *Clays Clay Miner.* **24**, 53.

Isphording W.C. (1975) *Am. Miner.* **60**, 840.

Kerr P.F., Hamilton P.K. & Pill R.J. (1950) Am. Petrol. Inst., Project 49, rept. 7.

MacEwan D.M.C. (1961) In: *The X-ray Identification and Crystal Structures of Clay Minerals*. Mineralogical Society, London.

Radoslovich E.W. (1962) *Am. Miner.* **47**, 617.

RÉSUMÉ: Un examen des distances 060 de smectites dioctaédriques a montré que pour les nontronites n'ayant que du fer sur les sites octaédriques, il existe une relation entre la dimension d'axe b et le nombre d'atomes de Fe^{3+} coordonnés tétraédriquement par maille du réseau contenant O_{20} $(OH)_4$. La pente, 0·0497 Å/Fe^{3+}, est plus fote que celle correspondant à l'accroissement de b résultant de Fe^{3+} sur les sites octaédriques, 0·0377 Å/Fe^{3+}, montrant l'importance plus grande de la substitution tétraédrique dans l'action sur b. On a introduit des facteurs tenant compte du nombre d'atomes Fe^{3+} sur les sites tétraédriques dans les formules de calcul des dimensions de maille sur l'axe b pour les smectites, mais celles-ci donnent généralement b d'une manière moins satisfaisante qu'une formule nouvelle utilisant seulement les quantités de fer tétraédrique et octaédrique.

KURZREFERAT: Wie ein Überblick über 060 Interferenzen von dioktaedrischem Smektit gezeigt hat, gibt es für Nontronite mit Eisen in oktaedrischen Lagen eine lineare Beziehung zwischen dem b-Achsenwert und der Zahl der Atome von tetraedrisch koordiniertem Fe^{3+} einer Zelleinheit mit $O_{20}(OH)_4$. Der Anstieg 0·0497 Å/Fe^{3+} ist grösser als

der für die Zunahme von *b*, wie er sich aus den Fe^{3+} in oktaedrischen Lagen ergibt, nämlich 0·0377 Å/Fe^{3+}, wodurch die grössere Bedeutung der tetraedrischen Besetzung für den Einfluss auf *b* gezeigt wird. Die Faktoren, welche die Zahl der Fe^{3+}-Atome auf die tetraedrischen Lagen berücksichtigen, sind in die vorhandenen Formeln für die Berechnung der *b*-Achsen Abstände für Smektite einbezogen worden, aber diese sind gewöhnlich weniger brauchbar *b* vorherzubestimmen als eine neue Formel, welche nur tetraedrische und oktaedrische Eisengehalte berücksichtigt.

RESUMEN: Un estudio de espaciamientos 060 de esmectitas dioctaédricas ha demostrado que en el caso de las nontronitas que sólo tienen hierro en sitios octaédricos existe una relación lineal entre la dimensión axial *b* y el número de átomos de Fe^{3+} coordenados tetraédricamente por cada malla que contiene O_{20} $(OH)_4$. La pendiente, 0·0497 Å/Fe^{3+}, es más pronunciada que la del aumento en *b* resultante del Fe^{3+} en sitios octaédricos, 0·0377 Å/Fe^{3+}, lo que demuestra la mayor importancia de la sustitución tetraédrica para influir en *b*. Los factores que tienen en cuenta el número de átomos Fe^{3+} en los sitios tetraédricos se han incorporado en fórmulas existentes para calcular las dimensiones de las mallas en el eje *b* para las esmectitas, pero generalmente tienen menos éxito en la predicción de *b* que una fórmula nueva en la que sólo entran en juego los contenidos de hierro tetraédrico y octaédrico.

Spectrochimica Acta, Vol. 34A, pp. 1151 to 1153. Pergamon Press Ltd., 1978. Printed in Great Britain

Lattice vibrations of boehmite (γ-AlOOH): evidence for a C_{2v}^{12} rather than a D_{2h}^{17} space group

J. D. RUSSELL and V. C. FARMER
Macaulay Institute for Soil Research, Craigiebuckler, Aberdeen, Scotland

and

D. G. LEWIS
Waite Agricultural Research Institute, Glen Osmond, 5064 South Australia

(*Received* 4 *November* 1977)

Abstract—The lattice vibrations of boehmite can be separated into O^{2-} translations, lying between 500 and 765 cm^{-1} and OH^- translations, lying between 300 and 410 cm^{-1}. Comparison of the i.r. spectra of random and oriented preparations of platy crystals allows the recognition of transition moments perpendicular to the plates. Bands additional to those required by the statistical symmetry indicated by diffraction (D_{2h}^{17}, *Cmcm*) establish that the true space group must be C_{2v}^{12} ($Cmc2_1$), each domain of which probably extends over an entire hydrogen bonded double hydroxyl sheet.

Progress in the identification of i.r. absorption bands arising from surface vibrations of hydrous oxides of aluminium and iron [1, 2] has made it desirable to assign also those arising from bulk vibrations. Single crystals suitable for i.r. study are generally not available, but a hydrothermally synthesized boehmite with a platy morphology has allowed the preparation of oriented deposits, which have assisted band assignments.

The space group of boehmite as determined by X-ray and neutron diffraction (D_{2h}^{17}, *Amam* or *Cmcm*) requires a centre of symmetry between pairs of hydrogen bonded hydroxyl groups (Fig. 1), but it is certain that this is only a statistical symmetry, since the hydrogen bond distances (2.70 Å) are too long for true symmetrical hydrogen bonds (normally less than 2.50 Å), and the OH stretching absorption does not show the characteristic features of symmetrical bonds [3]. Displacement of the proton from the centre of symmetry leads to the loss of xy symmetry planes, and so transforms space group *Cmcm* (D_{2h}^{17}) into $Cmc2_1$ (C_{2v}^{12}). FRIPIAT *et al.* [4] have assigned the proton vibrations of boehmite in terms of C_{2v} symmetry, but the same results are predicted for D_{2h} symmetry. A distinction between the two space groups should, however, be possible on the basis of lattice vibrations.

In the idealised D_{2h}^{17} (*Cmcm*) structure (Fig. 1) there are two AlO(OH) units in the primitive unit cell, and each Al^{3+}, O^{2-}, and $O(H)^-$ lies on C_{2v} sites with the two-fold axis parallel to y. The predicted lattice vibrations (Table 1) are $3A_g + 3B_{1g} + 3B_{3g} + 2B_{1u} + 2B_{2u} + 2B_{3u}$, of which the three last species are i.r. active with transition moments along the z, y, x directions respectively. For each i.r. active species, the higher frequency of the two should involve principally motion

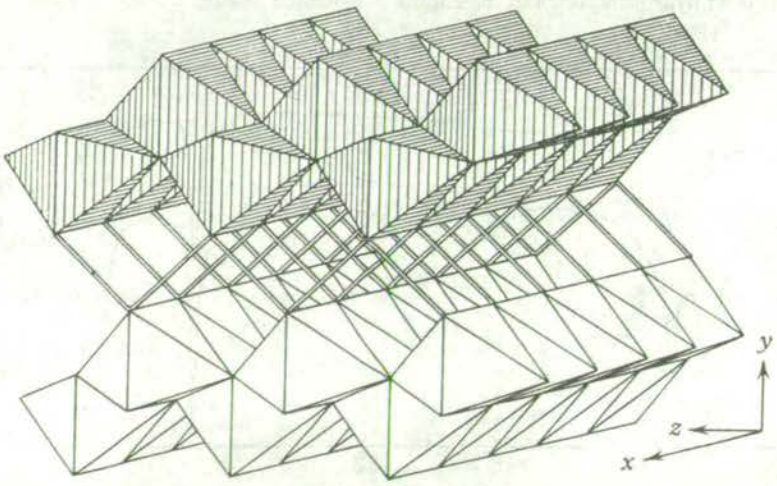

Fig. 1. Structure of boehmite, after EWING [5], with axes labelled according to the *Cmcm* configuration for consistency with the $Cmc2_1$ space group. Double lines indicate the zig-zag chains of hydrogen bonds that link the layers of edge-sharing octahedra to each other.

Table 1. Number and symmetry species of the vibrations of boehmite, for D_{2h}^{17} and C_{2v}^{12} space group symmetry, abstracted from the general D_{2h} table of FARMER [6].

Symmetry Species		Lattice Vibrations				Proton
Cmcm	*Cmc*2_1	Motion on C_{2v}^{y} sites				Vibrations
D_{2h}^{17}	C_{2v}^{12}	O^{2-}	OH^-	Al^{3+}	Total	C_{2h}^{x} sites
A_g	A_1	y	y	y	3	0
B_{1g}	A_2	x	x	x	3	0
B_{2g}	B_1	0	0	0	0	0
B_{3g}	B_2	z	z	z	3	0
A_u	A_2	0	0	0	0	γOH
B_{1u}	A_1	z	z	z	$2+T_z$	νOH+δOH
B_{2u}	B_2	y	y	y	$2+T_y$	νOH+δOH
B_{3u}	B_1	x	x	x	$2+T_x$	γOH

of the O^{2-} ion, and the lower motion of the OH^- ion, since the O^{2-} ions are more firmly bonded to four surrounding Al^{3+} ions, whereas the OH^- ions are bonded to only two. Inspection of the spectrum of randomly oriented crystals (Fig. 2(a) shows that there are indeed three strong bands assignable to O^{2-} translations at 765, 622 and 498 cm^{-1}, but there are four medium bands assignable to OH^- translations at 411, 398, 368 and 323 cm^{-1}, all of which are displaced in the spectrum of deuterated boehmite [4]. In the spectrum of oriented crystals (Fig. 2(b), obtained with the radiation incident along the y direction, the 765 cm^{-1} and 411 cm^{-1} absorption bands are weakened and so assignable to B_{2u} species.

Of the three in-plane OH^- translations, one, presumably the weakest at 398 cm^{-1}, must be ascribed to an antiphase A_g vibration which becomes active along z in C_{2v} symmetry (A_1 species). Its considerable intensity can be ascribed to the fact that this vibration shortens or lengthens all hydrogen bonds in the chains of hydrogen bonded hydroxyl groups that run parallel to the z-axis (Fig. 1), and so induces a displacement of the protons and of the electron clouds on the oxygens, giving rise to a considerable dipole oscillation. The sharpness of this activated vibration shows that the domains of ordered C_{2v}^{12} structure must extend over many unit cells. Considering the strong coupling within the double sheets of hydrogen bonded hydroxyl groups —by direct contacts and shared Al^{3+} cations along x, and by hydrogen bonds along z—it seems highly probable that such a double sheet has a consistent OH orientation, whereas the weak coupling between different double sheets would permit randomisation of OH orientations in the structure as a whole. Other weaker bands which can be assigned to activated antiphase vibrations lie at 572 and 278 cm^{-1}.

The effect of crystal orientation on the intensity of the absorption bands arising from proton vibrations confirms the assignments given by FRIPIAT *et al.* [4], as indicated in Fig. 2.

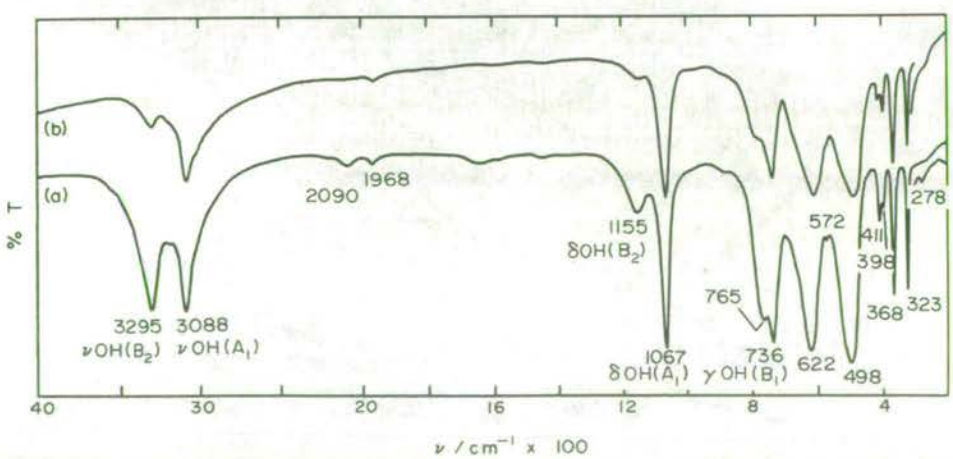

Fig. 2. Infrared spectra of boehmite: (a) randomly oriented crystals in a KBr disk, and (b) oriented film with the i.r. beam perpendicular to the platy (010) faces. Spectra recorded on a Perkin–Elmer 577 spectrometer.

REFERENCES

[1] J. D. Russell, R. L. Parfitt, A. R. Fraser and V. C. Farmer, *Nature* **248**, 220 (1974).
[2] R. L. Parfitt, J. D. Russell and V. C. Farmer, *J. Chem. Soc., Faraday Trans. I* **72**, 1082 (1976).
[3] Ya. I. Ryskin, in *The Infrared Spectra of Minerals* (V. C. Farmer, ed.), p. 137. Mineralogical Society, London (1974).
[4] J. J. Fripiat, H. Bosmans and P. G. Rouxhet, *J. Phys. Chem.* **71**, 1097 (1967).
[5] F. J. Ewing, *J. Chem. Phys.* **3**, 420 (1935).
[6] V. C. Farmer, in *The Infrared Spectra of Minerals* (V. C. Farmer, ed.), p. 515. Mineralogical Society, London (1974).

Clays and Clay Minerals, Vol. 27, No. 1, pp. 63–71, 1979.

INFRARED AND MÖSSBAUER STUDIES OF REDUCED NONTRONITES

J. D. RUSSELL, B. A. GOODMAN, AND A. R. FRASER

The Macaulay Institute for Soil Research, Craigiebuckler, Aberdeen, AB9 2QJ, U.K.

(Received 13 February 1978)

Abstract—Infrared and Mössbauer spectroscopy show that the extent of the reduction of nontronite is dependent on the chemical composition of the nontronite and on the nature of the reducing agent. Hydrazine reversibly reduces about 10% of the iron in all of the nontronites studied irrespective of composition and it is suggested that the resulting ferrous iron occurs only in distorted octahedral sites. Similar conclusions are reached for the dithionite reduction of the nontronites containing little tetrahedral iron, but for those with more than one in eight silicons replaced by iron, changes brought about by dithionite treatment are irreversible due to dissolution of appreciable quantities of iron. Results from both spectroscopic techniques suggest that iron in tetrahedral sites is preferentially dissolved and that up to 80% of the structural iron can be reduced.

Evidence is presented for the formation in these extensively reduced nontronites of a small amount of a mica-like phase resembling celadonite or glauconite, and, as dithionite is used for the pretreatment of soils, the implication of this observation is briefly discussed.

The use of deuterated hydrazine as a reducing agent has enabled the nontronite absorption band near 850 cm^{-1} to be assigned to a Si–O (apical) stretching vibration, which is inactive in the infrared for perfect hexagonal symmetry, but which is activated by distortions in the tetrahedral layer.

Key Words—Dithionite, Hydrazine, Iron, Nontronite, Smectite.

INTRODUCTION

The structural changes brought about in iron-containing smectites by chemical reducing agents such as hydrazine, sodium dithionite, and sodium sulphide have been investigated recently by several workers using infrared and Mössbauer spectroscopy. Rozenson and Heller-Kallai (1976a, b) concluded that the products of reduction depended on the mineral and on the reducing agent. They claimed that the reduction was completely reversible for $Fe^{3+}OHAl$ groupings but not $Fe^{3+}OHFe^{3+}$, reduction of both iron ions in the latter leading to irreversible dehydroxylation. In contrast, Roth and Tullock (1972) found no difference in reducing action between hydrazine and dithionite, and reported substantial reversibility in the reduction of $Fe^{3+}OHFe^{3+}$ groupings. Using electron spectroscopy for chemical analysis (ESCA), Stucki et al. (1976) observed a difference between hydrazine and dithionite in the extent of reduction of nontronite.

These studies were limited in that they considered only a nontronite from Garfield, Washington, and a biotite from Bancroft, Ontario, and were thus unable to illustrate the full effect of composition on the reduction. In order to widen the scope of such studies and perhaps rationalize the earlier findings, the effect of hydrazine and dithionite on the seven nontronites characterized by Goodman et al. (1976) was studied, using infrared and Mössbauer spectroscopy to assess the structural changes taking place.

EXPERIMENTAL

Materials

The nontronites used in this investigation were those studied by Goodman et al. (1976) from Grant County, Washington (Source Clay Minerals Repository, SWa-1) (WAS); Garfield, Washington (A.P.I. H33a) (GAR); Clausthal, Zellerfeld, Germany (CLA); a crocidolite deposit in Koegas, Cape Province, South Africa (KOE); an amosite deposit in Penge, Cape Province, South Africa); and Panamint Valley, California (CAL). The samples were purified by saturation with Na using NaCl solution, dispersion in water, separation of the <1.4-μm fraction, and then resaturation with Na.

For infrared studies, aqueous suspensions of this fraction containing 6–7 mg/ml were prepared and dried on either Irtran 2 windows or abraded polyethylene sheet to give deposits of reasonably uniform thickness (0.8–1.0 mg/cm^2). Films were exposed to the saturated vapor pressure of hydrazine hydrate at 20°C for 16 hr. In a modification of this technique, the fully deuterated analogue of hydrazine (hydrazinium hydroxide-d_6, N_2D_5OD) was used to assess the extent of OH/OD exchange accompanying reduction. Subsequent oxidation in air over D_2O prevented the OD groups from reexchanging on exposure to water vapor. Dithionite reduction of the nontronites consisted of immersing the deposits (6–7 mg) for various times (1–25 min) in 20 ml of freshly prepared 1% w/v aqueous sodium dithionite solution, pH 6, at 20°C, followed by a brief wash with unpurged distilled water, then drying at 30°C in a stream of O_2-free nitrogen to avoid reoxidation of the sample (Roth and Tullock, 1972). Once dry, the reduced nontronite was relatively stable in air at room temperature.

For Mössbauer studies the samples were in the form of randomly oriented freeze-dried powders. Hydrazine treatment consisted of adding a few drops of hydrazine hydrate to the mineral in a perspex container which was then sealed. The sample was studied without any fur-

Table 1. Si–O stretching frequencies and soluble Fe produced by dithionite and hydrazine treatments of various nontronites.

	Si–O(cm^{-1})				% total Fe^{3+}	
	Untr.[1]	N_2H_4	$Na_2S_2O_4$	Re-ox.[2]	Tet.[1]	$Na_2S_2O_4$-soluble[3]
1 WAS	1021	1004	1014	1022	6	16
2 GAR	1020	1006	1017	1020	9	7
3 CLA	1009	998	997	1017	15	37
4 CRO	1006	996	1005	1018	19	26
5 KOE	1006	996	1001	1018	27	17
6 AMO	1003	983	997	1016	28	26
7 CAL	1001	987	987	1000	32	16

[1] Goodman et al. (1976) Table 3.
[2] Reoxidized in moist air following dithionite treatment.
[3] 2 × 20 min treatments.

ther treatment. Reduction by dithionite was performed in a glove-box in an atmosphere of O_2-free nitrogen. Excess (2–3 ml) 1% w/v dithionite solution was added to 12–15 mg nontronite and allowed to stand for 10 min, then filtered, washed once with degassed water and partially dried under vacuum. The damp sample was then sealed in a perspex container for study by Mössbauer spectroscopy.

Instrumental techniques

Most of the infrared spectra of nontronite films were recorded on a Grubb Parsons Spectromaster. A Perkin Elmer 577 spectrometer, however, was used in the deuterohydrazine experiment. Dehydration of the samples and exchange with D_2O vapor was accomplished in a vacuum cell similar to that described by Angell and Schaffer (1965). The H-D exchange procedure involved repeated flushing of the sample with D_2O vapor and evacuation at $\sim 10^{-2}$ mm Hg. The temperature of the sample in the infrared beam was about 25–30°C.

Mössbauer spectra were recorded in 512 channels of a spectrometer (Harwell Scientific Services, Didcot, Berks., U.K.) incorporating an Ortec Model 6200 analyzer. A Co^{57} in Pd source of nominal strength 25 mCi was used with an argon-methane proportional counter as γ-ray detector. Velocity calibration was carried out with high purity metallic iron foil using the data of Preston et al. (1962). To minimize thickness effects all absorbers contained ~ 3 mg iron/cm^2, prepared as described above. Spectra were fitted to a sum of doublets having Lorentzian peak shapes using a least squares computer programme. The peaks of each doublet were constrained to have equal areas and widths. A parabolic baseline was assumed and χ^2 was used as a goodness-of-fit parameter. For statistically acceptable fits χ^2 is required to lie between the 1% and 99% limits of the χ^2 distribution, i.e., between about 416 and 561 for 486 degrees of freedom, where the number of degrees of freedom is equal to the number of channels fitted minus the number of variables in the fit.

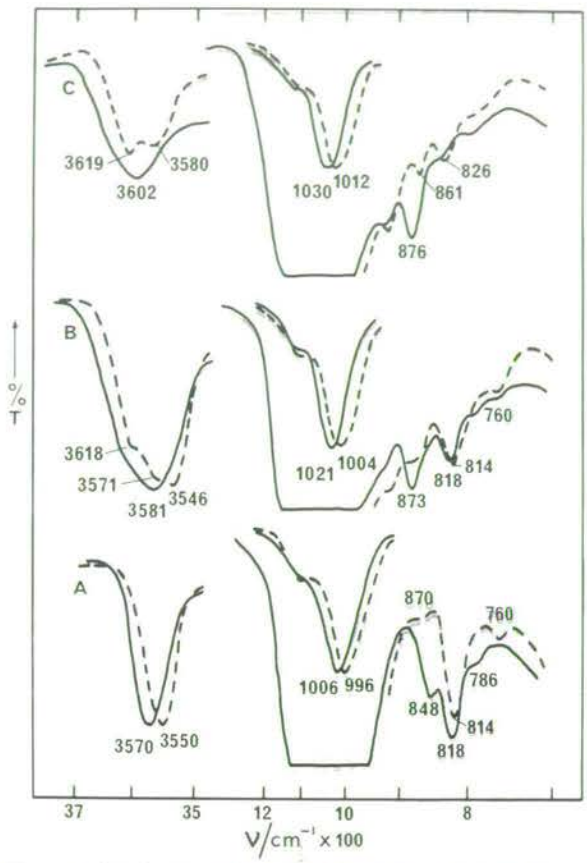

Fig. 1. Infrared spectra of smectite films on Irtran 2: A, CRO nontronite; B, WAS nontronite; C, Woburn Fuller's Earth. Full lines, untreated; broken lines, reduced by exposure to hydrazine vapor. ν, wave number; T, transmission.

RESULTS AND DISCUSSION

Striking color changes were produced in the nontronites following their treatment with sodium dithionite, the original pale yellow turning to emerald green in 1–2 min, then intensifying to blue-green in 5–10 min for the most ferruginous specimens. Hydrazine treatment produced only the emerald green color in all of the nontronites. Judging from color only, reduction by dithionite of nontronites CLA, CRO, KOE, AMO, and CAL was more rapid and more extensive than that of nontronites WAS and GAR. More detailed results relating to the reduction process were obtained from chemical analysis and infrared and Mössbauer spectroscopy.

Infrared

Hydrazine reduction. Spectral changes shown by CRO nontronite after hydrazine treatment (Figure 1A) are typical of those shown by the nontronites studied excluding the more aluminous WAS specimen. Bands previously assigned to librations of $AlFe^{3+}OH$ at about 850 cm^{-1} and $Fe^{3+}MgOH$ near 790 cm^{-1} (Goodman et

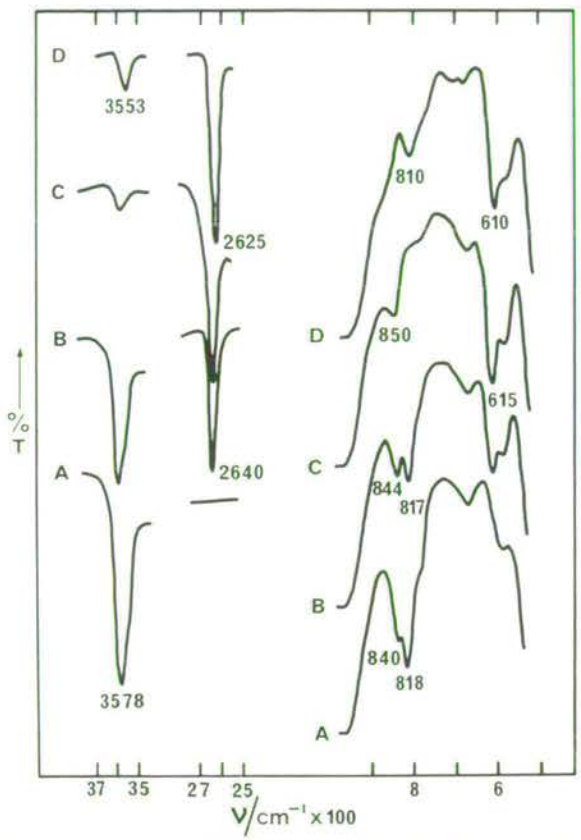

Fig. 2. Infrared spectra of self-supporting film of KOE nontronite: A, untreated; B, partially H/D exchanged by reduction with deuterohydrazine ($N_2D_4 \cdot D_2O$) vapor, then reoxidized in air/D_2O vapor; C, D, more completely exchanged by prolonged $N_2D_4 \cdot D_2O$ treatment, in reduced form (D) and reoxidized form (C). ν and T as Figure 1.

al., 1976) are lost, the former possibly shifting under the main $Fe^{3+}Fe^{3+}OH$ band at 818 cm^{-1} thus accounting for its intensification and shift to 814 cm^{-1}. New weak bands appear near 870 and 760 cm^{-1}. Frequencies of bands in the spectra of hydrazine-reduced nontronites vary only slightly within the ranges 880–864 cm^{-1}, 814–812 cm^{-1}, 760–756 cm^{-1} and intensity changes are generally comparable for all of the nontronites. Similar spectral changes were observed for the WAS sample (Figure 1B) but the absorbance of the 818 cm^{-1} band increased by almost 30% after hydrazine treatment compared with only about 5% for the others. This presumably is due to the intense band at 873 cm^{-1} shifting to about 814 cm^{-1} on reduction of the relatively abundant $AlFe^{3+}OH$ groupings to $AlFe^{2+}OH$. A similar result was obtained with Woburn Fuller's Earth (Figure 1C) whose composition (Heller et al., 1962) indicates that $AlFe^{3+}OH$ is the most abundant grouping. The OH stretching vibration shifted from 3581 cm^{-1} in WAS to 3546 cm^{-1}, and in the other nontronites from 3570 to 3550 cm^{-1}. These shifts agree with those reported by Roth and Tullock (1972) for a Garfield specimen, but in contrast, Rozenson and Heller-Kallai (1976a) reported that the OH stretching frequency of the WAS sample was not affected by hydrazine treatment. Absorption remaining at about 3620 cm^{-1} in WAS and the Fuller's Earth after hydrazine treatment (Figures 1B, C) is due to AlAlOH in these more aluminous samples.

These hydrazine-induced shifts in OH vibrations are consistent with reduction of some of the octahedral Fe^{3+} to Fe^{2+}, but the extent of the shift of the OH stretching band and the movement of the main Si–O stretching band to lower frequencies (Table 1) is surprising in the light of the estimated reduction of only about 10% of the Fe^{3+} from Mössbauer spectra (see later).

As observed by earlier workers, the hydrazine-reduced nontronites were completely reoxidized on exposure to moist air, their infrared spectra then being identical to those of the untreated nontronites.

Deuterohydrazine reduction. The reversibility of the hydrazine reduction enabled almost 95% replacement of OH groups by OD to be achieved by repeatedly exposing nontronite to deuterohydrazine vapor then to air saturated with D_2O vapor. This is in agreement with the observation of Roth and Tullock (1972) that reduction of nontronite in D_2O solution resulted in D for H exchange in structural OH groups. Spectra clearly show that the band at 840 cm^{-1} in the OH form (Figure 2A) is scarcely affected by D_2O exchange, shifting to 850 cm^{-1} in the OD form (Figure 2C). The slight low-frequency shift reported by Stucki and Roth (1976) could have resulted from a change in hydration of their sample, because we have observed that the band frequency drops by about 10 cm^{-1} when the specimen is partially dehydrated in the infrared beam. To try to eliminate problems arising from changes in hydration water, these authors attempted to dehydrate their nontronite by evacuation in a vacuum cell before recording spectra. But the high background absorption they show below 3500 cm^{-1} in Figure 1 for their oxidized nontronite indicates that the specimen is still substantially hydrated. The present results were obtained with the spectrometer purged with dry air. Spectra of the oxidized and reduced forms of OD nontronite (Figure 2C, D) show all of the spectral features reported by Stucki and Roth including the shift from 818 cm^{-1} for the $Fe^{3+}Fe^{3+}OH$ grouping to 615 cm^{-1} for $Fe^{3+}Fe^{3+}OD$, but in addition indicate that the 850 cm^{-1} band probably shifts to 810 cm^{-1} in the reduced form and not to 870 cm^{-1} as these authors suggested. They were unable to observe the new band near 810 cm^{-1} directly because of the overlapping $Fe^{3+}Fe^{3+}OH$ libration at about 820 cm^{-1}, but its presence must be part of the reason for the low-frequency shift and intensification of the $Fe^{3+}Fe^{3+}OH$ libration after hydrazine reduction (Figure 1).

It has been suggested by Goodman (1978) that the

presence of Fe^{3+} or Al^{3+} in the tetrahedral layer results in distortions which affect the electric field gradient at an octahedral cation bound to an O atom which is attached to the trivalent substituent. This concept of distortion of the tetrahedral oxygen atoms by Al and Fe^{3+} leads to a new and more acceptable assignment for the band near 850 cm^{-1} in nontronite spectra. It has been assigned by earlier workers to an $AlFe^{3+}OH$ librational frequency but the very low Al content of many nontronites (0.1–0.5% Al) and the observation that the band is little affected by D_2O exchange (Figure 2A, C) suggests that this may not be the most likely assignment for the band. More recently, Stucki and Roth (1976) assigned the band to an Fe–(OH) vibration but this seems unlikely for two reasons: first, the frequency is too high, Fe–O vibrations for both tetrahedrally and octahedrally coordinated Fe occurring below 700 cm^{-1} (Tarte, 1963); second, the reduction of only 10% of the Fe in nontronite by hydrazine does not agree with the complete disappearance of the band. It is suggested that the origin of this band is a b_1^2 Si–O(apical) stretching mode (Farmer, 1974), the vibration being inactive in the infrared for perfect hexagonal symmetry due to the stretching of one Si–O(apical) bond being exactly cancelled by compression of an adjacent Si–O(apical) bond. Any displacement of apical oxygens, such as that occurring when only two of the three octahedral sites are occupied or when Si is replaced tetrahedrally, is likely to make the vibration infrared-active due to imperfect cancellation of those two motions, giving a net change in dipole moment with a component in the Si–O *ab* plane. The band occurring near 850 cm^{-1} in nontronite spectra is, therefore, assigned to this vibration, its frequency being in reasonable agreement with the value of 779 cm^{-1} predicted for the ideal hexagonal array of oxygens (Farmer, 1974). In keeping with this assignment, the magnitude of the shift of the band to lower frequency on reduction (Figure 2D) is similar to those of other Si–O vibrations.

Dithionite reduction. Treatment of the nontronites with dithionite differentiated the WAS and GAR samples from the others. These two nontronites contain little or no tetrahedral Fe^{3+} (Goodman et al., 1976) and their spectra, illustrated by that of the GAR sample, showed changes (Figure 3A) that were similar to those observed for hydrazine reduction (Figure 1A) with only minor differences. The band at 756–760 cm^{-1} in spectra of the hydrazine-treated nontronites does not develop so strongly with dithionite treatment and the weak shoulder at 864–880 cm^{-1} is replaced by a well-resolved band at 864 cm^{-1}. The reason for the prominence of the latter feature is probably that the dithionite treatment of the nontronite results in a smaller low-frequency shift of the main Si–O stretching band than was observed for hydrazine treatment (Table 1).

The other nontronites have up to one Si in five replaced by Fe^{3+} and their spectra, illustrated by that of the CLA sample (Figure 3B), showed large decreases in intensity of the $Fe^{3+}Fe^{3+}OH$ libration at 818 cm^{-1}; the OH stretching bands showed similar displacements to those produced by hydrazine, but became broader and much weaker. These dithionite-treated nontronites did not revert completely to their original states on exposure to high-humidity air; their spectra, although qualitatively similar to those of the untreated nontronites, showed weaker OH bands. CRO nontronite treated with dithionite for 20 min recovered 70% of the intensity of its OH libration band but after two such treatments it showed little recovery of this band. The shifts of OH bands back to the original frequencies on exposure of the reduced nontronites to air are consistent with reoxidation of structural Fe^{2+}. The principal Si–O stretching band, however, did not show a consistent behavior; on reoxidation of WAS and GAR, it shifted back to its original frequency but for all of the other nontronites, i.e., those which underwent more drastic attack by dithionite, it shifted to frequencies higher than those of the untreated specimens (Table 1). The inverse relationship between the Si–O stretching frequency of nontronites and their tetrahedral iron contents described by Goodman et al. (1976) suggests that a shift to higher frequencies on reoxidation would be consistent with a loss of iron from the tetrahedral layer as a result of the dithionite treatment. In support of this, dithionite treatment dissolved less iron on average from the nontronites with low tetrahedral iron contents than from those with high (Table 1). Although the relationship is not perfect, it suggests that dithionite may be dissolving tetrahedral Fe^{3+} preferentially. The CAL nontronite was exceptional in that the Si–O band did

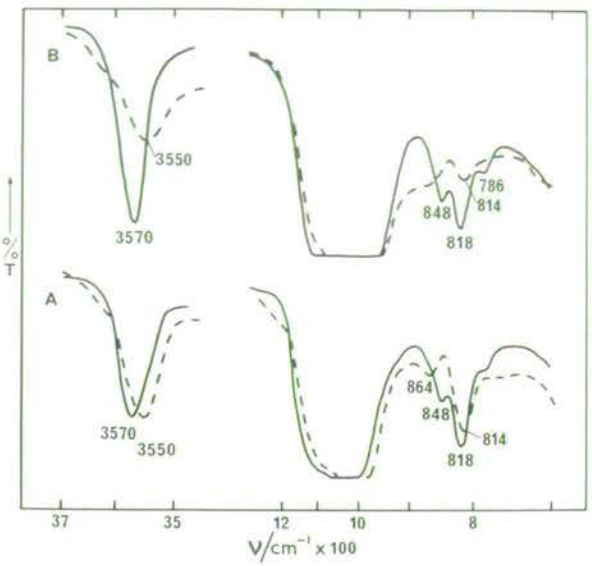

Fig. 3. Infrared spectra of nontronite films on Irtran 2: A, GAR; B, CLA. Full lines, untreated; broken lines, reduced by one 20-min treatment with dithionite solution. ν and T as Figure 1.

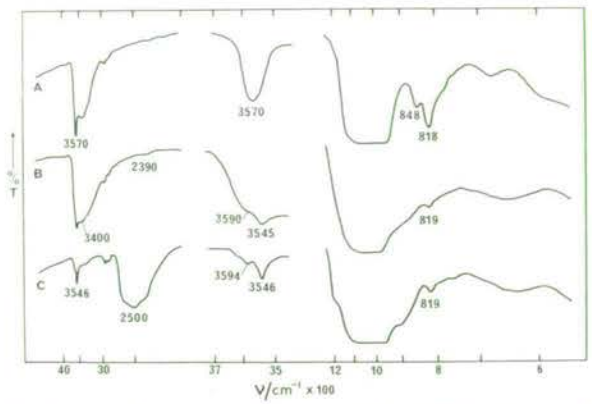

Fig. 4. Infrared spectra of self-supporting film of CRO nontronite: A, untreated; B, reduced by two 20-min treatments with dithionite solution; C, reduced film flushed with D_2O vapor. The center section is an expansion of the 3700–3500 cm^{-1} region. ν and T as Figure 1.

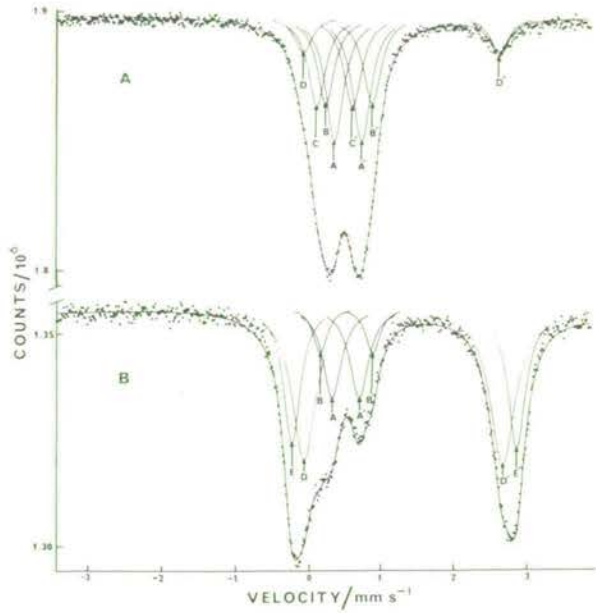

Fig. 5. Mössbauer spectra at 77 K of CLA nontronite reduced with (A) hydrazine and (B) dithionite.

not show the expected shift; and whereas the amounts of iron brought into solution in successive treatments of the other nontronites decreased sharply after the second treatment, for CAL they increased steadily, an additional 11% of the total iron appearing in the third extract. This suggests that the dithionite probably is causing general decomposition of the structure of the CAL nontronite. Dissolution of Fe^{3+} from the tetrahedral layer will create vacancies, negative charges on oxygen ions surrounding them being balanced by H^+ ions. The resultant OH groups would be expected to be strongly hydrogen bonded to each other with an O–O separation of about 2.6 Å and an OH stretching vibration near 2475 cm^{-1} (Nakamoto et al., 1955). This may be the origin of a weak broad band at 2390 cm^{-1} in the spectrum of dithionite-treated CRO nontronite (Figure 4B).

The low-frequency shifts shown by the Si–O bands of nontronites 3–7 (Table 1) on dithionite treatment are generally similar to those shown by specimens 1 and 2, and smaller than would have been expected for the greater reduction suggested by their spectra. This is probably due to the low-frequency shift caused by reduction of Fe^{3+} to Fe^{2+} being partially cancelled by the high-frequency shift resulting from dissolution of tetrahedral Fe^{3+} already discussed, the latter effect only becoming apparent on reoxidation. The small low-frequency shifts of 3 and 7 cm^{-1} shown by dithionite-reduced WAS and GAR nontronites respectively which contain little or no tetrahedral iron, suggests that the major part of the 10–20 cm^{-1} low frequency shift produced by hydrazine may be due to the effect of hydrazine as a base (Russell, 1978).

On longer treatment of the high-iron nontronites with dithionite the OH stretching and libration bands became much weaker, and broad diffuse absorption near 3400 cm^{-1} intensified as can be seen in the spectrum of CRO nontronite after two 20-min treatments with dithionite (Figure 4B). OH groups responsible for the broad diffuse band were readily exchanged by D_2O leaving a nonexchangeable component with relatively sharp OH stretching bands at 3546 and 3594 cm^{-1} and a weak OH libration at 819 cm^{-1} (Figure 4C); a perpendicular band near 678 cm^{-1}, not visible with the film at 0° incidence, was also present. These spectral features are similar to those reported for celadonite (Farmer et al., 1967; Russell et al. 1970), and for glauconites (Manghnani and Hower, 1964; Buckley et al., 1978) particularly those with a high Fe^{3+} content. The X-ray powder diffraction pattern of an oriented film of reduced nontronite showed a single moderately sharp spacing of 12.7 Å with no higher orders indicating interstratification of the nontronite possibly with the mica-like glauconite phase. This conclusion suggests that, at the higher temperatures used in the Mehra and Jackson (1960) dithionite pretreatment of soil clays that contain ferruginous smectites, considerable irreversible alteration of the smectite might occur.

Mössbauer

The Mössbauer spectra of untreated nontronites have been described in detail by Goodman et al. (1976). They were fitted to three doublets, two with isomer shifts, δ, consistent with octahedrally coordinated Fe^{3+} and the third with δ characteristic of tetrahedral Fe^{3+}. The two doublets from octahedral Fe^{3+} were assigned to the two crystallographically distinct types of coordination site (M1 and M2), with the component with the smaller quadrupole splitting, Δ, being assigned

to the site with *cis* OH groups (M2) since this site has the smaller electric field gradient on the basis of point charge considerations. The component with the larger value of Δ was assigned to the site with *trans* OH groups (M1) but, more recently, Goodman (1978) has suggested that it may arise in part from Fe^{3+} in distorted M2 sites, generated as a result of substitution of trivalent ions in tetrahedral sites.

High spin Fe^{2+} ions have one electron more than the half-filled d shell and as a result of increased shielding of s-electrons and the greater electric field gradient much larger values of both δ and Δ are generally observed than for Fe^{3+} ions. In the spectra of layer silicates the component with the larger Δ has conventionally been assigned to the site with *cis* OH groups (M2) again on point charge considerations (see Goodman, 1976a, in which a different convention for labelling the octahedral sites is used). However, the arguments presented above for the Fe^{3+} case also apply to Fe^{2+}, and consequently the component with the smaller value of Δ may contain a contribution from Fe^{2+} in distorted M2 as well as M1 sites (Goodman, 1976b).

Hydrazine reduction. The Mössbauer spectra obtained from the reduction of the nontronites with hydrazine were similar for all specimens examined. A typical spectrum is shown in Figure 5(A) and the results of the computer fits are summarized in Table 2. Peaks AA′ and BB′ arise from Fe^{3+} ions in sites with octahedral coordination and peaks CC′ from Fe^{3+} in tetrahedral sites as reported previously (Goodman et al., 1976 and also Figure 6[A]). Peaks DD′ are assigned to Fe^{2+} on the basis of the magnitudes of the isomer shift and quadrupole splitting. The amounts of iron reduced correspond to about 10% of the total with the exception of the CAL and WAS samples in which it was about 5 and 18% respectively. The widths of the Fe^{2+} peaks in these reduced samples are quite small, indicating that the reduction could be occurring selectively at one type of site. By comparing these results with those obtained from untreated specimens (Goodman et al., 1976), it appears that reduction takes place preferentially at sites with *cis* OH groups but, because of the large errors in computation of the areas of the Fe^{3+} components, definite conclusions cannot be made. Also the parameters for the Fe^{2+} ions, produced as a result of reduction, have similar values to those which were assigned to the more distorted site in dioctahedral micas (Goodman 1976a), but, as discussed above, this component could arise from Fe^{2+} in either an M1 or a distorted M2 site.

Dithionite reduction. The behavior of the WAS and GAR specimens with dithionite is similar to that with hydrazine (Table 2), but the other samples exhibit rapid and extensive reduction accounting for 60–80% of the iron (Figure 5B and Table 2). The spectra were fitted to four doublets (two Fe^{3+} and two Fe^{2+} components) although this must be an oversimplification since there were three Fe^{3+} components in spectra of each of the

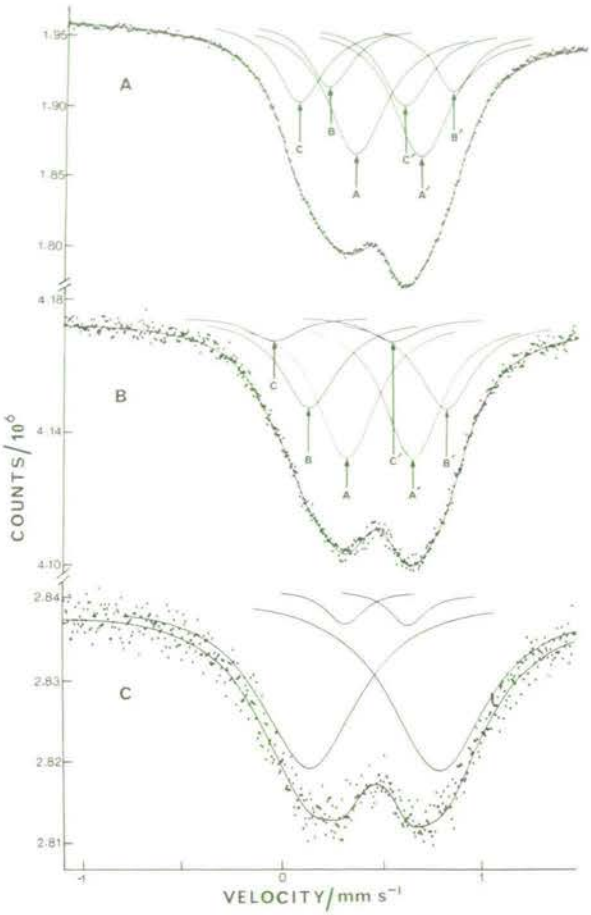

Fig. 6. Mössbauer spectra at 77 K of KOE nontronite: (A) untreated, (B) reoxidized after one 5-min treatment with dithionite and (C) reoxidized after two 20-min treatments with dithionite.

untreated nontronites. However, because of the low amounts of Fe^{3+} iron in many of these samples and the large degree of overlap of the Fe^{3+} peaks with one another, any attempt to fit further components was thought to be unjustifiable. Because they also contain a contribution from tetrahedral Fe^{3+} the parameters for the Fe^{3+} components in Table 2 have slightly lower values of δ than those previously reported for the octahedral components in nontronites (Goodman et al., 1976). The amounts of tetrahedral Fe^{3+} can be calculated if it is assumed that the isomer shifts for both octahedral and tetrahedral Fe^{3+} components are unaltered by reduction of the mineral and that the results in Table 2 represent a weighted average of the contributions. Approximate values for the percentage of the total iron as tetrahedral Fe^{3+} in these dithionite-reduced samples are then calculated as 8, 13, 5, 3, 8, 4, and 7 for WAS, GAR, CLA, CRO, KOE, AMO, and CAL, respectively. For WAS and GAR these values are similar to those obtained from untreated specimens but, for the other samples, they are much smaller. Thus, when extensive

Table 2. Computed Mössbauer parameters for reduced nontronites.

Nontronite sample and treatment	Fe^{3+}												Fe^{2+}								
	AA'				BB'				CC'				DD'				EE'				
	Δ	δ	Γ	%	Δ	δ	Γ	%	Δ	δ	Γ	%	Δ	δ	Γ	%	Δ	δ	Γ	%	χ^2
WAS + hydrazine[1]	0.37	0.45	0.38	61[4]	0.73	0.43	0.31	21									2.96	1.26	0.42	18	502
+ dithionite[1]	0.37	0.46	0.36	60[4]	0.72[3]	0.46	0.29[3]	14[4]									2.98	1.27	0.44	26	455
GAR + hydrazine[1]	0.36	0.47	0.34	59[4]	0.68	0.47	0.28	29[4]					2.58	1.22	0.33	13					533
+ dithionite[1]	0.36	0.47	0.34	61[4]	0.67	0.46	0.27	26[4]					2.65	1.23	0.39	13					466
CLA + hydrazine[2]	0.37	0.49	0.30	37	0.63	0.50	0.30	26	0.50	0.30	0.30	27	2.71	1.22	0.30	11					472
+ dithionite	0.37	0.46	0.32	20	0.72[3]	0.47	0.25[3]	8					2.74	1.26	0.41	44[4]	3.10	1.27	0.29	28	499
CRO + hydrazine[2]	0.34	0.49	0.29	34	0.61	0.49	0.29	29	0.48	0.30	0.29	28	2.72	1.25	0.29	9					481
+ dithionite	0.27[3]	0.46	0.33[3]	14[4]	0.57[3]	0.47	0.30[3]	10[4]					2.73[3]	1.27	0.40	46[4]	3.09	1.27	0.27	31[4]	459
KOE + hydrazine[2]	0.33	0.49	0.29	31	0.57[3]	0.49	0.29	32	0.50	0.30	0.29	25	2.77	1.24	0.29	11					400
+ dithionite	0.33[3]	0.46	0.31[3]	20[4]	0.62[3]	0.46	0.32[3]	17[4]					2.71	1.26	0.39	32	3.08	1.28	0.29	30	604
AMO + hydrazine[2]	0.34	0.49	0.30	34	0.60	0.49	0.30	29	0.51	0.31	0.30	27	2.77	1.24	0.30	10					456
+ dithionite	0.26[3]	0.45	0.29[3]	7	0.59[3]	0.47	0.36[3]	12					2.69	1.28	0.42	41	3.08	1.28	0.32	40	671
CAL + hydrazine[2]	0.33	0.49	0.29	35	0.61	0.49	0.29	31	0.46	0.30	0.29	29[4]	2.74[3]	1.29[3]	0.29	5					507
+ dithionite	0.33	0.45	0.33[3]	20	0.68[3]	0.46	0.25[3]	8					2.73	1.27	0.40	40[4]	3.07	1.27	0.28	33	505

All values are in mm s^{-1}, with the isomer shift, δ, relative to iron metal.

[1] These spectra were fitted to three doublets because of the low amounts of tetrahedral iron in the untreated specimens.

[2] The fits to these spectra assume that all components have equal values for the peak width, Γ.

[3] The standard deviations for the quadrupole splitting, Δ, isomer shift, δ, and peak width, Γ, are ≤0.02 mm s^{-1} except for those marked [3], where the standard deviations are in the range 0.03–0.07 mm s^{-1}.

[4] The standard deviations for the amounts of each component are ≤4%, except for those marked [4] where the standard deviations are in the range 5–10%.

reduction occurs, a considerable proportion of the tetrahedral Fe^{3+} is lost from the structure.

If the Fe^{2+} peaks were assigned in the conventional way, the component with the larger quadrupole splitting would correspond to Fe^{2+} in the M2 site and that with the smaller value of Δ to the M1 site. However, this simple approach can not be applied realistically to these spectra, because of the structural changes and decomposition which have been shown to occur as a result of reaction with dithionite.

Reoxidation. Samples of the KOE nontronite were subjected to treatments with 1% w/v sodium dithionite solutions for various times, after which they were allowed to oxidize by exposure to the atmosphere. The resulting spectra, which showed no evidence for any Fe^{2+} ions, are presented in Figure 6 in an expanded form to facilitate comparison with the untreated sample. It can be seen that the 5-min treatment produced a spectrum (Figure 6B) which bears a strong resemblance to that of the original nontronite (Figure 6A), although there is a decrease in intensity of the peaks (CC') from tetrahedral Fe^{3+}. In contrast the spectrum from the sample which had received two 20-min dithionite treatments (Figure 6C) shows little overall resemblance to that of the original nontronite. The weak central peaks have similar parameters to the main peaks (AA') of nontronite and probably correspond to this phase, but the spectrum is dominated by a pair of broad peaks which must correspond to a range of environments for the iron. The lower percentage absorption in the latter spectrum is caused partly by the lower iron content and partly because of the greater width of peaks from the phase formed as a result of the dithionite treatment. This observation of the change in form of the mineral after prolonged dithionite treatment is in agreement with the results from infrared spectroscopy presented above.

CONCLUSIONS

The Mössbauer and infrared results provide evidence that, under the experimental conditions used in this study, those nontronites that contain tetrahedral iron are much more extensively reduced by dithionite than are those that do not contain tetrahedral iron, and that this iron is preferentially dissolved during reduction.

This reaction, which produces glauconite- or celadonite-like components and a disordered iron-rich silicate may be significant in the context of pretreatment of minerals for analysis. The similarity between the intense blue-green colors formed during reduction and those observed in water-logged soils suggests that the reduction mechanisms described may occur in poorly drained soils that contain ferruginous smectites.

REFERENCES

Angell, C. L. and Schaffer, P. C. (1965) Infrared spectroscopic investigations of zeolites and absorbed molecules: *J. Phys. Chem.* **69**, 3463–3470.

Buckley, H. A., Bevan, J. C., Brown, K. M., Johnson, L. R., and Farmer, V. C. (1978) Glauconite and celadonite: two separate mineral species: *Mineral. Mag.* **42**, 373–382.

Farmer, V. C. (1974) *The I.R. Spectra of Minerals*: Mineral. Soc. London, p. 344.

Farmer, V. C., Russell, J. D., Ahlrichs, J. L. and Velde, B. (1967) Vibrations du groupe hydroxyle dans les silicates en couches: *Bull. Groupe Fr. Argiles* **19**, 5–10.

Goodman, B. A., Russell, J. D., Fraser, A. R. and Woodhams, F. W. D. (1976) A Mössbauer and I.R. spectroscopic study of the structure of nontronite: *Clays & Clay Minerals* **24**, 53–59.

Goodman, B. A. (1976a) The Mössbauer spectrum of a ferrian muscovite and its implications in the assignment of sites in dioctahedral micas: *Mineral. Mag.* **40**, 513–517.

Goodman, B. A. (1976b) The effect of lattice substitutions on the derivation of quantitative site populations from the Mössbauer spectra of 2:1 layer lattice silicates: *J. Phys.*, Colloq. C6 **37**, C6-819–823.

Goodman, B. A. (1978) The Mössbauer spectra of nontronites: consideration of an alternative assignment: *Clays & Clay Minerals* **26**, 176–177.

Heller, L., Farmer, V. C., Mackenzie, R. C., Mitchell, B. D. and Taylor, J. F. W. (1962) The dehydroxylation and rehydroxylation of triphormic dioctahedral clay minerals: *Clay Miner. Bull.* **5**, 56–72.

Manghnani, M. H. and Hower, J. (1964) Glauconites: Cation exchange capacities and I.R. spectra. Part II. Infrared absorption characteristics of glauconites: *Am. Mineral.* **49**, 1631–1641.

Mehra, O. P. and Jackson, M. L. (1960) Iron oxide removal from soils and clays by dithionite-citrate systems buffered with sodium bicarbonate: *Clays & Clay Minerals* **7**, 317–327.

Nakamoto, K., Margoshes, M. and Rundle, R. E. (1955) Stretching frequencies as a function of distances in hydrogen bonds: *J. Am. Chem. Soc.* **77**, 6480–6486.

Preston, R. S., Hanna, S. S. and Heberle, J. (1962) Mössbauer effect in metallic iron: *Phys. Rev.* **128**, 2207–2218.

Roth, C. B. and Tullock, R. J. (1973) Deprotonation of nontronite resulting from chemical reduction of structural ferric iron: *Proc. Int. Clay Conf.* 1972, 107–114.

Rozenson, I. and Heller-Kallai, L. (1976a) Reduction and oxidation of Fe^{3+} in dioctahedral smectites—1: Reduction with hydrazine and dithionite: *Clays & Clay Minerals* **24**, 271–282.

Rozenson, I. and Heller-Kallai, L. (1976b) Reduction and oxidation of Fe^{3+} in dioctahedral smectites—2: Reduction with sodium sulphide solutions: *Clays & Clay Minerals* **24**, 283–288.

Russell, J. D., Farmer, V. C. and Velde, B. (1970) Replacement of OH by OD in layer silicates and identification of the vibrations of these groups in infrared spectra: *Mineral. Mag.* **37**, 869–879.

Russell, J. D. (1978) Structural modification of nontronite and other ferruginous smectites by alkali metal hydroxides: *Clay Miner.* (in prep).

Stucki, J. W. and Roth, C. B. (1976) Interpretation of infrared spectra of oxidized and reduced nontronite: *Clays & Clay Minerals* **24**, 293–296.

Stucki, J. W., Roth, C. B. and Baitinger, W. E. (1976) Analysis of iron-bearing clay minerals by electron spectroscopy for chemical analysis (ESCA): *Clays & Clay Minerals* **24**, 289–292.

Tarte, P. (1963) Applications nouvelles de la spectrométrie infrarouge à des problèmes de cristallochemie: *Silic. Ind.* **28**, 345–354.

Резюме- Спектроскопия инфракрасных лучей и Моссбауэра показывает, что степень восстановления нонтронита зависит от его химического состава и природы восстановления. Гидразин обратимо восстанавливает около десяти процентов железа во всех изученных нонтронитах, независимо от состава, и предполагается, что двухвалентное железо встречается только в деформированных октаэдрических формах. Подобные заключения были сделаны и для дитионитового восстановления нонтронитов, содержащих немного тетраэдрического железа, но для тех, в которых больше, чем 1 из 8 силиконов, были замещены железом, изменения вызванные дитионитовой обработкой являются необратимыми, ввиду растворения значительного количества железа. Результаты исследований с помощью обоих спектроскопических методов показывают, что железо в тетраэдрических формах растворяется легче и что до восьмидесяти процентов структурного железа может быть восстановлено.

Приводятся доказательства, что в этих сильно восстановленных нонтронитах образуется небольшое количество слюдо-подобной фазы, напоминающей селадонит или глауконит, и, если дитионит используется для предварительной обработки почв, коротко обсуждается значение этих наблюдений.

Использование дейтерированного гидразина в качестве восстановителя способствует совмещению нонтронитовой абсорбционной связи вблизи 850см$^{-1}$ с Si-O /апикальной/ растягивающей вибрацией, которая инертна в инфракрасных лучах благодаря совершенной гексагональной симметрии, но которая активизируется в результате деформаций в тетраэдрическом слое.

Kurzreferat- Infrarot-und Mössbauerspektroskopie zeigen,daß der Ausmaß der Reduktion von Nontronit von der chemischen Zusammensetzung des Nontronit und von der Art des Reduktionsmittels abhängt.Hydrazin reduziert in umkehrbarer Reaktion ungefähr 10% des Eisens in allen Nontroniten,unabhängig von der Zusammensetzung und es wird vorgeschlagen,daß das resultierende Fe(II)-Eisen nur in verformten oktahedrischen Plätzen vorkommt.Ähnliche Beschlüsse wurden für die Reduktion mit Dithionit von Nontronit,welches ein wenig tetrahedrisches Eisen enthält,gemacht.diejenigen Nontroniten,die mehr als 1 unter 8 Silizium durch Eisen ausgewechselt haben,ist die Veränderung hervorgebracht durch Dithionitbehandlung,nicht reversibel wegen Auflösung von nennenswerten Mengen von Eisen.Resultate von beiden spektrokopischen Techniken schlagen vor,daß das Eisen in den tetrahedrischen Plätzen bevorzugt aufgelöst wird,und daß bis zu 80% des strukturellen Eisens reduziert werden kann. Beweise werden presentiert für die Formation in diesen ausgedehnt reduzierten Nontroniten,von einer glimmerartigen Phase,welche Keladonit oder Glaukonit gleichen und weil Dithionit für die Behandlung der Erden benutzt wird, wird die Implikation dieser Beobachtung kurz diskutiert.Das Benutzen von Deuterium-Hydrazin als Reduktionsmittel macht es möglich,das Nontronitadsorptionsband bei 850 cm^{-1} einer Si-O Streckschwingung zuzuschreiben. Für perfekte,hexagonale Symmetrie sind diese Schwingungen inaktiv,aber für Verzerrungen in der tetrahedrischen Schicht sind sie aktiv.

Résumé-La spectroscopie infrarouge et de Mössbauer montre que l'étendue de la réduction de la nontronite dépend de la composition chimique de la nontronite et de la nature de l'agent réducteur.L'hydrazine réduit réversiblement à peu près 10 % du fer dans toutes les nontronites étudiées irrespectivement de leur composition,et il est suggéré que le fer ferreux qui en résulte ne se trouve que sur des sites octaèdres déformés.Des conclusions semblables ont été tirées pour la réduction par la dithionite de nontronites contenant peu de fer tétraèdre,mais pour celles avec plus d'un silicium sur huit remplacé par le fer,les changements amenés par le traitement à la dithionite étaient irréversibles à cause de la dissolution de quantités appréciables de fer.Les résultats des deux techniques spectroscopiques suggèrent que le fer sur les sites tétraèdres est préferentiellement dissolu et que jusqu'à 80 % de fer de composition peut être réduit.Des preuves de la formation dans ces nontronites d'une petite quantité d'une phase pareille au mica ressemblant à de la celadonite ou à de la glauconite sont présentées,et,comme la dithionite est utilisée pour le pré-traitement des sols,l'implication de cette observation est brièvement discutée.L'emploi de l'hydrazine deutérée comme agent réducteur a permi à la bande d'adsorption de la nontronite près de 850 cm^{-1} d'être assignée à une vibration allongeante Si-O (apique),qui est inactive dans l'infrarouge pour la symmétrie hexagonale parfaite,mais qui est activée par des distortions dans le feuillet tétraèdre.

Clays and Clay Minerals, Vol. 27, No. 1, pp. 72–78, 1979.

SURFACE REACTIONS OF PARATHION ON CLAYS[1]

U. MINGELGRIN AND SARINA SALTZMAN

Institute of Soils and Water, Agricultural Research Organization,
The Volcani Center, Bet Dagan, Israel

(Received 6 February 1978)

Abstract—The adsorption-catalyzed degradation of parathion on clay surfaces is a hydrolysis process, proceeding either directly or through a rearrangement step. The rate and mechanism of degradation are dependent on the nature of the clay, its hydration status, and saturating cation. A mechanism for parathion degradation at adsorption sites on clay surfaces, in the absence of a liquid phase, is proposed.

Key Words—Adsorption, Catalysis, Hydrolysis, Insecticide, Parathion.

INTRODUCTION

Parathion (O,O-diethyl O-p-nitrophenyl phosphorothioate) is one of the most widely used plant and soil insecticides. Its metabolism in both biotic and abiotic media proceeds through one or more of the following reactions: isomerization, hydrolysis, oxidation, reduction (Melnikov, 1971). Clays are well known as potential catalyzers of various kinds of reactions of the adsorbed molecules (Mortland, 1970; Theng, 1974). As clay-parathion complexes are often formed, either in soils or in formulations using clays as carriers, their effect on parathion conversion may play an important role in parathion alteration in the environment.

The catalytic effect of clays on the metabolism of some organophosphate pesticides, such as malathion, dursban, diazinon, ronnel, zytron, and pyrimiphos ethyl, was reported by Polon and Sawyer (1962), Mortland and Raman (1967), and Mingelgrin et al. (1975). The only degradation mechanism observed in all these cases was the hydrolysis of the phosphate ester bond of the adsorbed molecule. Such factors as the nature of the clay, the moisture content, the saturating cations, and the incubation temperature, were found to affect the rate of the process. In recent years, some results on kaolinite-parathion interactions were reported. Kaolinite was found to enhance parathion degradation; this process also proceeds by the hydrolysis of the phosphate ester bond (Saltzman et al., 1974; Mingelgrin et al., 1977).

Rosenfield and Van Valkenburg (1965) observed that various homoionic bentonites, dried at elevated temperatures (300–950°C), induced the degradation of a thiophosphate (ronnel), the process occurring through a molecular rearrangement. The possible rearrangement products of parathion are known to be much more toxic to mammals than is the parent compound (Joiner et al., 1973). Therefore, it is important to check if such a process is possible in the case of clay-parathion complexes and, if so, to understand its mechanism and study the specific conditions favoring it.

MATERIALS AND METHODS

The clays used in this study were Wyoming bentonite (B-235, Fisher Scientific Co., Fair Lawn, N.J., U.S.A.) and kaolinite (Peerless No. 2, R. T. Vanderbilt, Export Corp., Norwalk, Conn., U.S.A.). The clays investigated were the natural commercial bentonite (which is a Na-saturated clay), and homoionic Ca-bentonite and Ca-kaolinite, prepared by a method described by Shainberg and Otoh (1968). Other materials used as adsorbents were silica gel and anionotrop and cationotrop aluminum oxide (chromatography grade, activity grade I, M. Woelm, Eschwege, W. Germany).

Parathion-^{14}C, labeled in the alkyl chain (Amersham Radiochemical Center, Arlington Heights, Illinois, U.S.A.), and high grade parathion (Analabs, Inc., North Haven, Conn., U.S.A.) were used; paraoxon (Koch Light Labs., England), diethyl thiophosphoric acid, ammonium salt (Ciba-Geigy, AG, Basle, Switzerland), and p-nitrophenol (BDH, Poole, England), were used as standards.

Procedure

The persistence of parathion when adsorbed on various adsorbents was investigated by two procedures:

a) Clay-parathion-^{14}C complexes were prepared by shaking for 30 min 0.3 g air-dried clay with 5 ml hexane solution containing 10,000 ppm parathion-^{14}C. The supernatant was checked for parathion, and discarded; the clay was washed with 5 ml hexane, which was also checked for parathion and discarded. The clay-parathion complex obtained was dried in an air stream, and divided into subsamples of 0.05 g, which were incubated in an oven, at different temperatures, for various periods of time. After incubation the samples were extracted twice, each time for 1 hr, with 4 ml hexane, together with 2 ml deionized water.

b) The clays were dried for 24 hr at 110° and 200°C and clay-parathion complexes were prepared by adding

[1] Contribution from the Agricultural Research Organization, The Volcani Center, Bet Dagan, Israel. 1977 Series, No. 216-E.

Clay Minerals (1979) **14**, 109.

INFRARED SPECTROSCOPY OF FERRIHYDRITE: EVIDENCE FOR THE PRESENCE OF STRUCTURAL HYDROXYL GROUPS

J. D. RUSSELL

Department of Spectrochemistry, The Macaulay Institute for Soil Research, Craigiebuckler, Aberdeen, AB9 2QJ, Scotland

(*Received 22 December 1978*)

ABSTRACT: IR spectroscopy has shown that adsorbed water is almost completely removed from ferrihydrite by evacuation at room temperature. Absorption bands at 3615 and 3430 cm^{-1} appearing thereafter are interpreted as arising from OH groups located respectively at the surface and deeper in the structure. These groups are readily converted to OD on treatment with D_2O vapour and this has allowed the OH deformation vibration to be identified at 800 cm^{-1}. It is proposed that OH groups in ferrihydrite are about half as numerous as those in akaganéite (β-FeOOH) and that they may occur in environments similar to those in this mineral. The formula for ferrihydrite proposed by earlier workers, $5\ Fe_2O_3.9H_2O$, should thus be amended to $Fe_2O_3.\ 2\ FeOOH.2{\cdot}6H_2O$ in order to indicate the presence of structural OH groups. A re-appraisal of the ferrihydrite structure appears desirable.

Naturally occurring ferric hydroxide gel has been studied by Chukhrov *et al.* (1971, 1972, 1973) using X-ray diffraction (XRD) and infrared (IR) spectroscopy. They proposed the name ferrihydrite and concluded that it had a defect-hematite structure, as proposed earlier by Towe & Bradley (1967) for a synthetic specimen. This structure was sustained by the failure of the latter authors to detect absorption bands assignable to deformation vibrations of structural OH groups in IR spectra. Schwertmann & Fischer (1973) arrived at a similar conclusion from IR spectra of naturally occurring ferric hydroxides. Chukhrov *et al.* (1971) further stated that the presence of OH groups was precluded by the typical bonding between Fe octahedra in this type of structure. Thus on the basis of characterization by XRD, DTA and IR spectroscopy, ferrihydrite was accepted as a distinct mineral species of formula $5Fe_2O_3.9H_2O$, containing no structural OH groups (Fleischer *et al.*, 1975). The IR results quoted by these authors are central to the elucidation of the structure of ferrihydrite, but the procedures employed all involved the use of KBr pressed disks. It is suggested that this may not have been the most appropriate technique, and in this study, the spectrum of a synthetic ferrihydrite is re-examined using a film technique in conjunction with D_2O exchange.

MATERIALS AND METHODS

Ferrihydrite was prepared by boiling a 0·01M aqueous solution of $Fe(NO_3)_3.9H_2O$, then dialysing it against distilled water. The product was isolated by freeze-drying. Its XRD pattern with peaks at 2·54, 2·25, 1·98, 1·74 and 1·47 Å matched closely that reported by Towe & Bradley (1967) for their synthetic ferrihydrite. No evidence of the more crystal-

line oxides or oxyhydroxides was detected in XRD patterns or IR spectra of the ferrihydrite.

For IR spectroscopy, a film of ferrihydrite was prepared by evaporating an aqueous suspension (1·2 mg/ml) on to an AgCl sheet to give a reasonably uniform deposit with a weight of 0·6 mg cm^{-2}. The film was placed in a vacuum cell and spectra were recorded on a Perkin Elmer 577 IR spectrometer with the sample either fully hydrated, evacuated at 0·002 torr for 30 min, or repeatedly flushed with D_2O vapour then evacuated.

RESULTS AND DISCUSSION

Because of the size of the ferrihydrite particles or aggregates, the film scattered IR radiation strongly, resulting in a pronounced slope of the background between 4000 and 2000 cm^{-1}. Nevertheless, it can be seen that the hydrated ferrihydrite has a broad absorption maximum at 3400 cm^{-1} due in part to adsorbed water which also gives rise to the band at 1635 cm^{-1} (Fig. 1a). Evacuation removes water, allowing absorption bands of OH groups to be seen at 3615 and 3430 cm^{-1} (Fig. 1b). A similar result was briefly reported by Parfitt *et al.* (1975) for what they called 'iron hydroxide gel', but no spectra were shown and no reference to ferrihydrite or its structure was made. Because the residual weak absorption band near 1640 cm^{-1} (Fig. 1b) is not removed by exchange with D_2O vapour (Fig. 1c) the contribution made by molecular water to this band must be very small. Even if all of its intensity were ascribed to water, this would account for a maximum of one-fourth of the absorbance at 3430 cm^{-1} in Fig. 1b by comparison with water in various environments (Russell & Farmer, 1964; Van der Marel & Zwiers, 1959). It is, therefore, concluded that the absorption band at 3430 cm^{-1} (Fig. 1b) must arise almost entirely from OH groups in the ferrihydrite structure. The appearance of a high-frequency

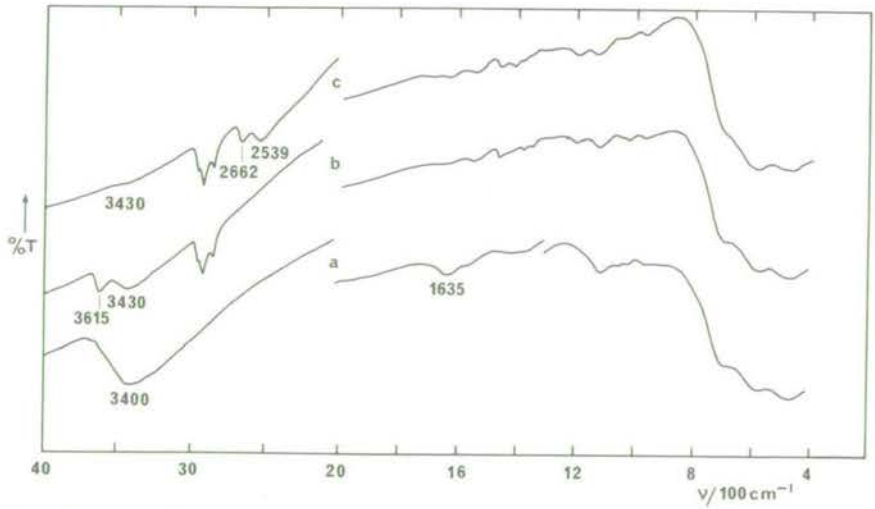

Fig. 1. IR spectra of film of ferrihydrite on AgCl plate in a vacuum cell: a, hydrated; b, after 30 min evacuation at 0·002 torr; c, after 18 D_2O vapour-evacuation treatments. T, transmission; ν, wavenumber; curves are displaced vertically. Sharp absorption bands in the 2850–2950 and 1350–1450 cm^{-1} regions are due to hydrocarbon rotary pump oil adsorbed from the vapour phase during evacuation.

band on removal of adsorbed water from ferrihydrite is analogous to that found for goethite (Russell *et al.*, 1974), and akaganéite (Russell, unpublished data), suggesting that the 3615 cm^{-1} band be assigned to relatively free surface OH groups. The half-width of this band however is some 60 cm^{-1} compared with about 13 for doubly and triply coordinated and 20–30 cm^{-1} for singly coordinated OH groups on the goethite surface, suggesting a much broader distribution of OH . . . O distances (i.e. a more disordered arrangement of OH groups) on the ferrihydrite surface.

Repeated flushing of the evacuated ferrihydrite with D_2O vapour exchanged both types of OH group as shown by the shift from 3615 and 3430 cm^{-1} to 2662 and 2539 cm^{-1} (Fig. 1c), isotopic ratios being 1·358 and 1·351 respectively. The surface OH groups underwent H-D exchange more rapidly than the bulk OH groups, weak absorption remaining at 3430 cm^{-1} after 18 cycles of D_2O vapour flushing followed by evacuation to 0·005 torr (Fig. 1c). The absorbance of this band is only 20% of that of the original (Fig. 1b). This suggests that the majority of OH groups in ferrihydrite are relatively accessible, but that some are located more deeply in the structure. The relative ease of exchange of the OH groups perhaps renders a distinction between surface and bulk types somewhat doubtful. Nevertheless, the higher frequency stretching vibration is indicative of relatively weak hydrogen bonds, 3615 cm^{-1} being equivalent to a O-H . . . O distance of just over 3·0 Å, and the lower frequency band to more strongly hydrogen bonded hydroxyls, O-H . . . O distance 2·86 Å (Nakamoto *et al.*, 1955).

The identification of OH groups in ferrihydrite from their stretching band is unambiguous, but even after D_2O exchange it is not clear where the corresponding OH deformation band absorbs although some loss of absorption may have occurred near 800 cm^{-1} (Fig. 1c). The band is likely to be weak and in order to identify it, a differential plot (Fig. 2b) between the OH and OD forms (Fig. 2a) was made over the range 1200–400 cm^{-1}. It can be seen clearly that positive absorption (OH) centred on 800 cm^{-1} is replaced by negative absorption (OD) at 600 cm^{-1} as a result of the D for H exchange. OH groups in ferrihydrite therefore exhibit a weak, broad, deformation band at 800 cm^{-1}: an inflexion near 1000 cm^{-1} probably arises from the deformation vibration of surface OH groups. The isotopic ratios of 1·358, 1·351 for the OH stretch and 1·33 for the OH bend for ferrihydrite are in good agreement with values for smectites (1·35–1·36 and 1·30–1·35 respectively (Russell, unpublished data)) and hydroxides of iron and aluminium (1·32–1·34 and 1·28–1·32 (Ryskin, 1974; Russell, unpublished data)).

Although it is not possible from IR spectra to measure directly the extent to which OH groups occur in ferrihydrite, an estimate may be made from a comparison between ferrihydrite and the three oxyhydroxides of iron, using the ratio of the areas of OH stretching bands to Fe-O bands. These results (Table 1), although approximate, suggest that the concentration of OH groups in ferrihydrite is significant and may approach one third to one half of that in crystalline iron oxyhydroxides. The frequency of the bulk OH groups (3430 cm^{-1}, Fig. 1b) and the ease with with they are exchanged by D_2O further suggests that they could be in an environment similar to that of OH groups in akaganéite which absorb at 3478 cm^{-1} (Russell, unpublished data).

Excluding adsorbed water, akaganéite may be formulated as $Fe_2O_3.H_2O$. From the observation made above, ferrihydrite might then be written $2Fe_2O_3.H_2O$. To take account of the structural OH, the formula put forward by Towe & Bradley (1967) could then be rewritten as $Fe_2O_3.2FeOOH.2{\cdot}6H_2O$.

The conclusions drawn here concerning the occurrence of OH groups in ferrihydrite are

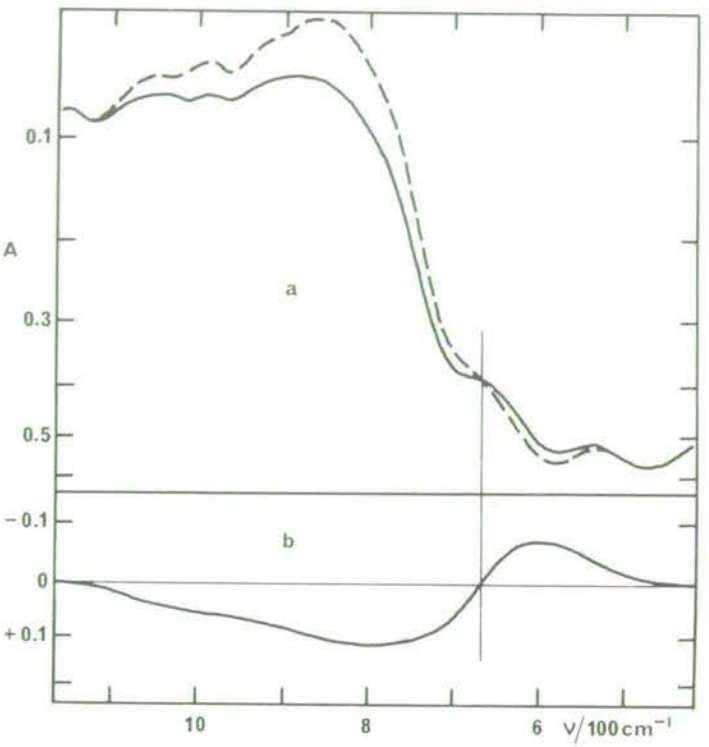

Fig. 2. IR spectra of ferrihydrite: a, OH form (solid curve) and OD form (broken curve) on same base line; b, differential plot between OH and OD forms, positive values of absorbance (A) indicating OH and negative values OD. ν, wavenumber.

TABLE 1. Areas of O-H stretching bands and Fe-O bands and the ratios of these areas for hydrated iron oxides

	Band area (Arbitrary units)*		
Hydrated oxide	O-H stretch†	Fe-O	Ratio
Ferrihydrite	322	935†	0·34
Goethite (α)	766	957	0·80
Akaganéite (β)	622	1118	0·60
Lepidocrocite (γ)	1176	1285‡	0·92

* Data from absorbance spectra of 0·5 mg sample in 13 mm diam. CsI pressed disks heated 24 h at 125 °C: no significant water absorption bands detectable near 1630 cm^{-1}.

† These areas include surface and bulk OH bands which are not resolved in alkali halide pressed disks.

‡ Small corrections (50–100 units) were made for overlapping OH deformation bands.

contrary to those of Towe & Bradley (1967) and Schwertmann & Fischer (1973) for synthetic and natural specimens respectively. The failure of these authors to observe a Fe-OH deformation band in their KBr disk spectra is due to its weakness and partial overlap by lower-frequency Fe-O bands. Towe & Bradley then concluded that the band occurring in the OH stretching region arose solely from adsorbed water without checking that this band was completely eliminated by heating the disk. Schwertmann & Fischer agreed with Towe & Bradley concerning the lack of an OH deformation band (although the relevant region of the former authors' spectrum was overlain by a broad silicate absorption band) and sought confirmation of this by heating the disk to remove adsorbed water. Unfortunately, Schwertmann & Fischer's samples contained organic matter and the 1300–1700 cm^{-1} region of their spectra was masked by the two broad absorption bands of carboxylate groups. This prevented them from making a direct observation of the 1625 cm^{-1} water band and necessitated the use of a graphical method of extrapolation to 0% carbon. Their observation of residual absorbance at 1625 cm^{-1} by this method must be considered to be of doubtful validity, but it led these authors to conclude that the absorption band at 3400 cm^{-1} in the spectrum of the heated disk of ferrihydrite was solely due to molecular water and, therefore, that their natural specimen of ferrihydrite, like Towe & Bradley's synthetic specimen, contained no structural OH groups. Unfortunately, this conclusion, based on weak evidence, became one of the principal structural characteristics listed by Fleischer *et al.* (1975) in the recognition of ferrihydrite as a distinct mineral species.

The IR evidence presented here for the presence of structural OH groups in ferrihydrite is unambiguous and indicates that a reappraisal of the ferrihydrite structure is necessary. This is particularly important if the role played by natural ferrihydrites and related phases in reactions with fertilizers in soils are to be understood fully.

ACKNOWLEDGMENTS

The author wishes to thank Dr D.G. Lewis, Waite Agricultural Research Institute, Glen Osmond, Australia, for providing the ferrihydrite, and Dr C.W. Childs, Soil Bureau, DSIR, Lower Hutt, New Zealand, for helpful discussion during the investigation.

REFERENCES

Chukhrov F.V., Zvyagin B.B., Gorshkov A.I., Ermilova L.P. & Rudnitskaya E.S. (1971) *Izv. Akad. Nauk. SSSR Ser. Geol.* (1), 3.

Chukhrov F.V., Zvyagin B.B., Ermilova L.P. & Gorshkov A.I. (1972) *Proc. Int. Clay Conf. Madrid* **1**, 397.

Chukhrov F.V., Zvyagin B.B., Gorshkov A.I., Ermilova L.P. & Balashova V.V. (1973) *Izv. Akad. Nauk. SSSR Ser. Geol.* (4), 23.

Fleischer M., Chao G.Y. & Kato A. (1975) *Am. Miner.* **60**, 485.

Nakamoto K., Margoshes M. & Rundle R.E. (1955) *J. Am. Chem. Soc.* **77**, 6480.

Parfitt R.L., Atkinson R.J. & Smart R.St.C. (1975) *Soil Sci. Soc. Am. J.* **39**, 837.

Russell J.D. & Farmer V.C. (1964) *Clay Miner. Bull.* **5**, 443.

Russell J.D., Parfitt R.L., Fraser A.R. & Farmer V.C. (1974) *Nature* **248**, 220.

Ryskin Y.I. (1974) The vibration of protons in minerals: hydroxyl, water and ammonium. *The Infrared Spectra of Minerals* (V.C. Farmer, editor) pp 137–181. Mineralogical Society, London.

Schwertmann U. & Fischer W.R. (1973) *Geoderma* **10**, 237.

Towe K.M. & Bradley W.F. (1967) *J. Colloid Inter. Sci.* **24**, 384.

Van der Marel H.W. & Zwiers J.H.L. (1959) *Silicates Ind.* **24**, 359.

RÉSUMÉ: La spectroscopie infrarouge a montré que l'eau adsorbée est presque entièrement éliminée de la ferrihydrite par mise sous vide à température ambiante. les bandes d'absorption qui apparaissent ensuite à 3615 et 3430 cm^{-1} sont interprétées comme provenant de groupements OH situés respectivement à la surface et plus profondément dans la structure. Ces groupements sont aisément convertis en groupements OD par traitement au moyen de D_2O en phase vapeur et ceci a permis d'identifier la vibration de déformation à 800 cm^{-1}. On considère que les groupements OH dans la ferrihydrite sont environ moitié moins nombreux que dans l'akaganéite (β-FeOOH) et qu'ils peuvent survenir dans des environnements analogues à ceux correspondant à ce minéral. La formule de la ferrihydrite proposée par les premiers chercheurs, 5 Fe_2O_3. $9H_2O$, devrait être modifiée en Fe_2O_3. 2 FeOOH. 2·6 H_2O, afin de mettre en évidence la présence des groupes OH de la structure. Il parait désirable que la structure de la ferrihydrite fasse l'objet d'un nouvel examen.

KURZREFERAT: Mit Hilfe der IR-Spektroskopie läßt sich zeigen, daß adsorbiertes Wasser durch Evakuierung bei Raumtemperatur fast ganz von Ferrihydrit entfernt wird. Die hernach erscheinenden Absorptionsbanden bei 3615 und 3430 cm^{-1} werden so interpretiert, daß sie von den oberflächlichen bzw. tiefer in der Struktur befindlichen Hydroxylgruppen stammen. Diese Gruppen werden bei Behandlung mit D_2O kaum in OD überführt, so daß die OH Deformationsschwingung bei 800 cm^{-1} identifiziert werden kann. Vorgeschlagen wird, daß OH-Gruppen in Ferrihydrit etwa halb so zahlreich sind, als die von Akaganit (β-FeOH) und daß sie eine ähnliche Umgebung wie dieses Mineral haben. Folglich sollte die Formel für Ferrihydrit früherer Arbeiten in folgender Weise berichtigt werden Fe_2O_3.2FeOOH $6H_2O$ um so die Anwesenheit von strukturellen OH-Gruppen anzuzeigen. Die Struktur von Ferrihydrit sollte neu bestimmt werden.

RESUMEN: La espectroscopia por rayos infrarrojos ha mostrado que el agua adsorbida se extrae casi por completo de la ferrihidrita por evacuación a la temperatura ambiente interior. Las bandas de absorción que aparecen luego a 3615 y 3430 cm^{-1} se interpreta que surgen de los grupos OH situados respectivamente en la superficie y más dentro de la estructura. Estos grupos se transforman fácilmente en OD mediante el tratamiento con vapores de D_2O y esto ha permitido identificar a 800 cm^{-1} la vibración de la deformación de OH. Se propone que los grupos OH en la ferrihidrita son aproximadamente la mitad de numerosos que los presentes en acaganeita (β-FeOOH) y que pueden darse en ambientes similares a los de este mineral. La fórmula propuesta para la ferrihidrita por investigadores anteriores, $5Fe_2O_3.9H_2O$, debe enmendarse pues a Fe_2O_3. 2FeOOH. 2·6H_2O, con objeto de indicar la presencia de grupos OH estructurales. Parece deseable hacer una reevaluación de la estructura de las ferrihidritas.

ADDENDUM

The author wishes to thank his colleague Mr E. Paterson for bringing to his attention, after this paper was accepted for publication, the thesis of Van der Giessen (1968) in which IR and NMR results were interpreted to show that iron III oxide hydrate (ferrihydrite) contained hydroxyl groups within its structure. The composition $Fe_2O_3.1·6H_2O$ was therefore re-written FeOOH.0·$3H_2O$, a formula which agrees very well with that proposed in this paper, FeOOH.0·$5H_2O$.

VAN DER GIESSON A.A. (1968) Chemical and Physical Properties of Iron III Oxide Hydrate. Thesis, 104 pp. Centrex, Eindhoven, Netherlands.

Clay Minerals (1979) **14**, 127.

AN INFRARED SPECTROSCOPIC STUDY OF THE INTERACTION OF NONTRONITE AND FERRUGINOUS MONTMORILLONITES WITH ALKALI METAL HYDROXIDES

J. D. RUSSELL

Department of Spectrochemistry, The Macaulay Institute for Soil Research, Craigiebuckler, Aberdeen, AB9 2QJ, Scotland.

(*Received 7 December 1978*)

ABSTRACT: IR spectroscopy has been used to study the interaction of alkali metal hydroxides with dioctahedral smectites having iron contents of 0·7% (montmorillonite) to 22% (nontronite), in connection with the alkali-stabilization of soils. The results have shown that the alkalis (LiOH, NaOH, KOH and CsOH) deprotonate hydroxyl groups co-ordinated to octahedral ferric iron, causing distortion of tetrahedral and octahedral layers. This concept of distortion is supported by a striking change in Mössbauer spectra and a large increase in *b* cell dimensions. The perturbation of the smectite structure, shown by shifts in the Si-O and O-H stretching vibrations, is greater for Na, K and Cs than for Li, suggesting that the larger cations interact with surface oxygens around the hexagonal hole. IR spectra suggest that the effect of NaOH on nontronite is substantially reversed by treating the smectite with CO_2 or acetic acid vapour or by washing it with dilute salt solution, although Mössbauer spectroscopy and XRD indicate that the structure of the regenerated smectite is more disordered than that of the original.

Alkali and alkaline earth hydroxides have been widely used as soil stabilizers and it has been shown that increased soil strength depends on chemical dissolution of, *inter alia*, kaolin minerals and montmorillonites (Ingles, 1970). This type of attack of silicates by alkali has been recognized by Dudas & Harward (1971) in the Hashimoto & Jackson (1960) procedure for the removal of amorphous alumino-silicates. Under even more drastic conditions, silicates are extensively dissolved and zeolites may be synthesized (Zhukova *et al.*, 1971). Only one study (Volkov *et al.*, 1976) has been made at low levels of alkali, this dealing with the dissolution and swelling kinetics of montmorillonite and kaolinite. This paper describes a preliminary investigation using infrared (IR) spectroscopy aimed at following the structural changes occurring during interactions between several alkalis and a series of smectites with a range of iron contents from 0·7% (montmorillonite) to 22% (nontronite).

EXPERIMENTAL

Materials

The smectites studied included the nontronites investigated by Goodman *et al.* (1976) and montmorillonites from Woburn and Wyoming (Heller *et al.*, 1962) and from Otay (Schultz, 1969). They were purified by standard procedures (Goodman *et al.*, 1976). Films

(0·6 mg cm^{-2}) of Li-, Na-, K- and Cs-saturated smectites were prepared by evaporating suspensions on to AgCl or Irtran 2 plates. The alkalis (analytical reagent grade LiOH, NaOH, KOH and CsOH) were used as 0·1M or 0·5M solutions prepared with freshly boiled water to minimize CO_2 content.

Methods

Alkali treatment. Appropriate volumes of the solutions of the various alkalis were added to air-dry films of the smectites and evaporated to dryness in a stream of nitrogen to minimize carbonate formation. Films were then transferred to the spectrometer sample compartment.

Hydrolysis treatment. Alkali-treated films of smectites were subjected to various treatments to reverse the effect of alkali: (a) washing with a 0·1M solution of the corresponding alkali chloride; (b) exposure to a mixture of 10% CO_2 in nitrogen at high humidity; (c) exposure to a flow of moist acetic acid vapour.

Infrared spectroscopy. IR spectra of the smectite films were recorded from 4000-200 cm^{-1} on a Perkin Elmer 577 spectrometer which was continuously purged with dry air containing substantially less CO_2 than normal air. Alkali-treated smectite films were relatively stable under these conditions.

RESULTS AND INTERPRETATION

Alkali hydroxide : nontronite ratio

Treatment of Na-nontronite with NaOH causes a colour change in the nontronite from yellow–green to red–brown, and leads to marked changes in IR spectra. Those shown by the Garfield specimen (Fig. 1) are typical of all the nontronites studied. All absorption bands are affected by the presence of the base, even at the lowest level used. Lesser amounts produced smaller shifts. The Si-O stretching at 1020 cm^{-1} shifts to 985 cm^{-1} with 5 and 10 mmol NaOH/g clay, to 970 cm^{-1} with 15 and to 950 cm^{-1} with 25 mmol/g, the band becoming progressively broader. Si-O-Si vibrations in the 500–400 cm^{-1} region are also modified, bands at 492, 427 and a shoulder near 450 cm^{-1} steadily coalescing to a broad diffuse band near 470 cm^{-1}. Perhaps even more striking is the effect on OH vibrations. The band due to OH deformation of FeFeOH groups at 818 cm^{-1} shifts to 811 cm^{-1} and becomes progressively weaker with increasing amounts of base, until at 15 mmol NaOH/g it is essentially absent. Bands near 840 cm^{-1} and 790 cm^{-1} previously assigned to Si-O apical (Russell *et al.*, 1979) and MgFeOH (Goodman *et al.*, 1976) also disappear. The OH stretching band near 3572 cm^{-1} shifts to 3544 cm^{-1} and becomes weaker, but at 15 mmol/g, when the 818 cm^{-1} band is absent, a medium intensity band still remains at 3535 cm^{-1}. This must be due to an OH stretching vibration of NaOH for which broad, more strongly hydrogen-bonded absorption steadily increases in intensity near 3000 cm^{-1}. The lack of the sharp absorption bands of crystalline NaOH in the spectrum of nontronite treated with 25 mmol NaOH/g and the complete absence of X-ray lines at 5·90 and 2·70 Å indicates that the excess NaOH is not present as a separate external phase, but is in the interlayer space. The presence of such an interlayer complex is indicated in the X-ray diffraction (XRD) pattern of Na-nontronite with 15 mmol NaOH/g by a rational series of orders out to $d(00,10)$ with a basal spacing of 15·00 Å,

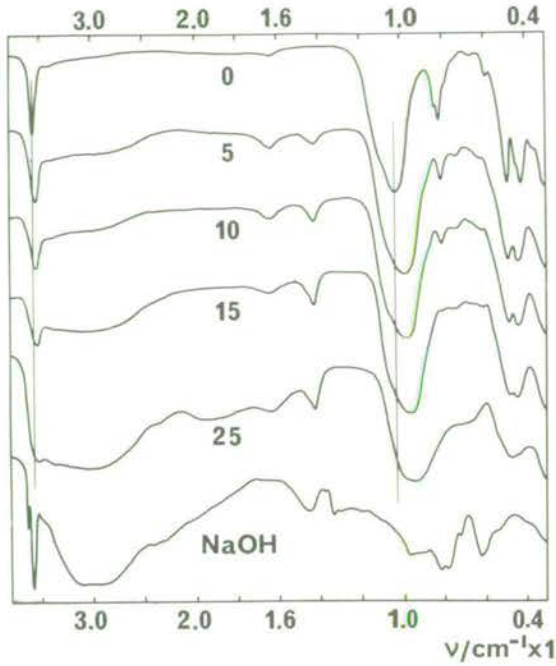

Fig. 1. IR spectra of films of Na-nontronite (Garfield) evaporated in N_2 in the presence of the indicated amounts of NaOH (mmol/g). The spectrum of solid NaOH in Nujol and Fluorolube (Nyquist & Kagel, 1971) is shown for comparison. *ν*-wavenumber

compared with 12·46 Å for the untreated Na-nontronite. This 15 Å spacing is consistent with a double layer containing Na^+, OH^- and H_2O molecules. Interaction between OH^- groups and H_2O causes a shift in the H_2O deformation band from 1630 cm^{-1} in the untreated nontronite to 1637 cm^{-1} for 5 and 10, and 1650 cm^{-1} for 15 mmol/g. A complex with a basal spacing of 14·87 Å was formed between NaOH and the least ferruginous of the montmorillonites studied (Otay) indicating that this is probably a general phenomenon that is independent of the iron content of the dioctahedral smectite.

The changes in Si-O and O-H bands described above are matched by marked effects on XRD and Mössbauer patterns. With increasing NaOH concentrations the 060 reflection becomes progressively weaker and broader indicating an irregular distortion of the layer structure, and also shifts markedly to higher spacings (Table 1) indicating an increase in the *ab* cell dimensions. The broadening is already obvious at 2 mmol alkali/g, before any significant shift is detectable. The Mössbauer spectrum showed a similar continuous change from that of the original (Fig. 2a) to that of the nontronite containing 15 mmol/g (Fig. 2b).

Effect of different alkali metal hydroxides

LiOH, NaOH, KOH and CsOH do not produce identical changes in IR spectra of the Garfield nontronite. At 5 mmol/g (Fig. 3), LiOH causes a decrease in intensity of OH stretching and bending bands but little or no shift in their frequencies or in those of the

TABLE 1. Values of d (060) for Koegas nontronite after treatment with NaOH and subsequent washing with 0·1M NaCl solution

NaOH (mmol/g)	d(060) (Å)	Washed with 0·1M NaCl
0	1·537	—
2	1·538	1·537
5	1·549	1·544
15	1·582	1·554

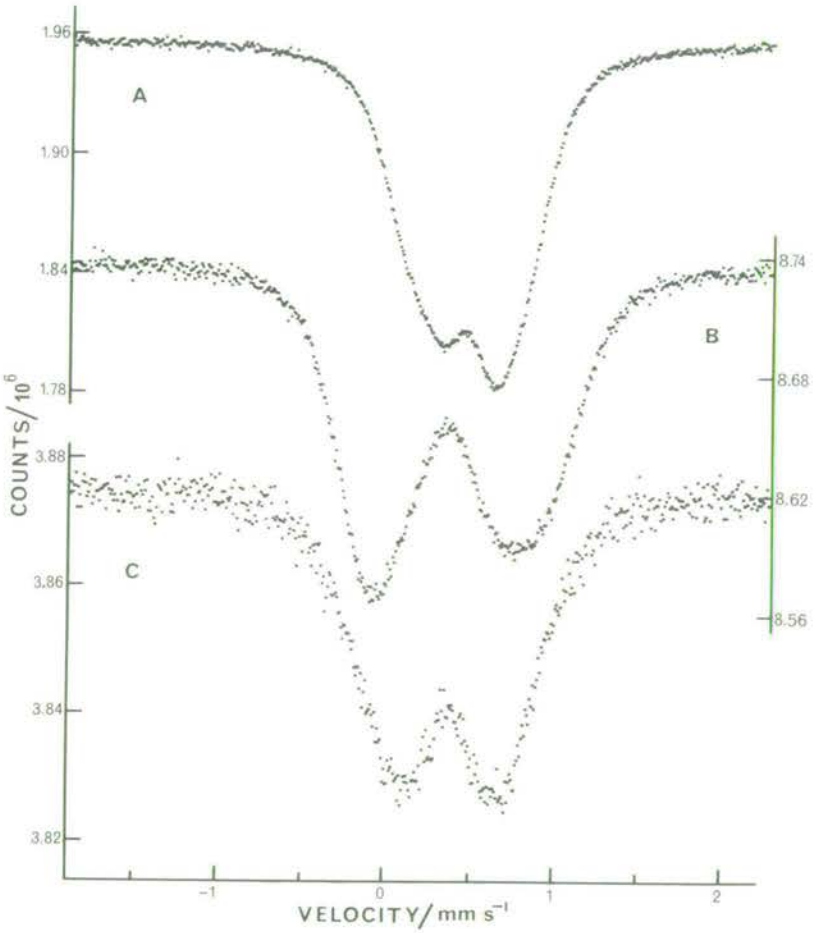

Fig. 2. Mössbauer spectra of Na-nontronite (Koegas) A, untreated; B, treated with 15 mmol NaOH/g; C, sample B washed with 0·1M NaCl solution. Spectra were recorded as described in Goodman *et al.* (1976).

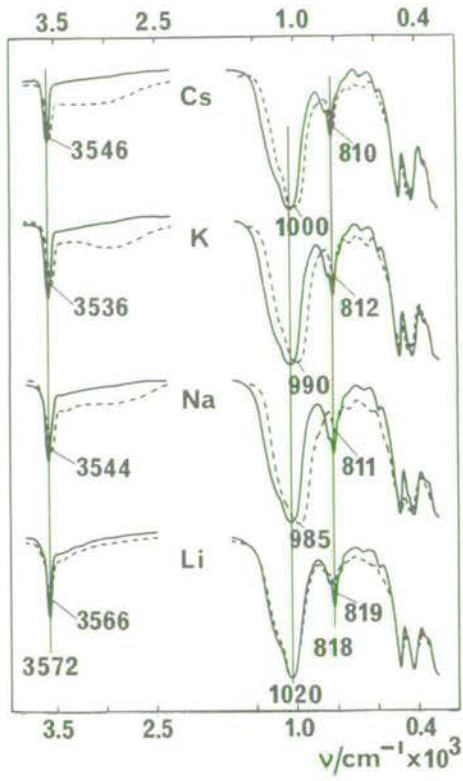

Fig. 3. IR spectra of films of Cs-, K-, Na- and Li-nontronite (Garfield) before (solid lines) and after (broken lines) evaporation in N_2 with 5 mmol/g of the corresponding alkali metal hydroxide.

Si-O bands at 1020, 492 and 427 cm^{-1}. In contrast, KOH and CsOH, like NaOH, produce large shifts in all of these bands, suggesting an effect specific to the larger cations. The shifts in Si-O bands for these cations follow the sequence Na > K > Cs which is the reverse of the order of increasing ionic radii. At 15 mmol/g, LiOH eliminated the 818 cm^{-1} OH deformation band, but shifted the Si-O stretch only 15–20 cm^{-1} to lower frequencies compared to 50 cm^{-1} for NaOH at this concentration (Fig. 1), and in keeping with this result the *b* dimension increased only slightly, the 060 reflection shifting from 1·537 Å to 1·539 Å compared with 1·582 Å for NaOH at 15 mmol/g (Table 1). The Mössbauer spectrum, however, shows an even wider splitting of the two major components than was observed for NaOH (Fig. 2b), indicating a more highly asymmetrical electric field gradient following LiOH treatment.

Reversibility

The spectral changes brought about by alkali at 2 mmol/g on nontronite are completely reversed by washing the nontronite film with water or dilute salt solutions, or by treatment with moist acetic acid vapour. Reversal becomes less complete for those nontronites treated with more alkali. At 5 mmol KOH on K-nontronite (Fig. 4), OH and

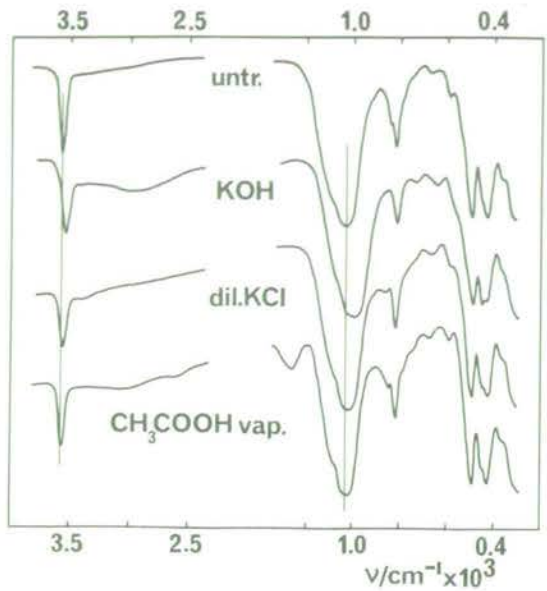

Fig. 4. IR spectra of film of K-nontronite (Garfield) treated in sequence with the indicated reagents, KOH at 5 mmol/g.

Si-O bands regain intensity and return to within a few wavenumbers of the original values of the untreated nontronite. When deuterated reagents were used in an analogous system structural OD groups were introduced into the nontronite lattice with absorption bands for OD stretch at 2640 cm^{-1} and FeFeOD bend at 615 cm^{-1} (Fig. 5) indicating that alkali

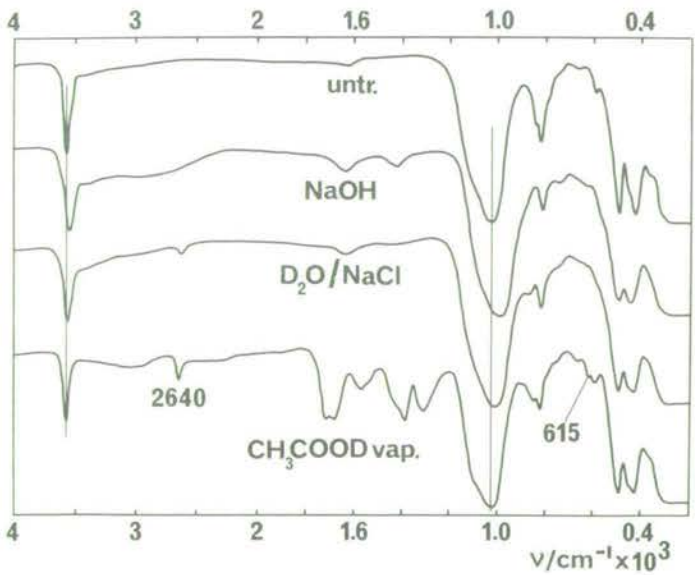

Fig. 5. IR spectra of film of Na-nontronite (Garfield) treated in sequence with the indicated reagents, NaOH at 5mmol/g.

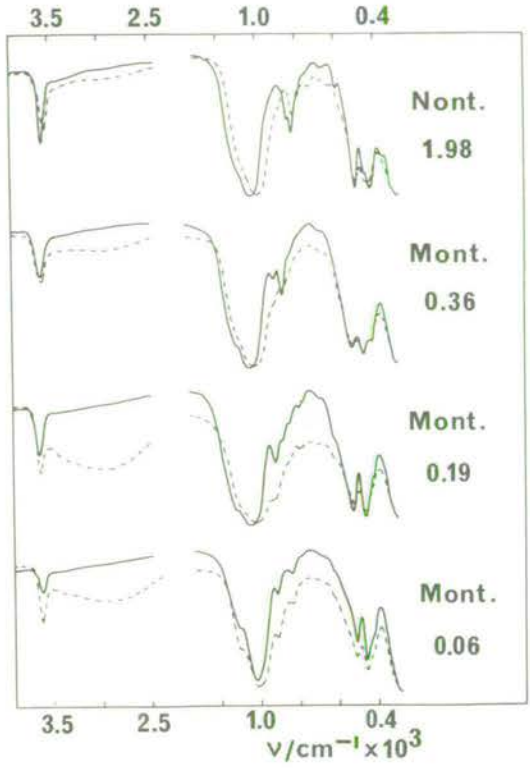

Fig. 6. IR spectra of films of Na-saturated smectites containing the indicated amounts of octahedral iron (atoms/$O_{10}(OH)_2$): solid curves before, broken curves after treatment with 5 mmol NaOH/g. Nont. 1·98–Garfield nontronite; Mont. 0·36–Woburn Fuller's Earth; Mont. 0·19–Wyoming montmorillonite; Mont. 0·06–Otay montmorillonite.

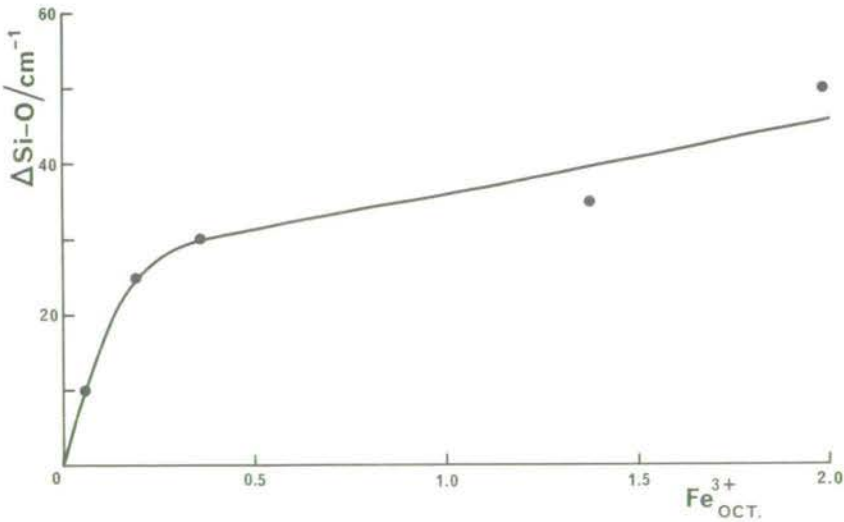

Fig. 7. Alkali-induced shifts in wavenumber (cm^{-1}) of the Si-O stretching vibration of smectites as a function of the half unit cell octahedral Fe^{3+} content.

had deprotonated structural OH groups. Reversal of the effect of alkali at 15 mmol/g is less complete than at 5 mmol/g, as judged by the failure of OH and Si-O bands to recover their original intensities or frequencies. This was particularly true of the band due to Si-O apical at 840–850 cm^{-1} (Russell *et al.*, 1979) which recovered only about 10–20% of its original absorbance.

The 060 spacings showed similar trends following washing of alkali-treated nontronite with salt solutions (Table 1). That for the nontronite containing 2 mmol/g regained its sharpness at 1·537 Å, while those for the nontronite containing 5 and 15 mmol/g shifted back towards the value of the untreated nontronite and became narrower and more intense. These changes are indicative of a tendency to re-ordering on removal of the alkali cation. Analogous changes were observed in Mössbauer spectra (Fig. 2b, c), leading to the conclusion that the higher concentrations of alkali produce some irreversible disordering of the nontronite structure.

Effect of NaOH on various smectites

The effect of alkali on other smectites has not been fully investigated, but spectral changes caused by NaOH at 5 mmol/g in ferruginous smectites are similar to those in nontronite (Fig. 6): deformation vibrations of OH coordinated to octahedral Fe^{3+}, near 870–890 cm^{-1}, disappear, and Si-O stretching bands shift to lower frequency. The OH groups in nontronite containing 1·98 Fe^{3+} per half unit cell are eliminated by 15 mmol NaOH/g. Proportionally, 5 mmol g^{-1} for the smectites with lower Fe^{3+} contents represents a considerable excess over Fe^{3+}–OH groups, and this accounts for the complete disappearance of bands due to these groups. A plot of the alkali-induced shifts in Si-O

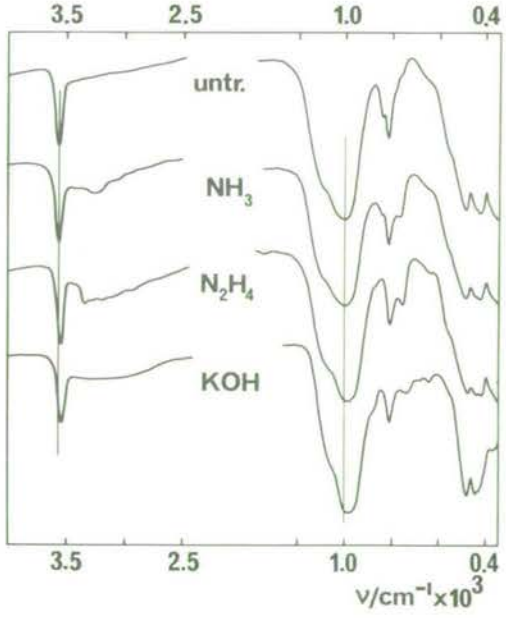

Fig. 8. IR spectra of film of K-nontronite (Koegas) before and after treatment with various bases: NH_3, N_2H_4-vapour for 24 h; KOH at 5 mmol/g.

stretching bands for the various smectites (Fig. 7) indicates that the size of the shift increases with increase in Fe^{3+} in octahedral coordination in the smectite.

Effects of other bases on nontronite

Similar, although less dramatic, shifts in absorption bands were observed following treatment of nontronite with ammonia or hydrazine vapours (Fig. 8). The former has a small effect on the OH deformation bands in the 820 cm^{-1} region, slightly decreasing intensities and frequencies, while the latter causes shifts in absorption bands of OH, and of Si-O bands near 1000 and 450 cm^{-1}, comparable with those produced by alkali. Hydrazine reduces only about 10% of the iron in nontronite, and this might account for some of the observed shifts, but the similarity between the spectra of the hydrazine- and the KOH-treated nontronite (Fig. 8) in both OH and Si-O vibrations suggests that these bases are producing the same effect.

DISCUSSION

A mechanism capable of explaining the results involves deprotonation of the structural OH groups by the alkali hydroxide under air-dry conditions as follows:

$$MOH + OH\ (\text{smectite}) \rightarrow M^{+}O^{-}\ (\text{smectite}) + H_2O$$

evaporation of the water produced by the reaction stabilizing the product. This mechanism is supported by the regeneration of OD groups when the reaction is reversed in the presence of deuterated reagents. The specificity of the deprotonation reaction to Fe^{3+}–OH groupings is presumably the result of the greater electron affinity of Fe^{3+} compared with Al^{3+} and Mg^{2+} and, therefore, the more acidic character of OH groups coordinated by Fe^{3+}.

Alternative mechanisms that have been proposed to explain shifts in frequency of structural OH groups caused by dehydration (Farmer, 1958; Russell & Farmer, 1964) are discounted because they do not give rise to loss of intensity of FeOH bands or to the large low-frequency shifts observed for Si-O vibrations.

Nontronites contain only about 4 mmol lattice OH groups per g (Goodman *et al.*, 1976), but require 15 mmol alkali hydroxide to remove them. The apparent non-stoichiometry of the reaction is due in part to the formation of carbonate which, although attempts were made to minimize it, could not be prevented at the higher levels of alkali, but more especially to the formation of a well-ordered 15 Å interlayer complex between the alkali and the nontronite. Formation of a complex with an almost identical spacing between NaOH and a montmorillonite of very low iron content (Cheto-type) indicates that the formation of such complexes may be general for alkalis and smectites which, to the author's knowledge, has not been reported previously.

To maintain electrical neutrality in the deprotonated nontronite, the alkali cations must be retained in the interlayer as close as possible to the oxide anions, thereby providing an explanation for the variation in effect of the different alkali hydroxides (Fig. 3) in terms of the ionic radii of the alkali metal cations in relation to the size of the hexagonal hole in the tetrahedral sheet. The Li ion because of its small size (0·78 Å radius) can approach the oxide ion through the hexagonal hole, neutralizing the negative charge with less disturbance of the positions of silicon or oxygen atoms in the tetrahedral sheet.

The larger Na, K and Cs ions (0·98, 1·33 and 1·65 Å radius respectively) cannot completely penetrate the hexagonal hole, but their approach to it is sufficiently close to perturb the Si-O framework, causing substantial low-frequency shifts of the principal Si-O stretching vibration. The order of these shifts, Na > K > Cs, is that anticipated for the order of penetration of these ions into the hexagonal hole. These shifts to lower frequencies contrast with those to higher frequency observed by Tettenhorst (1962) and Russell & Farmer (1964) for heated montmorillonites saturated with small exchangeable cations.

The migration of cations proposed here finds some support in the observed difference between Mössbauer spectra of LiOH- and NaOH-altered nontronite. The greater splitting of peaks in the former is consistent with a much more asymmetrical electric field gradient. This is presumably caused by the smaller Li ion approaching the deprotonated OH groups and localizing the negative charge there. The larger Na ion, being unable to penetrate the hexagonal hole, will attract the negative charge into the SiO_4 tetrahedron, distributing it more widely, and giving rise to a relatively more symmetrical electric field gradient. It appears that a deprotonation reaction of this type has not been reported previously in the literature. Its specificity to FeOH groups highlights another facet of the surface reactivity of dioctahedral smectites and provides a means by which they may be more completely characterized and their surface properties more fully understood.

ACKNOWLEDGMENTS

Thanks are due to Dr B.A. Goodman and Mr D.R. Clark for recording Mössbauer spectra and X-ray patterns respectively, to Mr A.R. Fraser for chemical analyses and to Drs V.C. Farmer and M.J. Wilson for helpful discussion of the work.

REFERENCES

Dudas M.J. & Harward M.E. (1971) *Soil Sci. Soc. Am. Proc.* **35**, 134.
Farmer V.C. (1958) *Miner. Mag.* **31**, 829.
Goodman B.A., Russell J.D., Fraser A.R. & Woodhams F.W.D. (1976) *Clays Clay Miner.* **24**, 53.
Hashimoto I. & Jackson M.L. (1960) *Clays Clay Miner.* **7**, 102.
Heller L., Farmer V.C., Mackenzie R.C., Mitchell B.D. & Taylor H.F.W. (1962) *Clay Miner. Bull.* **5**, 56.
Ingles D.G. (1970) *Aust. J. Soil Res.* **8**, 81.
Nyquist R.P. & Kagel R.O. (1971) *Infrared Spectra of Inorganic Compounds (3800–45 cm^{-1})*. Academic Press, New York.
Russell J.D. & Farmer V.C. (1964) *Clay Miner. Bull.* **5**, 443.
Russell J.D., Goodman B.A. & Fraser A.R. (1979) *Clays Clay Miner.* **27**, 63.
Schultz L.G. (1969) *Clays Clay Miner.* **17**, 115.
Tettenhorst R. (1962) *Am. Miner.* **47**, 769.
Volkov F.E., Zlochevskaya R.I. & Voronkevich S.D. (1976) *Vestn. Mosk. Univ., Geol.* **31**(3), 87.
Zhukova R.S., Kruglitskŭ N.N. & Glukovskŭ V.D. (1971) *Ukr. Khim. Zh.* **37**, 291.

RÉSUMÉ: La spectroscopie infrarouge a été utilisée pour étudier l'interaction des hydroxydes des métaux alcalins avec les smectites dioctaédriques de teneurs en fer comprises entre 0·7% (montmorillonite) à 22% (nontronite), en liaison avec la stabilisation alcaline des sols. Les résultats ont montré que les bases (LiOH, NaOH, KOH et CsOH) enlèvent les protons des groupements hydroxyle correspondant au fer ferrique octaédral, provoquant la distorsion des couches tétraédriques et octaédriques. Une modification marquée des spectres Mössbauer et une forte augmentation des dimensions de maille b viennent à l'appui de cette conception de la distorsion. La perturbation de la structure de la smectite, mise en évidence par les déplacements

des vibrations d'élongation de Si-O et O–H, est plus grande pour Na, K et Cs que pour Li, ce qui paraît indiquer que les cations les plus gros réagissent avec les oxygènes de surface autour du trou hexagonal. Les spectres infrarouge suggèrent que l'effet de NaOH sur la nontronite est nettement inversé en traitant la smectite avec du CO_2 ou des vapeurs d'acide acétique, ou en la lavant avec une solution saline diluée, bien que la spectroscopie Mössbauer et la diffraction des rayons X indiquent que la structure de la smectite régénérée est plus désordonnée que celle de l'original.

KURZREFERAT: Die IR-Spektroskopie wird angewendet, um in Verbindung mit der Alkalistabilisierung von Böden, die Wechselwirkung von Alkalimetallhydroxiden mit dioktaedrischen Smektiten zu studieren, wenn diese Eisengehalte von 0·7% (Montmorillonit) bis 22% (Nontronit) haben. Die Ergebnisse haben gezeigt, daß die Alkalien (Li OH, NaOH, KOH und CsOH) Hydroxylgruppen deprotonieren, wenn diese mit oktaedrischem 3-wertigen Eisen koordiniert sind und hierbei tetraedrische und oktaedrische Schichten verzerren. Unterstützt wird dieses Konzept einer solchen Verzerrung durch die auffallende Änderung im Mössbauer Spektrum und durch eine große Zunahme von b der Elementarzelle. Die Störung der Smektitstruktur, wie sie sich durch Verschiebung der Si-O und O–H Streckschwingungen bemerkbar macht, ist für Na, K und Cs größer als für Li, was vermuten läßt, daß die größerene Kationen von den Oberflächensauerstoffen um das hexagonale Loch entsprechend beeinflußt werden. IR Spektren lassen vermüten, daß die Wirkung von NaOH auf Nontronit ganz wesentlich aufgehoben wird, wenn der Smektit mit CO_2 oder Essigsäuredampf oder durch Waschen mit verdünnten Salzlösungen behandelt wird obgleich Mössbauer-Spektroskopie und Röntgendiffraktometrie anzeigen, daß die Struktur des regenerierten Smektits ungeordneter ist als die des ursprünglichen.

RESUMEN: Se ha empleado la espectroscopia de rayos infrarrojos para estudiar la interacción de hidróxidos de metales alcalinos con esmectitas dioctaédricas que tenían contenidos de hierro de 0·7% (montmorillonita) a 22% (nontronita), en relación con la estabilización de álcalis de los suelos. Los resultados han demostrado que los grupos deprotonados de álcalis (LiOH, NaOH, KOH y CsOH) see coordinaban en ion férrico octaédrico, causando distorsión de las capas tetraédricas y octaédricas. Este concepto de distorsión se ve apoyado por un notable cambio en los espectros de Mössbauer y un gran aumento de las dimensiones de la célula *b*. La perturbación de la estructura de la esmectita, puesta de manifiesto por desplazamientos en las vibraciones de estiramiento de Si-O y O-H, es mayor en el caso de Na, K y Cs que en el de Li, lo que sugiere que los cationes más grandes ejercen interacción con los de oxígeno de la superficie en torno al agujero hexagonal. Los espectros de infrarrojos sugieren que el efecto de NaOH en la nontronita se invierte tratando la esmectita con CO_2 o vapores de ácido acético, o lavándola con solución de sal diluída, aunquela espectroscopia de Mössbauer y la difracción de rayos X indican que la estructura de la esmectita regenerada es más desordenada que la de la original.

STRUCTURAL STUDIES ON SOIL POLYSACCHARIDE

M. V. CHESHIRE, J. M. BRACEWELL, C. M. MUNDIE, G. W. ROBERTSON, J. D. RUSSELL and A. R. FRASER

(The Macaulay Institute for Soil Research, Craigiebuckler, Aberdeen AB9 2QJ)

Summary

The polysaccharide extracted by alkali from a Countesswells series soil has been fully methylated and the hydrolysis products identified by GC–MS. The parent neutral sugars are galactose, glucose, mannose, arabinose, xylose, fucose and rhamnose and these constitute about 40 per cent of the polysaccharide. The analysis shows that hexose components are predominantly present in $1 \rightarrow 3$ and $1 \rightarrow 4$ linkages and pentose sugar in $1 \rightarrow 4$ linkages. About 20 per cent of the residues were in branching positions.

From the number of non-reducing terminal groups present the average molecular weight of the methylated material has been calculated to be about 1460 compared with a value of 2700 obtained by vapour pressure osmometry. This contrasts with much higher values reported for unmethylated soil polysaccharides.

The mixture of derivatives obtained supports the concept that soil polysaccharide originates in both plants and microorganisms.

Introduction

A WELL-KNOWN method of establishing the chemical structure of polysaccharide involves methylation followed by identification of the methylated sugars released on subsequent hydrolysis, but to enable the information acquired from the analysis of the methylation pattern to be fully interpreted, polysaccharides must be homogeneous. Although numerous attempts at fractionation of soil polysaccharide have been unsuccessful in separating polymers with compositions distinct from the unfractionated material, it is almost certain that soil polysaccharide is not homogeneous.

In spite of these difficulties it was thought that a structural study would be worthwhile because it should at least give an estimate of the degree of branching and show which types of linkage predominate.

Materials and methods

Soil

Soil of the Countesswells series developed on till derived from acid igneous rocks (Glentworth and Muir, 1963) was sampled to a depth of 25 cm. It was air-dried at 20 °C and screened through a 2 mm sieve.

Extraction and isolation of the soil polysaccharide

Soil (1 kg) in a glass jar was ball-milled for 1 h with 10 dm^3 0.1M HCl and allowed to stand for 15 h. The clear supernatant extract was decanted, discarded, and the residue milled for 1 h with 10 dm^3 0.2M NaOH and allowed to stand for 15 h. The suspension was centrifuged in an Alpha Laval centrifugal separator (10,000 *g*) and the supernatant solution filtered through a x3 porosity sintered glass filter to

remove floating debris. The solution was acidified by the addition of 600 cm^3 6M HCl; the precipitated humic acid was removed by centrifuging at 2000 *g* and the supernatant solution of fulvic acid was applied to a column 800 x 50 mm of Polyclar: Celite 1 : 1. The fulvic acid solution was pumped upwards through the column at about 3 cm^3 per min using an LKB Perpex pump. Much of the colour of the fulvic acid was retained on the column and the eluate, which contained most of the polysaccharide, was light yellow. Unadsorbed fulvic acid solution was displaced from the column by 1 dm^3 0.1M HCl and added to the eluate. The column was then restored for use by eluting with 0.2M NaOH until most of the coloured matter had been desorbed, and then with 0.1M HCl.

After the polysaccharide-containing eluate had been neutralized with NaOH to pH 7.0 and the precipitate of aluminium and iron hydroxides removed by centrifuging at 2000 *g* and decanting, the supernatant liquid (12 l) was concentrated to about 1 l by rotary evaporator at <40 °C, at which point some sodium chloride crystallized. Powdered disodium EDTA (7 g) was added to the suspension which was then dialysed against 5 dm^3 water containing 50 g disodium EDTA. After 24 h the outer EDTA solution was renewed, left a further 24 h and thereafter replaced daily by water for a week. This treatment removed some of the cations which might interfere later. If EDTA were omitted, the polysaccharide obtained by ethanol precipitation could not subsequently be completely redissolved, the undissolved matter being rich in Fe, Al and Si.

The dialysed fulvic polysaccharide fraction was evaporated to about 300 cm^3 and the polysaccharide precipitated by the addition of 3 volumes of ethanol. The precipitate was collected by centrifuging and decanting the supernatant. Excess ethanol was allowed to evaporate and the polysaccharide, dissolved in the minimum of water, freeze-dried. The average yield of polysaccharide was 0.137 per cent of the soil or 1.8 per cent of the soil organic matter. The reducing sugar content of the polysaccharide accounted for 2.6 per cent of the total soil reducing sugar as determined by alkaline ferricyanide.

Hydrolysis of soil and polysaccharides

Two methods of hydrolysis were employed. One, with 12M H_2SO_4 and 0.5M H_2SO_4 as described by Cheshire *et al.* (1974), was used for soil and polysaccharide and the other, in which about 10 mg polysaccharide was heated at 120 °C with 0.5 cm^3 0.2M trifluoracetic acid for 1 h in a sealed tube, was used for polysaccharide only.

Sugar analysis

Total reducing sugar content of hydrolysates was determined with alkaline ferricyanide (Hoffman, 1937) using a glucose standard in an Auto Analyzer, and the value quoted in Table 1 is expressed as glucose equivalent.

Amounts of individual sugars in hydrolysates were determined by gas liquid chromatography of the alditol acetates using *myo* inositol as an internal standard (Cheshire *et al.*, 1973).

Infrared absorption spectroscopy

Solid samples (0.8 mg) were incorporated in 12 mm diameter KBr pressed disks which were heated at 150 °C for 16 h to remove adsorbed water. Liquid samples were in the form of capillary films between KBr plates. Spectra were recorded from 4000 to 200 cm^{-1} in a Perkin-Elmer 577 spectrometer.

NMR spectroscopy

NMR spectroscopy was performed in a Perkin-Elmer R12B spectrometer using naphthalene as an internal standard.

Methoxyl group determination

Methoxyl groups were determined by the Zeisel method as described by Belcher and Godbert (1954).

Vapour pressure osmometry

This was performed on the methylated polysaccharide using a Knauer osmometer.

Experimental

Methylation of the polysaccharide

Polysaccharide dried over P_2O_5 at 35 °C (0.5 g) was methylated by the procedure of Hakomori (1964), modified as described by Conrad (1972). It was suspended in dry, redistilled dimethylsulphoxide (50 cm^3) under N_2 and the suspension heated at 60 °C with stirring until the polysaccharide had dissolved. This usually took about 1.5 h. After cooling the solution to 25 °C the methylsulphinyl anion (15 cm^3), prepared from 1 g sodium hydride and 15 cm^3 dry, redistilled dimethylsulphoxide, was added and the viscous mixture which resulted was stirred for 1 h. The solution was then cooled to 20 °C and three 1 cm^3 portions of methyl iodide added over a period of 8 min. The solution, which became less viscous, was stirred for 1 h before being dialysed against running tap water for 64 h. The small amount of precipitate formed was removed from suspension by centrifuging. The supernatant solution was evaporated to about 50 cm^3 and the mineral oil introduced with the sodium hydride removed by extraction in a Soxhlet apparatus with redistilled hexane for 24 h. The aqueous solution was then extracted with redistilled chloroform in a liquid–liquid extractor and the aqueous and chloroform phases treated as described below.

The chloroform-soluble material from three such methylations was combined and dissolved in 3 cm^3 redistilled dimethylformamide and 4 cm^3 methyl iodide, then 4 g silver oxide was added. The mixture was maintained at 50 °C for 5 h then left at 20 °C for a further 16 h. The solid matter was filtered from the reaction mixture, washed with redistilled acetone and discarded. The washings were combined with the filtrate which was evaporated to dryness. The residue, resuspended in water, was extracted with redistilled chloroform.

The chloroform-insoluble material which remained in the aqueous phase in the three methylations was combined, dried, and resubmitted to the methylation procedure described.

Treatment with diborane to remove carboxyl groups

In the fully methylated polysaccharide prepared as described above, ester groups are present. These were saponified by treatment with 0.01M NaOH at 3 °C for 3 h and the sodium ion removed by applying the solution to a small column of IR 120(H) resin. This treatment was repeated and the solution evaporated to dryness.

About 10 mg of the produce was reacted under N_2 with 1 cm^3 1M diborane in tetrahydrofuran stabilized with 5 per cent sodium borohydride. After 24 h an

additional 1 cm^3 diborane solution was added and the reaction allowed to proceed for a further 24 h. The solution was then diluted with methanol and evaporated to dryness. Two more evaporations of added methanol were performed to remove boric acid as methyl borate. This procedure is a modification of that described by Talmadge *et al.* (1973).

Analysis of the hydrolysis products of the fully methylated polysaccharide and its decarboxylation product

After hydrolysis of the polysaccharide by trifluoracetic acid, the hydrolysate was evaporated to dryness and reduced by treatment with 0.1 g sodium borohydride in aqueous solution. Excess sodium borohydride was destroyed by treatment with acetic acid and boric acid removed as methylborate by repeated additions, followed by evaporation to dryness, of 10 per cent acetic acid in methanol.

Separation and identification of the partially methylated alditol acetates

Gas chromatographic analysis was performed using two columns; (a) a 1.5 m x 5 mm i.d. glass column packed with 3 per cent w/w ECNSS-M on 100–120 mesh gas chrom Q and (b) a 15 m x 0.5 mm i.d. glass support coated open tubular column (S. C. O. T) of silicone OV-225 on fine diatomaceous earth. For quantitative estimation of the acetates using a flame ionization detector, the temperature was 160 °C and the nitrogen flow rate 30 cm^3 per min with column (a), and 2 cm^3 per min with column (b). Most peaks were integrated using an Infotronics CRS 309, but minor peaks were estimated by triangulation.

Identifications were made by a combination of GLC retention time and mass spectra obtained by GC-MS using the principles given by Bjorndal *et al.* (1970). The mass spectra and retention times of known, partially methylated standard derivatives of each of the seven sugars were identified for standardization. In addition, an aliquot of the samples was reduced with sodium borodeuteride to give a deuterium label on carbon 1, a procedure that proved useful in identifying the source of several fragment ions in the mass spectra. The instruments used were a VG MM12B single focussing (VG Organic Ltd.) and an MS 30 double focussing (AEI/Kratos Ltd.) mass spectrometers, which were interfaced to the chromatograph through jet separators. Spectra were scanned at 70eV electron impact energy.

Results

Characteristics of the isolated polysaccharide

The polysaccharide was a creamy white powder easily soluble in water. It had 36 per cent reducing sugar content and, besides neutral sugars, contained both uronic acids and amino sugars. Its sugar composition is shown in Table 1.

Small amounts of dicarboxylic acids including succinic, fumaric, malic and levulinic acids, were present in the hydrolysate. Amino acids were also present. Identified components accounted for only about 60 per cent of the material but the nature of the remainder is not known. Although hydrolysis is considered to destroy some of the uronic acid (Swincer *et al.*, 1968), this is probably not the explanation for the unaccounted material, because there was no measurable release of CO_2 during hydrolysis.

The infrared spectrum of the polysaccharide (Fig 1a) shows, in addition to the intense C–O stretching bands near 1000 cm^{-1} typical of carbohydrates, broad

TABLE 1
Composition of the isolated soil polysaccharide

Carbon %	*Nitrogen* %	*Hydrogen* %	*Phosphorus* %	*Sulphur* %	*Ash* %	*Reducing sugar content (ferricyanide method)* %
39.4	3.85	5.61	0.17	0.05	0.88	36.2

Sugar Residues

galactose %	*glucose* %	*mannose* %	*arabinose* %	*xylose* %	*rhamnose* %	*fucose* %	*glucosamine* %	*galactosamine* %	*glucuronic acid* %	*galacturonic acid* %
5.0	9.7	3.7	2.5	5.1	2.2	1.2	2.3	2.6	2.3	2.4

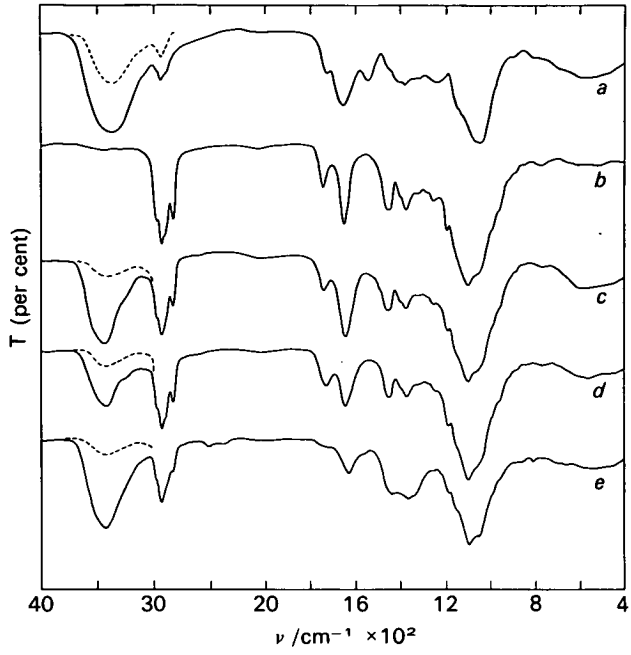

FIG. 1. Infrared absorption spectrum of KBr pressed disks (k) or capillary films (f) of soil polysaccharides: *a*, as isolated (k); *b*, fully methylated, $CHCl_3$-soluble (f); *c*, incompletely methylated, $CHCl_3$-insoluble (k); *d*, methylated then saponified, acid form (k); *e*, methylated, saponified then reduced (k). Broken curves refer to disks heated 16 h at 150 °C to remove adsorbed water. Absorption bands near 2400 and 1400 cm^{-1} in *e* arise from borate produced during the reduction with diborane. ν; wavenumber: T; transmission.

absorption near 2500–2700 cm^{-1} and bands at 1725 and 1230 cm^{-1} characteristic of carboxylic acid groups. The frequencies agree well with those observed for other acidic polysaccharides such as pectic acid. The spectrum also shows bands at 3080, 1655 and 1540 cm^{-1} indicative of secondary amide groups. Weak bands at 895, 805 and 800–750 cm^{-1} are not inconsistent with the presence of β-anomers in the polysaccharide (Barker *et al.*, 1954).

Methylation

Methylation of the polysaccharide was monitored by infrared spectroscopy and by determination of the methoxyl content at various stages. After a single methylation with methylsulphinyl anion and methyl iodide, analysis of the chloroform-soluble material, which was obtained in 23 per cent yield (equivalent to 16 per cent of the starting material), showed a methoxyl content of 30.1 per cent. After a further methylation with methyl iodide/silver oxide in dimethylformamide the methoxyl content was not significantly changed (30.4 per cent). As judged from the weakness of absorption in the OH stretching region of the IR spectrum (3500–3300 cm^{-1}), methylation is well advanced after the first treatment and is complete after the second (Fig. 1b). OH stretching bands are absent and strong ether bands from C–O–CH_3 groups are visible at 1100–1200 cm^{-1}. Absorption bands arising from C–H deformation of O–CH_3 groups and C=O stretch of methyl esters occur

at 1440–1460 cm^{-1} and 1740 cm^{-1}, respectively. The strong band at 1650 cm^{-1} is the C=O stretch of tertiary amide $-CO-N(CH_3)-$ (Bellamy, 1975) resulting from methylation of secondary amides.

The material insoluble in chloroform after the first methylation, 20 per cent (equivalent to 16 per cent of the polysaccharide), contained only 19.3 per cent methoxyl and the infrared spectrum clearly showed that the sample still contained a proportion of OH groups absorbing at about 3360 cm^{-1} and broad absorption near 1040 cm^{-1} arising from unmethylated polysaccharide (Fig. 1c). On re-methylation, a further 6 per cent of chloroform-soluble material was obtained which had a methoxyl content of 30.0 per cent and an infrared spectrum indistinguishable from that of the original $CHCl_3$-soluble methylated fraction (Fig. 1b). The overall recovery of chloroform-soluble methylated polysaccharide was 29 per cent, equivalent to 20 per cent of the polysaccharide.

A typical NMR spectrum of the fully methylated polysaccharide is shown in Fig. 2. Quantitative analysis of the spectrum in the region 3.25–3.75 ppm for two samples gave H contents of 3.483 and 3.548 equivalent to 35.98 and 36.66 per cent methoxyl respectively. Total hydrogen contents of 6.3 and 6.7 per cent were calculated for the 1–5 ppm region of the spectrum. On shaking the sample with a small amount of D_2O only one of the peaks, a minor one at 1.9 ppm, was affected (Fig. 2b). Absorption in the region 3.25–3.75 ppm was completely unaffected showing the absence of alcoholic hydroxyl groups.

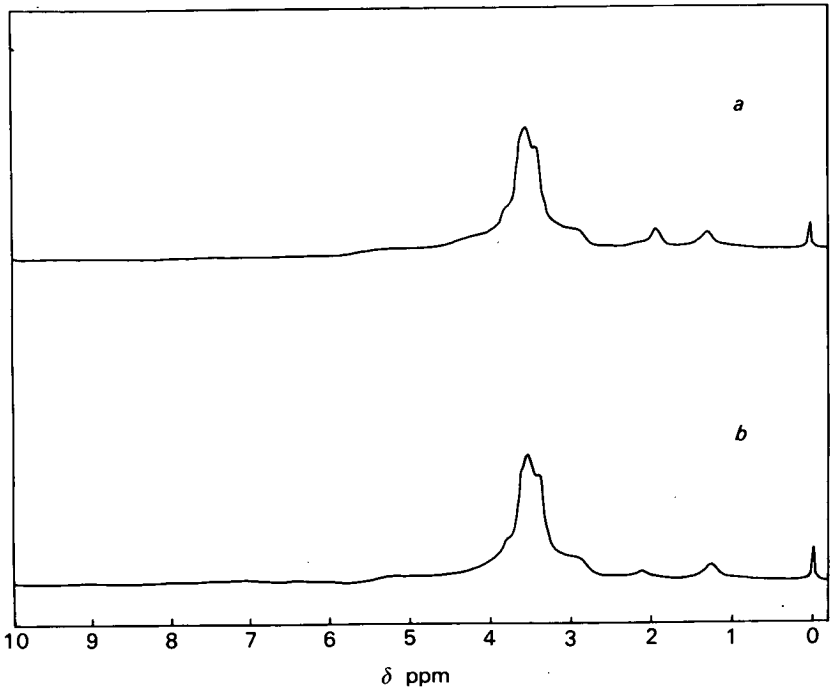

FIG. 2. NMR spectrum of fully methylated soil polysaccharide: *a*, In chloroform; *b*, After shaking with D_2O.

TABLE 2

Relative molar proportions of sugars obtained on hydrolysis of methylated soil polysaccharide

Relative retention time OV225	*Designation of methoxy derivatives*	*Relative molar proportion*	*Possible original structure*
55	2,3,5-Ara	2.7	terminal Ara (f)*
64	2,3,5-Xyl	3.7	terminal Xyl (f)
64	2,3,4-Rha	3.1	terminal Rha
64	2,3,4-Ara	0.6	terminal Ara (p)**
64	2,3,4-Xyl	4.3	terminal Xyl (p)
69	2,3,4-Fuc	1.3	terminal Fuc
69	3,5-Ara/Xyl	3.3	1→2 Ara (f)/Xyl (f)
74	2,5-Ara/Xyl	0.4	1→3 Ara (f)/Xyl (f)
74	3,4-Rha/Fuc	0.9	1→2 Rha/Fuc
87	2,3-Rha	0.8	1→4 Rha
87	2,4-Rha	1.4	1→3 Rha
87	2,4-Ara/Xyl	1.0	1→3 Ara (p)/Xyl (p)
87	2,3-Ara	1.9	1→4 Ara (p) or 1→5 Ara (f)
87	2,3-Fuc	0.4	1→4 Fuc
87	2,3-Xyl	12.0	1→4 Xyl (p)
100	2.3.4.6-Glc/Man	7.0	terminal Glc/Man
106	2,3,4,6-Gal	7.0	terminal Gal
114	2-Rha/Fuc	1.4	1→3 and 1→4 branched Rha/Fuc
114	4-Rha/Fuc	0.5	1→2 and 1→3 branched Rha/Fuc
114	3-Rha/Fuc	0.6	1→2 and 1→4 branched Rha/Fuc
114	2-Ara/Xyl	3.0	1→3 and 1→4 branched Xyl (p)/Ara (p) 1→3 and 1→5 branched Ara (f)
114	3-Ara/Xyl	0.7	1→2 and 1→4 branched Xyl (p)/Ara (p) 1→2 and 1→5 branched Ara (f)
137	2,4,6-Glc	6.7	1→3 Glc
137	3,4,6-Glc and/or Man	6.6	1→2 Glc and/or Man
137	2,4,6-Man	1.0	1→3 Man
143	2,3,6-Man	2.5	1→4 Man
143	2,4,6-Gal	2.5	1→3 Gal
143	2,3,6-Gal	1.2	1→4 Gal
143	2,3,4-Glc	1.2	1→6 Glc/Man
143	2,3,6-Glc	6.4	1→4 Glc
154	2,3,4-Gal	1.6	1→6 Gal
176	4,6-Man/Gal	1.4	1→2 and 1→3 branched Man/Gal
176	2,6-Gal/Man	1.4	1→3 and 1→4 branched Gal/Man
176	2,6-Glc/Man	1.4	1→3 and 1→4 branched Glc/Man
188	3,6-Glc/Gal/Man	2.5	1→2 and 1→4 branched Glc/Gal/Man
204	2,3-Man	1.5	1→4 and 1→6 branched Man
215	2,4-Glc	1.9	1→3 and 1→6 branched Glc
222	2,4-Man	0.3	1→3 and 1→6 branched Man
222	2,3-Glc	0.2	1→4 and 1→6 branched Glc
222	2,3-Gal	0.9	1→4 and 1→6 branched Gal
236	2,4-Gal	0.5	1→3 and 1→6 branched Gal

* (f) furanose.
** (p) pyranose.

Reduction of COOH groups

Saponification of the fully methylated polysaccharide required two treatments with alkali to hydrolyse all the ester groups as judged by the replacement of the infrared 1740 cm^{-1} C=O ester band by the COOH band at 1730 cm^{-1} (Fig. 1d). The recovery of saponified material was 76 per cent. On treatment with diborane almost complete removal of the COOH group was indicated by a considerable reduction in the intensity of the 1730 cm^{-1} and 1230 cm^{-1} bands (Fig. 1e).

Analysis of methylated sugars

The relative retention times and amounts of the alditol acetates obtained on GLC of the methylated and hydrolysed polysaccharide are shown in Table 2 which also includes the assignments made.

The relative proportions of the sugars have been expressed on a molar basis by use of the Effective Carbon Response theory (Sweet *et al.*, 1975). The methylated sugars identified in the hydrolysate confirm the complex composition shown in Table 1, the ratio of hexose to pentose to deoxyhexose by weight being 5.9:3.0:1 compared with 5.4:2.2:1 for the analysis of sugars. The percentages of the various types of linkage are given in Table 3. With the hexose components, methylated sugars corresponding to (1 → 3) and (1 → 4) linkages predominate. In each case the contribution from glucose is about 65 per cent of the total. Galactose makes the greatest contribution to the (1 → 6) linkages. With the pentose components there is a

TABLE 3
The percentage of various linkages indicated to be present in soil polysaccharides

Sugar linkage	*per cent*
Hexose	
1→2	6.6
1→3	10.2
1→4	10.1
1→6	2.8
1→2 and 1→3	1.4
1→2 and 1→4	2.5
1→3 and 1→4	2.8
1→3 and 1→6	2.7
1→4 and 1→6	2.6
Pentose	
1→2	3.3
1→3	1.4
1→4	13.9
1→3 and 1→4 or 5	3.0
1→2 and 1→4 or 5	0.7
Deoxyhexose	
1→2	0.9
1→3	1.4
1→4	1.2
1→2 and 1→3	0.5
1→2 and 1→4	0.6
1→3 and 1→4	1.4

comparatively large contribution from xylose in (1 → 4) linkage. The three types of bonds observed for deoxyhexoses occurred in similar amounts.

Unfortunately, because of very similar or identical retention times, not all the sugars could be separated. Xylose was present in both pyranose and furanose form because both 2,3,5-and 2,3,4-tri-methoxy xylitol acetate were identified in the hydrolysate in almost equal proportions. Much more arabinose was in the furanose than pyranose form.

No measurable difference in the amounts of methylated hexose derivatives was observed following treatment of the methylated polysaccharide with diborane to reduce carboxyl groups – a procedure that would have converted uronic acids to derivatives corresponding to (1 → 6) linked branched hexoses. This is in agreement with the small contribution made by uronic acid to the polysaccharide.

Substituted sugars representing terminal units accounted for 42 per cent of the sugars in the deoxyhexoses, 34 per cent in the pentoses and 25 per cent in the hexoses. The deoxyhexoses also had the greatest number of branching units, 24 per cent. The hexose branching units amounted to 21 per cent and the pentose, 11 per cent. From these values it is possible to calculate average molecular weights, and these are 660 for pentoses, 900 for deoxyhexoses and 5000 for hexoses. However, this assumes some degree of homogeneity, which may not exist. The overall average molecular weight comes to about 1460, equivalent to a molecule containing about 9 sugar residues. Values for the molecular weight of the fully methylated polysaccharide obtained by vapour pressure osmometry were in the region of 2700 confirming the order of magnitude of the value calculated from the fragmentation study. It is most likely that a mixture of polysaccharides of heterogeneous composition and with a range of molecular weights is present.

Discussion

Very few structural studies on carbohydrate components of soil have been reported. Majumda *et al.* (1974) isolated on oligosaccharide from the fulvic acid of an Indian soil rich in plant remains and, by periodate oxidation studies, established that five sugars were present in the sequence D-galacturonic-(1 → 3)-D-mannose-(1 → 3)-D-xylose-(1 → 3)-D-galactose-(1 → 3)-L-arabinose. This structure has not been encountered elsewhere in nature.

Partial hydrolysis of mineral soil with 0.05M H_2SO_4 or 1M acetic acid has liberated oligosaccharides which included 1 → 4 linked xylobiose and xylotriose (McGrath, 1973). These are probably derived from (1 → 4)-xylans of plant residues. Forsyth (1950) found that heating a solution of a peat polysaccharide in water was sufficient to release most of the constituent arabinose and some of the ribose. He concluded that the arabinose was attached to the polysaccharide by furanoside linkages.

Enzymic hydrolysis of a high molecular weight polysaccharide from an organic soil by an α-L-rhamnosidase (Barker *et al.*, 1967) released between 25 and 50 per cent of the rhamnose, leading to the conclusion that this sugar was present in α-linked end groups.

All the types of linkage observed by other workers have been observed in the methylation study of the soil polysaccharide isolated by us, but no information can be derived to show the sugars between which the linkages occur. Infrared data does suggest, however, that the anomeric form of these linkages is predominantly β. It is most likely that a large part of the xylose and glucose is present in linear chains of (1 → 4) linked units, since these are what would be expected from plant xylan and

glucan, known to be part of the soil polysaccharide. In plants, xylan side chains are frequently attached to either position 2 or 3 (Albersheim, 1976). Arabinose residues in plant cell walls are in highly branched polymers, the glycoside linkage being $1 \rightarrow 3$ and $1 \rightarrow 5$.

The hexose components of the plant cell wall are bonded with $1 \rightarrow 3$, $1 \rightarrow 4$, or $1 \rightarrow 6$ linkages and branching is quite common, particularly with galactans. In the plant, most polysaccharides are heterogeneous, containing two or more different sugars (examples are xyloglucan, arabinogalactan and galactoarabinoxylan), and this is possibly the form of a large part of the soil polysaccharide.

The polysaccharide of microorganisms, which must also contribute to the soil polysaccharide, shows a much more varied range of structures (Stacey and Barker, 1960; Gorin and Spencer, 1968). Hexose linkages frequently occurring are $1 \rightarrow 4$, $1 \rightarrow 3$ and $1 \rightarrow 6$ and often the polysaccharides are branched. Most species of fungi have a chitin-glucan cell wall composition, with $\beta(1 \rightarrow 3)$ the most common linkage in the glucan (Bartnicki–Garcia, 1968). Glucose also occurs in $\beta(1 \rightarrow 4)$ linked polymers such as cellulose, in $\alpha(1 \rightarrow 4)$ linked polymers such as glycogen and pullulan and also in $\beta(1 \rightarrow 3)$ and $\beta(1 \rightarrow 6)$ linked structures. Mannose occurs in mannan with both $\alpha(1 \rightarrow 2)$ and $\alpha(1 \rightarrow 6)$ linkages or $\beta(1 \rightarrow 3)$ and $\beta(1 \rightarrow 4)$ linkages, whereas galactose occurs in galactomannans and other heteropolymers. *Arthrobacter* and *Pseudomonas* species are the predominant bacteria in arable soils (Hepper, 1975) whilst *Flavobacterum* and *Achromobacter* are also common. *Bacillus* species are said to predominate in fallow soil. Polysaccharides produced by these organisms usually have hexose, deoxyhexose and uronic constituents. For example a polysaccharide containing glucose, mannose and glucuronic acid is synthesised by some *Bacillus* species (Forsyth and Webley, 1949). There is a dearth of information about pentose components because these are not often encountered in the polysaccharide of microorganisms but xylose occurs in $1 \rightarrow 4$ linkage in some yeasts.

It is clear from these considerations that the linkages present are not inconsistent with the presence of both plant and microbial, particularly fungal, polysaccharides.

The molecular weights obtained for the methylated soil polysaccharide are low compared with values of $5–43 \times 10^4$ for various soil polysaccharide preparations (Bernier, 1958; Mortensen, 1960; Finch *et al.*, 1966), suggesting that the methylation procedure leads to a partial hydrolysis. Alternatively, the higher values may be the result of association of molecules by weak chemical bonding not involving glycosidic linkages.

It is concluded that the mixture of methylated sugars which was found support the concept of soil polysaccharide as a mixture of polysaccharides of diverse composition and structure. It is intended to apply methylation and hydrolysis to fractions of soil polysaccharide in the hope of being able to identify different polysaccharides which it has not been possible to distinguish simply by their sugar composition.

Acknowledgements

We wish to thank Dr. Bryon Bache for the osmometry data, Robert Gordon's Institute of Technology for access to NMR equipment, and the Food Research Institute for part of the GC–MS analysis.

REFERENCES

ALBERSHEIM, P. 1976. The primary cell wall. In *Plant biochemistry* (eds J. Bonner and J. E. Varner), Chapter 9. London: Academic Press.

BARKER, S. A., BOURNE, E. J., STEPHENS, R., and WHIFFEN, D. H. 1954. Infrared spectra

of carbohydrates. Part II. Anomeric configuration of some hexo and pento-pyranoses. J. chem. Soc. 3468–73.

——, HAYES, M. H. B., SIMMONDS, R. G., and STACEY, M. 1967. Studies on soil polysaccharides. I. Carbohydrate Res. 5, 13–24.

BARTNICKI–GARCIA, S. 1968. Cell wall chemistry, morphogenesis, and taxonomy of fungi. A. Rev. Microbiol. 22, 87–108.

BELCHER, R. and GODBERT, A. L. 1954. *Semi micro quantitative analysis*. 2nd Edition. London: Longmans, Green and Co.

BELLAMY, L. J. 1975. *The infrared spectra of complex molecules*. Vol. 1, 3rd Edition. London: Chapman and Hall Ltd.

BERNIER, B. 1958. Characterization of polysaccharides isolated from forest soils. Biochem. J. 70, 590–8.

BJORNDAL, H., HELLERGVIST, C. G., LINDBERG, B., and SVENSSON, S. 1970. Gas–liquid chromatography and mass spectrometry in methylation analysis of polysaccharides. Angew. Chem. 9, 610–19.

CHESHIRE, M. V., GREAVES, M. P., and MUNDIE, C. M. 1974. Decomposition of soil polysaccharide. J. Soil Sci. 25, 483–98.

——, MUNDIE, C. M., and SHEPHERD, H. 1973. The origin of soil polysaccharide: Transformation of sugars during the decomposition in soil of plant material labelled with ^{14}C. Ibid 24, 54–68.

CONRAD, H. E. 1972. Methylation of carbohydrates with methylsulfinyl anion and methyl-iodide in dimethyl sulphoxide. In *Methods in carbohydrate chemistry VI*, (eds R. L. Whistler and J. N. BeMiller, pp. 361–4. London: Academic Press.

FINCH, P., HAYES, M. H. B., and STACEY, M. 1966. Studies on soil polysaccharides and on their interaction with clay preparations. Int. Congr. Soil Sci. II, 19–32.

FORSYTH, W. G. C. 1950. Studies on the more soluble complexes of soil organic matter. Biochem. J. 46, 141–6.

——, and WEBLEY, D. M. 1949. Polysaccharides synthesized by aerobic mesophilic, spore-forming bacteria. Biochem. J. 44, 455–9.

GLENTWORTH, R., and MUIR, J. W. 1963. The soils of the country round Aberdeen, Inverurie and Fraserburgh. Mem. Soil Surv. Scotl., Edinburgh. H.M.S.O.

GORIN, P. A. J., and SPENCER, J. F. T. 1968. Fungal polysaccharide. In Adv. in carbohydrate chemistry 23, 367–417.

HAKOMORI, S. 1964. Rapid permethylation of glycolipids and polysaccharides, catalyzed by methylsulfinyl carbanion in dimethyl sulfoxide. J. Biochem. 55, 205–8.

HEPPER, C. M. 1975. Extracellular polysaccharides of soil bacteria. In *Soil microbiology, a critical review*, (ed. N. Walker), pp. 93–110. Butterworths.

HOFFMAN, W. W. 1937. Photo-electric determination of glucose in blood and urine. J. biol. Chem. 120, 51–5.

MAJUMDA, S. K., BANERGEE, S. K., and RAO, C. V. N. 1974. Studies on soil humic substances Part 1. Fractionation of fulvic acid and characterization of sugar components. J. Indian Chem. Soc. 51, 686–90.

McGRATH. D. 1973. Sugars and uronic acids in Irish soils. Geoderma 10, 227–37.

MORTENSEN, J. L. 1960. Physico-chemical properties of a soil polysaccharide. Trans. 7th int. Congr. Soil Sci. II 14, 98–104.

STACEY, M. and BARKER, S. A. 1960. *Polysaccharides of microorganisms*. Oxford University Press.

SWEET, D. P., SHAPIRO, R. H., and ALBERSHEIM. P. 1975. Quantitative analysis by various G.L.C. response-factor theories for partially methylated and partially ethylated alditol acetates. Carbohydrate Res. 40, 217–25.

SWINCER, G. D., OADES. J. M., and GREENLAND, D. J. 1968. Studies on soil poly-saccharides I. The isolation of polysaccharides from soil. Austr. J. Soil Res. 6, 211–24.

TALMADGE, K. W., KEEGSTRA, K., BAVER, W. D., and ALBERSHEIM, P. 1973. The structure of plant cell walls I. The macromolecular components of the walls of suspension cultured sycamore cells with a detailed analysis of the pectic polysaccharides. Plant Physiol. 51, 158–73.

(Received 1 June 1978)

Reprinted from the *Soil Science Society of America Journal*
Volume 44, no. 1, January–February 1980
677 South Segoe Rd., Madison, WI 53711 USA

A Reinterpretation of the Infrared Spectrum of Sewage Sludge Fulvic Acid

The causes of environmental problems arising from the disposal of sewage sludge on soil can be understood only if the composition and properties of the sludge are known. Because organic matter is an important constituent of sludges it is necessary to know how it is involved in complexing and releasing potentially toxic heavy metals. This is particularly important for the water-soluble fulvic acids from sewage sludge and, in a recent study, it was these fractions which Sposito et al. (1976) sought to characterize using IR spectroscopy. Unfortunately, these workers have seriously misinterpreted their spectra by using band correlation data uncritically, and, as a consequence, they proposed unrealistic assignments for the absorption bands observed. The spectra can be more simply and correctly explained in terms of the absorption bands of sulfuric acid (cf. spectra shown by Giguère and Savoie, 1976) with a contribution from carboxyl groups of the fulvic acid. Variation in the intensities of the observed sulfuric acid bands at 1100–1200, 1045, 880, and 580 cm^{-1} follows the 4–12% content reported for these fulvic acids. The band positions observed by Sposito et al. (1976) in the spectrum of the metal complex of the fulvic acids are entirely consistent with carboxylate absorbing at 1580 and 1395 cm^{-1} and inorganic sulphate absorbing at 1125, near 1000, and 620 cm^{-1} (Bellamy, 1975; Nyquist and Kagel, 1971).

These observations have considerable relevance to recent work by Sposito and Holtzclaw (1977) and Holtzclaw and Sposito (1979) on the titration of sewage sludge fulvic acid, and the determination of carboxyl groups in this fraction. The titration behavior led these workers to the conclusion that SO_3H groups were present, and consequently, they used compounds containing these groups as models for assessing interference by SO_3H groups in the determination of the fulvic acid carboxyl groups. These compounds may not have been appropriate models for the sulfuric acid which is now known to be present in the sewage sludge fulvic acids studied by Sposito et al. (1976), and this may have led to errors in the estimation of carboxyl content.

Received 19 Sept. 1979

J. D. Russell

Department of Spectrochemistry
Macaulay Institute for Soil Research
Craigiebuckler
Aberdeen, Scotland AB9 2QJ

Literature Cited

1. Bellamy, L. J. 1975. The infrared spectra of complex molecules, Vol. 1, 3rd ed., p. 385–388. Chapman and Hall, London.
2. Giguère, P. A., and R. Savoie. 1960. Les spectres infrarouges de l'acide sulfurique et des oléums. Can. J. Chem. 38:2467–2476.
3. Holtzclaw, K. M., and G. Sposito. 1979. Analytical properties of the soluble, metal-complexing fractions in sludge-soil mixtures: IV. Determination of carboxyl groups in fulvic acid. Soil Sci. Soc. Am. J. 43:318–323.
4. Nyquist, R. A., and R. O. Kagel. 1971. Infrared spectra of inorganic compounds (3800–45 cm^{-1}). p. 265–299. Academic Press, New York.
5. Sposito, G., and K. M. Holtzclaw. 1977. Titration studies on the polynuclear, polyacidic nature of fulvic acid extracted from sewage sludge-soil mixtures. Soil Sci. Soc. Am. J. 41: 330–336.
6. Sposito, G., K. M. Holtzclaw, and J. Baham. 1976. Analytical properties of the soluble, metal-complexing fractions in sludge-soil mixtures: II Comparative structural chemistry of fulvic acid. Soil Sci. Soc. Am. J. 40:691–698.

Clay Minerals (1980) **15**, 205–206.

NOTE

ON SPURIOUS ABSORPTION BANDS IN IR SPECTRA OF CLAY MINERALS

Infrared spectroscopy is arguably the most powerful single technique available to chemists, but interpretation of spectra presents problems even for the most experienced investigators. Misinterpretations, and failure to recognize the presence of spurious absorption bands, can have serious consequences when such data appear in print, misleading and confusing particularly the non-expert. This is especially true when the

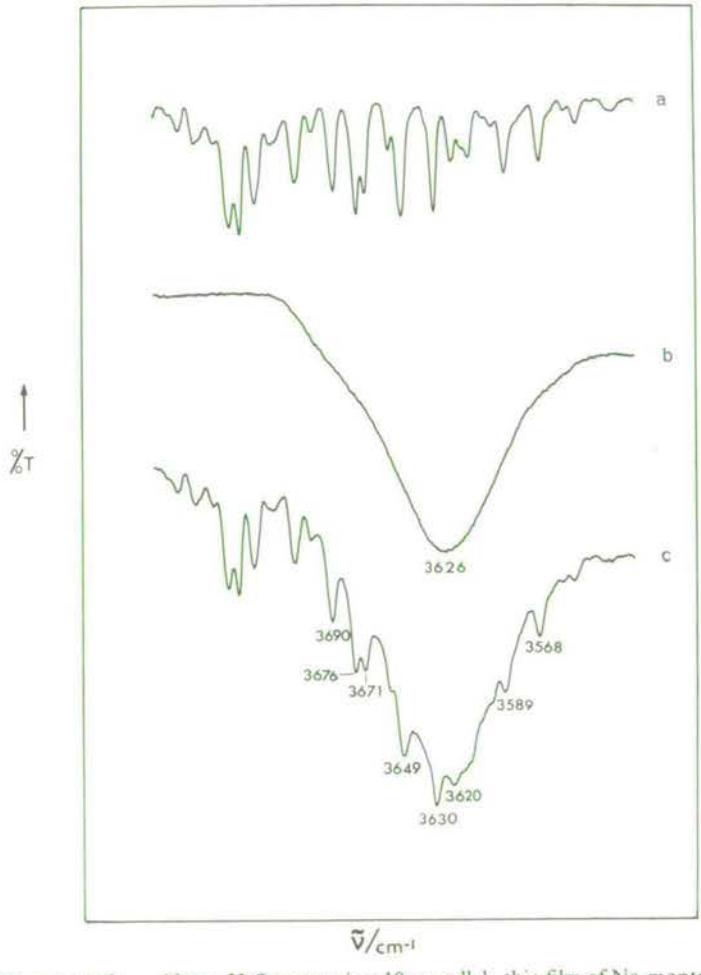

FIG. 1. IR spectra of a, ~10 torr H_2O vapour in a 10 cm cell; b, thin film of Na-montmorillonite; and c, a + b.

results are incorporated in authoritative textbooks. Recently, several examples of misinterpretation of IR spectra of soil organic matter fractions have been reported (Russell & Anderson, 1974, 1977a, b). Despite warnings concerning spurious bands in IR spectra (Launer, 1965; Russell, 1974), instances continue to appear in the literature, the most recent occurring in an XRD study of an illite-smectite by Alietti *et al.* (1979). They used IR spectroscopy as a complementary technique, and reported a spectrum showing the typical broad OH stretching band of the interstratified mineral near 3620 cm^{-1}, with a series of narrow, sharp absorption bands superimposed on it. The authors did not seek a detailed explanation of these sharp features, stating that they were characteristic of 'statistically well orientated bands', but made no statement that they were not due to the illite-smectite. It is shown here that the absorption pattern reported by these workers is precisely reproduced by inserting a cell containing H_2O vapour at a pressure of approximately 10 torr into the sample beam containing a smectite film (Fig. 1c), proving that the sharp bands in their spectrum arise from water vapour in the optical path of their instrument. The bands appear on the spectrum presumably because of imbalance between sample and reference beams. In this instance, as with the spectrum featured by Alietti *et al.*, the water vapour bands are positive on the absorption scale and are fairly readily identified, but they may be more difficult to detect should they appear in the negative direction, that is, when the imbalance results from an excess of water vapour in the reference beam.

Three instances are known (although there are probably many more) where water vapour bands arising in this way have been misinterpreted, Saksena (1964) ascribing them to OH groups arising from lattice imperfections in muscovite, and Chukhrov *et al.* (1964, 1965) assigning them to specific OH groups in allophanes.

It is hoped that the spectra presented here will make sufficient impact to prevent the future publication of this type of misleading spectroscopic data.

Department of Spectrochemistry,
Macaulay Institute for Soil Research,
Craigiebuckler,
Aberdeen

J. D. Russell

17 October 1979

REFERENCES

Alietti A., Brigatti M.F. & Poppi L. (1979) *Clay Miner.* **14**, 39.

Chukhrov F.V., Berkhin S.I., Ermilova L.P., Moleva V.A. & Rudnitskaya E.S. (1964) *Izvest. Akad. Nauk. SSSR. Ser. Geol.* **29**(4), 3.

Chukhrov F.V., Rudnitskaya E.S., Moleva V.A. & Ermilova L.P. (1965) *Izvest. Akad. Nauk SSSR. Ser. Geol.* **30**(3), 51.

Launer P.J. (1965) In: *Laboratory Methods in Infrared Spectroscopy* (R. G. J. Miller, editor), Heyden, London, pp. 13–17.

Russell J.D. (1974) In: *The Infrared Spectra of Minerals* (V. C. Farmer, editor) Mineralogical Society, London, pp. 11–25.

Russell J.D. & Anderson H.A. (1974) *Pl. Soil* **41**, 695.

Russell J.D. & Anderson H.A. (1977a) *Pl. Soil*, **47**, 263.

Russell J.D. & Anderson H.A. (1977b) *Pl. Soil*, **48**, 547.

Saksena B.D. (1964) *Trans. Farad. Soc.* **60**, 1715.

Geoderma, 24 (1980) 207—213
Elsevier Scientific Publishing Company, Amsterdam — Printed in The Netherlands

A PRELIMINARY STUDY OF FUNGAL MELANIN BY INFRARED SPECTROSCOPY

J.D. RUSSELL, D. JONES, D. VAUGHAN and A.R. FRASER

Departments of Spectrochemistry, Microbiology and Soil Organic Chemistry, Macaulay Institute for Soil Research, Craigiebuckler, Aberdeen, AB9 2QJ (Great Britain)

(Received September 3, 1979; January 25, 1980)

ABSTRACT

Russell, J.D., Jones, D., Vaughan, D. and Fraser, A.R., 1980. A preliminary study of fungal melanin by infrared spectroscopy. Geoderma, 24: 207—213.

Infrared spectra of melanin and methylated melanin have been interpreted to show the existence of carboxyl groups in two different environments in the melanin structure. In one, there are a small number of carboxyl groups with an absorption band at about 1700 cm^{-1}; these are relatively free and are capable of interaction with alkali to produce carboxylate in the normal way. In the other environment, the carboxyl groups, absorbing at 1615 cm^{-1}, are conjugated and strongly hydrogen bonded to presumably phenolic hydroxyl groups, and cannot be neutralized with alkali. They do, however, react with diazomethane, as do the free carboxyls, to produce methyl ester absorbing at 1728 cm^{-1}.

The significance of these conclusions for the survival of melanin in soil and its reactions therein, is briefly discussed.

INTRODUCTION

Melanins occur widely in nature in plant, animal and microbial tissue as melanoproteins (Nicolaus and Piattelli, 1965). They are extractable as such by water or alkali, but cleavage from the protein moiety renders the melanin insoluble in all solvents (Blois, 1978). This splitting is likely to occur enzymatically in soil, the melanin being only slowly metabolized further (Linhares and Martin, 1978). Melanins are therefore likely to persist in soil, but little is known about their structure or their contribution to soil organic matter and its reactions. To try to gain some information about the structure of this intractible biopolymer, a preliminary investigation of the melanin from the fungus *Sclerotinia sclerotiorum* described by Jones (1970) has been made using infrared spectroscopy, methylation and chemical analysis.

0016-7061/80/0000—0000/$ 02.25

MATERIALS AND METHODS

Sclerotia were obtained from cultures of *Sclerotinia sclerotiorum* (Lib.) de Bary, grown on a medium consisting of 4% (w/v) Oxoid malt extract and 1.2% (w/v) Oxoid No. 3 agar, and incubated for 2—3 weeks at 20°C (Jones, 1970).

Extraction of pigment

Two procedures were used:

(1) Whole air-dried sclerotia were ground to a fine powder using a mortar and pestle. These sclerotia may have autolysed to some extent. The powder, 50 mg, was boiled in 10 ml 0.5 *M* NaOH for 3 h giving a dark brown suspension which was centrifuged at 2000 *g* for 10 min. The debris, which was still pigmented, was discarded. The brown alkaline centrifugate was brought to pH 2.0 with 6 *M* HCl and the precipitated pigment washed with distilled water and dried at 50°C.

(2) The black rind containing the melanin pigment was removed from the sclerotia with a razor blade and washed in water. To remove the polysaccharide and protein, the rind from 200 sclerotia was boiled in 10 ml 1.5 *M* HCl for 1.5 h, washed twice in 10 ml water, then boiled in 10 ml 5.4 *M* KOH for 1.5 h, and washed twice in 10 ml water. To remove chitin, the residue was stirred in 10 ml 8 *M* HCl at 2°C for 2 h, washed four times in 10 ml water and finally dried at 50°C. The yield was 35 mg.

To remove residual protein, the pigments isolated by these methods were hydrolysed with boiling 6 *M* HCl for several hours. The insoluble residues were washed with water and dried at 50°C. Pigments treated in this way are in the acid form. Salt forms were prepared by subsequent treatment with NaOH followed by water washing.

Methylation of hydrolysed pigment

The pigment from procedure 2 was suspended in 2 ml re-distilled diethyl ether and methylated by distilling ethereal diazomethane (prepared by adding 5 g nitrosomethylurea to a mixture of 10 ml 9 *M* KOH and 10 ml re-distilled diethyl ether) into the suspension until the yellow colour of the reagent persisted. The ether was allowed to evaporate at room temperature. The sample was remethylated a further 5 times, then washed successively with chloroform, ether and water. Finally it was treated with 5% HF to remove silica which appears in some methylated products.

Chemical analysis

The total nitrogen contents of the pigments were measured in H_2SO_4 digests by the method of Searcy et al. (1967). The inorganic-P content in the acid digest was measured by the method of Allen (1940). The methoxyl content

of the methylated samples was measured by the Zeisel method (Belcher and Godbert, 1954).

Infrared spectrometry

I.R. spectra of samples (0.8 mg in 13 mm diameter KBr pressed disks) were recorded on a Perkin-Elmer 577 spectrometer over the range 4000—200 cm^{-1}. Disks were heated at 150° C for 16 h to remove adsorbed water.

RESULTS AND DISCUSSION

Alkaline extraction of the pigment from the ground sclerotia, followed by precipitation with acid (method 1), yields a melanoprotein whose spectrum (Fig. 1a) is characterized by the intense secondary amide absorption bands of protein at 1660 and 1520 cm^{-1}. Similar protein-dominated spectra have been obtained for so called fungal melanins (Filip et al., 1974) and for bacterial 'humic acids' (Kosinkiewicz, 1978). It is suggested that the use of these terminologies is unnecessarily misleading, and that the more correct melano-

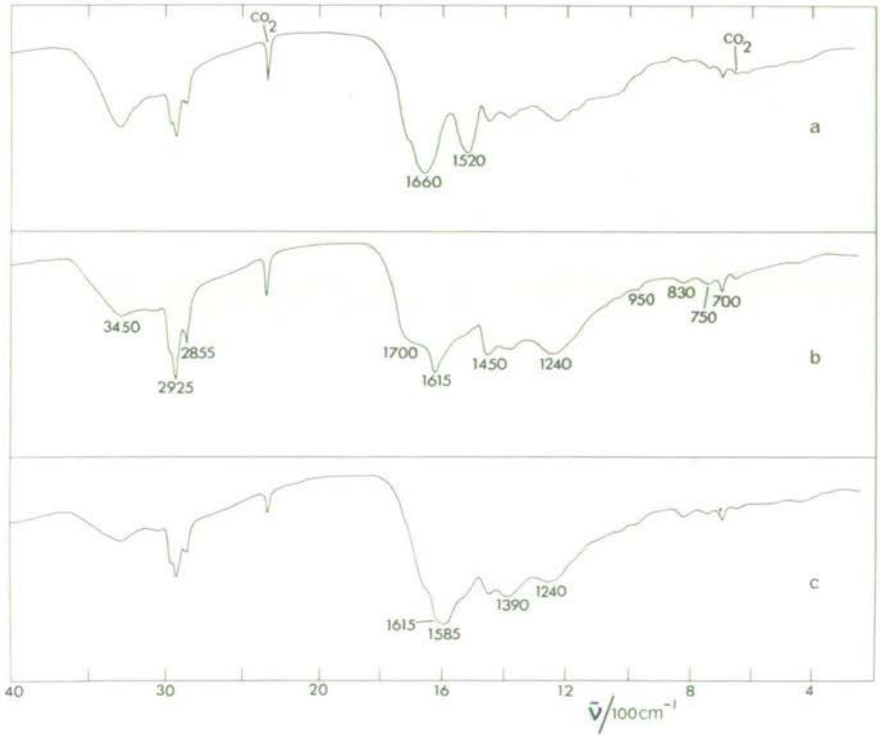

Fig. 1. Infrared spectra of heated KBr disks of sclerotinia pigment: a. isolated by procedure 1 in materials and methods; b. as a, hydrolysed with boiling 6 *M* HCl; c. as b, treated with NaOH then water washed.

protein should be used for all alkali-soluble biological pigments of this type: melanin, as defined by Blois (1978), should be reserved solely for the alkali-insoluble pigment which does not contain protein. Acid hydrolysis of the sclerotial melanoprotein yields an alkali-insoluble melanin which, from the absence of the 1660 and 1520 cm^{-1} secondary amide bands in its spectrum (Fig. 1b), contains little protein. The dominant absorption bands at 1615 cm^{-1} and 1240 cm^{-1}, with weaker bands at 3450, 1700 and 830 cm^{-1} and broad unresolved absorption in the range 3300—2400 cm^{-1} are all typical of melanin (Jones, 1970), but the spectrum contains stronger C-H absorption bands at 2850—2960 cm^{-1} and 1450 cm^{-1}, stronger C = O absorption at 1700 cm^{-1}, and weak bands of unknown origin at 950, 750 and 700 cm^{-1}. A preparation lacking the component(s) responsible for the last three absorption bands was obtained from extraction procedure 2. The initial HCl treatment used in this method, however, hydrolysed the native melanoprotein, rendering the melanin insoluble in the subsequent alkali treatment. Further purification was then only possible by removing nonpigmented wall components such as polysaccharide and chitin. The IR spectrum of the melanin prepared by this method (Fig. 2a) is the same as that shown by Jones (1970). The absorption pattern

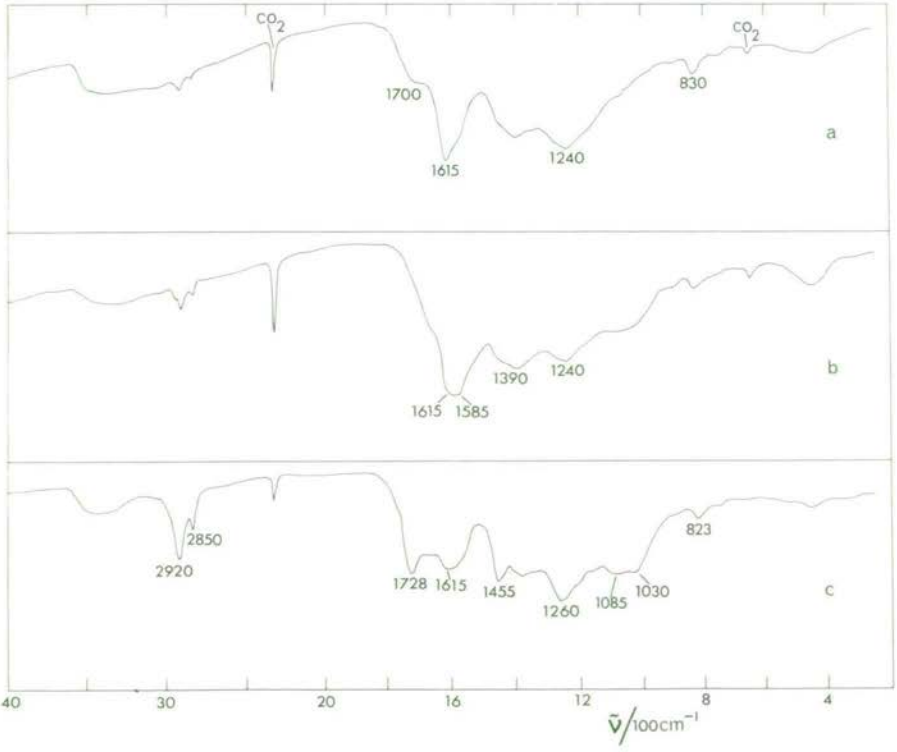

Fig. 2. Infrared spectra of heated KBr disks of sclerotinia pigment: a. isolated by procedure 2 in materials and methods; b. as a, treated with NaOH then water washed; c. as a, methylated 6 times with diazomethane.

TABLE I

Chemical Composition (%) of Melanins from *S. Sclerotiorum* and *Ustilago maydis*[*1]

Melanin source	C	H	N	P	OMe	Ash
S. sclerotiorum	60.3	3.7	1.2	0.06	—	0.6
HCl hydrol.			0.9	0.04	—	—[*2]
CH_2N_2 methylated					12.6	—[*2]
Ustilago maydis	62.8	3.4	1.0			
CH_2N_2 methylated					12.2	

[*1] Nicolaus and Piattelli, 1965.
[*2] Insufficient sample for ash determination.

is virtually unchanged on further HCl hydrolysis of the pigment, its N content decreasing from 1.2 to 0.9% (table I). Such a low nitrogen content suggests that the origin of the melanin, as proposed by Jones (1970), is probably catechol rather than DOPA, thus classifying the melanin with those of vegetable origin (Nicolaus and Piattelli, 1965). Indeed, the spectrum of the sclerotinia melanin resembles that of a synthetic pigment prepared by the enzymic oxidation of a mixture of simple phenols including catechol (Filip et al., 1974) and of catechol alone (Andrews and Pridham, 1967). The similarity is only superficial, however, in that the 1615 cm^{-1} band is weaker than that in the 1200—1300 cm^{-1} region for the synthetic polymers whereas in melanin the 1615 cm^{-1} band is stronger (Figs. 1b, 2a), and unlike natural melanins, these synthetic polymers are soluble in alkali. The above classification of the sclerotinia melanin as a vegetable pigment is apparently at variance with the findings of Liu et al. (1977) who showed that the pigment from the sclerotia of *Sclerotium rolfsii Sacc.* contained up to 8% N and yielded indole on alkaline fusion, suggesting that their melanin was of animal origin. However, its large N content and solubility at both high and low pH indicates that it is most probably a melanoprotein (Blois, 1978).

The spectra of melanin isolated from acidic media (Figs. 1b, 2a) differ considerably from those of the melanin treated with alkali (Figs. 1c, 2b). The band at 1700 cm^{-1} disappears, broad absorption at 3300—2400 cm^{-1} and the band at 1240 cm^{-1} become weaker, and simultaneously a new band appears at 1585 cm^{-1} and absorption at 1390 cm^{-1} becomes stronger. These changes are consistent with the conversion of a small proportion of free carboxylic acid groups to carboxylate by alkali, but it is significant that the principal band at 1615 cm^{-1} is not affected by this treatment, and that considerable intensity still remains at 1240 cm^{-1} and in the 3300—2400 cm^{-1} region.

To try to identify the origin of these three features, the melanin was repeatedly methylated with diazomethane to give a product with a methoxyl content (12.6%) close to that obtained by Nicolaus and Piattelli (1965) for methylated melanin from the spores of *Ustilago maydis* (Table I). The IR spectrum of the methylated sclerotinia melanin (Fig. 2c) shows considerable

weakening of both the 1615 cm^{-1} band and of absorption at 3300—2400 cm^{-1}, a shift of the 1240 cm^{-1} band to 1260 cm^{-1} and the appearance of a new band at 1728 cm^{-1}, spectra run at intermediate stages of methylation confirming that the enhancement at 1728 cm^{-1} occurred at the expense of the 1615 cm^{-1} band. The 1260 cm^{-1} and 1728 cm^{-1} bands arise from esters, possibly unsaturated or aryl (Bellamy, 1975), leading to the conclusion that the 1615 cm^{-1} band arises from carboxylic acid groups. An alternative assignment of the 1615 cm^{-1} band to carboxylate groups is untenable because of the very small ash content of the pigment (Table I). Ester groups derived from the small number of free carboxylic acid groups absorbing at 1700 cm^{-1} will also contribute to the 1728 cm^{-1} band. The 1615 cm^{-1} band lies outside the range of even internally hydrogen-bonded carboxylic acid groups in simple structures (Bellamy, 1975), but in complex, more highly oxidized systems, such factors as extended conjugation and hydrogen bonding to phenolic OH groups might combine to produce these low frequencies. Certainly, the presence of such groups is strongly indicated by the loss of absorption between 3500 and 3000 cm^{-1} in Fig. 2a on salt formation (Fig. 2b), and on methylation (Fig. 2c), and particularly by the appearance in the spectrum of methylated melanin (Fig. 2c) of new bands in the 1200—1020 cm^{-1} region which is characteristic for alkylarylether groups. The formation of a methyl ester which led to the assignment of the 1615 cm^{-1} band to conjugated, strongly hydrogen bonded carboxyl groups invalidates previous assignments of this band in melanin spectra solely to conjugated carbonyl groups (Bonner and Duncan, 1962) or to chelated quinones (Andrews and Pridham, 1967) because methylation of such systems would not give rise to a group absorbing at a frequency as high as 1728 cm^{-1}. For the same reason, an assignment to β-diketones, proposed by Theng and Posner (1967) for an analogous band at 1610 cm^{-1} in humic acid, is precluded, as is an assignment to graphitic structures suggested by Friedel and Carlson (1972) for a similar band in coal spectra. The results presented here suggest that the melanin structure might be similar to the oxidized polycyclic catechol polymer proposed by Nicolaus and Piattelli (1965) in which phenolic OH and carboxylic acid groups occur. The majority of both groups are mutually involved in strong hydrogen bonds, the remainder being relatively free. It is this latter type which participates in salt formation, a property studied by Bruenger et al. (1967) and more recently by Larsson and Tjalve (1978) who concluded that melanin behaves as a weak cation exchanger. In soil, melanin will therefore make a significant contribution to the movement and availability of metal ions in the soil through these readily available carboxyl groups. The strongly hydrogen bonded carboxyl groups are unable to participate in this reaction, but the observation that diazomethane can break this bond and produce ester and methoxyl groups suggests that these carboxyl groups may not be permanently unavailable. Indeed, Linhares and Martin (1978), while showing that, in soil, fungal melanins were almost as resistant to biodegradation as humic acids, nevertheless reported a loss of up to 15% of added ^{14}C in 12 weeks, indicating structural decomposition which might

alter the hydrogen bond status of the carboxyl groups making them more available in ion exchange reactions. The possible contribution of melanins to the humic fraction of soil organic matter is currently being actively investigated.

REFERENCES

Allen, R.J.L., 1940. The estimation of phosphorus. Biochem. J., 34: 858—865.

Andrews, R.S. and Pridham, J.B., 1967. Melanins from DOPA-containing plants. Phytochemistry, 6: 13—18.

Belcher, R. and Godbert, A.L., 1954. In: Semi-Micro Quantitative Analysis. Longmans, Green and Co., London, 2nd ed., pp. 155—159.

Bellamy, L.J., 1975. The Infrared Spectra of Complex Molecules, 1, Chapman and Hall, London, 3rd ed.

Blois, M.S., 1978. The melanins: their synthesis and structure. Photochem. Photobiol. Rev., 3: 115—134.

Bonner, T.G. and Duncan, A., 1962. Infrared spectra of some melanins. Nature, 194: 1078—1079.

Bruenger, F.W., Stover, B.J. and Atherton, D.R., 1967. The incorporation of various metal ions into *in vivo* and *in vitro* melanin. Radiat. Res., 32: 1—12.

Filip, Z., Haider, K., Beutelspacher, H. and Martin, J.P., 1974. Comparisons of IR-spectra from melanins of microscopic soil fungi, humic acids and model phenol polymers. Geoderma, 11: 37—52.

Friedel, R.A. and Carlson, G.L., 1972. Difficult carbonaceous materials and their infrared and Raman spectra. Reassignments for coal spectra. Fuel, 51: 194—198.

Jones, D., 1970. Ultrastructure and composition of the cell-walls of *Sclerotinia sclerotiorum*. Trans. Br. Mycol. Soc., 54: 351—360.

Kosinkiewicz, B., 1977. Humic-like substances of bacterial origin, I. Some aspects of the formation and nature of humic-like substances produced by *Pseudomonas*. Acta Microbiol. Pol., 26: 377—386.

Larsson, B. and Tjalve, H., 1978. Studies on the melanin affinity of metal ions. Acta Physiol. Scand., 104: 479—484.

Linhares, L.F. and Martin, J.P., 1978. Decomposition in soil of the humic acid-type polymers (melanins) of *Eurotrium echinulatum*, *Aspergillus glaucus sp.* and other fungi. Soil Sci. Soc. Am. J., 42:738—743.

Liu, T.M.E., Yu, P.H. and Wu, L.C., 1977. Isolation purification and identification of dark pigments in the sclerotia of *Sclerotium rolfsii Sacc.* Chih Wu Pao Hu Hsueh Hui Hui K'an, 19: 223—237.

Nicolaus, R.A. and Piattelli, M., 1965. Progress in the chemistry of natural black pigments. Rend. Acad. Sci. Fis. Mat., 32: 83—97.

Searcy, R.L., Reardon, J.E. and Foreman, J.A., 1967. A new photometric method for serum urea nitrogen determination. Am. J. Med. Technol., 33: 1—6.

Theng, B.K.G. and Posner, A.M., 1967. Nature of the carbonyl groups in soil humic acid. Soil Sci., 104: 191—201.

MINERALOGICAL MAGAZINE, SEPTEMBER 1980, VOL. 43, PP. 837–40

Glushinskite, a naturally occurring magnesium oxalate

M. J. WILSON, D. JONES, AND J. D. RUSSELL

Macaulay Institute for Soil Research, Craigiebuckler, Aberdeen

SUMMARY. Glushinskite, a dihydrate of magnesium oxalate, occurs at the lichen/rock interface on serpentinite colonized by *Lecanora atra* at Mill of Johnston, near Insch in north-east Scotland. It is found in a creamy white layer intermingled with the hyphae of the lichen fungus. It consists of crystals mainly 2 to 5 μm in size showing a distorted pyramidal form, often with curved and striated faces. X-ray, infrared, and chemical data are given.

SEVERAL oxalates occur as minerals, the most common being whewellite ($CaC_2O_4 \cdot H_2O$), weddellite ($CaC_2O_4 \cdot 2H_2O$), and humboldtine ($FeC_2O_4 \cdot 2H_2O$). The occurrence of magnesium oxalate as a mineral appears to have been reported only once, as colourless, platy aggregates in some Cretaceous coals in Arctic Russia (E. I. Nefedov in Zhemchuzhnikov and Ginzburg, 1960). Nefedov called the mineral glushinskite, and recorded the following data: hardness, 2; sp. gr. 1.85; α 1.365, β 1.530, γ 1.595; biaxial negative. Hey (1963) lists the mineral as a doubtful species, presumably because of the lack of X-ray diffraction and other data. The present study reports an occurrence of glushinskite together with X-ray diffraction, infrared, and electron-probe microanalysis data, all of which indicate glushinskite to be a definite mineral species.

Materials and methods. The mineral occurs in a creamy white, fine-grained layer at the rock/lichen interface (fig. 1) of a serpentinite outcrop (NJ 572247) directly opposite Mill of Johnston on the Clatt road approximately 6 km WSW of Insch. The outcrop is sparsely covered with various lichens, the mineral being found only at rock surfaces associated with *Lecanora atra* (Huds.) Ach; it is not found either with a foliose species, *Xanthoria parietina*, or with *Ochrolechia posella* (L.) Massal (identified by D. L. Hawksworth). The upper part of the lichen thallus was removed in the laboratory with a scalpel and the white material adhering to the rock surface scraped off and collected. A small quantity ($\approx$ 1 mg) of other material was also hand-picked from the undersurface of the lichen thallus, care being taken to avoid contaminating rock-mineral particles. For X-ray diffraction a Philips powder camera of 114.83 mm diameter was used with Fe-filtered Co-$K\alpha$ radiation. For infrared spectroscopy samples were incorporated in a 13 mm diameter KBr pressed disk and spectra recorded in a Perkin Elmer 577 instrument over the range 4000 to 200 cm^{-1}. Small fragments of material showing the rock/lichen interface were freeze-dried, coated with gold, and studied with a Cambridge S-4 scanning electron microscope equipped with an energy dispersive X-ray analyser.

X-ray diffraction. The white material scraped from the rock/lichen interface yielded a powder pattern showing it to be predominantly magnesium oxalate dihydrate with subordinate whewellite and trace amounts of serpentine and quartz. The pattern remaining after subtraction of the lines attributable to these impurities is shown in Table I and is in good agreement with the pattern for the dihydrate of magnesium oxalate given by Walter-Lévy *et al.* (1971). The crystallography of the dihydrated oxalates of the magnesium series (Mg, Mn, Fe, Co, Ni, and Zn) has been extensively discussed by Lagier *et al.* (1969) and Dubernat and Pézérat (1974) who showed that there is a three-dimensionally well-ordered phase isostructural with humboldtine and a disordered phase with stacking faults parallel to the (001) planes. These forms were termed the α and β forms, respectively, and they can be distinguished on the basis of their powder patterns. The naturally occurring form described here is closest to the β form although not all the weak reflections were observed.

Infrared spectroscopy. The infrared spectrum of the hand-picked white material from the rock/lichen interface (fig. 2*a*) is virtually identical with that of a sample of magnesium oxalate dihydrate (fig. 2*b*), synthesized by digesting magnesium hydroxide in an excess of oxalic acid in dilute aqueous suspension for 24 hours at 20 °C. In the spectrum of the natural material an additional weak, sharp band at 780 cm^{-1} is consistent with the presence of about 5% whewellite and a weak,

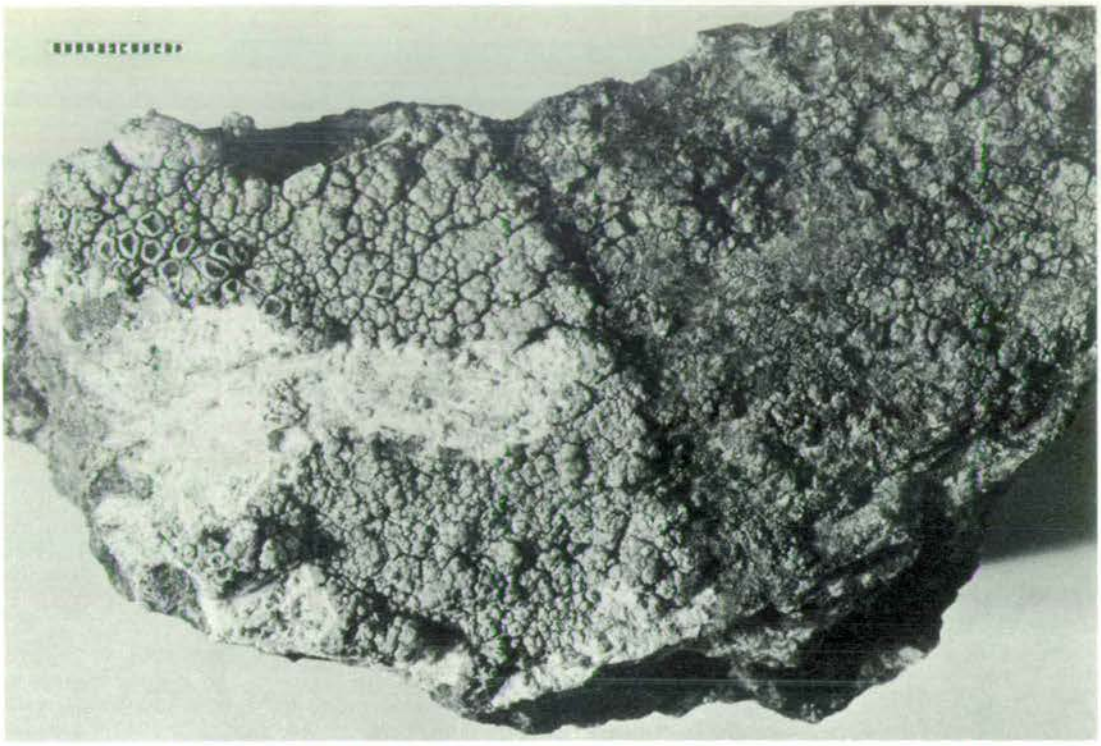

FIG. 1. Serpentinite encrusted with *Lecanora atra*, part of which has been scraped away to reveal white material, which contains glushinskite. Bar equals 5 mm.

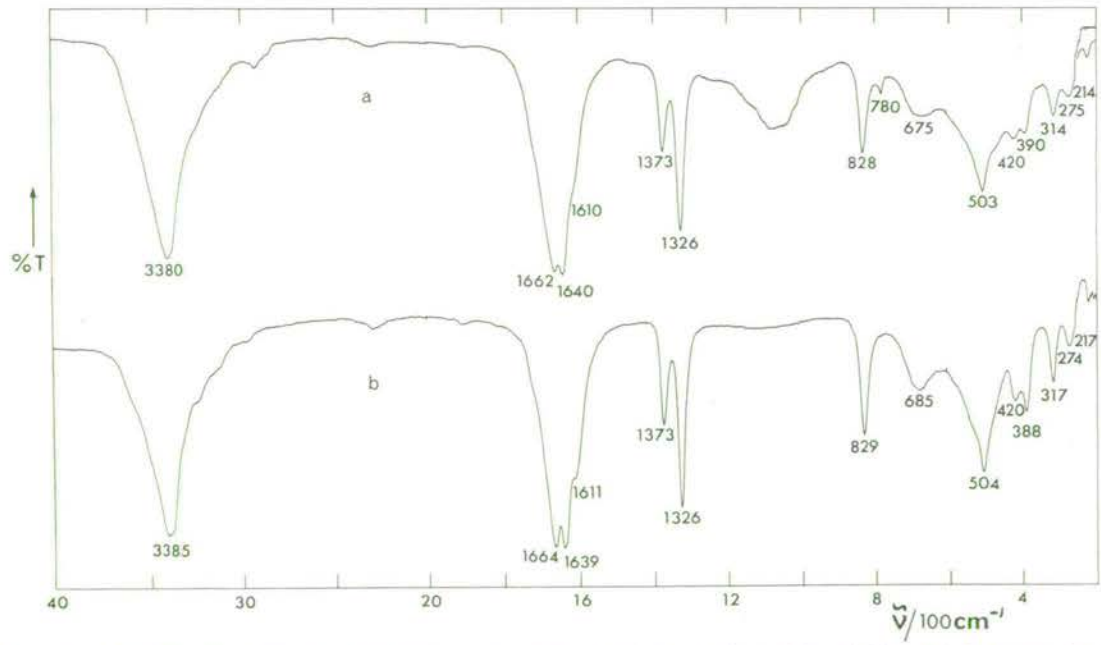

FIG. 2. Infrared spectra of (*a*) hand-picked material from the under-side of the lichen thallus and (*b*) magnesium oxalate dihydrate (β form synthesized by digesting magnesium hydroxide in an excess of oxalic acid in dilute aqueous suspension for 24 h) $\tilde{\nu}$ is wavenumber, T is transmission.

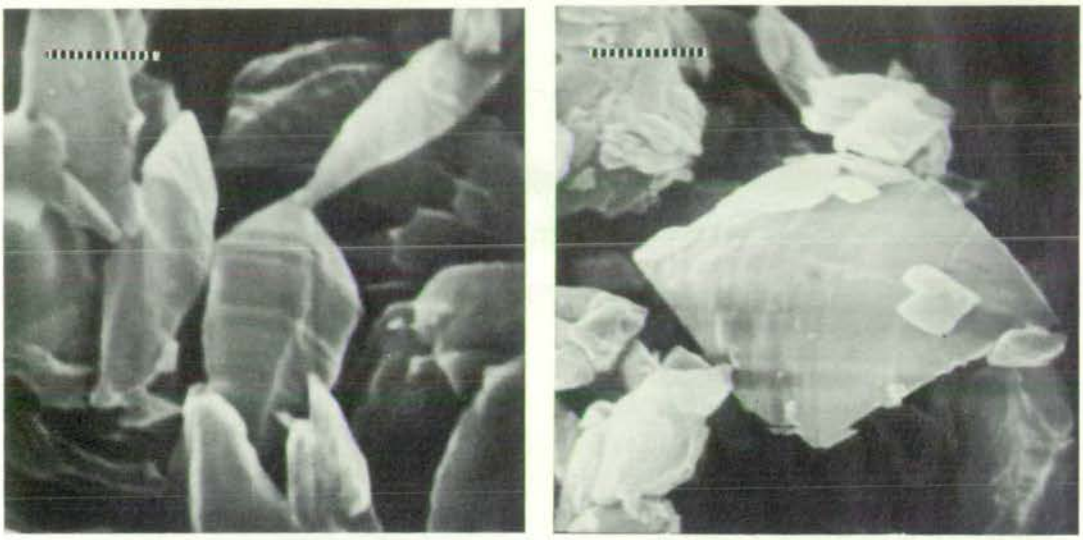

FIG. 3. Scanning electron micrographs of glushinskite crystals showing: *a*, *left*, distorted pyramidal form and *b*, *right*, curved and striated faces. Bar equals 1.25 μm and 2.5 μm respectively.

TABLE I. *X-ray powder diffraction data*

1		2		
d	*I*	*d*	*I*	*hkl*
4.89 Å	100	4.89 Å	100	200
3.849	10	3.853	20	002
*3.340	50	3.322	40 br	
3.179	70	3.168	80	$40\bar{2}$
2.541	40	2.551	40	021
2.492	10	2.487	10	$22\bar{1}$
—	—	2.447	10	$40\bar{4}$ }
—	—	—	—	400 }
2.379	50	2.379	60	202
2.086	40	2.090	40	$22\bar{3}$ }
—	—	—	—	221 }
2.039	60	2.036	60	$60\bar{2}$
1.861	50	1.863	40	023
—	—	1.782	5 br	—
—	—	1.663	5	$62\bar{3}$
—	—	1.647	5	$40\bar{6}$ }
—	—	—	—	402 }
—	—	1.606	20	$42\bar{5}$ }
—	—	—	—	421 }
—	—	1.585	10	$80\bar{4}$
1.526	30	1.529	40	$62\bar{5}$

1. Glushinskite from rock/lichen interface, Mill of Johnston, near Insch. * Partly quartz.

2. Synthetic magnesium oxalate dihydrate β form (Walter Levy *et al.* 1971). This form is monoclinic, space group $C2/c$ with $a = 12.675$ Å, $b = 5.406$ Å, $c = 9.984$ Å, $\beta = 129.45$. The unit cell parameters of glushinskite must be similar.

broad feature between 950 and 1200 cm^{-1} indicates a small amount of cellular polysaccharide from fungal hyphae and a trace of silicate. The spectrum of the sample characterized by X-ray diffraction was predominantly magnesium oxalate but contained about 10% of the total oxalate as whewellite, as well as some chrysotile and some material similar to silica gel.

Electron-probe microanalysis. Scanning electron microscope observations of the rock/lichen interface revealed an abundance of crystalline material ranging from about 2 to 5 μm in size. The majority of the crystals show a distorted pyramidal form (fig. 3*a*), often with curved and striated faces (fig. 3*b*). Lagier *et al.* (1969) have previously observed surface striations on synthetic magnesium oxalate crystals during transformation from the β to the α form. The X-ray spectrum obtained from these pyramidal crystals is dominated by magnesium but there is also appreciable iron and traces of nickel and manganese (fig. 4). The Mg:Fe ratio is approximately 20:1. Other crystals were observed to have a tabular or a well-developed tetragonal pyramidal form. These yielded a spectrum completely dominated by calcium—with no magnesium, iron, nickel, or manganese—and are, presumably, whewellite.

Discussion. The above observations show the occurrence of magnesium oxalate dihydrate—termed glushinskite by Nefedov (Zhemchuzhnikov and Ginzburg, 1960)—on the weathered surface of a lichen-encrusted serpentinite. Evidently, the mineral originates following reaction between the

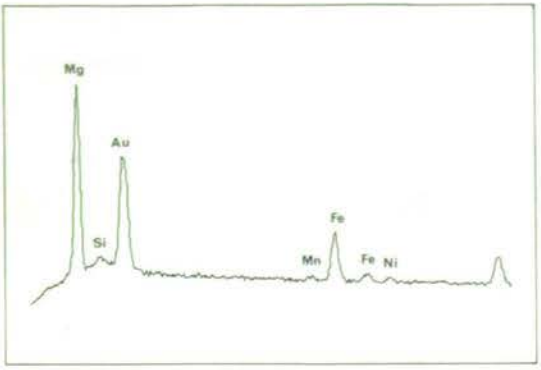

FIG. 4. X-ray spectrum from glushinskite crystals.

oxalic acid excreted by the mycobiont of *L. atra* and the magnesium-rich serpentine minerals in the substrate rock. In the same way, Jones *et al.* (1980) have recently shown that in lichen-covered basalt the decomposition of labradorite by the oxalic-acid producing mycobiont of *Pertusaria corallina* leads to the formation of crystalline calcium oxalate. It seems that glushinskite is likely to be a common weathering product where oxalic acid-producing lichens colonize magnesium-rich rocks; indeed, in the present instance the mineral was deliberately sought before it was known that it had been previously reported. The fact that the mineral contains significant quantities of ferrous iron and minor amounts of nickel and manganese is readily understandable since Lagier *et al.* (1969) have shown that the oxalates of these metals form a series with the magnesium form. Indeed, the small shifts in frequency shown by some of the absorption bands in the spectra in fig. 2, particularly those near 315 and 215 cm^{-1}, may reflect the isomorphous substitution of Mg by Fe^{2+}. All the evidence now available, therefore, indicates that glushinskite is indeed a valid mineral species.

Specimens will be donated to the Royal Scottish Museum and the British Museum (Natural History).

REFERENCES

Dubernat (J.) and Pézérat (H.), 1974. *J. Appl. Cryst.* **7**, 387–93.

Hey (M. H.), 1963. *Appendix to Chemical Index of Minerals.* British Museum (Nat. Hist.).

Jones (D.), Wilson (M. J.), and Tait (J. M.), 1980. *Lichenologist* (in press).

Lagier (J.-P.), Pézérat (H.), and Dubernat (J.), 1969. *Rev. Chim. Mineral.* **6**, 1081–93.

Walter Levy (L.), Perrotey (J.), and Visser (J. W.), 1971. *Bull. Soc. Chim.* 757–61.

Zhemchuzhnikov (Y. A.) and Ginzburg (A. I.), 1960. *The Principles of Coal Petrology.* Acad. Sci. USSR. [M. A. **16**–555].

[*Manuscript received 14 January 1980*]

IMOGOLITE AND PROTO-IMOGOLITE ALLOPHANE IN SPODIC HORIZONS: EVIDENCE FOR A MOBILE ALUMINIUM SILICATE COMPLEX IN PODZOL FORMATION

V. C. FARMER, J. D. RUSSELL and M. L. BERROW

(Department of Spectrochemistry, The Macaulay Institute for Soil Research, Craigiebuckler, Aberdeen)

WITH PLATE

Summary

Examination by infrared spectroscopy and electron microscopy of the fine clays (<0.5 μm) dispersed at pH 3.5 from H_2O_2-treated soil indicates that imogolite and proto-imogolite allophanes are concentrated in podzolic B_2 and B_3 horizons, and make up at least 6 percent of one B_2 horizon soil, which contains virtually no layer silicate clays. It is argued here that imogolite-type components are the principal source of extractable aluminium and silicon in such horizons, that they may act as cementing agents in indurated horizons, and that proto-imogolite, a soluble aluminium–silicate complex, is the predominant mobile form in which aluminium is transported to B_2 and lower horizons of podzols. Comparison of the amounts of aluminium extracted by acetic acid with those extracted by EDTA indicates that extractable aluminium in Bhg, Bh, and organic-rich A_2 horizons is present principally in organic complexes. It is proposed that the aluminium fulvates concentrated in these horizons are formed *in situ*.

Introduction

ALTHOUGH it is commonly argued that the formation of podzols involves transport of aluminium and iron as organic complexes from eluvial (A_2 or Ae) horizons to spodic horizons (Russell, 1973; McKeague *et al.*, 1976; Duchaufour, 1977), it is difficult to reconcile this theory with experimental findings indicating that the readily extractable aluminium and iron in B_2 or Bs horizons (as distinct from organic-rich Bh horizons) are predominantly in inorganic forms. For example, the investigations of McKeague and co-workers (1968, 1971) have shown that the atomic ratio of oxalate-extractable (Al + Fe) to pyrophosphate-extractable fulvate carbon averages about 0.4 in spodic horizons, much higher than the limiting ratio in soluble fulvate complexes (<0.03) at pH 4 (Schnitzer and Skinner, 1964), a pH characteristic of the upper mineral horizons of many podzols; again, Mössbauer spectroscopy has demonstrated that iron in podzolic thin iron pans is largely in the form of microcrystalline oxide phase (Goodman and Berrow, 1976); Brydon and Shimoda (1972) and Young *et al.* (1980) have established the presence of allophane in the lower part of podzol B horizons; and alkali-extractable SiO_2 and Al_2O_3 in such horizons are generally ascribed to allophanic material (Kirkman *et al.*, 1966; Loveland and Bullock, 1975). It is difficult to understand how

organic complexes of aluminium and iron, once precipitated in the Bs horizon, can be so completely converted to inorganic forms, in view of the long persistence (>10,000 years) shown by Al and Fe fulvates in buried A_1 horizons of volcanic ash soils (Wada and Higashi, 1976; Higashi and Wada, 1977).

The presumption of migration of Al and Fe as organic complexes has arisen largely from the lack of alternative plausible mechanisms. Recently, however, Farmer and co-workers (1977*b*, 1979) have shown that aluminium and silicon form a soluble complex (proto-imogolite), whose solutions are stable at pH less than 5, and Farmer (1979) has proposed that this complex could be the mobile form of aluminium in podzols, carrying aluminium and silicon to lower horizons or even out of the profile. In support of this proposal, he pointed to the almost universal occurrence of traces of imogolite in Bs horizons of Scottish soils (Tait *et al.*, 1978), the distribution of ortho-silicate groups in podzol horizons (Smith and Mitchell, private communication) and the deposition from an acidic spring water of proto-imogolite allophane, *i.e.* allophane with the same chemical composition and local structure as imogolite.

As this proposal requires that much of the extractable Al in Bs horizons should be present as imogolite or proto-imogolite allophane, the present investigation was undertaken to search for these components, using an acid dispersion technique which favours the dispersion of allophanic clays relative to layer silicate clays. The soils chosen were representatives of a group of podzols which were being examined for extractable trace elements, as it was thought the results might throw light on the very high concentrations of acetic-acid-soluble Al that had been found in their lower horizons. They included an iron humus podzol on gravel and two peaty podzols with thin iron pans, one on acidic gravels and the other on a basic igneous parent material. A cultivated brown forest soil on basic igneous parent material that gave high levels of acetic-acid-soluble aluminium was also examined.

Materials and Methods

Soils

The sites and soil characteristics (moist colours) are as follows:

(a) Tarbothill Series, Peaty Podzol with thin iron pan; Grid Ref. NJ 023135; fluvioglacial sands and gravel from schist and granite; elevation 350 m; slope 4°.

25–0 cm:	L, F, and H horizons.
0–5 cm:	A_2g; 5YR4/1 dark grey; stony loamy sand; weak medium subangular blocky; firm.
5–15 cm:	Bhg; 5YR2/2 dark reddish brown; organic stony sandy loam; weak medium subangular blocky; firm.
15 cm:	Thin iron pan.
15–38 cm:	B_2; 5YR5/8 yellowish red; loamy coarse sandy gravel; stone dominated; cemented.
38–91 cm:	B/C; 7.5YR5/4 brown; coarse sandy gravel; stone dominated; very slightly cemented.
91 cm+:	C; 10YR5/3 brown; coarse sandy gravel; stone dominated; loose.

(b) Baidland Series, Peaty Gleyed Podzol with thin iron pan; Grid Ref. NM 422488; drift from basalt; elevation 170 m; slope 4°.

43–0 cm:	Peat.
0–5 cm:	A_2g; 7YR2/2 very dark brown with humus staining; humose loam; massive.
5 cm:	Thin iron pan.
5–10 cm:	B_2; 10YR3/2 dark greyish brown; coarse sandy loam; massive; very firm.
10–18 cm:	B_3; 10YR4/3 brown; gritty loam; massive.
18 cm:	Shattered basalt rock.

(c) Corby Series, Iron Humus Podzol; Grid Ref. NJ 012547; fluvioglacial gravel from mainly quartz-biotite schist and sandstone; elevation 50 m; slope 2°.

16–0 cm:	L, F, and H horizons.
0–10 cm:	A_2; 5YR4/1 dark grey; stony sandy loam; weak medium subangular blocky; firm.
10–17 cm:	Bh; 5YR2/2 dark reddish brown; slightly organic gravelly sandy loam; medium angular and subangular blocky; friable.
17–36 cm:	B_{21}; 5YR3/4 dark reddish brown; gravelly sandy loam; structureless; friable.
36–62 cm:	B_{22}; 5YR4/6 yellowish red; loamy sandy gravel; stone dominated; loose.
62–110 cm:	B_3; 5YR3/4 dark reddish brown; humus stained in top 10 cm; sandy gravel; stone dominated; cemented.
110 cm+:	C_1; 7.5YR5/6 strong brown; sandy gravel; stone dominated; very slightly cemented, becoming loose.

(d) Insch Series, Brown Forest Soil (cultivated); Grid Ref. NJ 467297; basic igneous till on shattered rock; elevation 350 m; slope 5°.

0–25 cm:	Ap; 10YR4/4 dark brown; stony fine sandy loam; cloddy/crumb structure; soft.
25–40 cm:	B_2; 10YR5/6 yellowish brown; silty fine sandy loam; soft and friable.
40–81 cm:	B_3; 10YR6/4 light yellowish brown; stony sandy loam; compact.
81–96 cm:	C, 10YR6/6 brownish yellow; stony loamy till; compact.
96 cm+:	Rotten shattered basic igneous rock.

Acid-dispersable clays

5–10 g soil samples were boiled for 2 h with 100 cm^3 6 per cent w/v H_2O_2 to destroy organic matter, washed once with water on a centrifuge to remove soluble salts, and a clay fraction dispersed by ultrasonic treatment with 100 cm^3 dilute HCl, pH 3.5. Size fractions (<0.5 and <2.0 μm) were separated by centrifugation as supernatant liquids, which were concentrated by evaporation on a water-bath and then freeze-dried. Their infrared spectra were recorded on a Perkin Elmer 577 infrared spectrometer using 0.7 mg samples in 13 mm KBr disks, after heating the disks to 150 °C and 350 °C.

Acetic acid and EDTA extractions

Air-dry soil (20 g, <2 mm) was shaken overnight with 800 cm^3 of 0.43 M acetic acid on an end-over-end shaker. The extract was filtered through an

18.5 cm Whatman 540 filter paper and the residue washed with water before evaporating the filtrate to dryness. The dried extract was oxidized twice with 5 cm^3 16 M HNO_3, then treated with 10 cm^3 6 M HCl and evaporated to dryness. The residue was taken up in 10 cm^3 0.6 M HNO_3 containing Li and Cr as internal standards, filtered, and the Al determined by the porous-cup solution spark technique (Scott, 1960). Alternatively, Al was determined in the original filtrate by atomic absorption in a nitrous oxide-acetylene flame.

EDTA extracts were made with 0.05 M ethylene-diamine-tetra-acetic acid neutralized to pH 7 with ammonia. Air-dry soil (15 g, <2 mm) was extracted for 1 h with 75 cm^3 EDTA solution on an end-over-end shaker. The extract was filtered through an 18.5 cm Whatman 540 filter paper, and 50 cm^3 of the filtrate evaporated to dryness in a silica basin. The organic complex was destroyed by ignition, and the ash, moistened with distilled water, was twice treated with a few drops of 6 M HCl and taken to dryness. The residue was taken up in 10 cm^3 0.6 M HNO_3 containing Li and Cr as internal standards, filtered and the Al determined as above.

Results

Acid-dispersable clays

The B_2, B_3 and/or C horizons of all three podzols, and the iron pan of the Tarbothill Peaty Podzol, gave substantial yields of fine clay (<0.5 μm), all of which gave IR spectra indicating the presence of an imogolite-like component (Table 1). This material was the dominant component of the clay from the B_2 horizon of the Tarbothill profile: only traces of layer silicate clay and iron oxides could be detected by IR spectroscopy, X-ray diffraction, or electron microscopy. Electron microscopy (Plate 1) showed a considerable amount of well-ordered imogolite to be present, giving the

TABLE 1

Yields (mg/10 g) of <0.5 μm clay from one acid (pH 3.5) dispersion and their contents of imogolite type material (% Imog.) estimated from the 348 cm^{-1} IR absorption band, from four Scottish soils

	Tarbothill		Baidland		Corby		Insch	
Horizon	*Yield*	*% Imog.*	*Yield*	*% Imog.*	*Yield*	*% Imog.*	*Yield*	*% Imog.*
A_2/Ap	8[a,c]	0	300[a,f]	0	11[a]	0	86[a]	0
Bh	9[a]	0			1[a]	0	np	—
Fe pan	192[a,b]	39	39[a]	0	np	—	np	—
B_{21}	89	100	188[c]	54	65[c]	21	39[a]	0
B_{22} } B_2					42[c]	31		
B_3 or B/C	ne	—	115[c]	52	24[c]	55	15[d]	0
C	7	78	np	—	18[c]	48	17[a]	0

ne: not examined np: horizon not present

[a–c]: Other components present in the clay fractions include (a) complex oxalates, (b) ferrihydrite, (c) trioctahedral 16 Å layer silicate, (d) gibbsite, (e) dioctahedral layer silicates

[f]: This thin A_2g horizon incorporates the features of the Bhg horizon distinguished in the Tarbothill profile.

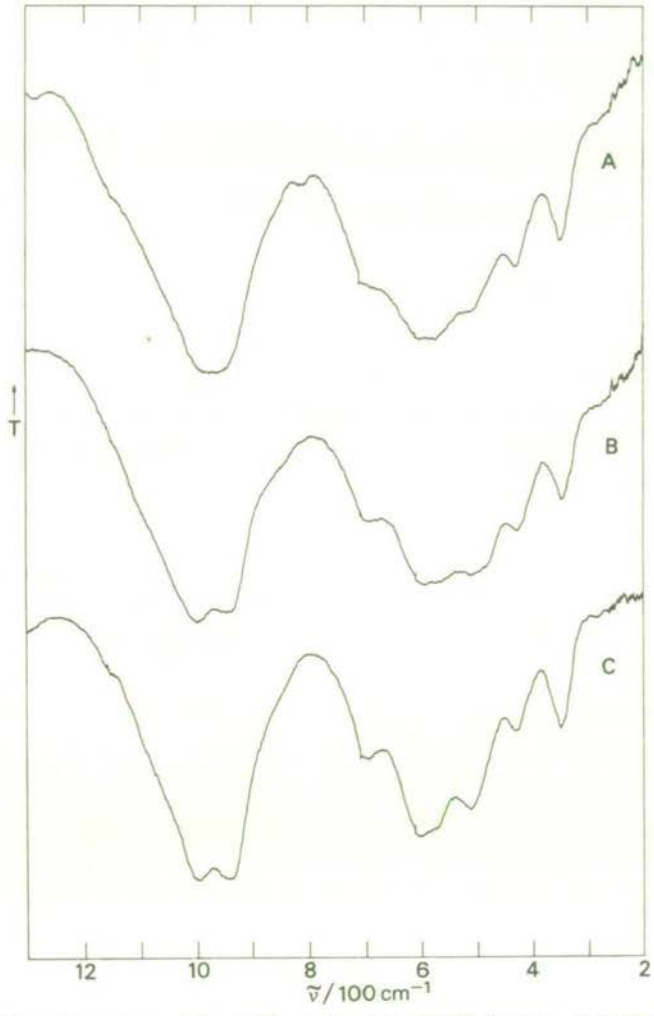

FIG. 1. A: Infrared spectrum of the <0.5 μm clay from the B_2 horizon of the Tarbothill Series profile; B: spectrum of this clay after treatment with 0.43 M acetic acid; C: spectrum of imogolite (Kurayoshi).

characteristic diffraction pattern for imogolite, associated with clumps of structureless material, probably allophane. Its infrared spectrum (Fig. 1A) was intermediate between those of proto-imogolite allophane and well-ordered imogolite (compare spectra in Parfitt and Henmi, 1980), and is consistent with a mixture of these components. After dispersing the clay (20 mg) in 0.43 M acetic acid (80 cm^3) for 16 h at 20 °C, a 40 per cent residue was obtained on neutralizing, which gave an infrared spectrum (Fig. 1B) approaching closer to pure imogolite (Fig. 1C), indicating preferential dissolution of the more poorly ordered allophanic component.

The imogolite-type material in the fine clays from the thin iron pan and

C horizons of this profile, and from the B_2, B_3 and C horizons of the other podzols, were associated with variable proportions of layer silicate clays, oxalates and iron oxide phases and so were more difficult to characterize precisely. Examination by electron microscopy of the Baidland B_2 clay and the Corby B_3 clay indicated, however, that fibrous imogolite was only a minor component of these clays, so their imogolite-type components are predominantly allophanic. The estimates given in Table 1 for the amounts of imogolite-type material (*i.e.* imogolite plus proto-imogolite allophane) present in the clays is based on the intensity of their absorption bands at 348 cm^{-1}, after correcting for any residual absorption remaining after heating the KBr disks to 350 °C, and taking the intensity given by the Tarbothill B_2 clay as corresponding to 100 per cent. The intensity of the characteristic band for imogolite structures at 348 cm^{-1} given by this clay was about 65 per cent of that given by well-ordered imogolite, which was re-measured as giving an absorbance of 0.36 for 1 mg air-dry freeze-dried clay in a 13 mm KBr disk (compare 0.27 previously reported by Farmer *et al.* (1977*a*) for material not freeze-dried).

The yields of fine clay listed in Table 1 are those obtained in a single dispersion, and, after allowing for their contents of imogolite-type components, give only an indication of the relative abundance of these components in different horizons. A second dispersion of the Tarbothill B_2 horizon gave a similar yield of fine clay, and imogolite-type components were present also in the coarse clay (0.5–2 μm) and silt (2–20 μm) fractions. An estimate by infrared spectroscopy of the total amount of imogolite-type material in all these fractions indicated a content of at least 6 per cent imogolite-type components in the soil sample (<2 mm). Layer silicate clays were scarcely detectable in any of these fractions, and a subsequent dispersion in 0.1 M Na-pyrophosphate, following exhaustive acid dispersion, yielded only traces of clay, consisting mostly of feldspars and quartz. The Baidland B_2 horizon, which is developed on more readily weatherable basalt, appears to contain even more imogolite-type material than does the Tarbothill.

Acetic acid and EDTA extractable aluminium

A comparison of the amounts of aluminium extracted by acetic acid and EDTA from the Tarbothill and Baidland Podzols (Table 2) indicates a sharp change in the nature of the extractable aluminium at the level of the iron pan. Above this horizon, EDTA extracts amounts of Al comparable to or greater than those extracted by acetic acid, but below this horizon, acetic acid extracts much more aluminium than EDTA, often ten times as much. A similar but less sharp transition occurs in the Corby Iron Humus Podzol at about the boundary of the Bh and B_{21} horizons. The fact that EDTA extracts more aluminium than does acetic acid from organic H horizons indicates that EDTA is an effective extractant for organically complexed Al, so the high amounts of EDTA-soluble Al from the Bhg horizons immediately overlying the thin iron pans, and from the Bh horizon of the Iron Humus Podzol point to an accumulation of Al-fulvates in them. On passing from these horizons into the B_2, Al soluble in acetic acid remains high or increases, whereas EDTA-extractable Al drops to

TABLE 2

Aluminium (ppm in air-dry soil) extracted by 0.43 M acetic acid (HA) and 0.05 M EDTA (pH 7) from four Scottish soils

	Tarbothill		*Baidland*		*Corby*		*Insch*	
Horizon	*HA*	*EDTA*	*HA*	*EDTA*	*HA*	*EDTA*	*HA*	*EDTA*
H[a]	120	1700	1000	1800	50	290	np	—
A_2/Ap	255	420	5490[b]	3800[b]	150	380	1800	460
Bh	4060	5700			1930	1080	np	—
Fe pan	4580	1360	3690	910	np	—	np	—
B_{21}	3790	410	6100	1200	3340	820	2600	430
B_{22} B_2					1800	610		
B_3 or B/C	600	40	4400	520	1450	340	1600	110
C	440	55	np	—	950	200	1800	130

np: horizon not present

[a]Organic horizon immediately above A_2

[b]This thin A_2g horizon incorporates the features of the Bhg horizon distinguished in the Tarbothill Peaty Podzol

much lower values, indicating that organic complexes play a minor role in these horizons.

This solubility behaviour points to the imogolite-type component as the principal source of Al in acetic acid extracts from B_2 and lower horizons. This material is not dissolved by the EDTA solution, but is partially dissolved by acetic acid, as reported in the previous section. To seek confirmation, the acid-dispersable fine clay (<0.5 μm) was isolated from the B_2 horizon of a Corby Series podzol after the soil had been extracted with acetic acid and then treated with hydrogen peroxide. IR spectroscopy indicated that the isolated clay still contained a high proportion of imogolite structures, and showed only a small increase in the proportion of layer silicate clays. Thus, although imogolite-like components could be an important, probably the major source, of acetic-acid-soluble Al in the B_2 and lower horizons of podzols, they are not quantitatively extracted, and appear to be present in a form that is partially protected from attack by acetic acid. This protection could well arise from natural organic matter adsorbed on their surface. The presence of such adsorbed material is indicated by the fact that, in preliminary experiments, no acid-dispersable fine clay (<0.5 μm) could be obtained from a Corby Series podzol B_2 horizon until it had been treated with hydrogen peroxide. This adsorbed organic matter also ensured that the acetic acid extraction procedure did not disperse significant amounts of imogolite: examination of the material dissolved by acetic acid, isolated by neutralizing, evaporating and freeze-drying the extract, showed that a complex aluminium acetate was the principal component from several B_2 podzolic horizons examined. Only in the Tarbothill B_2 extract was a small amount of imogolite-type material identified by its IR spectrum.

Imogolite-type material is not, however, the only possible inorganic source of acetic-acid-soluble Al in podzol B and C horizons. The Insch Brown Forest Soil (Table 2) shows high ratios of acetic-acid-soluble Al to

EDTA-soluble Al, but yielded no imogolite-like acid-dispersable component. Most of the acetic-acid-extractable Al was found to come from the clay fraction of this soil, which incorporated a chloritized-vermiculite from which the interlayer hydroxides could be leached by the acetic acid reagent (Berrow and Mitchell, 1980). Such clays commonly occur in podzolic Bs horizons (McKeague *et al.*, 1976) where they could form by interaction between vermiculites and percolating proto-imogolite solutions. Other possible sources of acid-soluble Al in the Insch soil are indicated in the Discussion.

Discussion

The finding of imogolite-type material in all the podzolic B_2 horizons, but more particularly the presence of an ordered imogolite in substantial amounts in the B_2 horizon of the Tarbothill Peaty Podzol, is strong evidence that aluminium migrates in podzols in the form of proto-imogolite, a soluble hydroxy-aluminium orthosilicate complex. Proto-imogolite allophane, with a spherical morphology, can form by transformation of pumice grains without translocation (Parfitt and Henmi, 1980), and proto-imogolite gels can form in the laboratory by interaction of orthosilicic acid with freshly formed aluminium hydroxide (Farmer *et al.*, 1979), but regular tubular imogolite structures can only form from solutions, as indicated by the site of precipitation of imogolite in nature and its mode of formation in the laboratory (Farmer and Fraser, 1978).

Farmer (1979) reported that fulvic acid forms stronger complexes with Al than does silicic acid. Fulvic acid in excess (COOH:Al $\geq$ 8) decomposed proto-imogolite solutions at pH 4.5 to give a soluble Al-fulvate plus silicic acid. At lower ratios of COOH:Al, fulvate and proto-imogolite coprecipitated at pH 4.5, and complete precipitation of all Al and all fulvate occurred at a molar ratio of COOH:Al of unity, with partial liberation of the silica from the proto-imogolite. It is difficult, therefore, to imagine how a soluble Al-fulvate could be converted to imogolite and proto-imogolite in B_2 horizons. Possible mechanisms of formation of a soluble proto-imogolite complex have been suggested by Farmer (1979) who pointed out that, in acid soils, aluminium released from primary minerals by non-complexing organic and inorganic acids would be immediately converted to proto-imogolite in the presence of low concentrations (>1 ppm) of silica. Complexes of aluminium with simple complexing acids, such as oxalic, citric and tartaric acid, would suffer biological degradation of the organic component to liberate the aluminium in a reactive form which could then combine with silica to form proto-imogolite. Deposition of allophane from such proto-imogolite sols is liable to occur in lower horizons of higher pH, or when the positive charges necessary to maintain dispersion are neutralised by absorbed anions, or when these positive colloids encounter negatively charged surfaces, such as those of smectites, illites, or vermiculites. Formation of well-ordered imogolite obviously requires particularly favourable conditions.

These formation mechanisms for proto-imogolite solutions are supported by analyses quoted by Vedy and Bruckert (1979) which show a large drop in the concentration of both complexing and non-complexing simple

organic acids on passing from capillary water to gravity water in an A_1 horizon of a podzol. These authors thought that the biologically liberated aluminium would be then transported to lower horizons as soluble fulvate complexes. However, in the early stages of podzolization, before the development of a leached Ae horizon, mobile aluminium, iron, and calcium will be relatively abundant in the A horizon, and any fulvic acid liberated will be precipitated *in situ* as an insoluble salt. Only after the formation of a well-developed Ae horizon will fulvic acid be in excess and able to pass through the Ae horizon. This mobile fulvic acid can carry only small amounts of complexed Al and Fe, but it will attack imogolite and proto-imogolite allophanes already deposited in the spodic horizon, liberating silica and forming an insoluble aluminium fulvate *in situ*. This mechanism can account for the absence of imogolite-type material in the Bh horizon of the Corby Iron Humus Podzol (Table 1). The thin iron pans of the peaty podzols provide effective barriers to the passage of fulvic acid solutions, so that in them imogolite persists up to the iron pan, and in the case of the Tarbothill profile into the iron pan. Organic matter is, however, sorbed on the imogolite-like material of the B_2 horizons, as preliminary experiments showed that no fine clay (<0.5 μm) could be dispersed from a B_2 podzolic horizon until it had been treated with H_2O_2.

These proposals for the formation of Bh horizons are by no means novel. Stobbe and Wright (1959) reported that, in humus podzols, large masses of dark organic matter have been observed descending after rains from the A_0, passing comparatively rapidly through the A_2, and finally being largely filtered out or absorbed in the B horizon. They considered this process to be active also in humus-iron podzols, and similar views have been expressed by Mattson and Gustafsson (1937) and by Stace *et al.* (1968).

Although the EDTA and acetic acid extraction procedures used in this work were developed to assess the availability to plants of trace elements in soils, the results are of considerable pedogenic interest. The results for the two peaty podzols in Table 2 are illustrative of those obtained for a larger group of peaty podzols with thin iron pans; they indicate that EDTA is as effective as, or more effective than, acetic acid for extracting aluminium complexed with organic matter, since the two reagents dissolve comparable amounts of Al from organic horizons, A_2, and Bhg horizons, with a very marked peak of EDTA solubility in the organic-rich Bhg horizons immediately overlying the thin iron pans. A similar peak of Al soluble in EDTA occurs in the Bh horizon of the Corby Iron Humus Podzol. The very high ratio of acetic-acid-soluble Al to EDTA-soluble Al in all the B_2 and lower horizons argues strongly for predominantly inorganic forms of Al in these horizons. Much of this acetic-acid-soluble Al can come from imogolite-type materials, which are partially dissolved by this reagent, but other sources must contribute to the high amounts of Al soluble in acetic acid from all horizons of the Insch Brown Forest Soil, which does not contain an imogolite-like component. However, the B_2 horizons of uncultivated Brown Forest Soils developed on Insch parent material do yield acid-dispersed clays containing imogolite (Tait *et al.*, 1978) and it is possible that liming the cultivated soil has altered the

original imogolite-type components. Synthetic studies (Farmer *et al.*, 1979) have indicated that the imogolite structure is potentially unstable at pH >6, as aluminosilicate gels precipitated in neutral or alkaline conditions have hydrous feldspathoid structures, containing polymerized silicate anions incorporating tetrahedral aluminium. Thus liming could convert imogolite-type materials to calcium feldspathoids or zeolites. This proposal accounts for the remarkably constant 2:1 ratio of acid-extractable Al:Ca reported by Berrow and Mitchell (1980) for horizons of this and another well-drained cultivated soil: each tetrahedral Al contributes a negative charge to the aluminosilicate anion, which must be compensated by a cationic positive charge, hence accounting for the 2:1 ratio of Al:Ca.

Finally, the possibility that imogolite-type components play a part in cementing indurated (duric) horizons should be considered. Such horizons are widespread in podzols in Scotland, sometimes coinciding with the B_2 horizon, as in the Tarbothill profile, sometimes lying at lower levels, as with the B_3 horizon of the Corby profile. McKeague and Sprout (1975), in a detailed study of Canadian cemented B_3 horizons, found that they yielded relatively high levels of Al and Si, frequently in an atomic ratio near 2:1 on extraction with hot 0.5 M NaOH, and concluded that these subsoils were cemented by amorphous or weakly crystalline secondary products containing Fe, Al and Si in various proportions. Imogolite-type material could well be the source of much of the NaOH-extractable Al and Si, and it will be noted (Table 1) that the yield of these components is as high from the cemented B_3 horizon of the Corby profile as from the B_2 horizon above. The looseness of the B_2 horizon could be ascribed, as suggested by Romans (1962), to the disruptive probing of tree roots, which seldom penetrate the B_3 layer.

The views on the podzolization process presented in this paper have some analogies with those expressed by Mattson (1933) and Mattson and Gustafsson (1937), who argued that aluminium and iron must migrate as positive colloids. They did not, however, realize that the aluminium silicate complex had a definite structure and limiting composition, and their belief that these sols could form by peptization from a pre-existing gel complex has not gained support. Their view that iron as well as aluminium migrated as a positive colloid is consistent with the diffuse distribution of iron oxide phases in B_2 and lower horizons, which largely parallels the distribution of allophane, and so suggests a transport and deposition mechanism analogous to that for aluminium. Indeed a negatively charged iron fulvate complex could not co-exist in solution with a positively charged proto-imogolite sol, as they would co-precipitate. Localized concentrations of iron oxides are more likely to form by oxidation-reduction mechanisms; for example, thin iron pans in podzols are probably both the result and the cause of a sharp boundary between an upper gleyed horizon and a lower oxidised B_2 horizon.

Acknowledgements

The authors thank A. D. Walker and J. S. Bibby for choosing and sampling the podzols, J. M. Tait for electron microscopy, and M. J. Wilson for X-ray diffraction examination of the isolated clays.

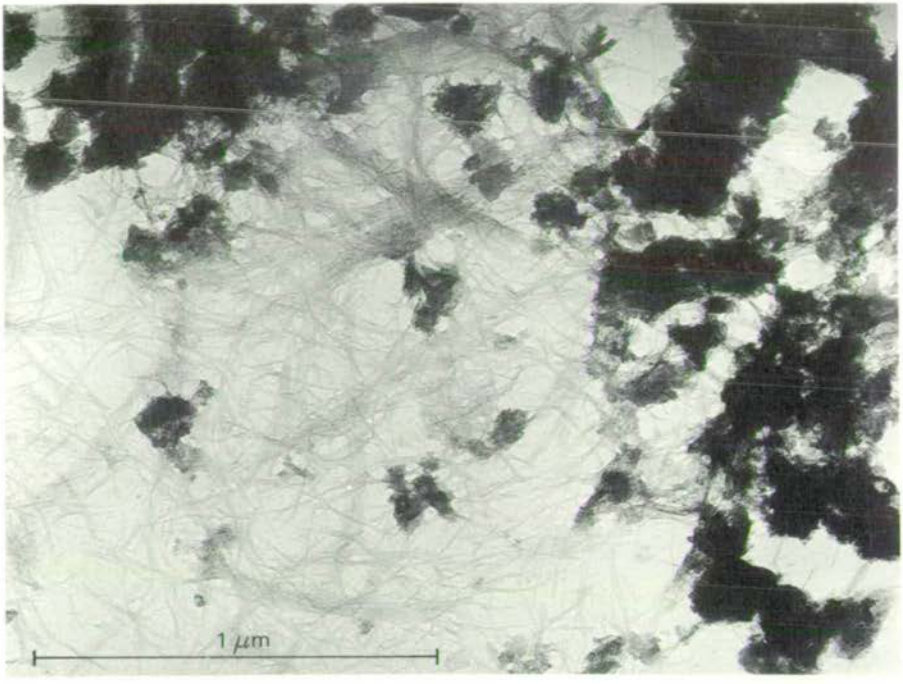

PLATE 1 Electron micrograph of the <0.5 μm clay from the B_2 horizon of the Tarbothill Series profile (Microscopist: J. M. Tait).

REFERENCES

BERROW, M. L. and MITCHELL, R. L. 1980. Location of trace elements in soil profiles: Total and extractable contents of individual horizons. Transactions of the Royal Society of Edinburgh: Earth Sciences **71**, 103–121.

BRYDON, J. E. and SHIMODA, S. 1972. Allophane and other amorphous constituents in a podzol from Nova Scotia. Canadian Journal of Soil Science **52**, 465–475.

DUCHAUFOUR, P. 1977. *Pédologie 1. Pédogenèse et classification*. Paris: Masson.

FARMER, V. C. 1979. Possible roles of a mobile hydroxyaluminium orthosilicate complex (proto-imogolite) in podzolization. In *Migrations organo-minérales dans les sols tempérés*. International Colloquium of C.N.R.S., Nancy. (in press).

FARMER, V. C. and FRASER, A. R. 1978. Synthetic imogolite, a tubular hydroxyaluminium silicate. In *International Clay Conference 1978* (eds. M. M. Mortland and V. C. Farmer) pp. 547–553. Amsterdam: Elsevier (published 1979).

FARMER, V. C., FRASER, A. R., RUSSELL, J. D. and YOSHINAGA, N. 1977*a*. Recognition of imogolite structures in allophanic clays by infrared spectroscopy. Clay Minerals **12**, 55–57.

FARMER, V. C., FRASER, A. R. and TAIT, J. M. 1977*b*. Synthesis of imogolite. Journal of Chemical Society, Chemical Communications 462–463.

FARMER, V. C., FRASER, A. R. and TAIT, J. M. 1979. Characterization of the chemical structures of natural and synthetic aluminosilicate gels and sols by infrared spectroscopy. Geochimica et Cosmochimica Acta **43**, 1417–1420.

GOODMAN, B. A. and BERROW, M. L. 1976. The characterization by Mössbauer spectroscopy of the secondary iron in pans formed in Scottish podzolic soils. Journal de Physique **37**, supplement C6, 849–855.

HIGASHI, T. and WADA, K. 1977. Size fractionation, dissolution analysis and infrared spectroscopy of humus complexes in Ando soils. Journal of Soil Science **28**, 653–663.

KIRKMAN, J. H., MITCHELL, B. D. and MACKENZIE, R. C. 1966. Distribution in some Scottish soils of an inorganic gel system related to allophane. Transactions of the Royal Society of Edinburgh 66(16), 393–418.

LOVELAND, P. J. and BULLOCK, P. 1975. Crystalline and amorphous components of the clay fraction in brown podzolic soils. Clay Minerals **10**, 451–469.

McKEAGUE, J. A. 1968. Humic–fulvic acid ratio, Al, Fe and C in pyrophosphate extracts as criteria of A and B horizons. Canadian Journal of Soil Science **48**, 27–35.

KcKEAGUE, J. A., BRYDON, J. E. and MILES, N. M. 1971. Differentiation of forms of extractable iron and aluminium in soils. Soil Science Society of America Proceedings **35**, 33–38.

McKEAGUE, J. A., ROSS, G. J. and GAMBLE, D. S. 1976. Properties, criteria of classification and concepts of genesis of podzolic soils in Canada. In *Quaternary soils: 3rd Conference on Quaternary research* (ed. W. C. Mahaney) pp. 27–60. Norwich: Geo Abstracts Ltd. (published 1978).

McKEAGUE, J. A. and SPROUT, P. N. 1975. Cemented subsoils (duric horizons) in some soils of British Columbia. Canadian Journal of Soil Science **55**, 189–203.

MATTSON, S. 1933. The laws of soil colloid behaviour: XI. Electrodialysis in relation to soil processes. Soil Science **36**, 149–162.

MATTSON, S. and GUSTAFFSON, Y. 1937. The laws of soil colloid behaviour: XIX. The gel and the sol complex in soil formation. Soil Science **43**, 453–473.

PARFITT, R. L. and HENMI, T. 1980. The structure of some allophanes from New Zealand. Clays and Clay Minerals. (in press).

ROMANS, J. C. C. 1962. The origin of the indurated B_3 horizon of podzolic soils in North-East Scotland. Journal of Soil Science, **13**, 141–147.

RUSSELL, E. W. 1973. *Soil conditions and plant growth*, 10th edn. London: Longman.

SCHNITZER, M. and SKINNER, S. I. M. 1964. Organomineral interactions in soils: 3. Properties of iron and aluminium-organic complexes prepared in the laboratory and extracted from soil. Soil Science **98**, 197–203.

SCOTT, R. O. 1960. Application of direct photometry to agricultural analysis. Journal of the Science of Food and Agriculture **11**, 584–592.

STACE, H. C. T., HUBBLE, G. D., BREWER, R., NORTHCOTE, K. H., SLEEMAN, J. R., MULCAHY, M. J. and HALLSWORTH, E. G. 1968. *A handbook of Australian soils* p. 369, Glenside, S. Australia: Rellim.

STOBBE, P. C. and WRIGHT, J. R. 1959. Modern concepts of the genesis of podzols. Soil Science Society of America Proceedings **23**, 161–164.

TAIT, J. M., YOSHINAGA, N. and MITCHELL, B. D. 1978). The occurrence of imogolite in some Scottish soils. Soil Science and Plant Nutrition **24**, 145–151.

VEDY, J. C. and BRUCKERT, S. 1979. Soil solutions: composition and pedogenetic significance. In *Pédologie 2. Constituants et propriétés du sol* (eds M. Bonneau and B. Souchier) pp. 161–186. Paris: Masson.

WADA, K. and HIGASHI, T. 1976. The categories of aluminium- and iron-humus complexes in Ando soils determined by selective dissolution. Journal of Soil Science **27**, 357–368.

YOUNG, A. W., CAMPBELL, A. S. and WALKER, T. W. 1980. Allophane isolated from a podsol developed on a non-vitric parent material. Nature, London **284**, 46–48.

(Received 4 March 1980)

Clay Minerals (1980) **15**, 445–451.

SWELLING MINERALS IN A BASALT AND ITS WEATHERING PRODUCTS FROM MORVERN, SCOTLAND: I. INTERSTRATIFIED MONTMORILLONITE-VERMICULITE-ILLITE

D. C. BAIN AND J. D. RUSSELL

The Macaulay Institute for Soil Research, Craigiebuckler, Aberdeen AB9 2QJ

(Received 1 April 1980; revised 30 April 1980)

ABSTRACT: The main clay mineral in weathered basaltic rubble has been shown by X-ray diffraction, chemical, infrared and differential thermal methods to be an interstratification of montmorillonite, vermiculite and illite in the approximate ratio 2:1:1, the montmorillonite having some degree of segregation and the vermiculite and illite being randomly interstratified. All three components are dioctahedral, the swelling ones having a high tetrahedral charge, a large aluminium content, and very little iron. Despite the 50% montmorillonite content of the mineral, its infrared absorption pattern is generally illitic in character.

In a study of the chemical, mineralogical and textural changes which have taken place in the weathering of a Tertiary basalt at Killundine, Morvern (Bain *et al.*, 1980) some unusual swelling minerals were found in the clay fractions of the rocks at the extremes of the weathering sequence. In the basaltic rubble, which represents the most highly weathered sample, the main phase was thought to be interstratified montmorillonite-illite and the geochemical processes involved in its genesis were discussed. The purpose of this paper is to expand on the brief details already published and to characterize the mineral in more detail both structurally and chemically; in part II (Bain & Russell, 1981), a swelling chlorite in the fresh basalt will be similarly characterized.

MATERIALS AND METHODS

The weathered material occurs at the top of the basalt flow as very friable red fragments consisting of clay and hematite and incorporating mottled material with white patches and spots. As these spots were found to consist of the swelling mineral of interest, the white material was hand-picked from crushed fragments under a binocular microscope, thus producing a purer separate than the clay fraction obtained by the usual sedimentation procedures.

X-ray diffraction traces were obtained from oriented aggregates and random powders using a Philips 2 kW diffractometer, iron-filtered CoKα radiation, divergent, receiving and scatter slits of 1°, 0·2 mm and 1°, respectively, and a scanning rate of 2° 2θ/min.

IR absorption spectra were recorded on a Perkin-Elmer 577 spectrometer over the range 4000–200 cm^{-1} using 13 mm diameter KBr pressed disks containing 1 or 0·25 mg sample. Weakly adsorbed water was removed by heating the disks for 16 h at 150°C.

The DTA curve was obtained on apparatus similar to that described by Mitchell &

Mackenzie (1959); a 150 mg sample was equilibrated at 56% relative humidity and heated at 10°C per minute in a nitrogen atmosphere.

The chemical composition was determined by X-ray fluorescence spectrometry using 0·167 g sample, the methods for sample fusion and corrections for background and inter-element effects being those of Norrish & Hutton (1969). The Kα lines were measured on a Philips PW 1540 spectrometer equipped with a 2 kW Cr tube and flow proportional counter with a 1 μm polypropylene window, using pulse-height discriminator settings specific to each wavelength.

Cation-exchange capacity (CEC) was determined by the neutral ammonium acetate method as modified by Mackenzie (1951).

RESULTS AND INTERPRETATION

The X-ray diffraction trace of the mineral separate after Mg-saturation displays a very strong peak at 14·2 Å with a moderate peak at 4·87 Å and weaker reflections at 4·48 and 3·545 Å (Fig. 1a). On treatment with glycerol, the main peak shifts to 18·0 Å with a

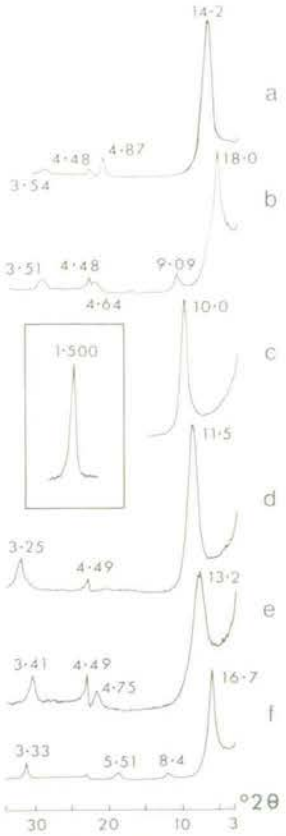

FIG. 1. X-ray diffraction traces of oriented aggregates at approximately 50% R.H., obtained using Co Kα radiation. Key: a, Mg-saturated; b, Mg-saturated, glycerol solvated; c, Mg-saturated, heated at 300°C; d, K-saturated; e, K-saturated, ethylene glycol solvated; f, Ca-saturated, ethylene glycol solvated. Inset: (060) region obtained from unoriented sample. All spacings are in Å.

shoulder at about 14 Å, and weaker peaks occur at 9·09, 5·95, 4·64, 4·48 and 3·51 Å (Fig. 1b). After heating at 300°C the main peak moves to 10·0 Å (Fig. 1c). Clearly the mineral is a swelling type which, from the 060 reflection at 1·500 Å (Fig. 1, inset) is dioctahedral and has similarities to montmorillonite. However, no integral series of basal reflections occurs (the 002 is absent) and the basal spacing is rather low for Mg-montmorillonite (usually 14·9–15·1 Å), indicating interstratification with at least one other component with a lower basal spacing.

Chemical analysis of the Ca-saturated mineral indicates a K_2O content of 1·80% (Table 1) which can only be due to an illite component in the interstratified phase as no other K-bearing mineral is present. The K_2O content of illites can vary from 4·78 to 11·0% and using the 7% average quoted by Weaver & Pollard (1973) for 24 illites, a value of about 25% illite is obtained for the interstratified mineral.

After K-saturation, the main peak occurs at 11·5 Å (Fig. 1d) and this moves to 13·2 Å on glycol solvation (Fig. 1e), an increase which is much too small for an interstratification of montmorillonite with 25% illite and most probably indicates the presence of a vermiculite component, since glycol-treated K-vermiculite remains collapsed at 10·4 Å.

Comparison of the diffraction trace of the Ca-saturated, glycol-treated sample (Fig. 1f) with the calculated diffraction curves of Cradwick & Wilson (1978) for three-component interstratification of illite, vermiculite and montmorillonite suggests that if there is 25% illite, there is probably an equal amount of vermiculite and about 50% montmorillonite. The calculated and actual spacings are not identical and the relative proportions of the components cannot be calculated exactly; however, comparison does suggest that the montmorillonite shows some degree of segregation and that the illite and vermiculite are randomly interstratified. Such segregation would explain the fully expanded montmorillonite spacing of 18·0 Å observed on the trace of the Mg-saturated, glycerol-treated sample.

Although the IR spectrum of the mineral separate (Fig. 2a) appears to resemble that of a typical illite (Fig. 2b) more closely than that of montmorillonite (Fig. 2c), there are some significant differences in both peak position and intensity. For the Killundine mineral, the

TABLE 1. Chemical composition of Ca-saturated mineral (in weight %).

SiO_2	48·2
TiO_2	0·18
Al_2O_3	24·5
Fe_2O_3*	1·44
MgO	2·62
CaO	2·81
K_2O	1·80
L.O.I.†	11·12
H_2O^-	8·30
	100·97

* Total iron as Fe_2O_3.
† L.O.I. = loss-on-ignition between 105 and 1000°C.

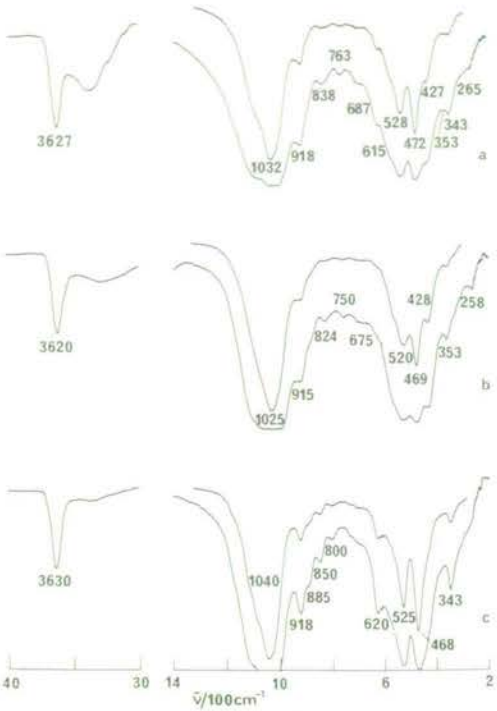

FIG. 2. Infrared absorption spectra of: a, Killundine mineral; b, Fithian illite; c, Wyoming montmorillonite. Spectra are recorded at concentrations of 1 mg (lower spectrum) or 0·25 mg (upper spectrum) in 13 mm diameter KBr pressed disks. $\tilde{\nu}$, wavenumber.

greater intensity of the AlAlOH deformation vibration at 918 cm^{-1}, the additional band at 838 cm^{-1}, the weak but well-defined band at 615 cm^{-1} and the sharp band at 343 cm^{-1} all indicate the presence of a montmorillonite. The weakness of the AlFeOH absorption near 885 cm^{-1} (Fig. 2a) compared with that shown by Wyoming montmorillonite (Fig. 2c) suggests that the montmorillonite in the Killundine mineral contains little structural iron.

Despite the overall similarity of the spectrum of the mineral to that of illite, the relative intensities of the illite 353 cm^{-1} and montmorillonite 343 cm^{-1} bands suggests that the montmorillonite may be as abundant as the illite-type minerals and this agrees generally with the estimates made from chemical analysis and XRD. The dioctahedral vermiculite which XRD suggests is also present cannot unambiguously be identified from the IR spectrum (Fig. 2a) but the presence of such a mineral whose spectrum closely resembles those of muscovite and illite is the reason for the illite-like absorption pattern observed (Kodama & Ross, 1972).

In the absence of other minerals, such as kaolinite, which absorb in the 350 cm^{-1} region, the absorbance of the band at 343 cm^{-1} in Fig. 2a can give an estimate of the amount of montmorillonite present. Using an average absorbance of 0·17/mg from four different montmorillonites as standard, a content of 56% was obtained for the Killundine mineral. Similarly, using an average absorbance value of 0·07/mg for the 353 cm^{-1} band of two illites, the interstratified mineral contains 43% illite-type layers, i.e. illite plus dioctahedral vermiculite. These amounts are in reasonable agreement with those estimated from XRD.

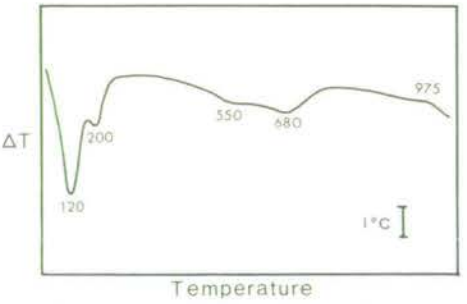

FIG. 3. DTA curve with temperatures indicated in °C.

The measured CEC of 93·7 mEq/100 g also agrees reasonably well with the value of 105 mEq/100 g calculated from average figures for montmorillonite, vermiculite and illite (Dixon & Weed, 1977) in the ratio 2:1:1.

The DTA curve of the untreated mineral (Fig. 3) displays a strong endothermic doublet at 120 and 200°C characteristic of montmorillonite saturated with a divalent cation (probably Ca^{2+}). Indeed, the whole curve strongly resembles that of a dioctahedral smectite, although the sharpness of the hygroscopic moisture peaks is more reminiscent of vermiculite than montmorillonite and the endotherm at 550°C could possibly be due to the illite component.

DISCUSSION

Although the Killundine three-component interstratified mineral is alumina-rich and iron-poor (Table 1), there are likely to be considerable differences in composition between the illite and swelling components. In order to calculate the structural formula of the swelling component (i.e. montmorillonite plus vermiculite), the analysis was corrected for the illite component using the average illite composition of Weaver & Pollard (1973). This correction accounts for nearly all the iron in the sample and the resulting structural formula (half cell) for the swelling component is:

$$Ca_{0\cdot30}(Al_{1\cdot72}Fe_{0\cdot01}Mg_{0\cdot29})(Si_{3\cdot60}Al_{0\cdot40})O_{10}(OH)_2.$$

Thus the number of ions in octahedral co-ordination is 2·02, confirming the dioctahedral character of both montmorillonite and vermiculite. The high tetrahedral charge is also reflected in the response of the mineral to the Greene-Kelly test (saturation with Li^+, heating at 300°C overnight, and treating with glycerol) which results in a strong diffraction peak at 17·2 Å and a moderate peak at 9·9 Å. A similar response to this test was obtained by Ross & Mortland (1966) for a clay from the A_2 horizon of a Michigan podzol. This clay contained about 25% mica interstratified with the swelling component and also had a similar CEC and chemical composition to the Killundine mineral. Interstratified mica-vermiculite-smectite has also been found in Ae horizons of Canadian podzols (Kodama & Brydon, 1968) where it represents a stage in the pedogenic weathering of mica.

The Killundine mineral illustrates the importance of applying various treatments, such as those used by Foscolos & Kodama (1974), to identify positively all the components in an interstratified system. For example, the XRD trace of the Killundine mineral (Fig. 1f)

compares favourably with the calculated curves of Reynolds & Hower (1970, Fig. 4a) for illite-montmorillonite interstratifications containing 20–40% illite, a value supported by the (002) illite/(003) montmorillonite spacing of 5·51 Å which suggests 34% illite. However, the K-saturation + glycol test provides strong evidence for an additional vermiculite component which, added to illite, means that probably about 50% of the layers are of the illite-type, thus explaining the general illitic nature of the infrared spectrum.

REFERENCES

Bain D.C. & Russell J.D. (1981) Swelling minerals in a basalt and its weathering products from Morvern, Scotland: II. Swelling chlorite. *Clay Miner.* **16** (in press).

Bain D.C., Ritchie P.F.S., Clark D.R. & Duthie D.M.L. (1980) Geochemistry and mineralogy of weathered basalt from Morvern, Scotland. *Miner. Mag.* **43**, 865–872.

Cradwick P.D. & Wilson M.J. (1978) Calculated X-ray diffraction curves for the interpretation of a three-component interstratified system. *Clay Miner.* **13**, 53–65.

Dixon J.B. & Weed S.B. (1977) *Minerals in Soil Environments*, pp. 242, 312. Soil Sci. Soc. Am., Wisconsin.

Foscolos A.E. & Kodama H. (1974) Diagenesis of clay minerals from Lower Cretaceous shales of north eastern British Columbia. *Clays Clay Miner.* **22**, 319–335.

Kodama H. & Brydon J.E. (1968) A study of clay minerals in podzol soils in New Brunswick, eastern Canada. *Clay Miner.* **7**, 295–309.

Kodama H. & Ross G.J. (1972) Structural changes accompanying potassium exchange in a clay-size muscovite. *Proc. Int. Clay Conf., Madrid*, **II**, 159–171.

Mackenzie R.C. (1951) A micromethod for determination of cation-exchange capacity of clay. *J. Colloid Sci.* **6**, 219–222.

Mitchell B.D. & Mackenzie R.C. (1959) An apparatus for differential thermal analysis under controlled-atmosphere conditions. *Clay Miner. Bull.* **4**, 31–43.

Norrish K. & Hutton J.T. (1969) An accurate X-ray spectrographic method for the analysis of a wide range of geological samples. *Geochim. cosmochim. Acta*, **33**, 431–453.

Reynolds R.C. & Hower J. (1970) The nature of interlayering in mixed-layer illite-montmorillonites. *Clays Clay Miner.* **18**, 25–36.

Ross G.J. & Mortland M.M. (1966) A soil beidellite. *Soil Sci. Soc. Am. Proc.* **30**, 337–343.

Weaver C.E. & Pollard L.D. (1973) *The Chemistry of Clay Minerals*, pp. 5–23. Elsevier Scientific Publishing Company, Amsterdam.

RÉSUMÉ: Le minéral argileux principal d'un basalte détritique altéré a été identifié par diffraction des rayons X, analyse chimique, spectroscopie infrarouge et analyse thermique différentielle; il s'agit d'un interstratifié montmorillonite, vermiculite et illite, dans le rapport approximatif 2:1:1, la montmorillonite possède un certain degré de ségrégation et vermiculite et illite présentent une interstratification gouvernée par le hasard. Tous le trois composants sont dioctaédriques, celui qui gonfle possède une charge tétrahédrique elevée, un fort contenu en aluminium et très peu de fer. Malgré une teneur de 50% de montmorillonite, le minéral présente le spectre d'absorbtion infra-rouge voisin de celui d'une illite.

KURZREFERAT: Das Hauptmineral in verwittertem basaltischen Grus wurde mittels Röntgendiffraktometrie, chemischer Methoden und Infrarot und Differential Thermoanalysen als ein Gemisch von Montmorillonit, Vermiculit und Illit im umgefähren Verhältnis von 2:1:1 identifiziert. Der Montmorillonit zeigt einige Anzeichen von Segregation, während Vermiculit und Illit in willkürlicher Wechsellagerung vorliegen.

Alle drei Komponenten sind dioktaedrisch. Die quellfähigen Tone haben eine hohe tetraedrische Ladung, einen hohen Aluminiumgehalt und sehr wenig Eisen. Trotz des 50%igen Montmorillonitanteils in dem Wechsellagerungsmineral hat das Infrarotabsorptionsspektrum einen illitischen Charakter.

RESUMEN: El mineral principal de arcilla en escombros basálticos meteorizados se ha demos-

trado por métodos de difracción de rayos X, químicos, infrarrojos y térmicos diferenciales, que es una interestratificación de montmorillonita, vermiculita e ilita en la proporción aproximada 2:1:1, en la que la montmorillonita tiene cierto grado de segregación y la vermiculita y la ilita aparecen interestratificadas aleatoriamente. Estos tres minerales constituyentes son dioctaédricos, y los que se hinchan tienen una carga tetraédrica, un gran contenido de aluminio y muy poco hierro. A pesar del contenido de 50% montmorillonita del mineral, su forma de absorción infrarroja es de carácter ilítico.

Manuscript for

CLAY MINERALS

August, 1980

SWELLING MINERALS IN A BASALT AND ITS WEATHERING PRODUCTS FROM MORVERN, SCOTLAND. PART II SWELLING CHLORITE

by

D.C. Bain and J.D. Russell

Swelling minerals in a basalt and its weathering products from Morvern, Scotland. Part II Swelling chlorite

D.C. Bain and J.D. Russell

The Macaulay Institute for Soil Research, Craigiebuckler, Aberdeen AB9 2QJ.

Abstract

A swelling chlorite from unweathered basalt has been characterised by XRD, IR, DTA and chemical analysis. Its 001 spacing of 14.9Å increases to 18.0Å on treatment with glycerol and decreases to 13.9Å with a broad diffraction effect at 13.9-10Å after heating to 550°C. The mineral has an 060 spacing of 1.537Å consistent with a trioctahedral composition, but its OH stretching band at 3638 cm^{-1} does not show the expected pleochroism, suggesting an anomalous hydroxide sheet which chemical analysis shows is incomplete. Although the mineral has a CEC of about 50 meq/100 g, smectite is not present, but all the techniques showed that the mineral has some saponitic character, indicating that it probably has a structure intermediate between swelling chlorite and saponite.

The weathering of a Tertiary basalt at Killundine, Morvern, to a red residual rubble dominated by secondary clay formed from labradorite has been described by Bain et al. (1980). In part I of this study (Bain and Russell, 1980) interstratified montmorillonite-vermiculite-illite, which is the main mineral in the weathered material, was characterised structurally and chemically, and this paper is devoted to a similar characterisation of a swelling chlorite type mineral which occurs in the fresh basalt.

Materials and Methods

The basalt, which is a hard, coherent rock showing no signs of weathering, contains irregular greenish patches, occasionally enclosing carbonate, of

chloritic material which seems to have formed from a late-stage fluid during the cooling of the lava (Bain et al., 1980). The fraction <2 μm was separated by standard sedimentation procedures from rock fragments ground under water by hand, and to obtain a larger quantity for chemical analysis, the <1.4 μm fraction was separated from material ground in a Tema mill for 2 minutes.

Details of the techniques and instruments used to obtain information by X-ray diffraction (XRD), infrared (IR) absorption spectroscopy, X-ray fluorescence spectrometry and differential thermal analysis (DTA) have been described in Part I (Bain and Russell, 1980) together with the method for determining cation-exchange capacity (CEC). Ferrous iron was determined on the <2 μm fraction using a modification of the colorimetric method of Wilson (1960) and ferric iron calculated by difference from the total iron subsequently determined on the same solution after reduction with ascorbic acid. In the solutions obtained by treating the clay according to the heating-extraction method of Ross and Kodama (1974), Mg was determined by atomic absorption spectroscopy and Si, Al and Fe were measured colorimetrically using the molybdenum blue, aluminon and orthophenanthroline methods, respectively.

Results and Interpretation

On the XRD trace of an oriented aggregate of the <2 μm fraction, there is only one strong peak, at 14.9Å, accompanied by a broad reflection at 7.3Å and a series of weak peaks due to feldspar between 4.61 and 3.19Å (Fig. 1a). Most of this pattern is unchanged on addition of glycerol except that the main peak shifts to 18.0Å and a second order reflection appears at 8.90Å (Fig. 1b). After heating at 550°C there is a broad reflection at 13.9Å and a weak, broad effect between 13.9 and 10Å (Fig. 1c). In the 060 region (70-75° 2θ) there is a single peak at 1.537Å (Fig. 1d). The 7Å peak, which is unaffected by glycerol but disappears on heating at 550°C, is thought to

be due to a small amount of normal chlorite as it is removed by treatment with warm HCl.

Saturation with Ca^{2+}, Mg^{2+}, Na^{+} and K^{+} produced no change in the XRD pattern (Fig. 2 a-d) although the 001 peak was slightly broader for the K-saturated sample (Fig. 2d) than for the others.

The chemical composition of the clay (Table 1) includes that of the feldspar, which, from the 2θ values for the $1\bar{1}1$ and $20\bar{1}$ reflections, is a labradorite of composition An_{60} (Van der Plas, 1966, p. 200-202). In order to obtain the composition of the swelling mineral, the CaO figure (1.47%) from the analysis of the K-saturated material was used to correct for the presence of labradorite, using the mineral with composition An_{60} listed by Van der Plas (1966, p. 39). This corrected composition yields the structural formula $(Si_{7.66}Al_{0.34})(Al_{1.72}Fe^{3+}_{1.96}Fe^{2+}_{1.50}Mg_{5.64})O_{20}(OH)_{16}$ when calculated as a normal chlorite. The octahedral filling of 10.22 is much smaller than the 11.36-11.58 recently reported for the so-called leptochlorites by Shirozu (1980), who concluded that the octahedral vacancies in the structure of these chlorites were concentrated in the interlayer hydroxide sheet giving a typical filling of approximately 5.4. To obtain further information on the nature of this sheet, the sample was heated to 560°C to dehydroxylate the hydroxide sheet and then treated twice with 0.2 M HCl and 0.2 M NaCl, a method shown by Ross and Kodama (1974) to remove more than 90% of the sheet. From the amounts of SiO_2, Al_2O_3, Fe_2O_3, and MgO in the extracts (Table 2), some 10% of the sample was removed in the first extract and another 11% in the second. Iron and magnesium were removed in roughly equal amounts with about half as much alumina and silica, the latter indicating that the 2:1 layer has been attacked to some extent. The XRD trace of the residue shows a peak at 14.5Å and a broad reflection between 14 and 10Å (Fig. 2e) (similar to the sample heated to 550°C with no subsequent treatment), part of the 14Å phase swelling to 17.8Å with glycerol (Fig. 2f), and apparently

all collapsing to 9.9Å after heating at 550°C (Fig. 2g). These results clearly show that virtually all the hydroxide sheet was removed by these extractions. Of the 21% removed, approximately 4% is assignable to the 2:1 layer indicating that the hydroxide sheet removed represents about 17% of the structure. This value is considerably lower than the theoretical 30-33% which the hydroxide sheet comprises in a normal chlorite, indicating that this sheet is incomplete in the Killundine mineral and, from the predominance of divalent ions in the extract (Table 2), that it is trioctahedral.

The decrease in CaO and increase in K_2O content on K-saturation (Table 1) is consistent with the CEC value for the <1.4 μm fraction of 41.9 meq/100 g. Allowing for 12.6% labradorite (as calculated from the CaO content) the CEC of the swelling phase would be at least 48 meq/100 g as a small amount of chlorite is also present.

Apart from the low temperature endotherm at 120°C, due to an appreciable content of adsorbed moisture, the DTA curve (Fig. 3) is quite characteristic of a chlorite which usually displays a large endotherm between 450 and 650°C, another around 700°C and an exotherm between 750 and 900°C (Caillère and Hénin, 1957; Phillips, 1963). It is also similar to that of corrensite (a regular alternation of swelling chlorite and chlorite) published by Lippmann (1954).

The IR spectrum of preground fresh basalt (Fig. 4a) shows generally broad absorption bands in the 4000-800 cm^{-1} range with sharper detail between 800 and 200 cm^{-1}. Most of the bands in the lower frequency range correspond with those reported by Lyon (1962) for a feldspar comprising 50% albite, 50% anorthite, in reasonable agreement with the composition of the feldspar calculated from XRD. The broad band at 3636 cm^{-1} belongs to the chlorite-type mineral indicated by XRD, but most of the rest of its absorption pattern is obscured by that of the feldspar. The feldspar pattern was still

obvious in the spectrum of the <1.4 μm fraction from the ground rock, but in a <0.5 μm fraction, the chloritic phase is dominant. Its IR spectrum (Fig. 4b), with an OH stretching band at 3638 cm^{-1}, OH deformation at 645 cm^{-1} and Si-O bands at 1008 and 454 cm^{-1}, and no detectable OH absorption near 920 cm^{-1}, is consistent with a trioctahedral layer silicate, and resembles that of the low-Al chlorite pennine (Fig. 4c).

Despite the overall similarity, there are several important differences, principally the general weakness of OH absorption bands at 3638 and 645 cm^{-1}, absence of an OH band near 3500 cm^{-1}, and the simpler contour and relatively high frequency of the Si-O stretching band at 1008 cm^{-1} in the Killundine mineral. Also, from a comparison between spectra of an oriented film and a random dispersion in a KBr pressed disk, the 3638 cm^{-1} OH band shows little or no pleochroism, contrasting sharply with the 3635, 3490 cm^{-1} pennine OH bands which are markedly pleochroic. Elimination of the 3638 cm^{-1} band by heating to 560°, a temperature known to dehydroxylate the hydroxide sheet of chlorites, clearly establishes its origin in this type of structure. Its failure to exhibit pleochroism despite the overall trioctahedral character of the mineral, does not appear to be due to the hydroxide sheet being dioctahedral because the cations extracted from the hydroxide sheet following heating to 560°C (Table 2) are predominantly divalent.

Another difference between the minerals is seen after heating them to 560°, the spectrum of the Killundine mineral showing weak OH bands at 3661 and 3623 cm^{-1} compared with 3673 cm^{-1} for pennine. These bands originate in the 2:1 layer, and in the Killundine mineral they arise from $Mg_2Fe^{2+}OH$ and possibly $Fe_3^{2+}OH$ groupings, respectively, indicating considerable Fe^{2+}-for-Mg substitution. This is at variance, however, with the position of the Si-O stretching band at 1008 cm^{-1}, Oinuma and Hayashi (1968) having shown that with increasing Fe^{2+} content, the Si-O band of chlorites shifts from

about 1000 cm^{-1} in pennine to 981 cm^{-1} in daphnite. Indeed, sheridanite and ripidolite, chlorites with Fe^{2+} contents that are similar to that of the Killundine mineral, show spectra (Post and Plummer, 1972; Farmer, 1974, p. 342) that are quite different, suggesting that the structure of the Killundine mineral is significantly different from that of normal chlorite.

The higher frequency of its Si-O stretching band (Fig. 4b) indicates that less of the tetrahedral Si is substituted by other ions in the Killundine mineral compared with pennine, and this is borne out by the composition calculated above. This lower level of substitution is more analogous to that present in smectites, and in agreement with this, the IR pattern of the Killundine mineral, with the exception of the broad 3638 cm^{-1} band of the hydroxide sheet, closely resembles that of saponite, illustrated here (Fig. 4d) by a spectrum that contains some Fe^{2+}-for-Mg substitution (Mitchell, 1954).

Despite this similarity to saponite, the Killundine mineral displays no spectroscopic evidence that saponite per se is present, in that no absorption band was observed near 3710 cm^{-1} (Fig. 4b), as would have been expected from the influence of K^+ ion (from KBr) in a collapsed interlayer on lattice OH groups of saponite (Farmer, Russell and Ahlrichs, 1968). This implies that K^+ ions are either unable to penetrate into the interlayer region, or, more probably, that they enter the interlayer and migrate towards exchange sites, but, because the hydroxide sheet prevents the interlayer from collapsing on removal of adsorbed water, they cannot approach lattice OH groups sufficiently closely to produce the high frequency band.

In the spectrum of a sedimented deposit of the Killundine mineral, the hydroxide sheet OH band shifts from 3610 cm^{-1} in the hydrated, air-dry state, to 3630 cm^{-1} after prolonged evacuation which removed most of the hydration water, and finally to 3638 cm^{-1} after heating to 200°C (Fig. 4b). This

progressive shift to higher frequency with removal of hydration water indicates the involvement of the OH groups of the hydroxide sheet in hydrogen bonding with interlayer water. Such an interaction provides proof that the hydroxide sheet is discontinuous, because only then, in the context of a 14Å basal spacing, could water molecules be suitably accommodated.

Discussion

The essential characteristics of swelling chlorite, as originally described by Stephen and MacEwan (1950, 1951), are that it has a 14Å basal spacing (with a series of orders) which contracts slightly on heating to 500°C and swells to 17-18Å with glycerol. The mineral in the clay fraction from the Killundine basalt matches this description in a general way, although there are minor discrepancies in spacings and there is no series of basal reflections. The similarities to chlorite are obvious, particularly in the spacing of 13.9Å after heating at 550°C, in the IR spectrum and in the DTA curve, and these, combined with swelling to 18Å with glycerol, all point to identification as swelling chlorite.

However, comparison of the chemical composition of the Killundine mineral (Table 1) with analyses of chlorites and saponites in the literature fails to indicate any strong affinity with either group. The contents of the two most common elements occupying octahedral positions - Fe and Mg - vary widely in chlorites and saponites and the amounts in the Killundine mineral fall within the limits of both mineral types. The lowest content of alumina in the chlorites listed by Foster (1962) is 10.14%, however, so that 8.33% is abnormally low for a chlorite but within the range of figures given by Weaver and Pollard (1973) for saponites (3.89-14.52%). The silica content, on the other hand, is slightly higher than that of the most siliceous chlorite (36.43% SiO_2) and lower than that of the least siliceous saponite (39.68% SiO_2). Similarly, the LOI figure is higher than for any normal chlorite and

about the same as the lowest figure quoted for saponite, all of which would tend to suggest some affinities with saponite.

Thus the XRD and IR ~~and DTA~~ results and the chemical analysis of the Killundine mineral all point to a structure which is intermediate between those of chlorite and saponite, with some of the properties of both minerals. Several observations, however, militate against the presence of saponite per se, at least in any significant proportion, namely: 1) no contraction in spacing on saturation with K^+ and Na^+; 2) no endotherm at about 200°C on the DTA curve as would be evident for a smectite saturated with a divalent cation; 3) no detectable high frequency band near 3710 cm^{-1}, produced by interaction between K^+ ions from the KBr disk matrix and lattice OH groups of saponite.

From the formula calculated above on the basis of a normal chlorite structure, the filling of the hydroxide sheet could be about 4.2, indicating that it ~~the sheet~~ is incomplete, and indeed from the Ross and Kodama treatment, only half of the hydroxide sheet of a normal chlorite appears to be present. This observation was used to recalculate the following structural formula on the basis of 50 negative charges:

$(Si_{6.84}Al_{1.16})(Al_{0.68}Fe^{3+}_{1.22}Fe^{2+}_{1.34}Mg_{5.04})O_{20}(OH)_{10}$

Assuming that the octahedral sheet in the 2:1 layer is fully trioctahedral, 8.28 octahedral cations in this formula would indicate only 2.28 cations in the hydroxide sheet, just over one third of the maximum value in a chlorite. It would appear, therefore, that between one half and one third of a complete hydroxide sheet is present.

Swelling chlorites are usually considered to be imperfect structures containing "islands" of hydroxide sheet between the 2:1 layers - i.e. the hydroxide sheet is discontinuous (Brindley, 1961). The extent of the hydroxide sheet will doubtless vary from sample to sample but presumably

the "islands" must be frequent enough to prevent collapse on heating, yet infrequent enough to allow glycerol molecules to fill the spaces between them and permit the structure to expand. The spaces must accommodate the exchangeable cations and their associated hydration water observed in the IR spectra. This type of interlayer structure may also account for the partial collapse of the Killundine mineral at 550°C, unfilled areas between the "islands" collapsing to produce a broad reflection between 14 and 10Å on the XRD pattern. Unlike the swelling chlorite as defined by Stephen and MacEwan (1950, 1951), the Killundine mineral does not produce a series of basal reflections, pointing to considerable disorder in the structure. Similarly, an electron diffraction pattern consisting of rings (at 4.55, 2.64, 1.74 and 1.54Å) rather than spots indicates a turbostratic structure. Failure of the IR bands of the hydroxide sheet to exhibit the pleochroism expected of a trioctahedral sheet further indicates that this disorder occurs in the hydroxide sheet, presumably due to size, frequency and arrangement of the "islands".

Acknowledgements

The authors wish to thank A.R. Fraser for providing the IR results on the dehydration of the mineral, J.M. Tait for electron diffraction data and B.F.L. Smith for chemical analyses of the extracts.

References

Bain D.C., Ritchie P.F.S., Clark D.R. & Duthie D.M.L. (1980). Geochemistry and mineralogy of weathered basalt from Morvern, Scotland. Miner. Mag. (in press).

Bain D.C. & Russell J.D. (1980). Swelling minerals in a basalt and its weathering products from Morvern, Scotland. Part I Interstratified montmorillonite-vermiculite-illite. Clay Miner. (in press).

Brindley G.W. (1961). Chlorite Minerals. Pp. 242-296 in: The X-ray Identification and Crystal Structures of Clay Minerals (G. Brown, editor). Mineralogical Society, London.

Caillère S. & Hénin S. (1957). The Chlorite and Serpentine Minerals. Pp. 207-230 in: The Differential Thermal Investigation of Clays (R.C. Mackenzie, editor). Mineralogical Society, London.

Farmer V.C. (1974). The Layer Silicates. Pp. 331-363 in: The Infrared Spectra of Minerals (V.C. Farmer, editor) Mineralogical Society, London.

Farmer V.C., Russell J.D. & Ahlrichs J.L. (1968). Characterization of clay minerals by infrared spectroscopy. Trans. 9th Int. Congr. Soil Sci. 3, 101-110.

Foster M.D. (1962). Interpretation of the composition and a classification of chlorites. Prof. Pap, U.S. geol. Surv. 414A, A1-A33.

Lippmann F. (1954). Uber einen Keuperton von Zaisersweiher bei Maulbronn. Heildelberg. Beitr. Min. Pet. 4, 130-134.

Lyon R.J.P. (1962). Evaluation of Infrared Spectrophotometry for Compositional Analysis of Lunar and Planetary Soils, Stanford Research Institute, California.

Mitchell W.A. (1954). An occurrence of saponite in vesicular lava. Clay Miner. Bull. 2, 207.

Oinuma K. & Hayashi H. (1968). Infrared spectra of clay minerals. J. Toyo Univ. Gen. Educ. (Nat. Sci.) 9. 57-98.

Phillips W.R. (1963). A differential thermal study of the chlorites. Miner. Mag. 33, 403-414.

Post J.L. & Plummer C.C. (1972). The chlorite series of Flagstaff Hill area, California: a preliminary investigation. Clays Clay Miner. 20, 271-283.

Ross G.J. & Kodama H. (1974). Experimental transformation of a chlorite into a vermiculite. Clays Clay Miner. 22, 205-211.

Shirozu H. (1980). Cation distribution, sheet thickness and O-OH space in trioctahedral chlorites - an X-ray and infrared study. Miner. J. 10, 14-34.

Stephen I. & MacEwan D.M.C. (1950). Swelling chlorite. Geotechnique 2, 82-83.

Stephen I. & MacEwan D.M.C. (1951). Some chloritic clay minerals of unusual type. Clay Miner. Bull. 1, 157-162.

Van der Plas L. (1966). The Identification of Detrital Feldspars, Pp. 39, 200-202, Elsevier, Amsterdam.

Weaver C.E. & Pollard L.D. (1973). The Chemistry of Clay Minerals, Pp. 77-86, Elsevier, Amsterdam.

Wilson A.D. (1960), The micro-determination of ferrous iron in silicate minerals by a volumetric and a colorimetric method. Analyst, Lond. 85, 823-827.

Table 1. Chemical composition, in weight %

	<1.4 μm	<1.4 μm K-sat.	Corrected for labradorite
SiO_2	37.9	38.8	36.5
TiO_2	0.13	0.15	0.17
Al_2O_3	10.7	11.0	8.33
Fe_2O_3†	7.32	7.64	8.61
FeO†	7.27	7.57	8.58
MnO	0.18	0.14	0.16
MgO	15.8	15.9	18.1
CaO	2.51	1.47	
Na_2O	1.47	n.d.	
K_2O	0.15	2.70	3.00
L.O.I.*	16.04	13.73	15.62
TOTAL	99.47	99.10	99.07

* L.O.I. - loss-on-ignition at 1000°C. <1.4 μm sample equilibrated at 56% relative humidity; K-sat. sample at room humidity.

† FeO and Fe_2O_3 measured on <2 μm sample and re-calculated for <1.4 μm sample assuming Fe^{2+}/Fe^{3+} is the same in both.

n.d. - not determined.

Table 2. Chemical analyses of extracts from HCl treatment after heating to 560°C

	% in first extract	% in second extract	Total
SiO_2	1.76	1.95	3.71
Al_2O_3	1.73	1.87	3.60
MgO	3.32	3.52	6.84
Fe_2O_3*	2.92	3.72	6.64
Total	9.73	11.06	20.79

* Total iron as Fe_2O_3

Legend for Figures

Fig. 1 XRD traces obtained at approximately 50% R.H. using CoKα radiation. Key: a - oriented aggregate; b - oriented aggregate, glycerol solvated; c - oriented aggregate heated at 550°C; d - unoriented sample.

Fig. 2 XRD traces of oriented aggregates obtained with CoKα radiation. Key: a - d - saturated with Ca^{2+}, Mg^{2+}, Na^{+} and K^{+}, respectively; e - g - after treatment by the heating-extraction method of Ross and Kodama (1974); e - room temperature; f - glycerol solvated; g - heated at 550°C.

Fig. 3 DTA curve of Ca-saturated sample, with temperatures indicated in °C.

Fig. 4 Infrared absorption spectra of a - Killundine basalt; b - <0.5 μm clay fraction from Killundine basalt; c - pennine (Farmer, 1974); d - saponite (Mitchell, 1954). 0.3-0.7 mg, in 13 mm diameter KBr pressed disks heated to 200°C. Sharp absorption bands near 3000 and 2300 cm^{-1} arise from C-H contamination and absorbed CO_2, respectively.

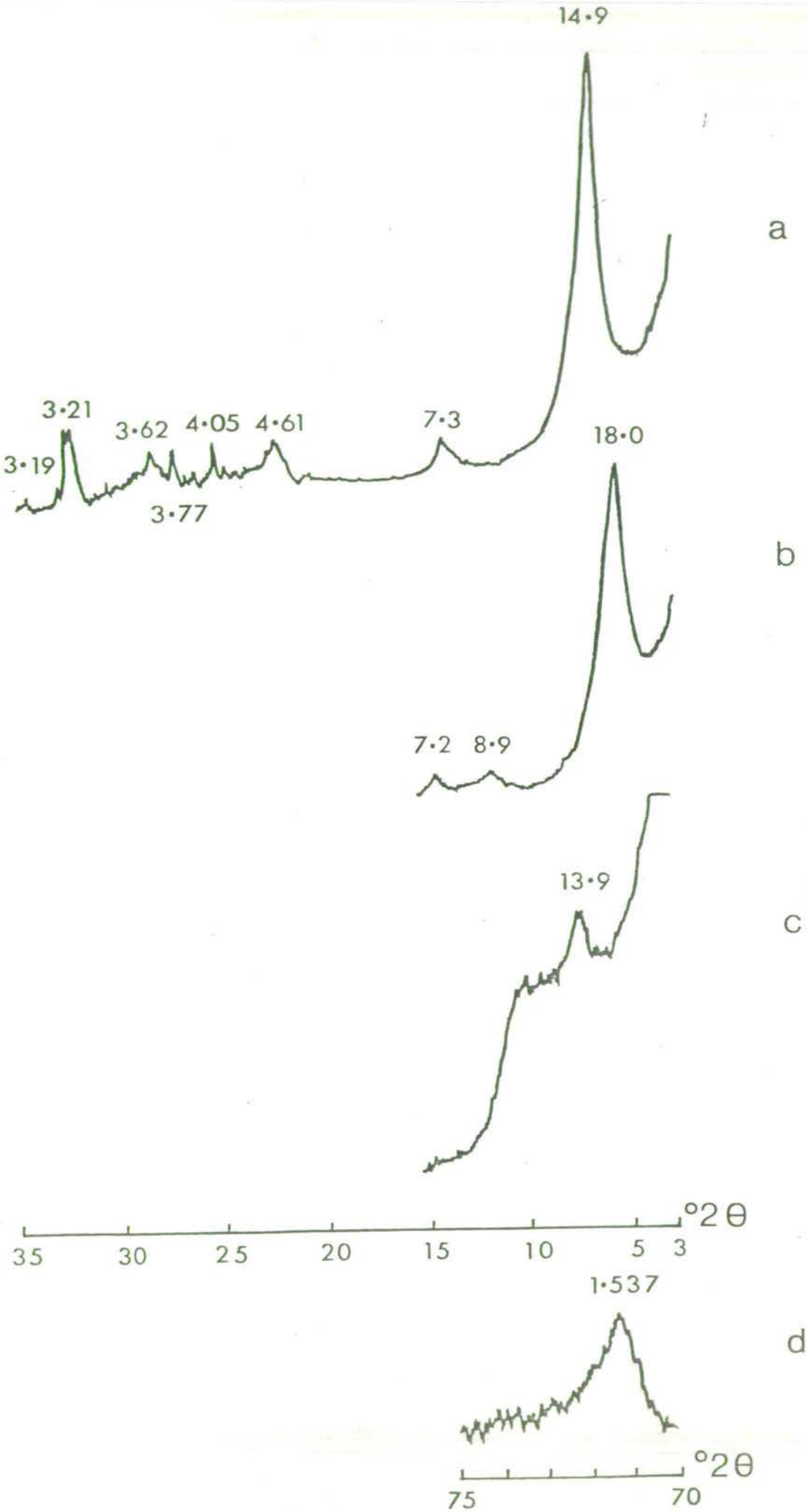
14·9
a
3·21
3·19
3·62
4·05
4·61
7·3
3·77
18·0
b
7·2
8·9
13·9
c
°2θ
35
30
25
20
15
10
5
3
1·537
d
°2θ
75
70

Fig 1

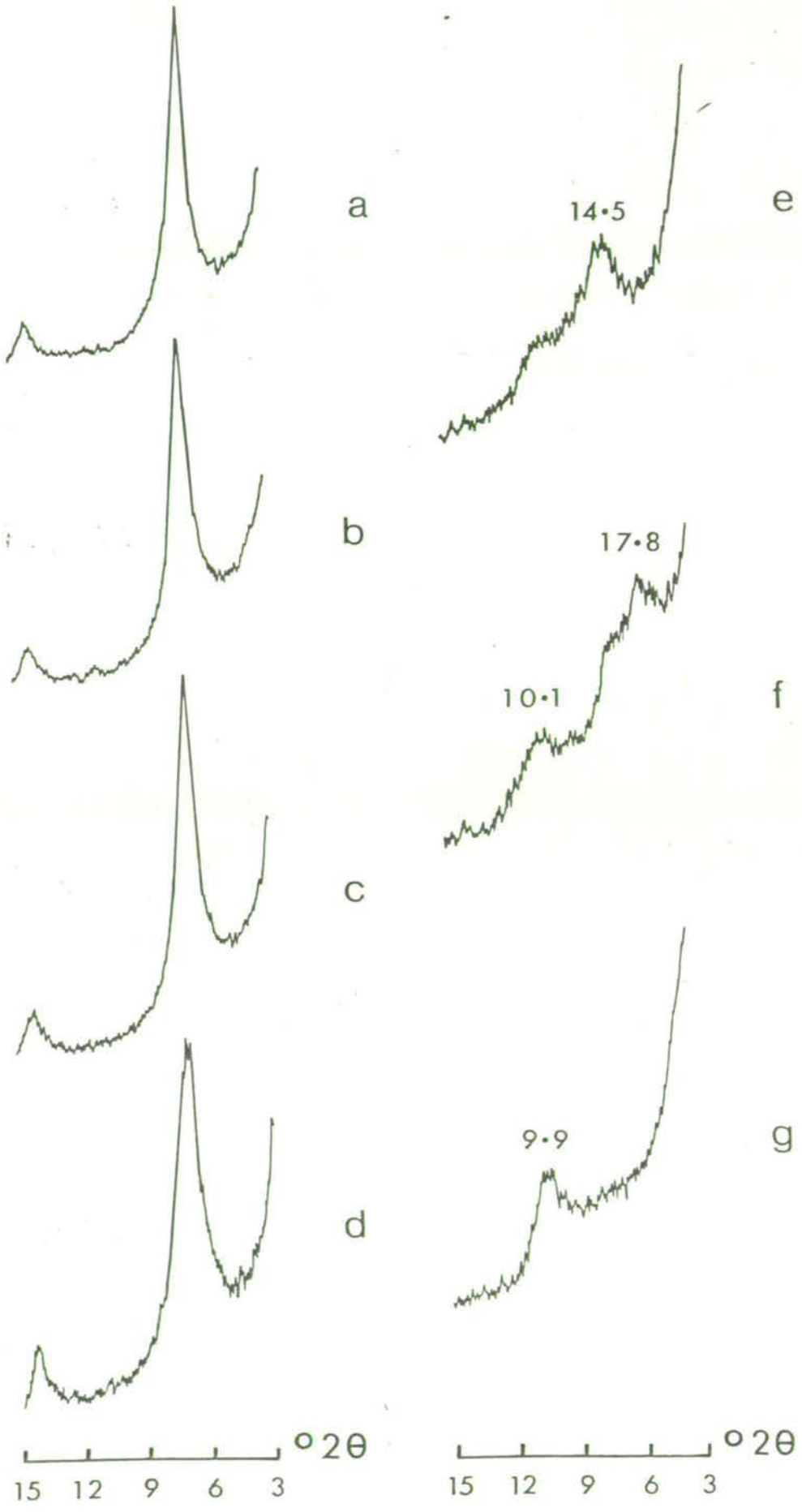

Fig 2

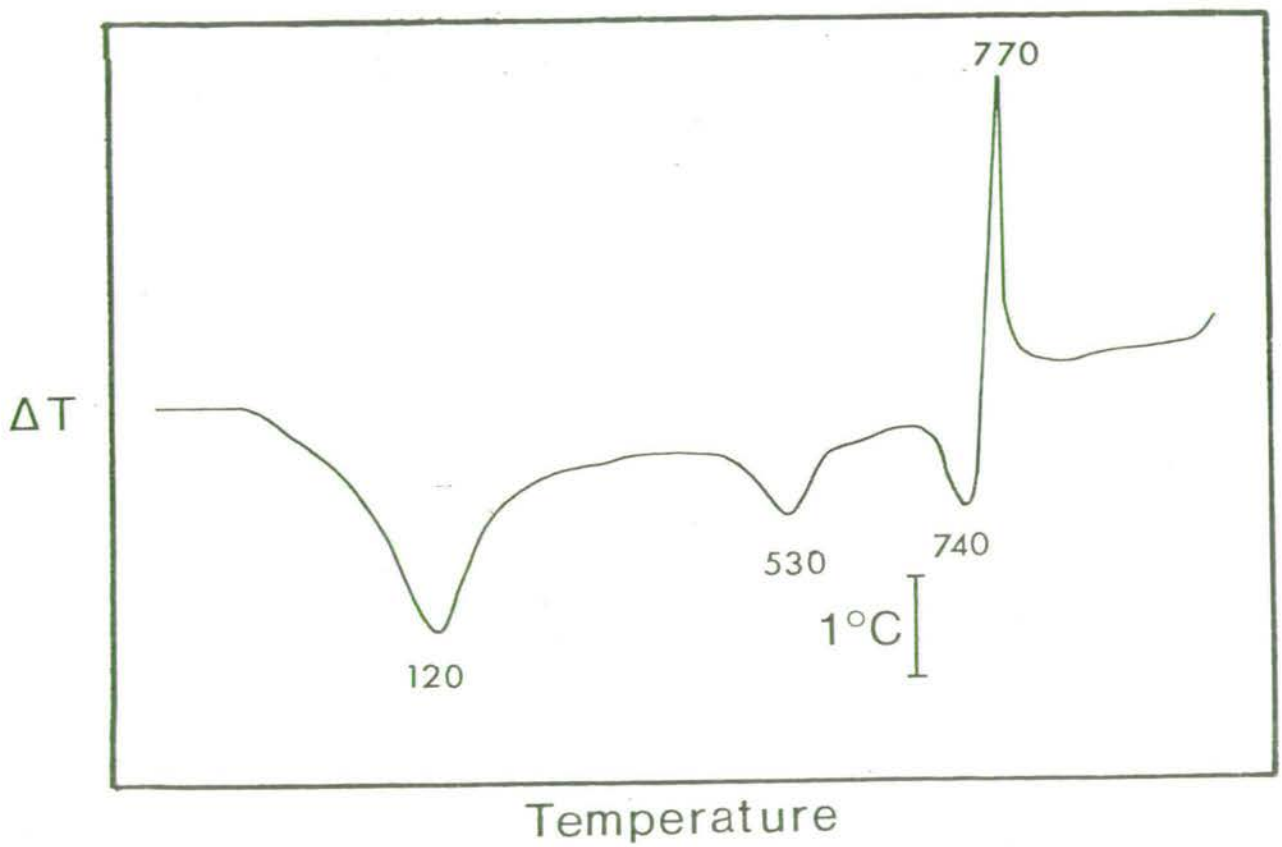

Fig 3

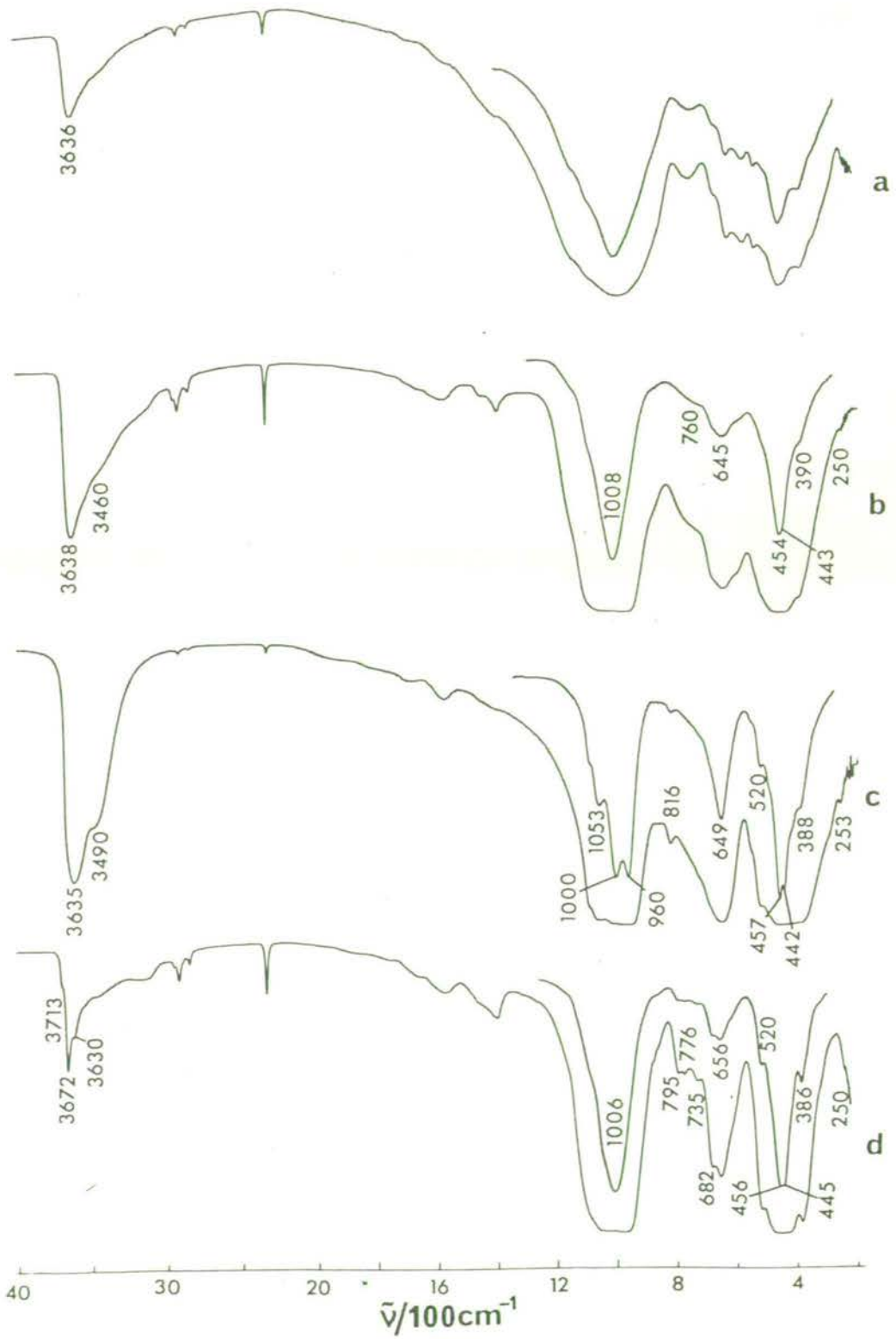
3636
a
3638
3460
1008
760
645
390
250
454
443
b
3635
3490
1053
816
649
520
388
253
1000
960
457
442
c
3713
3672
3630
1006
795
776
735
656
520
386
250
682
456
445
d
40
30
20
16
12
8
4
ν̃/100cm⁻¹

Manuscript for

CLAY MINERALS

November 1980

A SWELLING HEMATITE-SILICATE COMPLEX IN WEATHERED GRANITE

By

M.J. Wilson, J.D. Russell, J.M. Tait,

D.R. Clark, A.R. Fraser and I. Stephen

A SWELLING HEMATITE-SILICATE COMPLEX IN WEATHERED GRANITE

By

M.J. Wilson, J.D. Russell, J.M. Tait

D.R. Clark, A.R. Fraser and I. Stephen*

The Macaulay Institute for Soil Research, Craigiebuckler, Aberdeen, AB9 2QJ.

* Department of Soil Science, University of Aberdeen, Aberdeen.

Hematite is widespread in soils developed under tropical and sub-tropical climates. Recently, it has been found that the X-ray diffraction pattern of hematite separated from such soils is not always identical with that of reference samples from mineral deposits. In particular, X-ray patterns from soil hematite exhibit differential line broadening which is now accounted for in terms of disorder effects resulting indirectly from aluminium substitution within the structure (Schwertmann et al., 1977). In fact, iron oxides also act as sinks, adsorbing other ions common in the environment, such as silicate and phosphate, as well as a variety of trace elements. The effect of such foreign ions in general, and of the silicate ion in particular, is to inhibit crystallization of iron oxide minerals and to induce structural disorder (Kühnel et al., 1975; Schwertmann and Taylor, 1977). At present, the nature of the association between iron oxide and silicate is not clear; it is not known, for example, if silicate is adsorbed onto the surface of the oxide or if it is incorporated into the structure. In the present paper, a naturally occurring hematite-silicate complex is described in detail, thus enabling the nature of the iron oxide-silicate association to be specified.

MATERIALS

The material was separated from samples collected from an exposure of

ABSTRACT

A naturally occuring hematitic iron oxide-silicate complex has been found in red mottled patches of a deeply weathered granite in north-east Scotland. X-ray diffraction shows a basal spacing of 36Å - also observable by high resolution electron microscopy - which expands to 40Å with glycerol and contracts to 33.5Å on heating. Selected area electron diffraction reveals a composite hematite-layer silicate pattern with the a axis of hematite parallel to the b axis of the silicate. The infrared spectrum of the complex clearly shows the contribution made by each of the components. The silicate, with bands due to OH stretching at ~~3698~~ ~~and~~ 3602 cm^{-1}, OH deformation at ~~910 and~~ 855 cm^{-1}, and Si-O stretching at 1085, 1035, 540 and 471 cm^{-1} resembles ferruginous pyrophyllite, while the hematite, with a perpendicular band at 647 cm^{-1}, in-plane bands at 519, 438, 400, 302 and 227 cm^{-1} and a characteristic pattern of relative band intensities, is similar to a platy form of soil hematite. Electron microprobe analysis of individual particles gives the complex an (Fe + Al):Si ratio of 6:1, which is consistent with a structure made up of ~~a~~ twelve octahedral sheets terminated on both sides by a silicate sheet. It seems ~~possible~~ that the complex developed from a siliceous ferrihydrite which became progressively transformed with ~~geological~~ time.

deeply weathered granite at the foot of Bennachie, an upstanding granitic mass with tor-like features at its summit. Attention was focussed on these samples following a preliminary X-ray examination of the clay fractions separated from reddened, weathered granite where ~~the occurrence of~~ a 18Å reflection was observed in the untreated material. The outcrop is located at the eastern end of the Bennachie car park some 7 km WNW of Inverurie in north- east Scotland (NJ/682246). It is approximately 6 m high and shows 4 to 5 m of loose, weathered granite covered by 1 to 2 m of soliflucted, consolidated stony material upon which a podzolic soil profile has developed (Fig. 1a). Usually, the granite is completely friable, although the original fabric can easily be discerned. Occasional quartz veins and harder patches of rock also occur. This type of deep weathering is fairly widespread in north-east Scotland and is believed to represent the remnant patches of a weathered mantle of Tertiary age, most of which was eroded away during the Pleistocene glaciation. One of the most striking features of the weathered granite is its colour, with bright red mottling (Munsell Colour 10R 5/8) superimposed on a generally white or light brown background (Fig. 1b). The boundary between red and non-red parts is usually quite sharp; close examination of the white material often shows a faint, light red mottling with occasional patches of yellow-brown or black.

METHODS

Samples were collected from adjacent red and non-red parts of the weathered granite on several different occasions. The samples were dispersed in water using an ultrasonic probe at 20 KHz for 10 min followed by end-over-end shaking for 24 h; the <2μm faction was then separated by repeated siphoning off the top 10 cm of the suspension after sedimentation for 8 hours. Kaolinite,

which is the predominant mineral in the clay fraction, was removed by HF dissolution using the method described by Norrish (1968). For X-ray diffraction, clay/water suspensions were dried on to a glass slide and the oriented aggregate so obtained examined using a Philips 2 kW diffractometer with Fe-filtered CoK α radiation. At angles of <12°2θ divergent, receiving and antiscatter slits of ¼°, 0.1 mm and ¼° respectively were used, these being changed to 1°, 0.2 mm and 1° at angles >12°2θ. ~~The clay fractions were subjected to various treatments in order to study the responses of the characteristic basal reflection. Thus~~, The clays were examined air dry, in a wet state, after saturation with glycerol and ethylene glycol, after saturation with various ions and after heating at 300 and 500°C for 2 to 4 h. In addition, the effect of boiling 0.5 M NaOH for 2.5 mins (Hashimoto and Jackson, 1960), boiling 5 M HCl for 30 min, prolonged treatment with acid ammonium oxalate in the light ~~(Tamm, 1922)~~ and treatment with sodium dithionite-citrate-bicarbonate solutions (Mehra and Jackson, 1960) were also studied.

For electron microscopy the clays were dispersed in double-distilled water, a drop of suspension being dried on to a carbon-coated copper grid and then examined using a Siemens Elmiskop 102. Electron diffraction patterns were recorded using the same instrument. High resolution electron micrographs were also taken of randomly oriented clay particles embedded in Spurr's Resin and cut with an LKB Ultratome to a thickness of approximately 15.0Å. By this means the layer structure of the clay mineral crystallites could be clearly observed with a resolution of 10Å. Thin sections of resin-impregnated red and non-red weathered granites were also examined using optical microscopy.

Chemical analyses of untreated and HF-treated samples were carried out in a Kratos CORA analytical electron microscope equipped with a Link System energy-dispersive X-ray analyser. Integrated counts were determined for

each of the X-ray peaks for Al-K, Si-K, K-K_α and Fe-K_α. Sufficiently thin crystals were analyzed to render absorption and fluorescence errors negligible. Correction factors for losses in the detector were made.

For infrared spectroscopy the samples were either incorporated in 13 mm diameter KBr or CsI pressed disks or deposited from aqueous suspension onto CsI plates, and the spectra recorded on Perkin Elmer 577 or 580B spectrometers over the range 4000-200 cm^{-1}. The disks contained either 2 mg or 0.25 mg.

RESULTS

Optical Observations

Quartz and K-feldspar are the dominant minerals in the weathered granite with subordinate muscovite and small amounts of pleochroic biotite. ~~The distribution of clay minerals and iron oxides in the red and non-red parts of the outcrop was studied by optical microscopy.~~ Kaolinite is the dominant weathering product and occurs in coarse interlocking aggregates and as books, rouleaux and vermicules; in many places it completely replaces the original feldspar. Smectite and mica are much less abundant and in the drab samples, occur in small discrete patches and vein-like filaments, occasionally abutting against kaolinized feldspar (Fig. 2a). In the red samples the iron oxides seem to be preferentially associated with mica and montmorillonite rather than kaolinite which in many cases is relatively free ~~to~~ of pigment (Fig. 2b).

X-ray diffraction results

The mineralogy of the clay fractions separated from the red and non-red parts of the weathered granite was virtually identical with dominant kaolinite (both well-crystallized kaolinite and tubular halloysite occur in

this outcrop) and subordinate illite. The only difference is that the red clays show a relatively weak and somewhat broad reflection at 17.8Å (Fig. 3a). This reflection was observed using two different diffractometers with various slits and instrumental settings and thus represents a genuine diffraction effect. First observations showed that this high spacing increased on glycerol solvation, contracted on heating at 300°C and 600°C and remained stable after boiling with 0.5 M NaOH or 5 M HCl. The spacing was unaffected by acid ammonium oxalate treatment but disappeared after the dithionite treatment of Mehra and Jackson (1960), suggesting the possibility of an iron oxide-clay mineral complex. The existence of such a complex would be of even greater interest in this case because, despite the red colouration of the clay, no hematite was detectable by X-ray diffraction. The clay itself contains about 7 per cent dithionite citrate-extractable iron and X-ray diffraction of a 93 per cent kaolinite/7 per cent hematite mixture showed that ~~the~~ a crystalline iron-oxide should be easily detectable at this level. Thus, it may be that the red colour is imparted principally by an iron oxide complex rather than by discrete hematite.

Enriched samples of the complex were obtained after dissolution of the kaolinite in HF. The diffraction pattern after a 5 min treatment (Fig. 3b) shows a strong 17.8Å spacing, a weak subsidary reflection at 11.8Å and a clearly defined reflection at 36Å approximately, which had not previously been observed. The 36, 17.8 and 11.8Å spacing are therefore indexed as 001, 002 and 003 reflections, respectively; no other orders or spacings attributable to the complex could be seen. The basal reflections are still apparent after HF treatment for 2 hours but they then gradually become broader and weaker until after 8 hours they are completely eliminated from the diffraction pattern (Fig. 3c). The residue at this stage consists principally of well-crystallized mica, goethite and anatase, but there are also two very weak reflections characteristic of hematite at 2.70 and

2.52Å. The effects of the various treatments on the HF-concentrated material are shown in Table 1 and Figure 4.

Fig. 5 shows an X-ray powder photograph of the complex obtained from 450°C heated and 3 min HF-treated <0.2 μm material, which from infrared observations appeared to be relatively free of contaminating mica. It may be noted that the basal reflections of the complex are not observable in this photograph, the pattern being in general agreement with that of hematite (Table 2). However, there are two features which deserve further comment. Firstly, it can be seen that two of the lines - indexed as 110 and 300 for hematite - are much sharper than those of the rest of the pattern. Secondly, these reflections are more intense than the same reflections which are normally observed for hematite. This type of pattern is also characteristic of unheated material. The significa of these observations will be discussed later.

Electron Microscopy

Observations on untreated and HF-concentrated clay fractions showed the presence of poorly-shaped clay mineral particles with characteristic moiré fringes and prominent, irregularly distributed electron-dense areas (Fig. 6a), an aspect consistent with a close association between iron oxide and layer silicate minerals. Electron diffraction patterns of such particles (Fig. 6b) can be interpreted in terms of hematite and a layer silicate phase and also reveal an orientation relationship between these components. Thus, the silicate phase yields a hexagonal diffraction pattern, typical of layer silicates, the 11, 02 reflections close to the central beam being relatively weak. However, the 13, 20 reflections coincide with the 110 reflections of hematite, indicating that the $\underline{b}$ axis of the silicate sheet is parallel to the $\underline{a}_{hex}$ axis of the hematite. This orientation relationship is understandable in view of the fact that both phases would contain planes of oxygen atoms in hexagonal close packing parallel to the basal planes. The secondary diffraction effects surrounding the main hematite

reflections are due to the composite nature of the particles as well as to rotation of the layers, indicated also by the moiré fringes referred to previously.

High resolution lattice images of the HF-treated clay (Fig. 6c, d) show many areas with a pronounced 36Å layer structure - a spacing in agreement with the X-ray diffraction data. Moreover, the high-resolution micrographs graphically illustrate the complex nature of these lamellar structures and the ways in which they are affected by dislocations. Thus, variable layer thickness with prominent pinching out and swelling effects, sinuosity and bending of the layers, kinking of the layers and angular discordance between packages of layers are all prominent features. Other particles show 10Å lattice fringes indicative of mica.

Infrared Spectroscopy

Spectra of the red and non-red clays are very similar, being dominated by absorption bands of well-crystallized kaolinite (Fig. 7a, a'). Bands near 2900, 1730 and 1350-1550 cm^{-1} due to organic matter are also visible. In the red clay, however, there is an additional band at 305 cm^{-1} and a greater intensity at 643 cm^{-1} than would normally be expected for kaolinite (Farmer, 1974). These bands are eliminated by dithionite-citrate-bicarbonate treatment, which also decreases absorption in the 450-550 cm^{-1} region (Fig. 7b) resulting in the complete bleaching of the clay, and indicating that the red pigment is probably hematite-like.

A comparison was made of the red and non-red clay fractions after a 5 min HF treatment to remove the kaolinite. Both clays yield spectra consistent with finely-ground muscovite but the red clay is now characterized by strong hematite-like bands at 300, 440, 530 cm^{-1} with weaker bands at 225

and 650 cm^{-1} (Fig. 7c, c'). The spectrum of the red clay also shows enhanced absorption near 1050 cm^{-1} and weak bands at 3604 and 860 cm^{-1} in the OH stretching and deformation regions respectively, indicating the presence of a layer silicate other than muscovite. Prolonged HF treatment results in dissolution of much of the hematite pigment and virtually all of the silicate leaving a residue containing a small amount of the more usual type of hematite as found in specular ore (Estep, 1972; Farmer, 1974) with strong bands at 530, 450 and 315 cm^{-1} and weaker bands at 640, 400 and 230 cm^{-1} (Fig. 7d) as well as some weak bands that can be attributed to goethite. This treatment also concentrates organic matter and both clays show a complex absorption pattern due to peptide and polysaccharide.

In an attempt to obtain the spectrum of the hematite complex free from interference by the other components present in the clay, two approaches were used, one involving thermal decomposition followed by chemical dissolution of these components, and the other, avoiding chemical treatment, using differential spectroscopy to cancel their IR absorption bands. In the first, the red clay was subjected to four successive treatments consisting of heating to 450°C for 16h followed by a 3 minute HF extraction. This yielded a product which retained the 36Å basal spacing and contained no kaolinite and little detectable 10Å mineral. The IR spectrum (Fig. 8a) confirmed this composition, and clearly showed absorption bands of iron oxide and associated silicate. The silicate bands at 3597, 1110, 1075, 1053, 1030 and 854 cm^{-1} resemble those of ferripyrophyllite recently reported by Chukhrov et al. (1979). The relationship to pyrophyllite gains some support from the observation that, like pyrophyllite, which has a perpendicular band with an anomalously low frequency of 1052 cm^{-1} compared with other layer silicates, the silicate in the complex has a perpendicular Si-O band at 1030 cm^{-1} (Fig. 8a, b), the lower frequency in the complex being due, by analogy with the shift of this band from 1066 cm^{-1} in beidellite to 1034 cm^{-1} in nontronite (Farmer and

Russell, 1974), to the effect of octahedral Fe^{3+}. The Si-O bands expected in the 500 cm^{-1} region are overlapped by the strong bands of the hematite in the complex. The spectrum of the hematite component (Fig. 8a) is virtually identical with that of a platy form of hematite from the Scottish Old Red Sandstone (Fig. 8c) and shows the same perpendicular character for the band near 645 cm^{-1} (cf. Fig. 8b, and d) thought to be a longitudinal optical mode activated in the thin platy crystals. These results showing parallel orientation of the silicate and hematite components complement those described previously for electron diffraction. Transmission electron microscope analysis has, however, shown that the HF used in this method of concentration has attacked the complex, preferentially dissolving the silicate.

In the second method, a differential spectrum was recorded between a magnetic concentrate of the 0.2 - 2 μm red clay in the sample beam of the spectrometer and the untreated 0.2 - 2 μm fraction in the reference beam. The concentrate, prepared by the method of Schulze and Dixon (1979), contained 15 times more complex than the untreated clay. The differential spectrum (Fig. 9) was obtained by adjusting the concentrations of sample and reference until kaolinite and illite absorption bands were cancelled as far as possible. Perfect cancellation proved to be impossible by this technique as shown by the presence of weak bands of kaolinite at 3689, 3618, 1025 and 910 cm^{-1}, but it is sufficiently good to allow the principal silicate bands of the complex at 3602, 1110, 1087, 1045, and 855 cm^{-1} to be seen, and to show that the hematite bands are virtually identical to those of the HF concentrate (Fig. 8a). The kaolinite band at 1025 cm^{-1} obscures the silicate complex band at 1030 cm^{-1} but those at 1110 and 1087 cm^{-1} are more clearly resolved than their counterparts in the spectrum of the concentrate, suggesting that the structure of the complex has probably been slightly altered by the chemical method of isolation. Nevertheless, the HF concentrate has been useful in characterizing the 3602 and 855 cm^{-1} bands of the complex. These are unchanged

after treatment with D_2O vapour using the method described by Russell et al. (1974) and are therefore not due to external OH groups. On removal of adsorbed water by evacuation, the 855 cm^{-1} band shifts to higher frequency, and on exposure to hydrazine vapour, both bands shift to slightly lower frequency. These results are analogous to those observed for layer silicates, supporting the contention that the 3602 and 855 cm^{-1} bands originate in OH groups that are coordinated to Fe^{3+} in a layer silicate-like environment (Russell et al., 1979). After heating the complex to 1000°C, these OH bands are missing from the spectrum which nevertheless retains the pattern typical of platy hematite (Fig. 8a). In contrast, the platy soil hematite similarly heated shows a pattern consistent with a change to the more cubic specularite-type morphology in agreement with the findings of Estep (1972). Failure of the hematite component in the complex to undergo this transformation must be due to the restraining influence of the silicate component, providing further support for the conclusion that both components are linked in the same structure.

Composition

Preliminary XRF analyses were performed on the bulk HF-treated material which contained considerable amounts of mica. The complex was then removed by the dithionite-citrate treatment of Mehra and Jackson (1960) so that the composition of the residual could be determined and used for the calculation of a corrected analysis for the complex. This corrected analysis, calculated on a water-free basis, gave: Fe_2O_3 90.54, SiO_2 5.53, Al_2O_3 3.58, TiO_2 0.21 and MgO 0.14%. Colorimetric analysis of some purified material yielded the following: Fe_2O_3 91.03, SiO_2 7.52 and Al_2O_3 1.45%. Because of the possibility that HF treatment had extracted unknown and possibly considerable amounts of silica from the complex untreated, electromagnetically purified material was

analysed using a transmission electron microscope equipped for microprobe analyses (Table 3). Although the majority of the particles analysed looked similar by electron microscopy, on microprobe analysis, a small number gave either very large values for the Fe:Si ratio, due to the presence of free hematite, or occasionally very low values due to the presence of kaolinite. When the analyses of these particles were rejected, the mean from fourteen determinations was Fe_2O_3 73.6, SiO_2 19.7 and Al_2O_3 6.7%. From the composition it is clear that HF treatment has selectively dissolved SiO_2 from the complex. This mean composition leads to the following ratios Fe:Si:Al = 14.6:2.6:1 or (Fe + Al):Si = 6.0. An example of the spectrum upon which the above analysis is based is shown in Fig. 10.

INTERPRETATION

The above results demonstrate the existence of a hematite-silicate complex in the red mottled patches of a deeply-weathered granite and it now remains to consider how the results can be reconciled in terms of a particular structural arrangement. A central question in this respect is how a fundamental spacing of about 36Å can be generated from a sequence of hematite units and silicate sheets. Two possible structural models (in the dehydrated form) are shown in Fig. 11. In model 1 there are two hematite units - consisting of twelve octahedral sheets - with silicate sheets attached to both sides. In model 2, the same double hematite unit has a silicate sheet attached to one side only. Model 1 yields a calculated spacing of 34.5Å with an Fe:Si ratio of 6:1. Model 2 has calculated spacing of 32.3Å with an Fe:Si ratio of 13:1. Evidently, a choice between these models cannot be made on the basis of the observed spacing of the dehydrated complex, as it occurs at 33.4Å. However, the 6:1 (Fe + Al):Si ratio clearly offers support for an interpretation based on model 1.

Whatever the exact structure of the complex, electron diffraction indicate that there is an orientation relationship between the different components, with the b axis of the silicate sheet lying parallel to the a axis of the hemati unit. This observation could account for the anomalous X-ray diffraction patter in which the 110 and 300 reflections of hematite are sharper than the other reflections of the pattern and are, in addition, usually intense. Presumably, the sharp reflections originate from planes common to both hematite units and silicate sheets, so that in these directions the structure is well-ordered. In other directions, however, no such order exists between the hematite sub-units, leading to broadened lines. However, another interpretation is suggested by the fact that similar differential line broadening has also been observed in hematite separated from soils of tropical and sub-tropical areas. This has been attribute to the indirect effect of Al substitution which preferentially retards growth in the z direction but not in the x direction, thereby leading to very thin crystals (Schwertmann et al., 1977).

At present, the reasons for the swelling properties of the hematite-silicate complex are not clear, and apart from the fact that there are obviously weak bonds between the silicate sheets, there is no complete analogy with either smectite or halloysite. Thus, the X-ray spacings indicate that the complex is capable of absorbing two layers of water, glycerol or ethylene glycol, suggesting a resemblance to smectite rather than halloysite. On the other hand, in the natureal state, the complex appears to contain only a single water layer and yields the same X-ray spacing irrespective of cation saturation, observations more consistent with a halloysite-type interlayer space where there is little or no capacity for cation exchange. Intercalation tests are also somewhat abmiguous in that it seems to be possible to form an intercalate with K-acetate but not with hydrazine.

ORIGIN

Although statements on the origin of the hematite-silicate complex

are necessarily speculative, several inferences can reasonably be made. Comparison of the mineralogy of the red and non-red parts of the weathered granite, as revealed by optical microscopy, indicates that apart from the presence of pigmentary iron oxides there is little difference between them. In both cases, quartz and K-feldspar are dominant, the latter frequently being converted to kaolinite, with subordinate mica and montmorillonite. Minor amounts of pleochroic biotite also occur throughout the weathered outcrops, suggesting that the source of the pigmentary iron does not reside in altered ferromagnesian minerals within the reddened patches. It is considered more likely that, in pre- or interglacial times, the iron was complexed at higher levels of the weathered profile by waters percolating through organic surface horizons. Movement down the profile probably occurred along joint planes and other features in the weathered granite that allow ground water to move freely, and in these areas the iron-organic complex would be oxidatively degraded, possible microbially, leading to the precipitation of ferrihydrite. Typically, ferrihydrite is rich in adsorbed inorganic ions (including silica) and organic compounds, and although these may have an inhibiting effect on further crystallization, the ferrihydrite to hematite transformation can now be regarded as completely established in the appropriate environmental conditions (Schwertmann and Taylor, 1977; Schwertmann, 1978). The influence of silicate on ferrihydrite systhesis has been investigated by Schwertmann and Thalmann (1976). In their experiments they synthesized ferrihydrite containing up to 4.35% silica and undoubtedly the synthesis of even more siliceous ferrihydrite is possible. It seems likely, therefore, that the immediate precursor of the hematite-silicate complex was a siliceous ferrihydrite, the structure of which became more organized with geological time.

CONCLUSIONS

All the evidence indicates the existence of a hematite-silicate complex in the reddened patches of a deeply weathered granite in north-east Scotland. The most probable structural arrangement for this complex is one in which double hematite units are terminated on both sides by silicate sheets, the weak bonding between these sheets allowing expansion with water and glycerol. Although the hematite-silicate complex is unique, it is possible that a similar type of association of silicate sheets with hematite might be quite widespread, esepcially where the iron oxide results from weathering. Thus, the complex was detected only because a sufficient number of repeat units has built up to yield the anomalous, high X-ray spacings. In other circumstance there may not be enough silicate sheets to manifest any X-ray diffraction effects and consequently these would tend to go undetected.

REFERENCES

Chukhrov, F.V., Zvyagin, B.B., Drits, V.A., Gorshkov, A.I., Ermilova, L.P., Goilo, E.A. and Rudnitskaya, E.S., 1979. The ferric analogue of pyrophyllite and related phases in Proceedings 6th International Clay Conference 1978 Oxford, pp. 55-64. Edited by M.M. Mortland and V.C. Farmer. Published by Elsevier as Developments in Sedimentology Number 27.

Estep, P.A., 1972. Infrared spectroscopic studies of hematite. M.S. Thesis presented to West Virginia University.

Farmer, V.C., 1974. The Anhydrous Oxide Minerals, Chapter 10 in The Infrared Spectra of Minerals. Edited by V.C. Farmer. Mineralogical Society, London.

Farmer, V.C. and Russell, J.D., 1964. The infrared spectra of layer silicates. Spectrochim. Acta 20, 1149-1173.

Hashimoto, I. and Jackson, M.L., 1960. Rapid dissolution of allophane and kaolinite-halloysite after dehydration. Clays Clay Miner. 7, 102-113.

Kühnel, R.A., Roorda, H.J. and Steensma, J.J., 1975. The crystallinity of minerals - A new variable in pedogenetic processes: A study of goethite and associated silicates in laterites. Clays Clay Miner. 23, 349-354.

Mehra, O.P. and Jackson, M.L., 1960. Iron oxide removal from soils and clays by dithionite-citrate system buffered with sodium carbonate. Clays Clay Miner. 7, 317-327.

Norrish, K., 1968. Some phosphate minerals of soils. Trans. 9th Int. Congr. Soil Sci., Vol. III, 713-723.

Rooksby, H.P., 1961. Oxides and hydroxides of iron and aluminium. Chapter X in X-ray Identification and Crystal Structures of Clay Minerals (editor G. Brown) Mineralogical Society, London.

Russell, J.D., Parfitt, R.L., Fraser, A.R. and Farmer, V.C., 1974. Surface structures of gibbsite, goethite and phosphated goethite. Nature Lond., 248, 220-221.

Russell, J.D., Goodman, B.A. and Fraser, A.R., 1979. Infrared and Mössbauer studies of reduced nontronite. Clays Clay Miner., 27, 63-71.

Schulze, D.G. and Dixon, J.B., 1979. High gradient magnetic separation of iron oxides and other magnetic minerals from soil clays. Soil Sci. Soc. Am. J., 43, 793-799.

Schwertmann, U., 1979. Non crystalline and Accessory Minerals in Proceedings 6th International Clay Conference 1978, Oxford, pp. 491-499. Edited by M.M. Mortland and V.C. Farmer. Published by Elsevier as Developments in Sedimentology, Number 27.

Schwertmann, U. and Thalmann, H., 1976. The influence of [Fe(II)][Si], and pH on the formation of lepidocrocite and ferrihydrite during oxidation of aqueous $FeCl_2$ solutions. Clay Miner., 11, 189-200.

Schwertmann, U., Fitzpartick, R.W. and Le Roux, J., 1977. Al substitution and differential disorder in soil hematites. Clays Clay Miner., 25, 373-374.

Schwertmann, U. and Taylor, R.M., 1977. Iron Oxides. Chapter 5 in Minerals in Soil Environments. Edited by J.B. Dixon and S.B. Weed. Soil Science Society America, Madison, USA.

TABLE 1

Observed d(001) spacings (002 x 2) after various treatments

Treatment	dobs (Å)
Air dry	35.6
Wet	40.2
K^+ saturated	36.3
Mg^{2+} saturated	36.3
Mg^{2+} sat. glycerol	40.2
Mg^{2+} sat. ethylene glycol	39.4
300°C	33.4
550°C	33.3

TABLE 2

Partial X-ray diffraction data for (1) hematite-silicate complex from powder photograph in Fig. 5 and (2) hematite (Rooksby, 1961).

(1)			(2)		
dA	I	Attribution	dA	I	hkl
4.46	m	H.S. ?			
4.24	w	Q + HS ?			
3.70	m br	H.S.	3.67	35	012
3.31	vw	Q + HS ?			
3.06	vw	H.S. ?			
2.72	ms br	H.S.	2.69	100	104
2.52	vs sh	H.S.	2.514	75	110
2,224	mw br	H.S.	2.204	25	113/021
			2.072	3	202
1.842	mw br	H.S.	1.838	30	024
1.693	mw br	H.S.	1.692	45	116
			1.635	2	211
1.604	vw br	H.S.	1.597	15	018
1.491	mw br	H.S.	1.484	20	214
1.458	ms sh	H.S.	1.452	25	300

H.S. Hematite-silicate complex, Q Quartz, vs very strong, ms medium strong, m medium, mw medium weak, w weak, vw very weak, br broad, sh sharp.

CAPTIONS TO FIGURES

Fig. 1 Photographs showing: (a) exposure of deeply weathered granite covered by soliflucted material; (b) close-up of red mottled patches in weathered granite.

Fig. 2 Photomicrographs showing: (a) Area of non-red material with montmorillonite (Mo) containing flecks of iron oxide abutting sharply against kaolinized feldspar (KF), muscovite (Mi) is also partly kaolinized and shows a "fan-tail" appearance; (b) Area of red material consisting of coarse, interlocking kaolinite crystals (K) relatively free of iron oxides; the iron oxides (I.ox.) seem to be preferentially associated with veins and patches of micaceous and/or montmorillonite material. Q quartz. Bar 100 μm.

Fig. 3 X-ray diffraction traces of oriented aggregates of the <2 μm fraction separated from red weathered granite: (a) Untreated material; (b) treated with HF for 5 min; (c) treated with HF for 8 h.

Fig. 4 X-ray diffraction traces of oriented aggregates of the <2 μm fraction separated from red weathered granite and treated with HF for 5 min: (a) No further treatment; (b) solvated with glycerol; (c) heated at 300°C, for 4 h; (d) treated with dithionite-citrate-bicarbonate.

Fig. 5 X-ray diffraction powder photograph of randomly oriented complex after removal of kaolinite and illite by heating at 450°C followed by HF treatment.

Fig. 6 Electron micrographs showing: (a) particle of hematite-silicate complex with electron dense areas and moiré fringes; (b) electron diffraction pattern showing layer silicate and hematite reflections (the arrows shows the $\underline{a}^*$ direction of hematite and the $\underline{b}^*$ direction of the layer silicate); (c) and (d) structure with 36Å spacing and dislocation features. Bar equals 0.1 μm.

TABLE 3

Atomic ratios in particles of hematite-silicate complex calculated from transmission probe micro-analysis. [Multiple analyses refer to different areas of the same particle]

Particle	Fe:Si	Si:Al	Fe:Al	(Fe + Al):Si	
1	5.6	3.1	17.4	5.9	
	6.0	2.3	13.8	6.4	
2	5.2	2.9	15.1	5.6	
	5.3	2.5	13.3	5.7	
*3	2.6	2.6	6.8	3.0	
4	4.6	2.5	11.5	5.0	
	5.0	2.6	13.0	5.4	
*5	16.0	2.2	35.2	16.5	
	6.1	2.2	13.4	6.5	
	5.7	3.1	17.7	6.0	
6	5.1	2.4	12.2	5.5	
	6.1	2.3	14.0	6.5	
*7	9.3	1.8	16.7	9.8	
8	7.1	2.6	18.6	7.5	
9	5.9	2.9	17.1	6.2	
10	5.6	0.9	5.0	6.7	
*11	11.6	1.5	17.4	12.3	
12	5.9	1.3	7.7	6.7	
*13	20.0	2.0	40.0	20.5	
			13.6	6.1	mean
			3.8	0.7	S.D.

* Data for these particles not included in calculation of means because ~~of the possibility that~~ neither free hematite or Kaolinite was making a major contribution.

Fig. 7 Infrared spectra of KBr disks containing red clay (left) and non-red clay (right) from weathered granite: a,a' untreated; b, dithionite-citrate-bicarbonate extracted; c,c' 5 min HF extracted; d,d' 8 hrs HF extracted. (T, transmission; ν, wavenumber).

Fig. 8 Infrared spectra of HF concentrate (see text) of <0.2 μm red clay: (a) in CsI disk heated to 150°; (b) film on CsI plate at 0° incidence. Infrared spectra soil hematite; (c) in CsI disk heated to 150°; (d) film on CsI plate at 0° incidence.

Fig. 9 Differential infrared spectrum (see text) of hematite-silicate complex. (T, transmission; ν, wavenumber).

Fig. 10 X-ray spectrum of a particle of hematite-silicate complex.

Fig. 11 ~~Proposed~~ Possible arrangements of hematite-silicate complex.

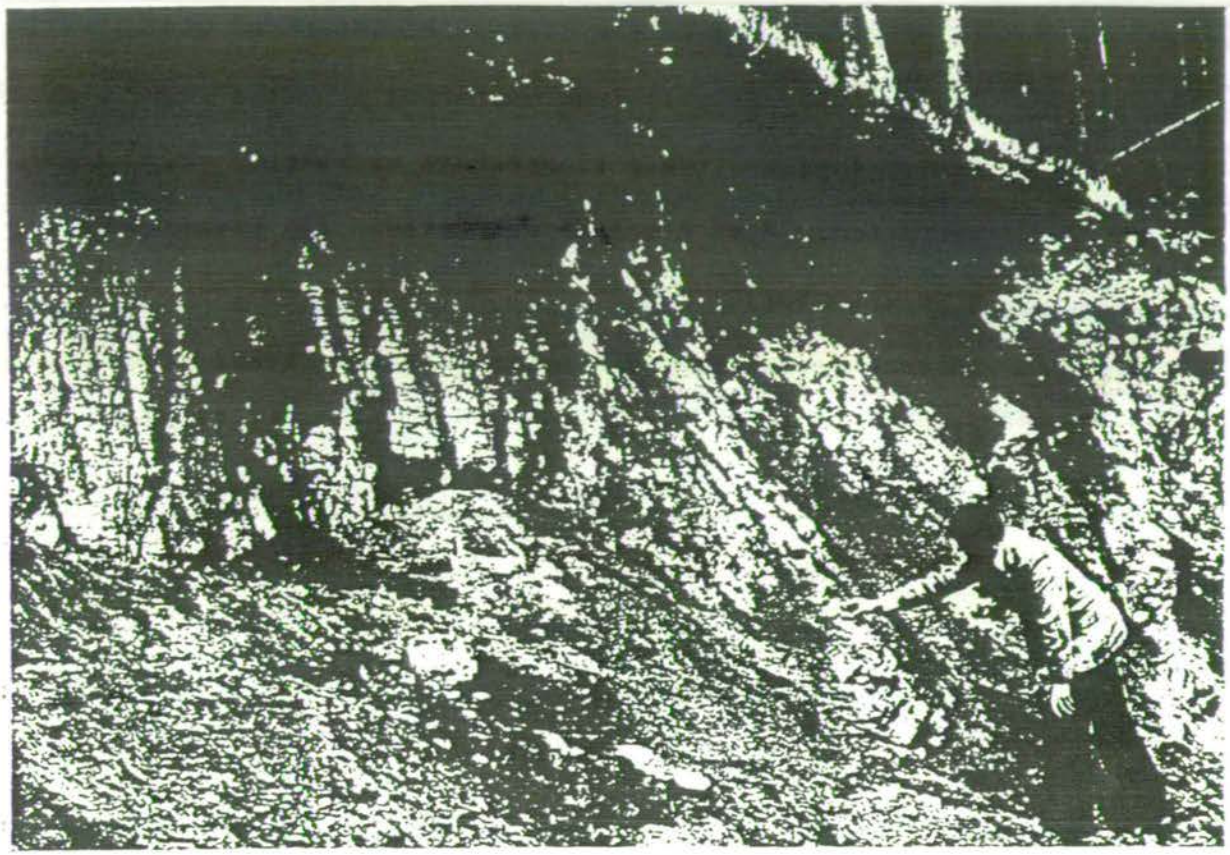

(a)

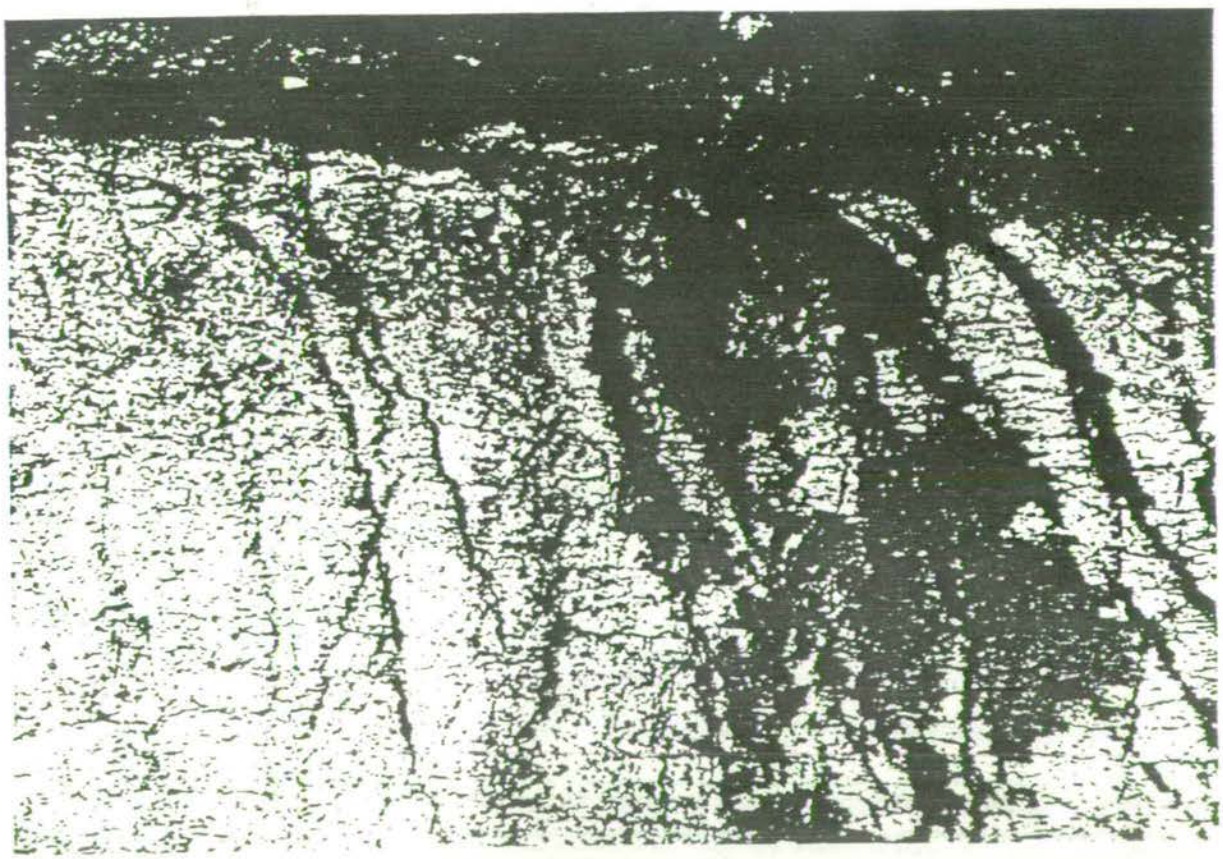

(b)

FIG. 2.

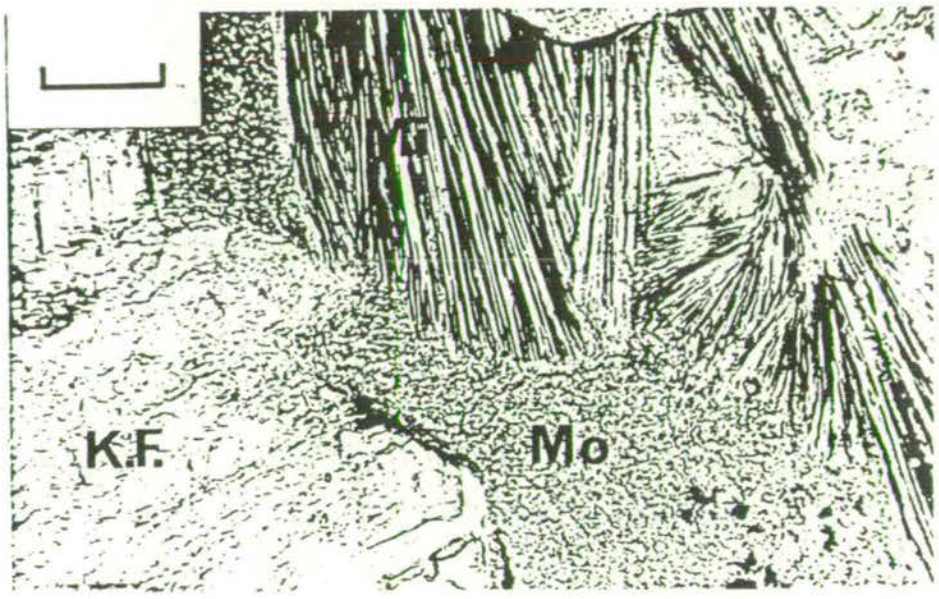

(a)

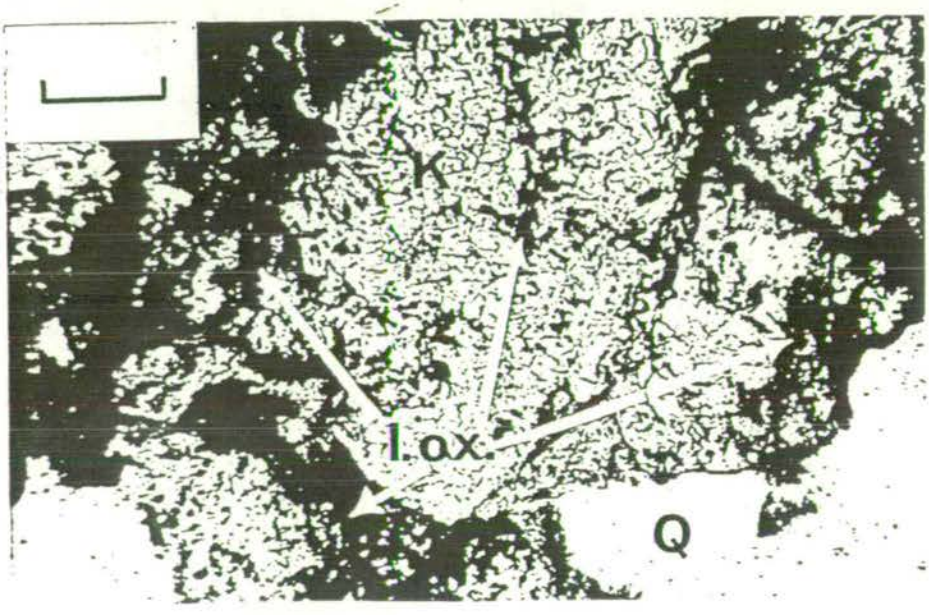

(b).

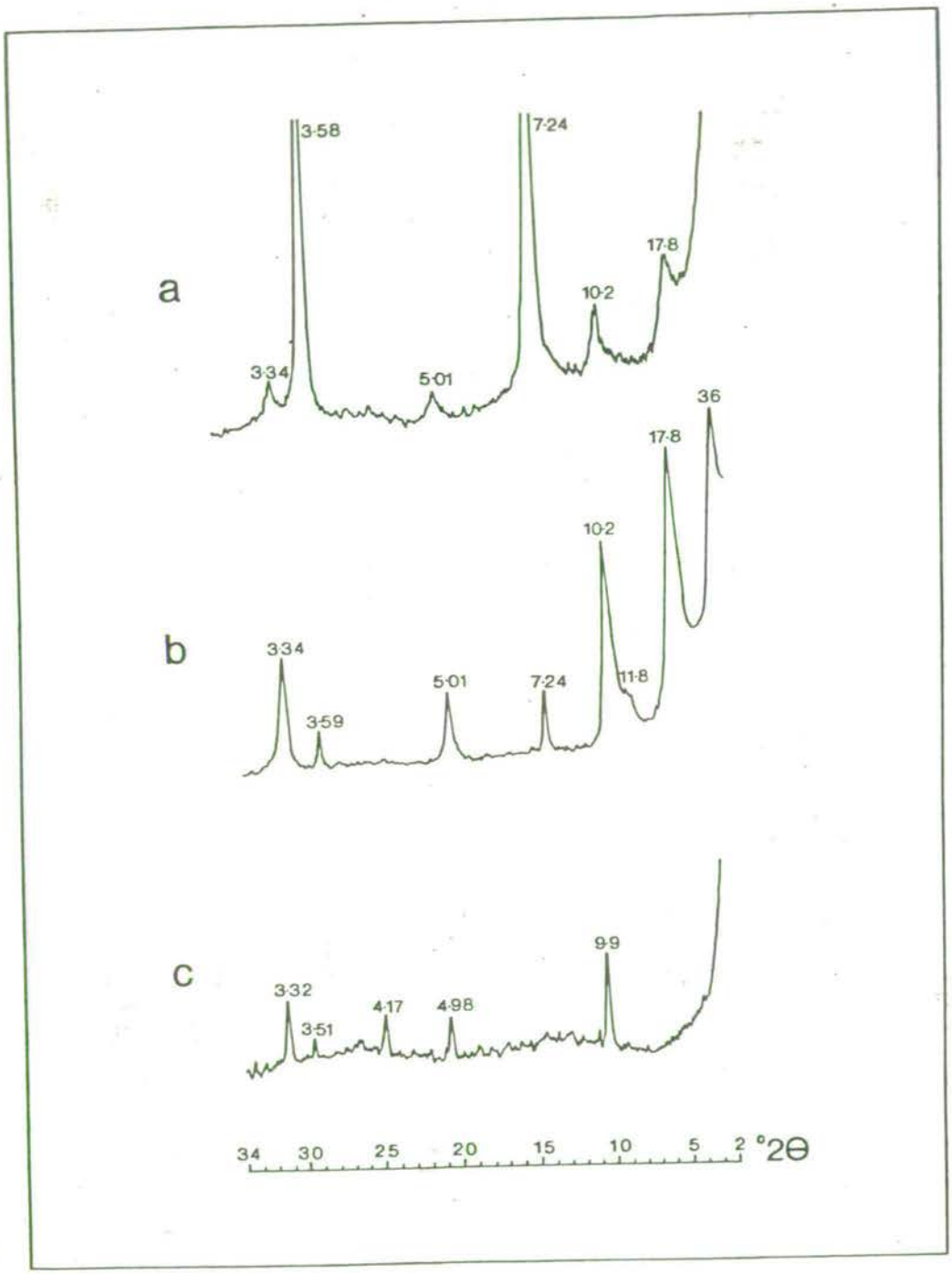
a
3·58
7·24
17·8
10·2
3·34
5·01
b
3·36
17·8
10·2
3·34
5·01
7·24
11·8
3·59
c
9·9
3·32
4·17
4·98
3·51
34 30 25 20 15 10 5 2 °2θ

Fig. 3.

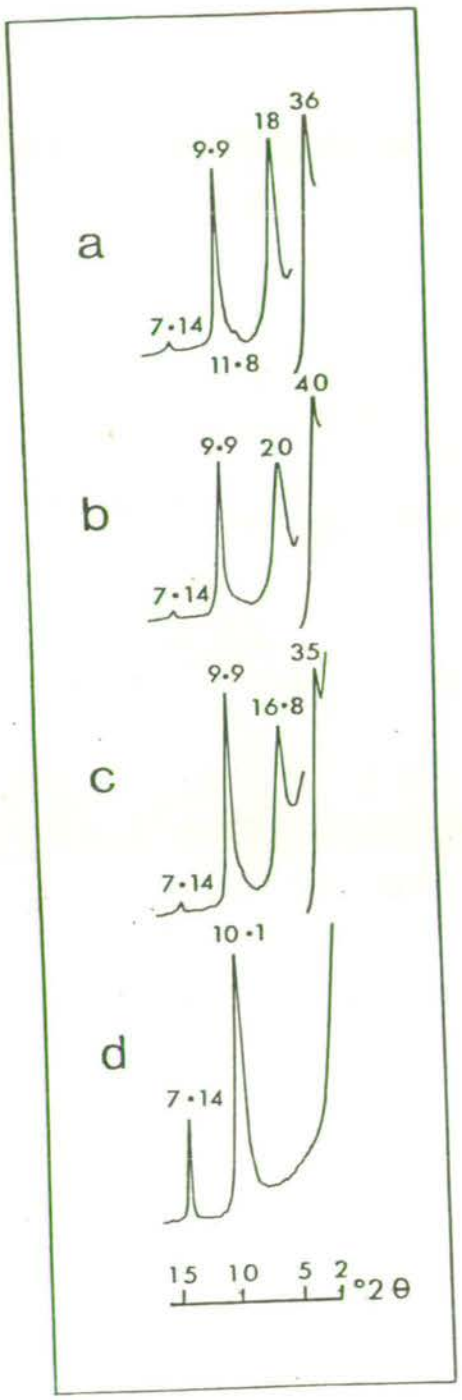

Fig. 4.

Fig 5.

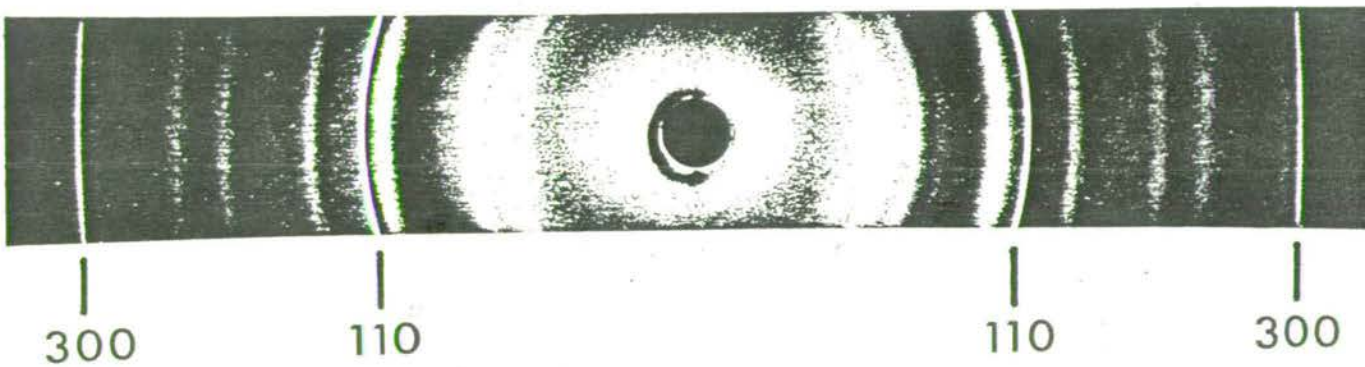

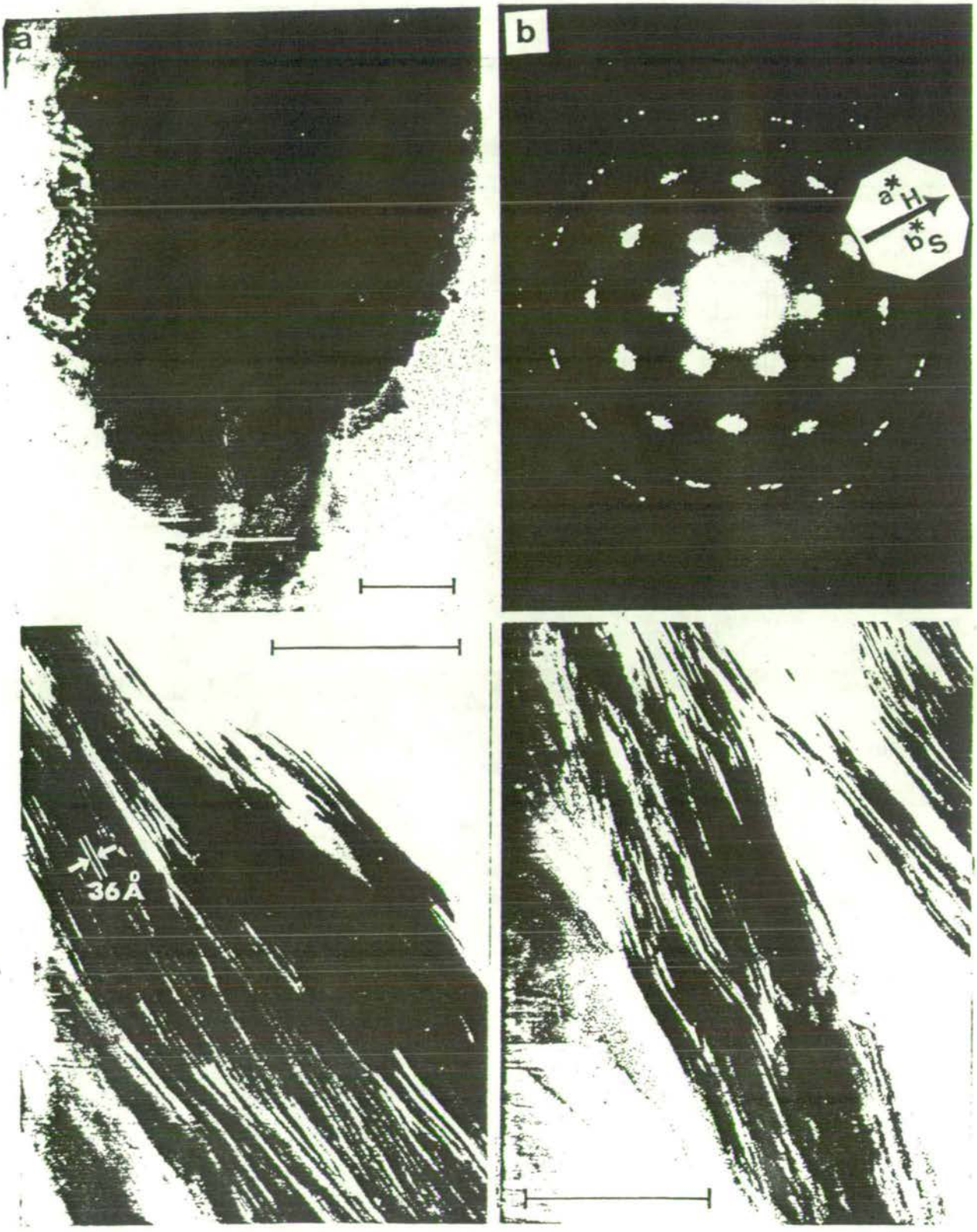

FIG. 6

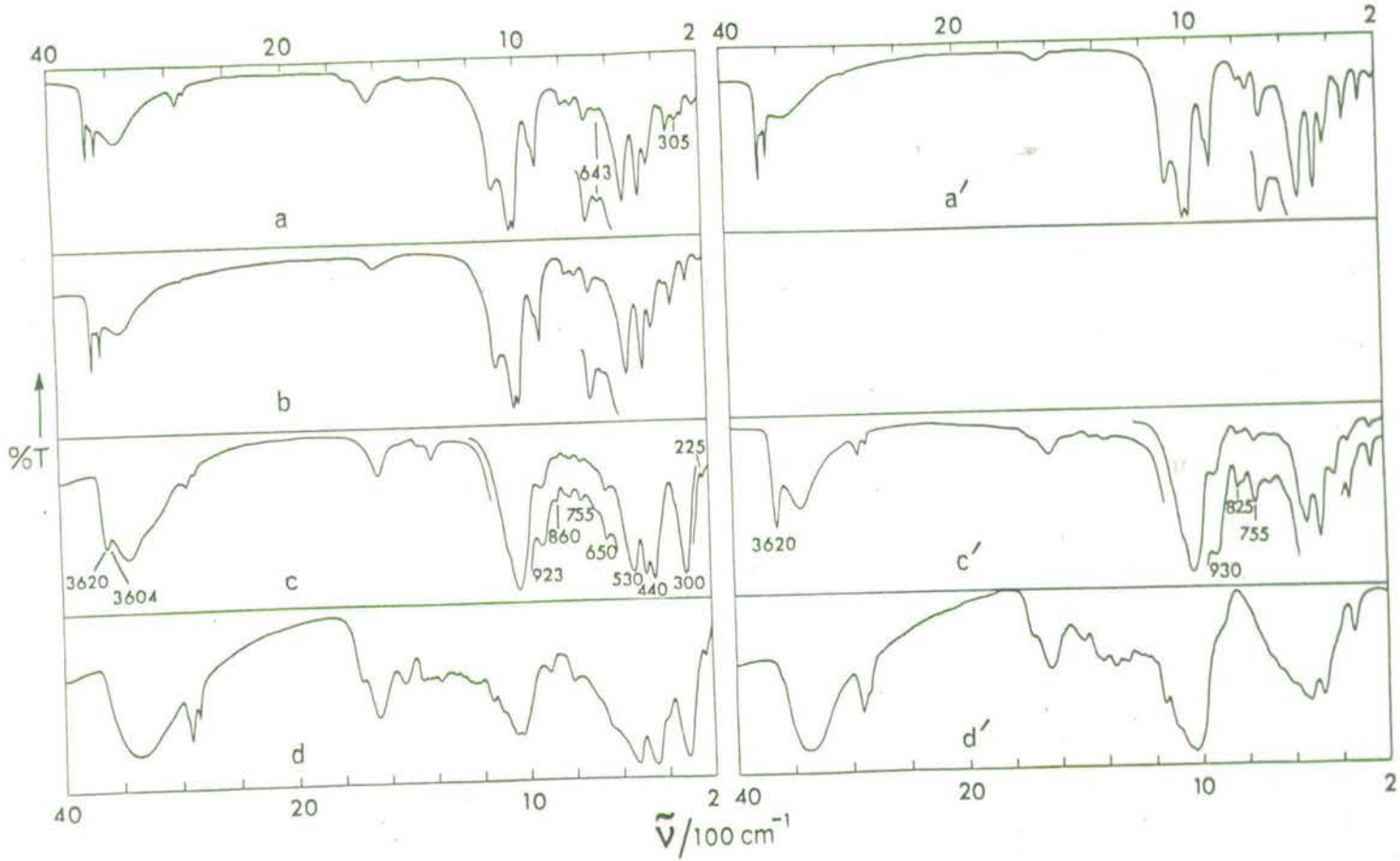
40
20
10
2
a
643
305
b
c
3620
3604
923
755
860
650
530
440
225
300
d
a′
c′
3620
825
755
930
d′
%T
$\tilde{\nu}$/100 cm^{-1}

FIG. 7.

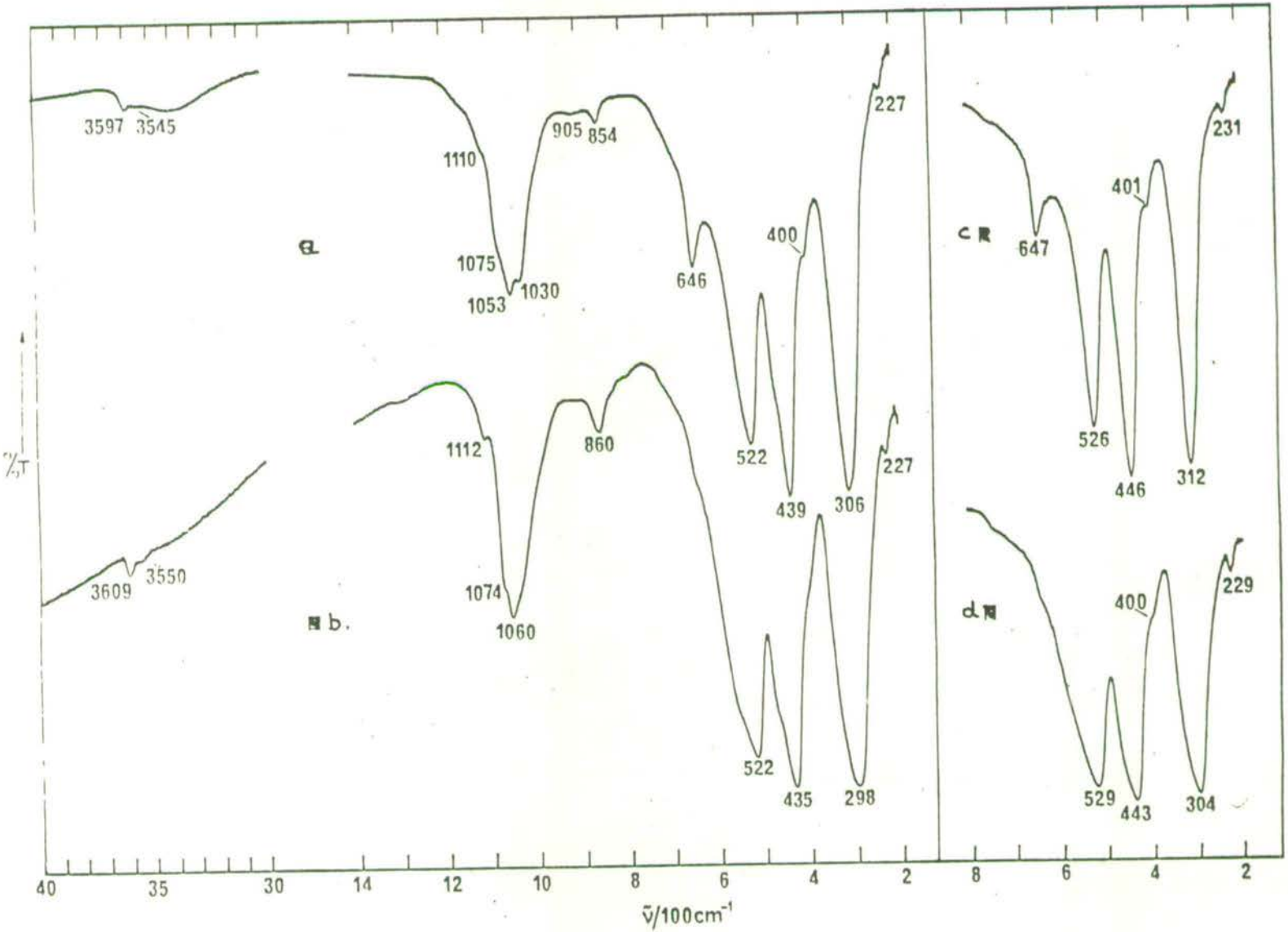
3597
3545
1110
905
854
1075
1053
1030
646
400
227
a
522
439
306
1112
860
227
1074
1060
3609
3550
b.
522
435
298
c
647
401
231
526
446
312
d
400
229
529
443
304
%T
40
35
30
14
12
10
8
6
4
2
8
6
4
2
ṽ/100cm⁻¹

Fig. 4

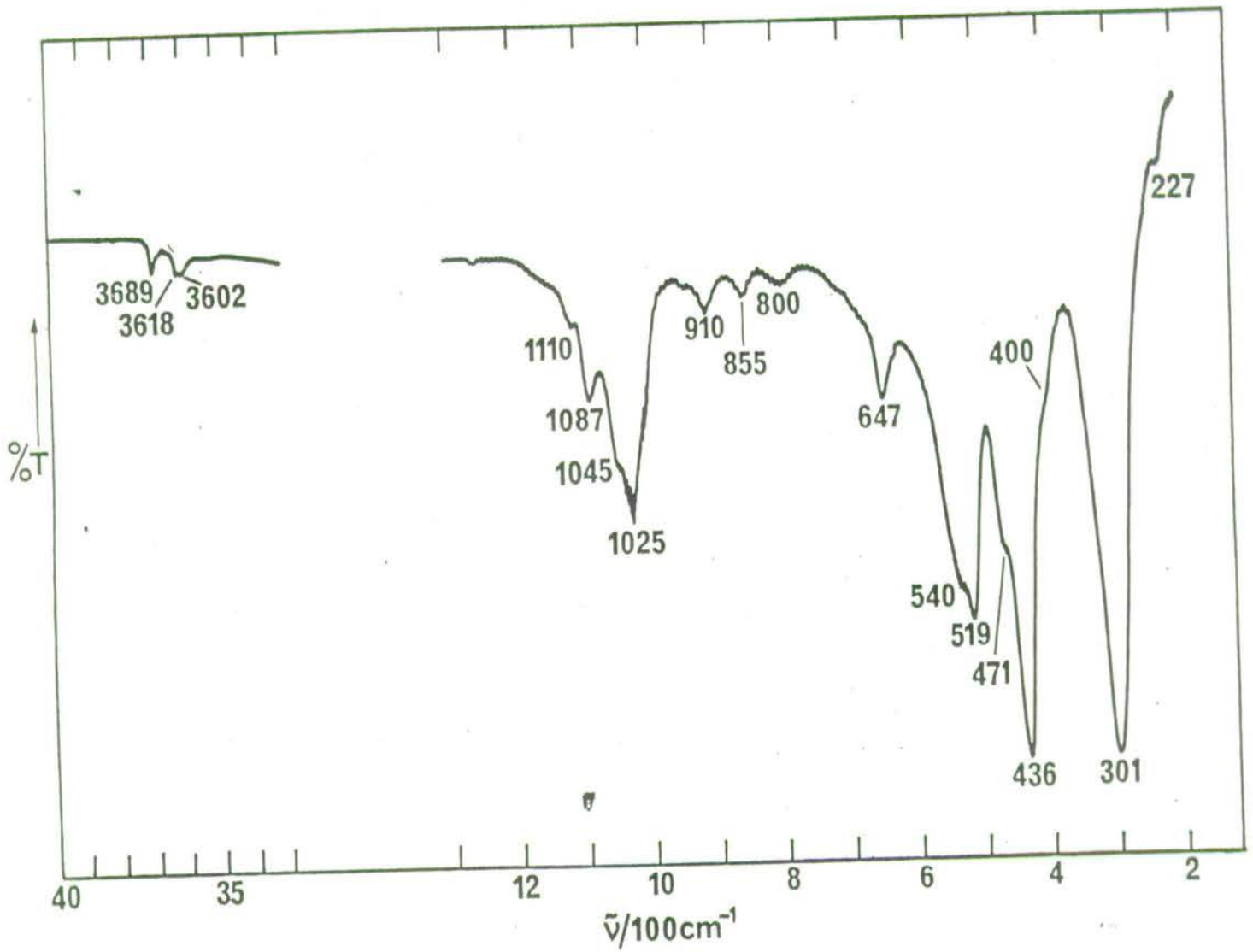
3689
3618
3602
1110
1087
1045
1025
910
855
800
647
400
227
540
519
471
436
301
%T
40
35
12
10
8
6
4
2
ν̃/100cm⁻¹

Fig 9.

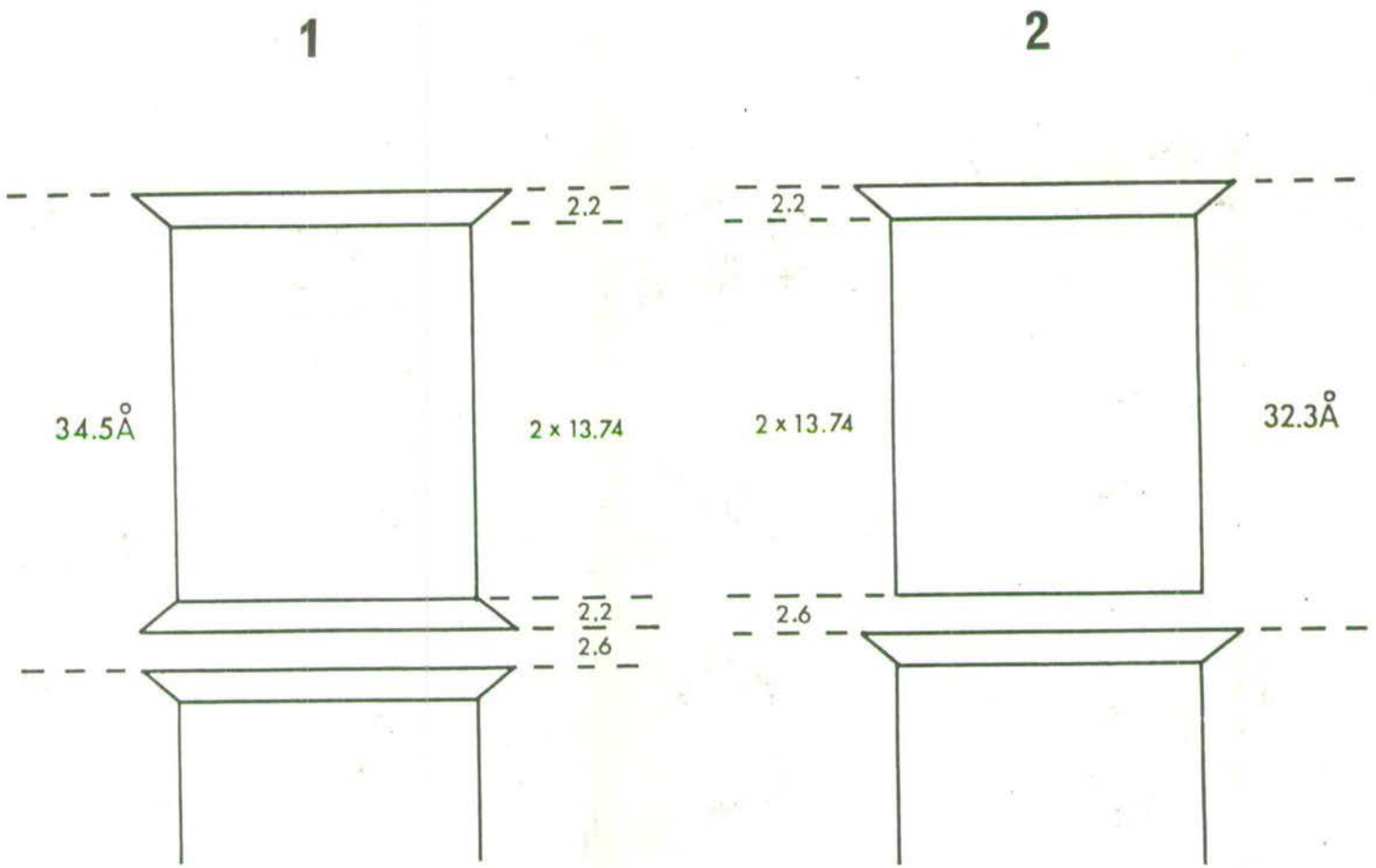

FIG. 11.

· FIG-10 ·